

AD-A 121 910

RIA-83-U51

AD A-121910

AGARD-CP-325

AGARD-CP-325

AGARD

ADVISORY GROUP FOR AEROSPACE RESEARCH & DEVELOPMENT

7 RUE ANCELLE 92200 NEUILLY SUR SEINE FRANCE

AGARD CONFERENCE PROCEEDINGS No.325

Advanced Casting Technology

TECHNICAL
LIBRARY

NORTH ATLANTIC TREATY ORGANIZATION



DISTRIBUTION AND AVAILABILITY
ON BACK COVER

NORTH ATLANTIC TREATY ORGANIZATION
ADVISORY GROUP FOR AEROSPACE RESEARCH AND DEVELOPMENT
(ORGANISATION DU TRAITE DE L'ATLANTIQUE NORD)

AGARD Conference Proceedings No.325
ADVANCED CASTING TECHNOLOGY

Papers presented at the 54th Meeting of the AGARD Structures and Materials Panel
in Brussels, Belgium on 4–9 April 1982.

THE MISSION OF AGARD

The mission of AGARD is to bring together the leading personalities of the NATO nations in the fields of science and technology relating to aerospace for the following purposes:

- Exchanging of scientific and technical information;
- Continuously stimulating advances in the aerospace sciences relevant to strengthening the common defence posture;
- Improving the co-operation among member nations in aerospace research and development;
- Providing scientific and technical advice and assistance to the North Atlantic Military Committee in the field of aerospace research and development;
- Rendering scientific and technical assistance, as requested, to other NATO bodies and to member nations in connection with research and development problems in the aerospace field;
- Providing assistance to member nations for the purpose of increasing their scientific and technical potential;
- Recommending effective ways for the member nations to use their research and development capabilities for the common benefit of the NATO community.

The highest authority within AGARD is the National Delegates Board consisting of officially appointed senior representatives from each member nation. The mission of AGARD is carried out through the Panels which are composed of experts appointed by the National Delegates, the Consultant and Exchange Programme and the Aerospace Applications Studies Programme. The results of AGARD work are reported to the member nations and the NATO Authorities through the AGARD series of publications of which this is one.

Participation in AGARD activities is by invitation only and is normally limited to citizens of the NATO nations.

The content of this publication has been reproduced
directly from material supplied by AGARD or the authors.

Published August 1982

Copyright © AGARD 1982
All Rights Reserved

ISBN 92-835-0314-6



*Printed by Technical Editing and Reproduction Ltd
5-11 Mortimer Street, London, W1N 7RH*

PREFACE

There is a strong drive among the NATO nations to reduce the cost of ownership of aircraft. Advances in manufacturing and fabrication technology can lead to lower manufacturing costs which reduces acquisition costs. These advanced manufacturing techniques may also lead to lower weight structures.

The Structures and Materials Panel held a Specialists' Meeting in 1978 on advances in fabrication processes and there was a high level of interest by the participants. The Panel decided to continue an activity in this area by selecting a particular area of advancing fabrication technology for more in-depth study.

Advances in casting technology can lead to a single casting replacing a complex fabrication of wrought components with consequent cost and weight benefits but there is traditionally a reluctance by designers to trust castings. The object of the Specialist Meeting was to present the current state of developments of advanced casting technology, and to bring together designers and materials and processing engineers for a full exchange of views.

The Meeting was attended by about 85 participants and discussion was lively. The papers presented a comprehensive review of the state of casting technology development, and illustrate the significant advances made over the last few years. It became clear from the discussion that the use of castings, especially aluminium alloy castings, for main structural applications is likely to increase significantly in the near future. The discussion highlighted areas needing further attention, which included:—

1. Designers need to design for casting, not convert a wrought fabrication.
2. There is need for greater liaison between designer and foundry before a casting is designed in detail.
3. Greater use could be made of the foundry science already known.
4. There is a need for foundries to prove that castings can be manufactured at repeatable quality, price and delivery.
5. There is a need to reduce the current costs of proof of quality.
6. There is scope for alloy development.

On behalf of the Structures and Materials Panel I would like to thank the Authors, Session Chairmen, Session Recorders and participants for their excellent contributions which made the Meeting so successful.

J.R.LEE
Chairman — Sub-Committee on
Advanced Casting Technology

CONTENTS

	Page
PREFACE by J.R.Lee	iii
	Reference
<u>SESSION I – REVIEW OF USE AND DEVELOPMENTS OF CASTINGS</u>	
ADVANCED CASTINGS IN THE DESIGN OF MILITARY AIRCRAFT by D.J.Duckworth and R.M.Shaw	1
ADVANCED CASTING – TODAY AND TOMORROW by D.Mietrach	2
SOME DEVELOPMENTS IN CASTING TECHNOLOGY by H.Nieswaag	3
DEVELOPMENTS IN ALUMINIUM ALLOY INVESTMENT CASTINGS by P.H.Jackson	4
DEVELOPMENT AND TRENDS IN MAGNESIUM ALLOY TECHNOLOGY by W.Unsworth and J.F.King	5
DISCUSSION SUMMARY – SESSION I by K.Verstraate	D-1
<u>SESSION II – DEVELOPMENTS IN CASTING THEORY AND PRACTICE</u>	
STRUCTURAL CONTROL IN SOLIDIFICATION PROCESSING by D.Apelian	6
NUMERICAL SIMULATION OF CASTING SOLIDIFICATION. APPLICATION TO THE SAND-COATED GRAVITY DIE CASTING PROCESS by G.Vanhoutte	7
THE SQUEEZE FORMING OF ALUMINIUM ALLOYS by G.Williams	8
DERNIERS DEVELOPPEMENTS DE LA COULEE EN SABLE SOUS BASSE PRESSION ADAPTES A LA REALISATION DE GRANDES PIECES DE STRUCTURES AERONAUTIQUES par G.Broihanne	9
NEW DEVELOPMENTS IN ALUMINIUM AND TITANIUM INVESTMENT CASTINGS by G.Wedeking	10
RESUME DES DISCUSSIONS – SESSION II par M.Dupont	D-2
<u>SESSION III – DEVELOPMENTS IN CASTING PRACTICE</u>	
AN EVALUATION OF VACUUM CENTRIFUGED TITANIUM CASTINGS FOR HELICOPTER COMPONENTS by L.J.Maidment and H.Paweletz	11
GRAIN REFINEMENT OF CAST NICKEL-BASE SUPERALLOYS AND ITS EFFECT ON PROPERTIES by A.F.Denzine, T.A.Kolakowski and J.F.Wallace	12
CAST TITANIUM COMPONENTS FOR ROTATING GAS TURBINE APPLICATIONS by B.A.Ewing	13

	Reference
REALISATION DE PIECES CRITIQUES EN FONDERIE DE PRECISION par M.Brun, G.Vandendriessche, D.Fournier et M.Meurtin	14
ELECTROSLAG CASTING EVALUATION by A.Mitchell and G.Sidla	15
DISCUSSION SUMMARY – SESSION III by D.Apelian	D-3
<u>SESSION IV – DEVELOPMENTS IN CASTING PRACTICE AND QUALITY CONTROL</u>	
A NEWLY DEVELOPED PROCESS (THE GKN + COSWORTH PROCESS) FOR THE PRODUCTION OF HIGH INTEGRITY ALUMINIUM ALLOY CASTINGS by J.Campbell and P.S.A.Wilkins	16
QUALITY ASSURANCE IN TITANIUM AND ALUMINIUM INVESTMENT CASTINGS by C.Liesner	17
QUALITE ET CONTROLE DES PIECES DE FONDERIE DE PRECISION POUR TURBOMACHINES par J.Thiery et J.Voeltzel	18
METALLURGICAL ASPECTS OF QUALITY CONTROL IN THE PRODUCTION OF PREMIUM QUALITY ALUMINIUM INVESTMENT CASTINGS FOR THE AEROSPACE INDUSTRY by S.Kenmerknecht	19
DISCUSSION SUMMARY – SESSION IV by C.A.Stubbington	D-4
DISCUSSION SUMMARY – GENERAL DISCUSSION by C.A.Stubbington	D-5

ADVANCED CASTINGS IN THE DESIGN OF MILITARY AIRCRAFT

by
 D. J. Duckworth
 R. M. Shaw
 British Aerospace P.L.C.
 Aircraft Group
 Warton Division
 Preston
 PR4 1AX
 U.K.

1. INTRODUCTION

The title of the meeting is 'Advanced Castings'. In writing this paper, we had to decide whether to concentrate upon castings which are being considered for our latest airframes, or alternatively, to review how we have used castings and what developments have taken place from the user point of view, over a period of years.

We eventually came down in favour of the latter, and as the luck of the draw has placed our paper as Paper 1, Session 1, we believe this decision to be correct for the purpose of the meeting.

Perhaps in reviewing our experiences we may pose several questions which hopefully will be answered by the later speakers on New Developments, Casting Practice and Quality Control.

In any new design the final shape used is always a compromise. Such factors as cost, structural efficiency, mechanical properties and quality must all be taken into account.

We will attempt to show how these factors interact and highlight what we believe to be the more important areas where development is required.

Finally, we will try to predict the future concerning the more extensive use of castings in modern airframes.

2. "USER" EXPERIENCE

The Military Aircraft Group of British Aerospace have designed and used castings for the last 35 years. During this time, castings made by all the well established processes e.g. Sand, Investment, Shaw, Gravity die, have been used with varying degrees of success.

In some cases, castings have been made for experimental development purposes which, although having performed in a satisfactory manner on test have been prevented from being introduced into airframes for a variety of reasons such as cost, too short a time scale, insufficient numbers to be made, lack of confidence in the process, etc.

When castings have been used, they have always been to established British Standard Aerospace Specifications if available. Where there is no British Standard available, we have written a Domestic Specification which is approved by the Ministry of Defence.

Many casting specifications have been written without any guarantee of strength within the casting itself. The castings are released from the foundry on the basis of test results obtained from separately cast test bars. In many cases "chilled" test bars are used which do not reflect the properties within the body of the casting. Fortunately, the more recently written specifications are giving properties for separately cast test bars and for properties within the casting.

The policy we are adopting at Warton, is where possible to use integrally cast test bars gated to the same running system, these test bars to be used for the purpose of heat treatment control. Then where size permits, test pieces are cut from actual castings at a frequency and location which is stated on the drawing.

In order to illustrate the type and size of castings that have been used throughout the years in our Military Aircraft we have assembled the following "figures". Also included are several illustrations of test components from which useful information has been derived.

Figure 1. This part is in low alloy steel to B.S. HC10, a Nickel, Chromium, Molybdenum steel of 1150 MPa tensile strength.

We have consistently had difficulties with castings in low alloy steel irrespective of the foundry or process used. Problems of porosity, distortion and occasionally decarburisation have lead us to the gradual change to the precipitation hardening stainless steels of the 17/4 PH type, with noticeable all round improvement.

Included in these improvements is our greater confidence in weld repaired casting. In our opinion, this point is of considerable significance. Some (American) foundries insist that weld repair is permitted by the drawings when quoting.

Figure 2. This figure shows a selection of light alloy castings used on one of our current aircraft.

It can be seen that in most cases, it is impractical to take reasonable test specimens from these parts. The castings are therefore represented by separately cast test bars.

Where separately cast test bars are used, it is essential that they are heat treated with the components they represent.

We have also had one bad experience where castings were not heat treated and found their way into structures.

Considerable effort was required to rectify the situation at a significant cost to the Company.

The recently introduced mandatory hardness checks into British Standards for all light alloy castings have now improved the situation in that some guarantee is given that the castings have been heat treated.

Figure 3. This shows our first production titanium casting in 6Al-4V alloy. Because this part was "a first", a high casting factor was used for design purposes. If the part were to be designed today, a lower factor would be used as the Ministry have now issued factors based upon statistical data collected from general sources, including "hipped" castings.

More will be said about design factors later.

The radiographic standard for this casting was based upon the ASTM-E-192 comparison radiographs for steel in the absence of such a standard for titanium. In our opinion, the defects shown in this standard equate more to titanium than those in ASTM-E-155, which is the radiographic standard for aluminium and magnesium castings, although this standard is still preferred by some foundries.

More development and production components have been made in the titanium alloy 6Al-4V and some are in service. These are illustrated in figures 4 to 7.

Figure 4. Shows a small Flap Track which is currently in production as a titanium forging machined all over. Although this component as a casting was not introduced into production, due mainly to insufficient numbers required at the time of completion of the development work, several interesting points are worth noting.

- 1) There is a reduction in the total machining time required to produce a fully machined component of 24 to 25 hours per plane set.
- 2) A suggested reduced cutter usage of 72%.
- 3) An increased material utilisation from 17% to 56% for the casting.

Full structural tests were made on three castings with the following results.

- 1) The castings all completed their fatigue test programme without failure.
- 2) A static test on one casting following fatigue testing did not fail the part at 140% of the ultimate design load and the test was terminated.
- 3) A third casting was used to repeat the fatigue test at 10% higher loads for another fully factored life, again, no failure occurred.

It must be noted however, that all the above assumes limited machining of the castings in question and in this particular case there was a significant weight penalty.

Figure 5. This figure shows the result of a static test made on a titanium casting assembly used as part of a flight refuelling probe. In this case, the casting on the right of the figure is electron beam welded to a wrought titanium 6Al-4V tube machined from bar. It is interesting to note the extreme permanent deformation adjacent to the failure although the casting contains extremely large grains.

Figure 6. This figure illustrates the current production casting used as the "Pitch and Yaw Nozzle" in one of our vertical take off aircraft. This component was originally made as a three piece welded stainless steel casting and is now made in one piece in case 6Al-4V titanium alloy with a weight saving of approximately 43%.

All the above figures illustrate the potential of titanium as a cast material, however, it is our belief that the full potential has yet to be exploited. For instance, the behaviour of cast titanium in torsion is extremely interesting.

Figure 7. This component was designed originally by the Royal Aircraft Establishment in order to obtain test results for tensile, bending, torsion and lug performance from one casting. The illustration shows the considerable torsional ductility exhibited by the 6Al-4V tube following test. During the test, a rotation of approximately 45 degrees was achieved in the tubular part of the casting without fracture.

It is suggested that this movement is achieved by the sliding of the "alpha" platelets within the "beta" grain which allows considerable movement before actual rupture occurs.

Moving on to larger cast components which are being considered for production, figure 8 shows what we believe to be a good example of the use of a light alloy casting for airframe structure.

Figure 8. This component is hollow, has a high degree of complexity and introduces a structural element which has to blend with the external profile of the aircraft.

The part is in A357 alloy, an Al-Si-Mg material. It is quenched from the solutionising temperature into "BREOX" (Poly Alkaline Glycol) to reduce distortion. This is followed by ageing to achieve its necessary tensile strength.

We believe that by using castings of this type or larger, the full potential of the casting process can be exploited for airframe manufacture. The larger the casting, the less parts there are to attach together by fasteners, fewer detail parts are involved and by good design, weight can be saved.

To illustrate this point, we currently manufacture an Airbrake of approximately 1.7m by 0.5m. This part, currently fabricated, is made up of 80 detail parts, all requiring individual planning, associated paper work, storage and most costly of all, assembly. As a casting, 60 of the component parts can be eliminated. The saving is therefore obvious, however, it is still necessary for the foundries to produce their castings at the right price, in the right timescale and for Design to commit themselves at an early enough stage to meet production build programmes.

3. DESIGN PHILOSOPHY

3.1 Present approach to the design of castings

In the initial design phase of any new project, the choice of which materials to use and in what form has to be made many times. With primary objectives of strength/stiffness, mass, time scale and cost, the resulting choice is almost invariably materials in the wrought condition.

The selection of wrought materials for most applications unfortunately leads to the subjective view that this should be the norm for all cases. This idea more than any other perhaps, explains why the use of castings on our Military Aircraft has not been more widespread.

At present, there is no formal requirement for the designer to even consider castings so, unless he has assessed the design requirements accurately and selected the material form objectively, castings are unlikely to be chosen.

All too often, castings are only used as a last resort when all other forms of manufacture have been eliminated, rightly or wrongly, on either complexity or cost grounds. This should not be so since castings obviously have their place.

3.2 An improved approach to the design of castings

The whole field of optimum material and manufacturing route selection could well be improved by formalising the process into a series of questions which when answered by the designer would lead to the correct solution. In this way, castings would at least get a fair chance of selection for the correct application.

For the designer to make the correct choice of a casting, he needs to be fully aware of contemporary casting properties (both good and bad!). A closer liaison between the designer, material specialist and founder should ensure this.

It is suggested that visits by designers to the foundries would stimulate an awareness of castings in a broader context than just mechanical properties. This would put the designer in a much better position to see the correct application when it came along.

At this stage however, the designer is in a "chicken and egg" situation where, perhaps due to his lack of the latest data, he is reluctant to call for the use of castings until he sees more evidence of service experience. The problem here of course is that he as the designer, is the only person who can initiate the process of gaining the experience he needs.

As an interim step to a more formal and objective process of making the correct choice, the designer should at least be persuaded to take a positive approach and ask the question, "Where can I use castings?" rather than the all too familiar, "How can I avoid using them?".

3.3 Factors which inhibit the use of castings

There is an extreme unwillingness in some cases, of both Design and Production to commit themselves to castings at a prototype stage of a new aircraft, due to Design Instability. This results in other routes of manufacture being chosen, such as machined from solid and fabricated. These methods of manufacture are often carried over into production for a variety of reasons, the main one being that once the design is "sealed" or frozen, our customers are reluctant to fund the introduction of castings, even though eventual cost savings can be demonstrated.

We decided to use castings as widely as possible on one of our aircraft and finished up being very disappointed for a variety of reasons involving Design, Manufacturing and Production. This bitter experience resulted in strong representations from Design and Production to design from solid or fabrication for prototype on the next project and change to castings later. We make the distinction here with the Design Instability argument mentioned previously.

3.4 Good design features of castings

The most obvious advantage a casting has over other forms of manufacture is the comparative ease with which complex shapes can be produced. It can prove to be very costly trying to produce these complex shapes by other means.

Again, from a cost point of view, it is often desirable to minimise the number of parts necessary to produce a given assembly. Here again, the casting has a lot to offer.

A third advantage which should be exploited fully is minimum machining. With good dimensional control and careful detail design, the amount of machining can be minimised which leads to cost and time savings.

Another point which is perhaps not realised by some designers is that in the case of titanium and steel castings, the basic cast material can have much the same strength as the wrought equivalents.

however, for aluminium and magnesium alloy, a reduction to approximately 60% and 75% respectively of the wrought strengths is fairly typical.

It is perhaps interesting to note that most of the advantages lie ultimately in the area of cost savings.

3.5 Poor design features of castings and possible solutions

The most serious penalties from a design point of view are in the need for casting factors in addition to the normal design factors of safety, also, the requirement for component strength testing and finally the costly non-destructive radiographic examination of each component.

AvP970, which is the British Ministry of Defence "Design Requirements for Service Aircraft", specifies obligatory casting factors. These factors can vary from 1.05 to 2.5 depending on such things as material, number of components to be strength tested, clearance by calculation only, etc.

Obviously, these factors introduce weight penalties, which in many cases are unacceptable in high performance military aircraft, where weight saving is at a premium.

Component strength testing allows some relief on casting factors by comparison with clearance by calculation, however, the testing increases the cost of the finished component.

The costly non-destructive radiographic examination of every component results in a financial penalty which is apparent throughout the whole of a production programme.

As mentioned previously, the strength of aluminium and magnesium alloy castings is somewhat less than the wrought equivalents. It is quite apparent that improvements here would be of benefit.

Finally, to complete the list of poor features, size limitations have restricted the use of castings in the past to some extent, however, it must be said that some quite large castings are now starting to appear which must be a step in the right direction.

Possible solutions to some of these poor design features lie in the judicious use of castings in the right applications. For example, there is little point in striving for the last gram of weight saving in a casting which is to be located in an area of the airframe where ballast is required for flight stability.

Similarly, more use of castings in Class 3 applications would be advantageous since this eliminates the need for expensive radiographic examination.

Perhaps most important of all, do we really need to carry out strength testing of each new design of casting? This AvP970 requirement has been inherited from the days when much less was known about casting and casting technology than is the case today. Elimination of this requirement would help significantly in the effort to make castings more competitive.

3.6 Modern techniques for machining from solid

Whether this is Design Philosophy or Company Policy is hard to say but the recent introduction of "Machining Centres" of the MOLINS type, for light alloy and the MITSUI for steel has influenced the number of small items made as castings. These Centres can produce from solid at a cost that is hard to match by castings. What these machines have effectively done is to remove a large slice of small parts (up to 300mm by 300mm by 50mm) from the casting area. They have had no bearing on larger items but to some extent can be said to have taken the smaller (easier?), "run of the mill" items away from the foundries and thus made their life more precarious.

4. PERFORMANCE, PROBLEMS AND REMEDIES

Considering all the variables involved in the use of castings and despite their apparent deficiencies, castings have performed very well in our airframes over the last thirty years or so. We can only recall one failure incident serious enough to have put an aircraft in danger. A diagnosis of the failure showed this to be the opening up of a "cold shut" causing a nose wheel of the aircraft to fold up on landing. Fortunately, the remaining piece of the nose wheel acted as a perfect "ski" and the aircraft landed without further damage.

One problem that has given considerable trouble over the years is the "oversell" by some foundry representatives. They will promise to cast any shape with unrealistic tolerances, in timescales which can never be met. If castings are to form a major contribution in the future for airframe structures it will be essential for the technical relationship between user and foundry to be considerably improved. There is also the possibility that there has been a tendency to under price castings.

The cost of material is relatively small when compared with labour and overhead costs which are necessary to build castings into airframes. We are convinced that the user would pay more for castings provided he could guarantee that he would receive a quality product in a timescale to meet build programmes.

It is vital for the foundry industry to establish its reputation and credibility with the user and thereby encourage designers to look more favourably upon this route of manufacture.

It is suggested that the foundry industry requires more technical men in the field who can guide potential users in detail matters concerning casting design at the onset of an airframe design. This will reduce the "old problem" of trying to reproduce components, originally drawn as machined parts, by castings, a formula which has inhibited the process from developing its full potential. In fairness, it must be added that a fundamental change in the attitude of Design and Production towards the use of castings on prototype aircraft is also required.

Up to the present time the majority of castings have been made using alloys and processes that have been established for many years. It is essential therefore, that if the use of castings is to make any significant impact in the future, for aerospace parts, that advantage is taken of newer areas and developments that can sway the designer away from thinking automatically of machined from bar or forged production routes.

Changes will have to be made, both in the foundries and in the attitude and knowledge of designers. There is no doubt that optimum use of castings in airframes can only be achieved if the "right" component is identified initially as suitable for casting, i.e. complex shapes, hollow shapes are ideal, and to be left with as little machining as possible prior to assembly within the airframe.

The following are therefore suggested as areas which can be exploited to the benefit of all :-

4.1 Provision of large castings

A recent programme in the United States has shown that with full commitment to the use of large aluminium castings, a minimum of 30% cost saving over a built up sheet metal structure with no weight penalty could be achieved for a primary structural component weighing approximately 82 Kg in its finished state.

4.2 Improved quality in order to eliminate or significantly reduce, casting factors

In order to achieve this it must be shown that variability of properties within the casting can be reduced. Possible ways of achieving this can be by :-

4.2.1 Increased use of "hipping"

4.2.2 Improvements in the surface quality for all forms of casting

4.2.3 The increased use of vacuum casting techniques

4.2.4 The introduction of additional technologies to the technique of casting e.g. Improved methods of metal entry into the mold cavity and the development of more sophisticated mold materials and chills.

4.2.5 A comprehensive re-evaluation of existing structural test data for as many "In service" castings as possible. The object being to highlight any conservatism in the choice of casting factors used during the original design.

While casting factors remain, castings are automatically penalised.

4.3 Improved tolerances

Traditionally, published "sand" casting tolerances have been large and imprecise in their application for aerospace use and "lost wax" tolerances have been small and seldom achieved.

Experience has shown that the Tooling point/Datum plane system is absolutely essential, together with a thorough analysis of subsequent "in-house" tooling requirements, i.e. for machining and drilling. Associated with this, we are moving towards the more general use of surface profile tolerances (ref. BS308).

The provision of checking fixtures, matched with tooling for mating parts, is almost essential. Normally these are duplicated - one at the foundry and one with the customer, and, if for reasons for example of Aerodynamic Accuracy, they locate the casting by other than their tooling points, then a precise method of use has to be spelled out for the foundry.

It is also sensible sometimes to describe on the drawing the interaction between flatness and thickness tolerances so that subsequent misunderstandings are prevented.

Regarding actual values, we use a general standard for small lost wax castings of $\pm 0.3\text{mm}$ up to 25mm with an additional $\pm 0.1\text{mm}$ for 25mm beyond. It will be recognised that this is lower than "brochure" standards but we have learned by bitter experience that these latter can only be achieved by lengthy iterative development programmes for which we never have time.

On sand castings, as our requirements from one job to the next are as varied as the tolerances proposed by the individual foundries, we usually negotiate tolerances on an ad-hoc basis.

Within the whole complex area of accuracy and tolerances our greatest need is for accuracy on thickness at the bottom of the range, say up to 5.0mm thick.

4.4 Cost saving, for instance, by reduction of radiography

Serious consideration could be given as to the need to fully radiograph castings, particularly if processes such as "hipping" or other defect healing processes have been used.

We would also suggest that in the majority of castings, certain areas are redundant from a real load carrying point of view. The elimination of radiography in certain areas in these times of high cost can help significantly.

4.5 Castings of lower weight

It is suggested that the use of magnesium castings should be seriously considered. Once more, providing the correct component has been chosen as being suitable for casting, in this case because of its liability to corrode if the protective coating is damaged. The important factors in the use of magnesium are :- Accessibility for inspection and replacement and elimination of moisture traps.

Advantages seen are the adequate supply of material, ease of casting, reduced distortion on heat treatment and with improved protective coatings, there could be a new lease of life for magnesium within airframes.

Lighter, stronger aluminium alloys should also receive serious attention. There is no doubt that low density, high strength alloys are feasible and these should be exploited if castings are to combat weight.

4.6 Other properties

A comparison with wrought alloys should be made to identify specific advantages which could be exploited. For instance, in some cases the Fracture Toughness is better. Do we use this feature?

5. ANOTHER "DIMENSION"

The foundry industry should be looking for another "dimension" in which to promote its castings. For example, thought is being put into the reinforcement of castings. The inclusion of fibre or particulate reinforcement, or whiskers could enhance such properties as stiffness, strength or elevated temperature characteristics.

Finally, we believe it is essential to introduce more dialogue between experts in the foundries and the designers AT AN EARLY STAGE of the design. If you as a specialist are the only individual who knows of your new wonder casting made from "unobtainium", PLEASE let the designer know because he is the only person who can turn your idea into a reality.

6. ACKNOWLEDGEMENTS

The authors wish to acknowledge the assistance given by their colleagues within British Aerospace and to thank the Directors for permission to publish this paper.

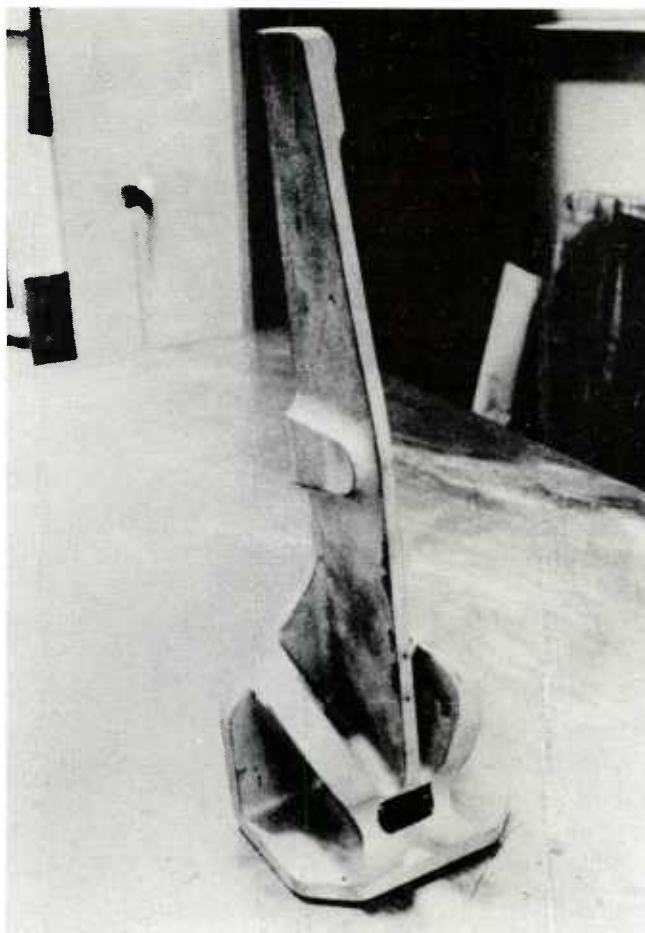


FIG. 1 LOW ALLOY STEEL CASTING IN A NICKEL CHROMIUM MOLYBDENUM STEEL OF 1150 MPa TENSILE STRENGTH



FIG. 2

SELECTION OF LIGHT ALLOY CASTINGS

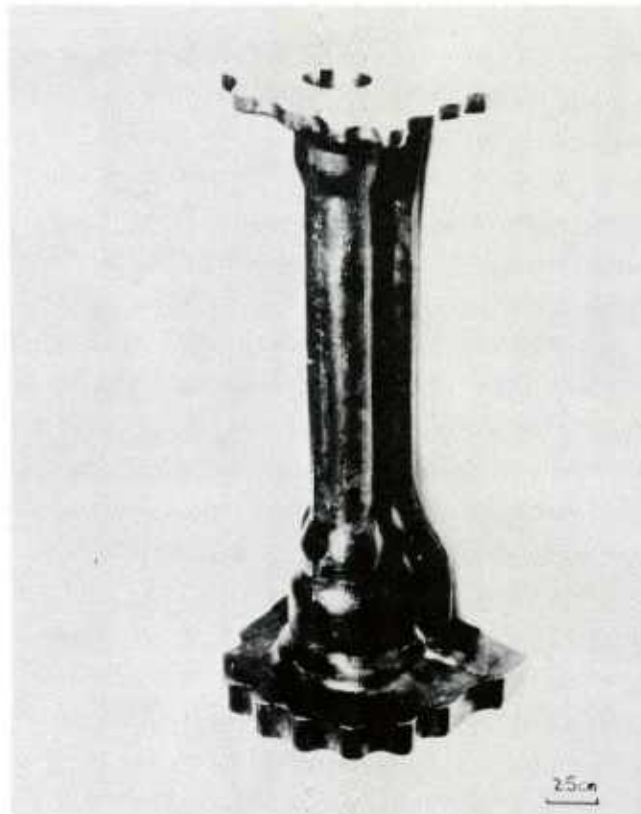


FIG. 3

FIRST PRODUCTION TITANIUM CASTING IN 6Al-4V ALLOY

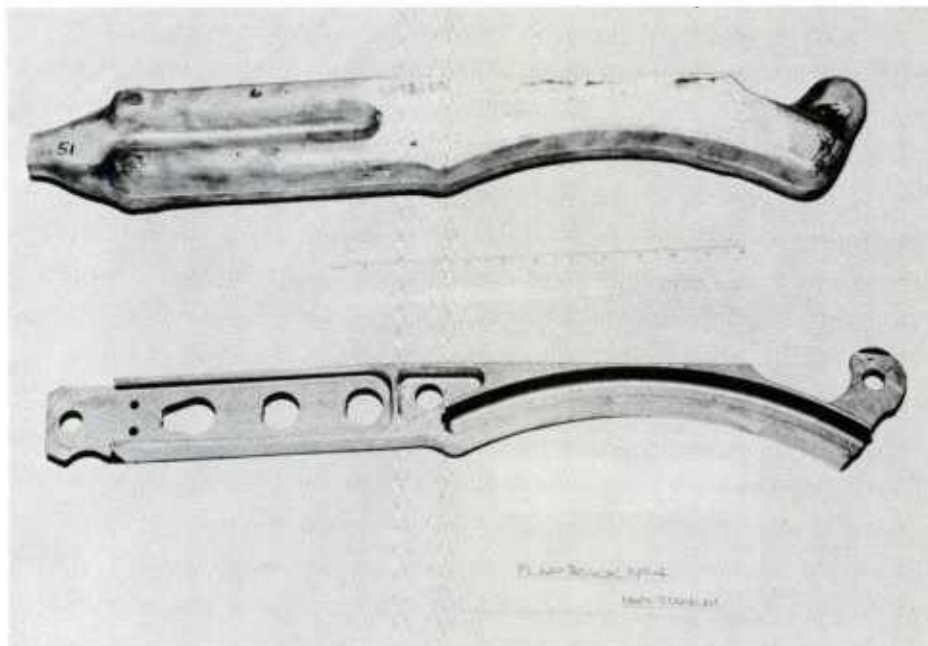


FIG. 4

CAST FLAP TRACK COMPARED WITH DIE FORGING MATERIAL TITANIUM 6Al-4V

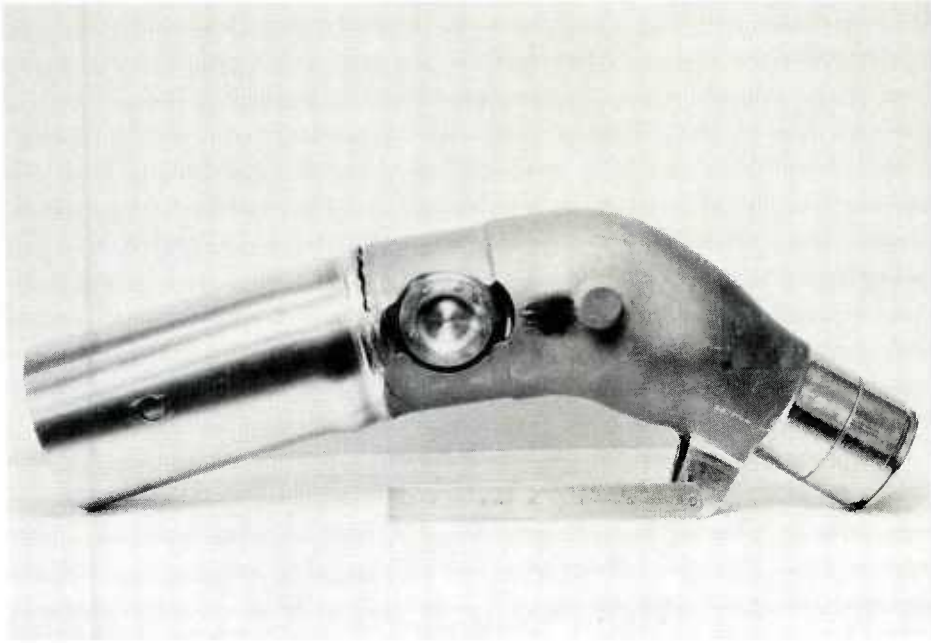


FIG. 5 RESULT OF STATIC TEST MADE ON TITANIUM CASTING EB WELDED TO WROUGHT TITANIUM

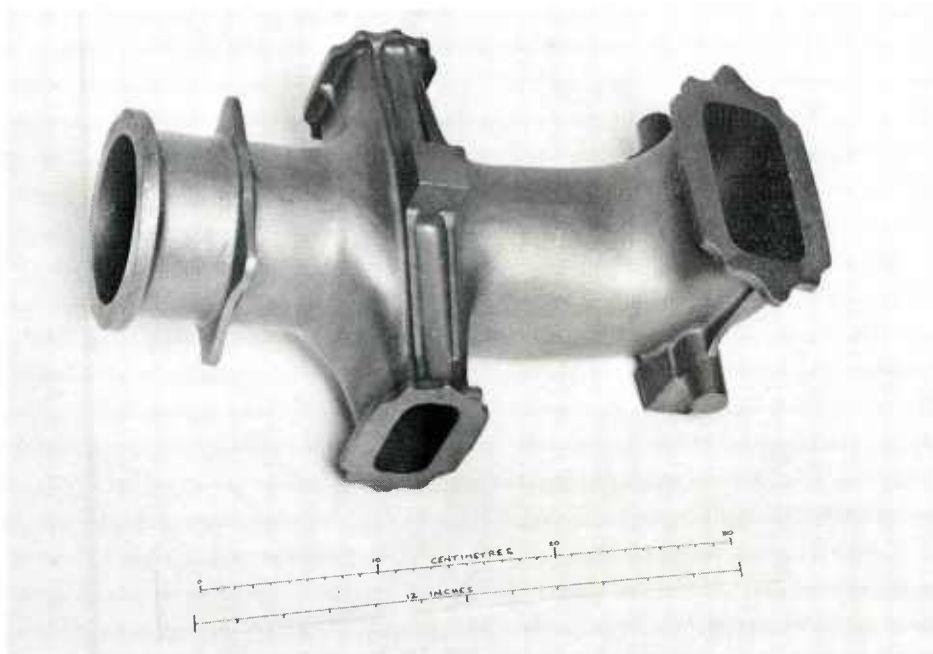


FIG. 6 PITCH AND YAW NOZZLE USED IN VERTICAL TAKE OFF AIRCRAFT

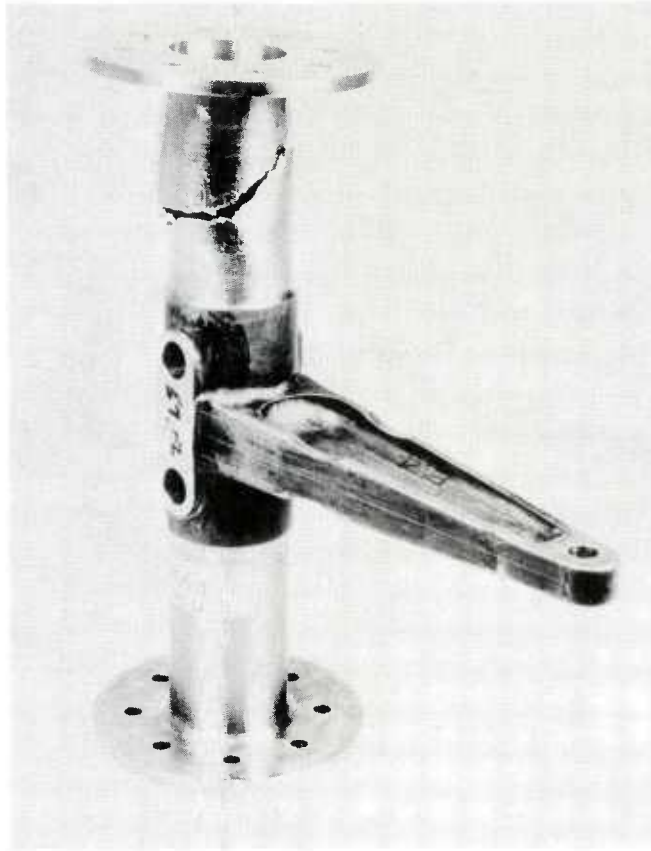


FIG. 7 TEST COMPONENT IN TITANIUM ALLOY 6Al-4V USED TO EVALUATE TORSION, BENDING AND TENSILE STRENGTH IN ONE COMPONENT

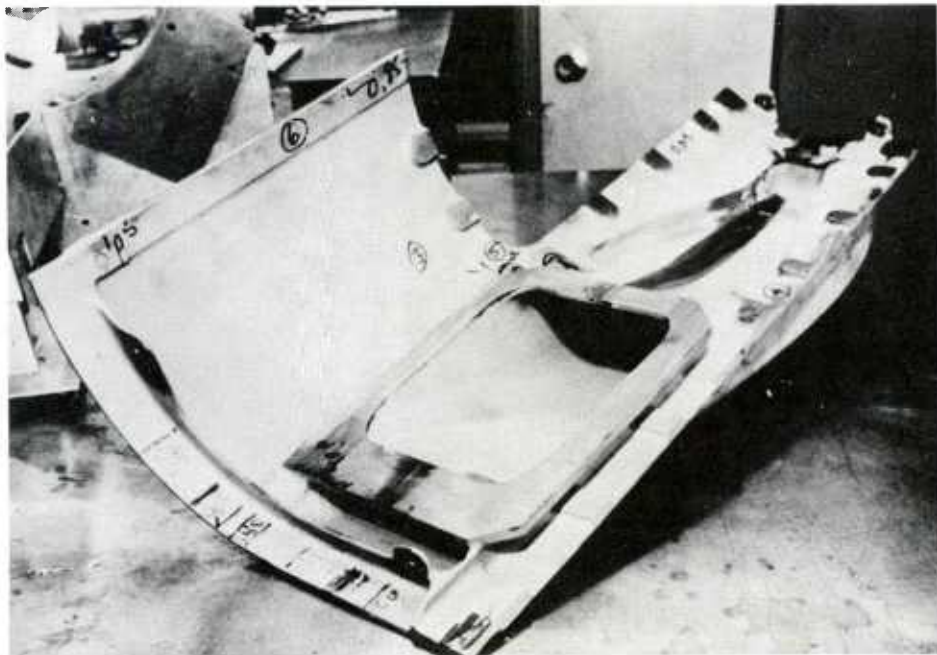


FIG. 8 CASTING IN A357 ALUMINIUM ALLOY

ADVANCED CASTING - TODAY AND TOMORROW

by

Dipl.-Ing. Dietmar Mietrach

VFW GmbH

Materials and Processes Development Department

Hünefeldstr. 1-5

D-2800 Bremen 1

Germany

Summary

A general summary of the state of foundries and limitations of foundry practice can be made as a result of personal visits to well-known foundries in the United States/Canada, France, Germany, Great Britain and Italy, and the discussions with and experience of these foundries. Components have been redesigned in cooperation with the foundries to make them more castable.

The aim of the WST-M-program (Economic Structures Technology-Metals) is not only to demonstrate the practicability of new technologies but also to put the economy in the foreground. Therefore a report will be given of cost-benefit analyses of different representative military components, castings of primary structure parts by chosen foundries and the mechanical values of static/dynamic tests.

Using this know-how and personal experience, it is possible to give a prognosis for use of castings in aviation industry, for the further development of casting techniques and materials in future.

1. INTRODUCTION

The call for an optimization of aircraft performance as well as the need to cut costs has in recent years led not only to the development of new materials but also to the further development of economic manufacturing processes and designs. This need has become all the more urgent due to the higher cost of raw materials, wages and energy.

Therefore a program entitled WST-M - Wirtschaftliche Struktur Technologien-Metallische Werkstoffe (meaning Economic Structures Technology-Metals) - funded by the FMoD (Federal Ministry of Defence) was launched at Vereinigte Flugtechnische Werke (VFW) in Bremen in 1978; this program concerns the development and demonstration of economic manufacturing processes in airframe construction, Fig. 1.

The aim is to achieve drastic cost reductions by developing and applying new economic manufacturing technologies such as: aluminium casting, hot isostatic pressing of titanium investment castings, economic riveting, welding of individual components, precision-forging and SFB/DB (Super-plastic Forming/Diffusion Bonding) [1], [2].

By placing subcontracts with other German manufacturers of aeronautical equipment and by cooperation with various institutes and the BWB (Federal Bureau for Weapons Technology and Procurement), the prime contractor VFW is able to ensure that the elaborated results will be applied widely to running projects and future programs.

2. TASK AND AIM

The casting technology is given high priority in the WST-M program, since it is a manufacturing process that is favourable in terms of cost and also offers the possibility of combining into one casting a whole number of material-intensive machining and sheet-metal parts which were previously joined by riveting at high cost. Moreover, the process affords the design engineer greater freedom of design. It should be noted that the design is made suitable for casting, i.e. the design engineer and foundry should get into touch as early as possible during component development. Only thus will it be possible to make maximum use of all the advantages of the process.

So far, the lack of confidence of design and stress engineers in castings has stood in the way of a more widespread use of castings for primary structures. Consequently, the program aims at manufacturing reproducible castings by suitable means [3].

The tasks of the program are:

- o to establish and compare the state of the casting technology in the USA, Europe and Federal Republic of Germany
- o using genuine components of the primary structure of MRCA Tornado and ALPHA Jet aircraft, classified according to the degree of difficulty during casting, to provide for a direct comparability between existing designs (riveted sheet-metal and machined parts) and the new cast version with regard to cost reduction and technical reliability
- o to compare by value analysis aircraft components cast in various foundries at home and abroad, to subject these to dynamic and static component tests and to carry out material-scientific investigations (Table 1 shows the chemical composition of selected aluminium casting alloys)
- o to make predictions on the use of castings in the aerospace industry.

The subject of aluminium castings will be dealt with in more detail below. The titanium casting technology will, however, not be elucidated as this would go beyond the scope of this article. Nonetheless, it should be noted that titanium castings will also be put to more extensive use in the aircraft industry in future. Comprehensive investigations are being carried out within the WST-M program.

3. PROCEDURE

The present state of the casting technology in terms of processes, component sizes, design and material-scientific data as well as mechanical characteristics has been established by way of personal visits to and extensive discussions with well-known foundries in the USA/Canada, France, Italy, Great Britain and the Federal Republic of Germany. At the same time, a prognosis was made [4], [5] in cooperation with the foundries of future tendencies for the years 1985 (stage 2) and 1995 (stage 3) with a view to design data and mechanical-technological values. These values are shown exemplarily in tables 2, 3 and 4.

Based on these data as well as on further boundary conditions such as tolerances, existing experience with castings and manufacturing know-how of the individual foundries [4], a number of MRCA components were selected according to various castings-related aspects to permit a comparison between modern casting technologies and conventional manufacturing processes at a genuine structure. These components and their adjacent areas were considered both technically and value-analytically, and designed as castings. It was here possible to combine into one part several milled parts which had initially represented one component but had broken down into individual parts for technical machining reasons.

The selected components are representative of a certain component type within the airframe. By demonstrating the economic and technical practicability of the individual representative component, demonstration is also furnished for the entire component type. Fig. 2 illustrates the possibilities available to cut the structural costs of future aircraft by introducing the casting technology.

4. STATE OF CASTINGS TECHNOLOGY

The casting processes sand casting, investment casting and precision casting are of significance for aerospace construction [1]. Depending on the respective technical or economic conditions for the individual components, either one or the other process will be more advantageous, whilst all 3 processes can be considered equal in the airframe.

Sand casting is the least expensive casting process for manufacturing large complex components, table 2. High mechanical values can be reached with iron chills specially placed in the mould, table 5. The disadvantage is that, in comparison with other casting methods, large tolerances of $+0.3/-0.5$ mm still exist and minimum wall thicknesses of only 2.5 mm are possible. Local machining or selective chemical milling offer a remedy to this problem.

The production of investment castings is slightly more expensive than that of sand castings. Investment casting, however, makes it possible to produce thin walls only approx. 1.6 mm thick at high tolerances ($+0.3/0.0$ mm). At present, components about 500 mm x 800 mm x 1500 mm can be manufactured, the size being limited not by the process but solely by the existing manufacturing facilities. Since no purposive cooling is possible during casting for reasons concerning the process itself, slightly inferior mechanical material properties are currently still to be expected in comparison with sand and precision casting, table 5. An improvement is possible by vacuum-degassing the molten metal, by casting under negative pressure or in a vacuum or by placing iron chills in the ceramic mould.

Precial casting is more expensive than sand and investment casting but makes it possible to manufacture components 3000 mm x 1000 mm x 1000 mm at minimum wall thicknesses of 1.6 mm and high tolerances (± 0.2 mm), table 4. By selective, local cooling, good metallurgic properties and thus high strength values can be achieved, table 5, similar to those achieved by sand casting.

It remains to be said that the present state of the casting technology is highest in the USA/Canada in terms of quantity, size and complexity of the parts, Fig. 3. However, in recent years considerable efforts have been made in Europe to reach this standard and, partly, as in the case of sand casting with minimum wall thicknesses of 2.5 mm, even to surpass the standard. German foundries will still have to make some progress.

Generally, the trend is noticeable that the sand casting and investment casting processes complement one another and that both processes are drawing closer to one another. For instance, investment castings are becoming ever bigger and have higher strength values thanks to the measures described above, whereas sand castings can have thinner walls and closer tolerances by applying investment casting measures (e.g. ceramic moulds) and refining sand casting techniques. These trends will grow even stronger in future.

5. CASTING MATERIALS

Preference is given to the casting alloys A 357, K01 and AVIOR Z, table 1, for primary structures in aircraft construction, for which the castings technology should mainly be used, on account of the high strength values of these alloys.

The siliceous standard casting alloy A 357 (G-ALSi7Mg0.6), a further development of A 356, has particularly good casting properties, producing strength values between $R_m = 310 \text{ N/mm}^2$ (investment casting) and $R_m = 350 \text{ N/mm}^2$ (sand casting/precial casting) depending on the casting process and component geometry, table 5.

The silver-alloyed and highly cupriferous material K01 (G-AlCu4Ag) is well suited for sand and investment casting processes when high demands are made on strength values of approx. $R_m = 420 \text{ N/mm}^2$ but is sensitive to heat-cracking during casting.

The cupriferous alloy Avior Z has a composition similar to that of K01. The main difference concerns the high magnesium content (up to 0.8%) and the alloying of zinc (up to 1.5%). Avior Z is cast only according to the precial casting process and has strength values of $R_m = 450 \text{ N/mm}^2$.

6. SELECTION AND CASTING OF REPRESENTATIVE COMPONENTS

An analysis of the MRCA production share was carried out within the WST-M program in order to establish cost-intensive factors and to find typical, improvable structures where a conversion to castings would appear sensible. Boundary conditions such as geometric dimensions, tolerances, strength values and castability have been taken into consideration in the new concept for casting. Preliminary designs of selected assemblies served as a basis for discussions with foundries at home and abroad, and were revised subsequent to the discussions with the manufacturers. This iterative course of action served not only to ensure that the drafted design corresponded to the latest castings standard but also to achieve considerable cost reductions.

The exemplary castings NIB, PYLON and INTAKE FLOOR by comparison increase in terms of size and complexity and continuously provide the result for present and future aircraft on the basis of the hardware examinations.

6.1 Exemplary component: NIB center structure

The NIB, being a primary component of the structure, serves to bear aerodynamic air loads as well as loads from the Krüger flap. The component is presently manufactured in series from 15 machined and sheet-metal parts as well as 164 fasteners, Fig. 4. The investment casting/precial casting versions of the alloy A 357 consists of only one part.

6.1.1 Value analysis

Comprehensive investigations and value analyses have revealed considerable cost savings for the cast version, Fig. 5. By introducing further design modifications, it was possible to exceed the original target data of 15% weight savings at the same cost - compared with the series-production component - by far with 20% weight savings and 25% cost savings, Fig. 6.

6.1.2 Design and stress, casting of components

The design data and strength values provided by the foundries, table 5, flowed into the component drawings. Savings from material overlappings for 164 fasteners and further weight-reducing measures led to a weight reduction of 20%. A weight reduction of approx. 25% in all is considered possible for the future by improving the casting process and material properties.

Two manufacturers each

- o a French foundry (precial casting) and
- o a German foundry (investment casting)

were commissioned to cast 20 components for the hardware program in order to demonstrate the practicability as well as to substantiate the cost savings calculated by value analysis.

The decision in favour of investment and precial castings rather than the far cheaper sand casting process was reached solely for reasons of weight. In designing the investment casting variant according to the 'cire perdue' process, it proved possible to have large thin-walled areas approx. 1.6 mm thick with close tolerances (+ 0.3/0.0 mm). The precial casting variant combines thin wall thicknesses (1.6 mm) and close tolerances (± 0.2 mm) with extremely good metallurgic properties and thus high mechanical values, table 5.

Fig. 7 shows a cast NIB. The results below refer to the precial castings.

6.1.3 Incoming inspection

The inspections and checks carried out by the manufacturer (foundry) and orderer (VFW) according to the test instructions served to check the quality standard of the casting. At the same time, it was possible to draw conclusions with regard to the reproducibility of the delivered castings. In order to demonstrate the reached mechanical/technological values, 'type sample verifications' were carried out on two components at the foundry and two further components at VFW. These verifications comprised

- o visual inspections
- o dimensional checks
- o checking of chemical composition
- o penetrant test
- o X-ray test as per ASTM-E 155
- o metallographic investigations
- o tensile tests on 13 specimens taken from the casting (LN 29512)

On the basis of the micrograph, it is possible to make a statement on the mechanical values [2], [6] and [7] using the DAS method (Dendrite Arm Spacing). An additional non-destructive quality assessment can thus be made at any part of the casting.

Precial and sand casting can be distinguished from one another by this method, Fig. 8. Statements of tendencies regarding DAS/tensile strength R_m are possible on the strength of the results in hand. In order to restrict the scattering range and to characterize the yield strength $R_{0.2}$ and elongation A_5 , a far greater number of samples has to be evaluated and additional criteria such as cell size, porosity and distribution of silicone particles must be taken into consideration [8].

Table 6 gives a table of the reached static strength values, determined at samples taken from two castings. The table shows that the values reached fully meet the requirements and that no single value differs distinctly.

To sum up, it can be said that the above tests have not given rise to any objections.

6.1.4 Component tests

The conventional design and castings of the NIB center structure were compared with one another under the same test conditions, Fig. 9 and 10, to permit a distinct comparison between the milled part/casting of a component. [3] gives a detailed description of the test set-up and performance at the precial casting.

The result of the static tests, Fig. 9, has shown that, in comparison with the conventional design, the cast version is sufficiently dimensioned statically, table 7, although the additional casting factor of 1.25 respectively 1.5 required by the certification authorities has not been introduced into the calculation.

Defined cumulative loads, Fig. 10, were applied during the dynamic tests. The load duration for one flight amounted to 8 seconds. Visual inspections were carried out continuously throughout the test. To sum up, it may be said that the cast version is by far superior to the conventional design on account of the fact that the possibilities offered by the casting technology have been exploited fully, Fig. 11 and table 7.

6.2 Exemplary component: PYLON

The Alpha Jet PYLON, Fig. 12, is another example of a structural component of A 357 having a high load-carrying capacity [2]. The aim is, by means of an improved sand or precast casting version, to reduce the mass of the structure by 25 to 30%, which will result in an increase of the useful value [1]. Higher strength values, thinner wall thicknesses and smaller tolerances as compared to the existing cast version are envisaged. The comparison [1] with the milled part shows clearly that all the examined cast versions have a higher useful value.

As in the case of the NIB, the individual cast versions of the PYLON were discussed with numerous foundries at home and abroad. The final decision as regards the casting of a large number of PYLONS to demonstrate the required values was reached in favour of the precast casting process on the one hand and the sand casting process on the other hand.

The first components will be delivered in mid 1982. The dimensional checks, specimen tests and component tests will then be carried out. A final value analysis will serve to complete this work package within the WST-M program.

6.3 Exemplary component: INTAKE FLOOR

The MRCA INTAKE FLOOR may serve as a representative exemplary component having a complex geometry and made of the aluminium casting alloy A 357. This part of the primary structure is located in the forward engine intake and bears the internal intake pressure. The component presently consists of a cost-intensive mixed design made up of 22 machined/sheet-metal parts and approx. 400 fasteners, Fig. 13. The casting will consist of one part only.

6.3.1 Value analysis

In comparison with the conventional design, cost reductions of more than 60% are possible by introducing selective design modifications, providing a design which is suitable for casting and applying the sand casting process, table 8. In other words, just where this component is concerned, costs of 15 million DM can be saved with the new technology for a new aircraft [2].

6.3.2 Design and stress

The data and statements provided by 9 foundries [2] with regard to wall thicknesses, tolerances and strength values, table 9, flowed into the design [9] of the existing MRCA component drawings, the low tolerances ensuing from the high aerodynamic requirements - which can, however, be mastered - for the casting and the tools.

6.3.3 Casting and component tests

After giving the INTAKE FLOOR a design suitable for casting, two selected foundries (sand and precast casting) were commissioned to cast the components. The first castings will be delivered in mid 1982. The value analysis, dimensional checks and component tests will then follow.

7. VERIFICATION OF STATIC AND FATIGUE CHARACTERISTICS

The mechanical-technological values of the castings for the sand, investment and precast castings processes (primarily for the alloy A 357) will be verified within the WST-M program. In parallel to component tests, specimens are taken from numerous castings in order to establish the static and fatigue characteristics (notched and unnotched specimens) as well as to carry out crack propagation and fracture-mechanics investigations [2].

Once these results are in hand, it will be possible to make available the required documents so as to use castings more extensively for primary structures and to minimize or eliminate the castings factor.

8. JOINING OF CASTINGS

A further task of the WST-M program consisted in checking to what extent it is possible to join components made of aluminium casting alloys by means of undetachable fasteners (solid, blind and special fasteners) or fusion welding (TIG or EB welding). The strength behaviour of such joints was established and compared with specimens made from an aluminium wrought alloy.

To sum up, the following may be said to apply to riveted casting specimens [2], [10]:

- o manufacture can be carried out according to the manufacturing procedures known for wrought alloys
- o the static strength behaviour of the riveted specimens of the aluminium casting alloy A 357 is equivalent where solid fasteners are installed, and less favourable than that of wrought alloys where blind and special fasteners are installed
- o depending on the specimen bar shapes and the fastener, the service life values (flight-to-flight load tests: FALSTAFF) of the aluminium casting alloy A 357 are slightly lower up to approx. $2 \cdot 10^4$ flights and slightly higher than the wrought alloy values up to approx. $5 \cdot 10^4$ simulated flights.
- o the fatigue strength behaviour (single step loading tests) of the aluminium casting alloy was slightly lower up to approx. $2 \cdot 10^4$ load cycles and slightly higher than of the wrought alloy from 10^5 load cycles onwards, Fig. 14.

As regards the TIG and EB welded cast specimens [2], [9] and [10], it can be said that:

- o aluminium casting alloy A 357 is to be considered well weldable
- o independent of the welding process, the static strength values of the fully heat-treated specimens correspond to the values of the basic material
- o contrary to the TIG welded specimens, no distinct difference of the fatigue strength behaviour was established between machined and unmachined specimens in the weld seam area of EB welded specimens

9. SUMMARY

The urgent need to cut structural costs in aircraft construction is increasingly leading to the development/further development of cost-reducing manufacturing processes.

In the past, it was not possible to use cost-saving castings extensively for primary structures in aircraft construction since there was a lack of confidence in the control of the casting process, in the reproducibility of the mechanical values and in the quality assurance methods in the aerospace industry. In order to force the introduction of high-strength aluminium castings, extensive hardware investigations and value analyses were carried out on genuine components of the MRCA-Tornado/Alpha Jet under the WST-M program at VFW in Bremen.

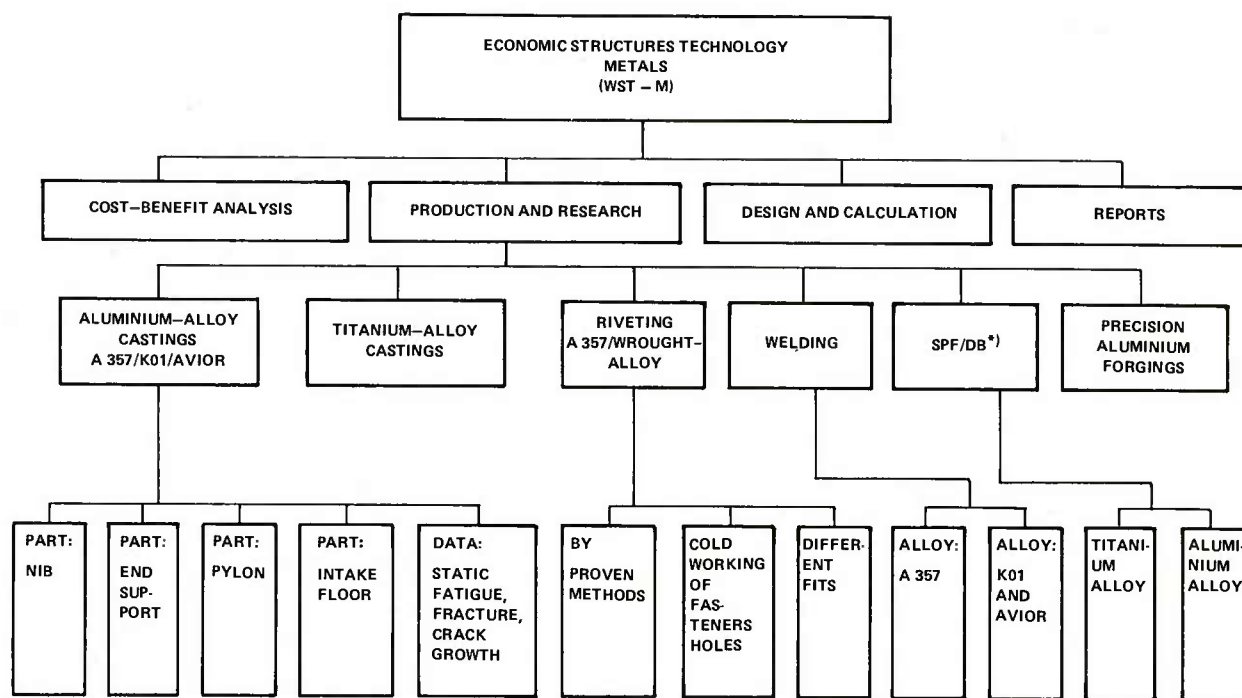
The investigations concluded positively in the first phase of the program revealed that cost savings of 25% and weight savings of 20% can be achieved by changing the existing NIB series component (15 single parts/164 fasteners) into a casting. The successful activities are being continued with the exemplary components INTAKE FLOOR and PYLON.

Finally, it should be noted that hot isostatic pressing of castings makes it possible to eliminate porosities and thus, amongst other things, to improve the mechanical characteristics. This process and the possibility of selective chemical milling at castings should be taken up and followed up further.

An important fact to bear in mind is that the success in applying the cost-saving castings technology depends on the quality of the foundry. Experience has shown that there is a distinct difference in quality so that orders cannot only be placed according to the principle of the cheapest bidder.

10. References

- [1] Mietrach, D., Lösungsansätze für den wirtschaftlichen Leichtbau von Flugzeugstrukturen, ALUMINIUM, Heft 6 und Heft 7 (1981)
- [2] -, Wirtschaftliche Struktur-Technologien, Entwicklung und Nachweis wirtschaftlicher Fertigungsverfahren im Flugzeugzellenbau, Abschlußbericht 1. Phase, VFW, Bremen May 1981
- [3] Mietrach, D. und J. Weilke, Erfolgreiche Einführung wirtschaftlicher und leichter Strukturen aus Aluminiumguß im Flugzeugbau, ALUMINIUM, Heft 2 und Heft 3 (1982)
- [4] -, Wirtschaftliche Struktur-Technologien, 1. Review, VFW, Bremen January 1979
- [5] Mietrach, D., Bauweisen für die metallische Flugzeugstruktur, insbesondere im Hinblick auf Werkstoffausnutzung und Fertigungskosten, Vortrag für die Bundesakademie für Wehrverwaltung und Wehrtechnik, Mannheim November 1980
- [6] Faber, J.W., Cast Aluminum Structures Technology, Summary Technical Report, Technical Report AFWAL-TR-80-3020, April 1980
- [7] D-XXXX "ALUMINUM ALLOY A 357 CASTINGS, DENDRITE ARM SPACING, PROCESS FOR DETERMINATION OF"
- [8] -, Aluminum Castings Technology, Manufacturing Methodology Improvement for Casting Ductility, Boeing, Seattle 1980
- [9] -, Wirtschaftliche Struktur-Technologien, 3rd Review, VFW, Bremen June 1980
- [10] -, Wirtschaftliche Struktur-Technologien, 4th Review, VFW, Bremen December 1980



* SPF/DB = SUPERPLASTIC FORMING/DIFFUSION BONDING

Fig. 1 Project structure plan "Economic Structure Technologies – Metals"

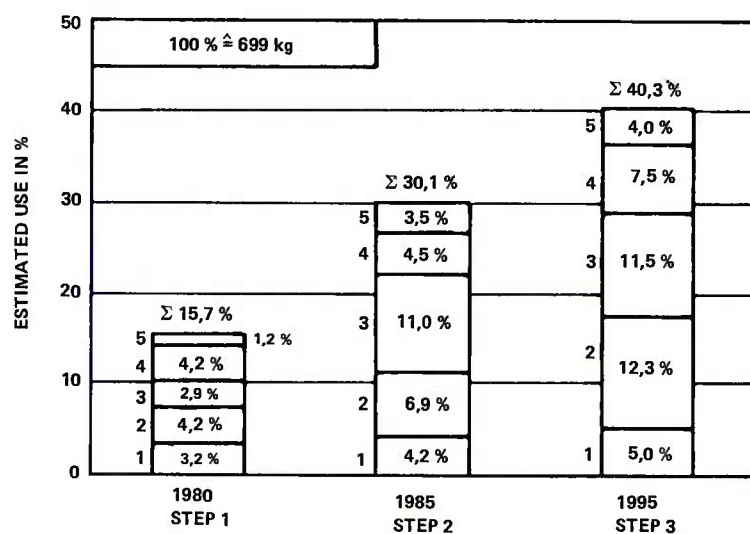


Fig. 2 Prognosis of the share of aluminium castings of various component types (1 NIB, 2 Frame, 3 Wall (INTAKE FLOOR), 4 Strap, Support Beam, 5 Panel) in a combat aircraft as a function of the stages of castings development

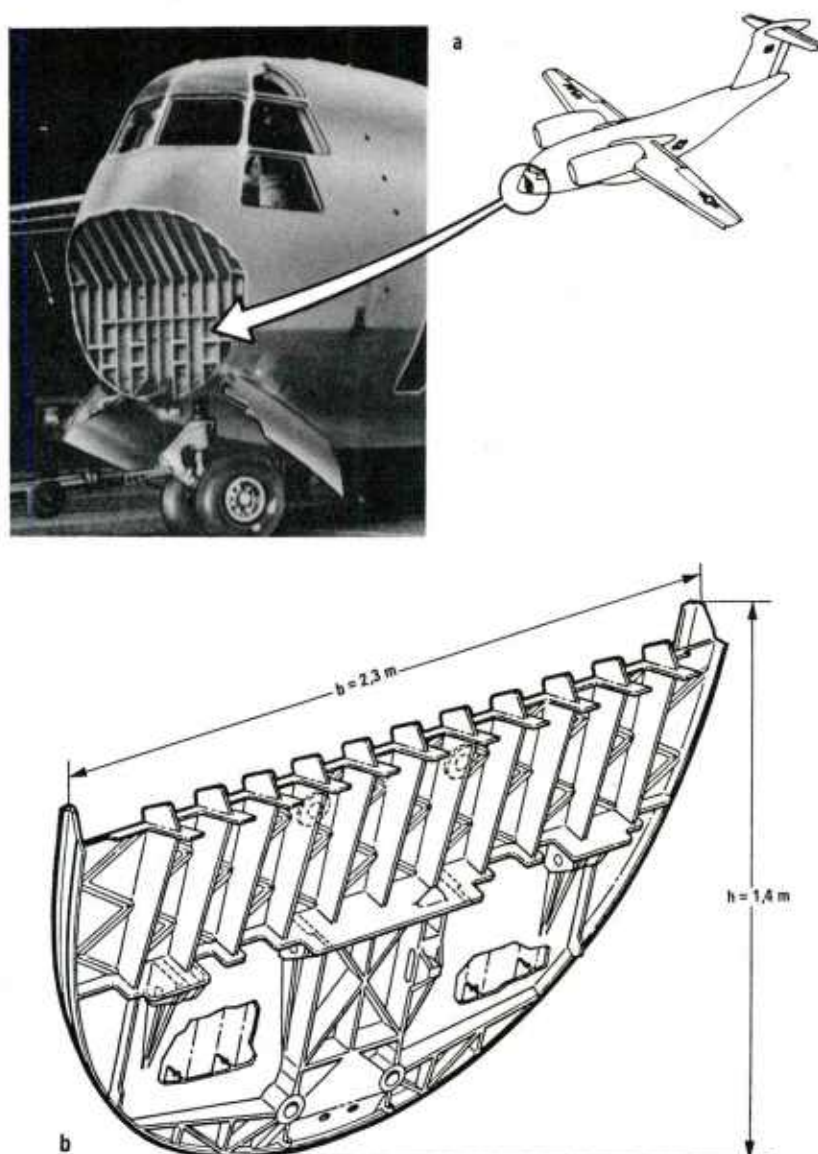


Fig. 3 Transverse frame of the Boeing YC-14 as a reference component for the CAST program in the USA: a – location of the component, b – shape and main dimensions of aluminium casting version A 357 [6]

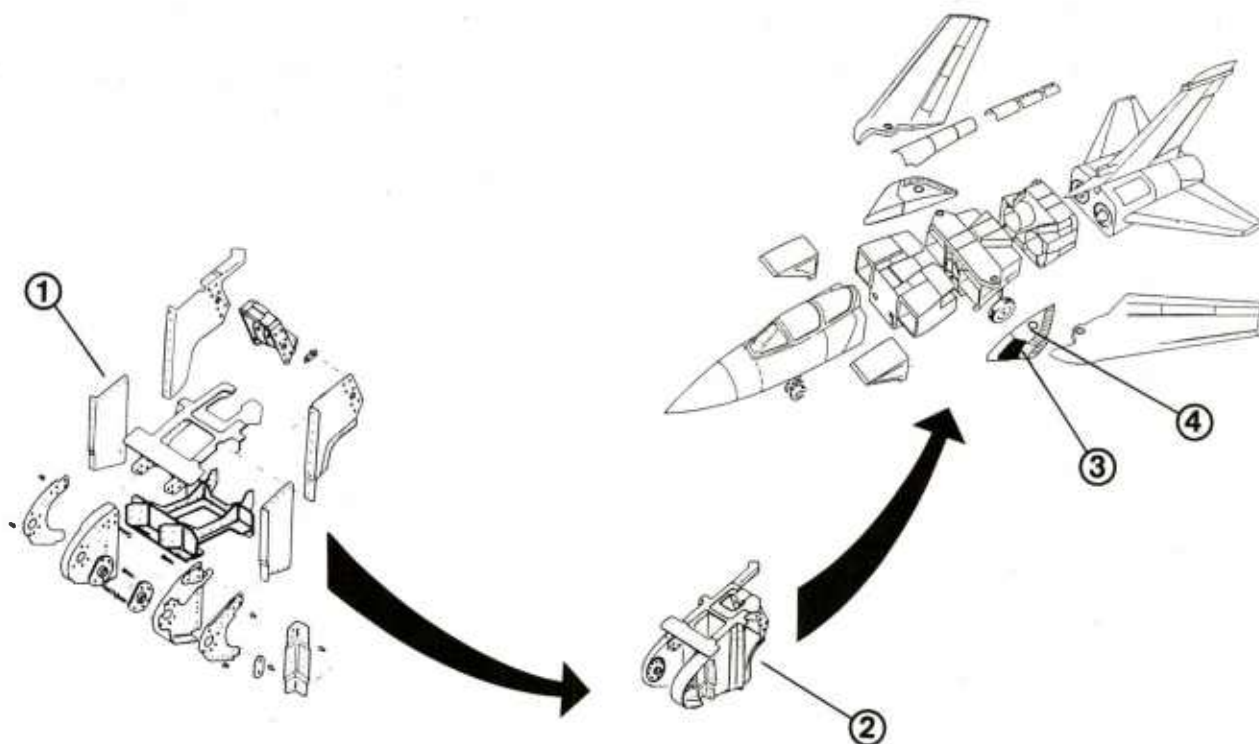


Fig. 4 The NIB, part of the MRCA Tornado primary structure, prior to the conversion:
1 NIB individual parts, 2 Assembled component, 3 Location in fixed wing, 4 Fixed wing

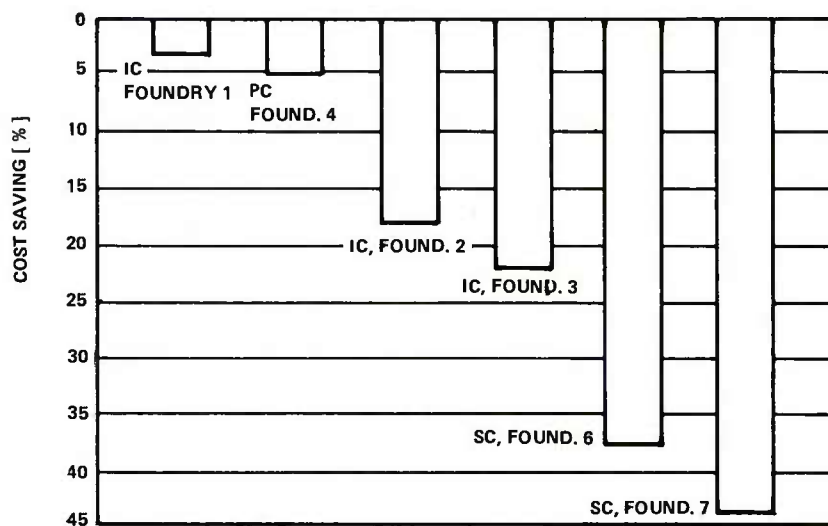


Fig. 5 Cost savings of NIB center structure in comparison with the basic component under series-production conditions: IC investment casting, PC precision casting, SC sand casting, material A 357, status: 1979

	OLD: MANY SINGLE PARTS	NEW: CASTING- VERSION		WEIGHT [%]	COSTS [%]
NUMBER OF PARTS	6 MACHINED PARTS 9 SHEET METAL PARTS 164 FASTENERS	1 CASTING	GOAL	- 15	± 0
WEIGHT [kg]	2,0	1,6	ACHIEVED	- 20	- 25

Fig. 6 Weight and cost calculation for the NIB center structure as investment/precision casting

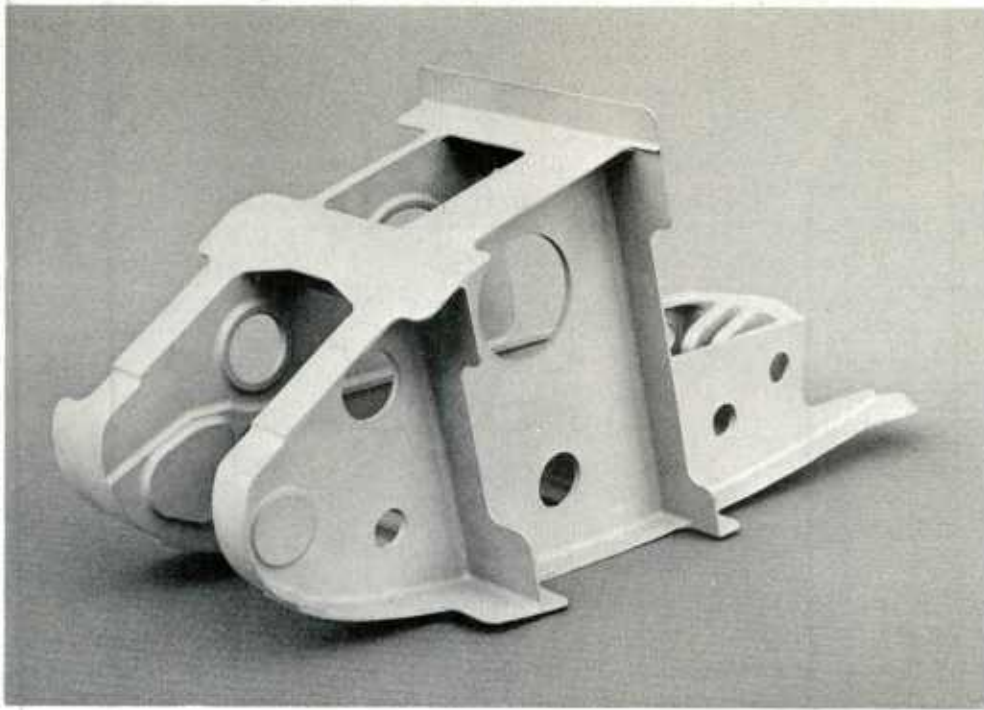


Fig. 7 NIB center structure: cast version in A 357. Approximate dimensions 500 mm length x 190 mm width x 300 mm height

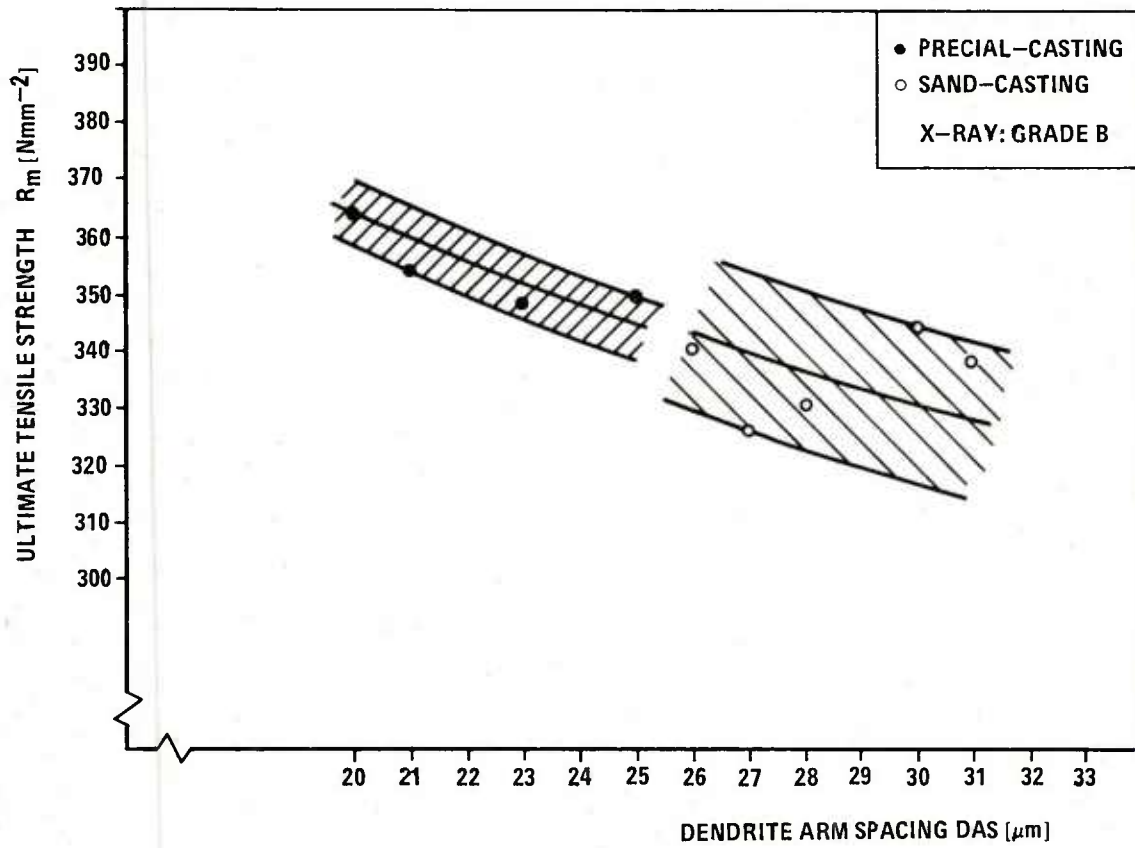


Fig. 8 Relationship between Dendrite geometry/tensile strength for precast and sand casting, material: A 357

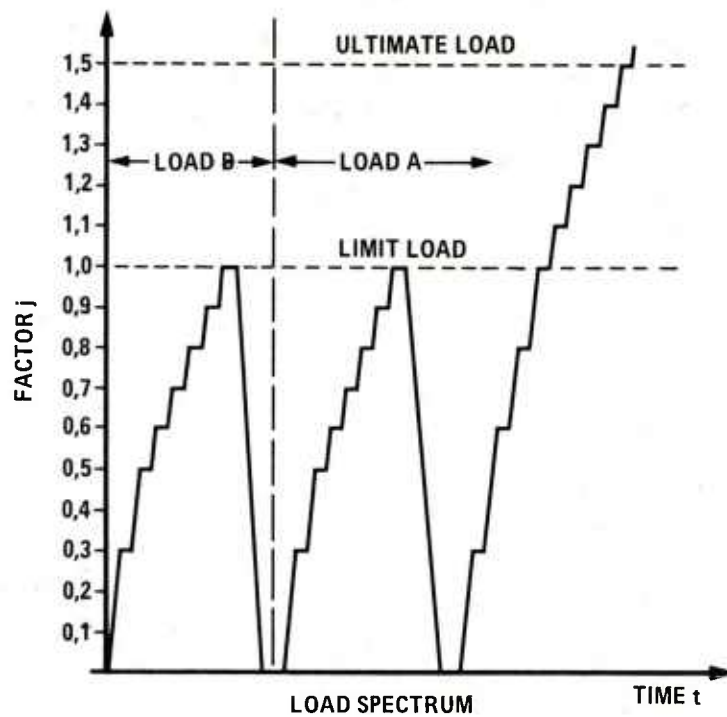


Fig. 9 NIB component test. Static test

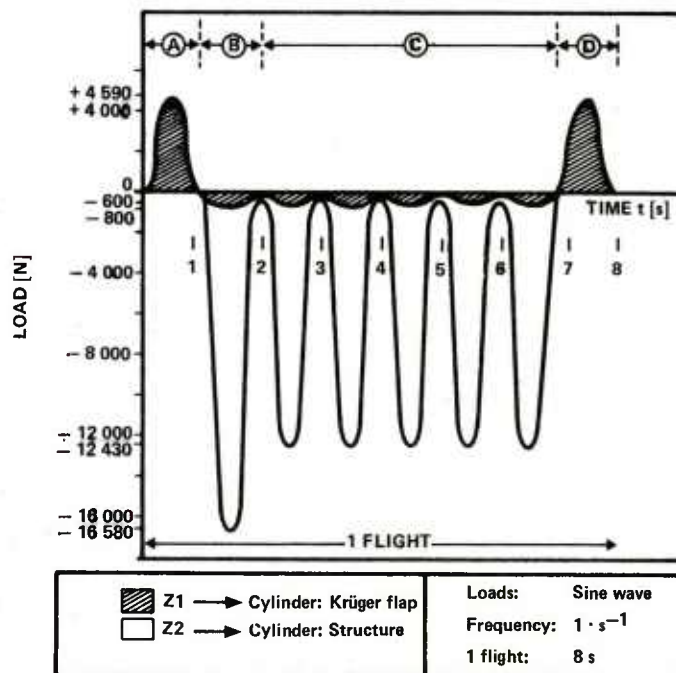


Fig. 10 NIB component test. Dynamic test

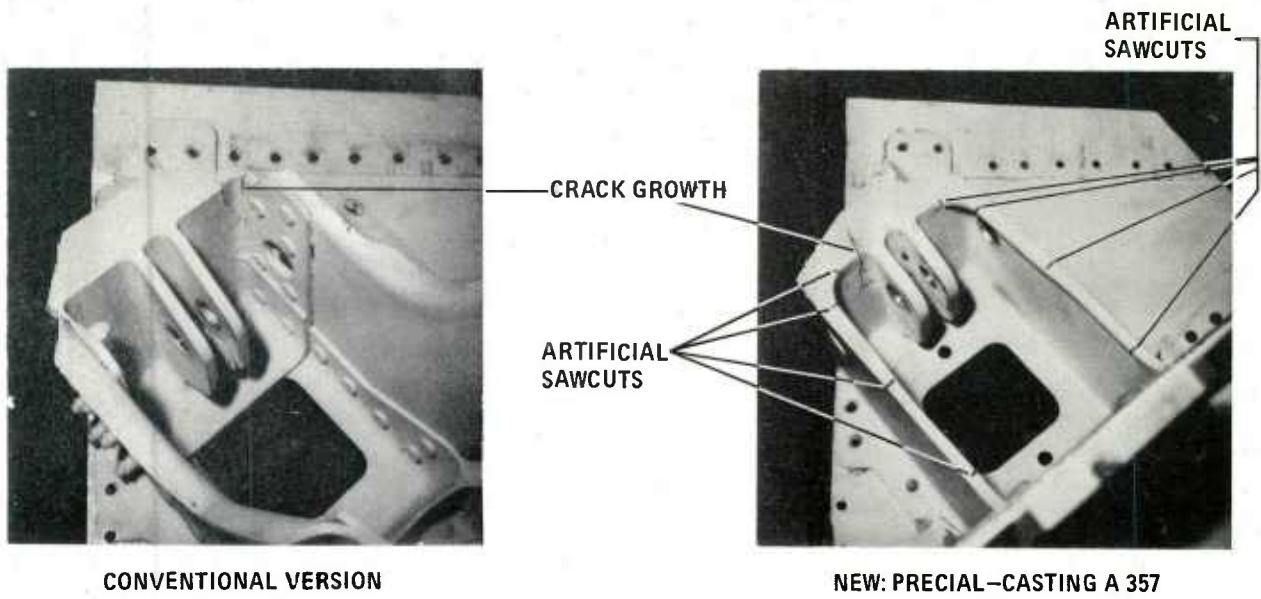


Fig. 11 Dynamic component test. Design and crack propagation at the NIB

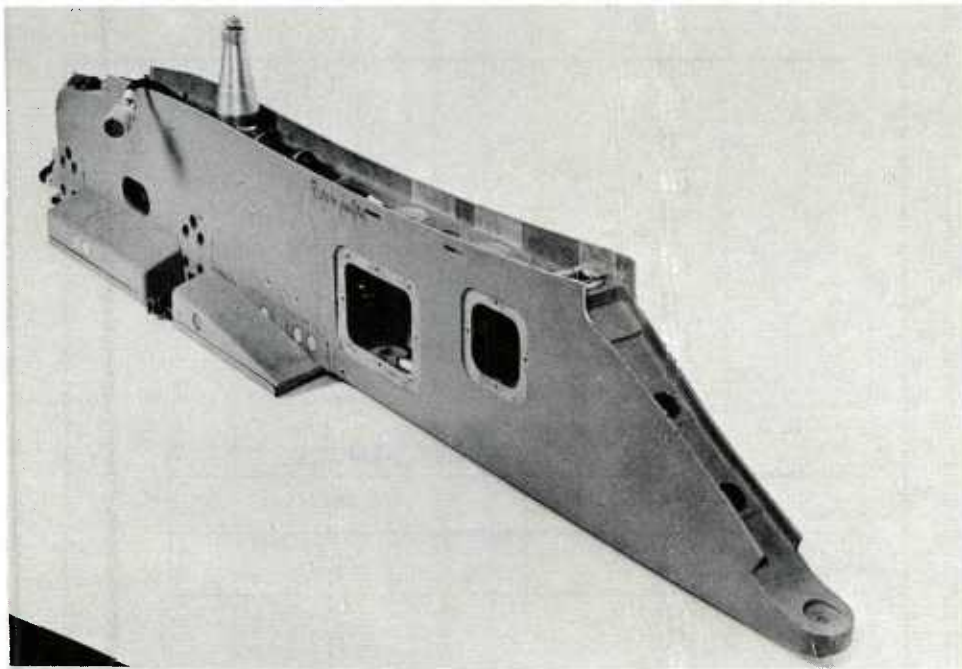


Fig. 12 Outer PYLON of Alpha Jet (sand casting). Approximate dimensions 1700 mm length x 80 mm width x 300 mm height

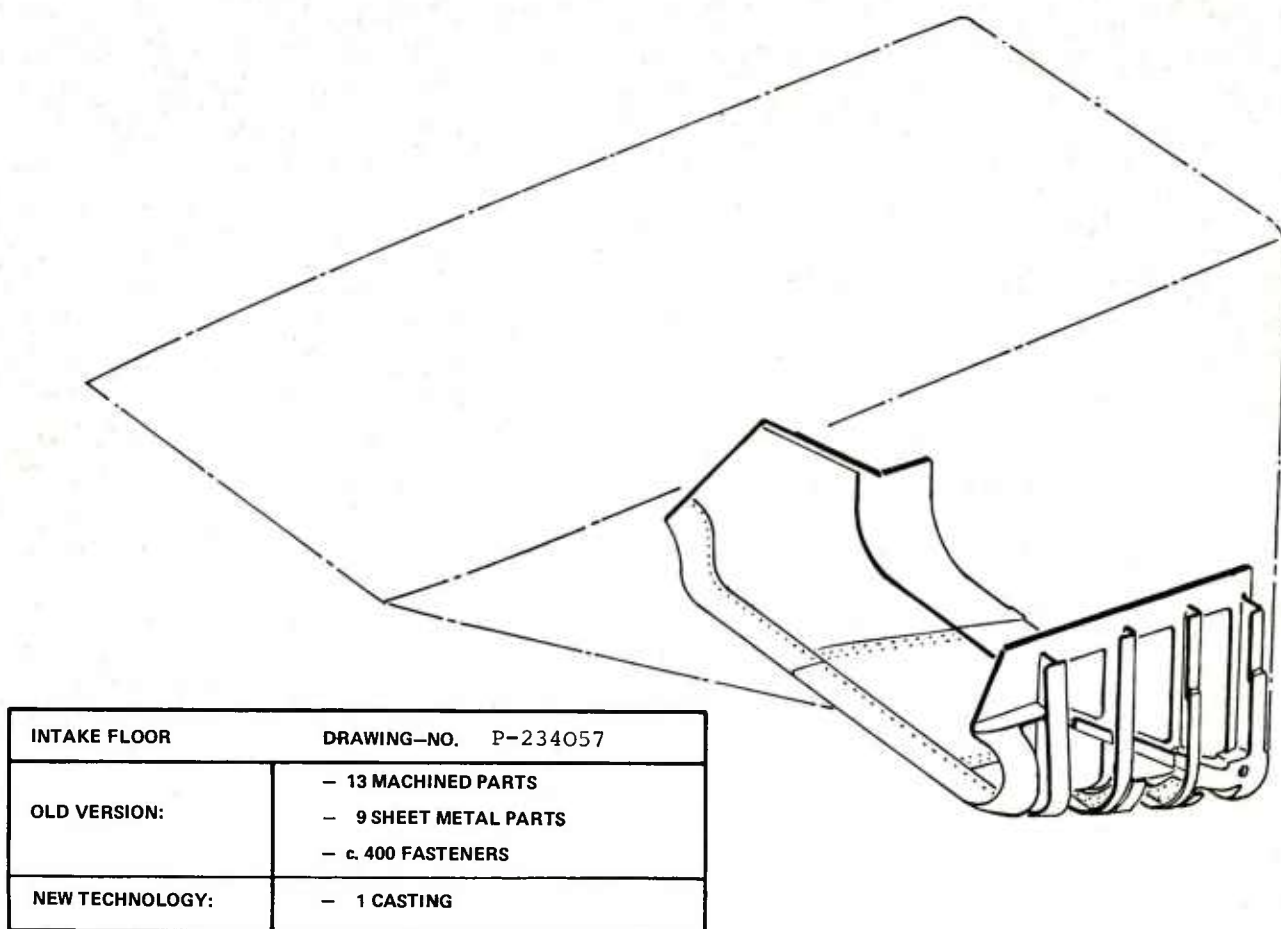


Fig. 13 Exemplary component: MRCA Tornado INTAKE FLOOR

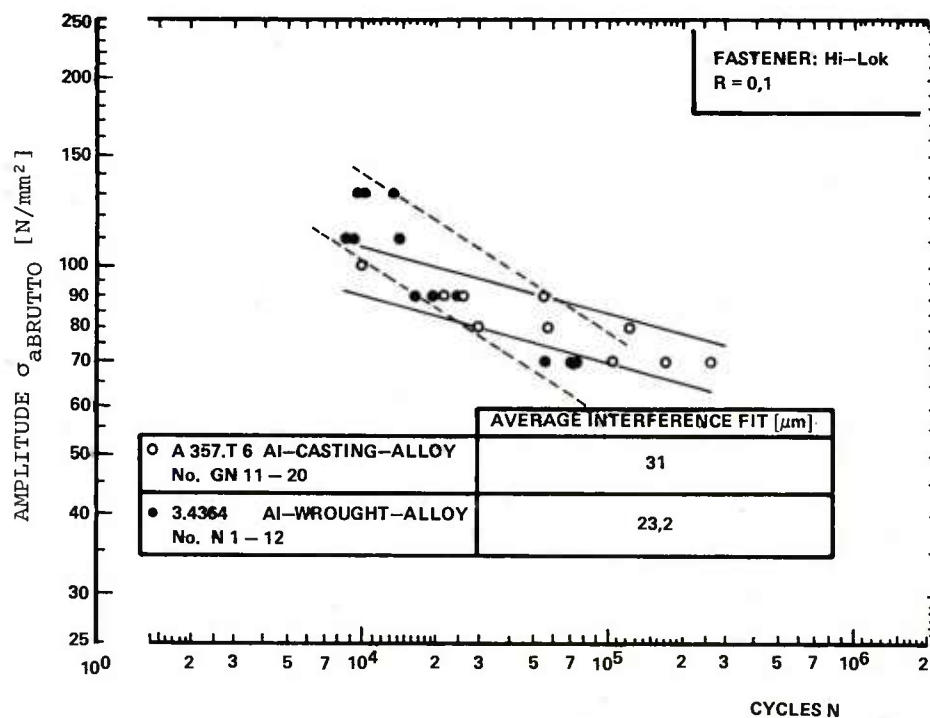


Fig. 14 Rivet investigations: Results of constant-amplitude fatigue tests (AGARD specimen). Comparison between casting and wrought alloy

ELEMENTS		Cu	Ag	Be	Mn	Mg	Ti	Fe	Si	Zn	Others each	Σ	Al
ALLOY		[%]	[%]	[%]	[%]	[%]	[%]	[%]	[%]	[%]	[%]	[%]	[%]
A356 (3.2374)	from	—	—	—	—	0,20	—	—	6,50	—	—	—	
	to	0,20	—	—	0,10	0,40	0,20	0,20	7,50	0,10	0,05	0,15	Bal
A357	from	—	—	0,04	—	0,40	0,10	—	6,50	—	—	—	
	to	0,20	—	0,07	0,10	0,70	0,20	0,20	7,50	0,10	0,05	0,15	Bal
K01	from	4,00	0,40	—	0,20	0,15	0,15	—	—	—	—	—	
	to	5,00	1,00	—	0,40	0,35	0,35	0,10	0,05	—	0,03	0,10	Bal
AVIOR	from	4,00	0,50	—	0,20	0,40	0,20	—	—	0,20	—	—	
	to	5,50	1,00	—	0,80	0,80	0,50	0,05	0,05	1,50	—	0,03	Bal

Table 1 Chemical composition of the aluminium casting alloys A 356, A 357, K01 and AVIOR

CRITERIA	SAND CASTING			
	STEP 1 (~1980)	STEP 2 (~1985)		STEP 3 (~1995)
MAX. SIZE [mm]	1500x800x4000	1500x1500x5000		2000x2000x5000
MIN. WALL THICKNESS [mm] IN LARGE AREAS	3,3/2,5 ²⁾	1,5		1,0
THICKNESS TOLERANCES [mm]	$\pm 0,5 \begin{cases} + 0,3^2) \\ - 0,5 \end{cases}$	$\pm 0,3 \begin{cases} + 0,3^2) \\ - 0,5 \end{cases}$		$\pm 0,30$
ALLOY	A 357	A357	K01	3)
MECHANICAL PROPERTIES 1) [N/mm ²] or [%]	R _m	350	370	420
	R _{p0,2}	280	290	350
	A ₅	5	7	5
1) In critical areas 2) Special process 3) New or modified aluminium alloys				

Table 2 Prognoses on the aluminium casting technology (sand casting) as a function of the stages of development

CRITERIA	INVESTMENT CASTING			
	Step 1 (~1980)	Step 2 (~1985)		Step 3 (~1995)
MAX. SIZE [mm]	500x500x850	500x800x1500		800x1000x2000
MIN. WALL THICKNESS [mm] IN LARGE AREAS	1,6	1,2		0,8
THICKNESS TOLERANCES [mm]	$\pm 0,3$ 0,0	$\pm 0,15$		$\pm 0,15$
ALLOY	A 357	A 357	K01	2)
MECHANICAL PROPERTIES ¹⁾ [N/mm ²] or [%]	R _m	310	340	420
	R _{p0,2}	220	260	350
	A ₅	5	6	5
1) In critical areas 2) New or modified aluminium alloys				

Table 3 Prognoses on the aluminium casting technology (investment casting) as a function of the stages of development

Although the reliability of a casting mainly depends on its shape, in other words on the design, the properties of the product are strongly related to the metallographic structure. This structure forms during the solidification of the liquid metal in the mould cavity, and after pouring it can only be modified in a limited way. In most cases therefore the structure should give the required properties already in the as-cast condition.

Apart from its structure, also the dimensional accuracy and the surface appearance should be mentioned as characteristics of the quality of a casting. These both factors are influenced by the moulding and pouring practice, that is common for a given foundry.

The demands required from castings are continually increasing. Guaranteed lifetime, higher strength, lighter in weight, applicable at increased temperatures, higher accuracy, are only a few examples. The production of such high-quality castings is only possible nowadays, as a result of careful processing in the foundry and modern knowledge of metallurgy and foundry technique. The term "casting technology" includes therefore many aspects; only a few of them will be discussed in the next paragraphs.

2. CRITICAL MOMENTS IN THE CASTING PROCESS

The shaping of a casting is schematically demonstrated in Fig. 1. A high-duty casting arises already in the design-stage, in a close co-operation between the designer and the foundryman. The exact shape of the product is determined, the alloy is chosen and the requirements written down into specifications, calculating the specific possibilities and restrictions of the casting method chosen.

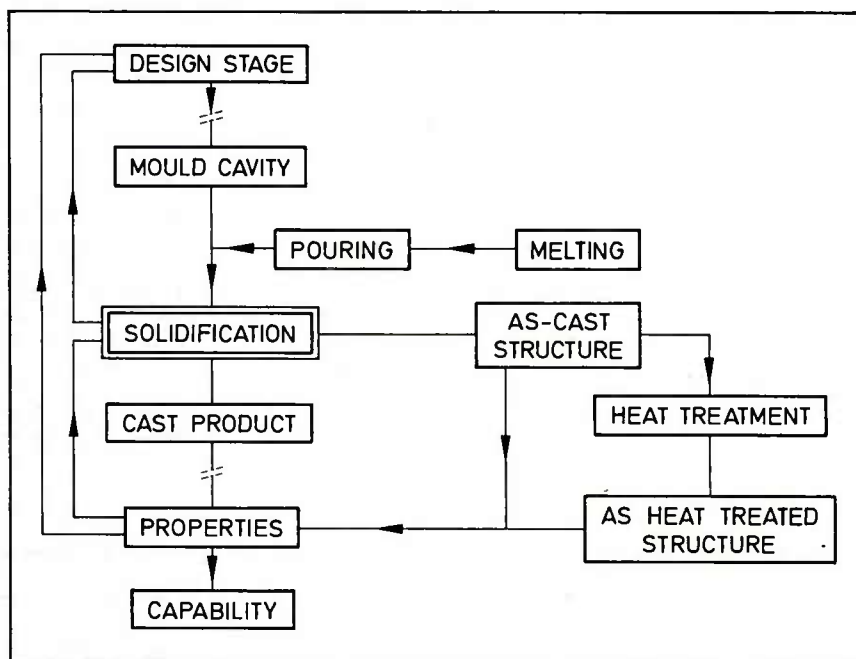


Fig. 1 Flow diagram of casting production and relation between structure and properties.

The foundryman has to fulfil the specifications, and must during the whole process pay attention to a number of critical moments, that could badly influence or even disturb the quality of the casting. In this respect must be mentioned:

- instability of the mould-wall during pouring and solidification, giving a lesser dimensional accuracy and sometimes the occurrence of internal porosity;
- metallurgical reactions during melting and pouring resulting in the pick-up of gases in the metal and the subsequent formation of oxides;
- turbulence of the liquid metal during pouring giving rise to a probable erosion of the mould, and entrapping of gases and slag;
- feeding behaviour of the alloy with the risk of shrinkage porosity.

These points are basically valid for all the casting methods, and for as well ferrous as non-ferrous alloys. However, the importance of each item depends on the alloy, the method, and the type of casting. There is a large difference in the rate of difficulty to produce a simple casting from normal cast iron or a high-duty component from a highly reactive titanium alloy.

From Fig. 1. it is obvious that the solidification of the casting takes the central-position of the problem, because the structure formed directly determines the properties and the reliability of the casting. Defects in this structure can badly influence the usability of the product. The question how to develop a qualified casting, can be transformed to how to achieve the good structure in the casting. The area "casting technology" consists therefore for the greater part in "solidification processing".

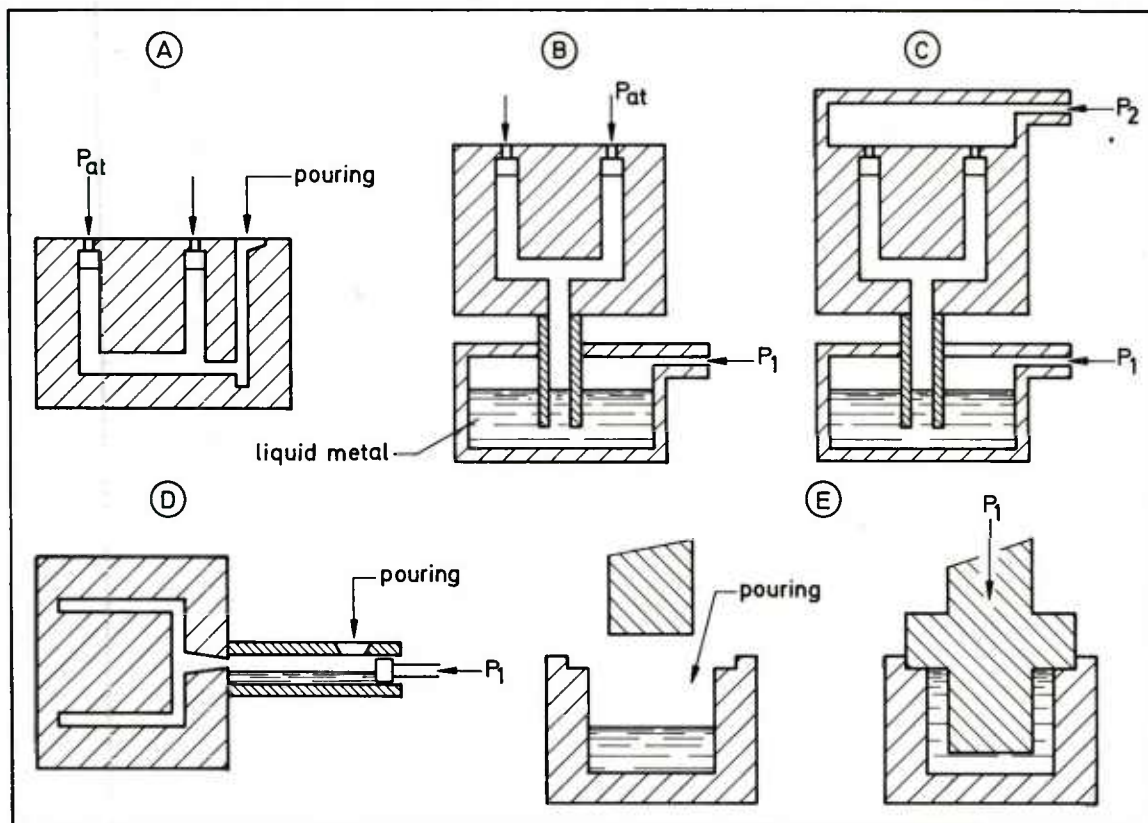


Fig. 2 Schematic representation of the different casting methods.

A = pouring by gravity
 B = low-pressure (die) casting
 C = counter-pressure (die) casting
 D = high-pressure die casting
 E = squeeze casting

Fig. 2. illustrates schematically the basic methods of casting classified according to the way in which the mould is filled (2) Fig. 2.A represents the traditional way of casting; the liquid metal is poured into an ingate and the mould cavity is filled by gravity. The mould itself can be made of moulding sand and is destroyed after the casting has solidified. Alternatively the mould is made from steel or cast iron (die) and can be used for a large number of castings. Cores, if necessary, are made of sand in these processes. Fig. 2.B refers to the low-pressure die-casting technique. The essential part in this process is the slow filling of the mould by adjusting the pressure P_1 , which exceeds P_{at} at about 0.05 MN/m^2 . The solidification of the casting occurs from top to bottom directed to the central ingate, which acts simultaneously as a feeder. This principle of mould filling is in fact also applied in the "CLA"-process for the manufacture of lost-wax investment castings (3). Under partial vacuum liquid metal is sucked into the cavity of the vertically positioned mould and remains there until the castings are solidified. The liquid metal, still present in the central ingate, drains back to the crucible. A refinement of the low-pressure die-casting process is shown in Fig. 2.C: the counter-pressure casting process invented in Bulgaria (4). The mould is carefully filled with liquid metal due to a controllable difference between P_1 and P_2 , which are appr. 1.6 MN/m^2 and 1.55 MN/m^2 resp. This higher than atmospheric pressure remains in the casting and the feeders during the solidification time. The high-pressure die-casting process with a cold chamber is illustrated in Fig. 2.D. Shortly after the metal has been poured into the chamber, it is pressed into the mould cavity. The pressure P_1 is rather high (about $50\text{--}200 \text{ MN/m}^2$), so the liquid metal enters the mould turbulent and with a very high speed. Fig. 2.E represents the so called squeeze casting process. Liquid metal is poured into the metal die, and next pressed into the final shape. The pressure P_1 is in the order of magnitude of 100 MN/m^2 (2,5,6).

The aim of this paper is on the one hand to discuss the developments in sand moulding with respect to the improvement of the quality of the casting, on the other hand it is concerned with the formation of the structure and structure control, mainly in the case of non-ferrous alloys.

3. DEVELOPMENTS IN SAND CASTING

Formerly only clay-bonded or greensand was used, because this mixture could cheaply be obtained mainly from natural deposits. The green strength was relatively low; increasing the strength necessitated an expensive and time consuming drying of the moulds. At that time cores were made with linseed oil or derivatives as binders. These cores should be baked in an oven to obtain the desired strength.

This situation has been fundamentally changed by the introduction of chemical binders, mostly resin-based, in the late 1950's and early 1960's (7). A number of new processes have been developed for the production of sand moulds: shell-moulding, the furan-sand process and the CO₂ sodium-silicate process. Among others the hot-box and cold-box methods can be mentioned for the production of sandcores.

Apart from the economic advantages due to a higher production rate, the biggest importance of these new processes for the foundry industry is the improvement of the dimensional accuracy and the higher reproducibility of the castings. Chemically-bonded sand has a higher strength than greensand, so the stability of the mould-wall is improved. The Figs. 3. and 4. demonstrate the influence of sand properties on the quality of iron castings (8). If the strength of the sand is low, as is the case for low-compacted greensand and under-cured resin, the mould-wall is not stable enough and will be moved by the solidifying casting. The result is a positive deviation from the mould cavity dimensions, coupled with the appearance of shrinkage porosity.

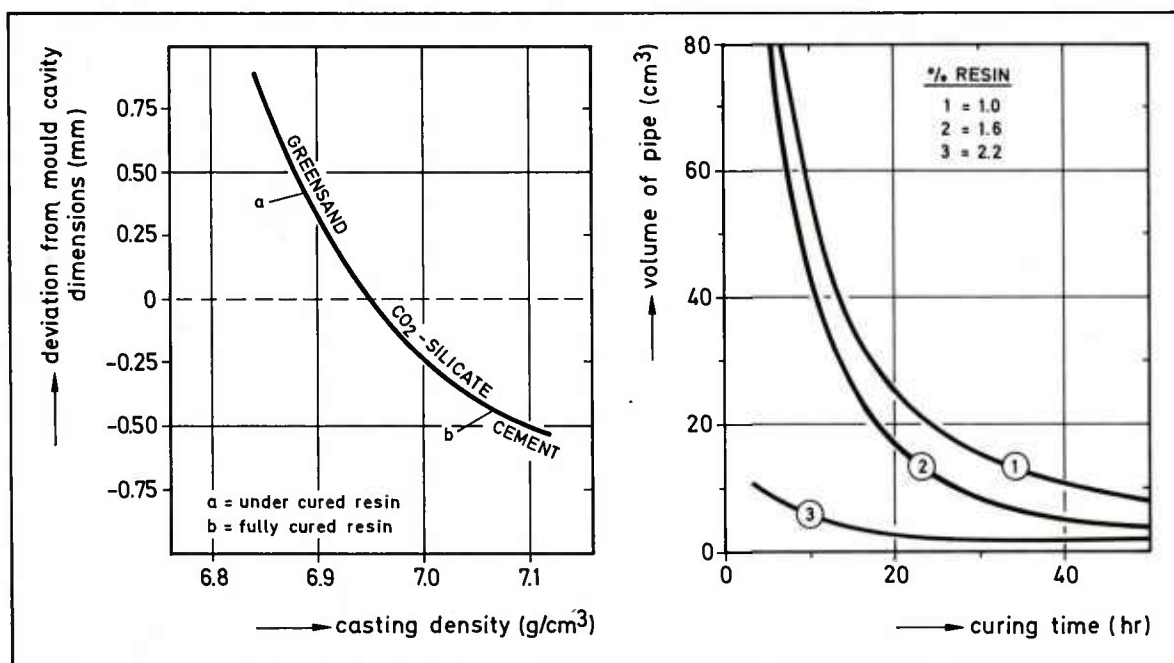


Fig. 3 Deviation from mould cavity dimensions of ductile iron 75 mm spheres related to the sand system used (ref. 8).

Fig. 4 Volume of a pipe formed in a ductile iron test casting poured in UF/FA resin bonded cold set moulds; 35% PTS catalyst (ref. 8).

Since cores are cured in the core-box itself, nowadays, more complicated core-shapes can be used with success (9). A representative example illustrating the possibilities at this moment, has been described by Skrivanek (10). It concerns the manufacture of complex thin passageways in components of turbo-jet engines and gear-boxes cast from the creep resistant magnesium alloy QH21. Using special air- or thermo-setting cores internal diameters of 2 mm or even less are possible in these passageways. The tolerances of diameter are ± 0.2 mm, and of position $\pm 0.4 - \pm 1.0$ mm, depending on the length of the core.

In spite of the progress in the application of chemically-bonded sand, the traditional greensand has not fully disappeared (11). On the contrary due to a better understanding of the behaviour of clay and an accurate mixing of the components into synthetic greensand, this moulding material has still its own place in the foundry practice. Nearly 50% of the total production in cast irons is manufactured in greensand. Concerning ferrous alloys Fig. 5. shows the different sand moulding techniques used. The selection of the method is clearly dependent upon the weight of the casting and the number of castings, that have to be produced. Three areas are indicated, although their boundaries are not well defined. Jobbing-work: single production or at best a small number of castings mainly of larger dimensions. Semi-jobbing: production of a larger number or of a small series of light and medium-sized castings. High-production: large scale production of castings, for instance for the automobile-industry.

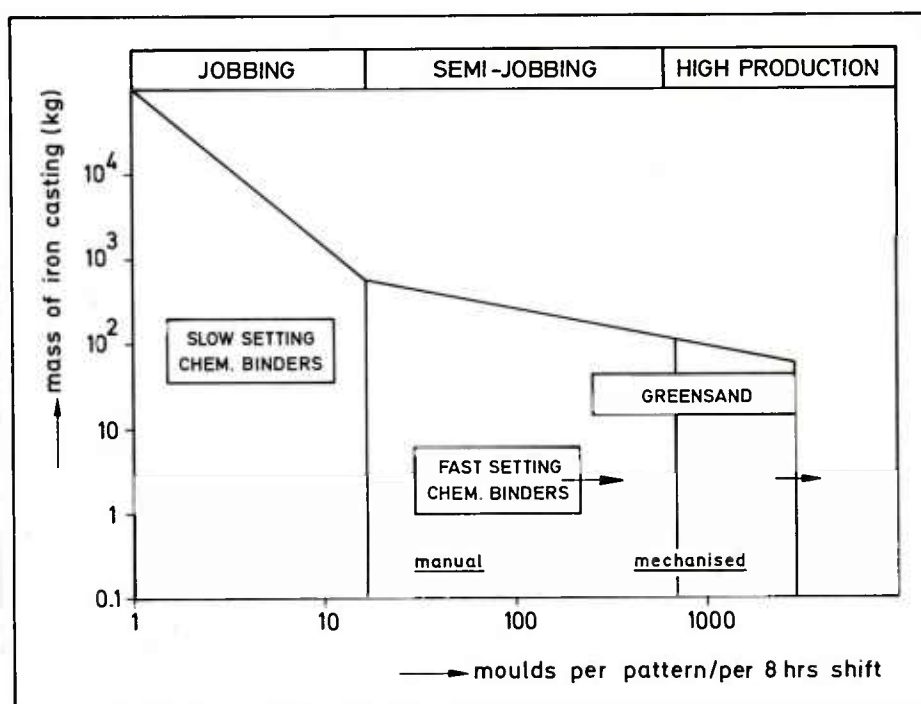


Fig. 5 Areas of application for different moulding sand systems (ref. 11).

Concerning ferrous alloys the greensand is pre-eminently suitable for the high-production area. This way of sand moulding is excellently suited for mechanization and automatization. Very sophisticated automatic moulding machines exist at this moment such as for instance the Disamatic, that have a production rate of 300 moulds per hour or even higher. Another advantage is the higher degree of compaction obtained with these machines, resulting in an improvement of the mould-wall stability. Compared with a production of moulds with normal machines the dimensional accuracy has been increased and the tendency to porosity diminished (Fig. 3.).

Almost all jobbing-work is done with chemically-bonded sand, in which cold-setting sodium silicate sand and furane sand takes a marked place. In the semi-jobbing foundry there is a competition between resin-sand and greensand. It depends on the local cost level of the binders and on the condition of the local silica sand which process is selected.

Roughly speaking Fig. 5. is also valid for aluminium and magnesium alloys. The only essential difference with the ferrous alloys is the application of die-casting techniques for mass-production and semi-jobbing if the shape of the casting is suitable. Table I illustrates the relative importance of the different casting methods in the production of aluminium and magnesium castings.

The development of highly automated moulding machines using greensand, and the introduction of the various chemically bonded sands has made it possible to produce more accurate castings more economically than with the traditional methods. Further developments can be expected in an increased automatization and mechanization, and in an improvement of the working conditions on the shop-floor. Very promising in this respect looks the so-called V-proces, in which the moulding sand is compacted by a vacuum, and binders are not necessary. This process competes with resin sand in the jobbing foundry (53,54).

4. SOLIDIFICATION AND FORMATION OF THE STRUCTURE

Shortly after the liquid metal has been poured into the mould cavity the solidification starts. Irrespective the moulding material two main types of solidification can be distinguished macroscopically:

- exogenous, that means that the crystallites grow from the mould-wall towards the center of the casting forming columnar crystals perpendicular to the wall;
- endogenous that means many crystallites are growing simultaneously across the whole wall-thickness forming equi-axed crystals.

Since there are a number of transitions between these types, the morphology of the solidification can be summarized into the schema of Fig. 6. (12,13,14). The way of solidification depends on the type of alloy, its composition and the cooling conditions. The arrows in Fig. 6. indicate the direction in which the solidification will change. The solidification behaviour of a number of aluminium alloys if cast in a sand mould, is summarized in Tabel II. Only high purity metals and some eutectics solidify exogenously with a smooth solid-liquid interface. Most high-strength aluminium alloys have, however, a long freezing range, and solidify according to type Va endogenously.

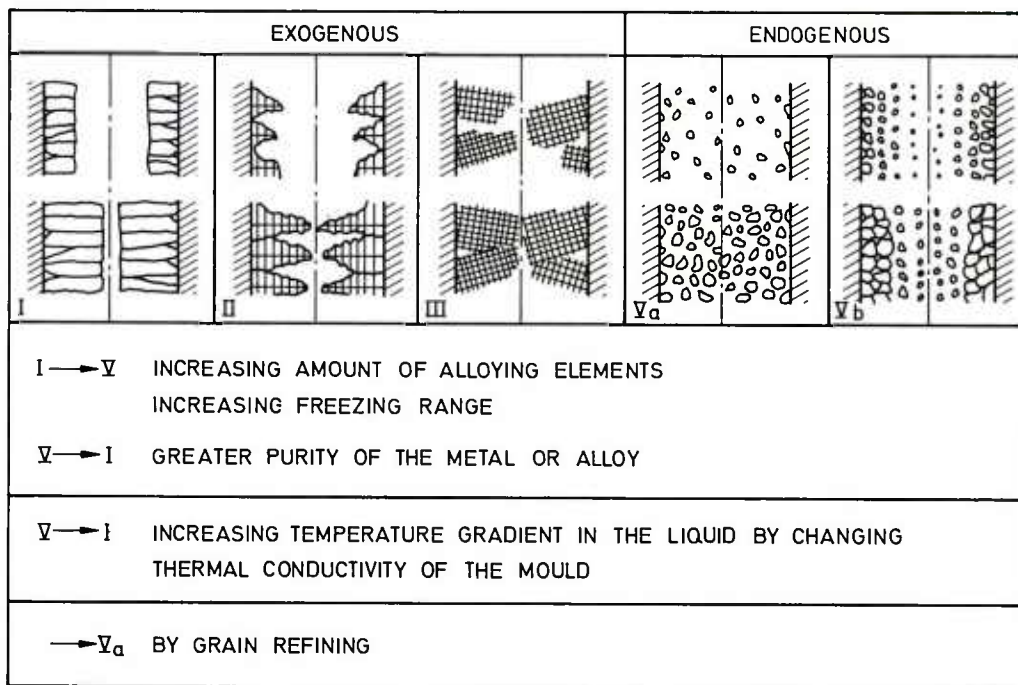


Fig. 6 The main types of solidification for metals and alloys.

Aluminium	Type	Al-Mg	Type	Al-Cu	Type	Al-Si	Type
99.999	I	3%Mg	III	0.5%Cu	IV	1.5%Si	Va
99.99	I	5%Mg	IV	1 %Cu	IV	4 %Si	Va
99.9	II	10%Mg	Va	4 %Cu	Va	10 %Si	Va
98.8	III			12 %Cu	Va	12.5%Si	Va
				33 %Cu	II	12.7%Si(Na)	Vb

Table II Solidification behaviour of sand cast aluminium alloys (ref. 14).

The type of solidification is primarily responsible for the macrostructure of the casting, especially with respect to the orientation of the grains: whether columnar or equi-axed. On the other hand, however, the way of solidification is decisive for a number of casting-properties of the alloy, as the shrinkage behaviour and the hot-tearing tendency. To obtain a high quality casting it is therefore very important to have full knowledge of the solidification characteristics to be able to control the structure in a proper way (55).

Most metals and alloys show a decrease in volume during solidification, that can go up to 5 or 6%. This shrinkage makes a continuous flow of liquid metal necessary to those points where the solidification occurs. As will be discussed in a next paragraph, the flow of liquid metal between the growing crystals is already blocked in an early stage of the solidification for alloys that solidify according to type III and V. To conclude it is important to note that long freezing range alloys tend to microporosity.

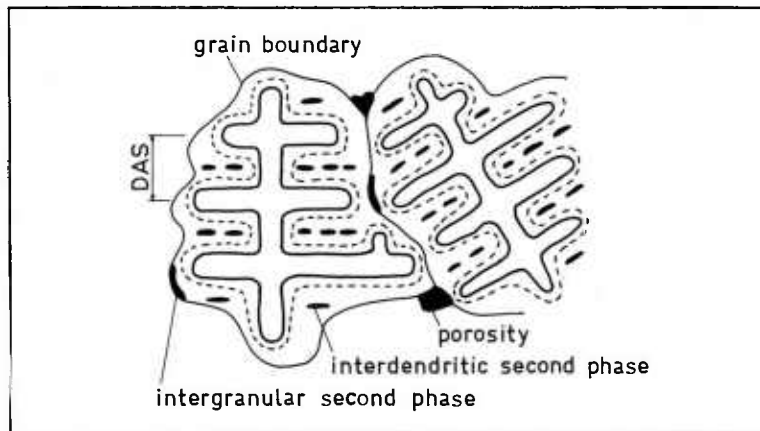


Fig. 7 Schematic representation of dendrite structure in hypo-eutectic alloys, showing dendrite-arm-spacing, and distribution of second phases and porosity.

The general appearance of the as-cast structure of an alloy with a small amount of eutectic is schematically shown in Fig. 7. Within the irregularly shaped grains a fine-structure is visible due to dendriteformation. Characteristic for a growing dendrite is the regular distance between the side-branches, the so-called dendrite-arm-spacing (DAS), that can be observed in the metallographic structure. During the growth of a primary dendrite, segregation of alloying elements and impurities occurs. This is responsible for two features in the structure: due to differences in composition coring takes place in the dendrite stems visible after etching and, due to an enrichment of alloying elements and impurities in the remaining liquid, a larger amount than expected of intermetallic compounds is formed. These inclusions are situated in the parts of the structure between the dendrite branches and at the grain boundaries, as indicated in Fig. 7. Fig. 8. summarizes the structural components which can be found in a casting. It is this complicated structure the foundryman has to optimize.

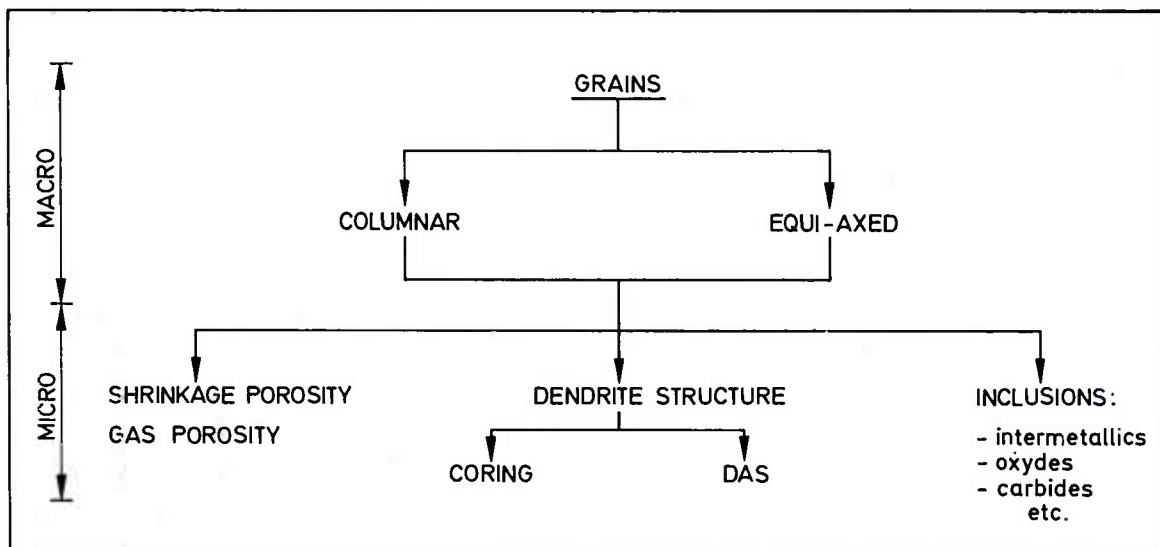


Fig. 8 Block diagram of the as-cast structure.

5. STRUCTURE CONTROL AND MECHANICAL PROPERTIES

Porosity and to a certain extent also the presence of inclusions are harmful for the mechanical properties of the casting. Neglecting a great scatter, Khan and Murthy (25) determined a relation between volume-percentage porosity (p) and tensile strength (R_m) for the alloy G-AlMg10, equal to:

$$R_m = 1.8p^2 - 45.2p + 321.5 \quad (1)$$

Eq.(1) shows that even a minor amount of porosity decreases the tensile strength strongly. So, the amount of porosity needs to be carefully controlled and measured. Arbenz (16) suggests a method based on specific density measurements. Castings or castingparts with an amount of porosity of 0.5% or even less can be qualified as very good. If the porosity equals 1% the quality of the casting is already fairly bad. So the margins in porosity are very narrow.

The metallurgical and foundrytechnical knowledge has made such a progress in the last two decades, that a number of methods for structure control are now available in the foundry (55). Apart from instruments for better chemical analysis, in this respect there can be mentioned:

- proper feeding to diminish the amount of porosity;
- increasing cooling-rate to obtain a finer dendrite structure;
- grain refining to obtain a more homogeneous distribution of the inclusions;
- providing a suitable morphology of the eutectic phase or more general the second phase by adding a restricted amount of an alloying element;
- excluding undesirable elements by a better control of raw materials and melting practice.

Only a number of these aspects will be discussed in the next paragraphs. There is assumed that the liquid metal before pouring has been brought in the proper condition by a well-controlled melting practice, refining- and degassing technique.

5.1. Influence of cooling on dendrite-arm-spacing

If the cooling rate during solidification is increased the dendrites will branch more frequently resulting in a smaller dendrite-arm-spacing. If the cooling rate is represented by the local solidification time t_1^* the following expression is valid for the dendrite-arm-spacing d :

$$t_1 = \left(\frac{d}{C}\right)^3 \quad (2)$$

The factor C is a constant, which depends on the alloy. Feurer (18) developed a model to calculate the value of C . The values of 11.0 and 12.4 respectively has been determined experimentally for the alloys G-AlSi5 and G-AlCu4Ti.

The dendrite-arm-spacing is a very useful metallographic quantity to determine the "thermal history" of a cast product. By measuring the dendrite-arm-spacing the foundryman can trace if for example the cooling rate of a test-bar is comparable with the one of the casting (19).

There is also a close relation between the dendrite-arm-spacing and the mechanical properties (18,20,21), that has been shown in Fig. 9.a and 9.b for two different aluminium alloys. Finer dendrites improve as well the static as the dynamic strength properties.

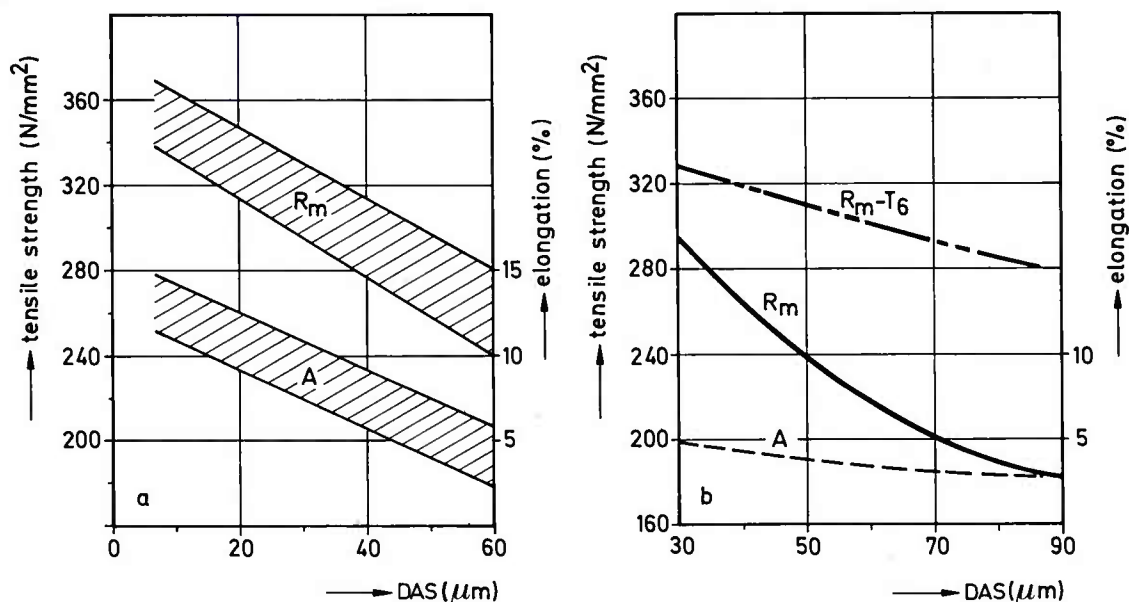


Fig. 9 Variation of mechanical properties with dendrite-arm-spacing (ref. 18,20,21)
 a. Alloy G-AlSi5 at equal porosity rating.
 b. Alloy G-AlSi7Mg in the as-cast and heat treated condition.

* Local solidification time is defined as the time required at a given location in the solidifying metal to pass from the liquidus temperature to the non-equilibrium solidus (17).

Oswalt and Misra (21) used the relation between DAS and the strength to develop a non-destructive testing method for estimating the strength in a casting. In the product shown in Fig. 10, the points are indicated, where the dendrite-arm-spacing is measured after the surface is prepared with a special technique. Using a standard relation between tensile strength R_m and dendrite-arm-spacing d , it is possible to calculate the strength in the casting test sites with Eq.(3)

$$R_m(x) = R_m(\text{test bar}) - m(d_1 - d_2) \quad (3)$$

with: $R_m(x)$: tensile strength of casting test site

R_m : tensile strength of the integral cast-on test bar

m : slope of the standard relation between tensile strength and DAS

d_2 : DAS of integral cast-on test bar

d_1 : DAS of casting test site

Basically the strength has been calculated with an integral cast-on test bar as a reference. According to the numbers cited in table III there is sufficient agreement between the measured and the calculated tensile strengths. So this method gives the foundryman a tool to control his castings, assuming, however that the measured DAS on the surface of the casting is representative for the inner parts of the casting test sites.

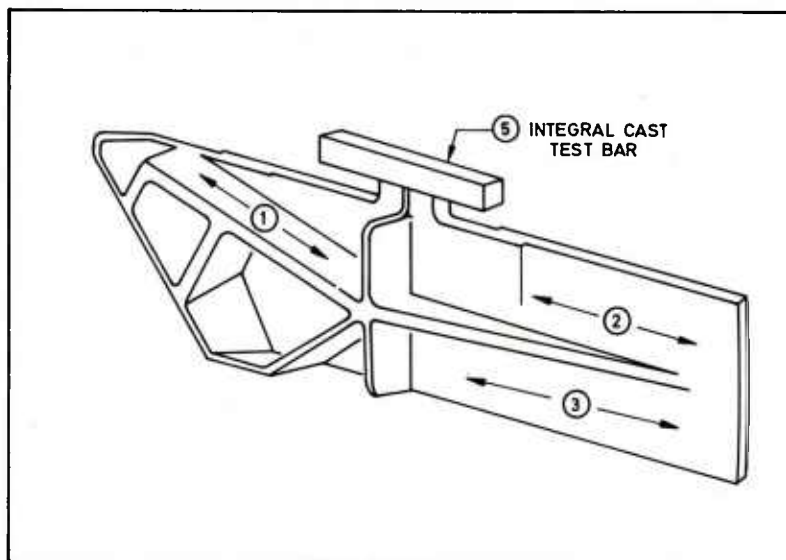


Fig. 10 Longeron fitting attach casting showing test locations; cast from alloy A 357-T6 (G-AlSi7Mg) in a greensand mould.

Casting	Test bar	DAS (μm)	Tensile strength (N/mm^2)	
			measured	calculated
A	ICTB	30.5	382	-
	ETB-1	43.2	362	364
	ETB-2	35.6	385	375
	ETB-3	38.1	372	365
	ETB-4	33.0	386	378
B	ICTB	50.8	339	-
	ETB-1	38.1	358	356
	ETB-2	38.1	354	357
	ETB-3	38.1	361	357
	ETB-4	43.2	352	350

Table III Measured and calculated tensile strengths of two sand cast longeron fitting attach castings made from A 357-T6 (ref. 21).

Note: ICTB = integral cast testbar

ETB = excised test bar

5.2. The feeding of a casting

The foundryman should take a lot of measures, called the feeding practice, and often a close co-operation between designer and foundryman is necessary before a sound casting can be obtained.

First of all the dimensions of the feeders have to be calculated with one of the equations which have been published in literature. The essential point in these equations is the condition that the solidification time of the feeder should be longer than the one of the casting to be fed. Solidification time depends on the type of metal and the shape of the casting (22) and can be expressed in the well-known Chvorinov's rule:

$$t = bM^n \quad (4)$$

with: b = constant, depending on type of metal, shape of casting and moulding material,
 $n \leq 2$.

Table IV summarizes for a number of alloys, sand cast, the values of the constants b and n in Eq.(4) (23).

Solidification time: $t = b.M^n$ t in min, M in mm				H = height D = diameter			
Alloy	Shape of casting	b	n	Alloy	Shape of casting	b	n
G-AlSi12	plate	0.103	2	G-AlCu4.5	plate	0.224	1.67
	cylinder H/D=1.0	0.076	2		cylinder H/D=1.5	0.092	1.93
G-AlSi4.5Cu3	plate cylinder H/D=1.5 cylinder H/D=1.0	0.221	1.86		cylinder H/D=1.0	0.106	1.85
		0.115	1.96	ductile iron	plate	0.089	1.86
		0.104	1.97		cylinder H/D=1.5	0.080	1.77
G-AlMg10	plate cylinder H/D=1.0	0.206	1.63		cylinder H/D=1.0	0.064	1.87
		0.119	1.77	carbon steel	plate	0.02	2

Table IV Solidification times of individually sand cast cylinders and plates.

Simply the feeder can be calculated from the equation $M_f = KM_c$, in which $K > 1$. In the case of low-carbon steels, which solidify exogenously, K will be equal to 1.2 (24). In the case of aluminium-alloys, especially the long-freezing range alloys, the value of K has to be increased. Better for such alloys, is to use a more general feeder-equation (23)

$$\frac{M_f}{M_c} = \frac{a}{1 - \frac{\beta}{v_f/v_c}} \quad (5)$$

in which the constant a has to be determined experimentally; tabel V shows some results of recent research.

$M_f = M_c \frac{a}{1 - \beta \frac{v_c}{v_f}}$			
Alloy	Feeder shape	a	β
G-AlSi12	H/D = 1.0	1.25	0.035
	H/D = 1.5	1.25	0.035
G-AlCu3Si4.5	H/D = 1.0	1.40	0.0417
	H/D = 1.5	1.34	0.0417
G-AlCu4.5	H/D = 1.0	1.36	0.0795
	H/D = 1.5	1.34	0.0795
G-AlMg10	H/D = 1.0	1.49	0.0575
	H/D = 1.5	1.44	0.0575
ductile iron	H/D = 1.0	1.55	0.036
	H/D = 1.5	1.70	0.036

Table V Feeder-equations for plate-like sand castings and cylindrical feeders (ref. 23).

A feeder with proper dimensions is necessary for obtaining a sound casting, but is however not a sufficient condition, since the passageway between feeder and place-to-feed also needs to stay open for a long time. In alloys with a long-freezing range this passageway is blocked soon after the start of solidification, as is demonstrated by Engler *et al* on the test casting in Fig. 11 (25,26). They determined the stagnation point for liquid flow during solidification. The ratio between the stagnation point and the total solidification time of the test casting, is called the relative feedability of the alloy.

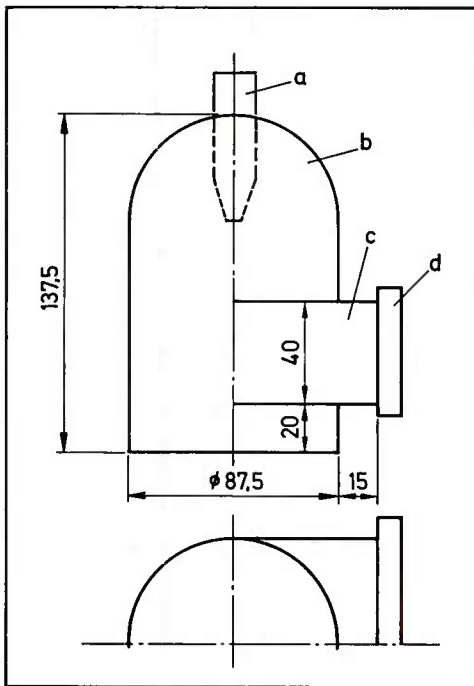


Fig. 11 Dimensions of the feeder test casting;
a: Williams-core, b: feeder,
c: slab trunk, d: heating plate.

As is illustrated in Fig. 12, the relative feedability passes through a minimum, exactly in the area of the long-freezing range alloys, in which a number of commercial high-duty aluminium-alloys is found: G-AlCu4Ti, G-AlSi7Mg, etc. It is obvious that special measures should be taken to obtain castings from these alloys with an acceptable low level of porosity. It appears that good feeding is only possible in such alloys if the solidification of the casting is directed towards the feeder, resulting in an open passageway for a long duration. A directed solidification occurs if the heat-extraction is controlled by either metallic chills or isolating materials, and if the shape of the casting is such that no hot spots can exist. So the designer has to keep in mind certain rules to model his design in the proper way. Many empirical rules can be found in the foundry literature for obtaining sound castings. Due to the development of modern computer techniques, however, it is possible to calculate from the heat-flow the progress of the solidification of the casting more conveniently, resulting in a proper siting of the chills or even in a redesign of the shape of the casting (27). This computer aided design of castings seems a quite important development, and will increase part reliability (28). Fig. 13. gives an example of a calculated solidification sequence for a steel wheel casting with two different web thicknesses.

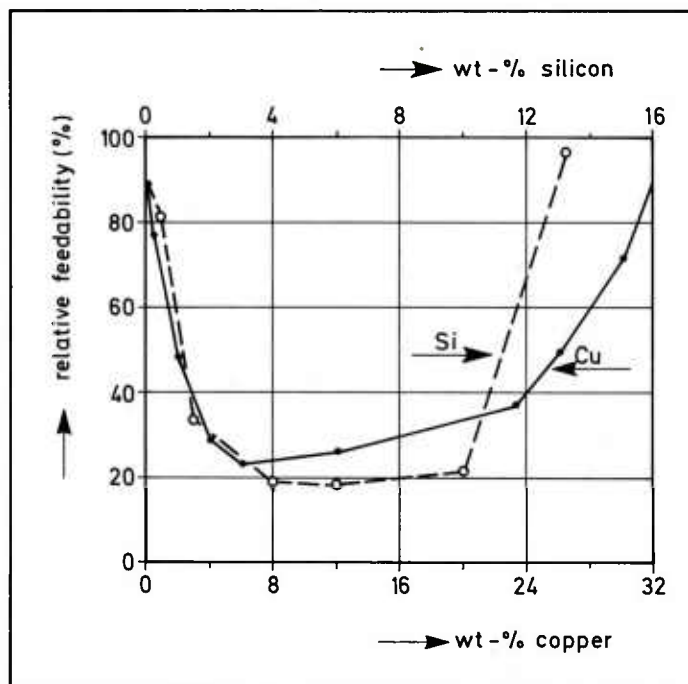


Fig. 12 Relative feedability of aluminium-copper and aluminium-silicon alloys.

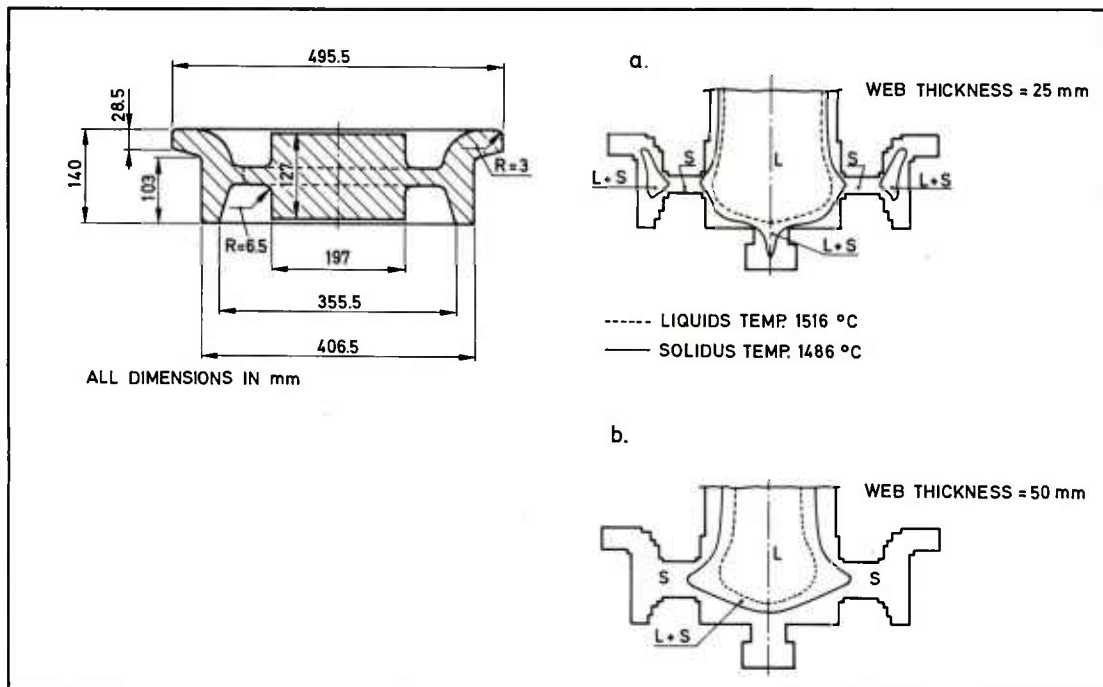


Fig. 13 Cross sectional view of rail wheel casting cast in steel. Computed isotherms of solidus and liquidus temperatures inside the casting at a time 2 min. after solidification.
 a. 75 mm thick chromite sand facing around rim and flange
 b. metal padding, greater web thickness (50 mm).

In the long-freezing range alloys the feeding is based on two mechanisms: mass-feeding, in which the whole mushy substance flows, and interdendritic feeding, in which the remaining liquid passes through the interdendritic channels (29). The interdendritic feeding can be improved by increasing the amount of eutectic residual melt during the last stages of the solidification. Since the amount of residual melt depends on the composition of the alloy, a number of special alloys has been developed with a better feedability by adding a small amount of an alloying element. As an example can be mentioned the addition of 0.75%Si to the alloys G-AlMg3 and G-AlMg5, or the addition of Mn, Cr, and Cd to the alloy G-AlCu5Ti (30,31,32).

5.3. Consequences for the mechanical properties

From the foregoing paragraphs can be concluded that the highest mechanical properties are obtained at relatively high cooling rates and under favourable feeding conditions. The influence of these two effects on the mechanical properties of the alloy A356 after heat treatment (G-AlSi7Mg0.3) is demonstrated in Fig. 14. (33). The test bars have been cut from a sand cast slab 19 mm thick, appr. 300 mm long and 125 mm wide. The slab is fed from one end, opposite the feeder a metallic chill has been placed. So a directed solidification occurs to the feeder, causing an increase in the local solidification time at greater distances from the chill (Fig. 15.). It appears that the yield strength ($R_{0.2}$) is almost insensitive to the cooling conditions, the ultimate tensile strength,

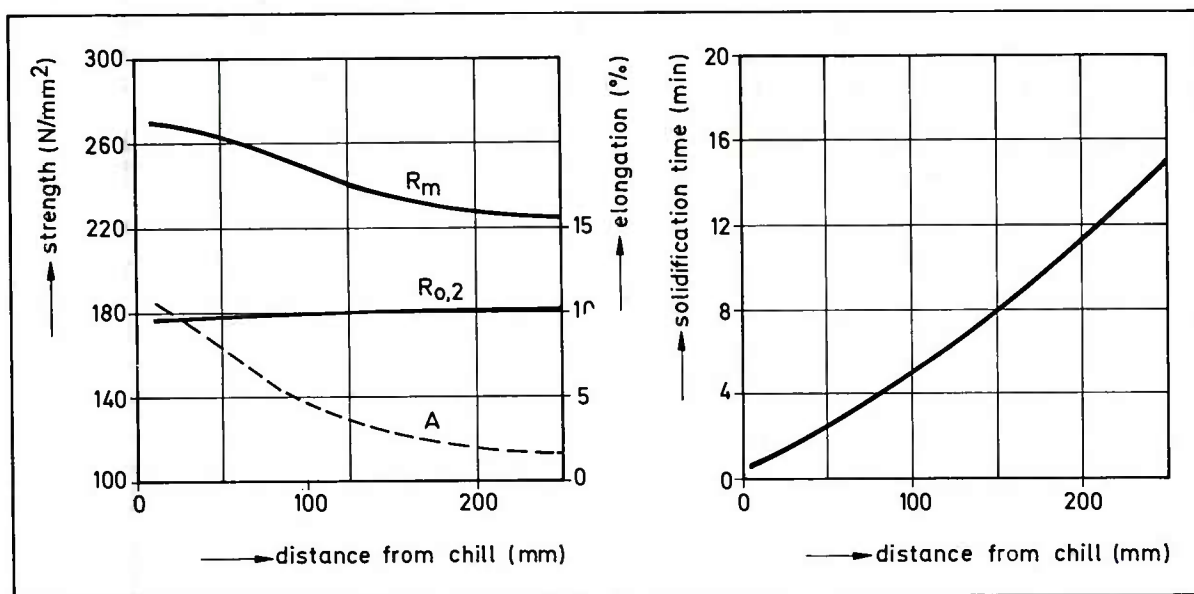


Fig. 14 Mechanical properties of alloy A 356-T6 versus distance from chill. 19 mm - thick test slab casting; quenched in boiling water, aged 5 hrs on 155°C.

Fig. 15 Time required for 19 mm thick test slab casting, poured in sand, to cool to solidus at various distances from chill.

however, and in particular the elongation decreases markedly in the direction of the feeder.

From this example it is obvious that the structure and the related mechanical properties of any casting alloy is sensitive to the wall-thickness. Important to note is the fact that small parts of the casting can endure the highest stresses, provided these parts are free from porosity. A separately cast test bar poured from the same ladle, as the slab from Fig. 14., yields the following mechanical properties:

$$R_m = 267 \text{ N/mm}^2, R_{0.2} = 185 \text{ N/mm}^2 \text{ and } A = 5.8\%.$$

These properties are quite different from those measured in the slab. Such test bars can thus only serve as a general alloy control, but say nothing about the properties of the casting itself. Therefore the attempts are understandable to develop non-destructive methods for measuring the mechanical properties directly on the casting.

The relation between the quality of the cast alloy, wall-thickness and feeding distance has been extensively studied by Drouzy *et al* (34-37); although the study was mainly done with the alloys G-AlSi7Mg0.3 and G-AlSi7Mg0.6, it has sense to discuss the results in this paper for their general validity. In agreement with Marsh and Reineman (Fig. 14.) Drouzy *et al* found, that the tensile strength R_m and the elongation A depend strongly on the structure, contrary to the elastic limit R_e , which is rather insensitive to the primary as-cast structure. The elastic limit could be estimated with good approximation from the tensile strength and the elongation with Eq. (6)

$$R'_e = R_m - 60 \log A - 13 \quad (6)$$

which is valid for elongations greater than 1%. In a $R_m - \log A$ -diagram, as shown in Fig. 16., lines of equal probable R'_e can be plotted.

Although different combinations of R_m and A will give the same elastic limit, it is at once clear that the quality of these different castings are not the same. Drouzy *et al* defined therefore a quality index by the general expression:

$$Q = R_m + c_1 \log A \quad (7)$$

with c_1 as a constant. In this case of the G-AlSi7Mg alloys c_1 is equal to 150, which gives the relation

$$Q = R_m + 150 \log A \quad (8)$$

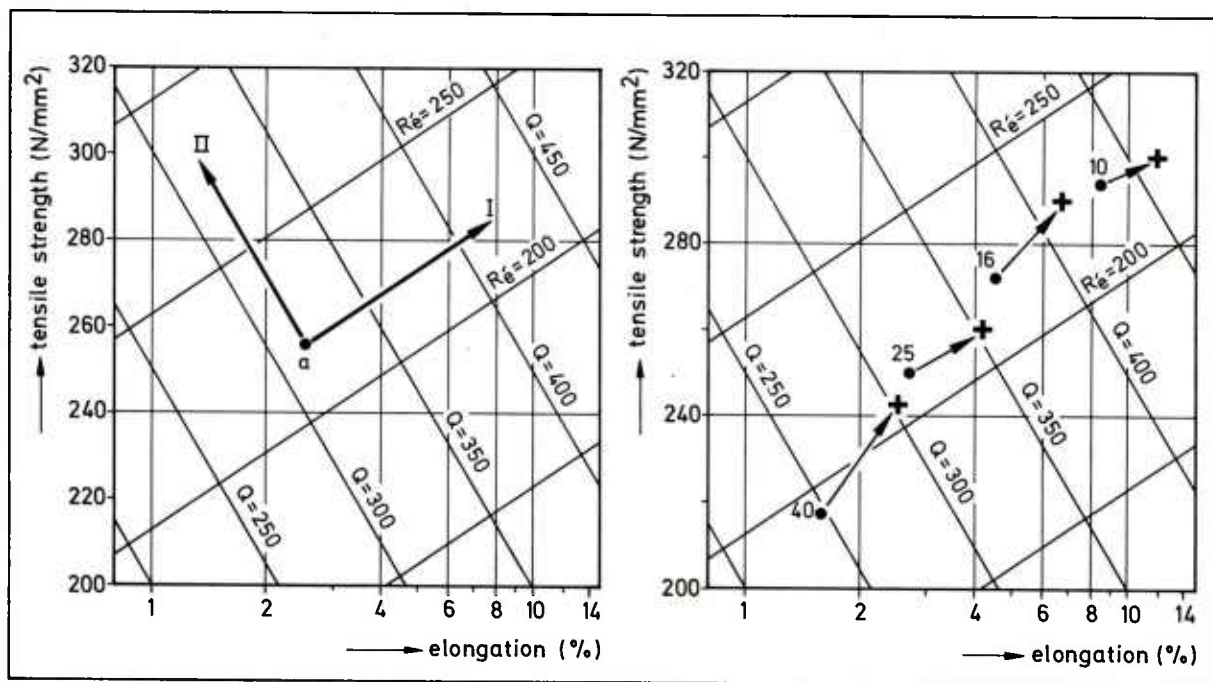


Fig. 16 Tensile strength - elongation diagram of heat-treated G-AlSi7Mg alloys with lines of equal quality index (Q) and lines of equal probable elastic limit (R_e).

Fig. 17 Influence of wall-thickness (in mm) and chilling (+) on the mechanical properties of sand-cast square bars from the alloy G-AlSi7Mg0.3 after heat treatment. Length to thickness ratio equals 5.

In Fig. 16, also a number of iso-Q lines has been constructed. From point a in this figure two main directions are important. Direction I (increasing Q) is covered if the density of the casting is increased by an efficient feeding, and if the dendrite-arm-spacing is diminished by a higher cooling rate. A lesser amount of iron or other impurities in the alloy increases also the value of Q. So, direction I depends upon the casting conditions and on the solidification processing.

A change of the mechanical properties in direction II can be realized by a more effective precipitation hardening, in these alloys caused by a higher magnesium content (0.6 instead of 0.3%) or by a better control of the heat treatment.

The influence of the dimensions of the casting, and so indirectly of the solidification conditions, on the quality of the alloy G-AlSi7Mg0.3 after heat treating is demonstrated in Fig. 17. It concerns horizontally sand cast square bars with a length to thickness ratio equal to 5. The bars are fed from one end. The crosses (+) in this figure represent the use of a metallic chill opposite to the feeder. It appears from these results that for the experimental conditions used and for a given wall-thickness the maximum value of Q, which can be obtained, has been fundamentally limited. The standard AIR 3380/C - class 2 dictates for the alloy G-AlSi7Mg0.3 an elongation greater than 2% and a tensile strength above 250 N/mm² (36). To satisfy this standard and referring to Fig. 17, the 25 mm bars has to be chilled; the 40 mm bar is not in agreement with the standard even in the chilled condition.

It might be concluded that a structure with high duty properties, satisfying a standard, only can be obtained in the smaller wall-thicknesses and with a relatively short feeding length. This maximum feeding length for two alloys can be read from the area a-b-c-d in Fig. 18., which should be read in combination with Fig. 17.

The quality index Q expressed in terms of R_m and A depends upon the shape of the casting and on the whole processing during the manufacturing of the casting (16). Fig. 19. gives an impression of the mutual relations. Only if all requirements, are simultaneously met, can this lead to a high quality casting. The successful application of these castings in many cases is the result of the necessary narrow co-operation between designer and foundryman.

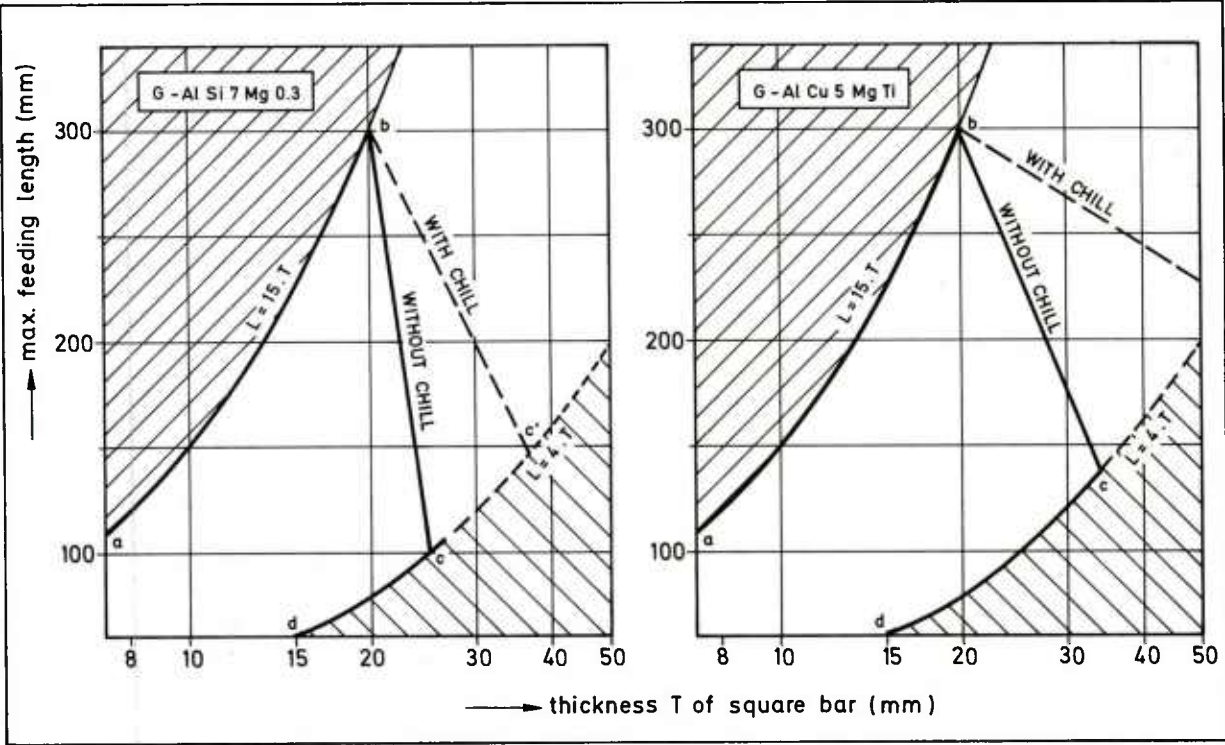


Fig. 18 Maximum feeding length for obtaining high duty sand cast square bars for two types of aluminium alloys.

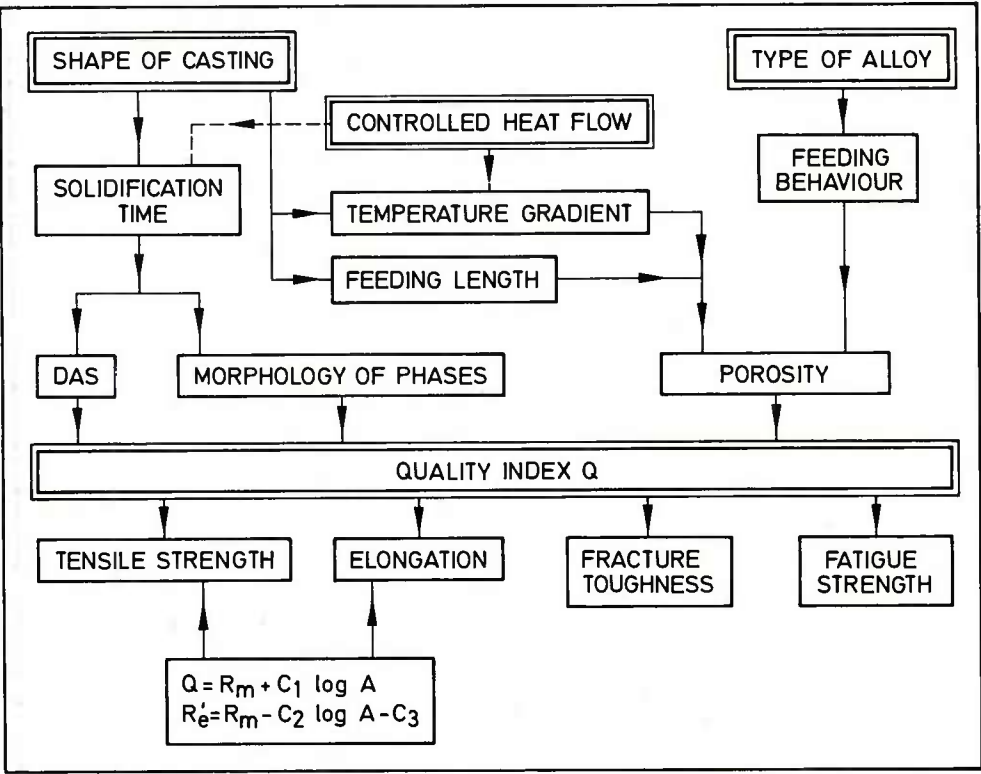


Fig. 19 Relationship between solidification parameters and mechanical properties for a given casting and alloy.

6. FURTHER IMPROVEMENT IN PRODUCTION AND QUALITY

It might be concluded from the foregoing paragraphs that only a careful foundry-practice can supply premium quality castings. For aluminium-alloys it is useful in that case to filter the liquid metal before it enters the mould cavity. Mollard and Davidson (38, 39) describe the successful application of ceramic foam filters. The amount of oxides and other inclusions is significantly reduced what results in a higher elongation and in a better X-ray density.

As another contribution to the improvement of the quality can be mentioned the constant development of alloys, coupled with metallurgical research. A good example is ductile cast iron, which is commercially produced since 1950. In this material the graphite crystallizes as spherulites, instead of the ordinary flakes in normal grey cast iron. This change in morphology of the graphite phase is the result of a small addition of magnesium to the liquid metal just before or during pouring. The mechanical behaviour of ductile iron is completely different from grey iron, as is illustrated in Figs. 20. and 21.; characteristic is the marked toughness of the material, which is for the ferritic grades comparable with low-carbon cast steel (8,40). The high quality properties can only be obtained with a careful metallurgical practice in the foundry, since small amounts of certain elements on ppm level can disturb the crystallization of the spherulites.

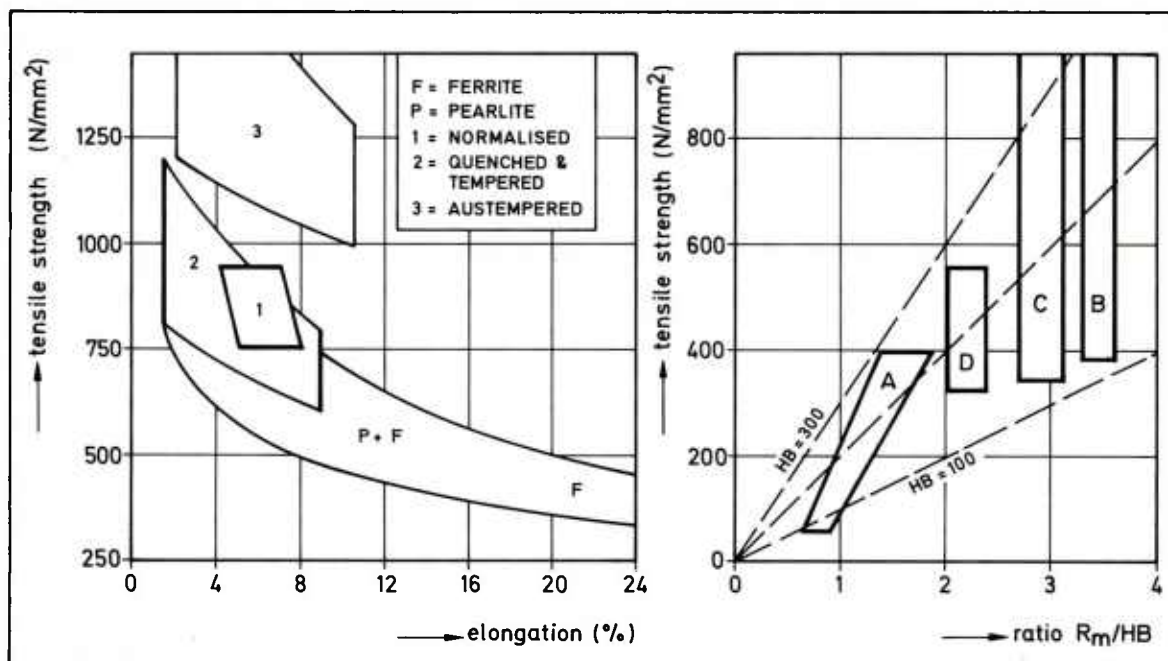


Fig. 20 Strength and ductility of different grades of ductile iron achievable as-cast and by heat treatment.

Fig. 21 Ratio between tensile strength and hardness for different grades of ferrous casting alloys

A = normal grey cast iron
B = cast steel
C = ductile iron
D = vermicular cast iron

In aluminium-silicon alloys the morphology of the second phase - in this case silicon - is as important to the mechanical properties, as graphite is in cast iron. The best ductility is measured if the silicon phase appears as fine, more or less rounded, flakes. A small addition of sodium, strontium or antimony promotes this structure. By a careful adjusting of the composition especially with respect to the impurity level, Aluminium Pechiney has been able to develop a new group of primary casting alloys with the trade name Calypso (41,42). The phosphorus content is less than 5 ppm. With these alloys it is possible to produce high duty castings with a greater reproducibility. Table VI shows a part of the alloys with their mechanical properties.

Aluminium-copper alloys with about 4.5% copper can endure very high stresses due to precipitation hardening. A large part of the development of these alloys has been devoted to an optimization of the precipitation. An addition of a number of elements is the result (43). So complex alloys appear, a few of them are listed in tabel VII. The composition of these alloys should be very carefully controlled in the foundry, especially the silicon and iron content should be kept as low as possible (<0.05%). With such a premium foundry-practice the alloy 201 for example has been applicated for high duty products. Stein and Tingley (44) describe some components of the Trident I missile, which should require to $R_m \geq 415 \text{ N/mm}^2$, $R_{0.2} \geq 345 \text{ N/mm}^2$ and $A \geq 3\%$. As a novelty can be mentioned that the design of the products was calculated accurately by an elastic-plastic stress analysis.

Calypso alloy		Mechanical properties			
		R_m (N/mm ²)	$R_{0.002}$ (N/mm ²)	A (%)	HB
25 A	G-AlCu5Zn2Mg	450	390	7	-
85 R	G-AlSi5Cu3Mg	400	300	2	125
67 N	G-AlSi7Mg0.3	290	200	18	90
67 N1	G-AlSi7Mg0.6	340	285	10	100

Table VI Mechanical properties of a few Calypso alloys after heat treatment (ref. 41).

Alloy	%Si	%Fe	%Cu	%Ti	%Mn	%Mg	%Ag	%V	%Zr
201	<0.05	<0.10	4.0-5.0	0.15-0.35	0.20-0.30	0.18-0.35	0.4-1.0	-	
204	<0.06	<0.10	4.5-5.5	<0.35	0.20-0.60	-	-	0.05-0.15	0.10-0.25
	Mechanical properties (cast test bars)								
	R _m (N/mm ²)			R _{0.2} (N/mm ²)				A(%)	
	201			204				201	
	204			201				204	
	440				370			8	
	370				280			7	

Table VII Chemical analysis and mechanical properties after heat treatment of the strong aluminium alloys 201 and 204 (ref. 43).

Another way of improving the quality is a further reduction of the porosity level, especially in alloys which are susceptible to microshrinkage. There are two approaches: improving the feeding during the solidification by external pressure, or increasing the density of the cast product by hot or cold isostatic pressing (HIP or CIP), or even a combination of the two. During "HIP-ping" the cast product is subjected to high temperatures and pressures in an inert atmosphere to seal up porosities, giving an increase in fatigue strength (45,46). Referring to Fig. 2, the squeeze casting process (2) and the counter-pressure casting process can also be mentioned in this respect. From the counter-pressure method can be said that the feeder-yield is higher, resulting in a greater density of the car wheels, which are among others manufactured with this process (47, 48).

Still in a stage of commercial development are the two processes propagated by Flemings *et al*: rheocasting and thixocasting (3,49-52). By intensively stirring the liquid metal in its freezing range a thixotropic solid-liquid slurry exists, which can be poured to a cold-chamber pressure die-casting machine. The advantages are a longer life-time of the die, due to a lower pouring temperature and a reduction of shrinkage porosity. Pressure die-casting of ferrous alloys seem also possible with this process. Problems are the careful control of the slurry and the fact that the fluidity of the slurry will rapidly decrease if the stirring action is stopped (51). So the slurry has to be immediately poured and transferred to the mould cavity by pressure.

7. EPILOGUE

Summarizing it may be concluded that the foundry-industry as a whole has developed itself to a modern process industry, that uses up-to-date production methods and that is able to meet the requirements the designers put forward. This is not an easy task, and needs skillful and qualified personnel in the foundries and a specialization between the foundries. In the casting process shapeless and amorphous liquid metal has to be transformed in a relatively short time to an often complicated product with the required structure. The foundry has to take many measures, inclusive the use of new techniques in certain cases, to prepare a structure which is free from defects or in which any defects do not diminish the usability. What defects are acceptable and what not, is not easy to decide, and needs in general more knowledge about the behaviour of a defect during the use of the casting. Measurement of the fracture-mechanical properties of cast alloys, together with a testing of the product itself (if possible), can give the necessary information. For a great number of cast alloys the fracture toughness and the crack growth rate are available for the designer. However, more data are necessary, to give the foundryman the possibility to optimize the as-cast structure in a still better way, and to prevent the foundry for an over-requiring from the designer.

8. REFERENCES

- 1) Goehler, D.D. - Structural castings for aircraft; a progress report from Boeing-Metal Progress, 113(1978), No 3, p. 38-43.
- 2) Ansprach, A. - Zum Flüssigpressen in der Giesserei - Giessereitechnik, 25(1979), p. 308-313.
- 3) Flemings, M.C. - New solidification processes and products - Metals Technology, 6(1979), p. 56-61.
- 4) Jorstad, J.L. - History of the low-pressure process - Die cast engineer, 1980, Jan./Febr., p. 16-21.
- 5) Chatterjee, S., A.A. Das - Some observations on the effect of pressure on the solidification of Al-Si eutectic alloys - Br. Foundryman, 66(1973), p. 118-124.
- 6) Weller, J., S. Remahne - Zur Festigkeitscharakteristik von AlSi12Cu1Ni1 - Pressguss - Giessereitechnik, 26(1980), p. 172-176.
- 7) Lemon, P.H.R.B. - The development of chemically bonded sands - Br. Foundryman, Special Suppl., June 1979, p. 15-27.
- 8) Hughes, I.C.H. - The developing technology of ironfounding; some recent contributions and opportunities - Br. Foundryman, 74(1981), p. 229-245.
- 9) Krömker, O. - Herstellung von Sandkernen für Fahrzeugguss aus Aluminium - Aluminium, 54(1978), p. 717-720.
- 10) Škrivanek, K. - Gestaltung mechanisch und thermisch hochbeanspruchter komplexer Leichtmetallgussstücke und ihre Herstellung in Sandformen - Giesserei, 68(1981), p. 702-711.
- 11) Williams, R. - The present status and future place of greensand in the foundry industry - Br. Foundryman, Special Suppl., June 1979, p. 53-62.
- 12) Patterson, W., S. Engler - Über den Erstarrungsablauf und die Grösse und Aufteilung des Volumendefizits bei Gusslegierungen - Giesserei techn. wissen. Beihefte, 13(1961), p. 123-156.
- 13) Engler, S. - Zur Erstarrungsmorphologie von Aluminium Gusswerkstoffe - Aluminium, 45(1969), p. 673-678.
- 14) Nieswaag, H. - Macro-stollingsverschijnselen in het gietstuk - De Gieterij, 8(1974), No 5, p. 5-9; No 6, p. 5-9.
- 15) Khan, R.H., K.S.S. Murthy - Solidification and feeding of aluminium-10% magnesium alloy casting in steel-shot-backed shell moulding - Aluminium, 54(1978), p. 392-395.
- 16) Arbenz, H. - Qualitätsbeschreibung von Aluminium Gussstücken anhand von Gefügemerkmalen - Giesserei, 66(1979), p. 702-711.
- 17) Bardes, B.P., M.C. Flemings - Dendrite-arm-spacing and solidification time in a cast aluminium-copper alloy - AFS. Trans., 74(1966), p. 406-412.
- 18) Feurer, U. - Influence of alloy composition and solidification conditions on dendrite-arm-spacing, feeding and hot tearing properties of aluminium alloys (Proc. Int. Symp. Quality Control of Engineering Alloys and the Role of Metals Science, ed. H. Nieswaag, J.W. Schut, Delft 1977; p. 131-145).
- 19) Wunderlin, R., U. Feurer - Schweiz. Masch. Markt, (1977), No 45, p. 74-75.
- 20) Radhakrishna, K., S. Seshan, M.R. Seshadri - Dendrite-arm-spacing in aluminium alloy castings - AFS Trans., 88(1980), p. 695-702.
- 21) Oswalt, K.J., M.S. Misra - Dendrite-arm-spacing: a non-destructive test to evaluate tensile properties of premium quality aluminium alloy (Al-Si-Mg) castings - AFS Trans., 88(1980), p. 845-862.
- 22) Sciamma, G., M. Jeancolas - Solidification times of simple shaped castings - AFS Cast Metals Res J., (1973), p. 1-7.
- 23) Prabhakar, K.V., H. Nieswaag - Stolling en voeding van aluminium-zand gietwerk - De Gieterij, 10(1976), No 2, p. 5-11; No 5, p. 5-14.
- 24a) Wlodawer, R. - Gelenkte Erstarrung von Gusseisen (Giesserei Verlag, Düsseldorf, 1977; 554 pp.).
- 24b) Wlodawer, R. - Die gelenkte Erstarrung von Stahlguss, 2^e Aufl. (Giesserei Verlag Düsseldorf, 1967; 228 pp.).
- 25) Engler, S., L. Henrichs - Feeding properties of Al-Cu casting alloys - AFS Cast Metals Res. J., 9(1973), p. 122-126.
- 26) Engler, S., G. Schleiting - Zum Speisungsverhalten bei Kokillenguss am Beispiel der Aluminium-Silicium-Legierungen - Giesserei, 30(1978), p. 65-72.
- 27) Jeyarajan, A., R.D. Pehlke - Application of computer-aided design to a steel wheel casting - Steel Furnace Montly, 1979, August, p. 280-282.
- 28) Trends in casting technology - Metal Progress, 119(1981), Jan., p. 96-100.
- 29) Engler, S., L. Henrichs - Interdendritische Speisung und Warmrissverhalten am Beispiel von Aluminium-Silicium-Legierungen - Giessereiforschung, 25(1973), p. 101-113.
- 30) Spektorova, S.I., c.s. - Al-Cu casting alloy of high dimensional stability - Russian Castings Pr., 1974, p. 424-425.
- 31) Höner, K.E., R. Wunderlin - Beeinflussung der Warmrissneigung, sowie der mechanischen Eigenschaften der hochtesten Aluminium-Gusslegierung G-AlZn5Mg durch Kornfeinung und Zusatz seltener Erden - Giesserei Pr., 1977, p. 249-262.
- 32) Henrichs, L. U. Hielscher - Das Fliessverhalten erstarrender Aluminium-Gusswerkstoffe als wesentliche Grösse für den Fehlerbedarf am Gussstück - Metall, 29(1975), p. 281-284.
- 33) Marsh, L.E., G. Reineman - Premium quality aluminium castings: theory, practice, and assurances - AFS Trans., (1979), p. 413-422.
- 34) Drouzy, M. - Interprétation des résultats de l'essai de traction des A-S7G à l'aide du diagramme R-A - Fonderie, 35(1980), No 402, p. 337-338.
- 35) Drouzy, M., S. Jacob, M. Richard - Interpretation of tensile results by means of quality index and probable yield strength - AFS Int. Cast Metals J., (1980), p. 43-50.

- 36) Jacob, S., M. Richard, M. Drouzy - Sensibilité à l'épaisseur et à la longueur des alliages d'aluminium moulés au sable - *Fonderie*, 33(1978), No 376, p. 91-98.
- 37) Drouzy, M., S. Jacob, M. Richard - Estimation de l'indice de qualité et de la limite d'élasticité des alliages A-S7G - *Fonderie*, 31(1976), No 360, p. 345-349 (see also: *Fonderie*, 31(1976), No 355, p. 139-147).
- 38) Mollard, F.R., N. Davidson - Ceramic foam: a unique method of filtering aluminium castings - *Modern Castings*, 69(1979), No 3, p. 64-65.
- 39) Mollard, F.R., N. Davidson - Experience with ceramic foam filtration of aluminium castings - *AFS Trans.*, 88(1980), p. 595-600.
- 40) Nieswaag, H. - Kenmerken van nodulair gietijzer - to be published: *Gietwerk Perspectief*, 2(1982), No 2.
- 41) Les nouveaux alliages de fonderie de la gamma Calypso - *Revue de l'Aluminium*, (1978), No 3, p. 121-128.
- 42) Etienne, C., L. Guillaume - Une nouvelle génération de pièces moulées en aluminium dans la construction automobile - *Revue de l'Aluminium*, (1980), p. 337-344.
- 43) Singh, G.B., G. Fleming - Superstrong aluminium alloys extend range of castings - *Metal Progress*, 107(1975), No 4, p. 79-82.
- 44) Stein, N., G. Tringley - Plastic bending analysis of type 201-T7 aluminium castings for Trident I missile - *Metal Progress*, 115(1979), No 3, p. 34-37.
- 45) Casting with titanium - *Engineering Materials and Design*, 1980, Oct., p. 51-54.
- 46) Trends in casting technology - *Metal Progress*, 119(1981), No 1, p. 96-100.
- 47) Balevski, A., I. Dimov - Methods for the treatment of materials with gas counter-pressure machines and applications - 48. Int. Foundry Congress, Varna Bulgaria, 1981; paper No 4 (16 p.).
- 48) Engels, G. - Anwendung des Gegendruck Giessverfahren in der Aluminium-Giesserei Pleven (Bulgarien) - *Giesserei*, 68(1981), p. 762-763.
- 49) Kievits, F.J., K.V. Prabhakar - Rheocasting of aluminium alloys (see ref. 18, p. 203-213).
- 50) Kattamis, T.Z. - Casting of semi-solid metals (see ref. 18, p. 189-201).
- 51) Asser, A., N.El. Mahallawy, M.A. Taha - Fluidity of stir-cast Al-10%Cu alloy - *Aluminium*, 57(1981), p. 807-810.
- 52) Sivaramakrishnan, C.S., R.K. Mahanti, R. Kumar - Stir cast morphology of aluminium-silicon alloys - *Aluminium*, 57(1981), p. 820-821.
- 53) Schaum, J.H. - Vacuum molding for clean quiet quality - *Modern Casting*, 71(1981), No 10, p. 50-53.
- 54) Engels, G. - Stand des Vakuumformverfahrens und seiner Mechanisierung - *Giesserei*, 67(1980), p. 757-763.
- 55) Nieswaag, H. - Improvement in product properties by solidification control (see ref. 18, p. 163-178).

DEVELOPMENTS IN ALUMINIUM ALLOY INVESTMENT CASTINGS

by

P.H.Jackson

Commercial Director

AICAL LIMITED (P.I.CASTINGS GROUP)

Davenport Lane Broadheath

Altrincham Cheshire WA14 5DS

England

SUMMARY

The paper sets out some of the main objectives in the development of aluminium alloy investment castings as seen by the Investment Foundry Industry, reviewing some examples of the successful utilisation of parts produced by the process for aerospace and high integrity applications, and illustrates the advantages to be derived from close collaboration between design engineers and the foundry.

Reference is made to developments taking place in investment casting technology and the possibilities for the extended use of investment cast parts in aerospace and defence equipment to which these could lead in the near future.

INTRODUCTION

Over the last fifteen years an entirely new field of application for investment castings has been opened up.

The market is essentially the aerospace and defence equipment manufacturers and the basic materials involved are aluminium alloys.

Throughout the aerospace and defence industries there is a demand for a wide range of component parts where the following criteria apply:-

Consistent mechanical properties

Minimum weight

Design freedom to achieve optimum functional requirements

Traditionally, aluminium alloys have been used as the materials best suited to achieve an acceptable combination of lightness, strength and low cost, and the most common techniques for forming the components required have been to machine from the solid or to fabricate from sheet metal.

The logical alternative of using castings to achieve the more complex forms was not overlooked, but such factors as poor surface finish, the need for draft taper, minimum section thickness and lack of confidence in the ability of foundries to achieve consistent metallurgical soundness, combined to prevent the exploitation of this approach.

Inevitably, as advances in aerospace and electronics technology created a demand for increasingly complex component shapes, so the pressure grew to find a metal forming method with the inherent capability of satisfying the criteria defined, without incurring the limitations of sand mould casting, while eliminating the need for extensive, and costly, machining operations.

This capability exists in the investment casting technique and, over the last few years, there has been a continuous development of the investment casting process with the aim of meeting the specific requirements of the aerospace and electronics industries for lightweight component parts.

Clearly the nature of these requirements is dynamic and as equipment designs continue to become more complex and exacting, so it is essential that the investment casting industry should plan the development of its own technology to ensure that future demands can be met.

For this to happen, the investment founders must be aware, not only of the present requirements of the design engineers, but also of the way in which these requirements are likely to develop over the next few years.

Equally, if the designers are to guide the founders along the lines they require, it is important that they should be aware of the state of the art as it exists at present. Understandably, there is a tendency for the potential user of investment castings to consult existing national standard specifications and to take these as defining the limits that can be attained in terms of mechanical properties. In fact most of these specifications were written some years ago and were based on the properties achieved in sand moulded castings at a time when processes and foundry practice were not controlled to anything like the degree applied today.

As an indication of the extent to which this applies, Figures 1, 2 and 3 show a summary of the actual results of mechanical tests on the last 20 batches of castings produced in the writer's foundry to the British Aerospace Specification 2L99.

The averages of these results expressed as a percentage of the specified figures are:-

0.2% Proof Stress:- 132% Ultimate Tensile Stress:- 124% Elongation:- 130%.

But these figures relate only to the basic criteria of mechanical strength at normal temperatures. Frequently the designer is concerned with a whole range of other factors such as operation at higher temperatures, resistance to various corrosive media, electrical or thermal conductivity; fatigue properties etc., none of which are defined in the standard specification available to him.

Similarly, there are no standard references to which he can refer which define the design configurations that can be achieved or the comparative costs of alternative types of design features (e.g. heatsinks, printed circuit board guides etc.).

In the hope that it will provide a stimulus for an active, definitive programme of investigation organised on a collaborative basis between the aerospace and the investment casting industries, it is proposed to indicate some of the main lines of development that the investment casting industry is at present pursuing, and to illustrate the stage that has been reached by showing examples from current production.

As major objectives the investment foundry industry is pursuing active development:-

1. of methods and process control to achieve better and more consistent mechanical properties in castings to existing material specifications,
2. of new alloys with improved and consistent mechanical properties,
3. of techniques to cast still thinner sections over larger areas to consistent metallurgical and dimensional standards,
4. of techniques to cast more complex configurations (e.g. enclosed heatsinks, complex small cross section passageways etc.).

Numerous examples of the degree to which progress has been made towards these objectives could be shown. Those which follow have been chosen as being entirely typical of current production. They are in no way considered to be "special cases" and are being produced in quantity to acceptable standards at the present time.

IMPROVED MECHANICAL PROPERTIES FROM EXISTING SPECIFICATIONS

1. Aircraft Structural Parts

Because of the limitations imposed by currently observed criteria, examples of the application of investment castings in aluminium alloy for structural parts of aircraft are rare, if not completely non-existent in the United Kingdom.

This is not the case to anything like the same extent in the United States and my first example (Figure 4) is a structural casting produced by the Hemet Casting Company of California for use on the McDonnell Douglas F-18 aircraft.

The casting is in aluminium alloy to Specification A356 heat treated to the T6 condition and released to the U.S. Military Specification MIL-A-21180, Class 10.

This specification demands an ultimate tensile stress of 262 N/mm^2 minimum with a yield strength of 193 N/mm^2 and 3% elongation. Our American colleagues have no difficulty in maintaining these figures.

The castings are tested non-destructively on a 100% basis to the standards set by MIL-C-6021, Class 2.

2. Artificial Hand Castings

Perhaps not surprisingly, a greater willingness to explore the possibilities of current practice often exists in industries which have had to employ a more empirical approach to their design problems, and the second example, produced in the writer's foundry, is not one for either the aerospace or the defence equipment industry.

It does, however, typify those requirements where the operating conditions are extremely arduous and virtually impossible to define, and where it appeared doubtful initially whether a cast aluminium alloy would possess adequate and sufficiently consistent mechanical properties.

The casting is the chassis of an artificial hand (Figure 5).

In initial discussion with the designers it became clear that the possibilities of abuse were such as to preclude any accurate assessment of the stress requirements. It was agreed, therefore, that an aluminium alloy to an established and well proven specification should be used (in this case A357) and that the foundry's efforts should be concentrated on producing the parts by a technique which would ensure the highest possible degree of metallurgical soundness in the actual castings on a consistently repeatable basis.

The extent to which this has been achieved and the advantages over the alternative approach of fabricating the chassis from steel parts are indicated in the report from the user which states:-

- i. New product tests give good strength and shock resistance. Endurance testing of hand mechanisms shows no significant wear on journals in casting.
- ii. Advantages are:-
 - (a) Removal of fasteners from high stress areas.
 - (b) No problems from loosening of structural fasteners.
 - (c) Quality control greatly simplified.
 - (d) Reduced weight of product.
 - (e) Product now far less labour intensive.

The successful outcome of this project demonstrates the possibilities of utilising aluminium alloy investment castings for quite highly stressed parts where the alternative would be to fabricate, since the one-piece design can be inherently stronger. At the same time it emphasises both the extent to which specification figures can be consistently bettered and the importance of considering the properties that are obtained in the actual casting as distinct from a separately cast test piece.

The need for a closely collaborated programme to investigate the extent to which current design factors could be safely reduced in this context becomes apparent. In general these design factors have also been established many years ago from statistical data related to sand moulded casting and have little relevance to investment castings.

NEW ALLOYS

Over and above the possibilities inherent in improvements to the basic properties attainable consistently from alloys to specifications in general use today, the investment casting industry is not ignoring the potentialities of new alloys.

Noteworthy among these are the silver bearing aluminium alloys. First developed in the United States, such an alloy began to receive general recognition around 1969.

As often occurs with a new concept, the initial claims made for the mechanical properties of the alloy were not always substantiated. The alloy has a strong tendency to be "hot-short" so that special care has to be exercised in establishing the detailed casting technique and indeed most foundries offering castings in this material appear to be selective as to the design configurations that they consider suitable.

In view of the possibilities, it would seem that a pooling of the experience gained to date and a collaborative programme of development would be of benefit to both the investment foundry industry and potential users.

THIN WALLED CASTINGS

Turning now to developments related to design features, our next examples illustrate the possibilities of weight reduction by reducing wall sections over extensive areas.

Difficulties can arise where large surface areas are unbroken by holes or protruding features such as bosses, lugs, webs etc., since the mould surfaces are then not secured to one another and, particularly where the section of the casting is very thin, this can give rise to variations in the mould cavity resulting in variations in thickness.

Over the last year or two the founder has made considerable progress in surmounting these problems as witnessed by the example shown in Figure 6, of a Dome cover for an airborne missile sight.

The wall thickness of this casting is $1.78 \text{ mm} \pm 0.5$, unbroken by holes or other features over an area of approximately 3500 sq.cm.

Over smaller areas, sections down to 1 mm thick are being cast satisfactorily and one simple way in which design collaboration can assist in exploiting this possibility is shown by the next example (Figure 7) where panels of reduced thickness enable a weight saving to be achieved while maintaining greater rigidity of form.

Both the examples shown are for relatively low stressed applications, but what happens where a requirement exists for a component with minimum weight but highly stressed?

The designer has no choice, apparently, but to utilise the minimum figures stipulated in a standard specification and to apply the design factors originally established for castings produced by sand moulding techniques.

Bearing in mind the extreme flexibility of the investing casting technique in terms of the ease of modifying the wax pattern die, it is suggested that a viable practical approach might well be made by producing castings of the component at differing wall thicknesses which could be subjected to appropriate testing in respect of the actual load criteria that would apply.

COMPLEX CONFIGURATIONS

The advantages of combining what would otherwise have been a fabrication of two or more individually made parts into a one-piece structure that were suggested by the hand chassis casting can be exploited to an even greater extent in the casting of boxes for electronic and avionic requirements.

Here, where the need for screened compartments, printed circuit board guides, heatsinks and shaped holes makes machining and fabrication unacceptably costly, the flexibility of investment casting is particularly relevant as can be seen by the cast-in features of the example illustrated in Figure 8.

The criterion in such cases is almost invariably geometrical accuracy rather than mechanical strength, but the need for close liaison between user and founder is equally important. Definition of the maximum dimensional variations acceptable on a practical basis is an obvious first requirement, but the importance of establishing the datum faces, and the tooling points for any finishing operations, in such a way as to relate the foundry's inspection of the castings directly to the way in which they will be picked up for machining, and the manner in which they will be assembled with other parts, cannot be overemphasised.

Just how far can the integration of a number of parts into a one-piece casting be taken? Every investment foundry equipped to serve the defence market can show its "pièces de résistance" but all have one feature in common; they are the result of an initial dialogue between designer and founder during which an interaction of ideas pushed the possibilities another small step forward.

CONCLUSION

In illustrating these examples of what is currently being produced by investment casting in aluminium alloys, it is hoped that some idea of the current state of development, and the directions in which this is moving, has been established, but the objective in mind is to emphasise the possibilities that exist to be exploited if the designer will accept the founder as a co-partner, and if the responsible bodies of the two industries with the most to gain; aerospace and investment castings; will collaborate in development programmes for the future.

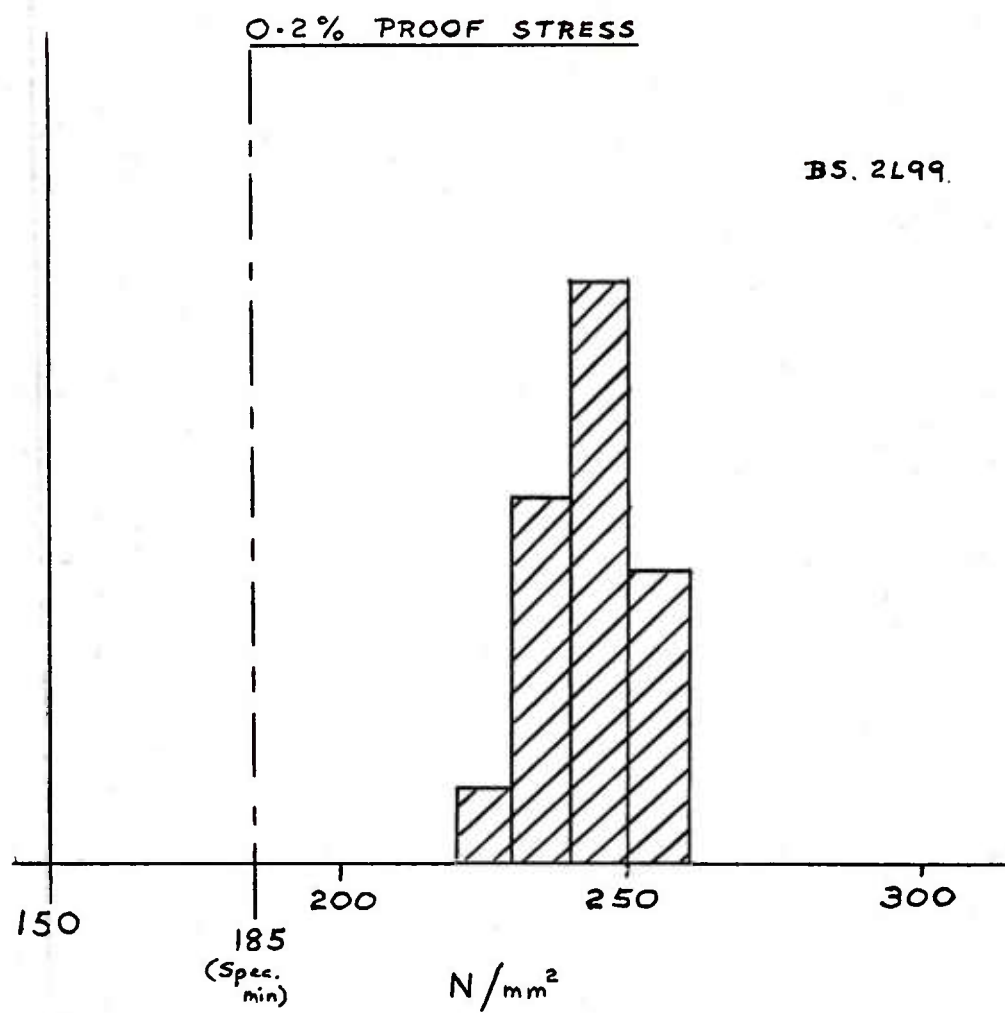


Figure 1

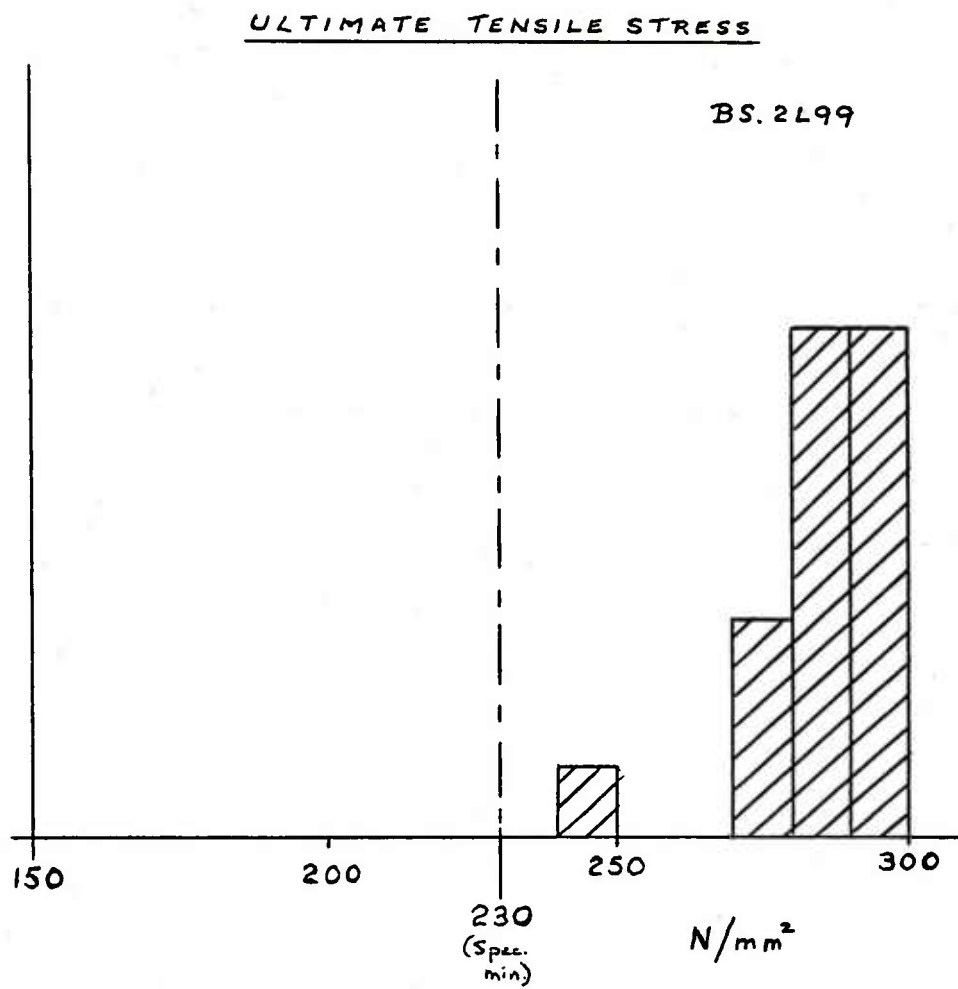


Figure 2

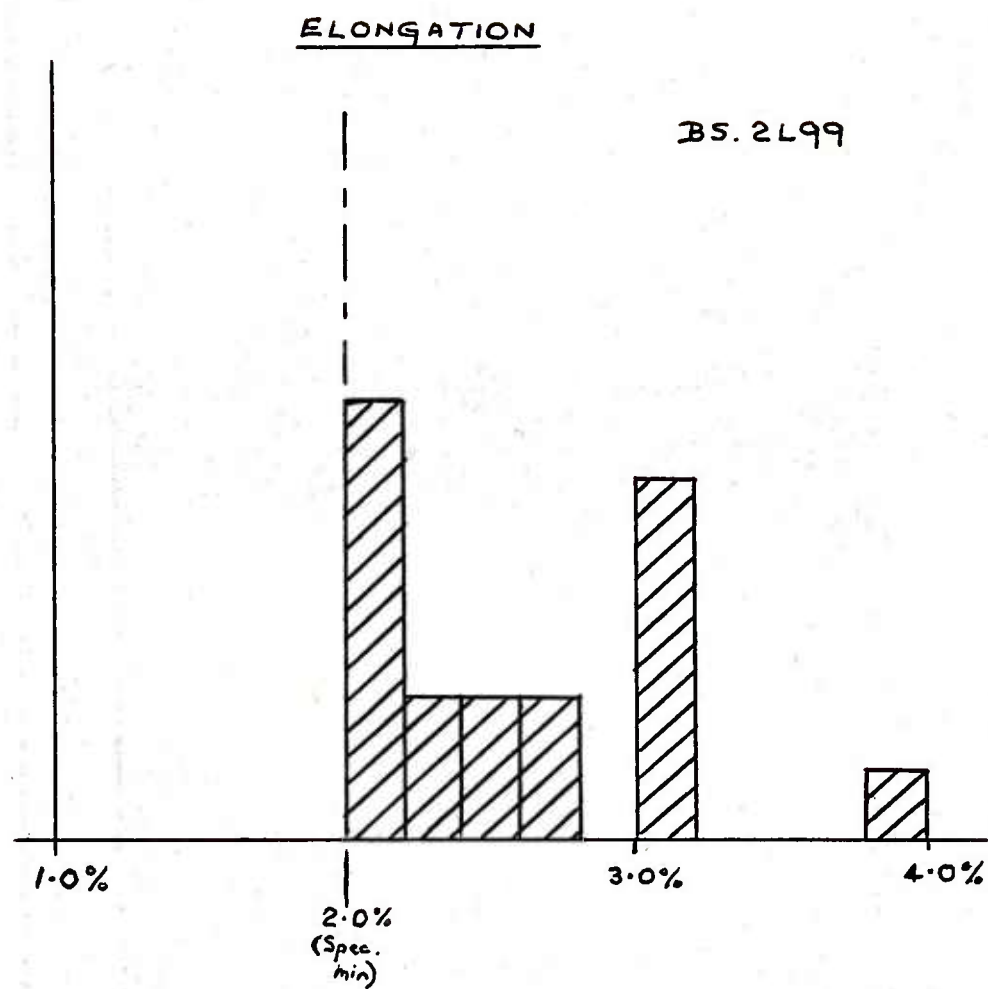


Figure 3

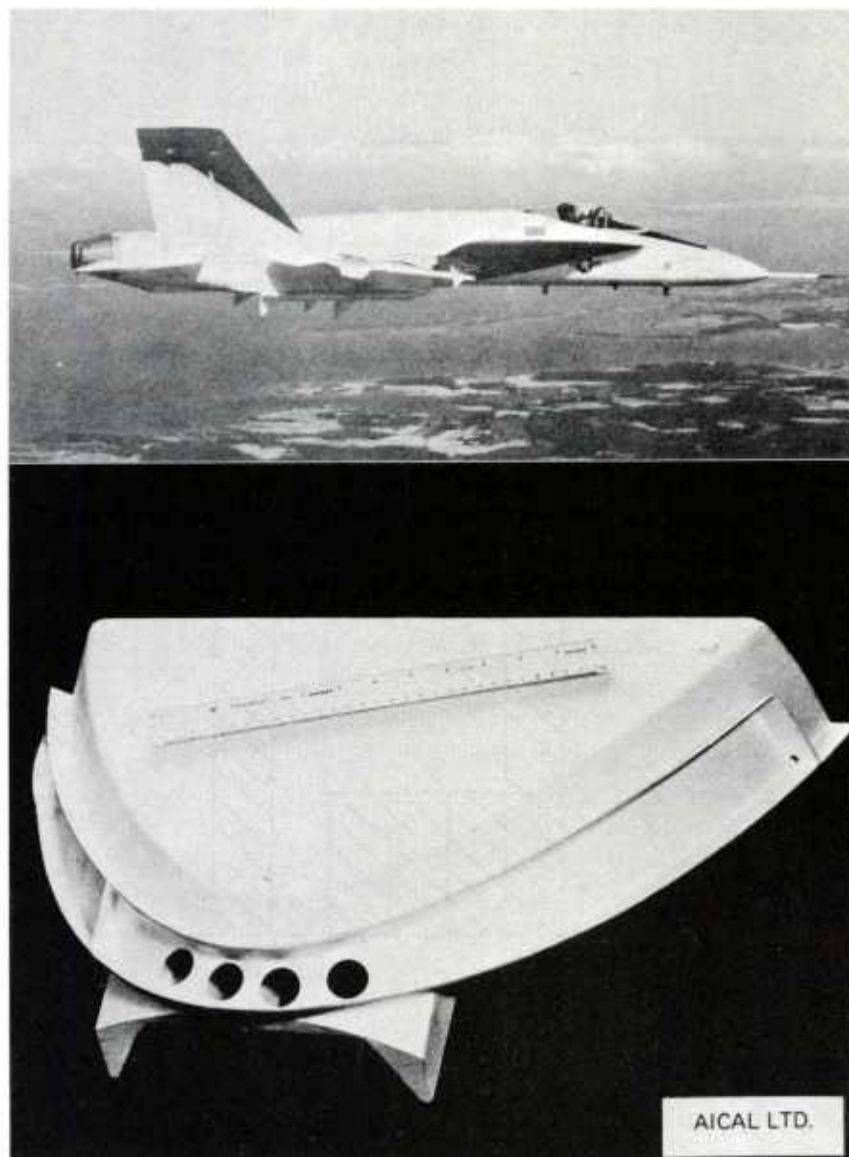


Figure 4. An example of an investment cast aluminium structural component for a military aircraft.

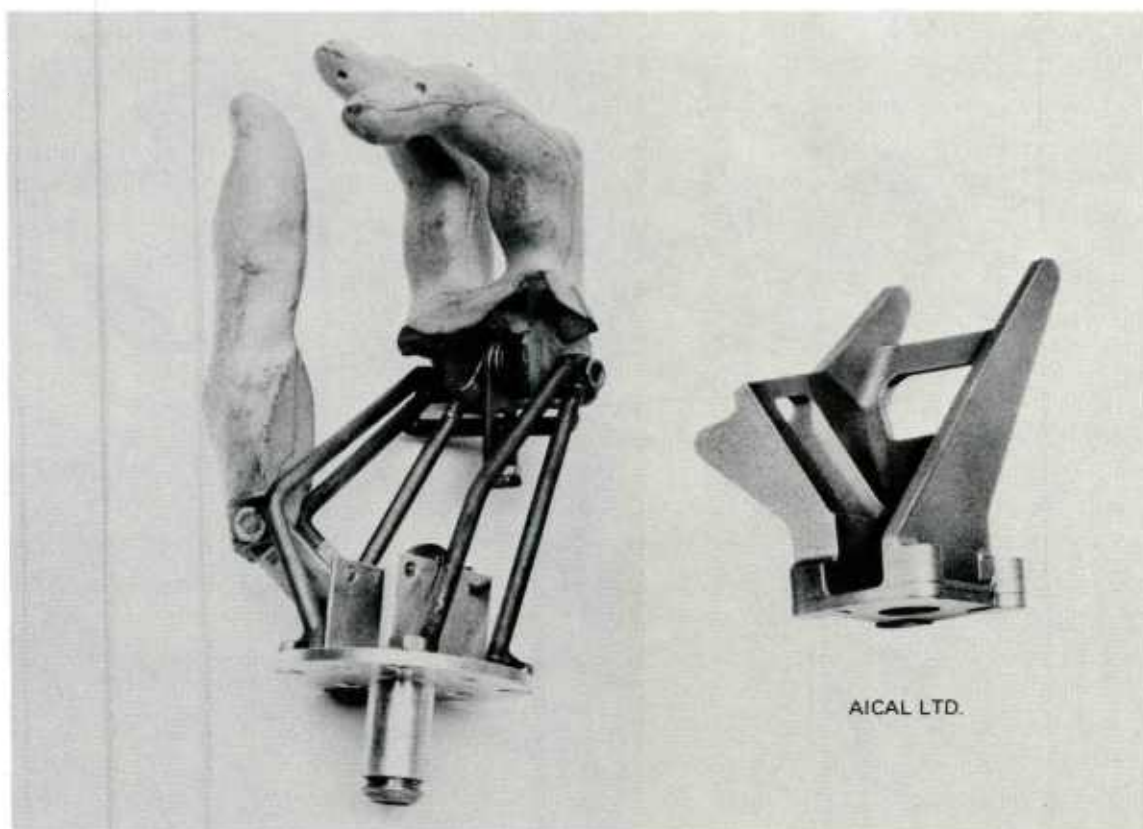


Figure 5. Comparison of the original fabricated structure of an artificial hand with the integral investment cast aluminium alloy chassis.



Figure 6. Large, thin-walled aluminium alloy investment casting for an airborne missile sight.

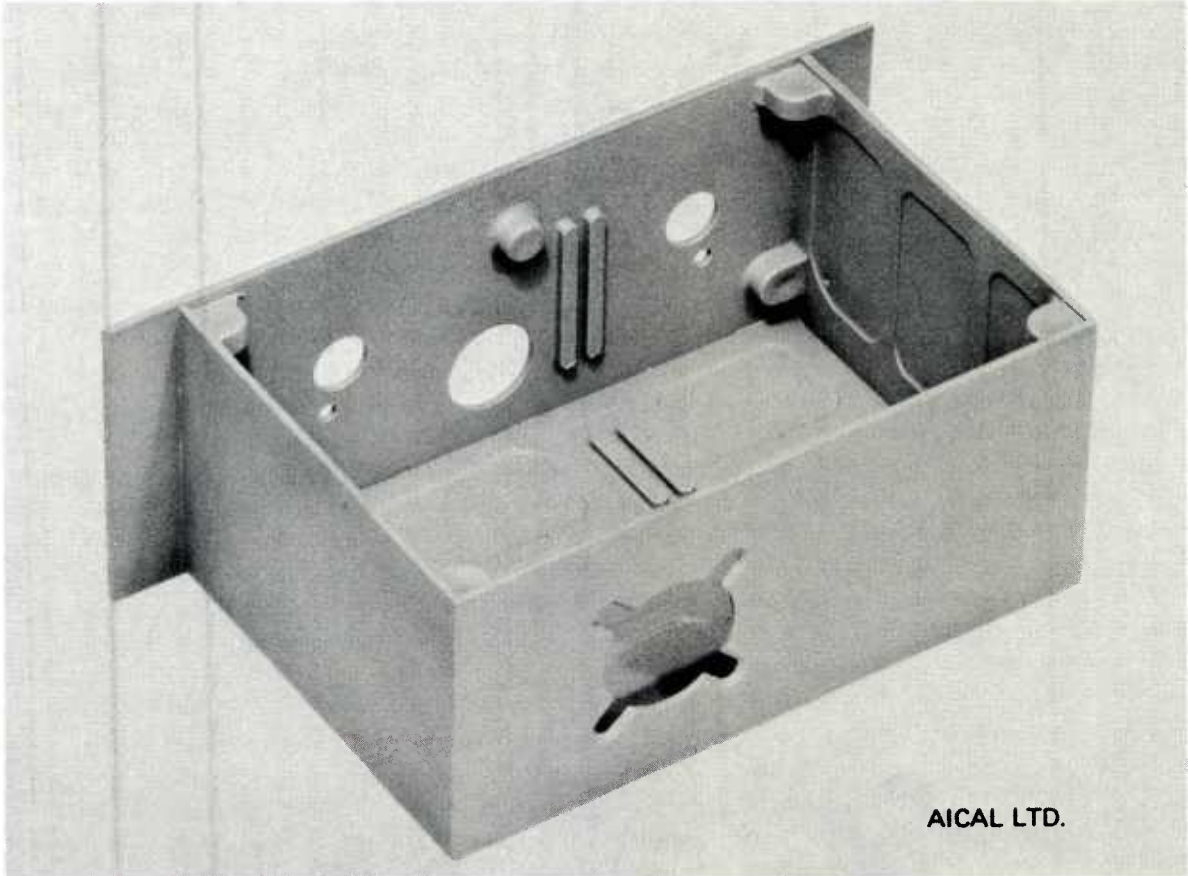


Figure 7. Small electronic box casting showing the weight saving achieved by panelling down to 1 mm thick.

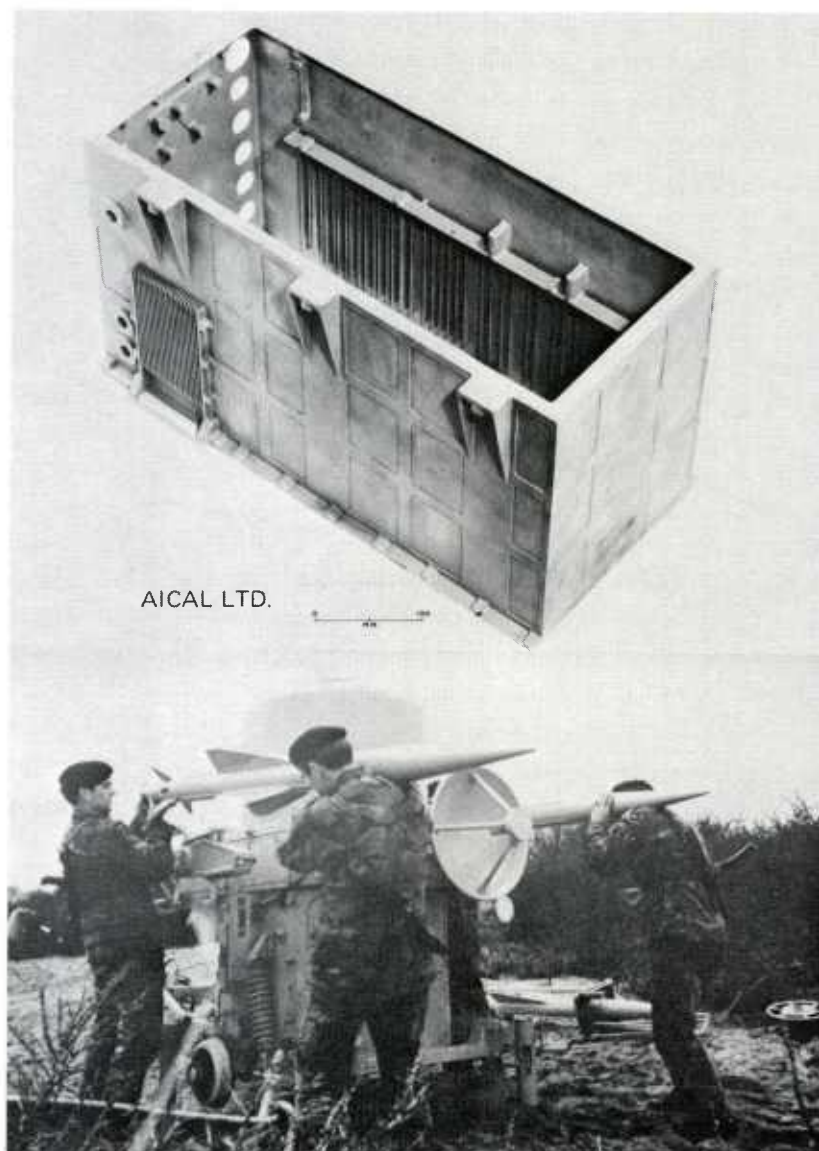


Figure 8. Large aluminium alloy investment casting showing potentialities of integrating numerous functional design features.

DEVELOPMENT AND TRENDS IN MAGNESIUM ALLOY TECHNOLOGY

W. Unsworth: Development Manager
 J.F. King: Senior Development Officer
 Magnesium Elektron Limited,
 P.O. Box 6,
 Swinton,
 Manchester, M27 2LS,
 England.

SUMMARY

Recent developments in Magnesium alloys, casting technology and corrosion protection are examined and probable future trends reviewed.

Alloys with improved ambient and elevated temperature capability to meet specific user requirements are described. High strength alloys with useful properties up to 250°C are available. Continuing developments indicate that significant improvements in temperature stability are possible giving alloys with strength at least comparable with current used aluminium alloys on an equal volume basis.

Adoption of resin bonded sands and the simultaneous development of techniques for producing longer and thinner cored passageways has enabled foundries to meet the aerospace industries requirements for more complex and larger castings. Further development of these techniques along with improved melting and casting techniques now being investigated should give the capability for thinner walled, closer tolerance castings offering additional weight saving advantages.

Current protective techniques are reviewed and possible developments to improve cost effectiveness of protection are discussed.

INTRODUCTION

Major requirements of a casting alloy for aerospace applications are:-

- [1] Minimum weight.
- [2] High Strength.
- [3] Good castability.
- [4] Good corrosion resistance.
- [5] Minimum cost.

Along with these are numerous special requirements such as stability at elevated temperatures, pressure tightness, ability to cast into very thin sections etc. Very few materials possess all the above qualities, and a number of compromises inevitably have to be made.

However, one attribute which magnesium alloys possess beyond all other structural alloys is light weight, and it is primarily this which has provided the incentive to its use in the aerospace industry.

To achieve the further requirements of high strength, good castability, corrosion resistance and minimum costs has required continuous development effort, which is still ongoing today.

ALLOY DEVELOPMENT

Background

Most designers with any knowledge of magnesium alloys will be familiar with the first major advance in magnesium casting alloy technology arising from the development in the U.K. of a technique for producing extremely fine grained magnesium alloys by Zr additions. This made possible the reliable production of castings with significantly better uniformity of properties and freedom from microporosity inherent in the then available Mg-Al-Zn type alloys. It also permitted the addition of a range of elements not previously useful with Mg-Al alloys, and opened the way to alloy design to produce specific combinations of properties. Early alloys developed during the 1950's based on

Mg-Zn-RE-Zr and Mg-Zn-Th-Zr systems are well known [e.g. EZ33, ZE41, HZ32, ZH62] and have been in use in aerospace applications for many years.

The development of engines with increasing power and efficiency, and consequently higher temperatures generated a continuing requirement for increasing strength and elevated temperature stability. Reduction in overall aircraft weight also indicated a move towards higher strength alloys which could be used in lighter castings. It is therefore in the area of high strength and temperature stability that most alloy development has been concentrated.

Figure 1 indicates the specified minimum room temperature tensile properties of magnesium alloys currently used in aerospace applications, with their approximate year of introduction. This shows some upward trend with time. Although use of Mg-Al-Zn alloys such as AZ91 has also continued, particularly in commercial aerospace applications where cost is a more important factor, considerable skill and experience is required to achieve consistent quality, and conversion of long established castings from AZ91 to ZE41 [RZ5] still continues today. However, if we consider the best available alloys for operation at 200°C [Figure 2], it is clear that a significant and continuous improvement has taken place.

Development of High Strength-High Temperature Silver Containing Alloys

A major advance arose from the discovery that alloys containing silver and a high Nd fraction rare earth could be solution treated, quenched and artificially aged to give high tensile properties at room temperature, which were well maintained to around 200°C. [1] Commercial alloys MSR-A [Mg-2.5% Ag - 1.7% Nd RE-Zr] and MSR-B [Mg-2.5% Ag-2.5% Nd RE-Zr] were introduced in 1960. MSR-B proved to have superior castability, and along with a slightly lower RE version [QE22 Mg-2.5% Ag-2.0% Nd RE-Zr] has been widely used for aerospace castings. They have good castability, are fully weldable and can be cast into relatively thin sections without difficulty [e.g. Figure 3].

However, this level of properties was still insufficient for some engine developments, and further development work was undertaken. It was found that by substitution of some of the Nd-RE component by Th within defined limits, a slight increase in yield strength could be achieved, but with a significant increase in elevated temperature properties. [2] An alloy QH21 [3] was introduced in 1976, with the compositional range:-

Ag	2.0 - 3.0%
Th	0.6 - 1.6%
Nd RE	0.6 - 1.5%
[Th + Nd RE]	1.5 - 2.4%
Zr	0.4% min.

Figure 4 shows the variation of tensile properties with temperature for QH21 compared with QE22, ZE41, and a typical Al casting alloy A356. Creep properties of QH21 at 200°C and 250°C also showed a significant improvement over previously available alloys [Table 1], and the alloy increased the maximum operating temperature for magnesium alloys by a further 30-40°C. Castability and weldability of QH21 is good, similar to QE22, and difficult castings can be made, as exemplified by the air intake bell for the Canadair drone CL289 [Figure 5].

Mechanical properties of QH21 represent the maximum available at this time, although higher strength alloys have been developed experimentally with significantly better properties. For example Table 2 compares the mechanical properties of QE22 with Yttrium additions to those of standard QE22 and QH21 alloys. These alloys combine excellent mechanical properties up to at least 250°C with superior castability to QE22 or ZE41, but unfortunately at a cost which precludes their use for commercial castings other than in very special price insensitive applications.

Recognising the effect of silver on the cost of these alloys, efforts were made to find some means of reducing silver content without impairing properties. Use was made of previous research work [4] which indicated that:-

- [a] Two precipitation modes were possible during the artificial ageing of Mg-Ag-NdRE-Zr alloys. [Figure 6]. Mode B, which occurred in alloys containing more than 2% Ag gave the preferred mechanical properties.
- [b] When some of the silver was substituted by Cu [e.g. 0.05-0.15%] the preferred mode B could be preserved even at silver levels as low as 1%, with only very slight reduction in tensile properties [Figure 7].

On this basis a new alloy designated EQ21 [5] has recently been introduced in which silver content has been reduced by 32% by controlled Cu addition i.e.:-

Ag	1.3 - 1.7%
Nd RE	0.5 - 3.0%
Cu	0.05- 0.10%
Zr	0.4% min.

Figure 8 and Table 3 compare the properties of EQ21 with QE22 and show that no significant sacrifice has occurred. Of particular interest is the observation that the short term elevated temperature properties of EQ21 are better than the original QE22, and rival those of QH21 in the 200-250°C range. Work is still in progress to investigate the longer term high temperature stability of the alloy. Castability of EQ21 is as good as that of QE22.

Development of High Strength Magnesium-Zinc-Rare Earth Alloys

In parallel with the development of silver containing alloy systems, further improvements were obtained from the Mg-Zn-RE-Zr system by the use of a hydrogen heat treatment [hydriding]. The effect of hydrogen in forming Zirconium Hydride in a Mg-Zr alloy had been known for some time. It was found that in zinc-rare earth containing alloys, hydrogen would diffuse into the metal, forming RE hydrides from the RE present in the Mg-Zn-RE eutectic phase, forming discrete particles [Figure 9] and permitting the Zn from the eutectic phase to diffuse into the matrix where it could be fully precipitated by a T6 type heat treatment to provide high strength. This permitted the use of a high zinc, high rare earth alloy, which although brittle and with low strength, in the as-cast state, had excellent castability and could be subsequently hydrided and heat treated to give high mechanical properties, particularly tensile strength and ductility. [6] The alloy introduced commercially in 1965 was designated ZE63, with a composition:-

Zn	5.5 - 6.0%
R.E.	2.0 - 3.0%
Zr	0.4 - 1.0%

Initial problems of non-reproducibility of hydriding were overcome by determination of suitable surface conditions for hydriding and use of controlled moisture content in the hydriding gas. [7]

Properties obtainable are shown in Table 4.

One limitation to the wider use of this alloy was that the hydriding rate is diffusion controlled and relatively long heat treatment is required to obtain full penetration [e.g. 40-50 hours @ 480°C at ambient pressure for 20 mm section]. This restricted the range of castings in which the alloy could be used to advantage to those with section thickness not exceeding say 20 mm. Where such criteria can be met, the alloy has been used extremely successfully. Figure 10 shows one of the castings which makes up the thrust reverser of the RB211 engine. The excellent castability of the alloy ensures that minimum machining is required, the aerofoil sections being cast to size.

Since gaseous diffusion rates are proportional to the square of the diffusing gas pressure, hydriding rate can be increased by hydriding in a pressurised furnace. Such furnaces are now commercially available and for example, the 40-50 hours indicated above can be reduced to less than 20 hours by increasing pressure from 1 to 2½ bar. This could make the alloy more attractive, particularly in view of the developing emphasis on production of thin walled castings.

Future Developments

Two major areas identified for future developments are:-

[a] Continuing requirement for minimum weight

This means a continuous requirement for maximum strength alloys which can be cast with high integrity into complex thin walled castings. The increasing ability of foundries to cast thinner Al alloy castings means that magnesium alloys must compete directly not only on a strength to weight basis, but on a strength to volume basis in normal casting configurations. Many applications in engines and gearboxes will also require maintenance of high properties at temperatures of 250°C and beyond.

[b] Minimum cost

Although the cost of the input material may be relatively low in relation to the finished cost of many complex aerospace castings, magnesium alloys are inherently more expensive than competitive aluminium alloys. Unless the advantage of using magnesium alloys can be clearly defined in terms of weight saving, ease of machining, or other factors, there may be a disincentive to use of magnesium. Current high strength alloys containing silver are expensive, and considerable effort is being made to develop silver free alloys with properties equal to, or better than the best available today.

Figure 11 shows an example of what may be available commercially in a relatively short time scale of 1 to 2 years on the basis of current development. The alloy indicated is silver free, and would cost less than the silver containing alloys currently available while giving higher strength and better temperature stability than commonly used Al alloys. An alloy with high temperature properties matching those of the high temperature Al alloy L119 [RR350], but with castability much superior to that alloy may also be achievable.

We may now extrapolate the earlier Figure 2 to the mid 1980's [Figure 12] showing that we have not yet reached the end of the line and that designers will have a still wider envelope of conditions in which magnesium alloys can be used.

CASTING DEVELOPMENT

Introduction

The magnesium foundry industry has tended to follow that of aluminium in developing and adapting new technology and processes. In only two areas is technology specific to magnesium being developed; the first of these, hot chamber pressure die casting, has little relevance to aerospace application, but the second, fluxless melting, will become significant in the short to medium term. Recent and possible new developments are summarised below.

Moulding and Core Making

"Dry sand processes" offer advantages with magnesium because of the latter's chemical reactivity, particularly to moisture. The adoption of the CO₂-silicate process in the 1960's, initially for core making but subsequently extended to general moulding, permitted a marked increase in the complexity of castings that could be produced. More recently cold set and air-set systems using resin bonded sands are replacing the CO₂-silicate system for both moulds and cores. This change has been a significant factor in enabling the magnesium foundries to meet the aerospace industries requirements for more complex and larger castings. The latter is exemplified by Figure 13 which shows the largest casting currently produced in Europe. This casting produced in ZE41A [RZ5] and weighing 280 Kg is for the main gearbox of the Westland WG34 helicopter.

The 'cold set' or 'self set' process uses synthetic organic resin binders which polymerise at room temperature through the addition of acid catalysts. [8,9] Binders used include mixtures of urea or phenol formaldehyde with furfuryl alcohol and the catalyst is a reactive aromatic sulphonic acid such as para toluene sulphonic acid or phosphoric acid. Another system utilises the formation of polyurethanes by reaction of phenolic novolac resins with methylene diphenyl-diisocyanate using a tertiary amine such as dimethyl ethyl amine as accelerator. [10] An alternative cold box technique, the SOFAST process, utilises phenolic or furan resins and peroxides gased with SO₂. [11,12]

The adoption of these new moulding techniques has resulted in better surface finishes in the as-cast condition and better dimensional accuracy; castings can now be produced to tolerances which would not have been considered possible a decade or so ago. The production of castings with thinner sections is also possible with consequent benefits in weight saving.

As far as the magnesium foundry industry is concerned the adoption of these techniques has brought a number of benefits. There has been a marked reduction in the number of sand compositions required for moulding and core making in a given foundry. Furthermore it has been claimed that the same sands can be used for both magnesium and aluminium. This reduction in the number of different sands in use has facilitated reclamation and recycling with obvious benefits. Another advantage is that the amounts of inhibitors required is lower than with the CO₂-silicate process and considerably lower than those necessary with 'green sands' with consequent environmental benefits.

The adoption of the new core materials and core making techniques has proved particularly beneficial for the production of cored passageways. A number of proprietary techniques have been developed which has enabled longer and thinner passages down to 2-3 mm dia., to be produced. Figure 14 is a gearbox casting sectioned to show the cored passageways and illustrates what can be achieved using present technology.

While the use of resin bonded sands will increase, the vacuum sealed moulding or 'V-process' is intriguing. [13,14] This process, developed in Japan, represents a new concept in foundry technology using dry, unbonded sand, a vacuum being applied to the moulding box to bind the sand. The stages in the production of a mould are summarised in Figure 15. While the process has been used for aluminium it does not appear to have yet been tried with magnesium. A number of problems are foreseen but if these can be overcome it may have some useful applications.

Other novel moulding techniques such as the 'full mould' process employing expendable foamed polystyrene patterns or the Effset or Freeze moulding process [15] using a clay bonded silica sand which is frozen, e.g. using liquid nitrogen, to improve its 'green strength', have not apparently been tried with magnesium.

Melting and Casting Processes

A significant innovation in magnesium foundry technology is that of fluxless melting which has developed from original work by J.W. Fruehling. [16] The technique involves the use of semi closed crucibles and protective atmospheres containing a small percentage of sulphur hexafluoride instead of fluxes for melting and alloying, the melts subsequently being cast under a shroud of protective gas. SF₆ concentrations of ½-2% by volume are usually sufficient to completely inhibit oxidation of the magnesium alloy at temperatures up to around 800°C. Various carrier gases can be used, e.g. air, nitrogen, argon, CO₂, or air/CO₂ mixtures [17]. The advantages offered by the process include:-

- [1] Lower melting losses and better material efficiencies.
- [2] Better environmental conditions since SF₆ is non-toxic.
- [3] The virtual elimination of risk of flux inclusions in the final casting.

While the process has been used commercially for a number of years for pressure die casting of magnesium aluminium alloys, e.g. AZ91, it has only recently been applied to sand castings. [18] Development work is continuing with particular reference to the magnesium-zirconium alloys.

The low pressure casting process, which utilises a positive pressure of around 0.5 bar to transfer molten metal from a holding crucible to a permanent mould, has been in commercial use for a number of years. However the recent developments in moulding and core making referred to earlier have enabled the low pressure casting technique to be used with conventional sand moulds. Two techniques, the EDEM and COSWORTH processes, [19] have recently been developed and used with aluminium, to produce aerospace components.

These processes have not yet been applied to magnesium but the adaptation of such semi-automated techniques involving pressure or vacuum assisted pouring, probably in combination with fluxless melting, would seem to be a logical development. The benefits to be gained include:-

- [1] Better material efficiencies and improved yields.
- [2] Better casting integrity resulting from improved feeding and the elimination of microporosity.
- [3] The ability to produce thinner walled castings with consequent weight saving.

Techniques for precision casting of both Mg-Al and Mg-Zr alloys have been available for a number of years but the quantities produced have been small and the size of the casting produced limited to around $\frac{1}{2}$ Kg. [20] Recent developments in plaster casting technology have enabled much larger parts to be cast satisfactorily in magnesium. Figure 10 showed the RB211 thrust reverser casting produced by this method.

The next decade will see greater emphasis placed on the adaptation and application of the processes outlined above to magnesium. The objectives will be to produce castings exhibiting:-

- [1] Better overall integrity.
- [2] More consistent properties in thick and thin sections.
- [3] Minimum section thickness consistent with service requirements.

These processes will be inherently more expensive than the older more conventional process but the increase in cost should be offset, at least in part, by improved material efficiencies, lower reject rates in the foundry and better operational performance.

Hot Isostatic Pressing

While this subject does not strictly fall under the heading of casting development it is worthy of mention. The technique is well known since it is used to upgrade aerospace components cast in super alloys or titanium. [21] Little work appears to have been done with magnesium castings although it is understood that an improvement of around 20% in fatigue strength was achieved on a casting made in QE22A. Further investigation of the effect of HIPping of magnesium alloy castings would clearly be worthwhile.

DEVELOPMENT OF ANTI-CORROSION TREATMENTS

Introduction

Magnesium is a reactive metal, as shown by its position in the electrochemical series, and a considerable amount of work has been done to develop protective techniques. Various treatments are now available which will provide satisfactory protection over a wide range of environmental conditions. The old concept of a chromate conversion coating plus a chromate containing primer and top coat is the cheapest and simplest system which performs effectively in mildly corrosive environments. However by inserting a water proof film of stoving resin between the conversion coating and the primer [i.e. surface sealing] the protective capability is considerably enhanced and this will provide satisfactory protection in aggressive environments. [22] Special coatings to provide wear resistance [e.g. nylon] and erosion/abrasion resistance [anodic coatings] are now available.

Figure 16 demonstrates what can be achieved with currently available protective treatments. This is a deep sea diving suit, affectionately known as Jim, who's body and boots are made in ZE41A [RZ5]. Jim has proved so successful that at the last count he had seven brothers operating in different parts of the world.

Some of the more recent developments in anti-corrosion protection are summarised below:

Anodic Treatments

The Dow 17 and HAE anodic treatments have been used for a number of years to produce hard erosion/abrasion resistant coatings. These anodic films are inherently porous, and do not provide maximum corrosion resistance without some form of sealing treatment. Although some authorities [23] require that the films be 'sealed' with inorganic salts such as silicates, or chromate/bifluoride mixture, the benefits of such treatments is questionable when overcoated with a paint system. A more waterproof seal may be obtained by the use of organic resins.

It has been shown [24] that anodic films can be successfully impregnated using various solvent free and solvent containing resins using simple dip or vacuum techniques. The best results were obtained by dip impregnation in a solution of an epoxy resin [Araldite 985E]. This is a convenient system to use since the two component mix has a long pot life and the curing schedule is rapid and simple. However for optimum results the anodic film should not be less than 25 μm [0.001 inch] thick, e.g. Type II, Class D.U.S. MIL-M-45202B. Such films are satisfactorily resin impregnated without any measurable build up. The very thin 2.5-5 μm greenish buff Dow 17 film cannot be resin impregnated. Furthermore the adhesion of resins to the thin film is not as good as that to a chromate conversion coating such as chrome manganese.

The benefits offered by a resin impregnation of HAE and Dow 17 films is that the impregnated film is harder, more erosion resistant and less prone to creepage corrosion from damaged areas. Furthermore the adhesion and overall corrosion resistance of the film is improved considerably.

The Dow 17 process itself has very good throwing power and has recently been shown to be capable of coating the bores of integral pipe cores. Table 5 shows the extent to which a full Dow 17 coating can be achieved in blind bores. Figure 17 shows a section cut from a casting in which a bore approximately 750 mm long and 8 mm diameter has been fully Dow 17 treated and impregnated with epoxy resin, although inlets or outlets for electrolyte were up to 300 mm apart. The ability to protect bores in this way could be important in extending the use of magnesium alloys in, for example, high temperature gearboxes where ester lubricants can cause some attack on magnesium or aluminium based alloys.

Other anodising treatments such as MGZ [25] and Magnadize [26] have been developed more recently. The former is claimed to give faster build up than Dow 17 or HAE, and to give better protection without sealing than inorganic 'sealed' Dow 17 or HAE. Magnadize coatings involve an anodising step followed by 'infusion' of a range of materials, including PTFE and MoS_2 for special applications. Neither coating has yet had significant application in aerospace applications and their performance in relation to the established HAE or Dow 17 is not known.

High Temperature Coatings

The majority of conventional protective schemes used for magnesium have maximum operational temperatures of approximately 200°C. This temperature is low when compared with the high temperature capabilities of some of the magnesium-zirconium alloys.

A number of commercially available high temperature resistant coatings have been examined [27]. Of these an aluminium silicone coating [Goodlass Wall 172/84] proved satisfactory at 250°C and maintained satisfactory corrosion protection for limited [up to 100 hours] exposure at 300°C when applied over a chrome manganese pretreatment. Application to a 25 μm Dow 17 film in place of the chrome manganese pretreatments or the use of strontium chromate pigmented resin as primer increased the permissible exposure at 300°C by a factor of ten.

Unfortunately, straight aluminium-silicone coatings have not been widely used in the aerospace industry because of doubts about their resistance to hydraulic fluids, and incompatibility with some other commonly used coating systems. Where elevated temperature protection is required, use is made of phenolic, epoxy-amino-silicone and polyimide based coatings, none of which are entirely satisfactory at temperatures above 200°C.

Although the chemical stability of polyimide films suggests that they should give excellent high temperature protection, this was found not to be so, major difficulties being in application of uniform coatings, and adhesion failure on chromate coating after temperature exposure. [27] Similar problems are still experienced today, and it is evident that further work is required to identify coating systems to give adequate protection to the maximum operating temperature of current and future magnesium alloys.

Galvanic Couples and Joints

The range of anti-corrosion treatments now available are capable of providing satisfactory protection on open surfaces over a range of operating environments provided:-

- [1] The correct treatment consistent with the operating environment is chosen.
- [2] That the treatment is properly applied.
- [3] The design of the component ensures freedom from sharp corners, moisture traps etc.

Furthermore the corrosion risk resulting from accidental damage of the protective film, particularly on open surfaces, has been over exaggerated since the magnesium alloys, unlike some of the aluminium alloys, are not susceptible to intergranular corrosion.

Major consideration must be given to eliminating galvanic corrosion at dissimilar metal contacts and moisture entrapment at joints and mating surfaces. It has long been recognised that these areas can be satisfactorily protected provided they are wet assembled using suitable polymeric jointing compounds. These methods are however messy and their success is to some extent operator dependant.

One method developed to overcome these problems was the technique of micro encapsulating the sealants. [28] The sealant whether air curing or two pack system, is enclosed in thin walled spheres about 20-50 micron in diameter; the wall material is usually not more than 10% of the capsule content. These can be applied to the fasteners prior to insertion and closure, but some precoated fasteners can be obtained commercially. On closure of the fasteners [Figure 18] capsules rupture releasing the contents which provide a seal against moisture ingress, the sealant exuding round the head of the fastener providing a fillet which increases the electrical path between fastener and substrate and reduces the risk of galvanic corrosion. While the practical and technical benefits can be readily recognised we have not been able to find any evidence of their use in the aerospace industry.

Future Developments

It has frequently been argued that the anti-corrosion schemes available for magnesium are considerably more complicated and costly than those used on aluminium. While this is accepted it is equally clear that serious problems still exist with some widely used aluminium alloys e.g. stress corrosion, intergranular and exfoliation corrosion. Furthermore the cost of the present magnesium anti-corrosion treatments amortised over the working life of the component may be small in relation to benefits resulting from weight saving.

It may be useful to quote from the guidance document on Aircraft design against corrosion issued by IATA in 1979 [29].

"The primary reason for the corrosive problems on aircraft today, prior to five years in service, is not inadequate technology, but inadequate use and application of existing technology during the basic design and manufacturing stages".

While accepting that better factory installed protective schemes may incur some penalties in terms of cost, or added weight, the document suggests that the costs are generally small compared to those associated with corrosion repair activity and downtime during service.

Obviously the cost effectiveness of anti-corrosion treatments for magnesium needs to be improved, but equally important is to ensure that adequate protective treatments are efficiently and reliably applied to castings to match the projected environment.

Resin impregnation of anodic coatings such as Dow 17 or HAE can be regarded as a step in this direction since it offers:-

- [a] A considerable improvement in performance for a small increase in cost compared to other available treatments.
- [b] Although requiring anodising equipment, processing steps can be simplified and reduced compared to other currently used high grade protection schemes [e.g. DTD911C recommendations].
- [c] Coloured anodic coatings provide visual evidence of correct treatment, easing inspection and increasing reliability.
- [d] Benefits such as better build up on corners, improved damage resistance etc. can be obtained.

Further work in these areas is required with the objectives of reducing the overall cost and simplifying the process consistent with maintaining, and where possible improving service performance. Particular consideration needs to be given to protection of close tolerance areas, e.g. machined surfaces/mating faces since these areas tend to receive least protection.

Environmental considerations may dictate the replacement of chromates in pretreatments and primers by less toxic materials. Work is already in progress to develop suitable alternatives.

Another area where work is required relates to protection at dissimilar metal contacts and joints. Further development of microencapsulation of sealants, or some other means of isolating galvanic contacts, to a stage where they are accepted as standard production procedures by the aerospace industry would be of significant benefit not only for magnesium components, but for a number of other metals as well.

The possibility of novel anti-corrosion treatments being developed based on modern techniques such as ion plating, ion implantation and surface micro-alloying cannot be ruled out. However even if successful such techniques would probably be restricted to limited, specialised applications.

The question of improving the inherent corrosion resistance of magnesium by alloying additions which have a general beneficial effect or merely modify the surface oxide to make it less chemically reactive, i.e. stainless magnesium, has often been the cause of speculation. On present knowledge the possibility of any significant achievements in developing an alloy which would remain stainless even under galvanic corrosion conditions must be remote in the foreseeable future.

REFERENCES

- 1] R.J.M. Payne, N. Bailey. J. Inst. Metals Vol. 88 Pt. 10 1959/60 pp 417-427.
- 2] W. Unsworth, J.F. King, S.L. Bradshaw. Light Metals Vol. 1 1977 pp 529-543.
- 3] British Patent 1,463,610.
- 4] K.G. Gradwell PhD Thesis, University of Manchester 1972.
"Precipitation in a High Strength Magnesium Casting Alloy".
- 5] British Patent 1,463,608.
- 6] P.A. Fisher, P.C. Meredith, P.E. Thomas. Foundry August 1967 pp 68-72.
- 7] British Patent 1,465,687.
- 8] P.H.R.B. Lemon. British Foundryman. Special Supplement, June 1979 pp 15-27.
- 9] J.A. Hufton, K.W. Cowlam. Foundry Trade Journal, February 2nd 1978 pp 193-207.
- 10] R.L. Naro, J.F. Hart. Trans AFS 1980 Vol. 55 pp 57-66.
- 11] W. Ellinghaus. Giesserei 68 [1981] Nr 6 16th March pp 135-143.
- 12] I. Strachan, H.J. Proffitt. Modern Casting December 1981 pp 42-43.
- 13] A.J. Clegg. Foundry Trade Journal March 31st 1977 pp 662-667.
- 14] P. Schneider. Foundry Trade Journal 1974-136 pp 723-733.
- 15] F.H. Hoult, C. Moore. Seminar on Engineering Equipment for Foundries.
Geneva 28th November-2nd December, 1977.
- 16] J.W. Fruehling, J.D. Hanawalt. Trans AFS 1969 Vol. 77 p 59.
- 17] S.L. Couling et. al Proc. International Magnesium Association, Oslo, 1979.
- 18] H.J. Proffitt. Proc. International Magnesium Association Meeting, Houston, 1981
pp 53-58.
- 19] P.S.A. Wilkins. Foundry Trade Journal, October 8th 1981.
- 20] G. Richards. British Foundryman Vol. 72 Pt. 7, July 1979 pp 162-167.
- 21] R.M. Conaway. Precision Met. April 1977 35[4] pp 39-40.
- 22] K.G. Adamson, W. Unsworth. Proc. Ann. Technical Conference. Institute Metal
Finishing, Llandudno May 13-17 1980 pp 48-57.
- 23] U.S. Military Specification MIL-M-45202.
- 24] J.F. King, K.G. Adamson, W. Unsworth. Ministry of Defence D. Mat Report 193
February 1973. "Impregnation of Anodic Films for the Protection of Magnesium Alloys".
- 25] G.R. Kotler, D.L. Hawke and E.N. Agua. Proc. International Magnesium Association,
Montreal, May 1976, pp 45-48.
- 26] C.P. Covino. Light Metal Age. February 1979 pp 32-33.
- 27] K.G. Adamson, J.F. King, W. Unsworth. Ministry of Defence D. Mat Report 196,
July 1973. "Evaluation of High Temperature Resistant Coatings for Protection of
Magnesium Alloys".
- 28] Engineering January 1974 pp 31.
- 29] IATA DOC. GEN/2637. February 1979.
Guidance Material on Design and Maintenance against Corrosion of Aircraft Structures.

ACKNOWLEDGEMENTS

Acknowledgement is gratefully made to the individuals and organisations who have supplied information and visual material for this paper, and to the Directors of Magnesium Elektron Limited for permission to present this paper.

STRESS IN N/mm ² FOR 0.2% CREEP STRAIN AT		QH21A-T6	QE22A-T6
200°C	100 hours	97	85
	1000 hours	60	55
250°C	100 hours	38	32
	1000 hours	21	16

TABLE 1: CREEP PROPERTIES OF QH21A, QE22A

ALLOY DESIGNATION	NOMINAL ANALYSIS					R.T. MECH. PROPS. [N/mm ²]			250°C MECH. PROPS. [N/mm ²]			
	Ag	RE	Th	Y	Zr	Y.S.	U.T.S.	E. %	Y.S.	U.T.S.	E. %	σ^*
QE22	2.5	2.0	-	-	0.6	205	266	4	122	160	30	32
QH21	2.5	1.0	1.0	-	0.6	210	270	4	167	185	16	39
QE22 + 4 Y	2.5	2.0	-	4.0	0.6	227	299	2	170	252	7	66
QE22 + 7 Y	2.5	2.0	-	7.0	0.6	236	326	2	189	291	5	ND

* indicates stress required to produce 0.2% creep strain in 100 hours.

N.D. - Not Determined.

TABLE 2: EFFECT OF YTTRIUM ADDITIONS TO QE22 ON MECHANICAL PROPERTIES

TEMP °C	PROPEETY	UNITS	QE22A	EQ21A																							
20	TENSILE	YS/UTS [N/mm ²] Elong. [%]	205-266-4	195-261-4																							
	FATIGUE LIMIT [UNNOTCHED]	N/mm ² at 5 x 10 ⁷ cycles rotating bend	93	89																							
	FRACTURE TOUGHNESS	K _{IC} MNm ^{-3/2}	14	16.5																							
200	TENSILE	YS/UTS [N/mm ²] Elong. [%]	165-185-24	170-192-16																							
	CREEP	Stress [N/mm ²] to produce indicated creep strain in stated time	<table><tr><td></td><td>100</td><td>500</td><td>1000 hrs</td></tr><tr><td>0.2%</td><td>87</td><td>65</td><td>56</td></tr><tr><td>0.5%</td><td>104</td><td>82</td><td>73</td></tr></table>		100	500	1000 hrs	0.2%	87	65	56	0.5%	104	82	73	<table><tr><td></td><td>100</td><td>500</td><td>1000 hrs</td></tr><tr><td>0.2%</td><td>95</td><td>72</td><td>62</td></tr><tr><td>0.5%</td><td>116</td><td>88</td><td>76</td></tr></table>		100	500	1000 hrs	0.2%	95	72	62	0.5%	116	88
	100	500	1000 hrs																								
0.2%	87	65	56																								
0.5%	104	82	73																								
	100	500	1000 hrs																								
0.2%	95	72	62																								
0.5%	116	88	76																								
250	TENSILE	YS/UTS [N/mm ²] Elong. [%]	122-160-30	152-167-15																							
	CREEP	Stress [N/mm ²] to produce indicated creep strain in stated time	<table><tr><td></td><td>100</td><td>500</td><td>1000 hrs</td></tr><tr><td>0.2%</td><td>32</td><td>21</td><td>16</td></tr><tr><td>0.5%</td><td>40</td><td>27</td><td>22</td></tr></table>		100	500	1000 hrs	0.2%	32	21	16	0.5%	40	27	22	<table><tr><td></td><td>100</td><td>500</td><td>1000 hrs</td></tr><tr><td>0.2%</td><td>36</td><td>24</td><td>19</td></tr><tr><td>0.5%</td><td>42</td><td>29</td><td>24</td></tr></table>		100	500	1000 hrs	0.2%	36	24	19	0.5%	42	29
	100	500	1000 hrs																								
0.2%	32	21	16																								
0.5%	40	27	22																								
	100	500	1000 hrs																								
0.2%	36	24	19																								
0.5%	42	29	24																								

TABLE 3: MECHANICAL PROPERTY COMPARISON EQ21A v QE22A

TEMP °C	PROPERTY	UNITS	RZ5 [ZE41A]-T5	ZE63A-T6
20	TENSILE	YS/UTS [N/mm ²] Elong. [%]	154-229-5	173-289-10
	FATIGUE LIMIT [UNNOTCHED] [U-NOTCH]	N/mm ² at 5 x 10 ⁷ cycles rotating bend " " " " [SCF2]	95 80	117 71
	FRACTURE TOUGHNESS	K _{IC} MNm ^{-3/2}	15.5	21
100	TENSILE	YS/UTS [N/mm ²] Elong. [%]	138-201-7	135-235-30
	CREEP	Stress [N/mm ²] to produce indicated creep strain in stated time	100 500 1000 hrs	100 500 1000 hrs
			0.2% 111 106 103	0.2% 64 49 42
			0.5% 117 116.5 116	0.5% 103 82 79
150	TENSILE	YS/UTS [N/mm ²] Elong. [%]	129-173-15	111-187-34
	CREEP	Stress [N/mm ²] to produce indicated creep strain in stated time*	100 500 1000 hrs	100 500 1000 hrs
			0.2% 94 87 82	0.2% 47 39 36
			0.5% 101 95 90	0.5% 51 - -

* Note: Stress values for ZE63A are total strain, not creep data.

TABLE 4: COMPARISON OF MECHANICAL PROPERTIES OF ZE63A AND RZ5 [ZE41]

BORE		DOW 17		
DIA. [mm]	LENGTH [mm]	VARIATION OF FILM AT BOTTOM OF BORE FROM UNIFORM DARK GREEN EXTERNAL FILM	THICKNESS [mm]	
			EXTERNAL	INTERNAL
12.3	80	No difference	0.030	N.D.
	120	Medium green - slightly mottled	0.030	N.D.
9.3	80	Medium green - uniform	0.030	N.D.
	100	Medium green - slightly mottled	0.030	0.020
6.3	80	Medium green - uniform	0.030	N.D.
3.8	45	Uniform medium green - uniform	0.030	N.D.
	90	Light Green - mottled	0.040	N.D.
2.7	85	Light Green - mottled	0.040	0.016

N.D. - Not Determined

TABLE 5: PENETRATION OF DOW 17 TREATMENT IN BORED HOLES

FIGURES

- 1] R.T. tensile properties of commercially available Magnesium alloys v year of introduction.
- 2] Improvement of elevated temperature properties of Magnesium alloys v year of introduction.
- 3] Typical QE22 casting.
- 4] Graph of tensile properties of QH21 v QE22, ZE41, A356 v temperature.
- 5] Air intake bell - Canadair drone CL289 in QH21 alloy.
- 6] Precipitation modes in Mg-Ag-RE-Zr alloys.
- 7] Effect of Cu and Ag levels on tensile properties of Mg-Ag-RE-Zr alloy.
- 8] Tensile properties v temperature for EQ21, QE22, QH21.
- 9] Microstructure of Mg-Zn-RE-Zr alloy as-cast and after hydriding.
- 10] Thrust reverser casting for RB211 engine.
- 11] Potential properties of Magnesium based alloy v comparable Al alloys.
- 12] Projected improvements in elevated temperature properties of Magnesium alloys.
- 13] Gearbox casting for Westland WG34 helicopter.
- 14] Gearbox casting for F16 fighter aircraft.
- 15] Moulding and castings using the 'V'-process.
- 16] Deep sea diving suit made in Magnesium alloy.
- 17] Section of casting showing anodised and impregnated bore.
- 18] Applications of microencapsulated sealants.

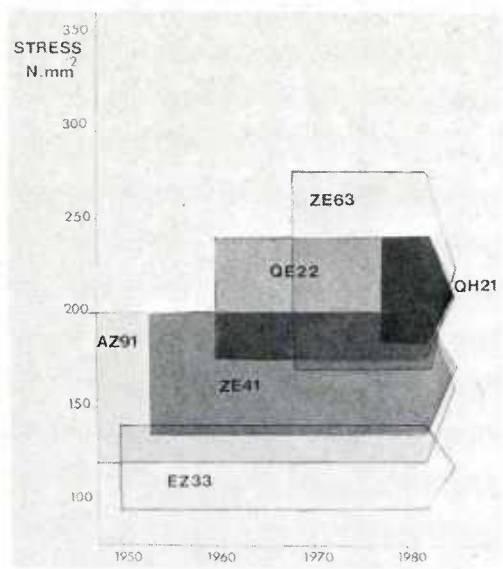


FIGURE 1

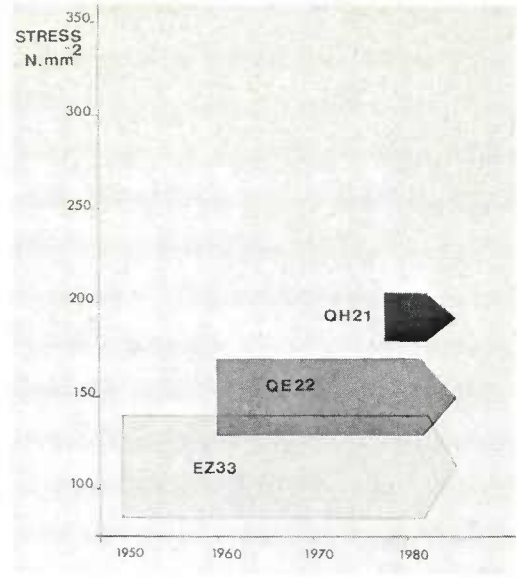


FIGURE 2

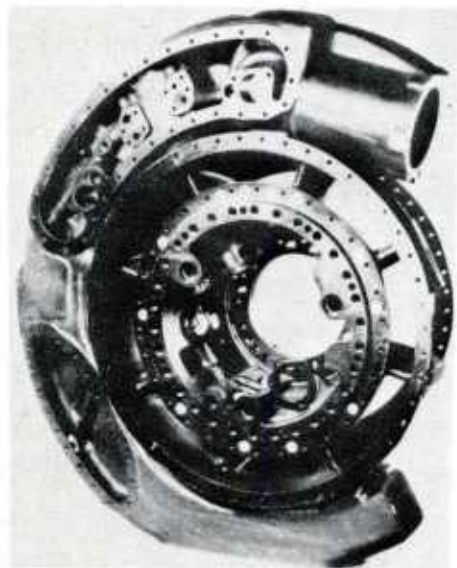


FIGURE 3

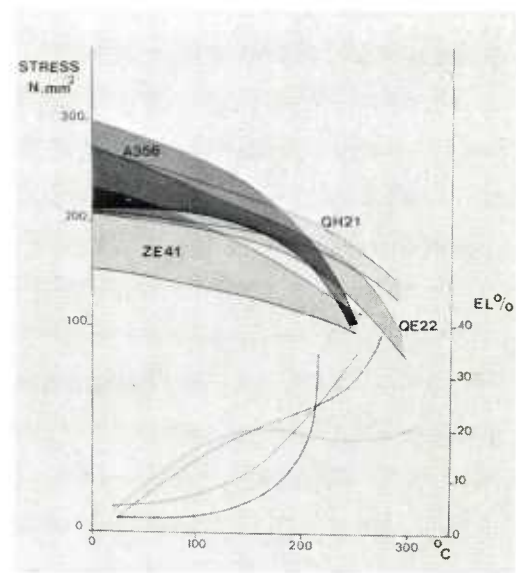


FIGURE 4

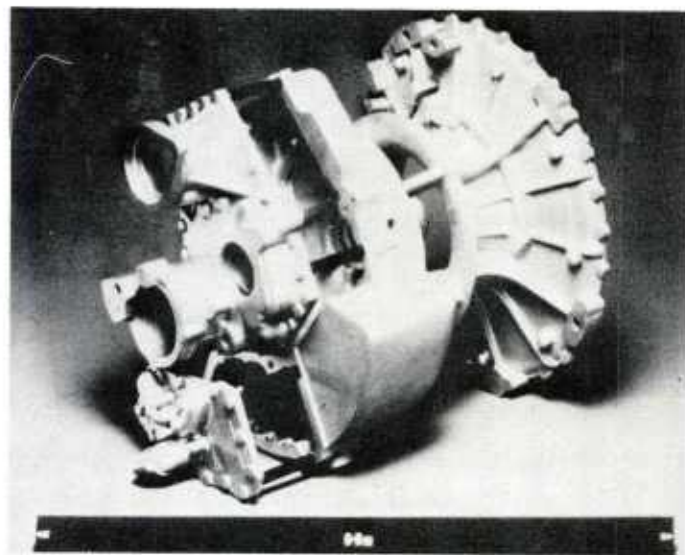


FIGURE 5

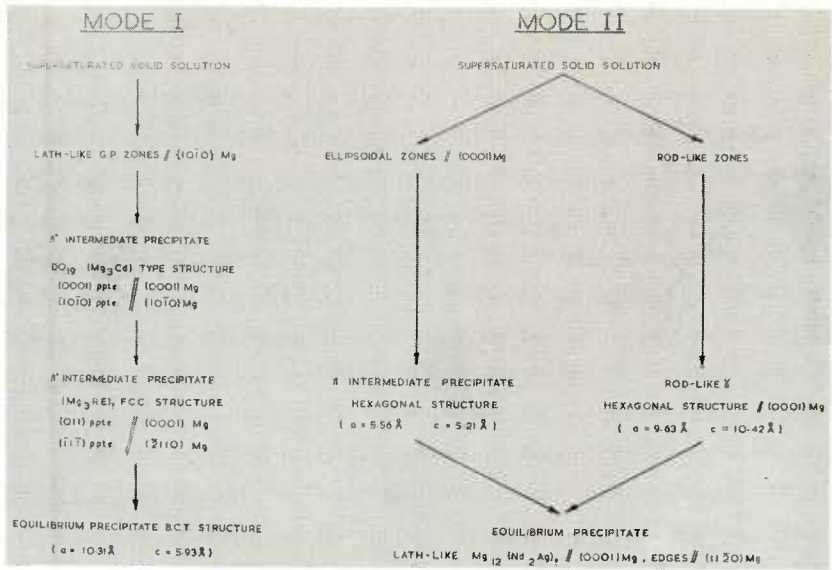


FIGURE 6

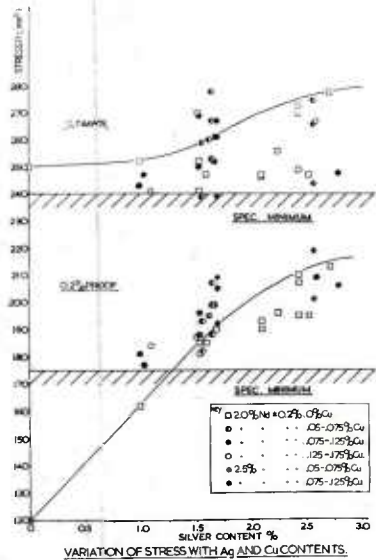


FIGURE 7

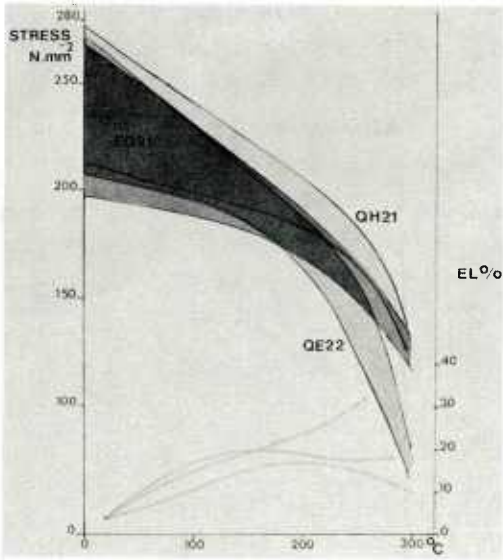


FIGURE 8

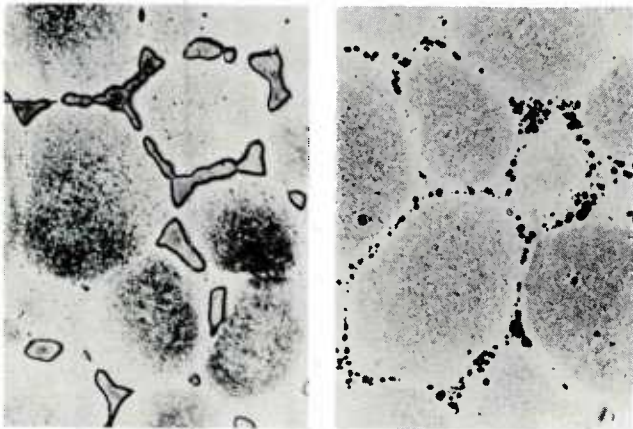


FIGURE 9

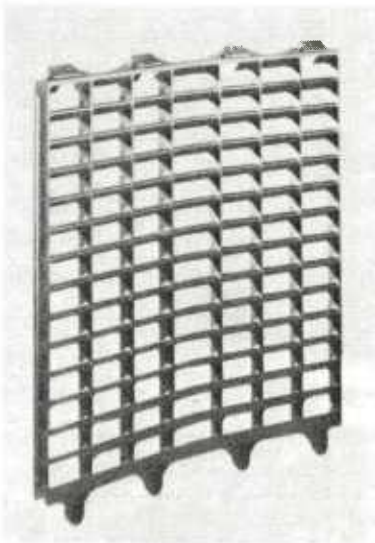


FIGURE 10

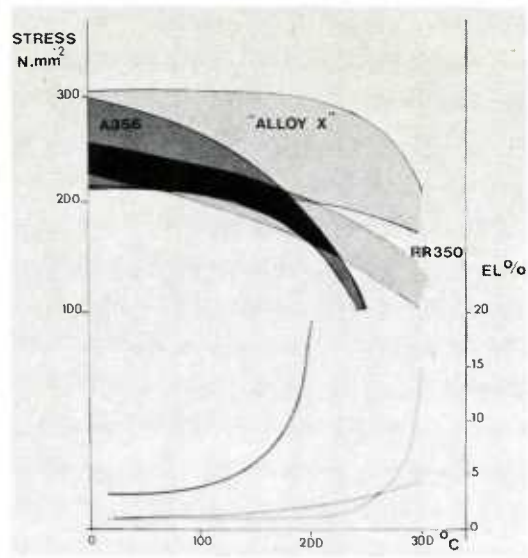


FIGURE 11

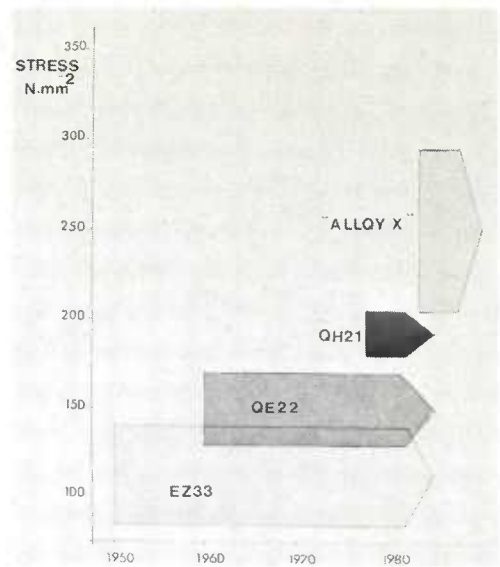


FIGURE 12

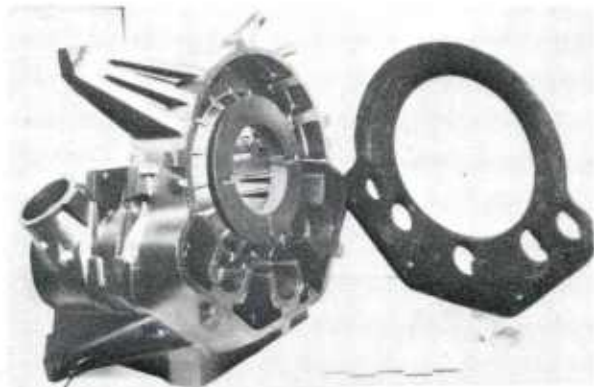


FIGURE 13

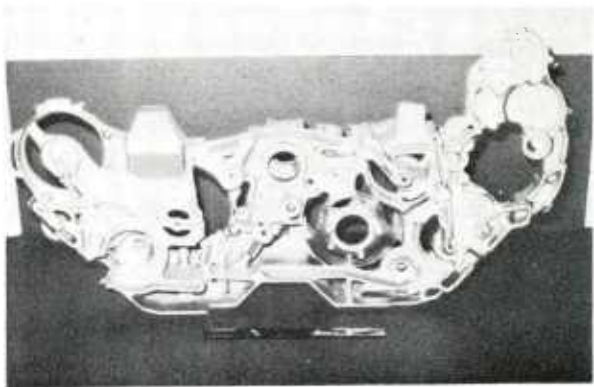


FIGURE 14

"V"-PROCESS - MOLDING AND CASTING PROCEDURE

A:	PATTERN MOUNTED ON VACUUM BOX PATTERN PLATE.
B:	SPECIAL PLASTIC FILM HEATED AND APPLIED TO PATTERN PLATE AND PATTERN.
C:	AIR AROUND PATTERN EVACUATED VIA PATTERN PLATE, ALLOWING FILM TO CONFORM TO PATTERN SHAPE.
D:	MOLDING BOX PLACED OVER FILM COVERED PATTERN, FILLED WITH DRY UNBONDED SAND.
E:	DOWNGATE AND RISERS FORMED IN LOOSE SAND, PLASTIC FILM PLATED OVER TOP OF MOLD, AND VACUUM APPLIED TO MOLDING BOX, EFFECTIVELY BINDING THE SAND IN THE BOX.
F:	VACUUM RELEASED FROM BELOW PATTERN, ALLOWING MOLD TO BE STRIPPED FROM PATTERN.
G:	COPE AND DRAG HALVES MADE SAME WAY, CLOSED BY CONVENTIONAL MEANS.
H:	VACUUM MAINTAINED ON MOLDING BOXES WHILE METAL IS Poured AND SOLIDIFIED.
I:	WHEN CASTING CDDL, VACUUM RELEASED, SAND BECOMES FREE FLOWING AND DRIPS OUT OF MOLD FOR REUSE.

FIGURE 15



FIGURE 16

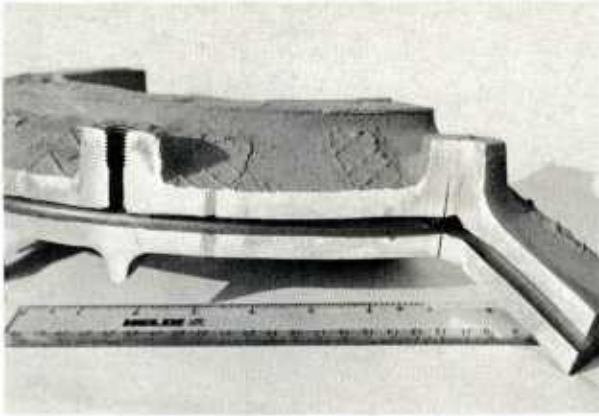


FIGURE 17

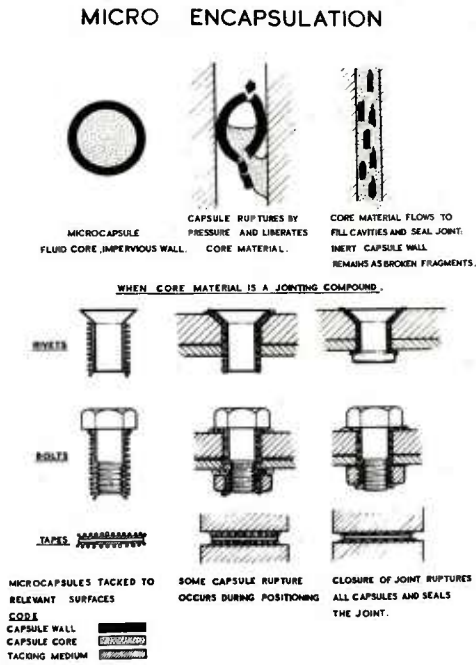


FIGURE 18

SESSION I

DISCUSSION SUMMARY

by

K.Verstraate

General Introduction

Mr John R.Lee, *Meeting Chairman*, opened the meeting by saying that the previous AGARD Specialists' Meeting was held in 1978, a conference that discussed fabrication technology in general. He drew attention to the theme 'Advanced Casting Technology', emphasising the necessity to bring together designers and materials and process engineers in this field for a full exchange of views so that areas of lack of knowledge that were limiting the use of castings could be highlighted.

Mr Lee then introduced the subjects of the different sessions, their chairman and recorders. He asked Dr Ir. J. van Eeghem to take the chair for Session I: 'Review of use and Developments of Castings'.

Summary of Discussions

- (1) The first paper of this session was that on 'Advanced Castings in the Design of Military Aircraft' by D.J.Duckworth and R.M.Shaw. The so-called 'hipping' became a major point of discussion in response to a statement and a question by Mr Lee concerning the possibilities and the necessity of cost reduction. The philosophy and experience of the authors was that an improved quality of casting could be achieved by foundries through a reduction in the variability of properties within the casting. Only in this way could a good assessment be made of the extent by which the life of castings was affected by casting defects and/or mis-handling in service.
- (2) After presentation of the second paper 'Advanced Casting – Today and Tomorrow' the speaker/author D.Mietrach explained extensively, at the request of Dr Ir. H.Nieswaag, what exactly was the meaning and significance of 'precial' casting. Apparently this term was quite new to the greater part of the audience, and had not been explained in the written and spoken text of the paper. Precial casting was defined as a method of casting production in which the dendrite arm spacing (DAS) was nearly identical to the volume of the whole casting. Mr R.Huet, the metallurgist/specialist of Fonderie Merlin-Gérin took the initiative to hold a 'tutorial' of about 10 minutes on the techniques of achieving this uniform occurrence of DAS.
- (3) Dr Ir. H.Nieswaag presented his knowledge and experience of 'Developments in Casting Technology – A Review' in the next paper. During the ensuing discussion, the level of porosity of the aluminium casting alloy G-AlCu3 received particular attention, with reference to Figure 12 of his written paper in which the relative feedabilities of Al-Cu- and Al-Si-alloys were compared. The audience were also very interested in the possibilities of computer-aided design (CAD) for other types of casting alloys, especially steel (see Figure 13) which belonged to the 'ferrous sector'.
- (4) P.H.Jackson reviewed 'Development in Aluminium Alloy Investment Castings' and stressed in both his paper and its discussion the following facts, expectations, wishes and necessities:
 - most official government material specifications were written many years ago, were therefore outdated, and no longer conformed to 'the state of the art';
 - most material specifications were in fact based on the original unique production method of the 'classic' sand casting; what was badly needed here by designers as well as foundrymen was a number of specifications with an up-to-date relationship between processes, materials and properties;
 - though normally material specifications referred only to static mechanical properties at room temperature, based on the testing of separately cast bars, designers needed data from which the behaviour of the casting as a whole could be predicted under *dynamic* conditions in high(er) temperatures, and/or in corrosive media, etc.
- (5) The authors W.Unsworth and J.F.King in the 5th and last paper of Session I paid considerable attention to the 'Developments and Trends in Magnesium Alloy Technology'. In the discussion the following 2 major requirements

(out of 5) were highlighted: *minimum weight* (= ability to cast into very thin sections: conclusion of Dr van Eeghem) and *good corrosion resistance* (= anodic treatments of and high temperature coating for magnesium alloy castings containing Ag and/or the rare earth metals Th and Zr as alloy elements).

Mr Lee stressed the need for the development of castings applicable to helicopter components. Apparently the vacuum moulding method ('V process') could not be used for the production of these types of castings, because corrosion problems might subsequently occur in service.

Dr van Eeghem then thanked all authors for their papers and contributions to the discussion, and closed Session I.

STRUCTURAL CONTROL IN SOLIDIFICATION PROCESSING

Prof. D. Apelian
Materials Engineering Department
Drexel University
Philadelphia, PA 19104, USA

SUMMARY

Control of heat flow, fluid flow and mass flow during solidification allows structural control of the cast product. The importance of the mushy zone width and local solidification time while in the mushy zone are discussed. Three recently developed processes - Rheocasting, Diffusion Solidification and the VADER melting process - are discussed in terms of solidification fundamentals, process advantages and applications.

1. INTRODUCTION

Control of the cast structure is the underlying object of solidification processing. It is through the careful control of heat, fluid and mass flow that one manipulates the resultant cast structure. In general, cast microstructures can be classified as shown in Figure 1. Microcrystalline and amorphous microstructures are obtained via the recently developed rapid solidification technologies (RST) (1,2). Of the conventional and refined microstructures, the vast majority of industrially produced castings have dendritic structures and the emphasis of this paper will be the control of dendritic solidification.

A schematic illustration of an engineering alloy freezing over a range of temperatures, solidifying in a columnar fashion in a static ingot mold is shown in Figure 2. This is a sketch of the basic solidification model; for illustration purposes, the dendrite arms are drawn out of proportion relative to the mold! A fully solid zone is present near the ingot surface, and a fully liquid zone exists at the center. Between these two zones exists a liquid/solid mushy zone. Control of this mushy zone is of paramount importance in controlling the resultant cast structure. Specifically, the width of this mushy zone and the time spent to solidify in this two phase region have pronounced effects on the resultant cast structure. These two parameters are further illustrated in Figure 3b which shows the progress of the liquidus and solidus isotherms (T_L and T_S - see Figure 3b) during unidirectional solidification...solidification progressing from the bottom to the top of the ingot. The vertical distance between the liquidus and solidus curves represents the region of the ingot over which solid and liquid phases coexist at a given time during solidification. This vertical distance is the width of the mushy zone; casting characteristics such as feeding, hot tearing and macrosegregation are strongly influenced by the width of this zone. The horizontal distance between the solidus and liquidus curves, shown in Figure 3b, is a measure of the local solidification time, t_f . The latter is inversely proportional to the average cooling rate at a given location during solidification and has a dominant effect on the scale of microsegregation throughout the structure.

Three recent developments - rheocasting, diffusion solidification (SD) and the VADER melting process - offer novel means of structural control during solidification. These processes are subsequently discussed.

2. RHEOCASTING/COMPOCASTING/THIXOFORGING

2.1 Background

Rheocasting was invented and developed at MIT by Flemings, Mehrabian and Spencer. The concept of rheocasting can be described by Figure 4 which shows that fractionally solidified melts (Sn-15% Pb model system) which are continuously and vigorously sheared during cooling will be fluid (3) at considerably high fraction solid values, i.e., $\approx 50\%f_S$. Simply, the shear stresses required for flow are reduced by about three orders of magnitude and the solid-liquid mixture behaves as a fluid slurry. The concept of rheocasting is shown in Figure 5. Here, alloy X is cooled to a temperature within the mushy zone such as T_2 ; during cooling the "melt" is agitated and stirred in addition to isothermal shearing at T_2 . The solid-liquid non-dendritic mixture consists of liquid phase of composition C_L of an amount f_L , and solid phase of composition C_S of an amount f_S , such that $f_S C_S + f_L C_L = X$.

The imposed vigorous agitation breaks up the dendritic structure and the result is an equiaxed non-dendritic structure as shown in Figures 6a and 6b. Thus, typical rheocast microstructures (Figure 6c) contain "nuclei" of the primary solid phase which are non-dendritic (due to the stirring action) surrounded by the liquid phase which solidifies with a dendritic structure.

Spencer's (3) work showed that partially solidified slurries exhibit a type of shear thinning - that is the apparent viscosity decreases with increasing shear rates. This is because the primary solid particles become ellipsoidal in shape and orient themselves in the shear direction with increasing shear rates. This particular characteristic is called thixotropy and thus the name thixocasting. In general, there are two types of fluids, Newtonian and non-Newtonian. Newtonian fluids obey a linear relationship between the shear stress in the fluid (τ) and the shear rate applied ($\dot{\gamma}$) where the coefficient is the apparent viscosity, μ - i.e., $\tau = \mu \dot{\gamma}$. Whereas in non-Newtonian fluids, this linear relationship is not observed. There are several distinct classes of non-Newtonian fluids such as Bingham flow, pseudo-plastic bodies and thixotropic fluids (4). Metals which are continuously cooled and sheared at a particular fraction solid are thixotropic in that they exhibit a reversible, isothermal, time dependent decrease in viscosity upon the application of a shearing strain (5).

2.2 Process Advantages

There are several inherent advantages to the rheocasting process. These are outlined below:

- (i) Reduced attack of the shot chamber and die because of lower casting temperatures and excellent fluidity of the slurry. This leads to improved die life.
- (ii) Reduced shrinkage and potential of cracks to develop since the slurry is already partially solidified prior to casting.
- (iii) The need for risers is reduced.
- (iv) Composite structures can successfully be made by adding second phase particles to the rheocast slurry. This process is termed compoasting.
- (v) Material handling systems are optimized. For example, instead of transferring molten metal into the die chamber one now inserts a rheocast slug which has been preheated to the isothermal shearing temperature (T_2 , Figure 5). This is called thixocasting because one takes advantage of the thixotropic nature of the system.
- (vi) The rheocast slug preheated to the isothermal shearing temperature can be forged in a die, and this process is called thixoforging. The analog here is squeeze casting, however in the latter the starting material is liquid metal instead of the partially solidified slurry.

2.3 Applications

Rheocasting has potential applications in batch type casting as well as continuous casting operations. The resultant rheocast microstructure has a reduced level of segregation. In addition, one can produce unique composite structures where the primary phase is hard and the liquid phase upon solidification is ductile. At present, we are evaluating the effect of rheocasting on the crack propagation behavior of IN-100 super alloy.

In the compocasting process, one takes advantage of the rheological behavior and structure of a partially solidified, and agitated slurry. The non-metallic second phase particles or fibers are added to and retained as a relatively homogeneous dispersion by the partially solid alloy slurry regardless of wetting. A schematic of the compocasting apparatus illustrating the fabrication steps (6) is shown in Figure 7. As the particles are added to the slurry, the high apparent viscosity of the slurry, and the presence of a high volume fraction of primary solid in the slurry prevents the non-metallic particles/fibers from floating, settling or agglomerating. With increasing residence times of the non-metallic particles interaction between the particles and the slurry matrix promotes bonding. Levi and Mehrabian (6) have shown that continuous agitation in the liquid portion of the slurry allows for bond formation to take place even though the melt does not wet the added particles. Table I lists the various aluminum systems which have been compocast and evaluated (7,8).

TABLE I. COMPOCAST ALUMINUM ALLOY SYSTEMS

Matrix Alloy	addition	Second Phase Added	
		size, μm	wt pct charged, %
Al-4 Cu	Al_2O_3	46	7
Al-4 Cu-0.75 Mg	Al_2O_3	3	15
Al-4 Cu-0.75 Mg	SiC	5;20;46	10;15;15
Al-4 Cu-0.75 Mg	MgO	40	10
Al-4 Cu-0.75 Mg	glass beads	100	30
Al-4 Cu-0.75 Mg	slag	<150	20-30
Al-4 Cu-0.75 Mg	Si_3N_4	46	10
Al-4 Cu-0.75 Mg	TiC	46	15

Experimental results show (6) that during compocasting strengthening occurs when a strong particle matrix bond is formed. This allows support of the local strain field which develops under load. In the case of Al-Mg alloys, bonding was achieved through formation of a MgAl_2O_4 (spinel) layer by reaction between the fiber and the Mg in the liquid Al. The Al-Cu-Mg alloys were observed to have MgAl_2O_4 , $\alpha\text{-Al}_2\text{O}_3$ and possibly CuAl_2O_4 coexisting in the interaction zone. It has been postulated that a compound of the aluminate type is formed on the fiber surface and thus provides the necessary bond with the surrounding matrix (6). Examination of composite fracture surfaces show that failure does not occur at the interface but rather by plastic flow at the matrix around the fibers. Composite strength is then dependent on particle-matrix bonding and is independent of the type of particles added. In contrast, ductility (as measured by reduction in area) is shown to be a strong function of the volume fraction of the particles added and seems to be independent of particle size (9).

Wear properties of the compocast aluminum alloys have been extensively evaluated (7,9). Aluminum matrices containing high weight percent of hard non-metals exhibit excellent friction and wear properties when tested against an AISI 52100 ball bearing on a pin-on-disk machine. For example, composites of 2024 containing 20 w/o of 142 μm size Al_2O_3 particles showed a weight loss of ~ 2 orders of magnitude less than the matrix alloy prepared and tested under identical conditions. Moreover, aluminum alloys containing SiC

particles had even better wear resistance due to the hardness of the SiC particles. Hosking has shown that a change in the wear mechanism takes place; the wear mechanism in the matrix aluminum alloys is adhesive in nature whereas in the composites (compcast) an abrasive wear mechanism is observed (9).

When the rheocast slurry is reheated to the two phase region, it can then be forged or thixoforged. The application of pressure ($8-9 \times 10^7$ Pa) results in significant refinement of the microstructure in addition to closure of existing porosity in the rheocast slug. The one drawback is that if the thixoforging is improperly done, oxide from the ingot or slug surface can be entrapped in the forgings reducing the overall measured ductility. Table II lists the mechanical properties of thixoforged and squeeze cast commercial 2024 Al alloy heat treated to T-6 condition (10). It is interesting to note that the mechanical properties of the squeeze cast and thixoforged 2024 alloy are comparable to that of the wrought material.

TABLE II. MECHANICAL PROPERTIES OF THIXOFORGED AND SQUEEZE CAST COMMERCIAL 2024 ALUMINUM ALLOY (Heat Treated to T-6 Condition)

	Ultimate Tensile Strength, Kg/mm ²	0.2% Offset Yield Strength Kg/mm ²	% Elongation
Thixoforged	46.4 (~65.9 Ksi)	34.7 (~49.3 Ksi)	11.2
Squeeze Cast	48.3 (~68.6 Ksi)	36.2 (~51.4 Ksi)	13.4
Wrought Alloy (from Ref. (11))	48.5 (~69 Ksi)	~40 (57 Ksi)	10

3. DIFFUSION SOLIDIFICATION

3.1 Background

In diffusion solidification casting of steel, high-carbon liquid iron is brought into contact with a low-carbon solid iron isothermally, and the liquid solidifies by rejecting carbon to the surrounding solid iron. The mold is first filled with uniform-sized low-carbon steel shot, then heated and subsequently quickly infiltrated with liquid cast iron (2-4% C) under moderate pressure.

Consider the liquid and solid region of the phase diagram shown in Figure 5, which compares conventional casting, rheocasting and casting by diffusion solidification (SD). In the rheocasting process, solidification occurs by manipulation of temperature on an isocomposition line, whereas the diffusion solidification process is carried out isothermally by manipulation of composition, i.e., by solute rejection from the liquid phase. The general process steps for diffusion solidification are:

- The liquid is initially held at its liquidus temperature, which is the process temperature. In Figure 5, this corresponds to an f_L' amount of liquid of composition C_L' ... at T_1 .
- The solid particles (f_S' amount of composition C_S') are heated and held at the same process temperature, T_1 .
- The liquid is rapidly infiltrated into the solid particles, filling the mold before significant SD takes place and thus blocking further infiltration.

In practice, a refractory mold is filled with low-solute shot, a barrier of coarse refractory particles is placed on top, and then the melt charge is added as shown in Figure 8. The particle valve (12) between shot and melt prevents premature infiltration between the two until sufficient pressure is exerted above the melt to break the liquid's surface tension; the particle valve and shot are then infiltrated and SD proceeds. The necessary sequence of operations for the entire process (using a wax pattern/investment mold logic) is:

- Make the core.
- Place the core in an injection molding machine and form the wax pattern around it.
- Invest the pattern and core with a refractory slurry to make the mold.
- Dewax and bond the mold.
- Emplace the low solute shot, particle valve, and the high solute melt charge.
- Heat the total assembly to the casting temperature in vacuum.
- Pressurize the casting vessel to infiltrate the casting.
- Homogenize.
- Cool to room temperature and remove mold, core and particle valve.

The general casting logics which utilize the SD concept and can thus lend themselves to rapid cycle casting of metallic components are the permanent mold logic and the investment mold logic. These are shown in Figures 9 and 10, respectively.

3.2 Process Advantages

In conventional casting solidification occurs via heat transport over a temperature range, and the final structure is dendritic. In SD casting, solidification occurs via mass transport, the process is isothermal and the liquid-solid front is planar. These fundamental differences result in totally unique microstructures; the source of conventional macrosegregation is no longer the interdendritic fluid and solute mass flow dictates the resultant structure.

Advantages of the SD process are that casting takes place at temperatures reduced by 150–200°C and the process can be carried out isothermally to cause 100% solidification and to obtain complete homogenization of the resulting casting, all without rejecting any heat to the mold.

Solidification time in conventional casting processes depends on casting dimensions and mold characteristics. In SD casting, the solidification time is essentially independent of casting dimensions and is controlled by the infiltrable shot size. Furthermore, the mold characteristics do not control the solidification time in SD casting. In brief, solidification time and mold-filling time in the SD process are shorter than in conventional casting.

In conventional casting, t_s , time for solidification, is proportional to ℓ^2 , where ℓ is the dimensional term, length (Chvorinov's Rule). In SD casting, on the other hand, t_{sd} , time for solidification, is proportional to $(\ell^6/5/p^2)^{1/5}$, where P is the infiltration pressure available (13).

The weaker dependence of solidification time on workpiece dimension can be advantageous when considering the SD process for automation. Cycle times comparable to die casting ought to be achievable with the SD process. There is much less of a problem of thermal shock to the "die" (mold), and the microstructure of the resultant casting is homogeneous with respect to carbon because of its rapid diffusion over these short distances.

In SD, the preheated solid particles occupy approximately 5/8 of the final volume of the casting prior to infiltration of the liquid phase; therefore, solidification shrinkage and heat of solidification to be accommodated are at least proportionately reduced. Although in conventional castings a riser is needed and the solidification shrinkage is concentrated in the last liquid to freeze, no riser is needed in SD and the solidification shrinkage is isolated, uniformly distributed, and smaller in amount. If the workpiece will subsequently be worked or hot isostatically pressed, or if it must be free of connected porosity, this better control of the shape and distribution of casting porosity is an advantage.

Diffusion solidification as a casting technique produces unique properties and microstructures without resort to extreme pressures, and it may therefore compete favorably with hot isostatic pressing as a way of consolidating atomized metal powder (shot). The atomized shot has the benefits of rapid solidification and of the controlled melting and solidification environments; the infiltrating liquid has the benefits of vacuum melting and of filtration by the particle valve. The distribution and magnitude of shrinkage cavitation are controlled by the particle-size distribution of the shot and by the content of inclusions (such as aluminum oxide or silicates, in steel). Steel castings have been made by SD with more than 99% of theoretical density, for example (14,15).

Since solidification proceeds simultaneously throughout the casting during SD, hot tearing and macrosegregation of impurities and alloying elements are decreased. The microstructure of diffusion-solidified steels is more like that of wrought steels than of cast steels – there is no columnar zone (13,15). The grain size and grain orientation of the diffusionally solidified casting is instead controlled by the grains in the initially solid portion of the charge.

It is possible to produce completely homogeneous microstructures free of microsegregation by SD since the initial shot particle size is chosen so as to minimize the freezing time by minimizing the diffusion distance consistent with successful forced infiltration under a reasonable external pressure. Most alloy systems to which SD can be applied are nearly completely homogenized soon after the completion of freezing. Design nomograms giving the infiltration depth and time at casting temperature to achieve a level of casting macrosegregation and homogeneity have been published (14,15,16).

There are other advantages for SD castings. Pieces with small surface-to-volume ratios or those with drastic changes in cross section can easily be produced because the casting solidifies without rejecting heat to the surroundings. Also, the casting will be free of laps and cold shuts because the mold is heated prior to infiltration.

The major limitations of SD castings are: (i) the initial shot should be of high metallurgical quality for the assurance of good mechanical properties; (ii) in addition, not all alloy systems can be SD cast. There are certain criteria which must be met. One needs a distribution ratio (C_S/C_L) above 0.4 and preferably close to 1.0 so that solidification can occur isothermally or even adiabatically. Also, a steep solidus line is desirable so that the shot does not have to be heated too close to its melting point. Lastly, rapid diffusion of the SD alloying element in the solid compared to the self-diffusion of the principal element is needed so that the shot will not sinter excessively.

3.3 Applications

The iron-carbon system is ideal for SD because of the large interstitial solubility of carbon in face-centered-cubic austenite. Therefore, the particle size of the low-carbon shot and the low process temperature relative to the melting point of the shot combine to eliminate any chance of sintering shrinkage by bulk diffusion of the iron from the shot/shot grain boundaries to the free surfaces of the shot. Diffusion solidification casting and welding have been applied (15) to plain-carbon steels from 0.1 to over 1% C, Figure 11; current research at Drexel University continues to emphasize this system.

Excellent ductility of SD steel castings can be obtained if they are adequately infiltrated and if metallurgical bonding is achieved at the original solid-liquid interface. Surface and subsurface scales such as silicates are especially harmful and lead to dotted-line fractures along the particles outlining the original shot surface. All that is necessary to correct this fault is to leave sufficient carbon in the original shot to reduce the silicates during heating to the process temperature. On the other hand, if one is interested in making castings/structures having a specifically "designed" fracture path, then the SD process is one attractive alternative.

In conventional solidification, at moderate rates of heat rejection and growth rates the solubility differences between the liquid and the solid phases cause natural partitioning; and equilibrium solid/liquid interfaces result due to the slow movement of the interface relative to the thermal motion of the atoms. The partitioning of the solute element at the solid/liquid interface is a function of the growth velocity and also the energy of the solute atoms in the solid and liquid phases at the interface; consequently deviation from equilibrium at the interface occurs during thermal solidification at high growth velocities (17,18). In contrast, in the SD the initial solid and liquid compositions at the interface are not the equilibrium values dictated by the phase diagram because of the arbitrarily chosen compositions of the solid and liquid phases. Langford and Cunningham (15) have reported significant segregation of Si, Mn, Mo and V in a diffusionally solidified weld between two pieces of low carbon steel when the high carbon melt (infiltrant) contained these alloying elements. Non-equilibrium compositions at the solid/liquid interface are automatically attained in diffusion solidification because the pre-existing solid and the infiltrated liquid need not and usually do not have the same kind and amounts of alloying elements. We have found that some alloying elements (Ni, Co, Mn and Mo so far) can be made to segregate either positively or negatively during diffusion solidification by appropriately choosing the relative compositions of the low carbon austenite and the high carbon melt (19). For example, in a plain Fe-C-Mn-Si steel, the element manganese can have positive microsegregation (more Mn in the last metal to freeze), negative or even neutral microsegregation depending on whether the shot has low, high, or the same manganese concentration as the liquid. The sharp carbon differential at the solid-liquid interface and elastic interactions due to difference in size of Fe and X atoms act to defeat the mechanisms which usually lead to microsegregation (slow diffusion in the solid, rapid mixing in the liquid).

There are other potential SD candidate systems. Carbon SD casting offers a way of making homogeneous ultrahigh carbon tool steels up to the maximum solubility of carbon in austenite (2.2%), which is quite difficult to do conventionally without obtaining a graphitic or white cast iron microstructure (14).

Stainless steels have been made at Drexel University by SD casting; the solidification can be made to occur either by carbon diffusion (martensitic types) or by chromium or nickel (or both) diffusion; we are not yet sure which will give the best results and further work is needed.

Malleable castings with 1.5-2% C have been made at Drexel University by SD infiltrating Fe-0.1% C-2% Si shot with Fe-3.5% C - 2% Si liquid to make a homogeneous austenite, and then graphitizing the casting. The high silicon content speeds graphitization, and there are not graphite flakes in the original SD casting to cause internal stress risers. The process temperatures (both for casting and heat treating) are similar to those used for conventional malleable iron. The SD process offers a way of making larger nodular graphite castings than can be done conventionally by casting white iron, and the uniform and stable composition of the shot and liquid make SD casting a more reliable method than inoculation to obtain nodular graphite.

4. VADER CONTROLLED MELTING PROCESS

The VADER controlled melting process allows one to produce equiaxed dendritic superalloy castings having a fine grain size, and castings which subsequently can be forged. This is a tremendous achievement; in the past, to produce complex superalloy components which could subsequently be forged, one had to resort to powder metallurgy and sophisticated forging technologies. The VADER melting process was developed and patented by Special Metals Corporation of New Hartford, N.Y., 13413, USA (20).

A schematic of the VADER melting process is shown in Figure 12. Two consumable electrodes are arced against each other, and the molten metal is allowed to drip into a stationary, rotating or a withdrawal mold located under the electrode. The VADER melting process enables one to manufacture fine grained superalloy ingots which subsequently can be forged to gas turbine components. Comparable size VIM-VAR (vacuum induction melted and vacuum arc remelted, respectively) products have large grains or irregular shape and internal cracking is prevalent. The contrasting structural features between VIM-VAR and VADER controllably melted ingots are shown in Figure 13. The VADER melting process produces superalloy ingots having equiaxed grains (4-8 ASTM).

In the VAR process, droplets from the electrode are superheated to form a molten pool which solidifies in a columnar dendritic mode. Rejection of phases along solidification fronts and other mechanisms may generate areas of macrosegregation. Vapor which deposits on the mold wall can fall into the molten pool and thus cause surface or internal defects in the ingot. In addition large amounts of energy are required to offset the losses to the water cooled mold. In contrast, in the VADER melting process droplets form as a result of arc melting between the two horizontal electrodes. The droplets fall with no superheat. Drop temperature measurements indicate that they are slightly below the liquidus temperature of the alloy (21). Drop measurements on IN-718 alloy were found to be 20°F below the liquidus as measured by DTA techniques. Figure 14 schematically illustrates the contrasting features between the VAR process and the VADER melting process. As pointed out earlier, the control of the width of the mushy zone and the local solidification time within this zone have pronounced effects on the resultant cast structure.

There are additional advantages to the VADER melting process. About 40% less energy is required in the VADER melting process for a comparable melt rate with the VAR process. Moreover, melt rates of at least 3 times that of VAR are feasible. Another subtle feature of the VADER melting process is that it offers flexibility in manufacturing in terms of electrode preparation and conditioning.

Tensile properties (at room temperature and 650°C) and stress-rupture property data of VADER U718 alloy specimens are shown in Figure 15. The observed increase in reduction in area and elongation are impressive.

REFERENCES

1. R. Mehrabian, B.H. Kear, M. Cohen: "Rapid Solidification Processing - Principles and Technologies", Proceedings of the Int. Conf. on Rapid Solidification Processing, November, 1977; Baton Rouge, Claiborne's Publishing Division.
2. R. Mehrabian, B.H. Kear, M. Cohen: "Rapid Solidification Processing - Principles and Technologies II", Proceedings of the Second Int. Conf. on Rapid Solidification Processing, March 1980; Baton Rouge, Claiborne's Publishing Division.
3. D.B. Spencer, R. Mehrabian, M.C. Flemings: Met. Trans. 1972, Vol. 3, pp. 1925-32.
4. G. Geiger, D. Poirier: Transport Phenomena in Metallurgy, Addison Wesley, Reading, Mass.
5. P.A. Joly, R. Mehrabian: Journal of Materials Science, 11 (1976), pp. 1393-1418.
6. C.G. Levi, G.J. Abbaschian, R. Mehrabian: Met. Trans., 1978, Vol. 9A, pp. 697-711.
7. A. Sato, R. Mehrabian: Met. Trans., 1976, Vol. 7B, pp. 443-451.
8. D. Boldy, B.S. Thesis, Drexel University, June 1976.
9. F.M. Hosking: M.S. Thesis, University of Illinois, June 1980.
10. R. Mehrabian et al.: "Structure and Deformation Characteristics of Rheocast Metals", AMMRC report TR 79-2 (Interim report DAAG46-76-C-0046), 1979.
11. Aluminum, Vol. I, ASM, Metals Park, Ohio.
12. M. Paliwal, D. Apelian, G. Langford: Met. Trans., 1980, Vol. 11B, pp. 39-50.
13. D. Apelian, G. Langford: Drexel University, unpublished work.
14. G. Langford, D. Apelian: Journal of Metals, Vol. 32, September 1980, pp. 28-33.
15. G. Langford, R.E. Cunningham: Met. Trans., 1978, Vol. 9B, pp. 5-19.
16. C. Lall, D. Apelian, G. Langford: "Aluminum-Lithium Castings Made by Diffusion Solidification", 109th AIME Annual Meeting, Las Vegas, Nevada, February 1980.
17. J.C. Baker: Interfacial Partitioning During Solidification, Ph.D. Thesis, MIT, 1970, Chapter V.
18. R.W. Chan, S.R. Coriell and W.J. Boettinger: "Rapid Solidification", in Proceedings of Laser Electron Beam Processing of Materials, W.W. White, P.S. Pearcy, eds., Academic Press, 1980.
19. M. Paliwal, D. Apelian, G. Langford: "Microsegregation of Ternary Alloying Elements During Diffusional Solidification of Iron-Carbon Based Alloys"; submitted to Met. Trans. (AIME).
20. F.H. Soykan, J.S. Huntington: U.S. Patent 4,261,412, April 14, 1981.
21. J.W. Pridgeon, F.N. Darmara, J.S. Huntington, W.H. Sutton: "Principles and Practices of Vacuum Induction Melting and Vacuum Arc Remelting", in Metallurgical Treatises, J.K. Tien and J.F. Elliott: editors, November 1981.

ACKNOWLEDGMENTS

The author is grateful to colleague and past student, Dr. G. Langford and Dr. M. Paliwal for their collaborative work on the SD process. The assistance of Dr. S. Reichman, W. Sutton, B. Boesch and C. Adaszczik of Special Metals Corp., New Hartford, N.Y., 13413 in preparation of the VADER melting process is much appreciated.

CONVENTIONAL
AND REFINED
MICROSTRUCTURES



* PLANAR
* CELLULAR
* DENDRITIC

NOVEL
MICROSTRUCTURES



* MICROCRYSTALLINE
* AMORPHOUS

Figure 1: Classification of Solidification Structures.

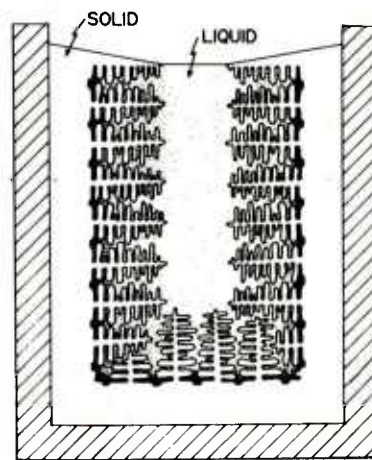
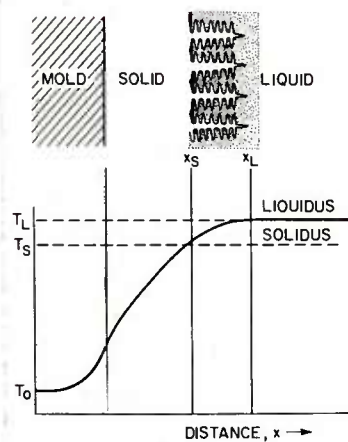
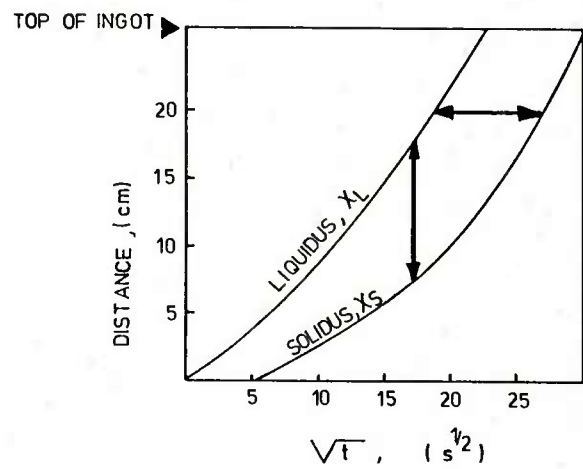


Figure 2: Dendritic solidification model.



(a)



(b)

Figure 3: (a) Temperature profile across the solidifying ingot; (b) Progress of liquidus and solidus isotherms during unidirectional solidification.

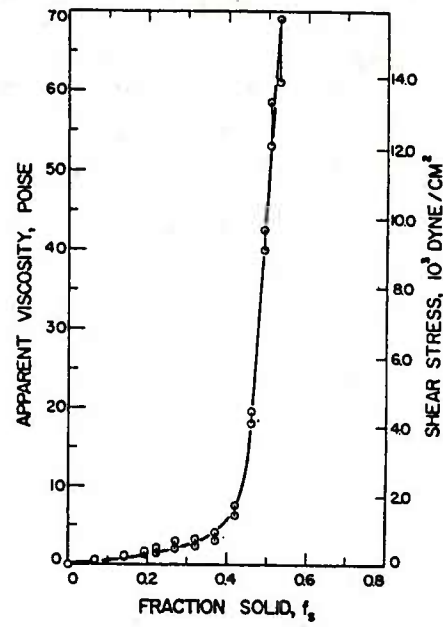


Figure 4: Apparent viscosity versus fraction solid curve for Sn-15 w/o Pb alloy at a given shear rate (3).

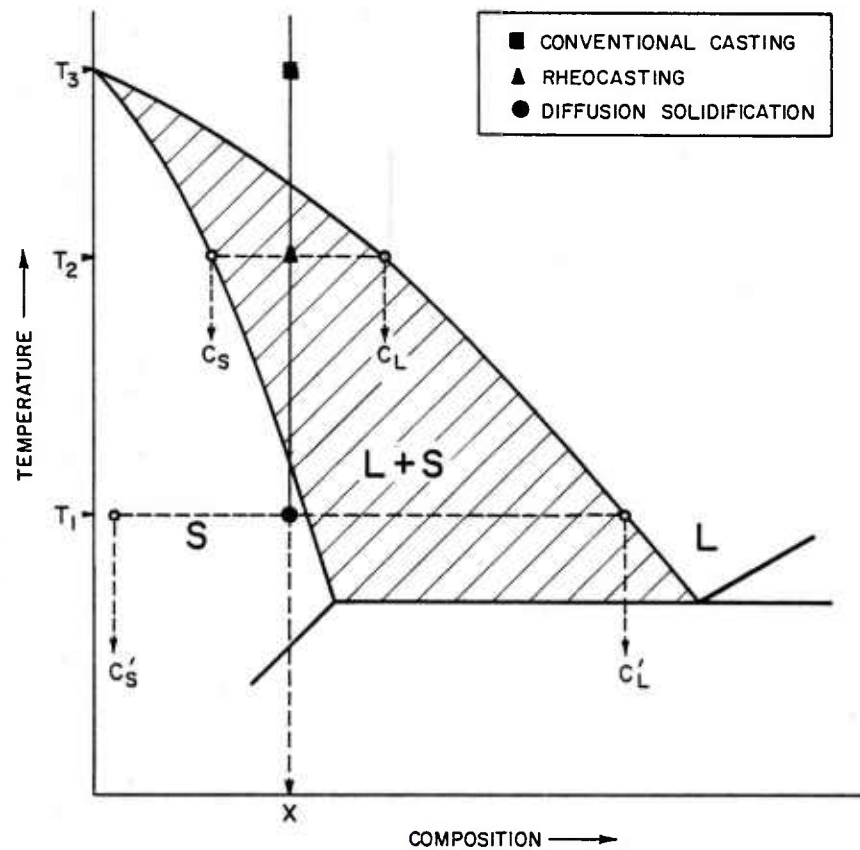


Figure 5: Phase diagram showing conventional casting at T_3 , rheocasting at T_2 and diffusion solidification at T_1 .

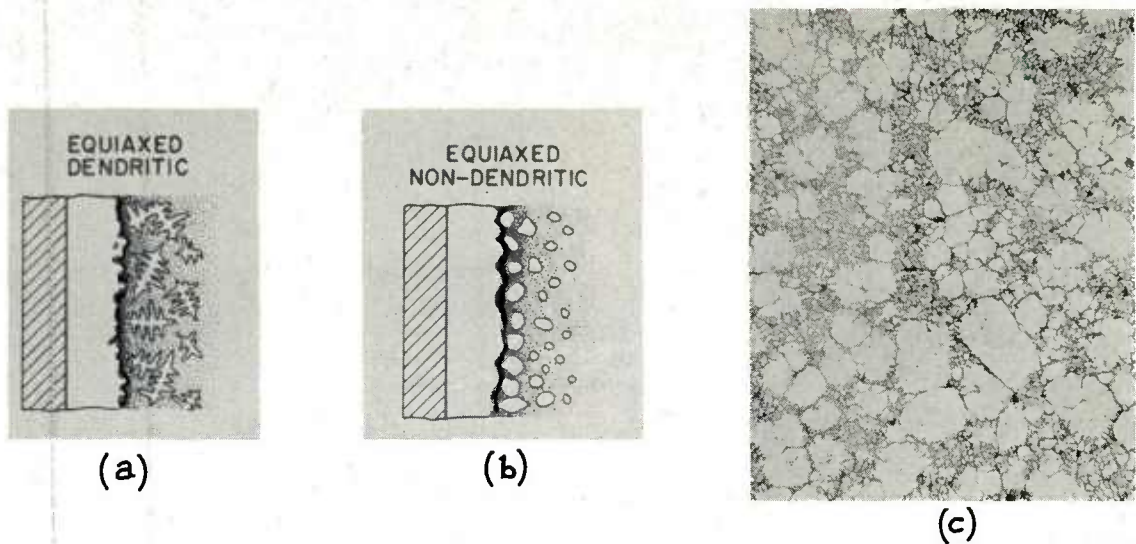


Figure 6: (a) Schematic model of an equiaxed dendritic structure; (b) Schematic model of an equiaxed non-dendritic structure; (c) Typical structure of rheocast and water quenched commercial 2024 Al alloy, 70X.

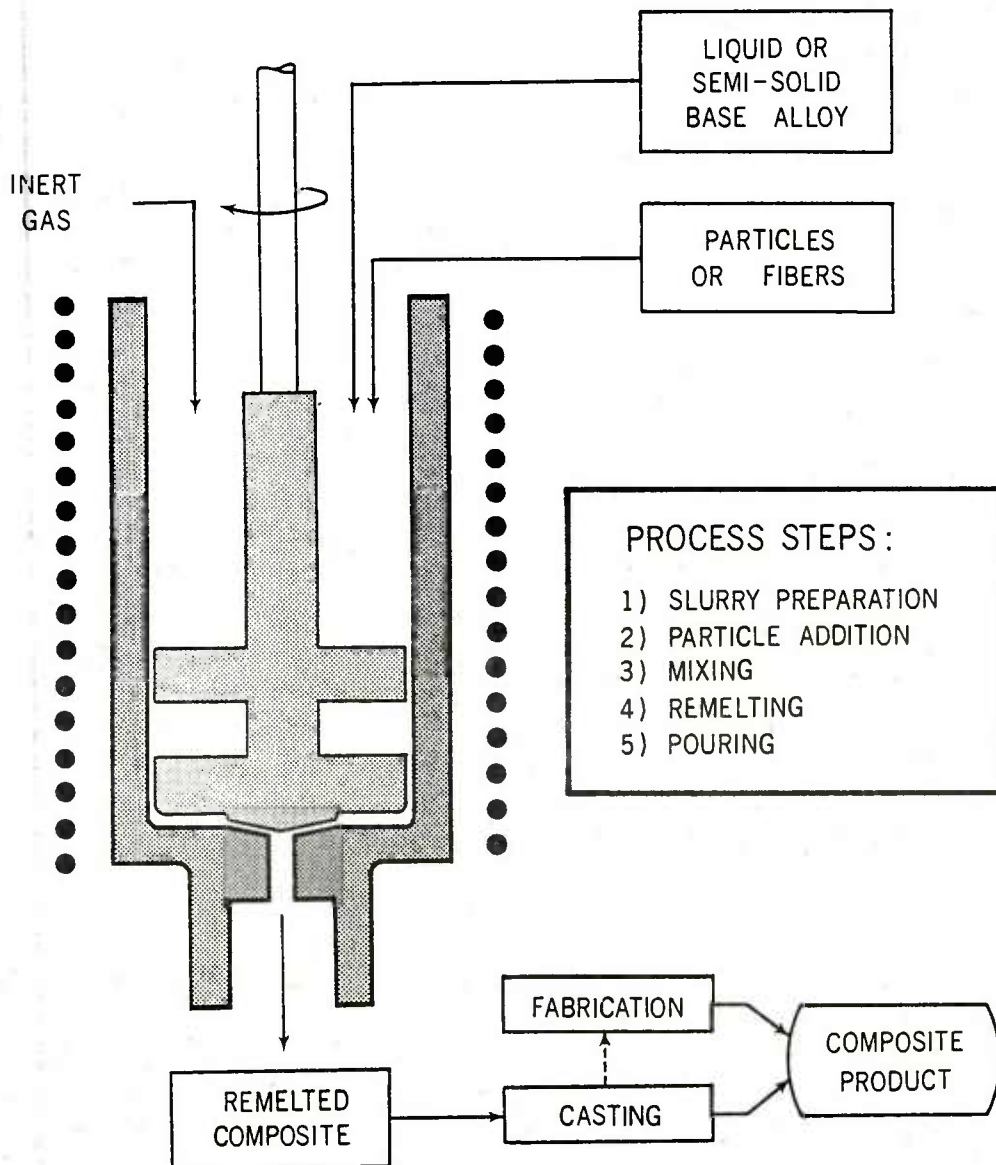


Figure 7. Schematic of the apparatus for fabrication of aluminum matrix composites.

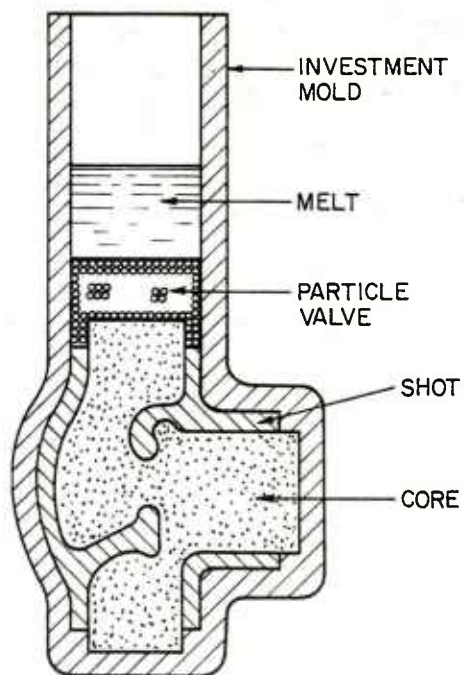


Figure 8: Sectional drawing of assembled mold for SD casting.

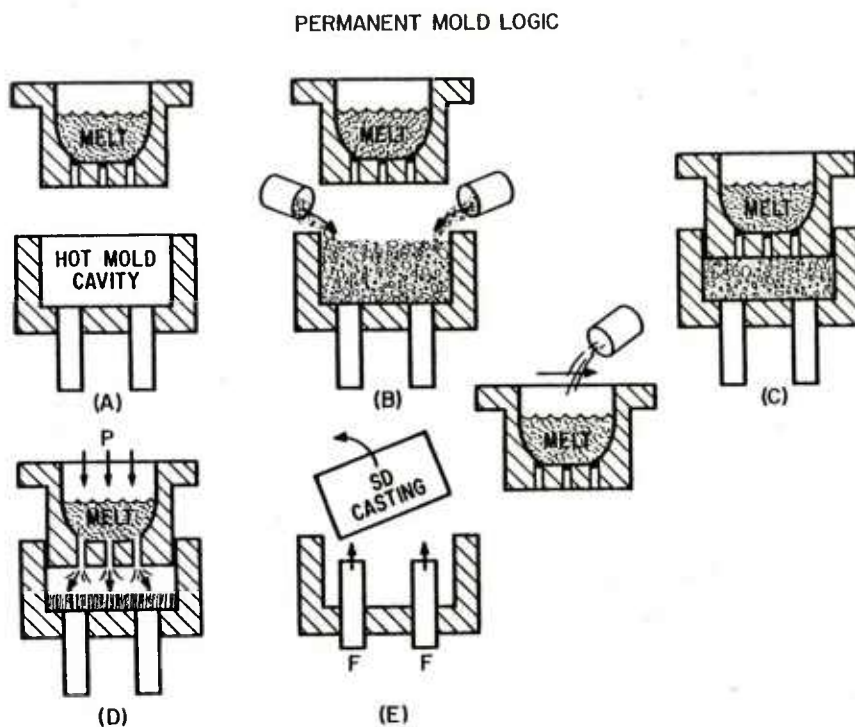


Figure 9: SD permanent mold logic; (A)-(E) indicate the sequence of events.

INVESTMENT MOLD LOGIC

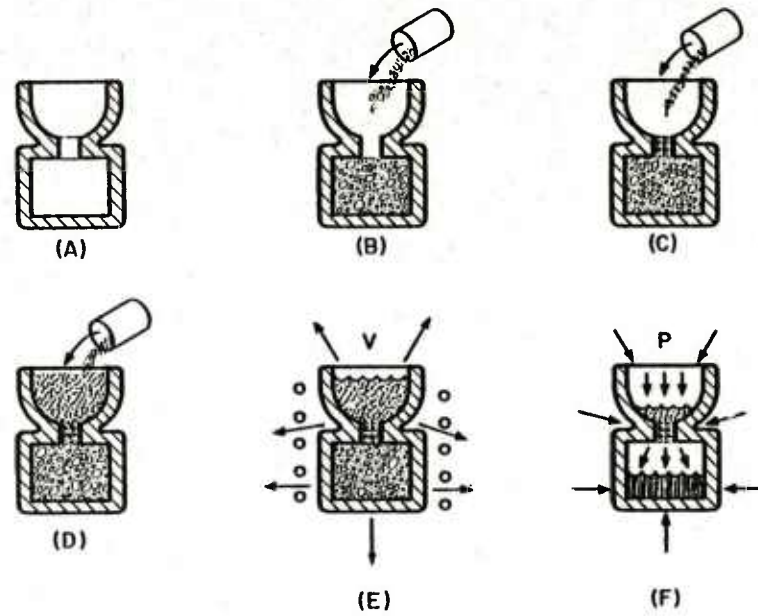


Figure 10: SD investment mold logic where (A)-(F) indicate the sequence of events. In (B) the mold is filled with the shot; in (C) the particle valve is inserted; in (D) the infiltrant is emplaced; (E) the setup is evacuated and heated to process temperature; (F) infiltration takes place.



Figure 11: Microstructure of diffusionally solidified 0.85 w/o plain carbon steel.

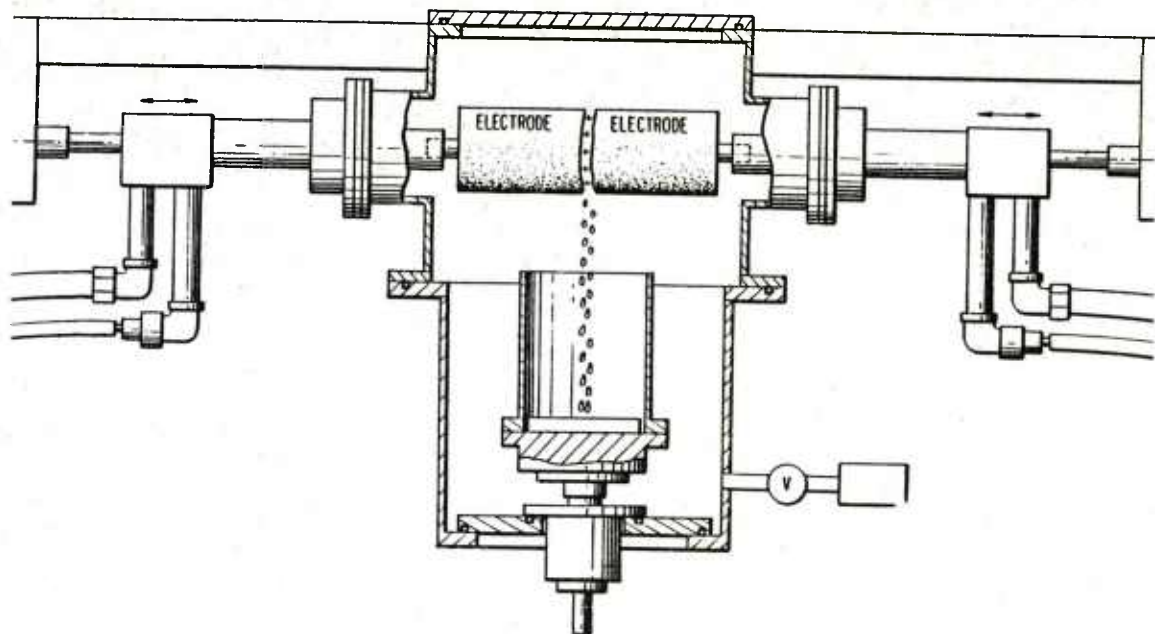


Figure 12: Schematic diagram of the VADER controlled melting process.

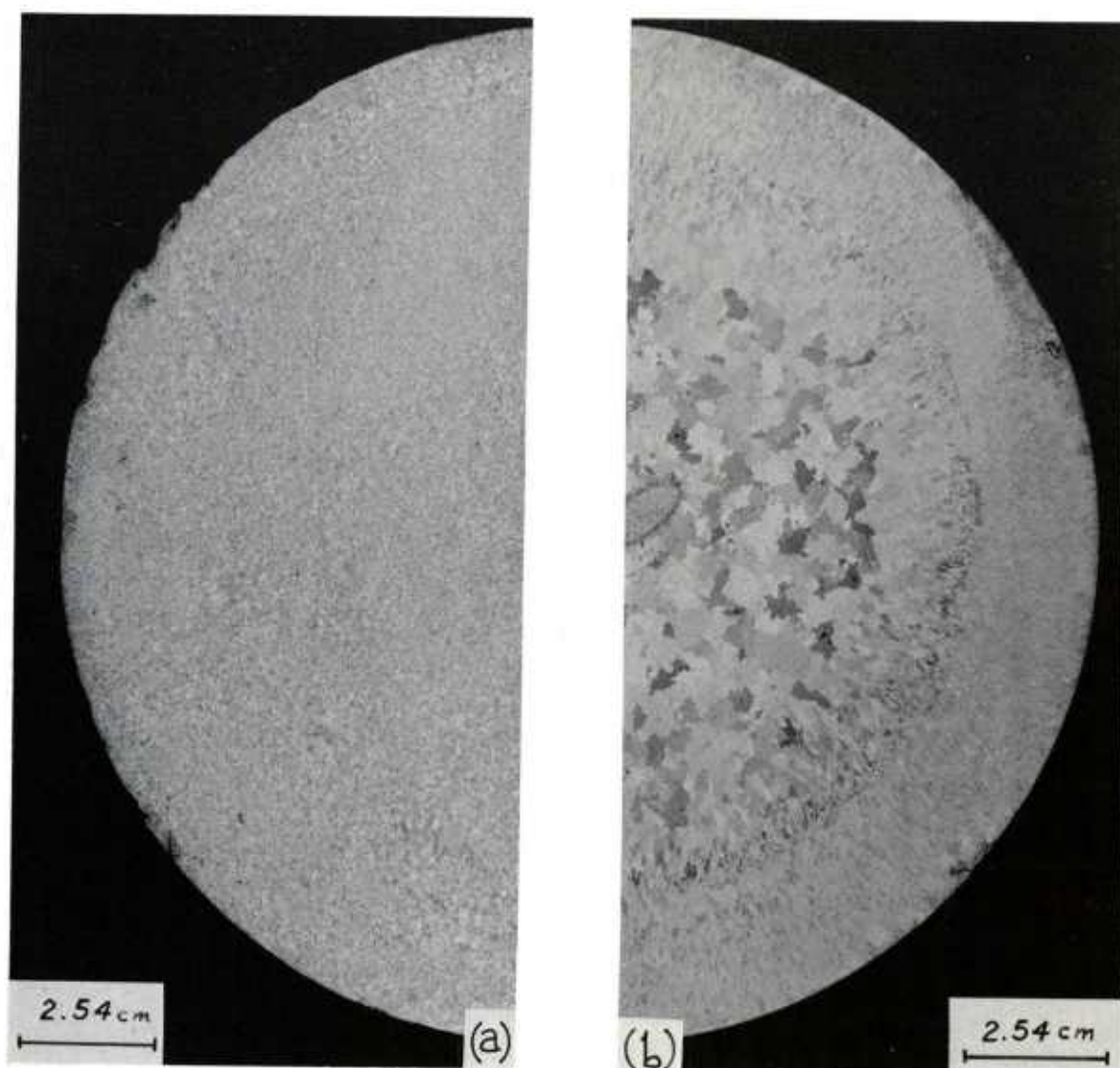
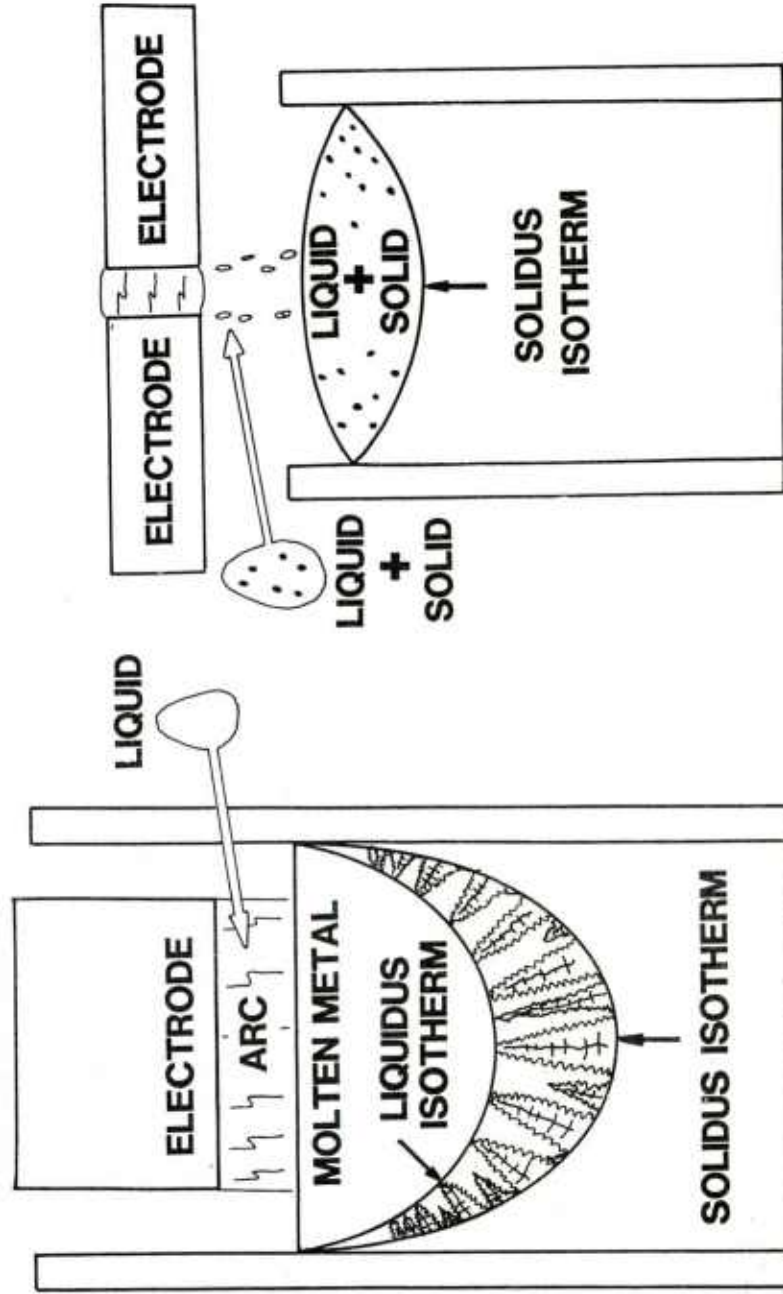


Figure 13: Macrostructure of (a) VADER IN-718 ingot and (b) VIM-VAR IN-718 ingot.

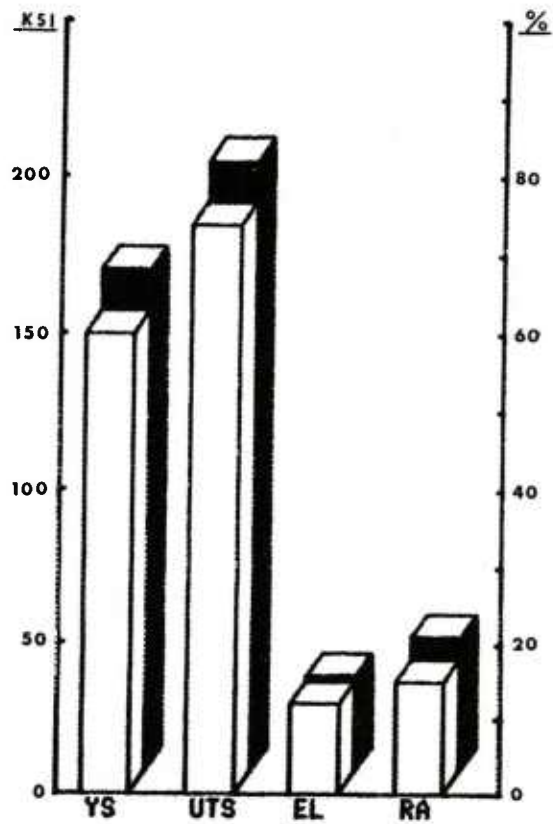
SCHEMATIC ILLUSTRATION OF SOLIDIFICATION

VAR VADER

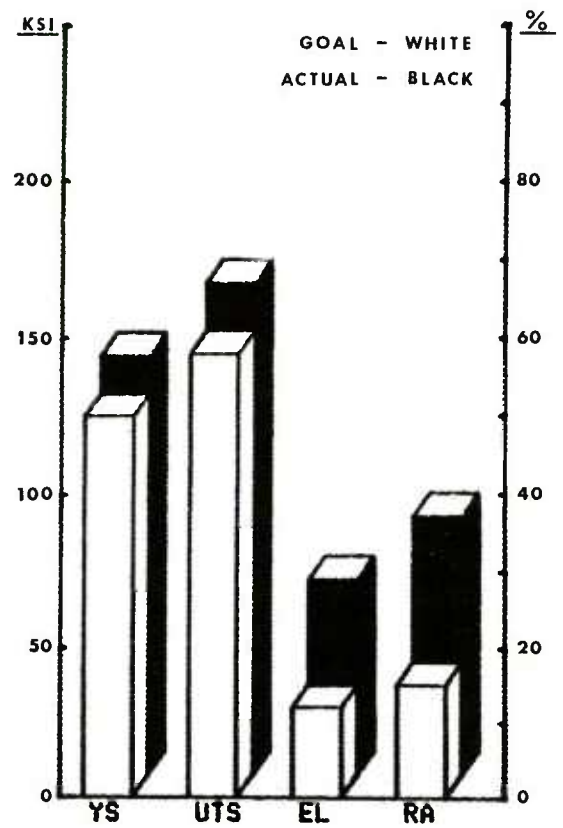


COLUMNAR DENDRITIC SOLIDIFICATION EQUAXED DENDRITIC SOLIDIFICATION

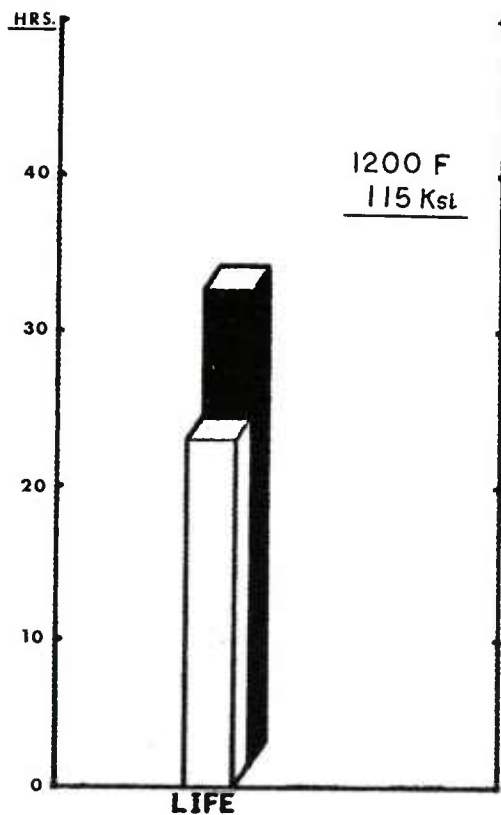
Figure 14: Model of columnar dendritic solidification in the VAR melting process and the VADER controlled melting process, respectively.



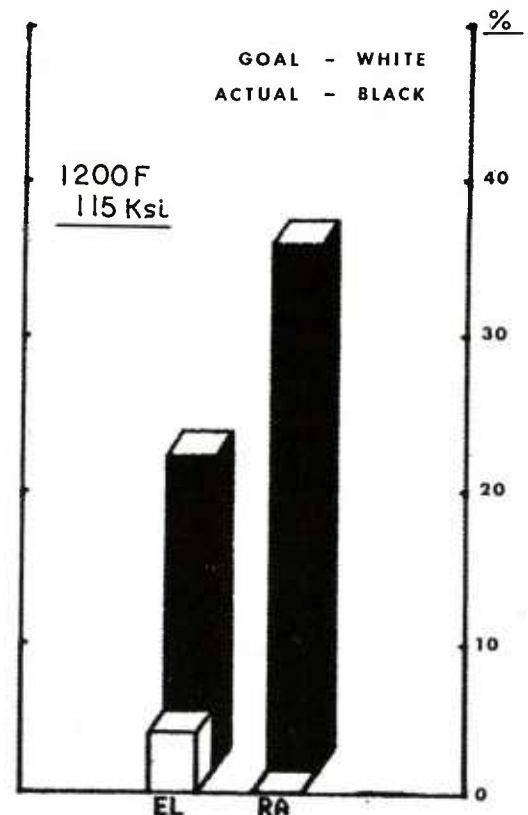
(a)



(b)



(c)



(d)

Figure 15: Properties of VADER U718 material; white regions indicate the goal and black shaded regions indicate actual measured values. (a) Room temperature ingot-roll down tensile properties; (b) 1200°F ingot-roll down tensile properties; (c) and (d) ingot-roll down stress rupture property data.

NUMERICAL SIMULATION OF CASTING SOLIDIFICATION
APPLICATION TO THE SAND-COATED GRAVITY DIE CASTING PROCESS

ir. G. Vanhoutte
CRIF Foundry Research Centre
Grotesteenweg-Noord 2
B-9710 Zwijnaarde (BELGIUM)

ABSTRACT

Numerical simulation of casting solidification has been carried out as part of a project with the objective of developing design rules for the production of sound S.G. iron castings through directional solidification in sand-coated gravity dies. To achieve this, one had to assess the parameters that govern heat transfer during solidification and subsequent cooling. Heat transfer during the freezing of an alloy in a sand-coated metallic mould is fairly complex and cannot be described analytically. Using the finite difference method for approximating the partial differential equations, a mathematical model was first set up for one-dimensional heat transfer phenomena in cartesian coordinates. Good agreement was obtained between the calculated temperature distributions and the real, experimentally determined, temperature profiles.

INTRODUCTION

This paper is a progress report on a project running at CRIF Foundry Research Centre with the objective of establishing design rules for the production of sound S.G. iron castings through directional solidification in sand-coated gravity dies.

A sand-coated gravity die combines the advantages of both a permanent mould and a sand mould : rigidity of the mould cavity, increased speed of solidification, reduction of molding sand consumption and prolonged lifespan of the die.

Heat transfer during the freezing of an alloy in a sand-coated metallic mould is fairly complex, since it involves heat conduction through the casting itself, internal heat generation (release of latent heat of solidification), heat transfer through the casting/sand interface, through the sand coating, through the sand/die interface, through the metallic mould, and finally convective heat transfer to the ambient space.

Heat transfer in a sand-coated gravity die can be influenced both by geometric parameters such as the relative thickness of the casting, sand coating and die, and by intrinsical material properties such as the nature of the sand (silica, chromite, zircon) and the binder system (clay or resin bonded).

Faced with this multiplicity of parameters, it was felt that a numerical simulation of the cooling and freezing phenomena by means of a mathematical model of heat transfer would enable us to evaluate the relative importance of each parameter.

The purpose of this paper is to describe initial efforts to establish such a model for the sand-coated gravity die, and to point out some technical problems encountered in its development.

EXPERIMENTAL PROCEDURE

The test casting selected for experimental work and computer simulation was a 200mm x 200mm square plate of 20mm thickness, as shown (together with its gating system) in fig.1. The casting was surrounded on all sides by a layer of cold setting resin-bonded sand of uniform thickness, which in turn was backed by a cast iron permanent mold of 50mm wall thickness. A cross-sectional view of the arrangement is presented in fig.2. Experiments were conducted with different thicknesses of the sand coating which varied from 5mm to 25mm. The castings were poured in nodular cast iron of eutectic composition (average composition was : 3.6%C, 2.4%Si, 0.02%Mn, 0.025%P, 0.010%S, 0.8%Ni, 0.06%Mg). Thermocouples were located in the casting and the mold for monitoring the temperature/time relationship until completion of solidification.

HEAT TRANSFER MODELING

Talking in terms of heat transfer theory, the freezing of a metal in a mold involves unsteady-state heat transfer with internal heat generation through change of state. The equations for solidification are of a non-linear type, caused by the boundary conditions at the moving solid/liquid interface. In addition, for a mathematical approach to be realistic, temperature dependent material properties must be taken into account. Finally, when thermal resistances at the various interfaces are involved, the analytical approach becomes unfeasible.

For mathematical treatment of similar complex heat transfer problems one is therefore committed to numerical approximation techniques which describe a problem by means of finite-difference equations instead of partial differential equations. Time and space are hereby discretized in small steps Δt , Δx , Δy , Δz respectively.

To summarize, numerical simulation of solidification involves three stages :

- formulating an accurate physical description of the casting and solidification process in mathematical form
- finding accurate values for the temperature-dependent thermal properties of all the materials involved
- finding a suitable algorithm for implementation of the model on a digital computer, i.e. computing the temperature/time relationships at specified space coordinates in casting and mold.

THE PHYSICAL MODEL

Several simplifying - however realistic - physical assumptions concerning the casting process had to be adopted in order to facilitate the mathematical treatment.

Filling transients were disregarded, so it was assumed that the mould cavity was filled instantaneously and that no convective heat transfer prior to solidification took place in the liquid metal. Initial liquid metal temperature was taken to be uniform throughout the casting and was derived by extrapolation from the experimentally recorded temperature at the casting centerline. The initial temperature at the metal/sand interface was equally taken to be uniform and was reasonably approximated by the so-called "contact temperature" as derived by classical heat transfer theory from material thermal properties.

Because of the volume expansion occurring during the solidification of nodular cast iron, it was felt reasonable to assume perfect thermal contact between metal and sand so that no particular thermal resistance was introduced at the metal/sand interface.

However, at the sand/permanent mold interface, a special situation arises from the limited thermal contact area between sand grains and a smooth metal surface, as can be seen on the idealized arrangement shown in fig.3. It was assumed here that the voids between the sand grains were filled with air and that heat transfer took place essentially by conduction through a fictitious air gap of uniform thickness, which was calculated from the total void volume in accordance with the average sand grain size.

Finally, a thermal resistance was considered at the mold/air interface, where heat transfer was assumed to take place essentially by natural convection to the surroundings.

MATERIAL THERMAL PROPERTIES

Specific heat (c), thermal conductivity (λ) and thermal diffusivity (α) (which is defined by $\alpha = \frac{\lambda}{\rho \cdot c}$) are all known to be temperature dependent, a fact which has to be taken into consideration for any simulation to be performed realistically. However, obtaining reliable numerical data for the thermal properties of sand and nodular iron turned out to be a cumbersome task : high temperature data are scarce and often conflicting.

For the permanent mould, in which temperature varied only over a limited range (some 100°C), constant thermal properties were adopted for simplicity. For the same reason, constant properties were assumed for the cast metal in the superheat region (from 1300°C to about 1150°C). The values adopted are summarized in fig.4.

It was soon realized that the success of the simulation depended essentially on the accuracy of the thermal properties of the sand coating in which steep thermal gradients were present. Reported values for moulding sand thermal properties show wide scatter since they depend largely on grain size, binder type and ramming density. Literature data were therefore chosen at random and systematically adapted by trial and error through comparison of calculated and experimentally determined temperature distributions.

The specific heat relationship was approximated by three straight line segments as shown in fig.5. The values that were finally adopted for resin-bonded sand are somewhat higher than those reported for clay-bonded sand, to account for the endothermic cracking of the binder system over a wide temperature range.

Thermal conductivity of the sand as a function of temperature was approximated for convenience by a third degree polynomial fit (fig.6), which is in agreement with physical reality : it must be emphasized here that the thermal conductivity of the sand is a modified or "apparent" conductivity which accounts for high-temperature radiative heat transfer. Thermal diffusivity was simply calculated from the assumed values of thermal conductivity, specific heat and density (taken as a constant).

Another major problem in the development of the model was the treatment of the release of latent heat of solidification. Option was made for the so-called " C_p -method" in which the latent heat of solidification is added to the specific heat over some pre-determined temperature range. Calculations are then performed on an "effective" rather

than a true specific heat. The most logical approach was to relate the fraction of the heat of solidification released to the fraction solidified. For nodular cast iron, the latter has been determined by other researchers, and the corresponding relationship is shown in fig.7.

THE MATHEMATICAL MODEL

1. As a first approximation the plate casting, whose thickness is small compared to its other dimensions, was associated to a theoretically infinite plate in 2 dimensions. Heat transfer under these circumstances is essentially 1-dimensional, at right angles to the plate surface. This 1-dimensional space was divided into discrete lumps with nodes representing the locations where temperatures were defined. This situation is represented in fig.8.

Each node has an inherent thermal capacity and is connected to its neighbours through thermal resistances. Nodes and boundaries were made coincidental to minimize difficulties in setting up the heat transfer equations. The symmetric nature required that only half the actual casting and mould assembly be modeled, thus drastically decreasing the computing effort. The casting centerline was considered to be an adiabatic boundary.

The 1-dimensional cooling problem is governed by the following partial differential equation :

$$\frac{\partial T}{\partial t} = \alpha \cdot \frac{\partial^2 T}{\partial x^2} \quad \text{with} \quad \alpha = \frac{\lambda}{c \cdot \rho} \quad \text{as mentioned earlier.}$$

This equation, with its numerous boundary conditions prevailing at individual nodal points, was solved using finite-difference approximation techniques. In these methods, derivatives are replaced by appropriate finite-difference expressions involving discrete values of Δx and Δt .

For example, for any general grid point in the mold or casting, the following expression holds :

$$\frac{T_{i,n+1} - T_{i,n}}{\Delta t} = \alpha \cdot \left[\frac{T_{i-1,n+1} - 2T_{i,n+1} + T_{i+1,n+1}}{(\Delta x)^2} \right]$$

where $T_{i,n}$ denotes temperature at node i at time n . This is the so-called "implicit" form of the finite-difference approximation ^(*). This leads to a so-called tridiagonal system of algebraic equations, where the number of equations as well as the number of unknown temperatures equal the number of nodal points considered.

It must be emphasized that particular boundary conditions prevail at any interface between two materials. This necessitated a separate finite-difference approximation to be derived for any singular type of nodal point. Boundary conditions were expressed using the pseudo-steady state technique which is a valid finite-difference approximation to the transient heat conduction problem. For those special nodal points, equations were derived by energy-balance considerations : a heat balance equation was written using simple algebraic equations for steady-state heat transfer by conduction or convection.

(*) In the implicit form, new temperatures at each nodal point i are solved in terms of new temperatures at adjoining nodes which are themselves unknown. By contrast, in the explicit form, new temperatures are computed in terms of earlier temperatures at adjoining grid points, all of which are known.

The technique is illustrated in appendix A for a nodal point at the interface between cast metal and sand.

Solution of the set of simultaneous equations by means of an appropriate algorithm yielded the 1-dimensional temperature profile in casting, sand layer and permanent mould at a specified time step. This procedure was repeated for successive time steps until solidification was complete. (For practical reasons, computations were interrupted when the casting centerline had cooled to 1000°C).

The real, experimentally determined temperature profiles were compared to the calculated distributions, and the numerical values of the material thermal properties were modified appropriately until satisfactory agreement was obtained.

With this simple 1-dimensional model, the relative deviation between calculated and experimental solidification times of the plate casting was of the order of 5 %.

2. An infinite plate is of course but a rough approximation for the plate casting represented in fig.1. For a more realistic simulation and especially with the treatment of other, more complex geometries in mind, a 2-dimensional solidification model was developed for the same test casting and mould arrangement as discussed earlier, in order to investigate heat transfer in a central plane normal to the plate surface.

This new situation is represented in fig.9. Obviously, only one quarter of the assembly needed to be modeled because of symmetry considerations. The X,Y-plane was subdivided into a network of nodal points, a distance ΔX apart, where temperatures were defined. Unsteady-state heat conduction in 2 dimensions is now governed by the parabolic differential equation :

$$\frac{\partial T}{\partial t} = c \cdot \left[\frac{\partial^2 T}{\partial x^2} + \frac{\partial^2 T}{\partial y^2} \right]$$

Different finite-difference approximation algorithms have been reported in literature. In this work the implicit-alternating-direction or IAD-method was selected because of its ease of implementation in a computer program. To summarize, the IAD-method subdivides each time interval Δt into half time steps $\Delta t/2$. The space derivatives of the partial differential equations are approximated implicitly (i.e. in terms of the future unknown temperatures) in the X-direction, and explicitly (i.e. in terms of prior, known temperatures) in the Y-direction over the first half interval. This procedure is then reversed in the second half interval.

Obviously, for any type of nodal point, two finite-difference equations had to be derived. For example, an internal general grid point is now characterized by the following two equations :

$$(1) \quad \frac{2}{\alpha_{i,j,n}} \cdot \frac{T_{i,j}^* - T_{i,j,n}}{\Delta t} = \frac{T_{i-1,j}^* - 2T_{i,j}^* + T_{i+1,j}^*}{(\Delta x)^2} + \frac{T_{i,j-1,n} - 2T_{i,j,n} + T_{i,j+1,n}}{(\Delta y)^2}$$

$$(2) \quad \frac{2}{\alpha_{i,j}^*} \cdot \frac{T_{i,j,n+1} - T_{i,j}^*}{\Delta t} = \frac{T_{i-1,j}^* - 2T_{i,j}^* + T_{i+1,j}^*}{(\Delta x)^2} + \frac{T_{i,j-1,n+1} - 2T_{i,j,n+1} + T_{i,j+1,n+1}}{(\Delta y)^2}$$

for the first and the second half interval respectively.

Here $T_{i,j}$ denotes the intermediate temperature at node (i,j) at the end of the 1st half interval. Material properties (condensed in α) must be evaluated at the prevailing

temperature.

As mentioned earlier, boundary and interfacial grid points required special attention. The introduction of a 2nd dimension however considerably increased the number of singular types of grid points. For example : symmetry, convection, interfaces and air gap all had to be considered both in X and Y direction, and at corner points.

As can be seen from fig.10 the assumption of a fictitious or equivalent air gap as a thermal resistance between sand layer and permanent mould created some additional complications : for the continuity of the grid system, the IAD method necessitated additional nodes along the extensions of the air gap. Thus, in the final version, some 30 types of singular grid points were taken into account.

The heat-balance method was again used for deriving the appropriate finite-difference equations. In some special cases the equations turned out to be pretty complicated as is illustrated in appendix B for a nodal point at the intersection of the X and Y interface between cast metal and sand.

The IAD algorithm was then implemented into a Fortran computer programme, which enabled the calculation of the 2-dimensional temperature field that is established during the solidification of a flat plate with finite dimensions in a sand-coated gravity die.

The printout of this programme consists of this 2-dimensional temperature field on successive time steps.

As before, calculated and experimentally determined temperature distributions were matched by modifying some thermal properties appropriately. Thus, the relative deviation between the real and the computed solidification time could be reduced to below 2 %.

NUMERICAL SIMULATION OF DIRECTIONAL SOLIDIFICATION

One of the techniques for achieving directional solidification in a casting using a sand-coated gravity die, consists of gradually varying the relative thickness of sand layer and permanent mould. In this way a thermal gradient can be created which is directed towards the point where the chilling effect (i.e. the thickness ratio of permanent mould to sand layer) is the highest.

In the case of the test casting for instance, upward directional solidification could be achieved by gradually increasing the sand layer thickness as is illustrated in fig.11.

An inclined surface however, as encountered here, is definitely unsuitable for mathematical modeling in cartesian coordinates where the space domain is subdivided stepwise. It can be approximated by a jagged series of steps constructed from the rectangular grid employed in the simulation.

Taking into account the existence of a thermal resistance, approximated as an extremely thin gap at the sand/permanent mould interface, this geometry can be modeled by a network of grid points as is illustrated in fig.12. Modeling a jagged interface - apparently an unsophisticated artefact - adds considerably to the complexity of the model, not only because the total number of nodal points increases markedly, but merely because a whole set of new types of nodal points must be defined along the extensions of the gap boundaries. About 50 different types of nodal points were considered for this casting and mould assembly.

Numerical simulation was performed using the IAD algorithm as before. Advantage was taken from the modular framework of the previous program, which necessitated only adding a set of new subroutines corresponding to the newly defined nodal points.

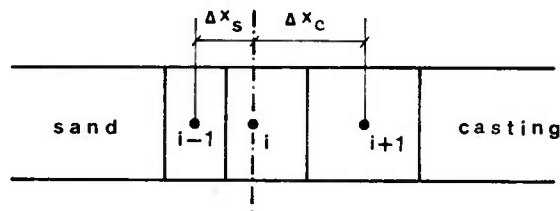
Output from the simulation is in the form of printouts of temperature at each nodal point. Fig.13 illustrates the temperature field at a specified time step, where the whole plate casting has cooled to just below 1000°C. The straight lines represent the sand/metal interface, the jagged lines stand for the sand/permanent mould interface. The simulation pertains to the test casting moulded in a gravity die with a sand coating of 5mm thickness below and 25mm above.

CONCLUSION

The sand-coated gravity diecasting process was numerically simulated in the simple case of a plate casting. Temperature fields in casting and mould assembly at predetermined time steps were calculated using a finite-difference technique. The method was used to investigate directional solidification based on sand coating thickness variations. A computer program that was developed for that purpose could easily be adapted to handle more complex casting geometries as well as different mould assemblies, e.g. sand casting alone. It was pointed out that the accuracy of computer simulation was strongly dependent on knowledge of materials thermal properties as well as on reasonable assumptions concerning interfacial heat transfer and internal heat generation phenomena.

APPENDIX A

1-dimensional heat transfer at interface between sand and casting



Consider a node i at the interface between sand and casting, with subdivisions Δx_s and Δx_c respectively. With heat transfer through a unit surface, a heat balance yields :

$$\lambda_s \cdot \frac{(T_{i-1,n+1} - T_{i,n+1})}{\Delta x_s} \cdot \Delta t + \lambda_c \cdot \frac{(T_{i+1,n+1} - T_{i,n+1})}{\Delta x_c} \cdot \Delta t$$

$$= (C_s \cdot \rho_s \cdot \frac{\Delta x_s}{2} + C_c \cdot \rho_c \cdot \frac{\Delta x_c}{2}) (T_{i,n+1} - T_{i,n})$$

which can be rearranged to the following implicit F.D.A. equation :

$$- 2Z_s \cdot T_{i-1,n+1} + [Z_s(2+M_s) + Z_c(2+M_c)] T_{i,n+1} - 2Z_c \cdot T_{i+1,n+1}$$

$$= (Z_s M_s + Z_c M_c) T_{i,n}$$

where $Z_s = \lambda_s \cdot \Delta x_c$

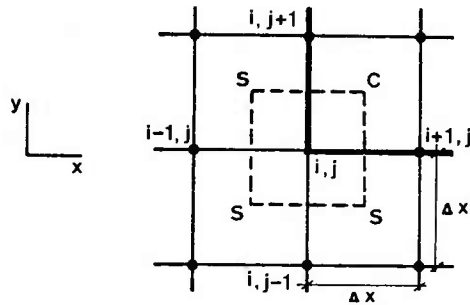
$Z_c = \lambda_c \cdot \Delta x_s$

$M_s = \frac{C_s \cdot \rho_s \cdot (\Delta x_s)^2}{\lambda_s \cdot \Delta t}$

$M_c = \frac{C_c \cdot \rho_c \cdot (\Delta x_c)^2}{\lambda_s \cdot \Delta t}$

APPENDIX B

2-dimensional heat transfer at intersection of X and Y interfaces between casting and sand



Consider a node (i,j) at the intersection of the X and Y interfaces between casting and sand. With $\Delta x_s = \Delta x_c = \Delta x$ for simplicity, and assuming that the lumps have unit length in Z direction, a heat balance over the first half interval $\frac{\Delta t}{2}$ according to the IAD algorithm yields :

$$\begin{aligned} & \lambda_s \cdot \frac{(T_{i-1,j}^* - T_{i,j}^*)}{\Delta x} \cdot \Delta x \cdot \frac{\Delta t}{2} + (\lambda_s + \lambda_c) \frac{(T_{i+1,j}^* - T_{i,j}^*)}{\Delta x} \cdot \frac{\Delta x}{2} \cdot \frac{\Delta t}{2} \\ & + (\lambda_s + \lambda_c) \cdot \frac{(T_{i,j+1,n} - T_{i,j,n})}{\Delta x} \cdot \frac{\Delta x}{2} \cdot \frac{\Delta t}{2} \\ & + \lambda_s \frac{(T_{i,j-1,n} - T_{i,j,n})}{\Delta x} \cdot \Delta x \cdot \frac{\Delta t}{2} \\ & = (3C_s \cdot \rho_s + C_c \cdot \rho_c) \cdot \frac{(\Delta x)^2}{4} \cdot (T_{i,j}^* - T_{i,j,n}) \end{aligned}$$

which can be rearranged to the following implicit F.D.A. equation :

$$\begin{aligned} & 2Z_s \cdot T_{i-1,j}^* - [3Z_s(M_s+1) + Z_c(M_c+1)] T_{i,j}^* + T_{i+1,j}^* \\ & = -2Z_s \cdot T_{i,j-1,n} - [3Z_s(M_s-1) + Z_c(M_c-1)] T_{i,j,n} - T_{i,j+1,n} \end{aligned}$$

where

$$Z_s = \frac{\lambda_s}{\lambda_s + \lambda_c}$$

$$Z_c = \frac{\lambda_c}{\lambda_s + \lambda_c}$$

$$M_s = \frac{C_s \cdot \rho_s \cdot (\Delta x)^2}{\lambda_s \cdot \Delta t}$$

$$M_c = \frac{C_c \cdot \rho_c \cdot (\Delta x)^2}{\lambda_c \cdot \Delta t}$$

A similar equation can be obtained over the 2nd half interval.

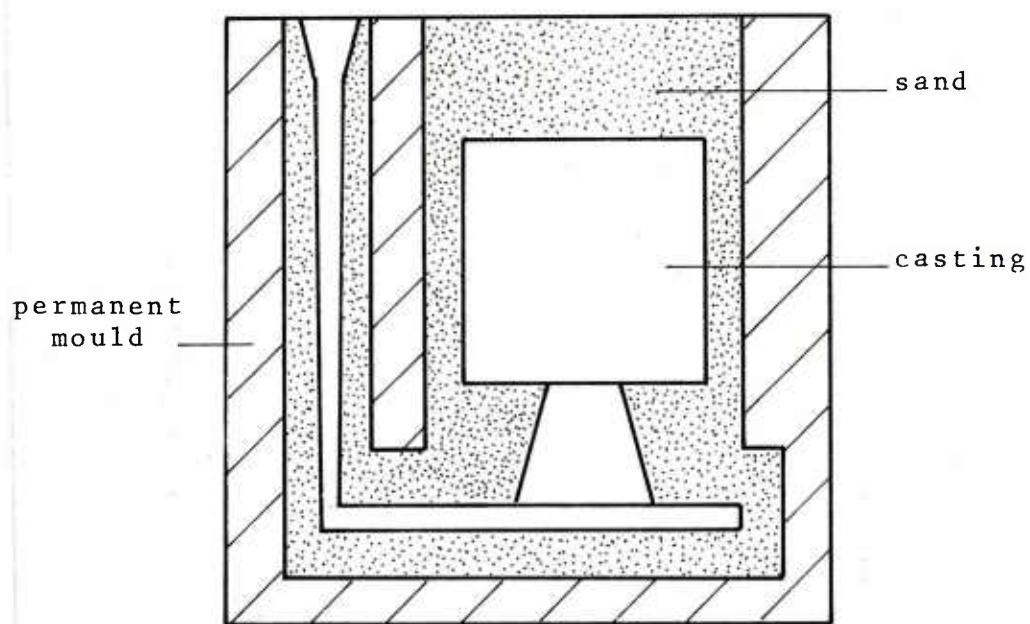


Fig.1 Schematic representation of test casting and mould assembly

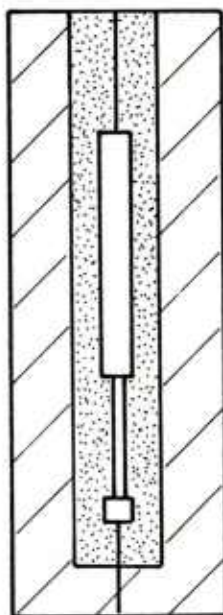


Fig.2 Cross-sectional view of test casting and mould.

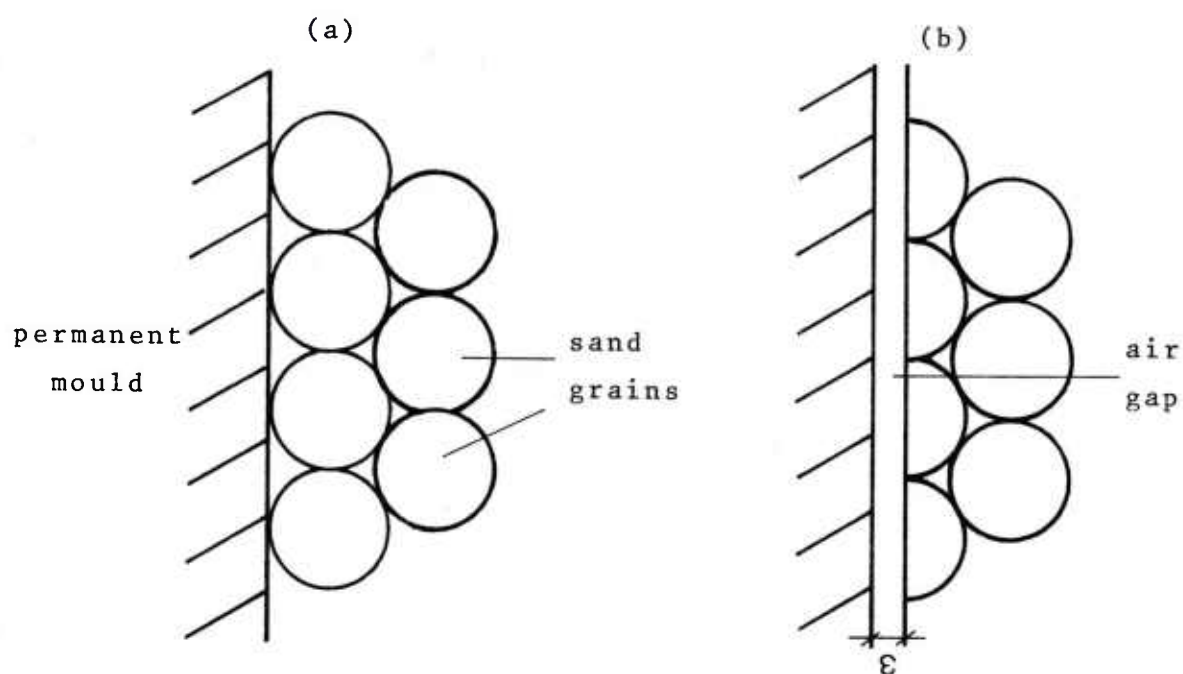


Fig.3 Schematic representation of sand/permanent mould interface : (a)idealized (b)as modeled.

	Permanent mould	casting
Material	grey cast iron	S.G. iron
Temp. range	0 - 200°C	1000 - 1300°C
Thermal conductivity $[\frac{W}{m \cdot K}]$	46 (0,11)	12.5 (0,03)
Specific heat $[\frac{J}{kg \cdot K}]$	565 (0,135)	837 (0,20)
Density $[\frac{kg}{m^3}]$	7250 (7,25)	7000 (7)

Fig.4 Constant material properties adopted for casting and mould.
(values between brackets are in C.G.S. units)

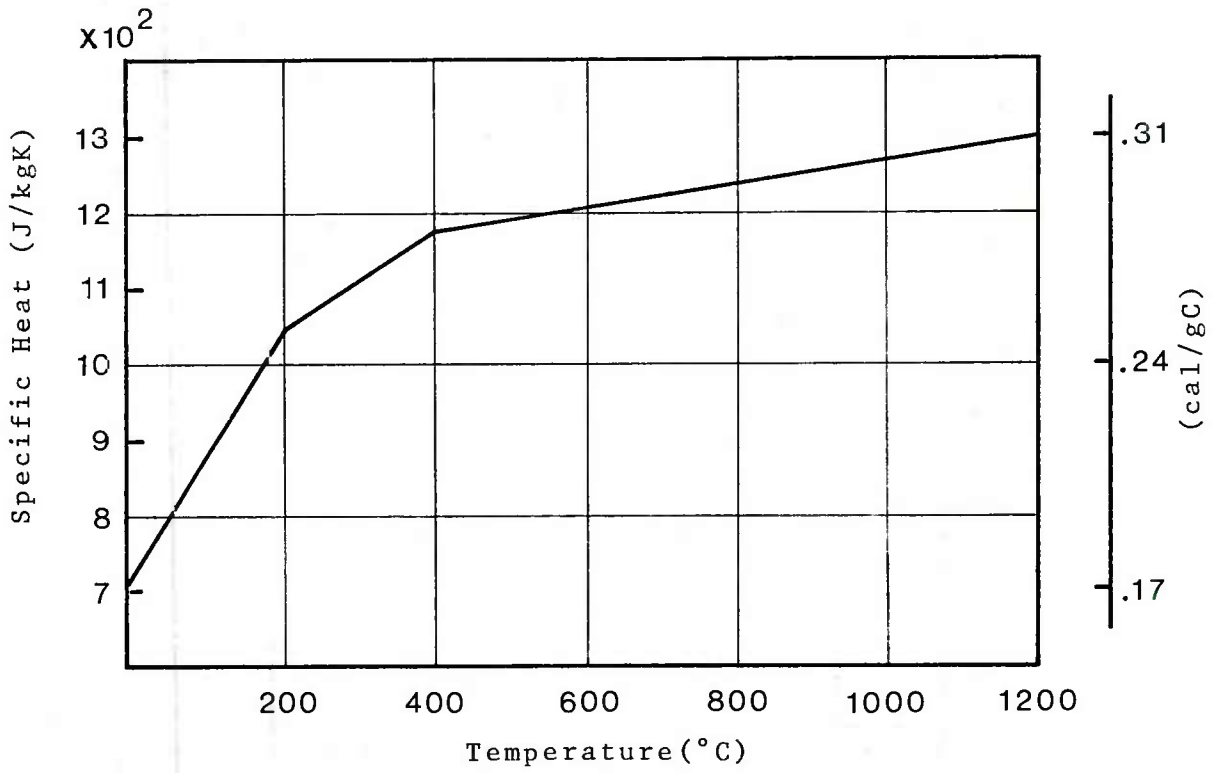


Fig.5 Functional relationship for specific heat of moulding sand.

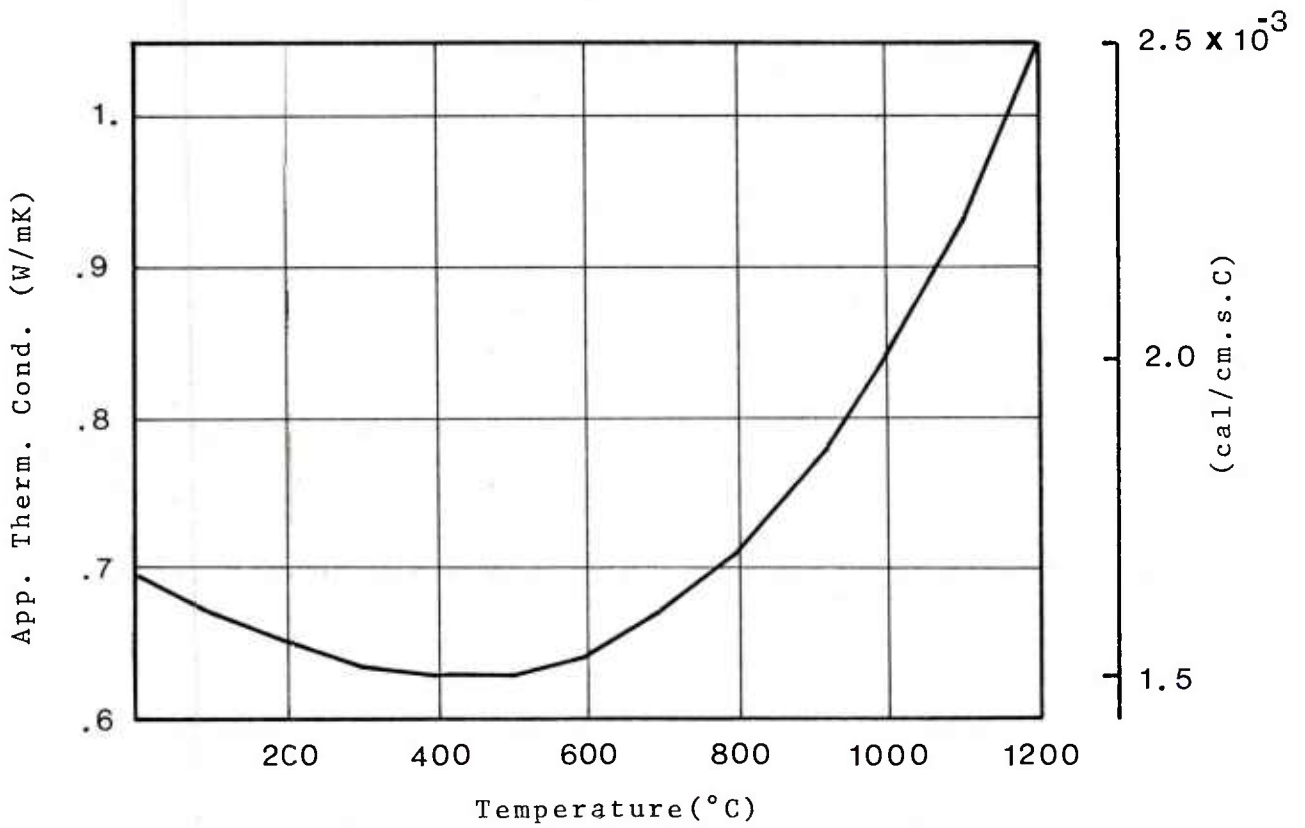


Fig.6 Functional relationship for apparent thermal conductivity of moulding sand.

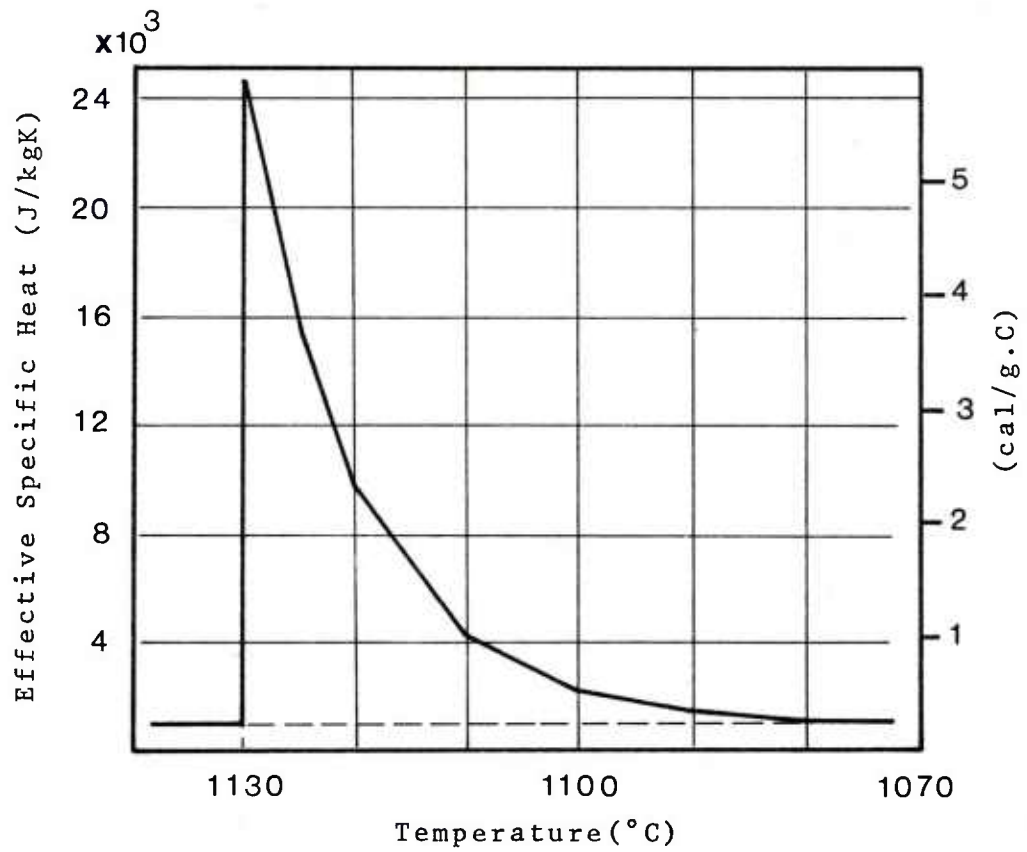


Fig.7 Effective specific heat of S.G. iron : treatment of latent heat of fusion.

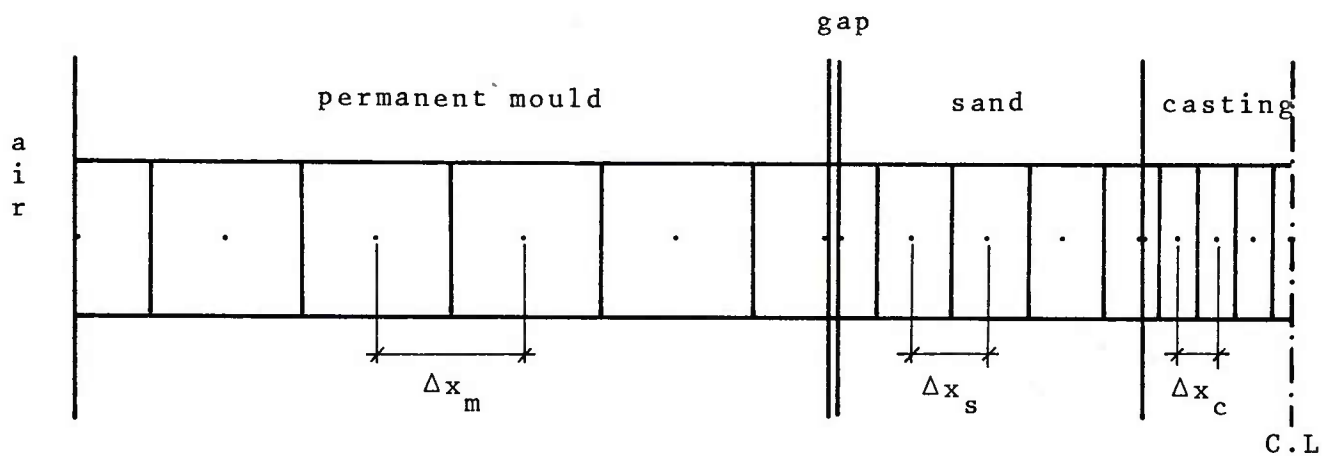


Fig.8 Geometric model for 1-dimensional heat transfer in a sand-coated gravity die.

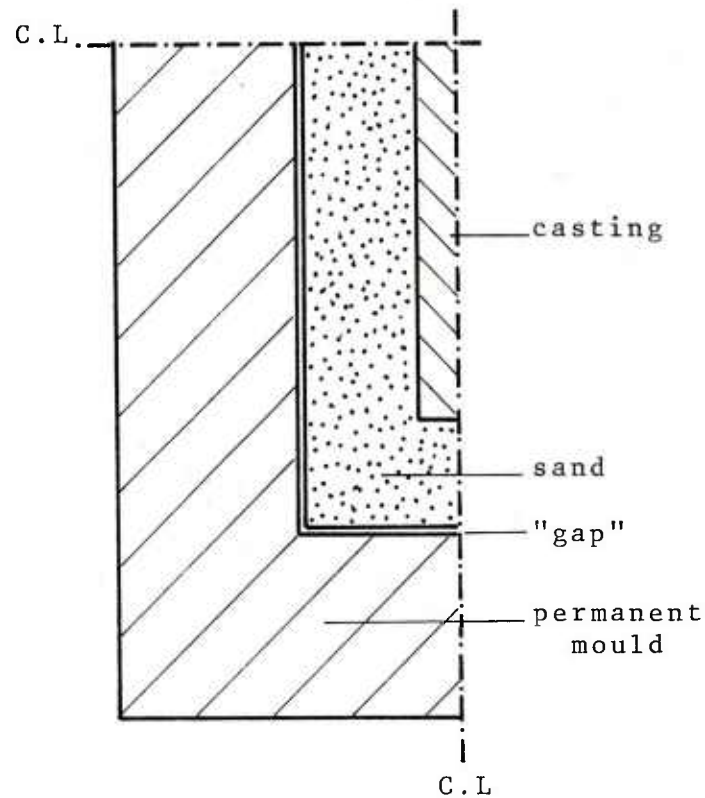


Fig.9 Space domain for 2-dimensional model of heat transfer in sand-coated gravity die.

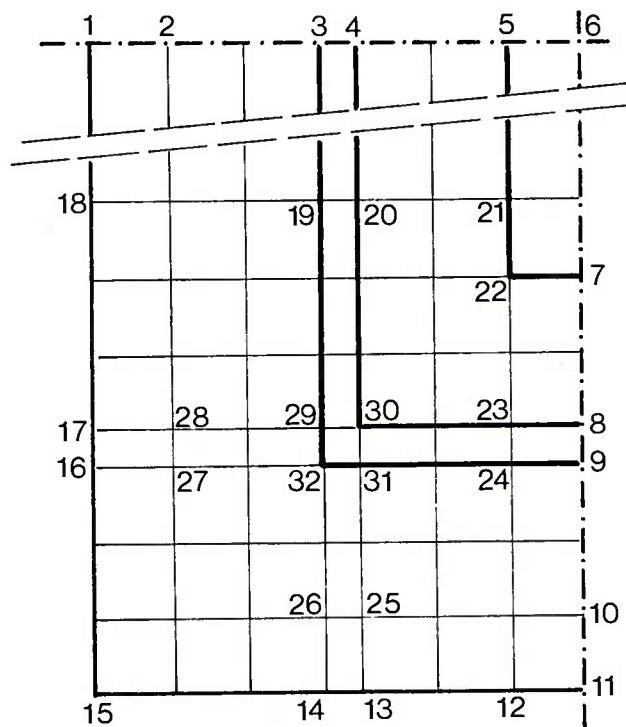


Fig.10 Illustration of singular types of nodal points in 2-dimensional model.

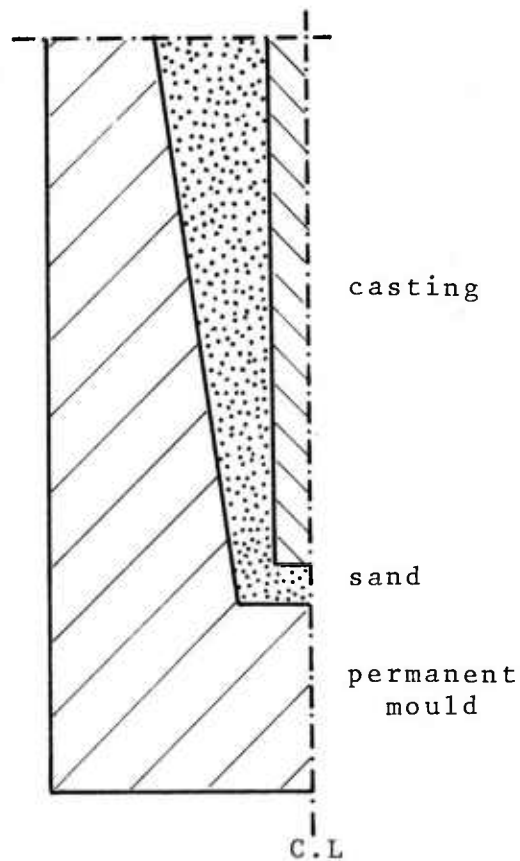


Fig.11 Schematic representation of mould assembly for directional solidification in sand-coated gravity die.

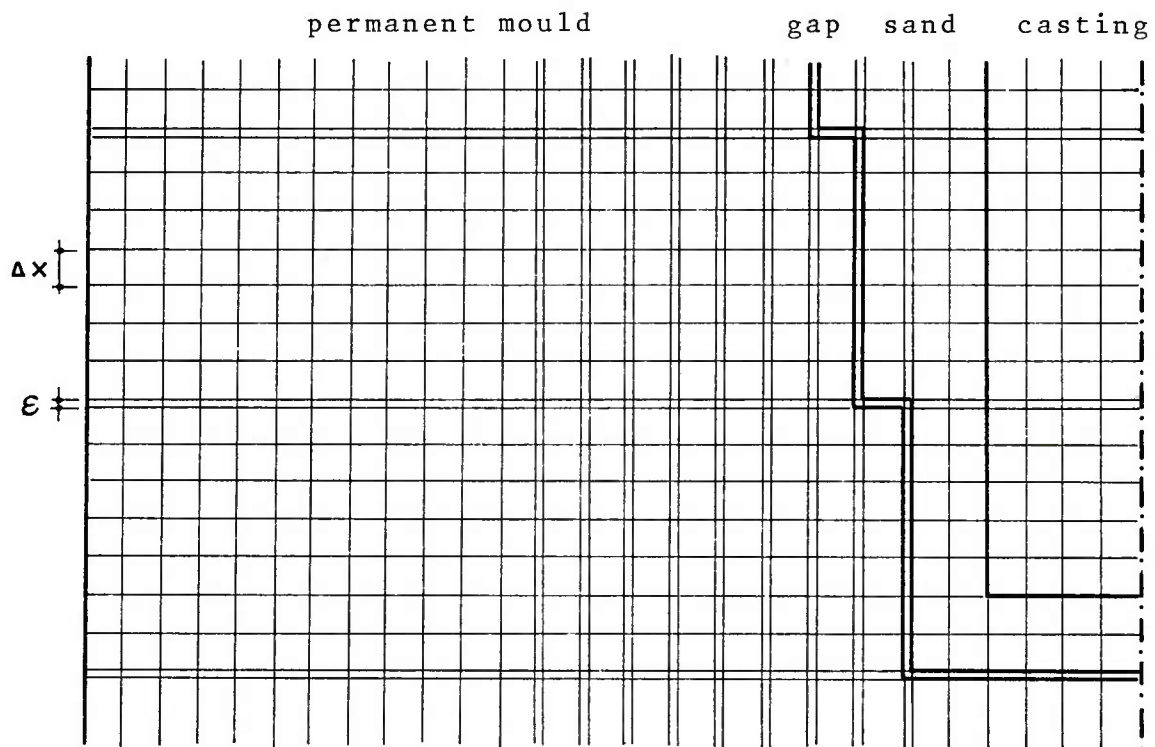


Fig.12 Network of nodal points used to simulate directional solidification.

TAU= 474. SEC

112	53.	11	198	174	176	252	254	335	337	423	425	516	517	612	613	709	711	806	808	900	987	992	996	998	998
111	58.	20	106	174	175	251	253	334	336	422	424	515	517	611	613	709	711	806	808	900	987	992	995	998	998
110	58.	70	106	171	172	248	250	332	333	421	422	514	516	610	612	708	709	805	807	900	987	992	995	998	998
109	58.	70	99	165	167	243	244	327	329	417	419	511	513	609	611	707	709	805	807	899	987	992	995	997	998
108	53.	70	96	152	153	233	234	321	322	413	415	509	510	607	609	706	708	804	806	899	987	992	995	997	998
107	53.	31	88	146	151	219	220	313	315	408	410	505	507	605	606	704	706	803	805	898	987	991	995	997	998
106	58.	71	74	121	121	218	220	313	314	408	410	505	507	604	606	704	706	803	805	898	987	991	995	997	998
105	58.	72	72	115	115	211	213	317	309	403	405	502	504	602	604	703	705	802	804	898	986	991	995	997	998
104	58.	72	72	113	113	207	209	303	305	400	402	499	501	600	602	701	703	801	803	897	986	991	994	997	998
103	58.	72	72	113	113	205	207	300	302	397	399	497	499	598	600	700	702	800	802	896	986	990	994	996	998
102	58.	72	72	112	112	203	205	298	300	395	397	495	497	596	598	698	700	799	801	896	985	990	994	996	998
101	58.	73	73	112	112	202	203	295	297	392	394	492	494	594	596	696	698	797	799	895	985	990	994	996	998
100	58.	73	73	112	112	199	201	292	294	389	391	489	491	591	593	694	696	796	798	894	984	989	993	995	996
99	58.	73	73	111	111	195	197	287	289	384	386	485	487	588	590	692	694	794	796	893	984	989	992	995	995
98	58.	74	74	111	111	193	195	285	287	382	384	483	485	586	588	688	690	792	794	892	983	988	992	994	995
97	60.	74	74	106	106	172	174	267	269	369	371	474	476	580	582	686	688	790	792	890	982	988	991	993	994
96	60.	75	75	106	106	172	174	267	269	369	371	474	476	580	582	686	688	790	792	890	982	988	991	993	994
95	60.	75	75	106	106	172	174	267	269	369	371	474	476	580	582	686	688	790	792	890	982	988	991	993	994
94	61.	76	76	106	106	172	174	267	269	369	371	474	476	580	582	686	688	790	792	890	982	988	991	993	994
93	61.	76	76	106	106	172	174	267	269	369	371	474	476	580	582	686	688	790	792	890	982	988	991	993	994
92	61.	76	76	106	106	172	174	267	269	369	371	474	476	580	582	686	688	790	792	890	982	988	991	993	994
91	62.	77	77	79	79	80	81	125	125	233	233	343	343	453	453	563	563	673	673	783	883	983	988	990	991
90	64.	80	80	82	82	83	84	125	125	233	233	343	343	453	453	563	563	673	673	783	883	983	988	990	991
89	64.	81	81	82	82	83	84	125	125	233	233	343	343	453	453	563	563	673	673	783	883	983	988	990	991
88	64.	81	81	82	82	83	84	125	125	233	233	343	343	453	453	563	563	673	673	783	883	983	988	990	991
87	63.	79	79	80	80	81	82	125	125	233	233	343	343	453	453	563	563	673	673	783	883	983	988	990	991
86	63.	79	79	80	80	81	82	125	125	233	233	343	343	453	453	563	563	673	673	783	883	983	988	990	991
85	64.	81	81	82	82	83	84	125	125	233	233	343	343	453	453	563	563	673	673	783	883	983	988	990	991
84	64.	81	81	82	82	83	84	125	125	233	233	343	343	453	453	563	563	673	673	783	883	983	988	990	991
83	64.	81	81	82	82	83	84	125	125	233	233	343	343	453	453	563	563	673	673	783	883	983	988	990	991
82	65.	81	81	82	82	83	84	125	125	233	233	343	343	453	453	563	563	673	673	783	883	983	988	990	991
81	65.	81	81	82	82	83	84	125	125	233	233	343	343	453	453	563	563	673	673	783	883	983	988	990	991
80	65.	81	81	82	82	83	84	125	125	233	233	343	343	453	453	563	563	673	673	783	883	983	988	990	991
79	66.	82	82	84	84	85	86	125	125	233	233	343	343	453	453	563	563	673	673	783	883	983	988	990	991
78	66.	82	82	84	84	85	86	125	125	233	233	343	343	453	453	563	563	673	673	783	883	983	988	990	991
77	67.	83	83	85	85	86	87	125	125	233	233	343	343	453	453	563	563	673	673	783	883	983	988	990	991
76	67.	83	83	85	85	86	87	125	125	233	233	343	343	453	453	563	563	673	673	783	883	983	988	990	991
75	68.	83	83	85	85	86	87	125	125	233	233	343	343	453	453	563	563	673	673	783	883	983	988	990	991
74	68.	83	83	85	85	86	87	125	125	233	233	343	343	453	453	563	563	673	673	783	883	983	988	990	991
73	68.	83	83	85	85	86	87	125	125	233	233	343	343	453	453	563	563	673	673	783	883	983	988	990	991
72	68.	83	83	85	85	86	87	125	125	233	233	343	343	453	453	563	563	673	673	783	883	983	988	990	991
71	69.	83	83	85	85	86	87	125	125	233	233	343	343	453	453	563	563	673	673	783	883	983	988	990	991
70	69.	83	83	85	85	86	87	125	125	233	233	343	343	453	453	563	563	673	673	783	883	983	988	990	991
69	69.	83	83	85	85	86	87	125	125	233	233	343	343	453	453	563	563	673	673	783	883	983	988	990	991
68	69.	83	83	85	85	86	87	125	125	233	233	343	343	453	453	563	563	673	673	783	883	983	988	990	991
67	69.	83	83	85	85	86	87	125	125	233	233	343	343	453	453	563	563	673	673	783	883	983	988	990	991
66	69.	83	83	85	85	86	87	125	125	233	233	343	343	453	453	563	563	673	673	783	883	983	988	990	991
65	69.	83	83	85	85	86	87	125	125	233	233	343	343	453	453	563	563	673	673	783	883	983	988	990	991

Fig. 13 Calculated 2-dimensional temperature field.

THE SQUEEZE FORMING OF ALUMINIUM ALLOYS

By

Mr Gwynne Williams
Projects Manager
Process Technology Department
GKN Technology Limited
Birmingham New Road
Wolverhampton
ENGLAND
WV4 6BW

SUMMARY

The Squeeze Forming Process is a hybrid manufacturing technology which involves the pressurised solidification of liquid metal in reusable dies. The basic process is described and the importance of various process parameters is discussed. A range of aluminium alloy components which have been made by GKN Technology Ltd using this technique, is shown. Details are given of the types of components geometry amenable to the process, and reference will be made to several components which have found defence application e.g. tank wheels. Mechanical property data determined in several of these components is presented for a number of aluminium alloys. It is observed that both "forging" and "casting" alloys can be successfully squeeze formed, and of the mechanical properties achieved compare favourable with conventional properties. It is concluded that the work performed at GKN Technology Ltd has shown squeeze forming to be a potentially powerful technique for the manufacture of a wide range of structural aluminium components in competition with more conventional production methods.

1. INTRODUCTION

Aluminium alloy components have been widely used in aerospace and defence structures for many years. In general, these components are produced by the various classical casting and mechanical working techniques. Wrought products are employed where strength and soundness are of paramount importance. Castings are used in areas which are less structurally significant, and where the shape capabilities of the casting processes can be exploited to economic advantage.

The general engineering applications of aluminium alloy parts have been largely restricted to extrusions or castings. The dominant factor has been the component price, so that the structurally significant products have almost always been made of steel or cast iron. There are now increasing market requirements for aluminium alloy components which can cope with arduous service conditions, but which are capable of optimum economics in production. A typical driving force for this market trend in general engineering is the requirement to save weight in automotive vehicles, and other structures.

Forging processes can employ aluminium alloys covering the whole spectrum of strength capabilities. Forgings are, however, generally expensive to produce and often require significant amounts of machining to bring the forged piece to a usable configuration.

The casting processes are capable of generating highly shaped parts, and at costs which are much less than those involved in forging. The correct selection of casting process, and strict control in manufacture, will produce components of good integrity. However, the conventional casting processes cannot employ the very high strength alloys and achieve the same structural performance as forgings.

There is a significant potential, therefore, for a manufacturing route which can combine the strength and confidence levels of forgings with the economics and shape capabilities of castings. Squeeze Forming is such a hybrid process. This paper describes the basis of the Squeeze Forming process, and presents results achieved by GKN. The development work to date has been carried out by GKN Technology Ltd in collaboration with GKN Sankey Ltd. A pilot production plant is coming on stream at GKN Sankey Ltd, in January 1982.

2. PROCESS DESCRIPTION

Squeeze Forming^{1,2,3} may be regarded as a hybrid casting/forging process: it is based upon the principle of pressurised solidification. The process has been reported in the literature by other workers, who have used several synonyms. Examples are Squeeze Casting^{4,5,6,7}, Extrusion Casting⁸, Liquid Pressing^{9,10}, Pressure Crystallisation^{11,12} and Cothias Casting¹³.

The literature suggests that the process may be used with a variety of feedstock materials, such as alloys of copper, nickel and iron^{5,6,8,9,11}, but the work as reported here has concentrated upon aluminium alloys.

There are several stages in the basic processing cycle:-

- a) A suitable dieset is mounted in a hydraulic press. The tools are preheated to a working temperature before the squeeze forming cycles begin.
- b) Liquid alloy is accurately metered into the lower part of the open dieset.
- c) The press cycle is activated, bringing the upper and lower tools together. The closure of the toolset causes the metal to be displaced and fill the cavity defined by each part of the mould. When the cavity has been filled, the press cannot close further, and is thus stalled in its movement. This causes the liquid metal to become pressurised. The dieset is closed as soon as possible after pouring of the liquid metal, so that only a limited amount of solidification can occur without pressure.
- d) The press is kept closed and the load upon the metal, until solidification has been completed. The pressure forces the metal into intimate contact with the die surfaces; this ensures faithful reproduction of detail, and a significant increase in the heat flow rate. The pressure also encourages any would-be shrinkage cavities to be forced with the vestiges of the liquid metal prior to complete solidification.
- e) The press ram is withdrawn to open the toolset when solidification has been completed. The component is then ejected and removed for the next cycle to begin.

There are many tooling concepts which may be used to utilise the benefits of pressurised solidification^{1,2,3,8}. The most usual form of the process is illustrated in Figure 1, which shows a backward extrusion mode of die filling during the tool closure. Other forms of the process may involve virtually zero displacement, or complex metal movement with backward and forward displacement.

The pressures which are used are expressed as the simple ratio load: projected plan area of the component. The value depends upon the component configuration, but generally falls within the range 31 MN/m² (2 tsi) to 108 MN/m² (7 tsi). Tall, slender components require higher pressures than those which tend to be more squat. It will be noted that this pressure range is lower than that used in forging aluminium alloys. The press capacity required to make sound components is therefore significantly lower than that needed for forgings. A single dieset only is required for squeeze forming, whereas several may be required for different stages of a forging process.

The pressure which is maintained throughout solidification encourages a particularly faithful reproduction of the dieset surface detail. The air gap which often forms at the mould/metal interface in other casting processes is suppressed, leading to a heat flow rate which is at least an order of magnitude greater than in gravity diecasting^{12,14}. Solidification times are therefore much shorter than in any process other than high pressure diecasting. Fine grained structures with small dendrite cell sizes result.

The dies are made of conventional hot working die steels such as H13. They are sprayed with a thin coating of a parting agent, e.g. graphite in water, before each cycle. The dies are kept at a controlled temperature; under heating leads to surface defects such as cold laps whereas overheating can lead to metal/mould reactions such as welding and soldering. Close temperature control can also optimise the inherently good dimensional reproducibility of the process.

The die temperature is usually in the range 200/250°C, and given adequate thermal control the dimensional tolerances can generally be held to 0.20 mm/100 mm (0.002 inch/inch). A slightly wider band is preferable if the component is to be heat treated, to allow for any possible distortional effects.

The most variable dimensions are those governed by the partline of the tools. This is because the final rest position of the die movement is determined by the amount of metal put into the die. Tolerances in this region are thus a function of metal metering accuracy.

There are several metal metering systems which may be employed in production - eg. automatic ladling or commercially available metal metering pumps. These will generally maintain a weight tolerance of 2% which is adequate for most applications. Particularly close control of across-the-partline dimensions can be achieved by the use of overflow systems built into the toolset.

Overflows may generally be avoided, and thus the process is capable of excellent material yield. Squeeze forming does not normally require a runner system, and the requirement for feeders is obviated by the pressurised mode of solidification. Therefore, except for limited machining operations (eg. bolt holes, critical parallel bores etc) or the removal of sharp edges, the metal which is placed into the die is used in its entirety.

3. EXAMPLE COMPONENTS

Circular shapes are ideally suited to the squeeze forming process, but a variety of non-axisymmetric configurations may be readily produced. As with all manufacturing processes, the best use of its capabilities is achieved when the component designer consults the squeeze forming operator at the earliest stage. Appendix 1 of this paper summarises the principle considerations for designing a squeeze formed component.

Components which have been made during the development programme range from 180 grammes to 34 kilogrammes in weight. The pilot plant of GKN Sankey will initially employ a 1500 tonneff. press more suited to the larger components: the lower weight limit should thus be regarded as 2 kg at present.

The early components were round in shape, because of the ease of maintaining working tool clearances at that stage of the development. Figure 2 illustrates a tank wheel made in the high strength 7075 alloy. This component was designed with a T-section for maximum structural efficiency of the metal. Tank wheels which are forged are usually L-section, because of the constraints of the forging process. This leads in this case to a squeeze formed product which is lighter by several kilogrammes than an equivalent forging. The design of the tank wheel is also one which gives a fairly even section in order to achieve a sensibly uniform pattern of solidification.

Wheels of this type have undergone extensive rig tests and are being subjected to arduous service evaluation. Work continues, but the structures are performing extremely well after a significant amount of service testing.

Split die technology can be employed to generate more complex shapes. Figure 3 shows an experimental car wheel form. A dieset with vertical splits was required in order to be able to make the externally undercut form of the tyre well. The wheel section shows a marked variation in sectional thickness within the one component, which was possible because the greatest sectional differences are in different planes. The effect of pressure can have a marked influence on the ability to feed limited sectional changes within the one plane.

Lateral holes can be incorporated into components by the use of retractable side cores. A prototype component made using this principle is shown in Figure 4. The initial feasibility of using disposable cores made of a soluble salt has also been shown. This type of core will enable more complex internal forms to be generated, to be considered against the machining of an internal feature.

Several components which are far from round have now been made. Two examples which are basically rectangular in form, are shown in Figure 5. Both of these components fit onto a prototype military bridging structure, the larger one by welding, and the smaller by bolting.

The components which have been made to date, some of which are illustrated in this paper, have been produced in a wide range of alloys. Squeeze forming can utilise material compositions which are both "casting" and "forging" types. The process may therefore be considered for components which are currently produced by various types of casting, forging, extrusion or fabrication. The ability to use the higher strength wrought-type alloy compositions is also quite important for structural applications, and when considering a possible change to aluminium from a steel or cast iron in order to save component weight. The range of alloys which have been examined is discussed below.

4. MECHANICAL PROPERTIES

Virtually the whole range of aluminium alloy types which are currently in use may be used to manufacture components by the squeeze forming process. To date, over 20 alloy compositions have been successfully squeeze formed. Table 1 is the current list, which includes 11 wrought alloy compositions, and many alloys which are heat treated after forming. The mechanical properties obtained from squeeze formings of all these alloys have been comparable to, and in some cases significantly better than, the mechanical properties of alloy components made by the conventional methods.

4.1 Casting Alloy Types:

Table 2 lists the tensile data obtained from five of the aluminium casting-type alloys studied in the squeeze forming programme. The figures quoted represent average values obtained from a number of tensile test pieces taken from actual squeeze formed components.

In the Table the tensile data are compared with the specified minimum properties for each alloy type and temper condition¹⁵, and with typical chill cast conventional properties¹⁵. It is clear from the Table that the mechanical properties of squeeze formed material are superior in all respects to those obtained from conventionally cast material. This is true for all eleven of the casting type specifications studied to date. The proof stresses have been improved by squeeze forming, and of particular significance is the marked improvement in the elongation to failure, which is a measure of the toughness and ductility of the material. These improvements reflect both the fine-grained structure and more importantly the elimination of microporosity in the squeeze formed material. This is illustrated in Figure 6 which

shows a photomicrograph of an LM25 alloy, as cast, taken from a squeeze formed component. There is clearly no sign of microporosity, and the secondary arm spacing of around 20 microns and average grain size of around 120 microns indicate a fine microstructure. The silicon phase in the microstructure appears in its modified morphology because of strontium additions to the melt. It is our experience that squeeze forming pressures are not sufficient alone to cause complete modifications of the silicon phase, particularly in the thicker sections.

The LM25 alloy shown in Figure 6 had an iron content of 0.40 wt %, and the mechanical property data given in Table 2 for squeeze formed LM25 also relates to material with this iron content. In conventional casting processes the presence of iron in aluminium alloys can reduce alloy ductility and impact resistance, due to the formation of coarse iron aluminide needles and other iron bearing phases in the alloy microstructures. Consequently when aluminium casting alloys are used to produce components where ductility and impact resistance are important, it is necessary to employ primary quality alloys with the iron content typically restricted to below 0.2 wt %. In squeeze forming the formation of coarse iron bearing phases is, however, prevented by the rapid solidification rates involved. Although intermetallic iron compounds are still present in the microstructure, they are very finely divided and so rendered relatively harmless. It is therefore possible to consider the possibility of squeeze forming critical components from secondary quality aluminium alloys.

Figure 7 shows the improvement obtained in fatigue properties for an LM25-T6 alloy when squeeze formed rather than conventionally cast. Samples for testing were cut from actual squeeze formed components, the testing being performed on a servohydraulic, constant strain amplitude fatigue machine. The iron content of the alloy was in this case 0.29 wt % Fe.

4.2 Forging Alloy Types:

Alloy specifications in three families of wrought aluminium alloys have been investigated. These include the standard specifications 2014 and 2024 (H15) in the AA.2000 series (Al-Cu base); 6061, 6066 and 6082 (H30) in the AA.6000 series (Al-Mg₂Si base); and 7020 (H17), 7050, 7075 and 7475 in the AA.7000 series (Al-Zn-Mg base). In addition the non standard alloys SF1 (Al-4Zn-2Mg) and SF3 (Al-5Zn-1Mg), have been extensively studied, both being weldable 7000 series type alloys.

Table 3 lists the tensile data obtained from some of these alloys in the squeeze formed conditions. These figures were acquired from samples cut from actual squeeze formed components. Table 3 also lists comparative tensile data for each alloy type after conventional forging operations¹⁶. It is important to be well aware of the inhomogeneities in properties which are introduced after forging operations. Table 3 therefore contains data for minimum tensile properties in the longitudinal and transverse directions for those alloys where this information was available.

Squeeze formed components are isotropic in their tensile properties, and are not subject to the directionality which often affects a forging. It may be seen from the data presented in Table 3 that in general the tensile properties of the squeeze formed alloy components compare extremely well with conventional forgings. In all cases, there is a good comparison between the isotropic squeeze formed tensile strength and 0.2% proof strength with those measured in the longitudinal direction of a conventional forging.

The ductility, as measured by the percentage elongation to failure, is, in fact, the only tensile property which is in any way inferior in squeeze formed material when compared with the longitudinal properties of forged material. This is a consequence of the isotropic nature of the microstructure of squeeze formed material, an example of which is shown in Figure 8 for alloy AA.6066 - as formed. The grain boundary precipitates seen in this microstructure cannot be removed totally by subsequent heat treatments, and clearly they do not have the favourable elongated appearance of precipitates in a longitudinal section of a forging. Consequently there is less scope for elongation of the structure prior to failure. However, it is important to note that conventionally forged material is much less ductile in its transverse direction than in the longitudinal direction. In fact, as may be seen from Table 3, the ductility values of squeeze formed material normally lie somewhere between the longitudinal and transverse values of conventionally forged material. Alloy development work with alloy SF1 (Al-4Zn-2Mg) has achieved good ductility values. Similar work is in progress with other forging alloys (e.g. AA.2014, Al-45Cu-Si-Mg-Mn) to improve their ductility.

The microstructure shown in Figure 8 is typical of the microstructures found in squeeze formed, forging grade aluminium alloys. The structure is equi-axed with a grain size of around 120 microns. Any intermetallic phases which form in the alloy are finely dispersed within the grain boundary precipitates, many of which disappear on subsequent solution heat treatment. The macrostructure of the component from which this photomicrograph was prepared is shown in Figure 9. Clearly the component was fully dense with no macro or micro-porosity and the structure was fine grained and equi-axed throughout.

Figure 10 gives a comparison of fatigue properties for two squeeze formed alloys with conventionally worked material (longitudinal direction). It is clear from the figure that the fatigue performance of the squeeze formed material was equivalent in both

cases to that of conventional material.

From the results presented in this section it seems fair to suggest that squeeze formed materials compare well with conventionally worked and forged material in all mechanical respect, and that they can be superior if isotropic properties are important. Particularly noteworthy is the ability to produce satisfactory components from AA.7000 series alloys which are the highest strength aluminium alloys currently available.

5. CORROSION AND STRESS CORROSION

Several components, and test pieces cut from components, have been subjected to various forms of corrosion testing.

Pieces of tank wheel in Al-5Zn-2Mg-Cu (AA.7075) alloy have been subjected to salt spray and hot chamber accelerated corrosion. The results are comparable with conventionally forged material.

Welded structures incorporating the larger bridge component in Al-4Zn-2Mg alloy have also been subjected to hot chamber accelerated corrosion, with satisfactory results. Examples of this welded structure have also been subjected to marine corrosion in a warm climate for over a year with no signs of problems.

Many test pieces of both Al-Zn4-Mg2 (SF1) and Al-Zn5-Mg2-Cu (AA.7075) in the T73 type of heat treatment condition have been subjected to stress corrosion susceptibility testing using a four-point bend method. The test laboratory was Ministry of Defence Q.A.D. approved.

The stress corrosion tests were carried out in hot saline medium, with stress in the outer fibres of 80% of 0.2% proof stress for the material. Satisfactory behaviour of several hundred hours survival has been observed for both alloy systems. The results with the Al-4Zn-2Mg alloy (SF1) have been correlated with service data for similar wrought material, and the results indicate a normal life expectancy of 20+ years.

It should be noted that the isotropic nature of a squeeze formed component indicates that satisfactory stress corrosion performance will be non-directional. This is not always the case with forgings, which can have marked variations for the longitudinal and short transverse directions.

Further work is in hand to substantiate the performance of alloy systems which are of interest to the aerospace industries eg. Al-Cu4.5-Si-Mg-Mn (AA.2014).

6. SPECIFICATIONS

Squeeze forming is a comparatively new manufacturing process. It is a hybrid casting/forging process, and as such does not comply with the full specifications and inspection standards for either forgings or castings made by traditional methods. Careful records are kept by GKN of all manufacturing conditions, component quality etc and work is in hand to compile full material specifications for compositional limits, spread of mechanical property results etc. Corroborative materials evaluation programme are also being conducted by certain potential customers.

It is therefore anticipated that a set of relevant specification and inspection standards will emerge in the fullness of time. Meanwhile, all products are subjected to rigorous inspection procedures and at least one component per heat treatment is taken for mechanical property evaluation. Several mechanical property test pieces are taken from different locations within the component, so that a mechanical test report can give both mean results and the standard deviation. A reasonable guarantee of minimum mechanical properties can thus be given.

7. CONCLUSIONS

- 1) Squeeze forming is a potentially powerful technique for manufacturing a wide range of aluminium components intended for structural applications. It combines the strength and confidence levels of forgings with the economics and shape capability of castings.
- 2) The process produces sound components with excellent finish and dimensional reproducibility, and with very good material utilisation.
- 3) A wide variety of component shapes and geometries have been successfully squeeze formed, with component weights ranging from 180 gms to 34.0 kg.
- 4) The squeeze forming process has been successfully applied both to casting grades and wrought grades of aluminium alloy.
 - a) For casting alloys the mechanical properties of the squeeze formed material were found to be superior in all respects to conventionally cast material. There were particularly large improvements in ductility, toughness and fatigue performance. In addition it was found that squeeze formed material was far less susceptible to the embrittling effects of iron compounds than was conventionally cast material,

due to the rapid solidification rates involved.

- b) For wrought grade alloys it was found that the mechanical properties of squeeze formed material were comparable with those of forged material particularly when the anisotropy of the latter were taken into account. Squeeze formed material has isotropic mechanical properties.

8. ACKNOWLEDGEMENTS

The author wishes to thank the management of GKN Technology Ltd and GKN Sankey Ltd for the facilities provided, and permission to publish this paper.

7. REFERENCES

1. G Williams and K M Fisher. "Solidification Technology in the Foundry and Casthouse", Conference, 1980, Metal Society. Proceedings to be published.
2. G Williams and K M Fisher. Metals Technology. July 1981, p.263.
3. G Williams, J Barlow, K M Fisher, P H Evans and L F Taylor. Int. Congress held on Metals Engineering. University of Aston in Birmingham. September 1981.
4. Y Kaneko, H Murakami, K Kuroda and S Nakasaki. 10th SDCE International Die Casting Congress, 1979, Society of Die Casting Engineerings Inc. Also Foundry Trade Journal 1980, 148 (3183), 397.
5. J C Benedyk; 6th SDCE International Die Casting Congress, November 1970, Paper 86, Society of Die Casting Engineerings Inc.
6. K M Kulkarni. Foundry Man. Technol. August 1974, 76.
7. R F Lynch, R P Olley and P C J Gallagher. Trans. AFS. 1975, 83, 569.
8. V M Plyatskii. Extrusion Casting. 1975 New York, Primary Sources.
9. V P Severdenko and T P Mallei. Dukl, Akad, Nauk, SSSR. 1961, 5.253.
10. A F Astashov and S I Tishaev. Kuznechno-Shtampov. 1967 (8), 16.
11. B B Gulyaev et al. Literino Proizvod, December 1960, 12, 33.
12. S Chatterjee and A A Das. Br. Foundryman, 1973, 66 (4), 118.
13. L W Chambers. Foundry Trade Journal, 1980, 148 (3187), 802.
14. V Nishida and H Matsubara. Br. Foundryman. (1976), 69, 274.
15. The Properties of Aluminium Casting Alloys. (1971). Handbook of the Association of Light Alloy Refiners and Smelters, U.K.
16. Aluminium Standards and Data (1976). The Aluminium Association U.S.A.

APPENDIX 1

GUIDE TO DESIGN CONSIDERATIONS FOR SQUEEZE FORMED COMPONENTS

1. MATERIALS:

A wide range of aluminium alloys may be considered for squeeze forming applications (see mechanical property data provided).

2. SIZE of COMPONENT:

The largest component made to date is a large vehicle wheel - 720 mm diameter and weighing 34 kg.

The largest projected area of component should be currently considered as 483870 sq.mm (750 sq. ins) but in due course LARGER components can be considered.

The lower weight limit should be considered as 2 kg at present, because of the production equipment available.

3. SECTION THICKNESSES:

The sectional thicknesses permitted in the component are very much particular to each case. In general terms, sections in the range 3-50 mm are permissible. Components should be designed to have fairly even sections in order to balance the solidification process heat flow. In certain cases, however, it will be possible to combine thin and heavy sections in the one component, especially if a slight element of central porosity can be tolerated.

4. SHAPES:

Circular shapes are the easiest to produce, and usually imply lower tool costs.

Square and rectangular shapes have been made successfully and more complex shapes can be considered on merit.

The usual considerations of mechanical design should be borne in mind with respect to minimising stress raisers etc.

Extraction of the component is eased by tapers, generally of the order of 2° . These should be allowed for in the component design. The seal of the toolset relies on a parallel fit of punch and die, and so no taper is necessary at this point.

5. CORES:

Simple side cores can be used to effectively generate through holes and external undercut forms (cf. tubeless wheel form, and yoke).

Recent experiments with disposable cores indicate that there is some potential for generating long holes and more complex internal profiles, but the cost penalties must be considered.

6. CAST-IN INSERTS:

Squeeze forming is particularly effective in achieving good bonding of cast-in inserts.

The process has also been used to cast-in steel and iron rings, and electric heating elements.

7. DIMENSIONAL TOLERANCES:

General tolerances before heat treatment can be 0.20 mm/100 mm (0.002 inch/inch) but wider limits should be aimed for to minimise possible production problems and allow some heat treatment distortion.

Dimensional tolerances across the partline will need to be greater, because of the control requirements on the supply of liquid metal. Thickness dimensions across the partline should be opened to ± 0.25 mm tolerance.

8. SURFACE FINISH:

The squeeze forming process ensures that the component largely mirrors the surface texture which is on the die, even to the point of picking up the smallest of scratch marks. Textured die finishes will therefore be well produced.

The dies are at present treated with a graphitic release agent, which stains the components. An oxide film is produced during heat treatment. It will be usual therefore to bead-blast the surface as a finish treatment: this can be quite a fine process, bringing out the surface detail, or a coarse finish to mask minor blemishes etc.

TABLE 1. ALUMINIUM ALLOYS WHICH HAVE BEEN SQUEEZE FORMED TO DATE

<u>A. CASTING TYPE</u>		<u>B. FORGING TYPE</u>		
<u>BS 1490</u>		<u>AA Alloy Number</u>		
LMO	Al-99.5%	2014	Al-Cu4½MgMnSi	British Equivalent H15
LM4	Al-Si5Cu3	2024	Al-Cu4½MgMn	
LM5	Al-Mg5	3004	Al-Mn-Mg	British Equivalent H20
LM13	Al-Si11MgCu	6061	Al-SiMgCuCr	
LM18	Al-Si5	6066	Al-Si1MgMnCu	
LM25	Al-Si7Mg	6082	Al-Si1MgMn	British Equivalent H30
		7018	Al-Zn5Mg1	
		7050	Al-Zn6Mg2½Cu2½	
		7075	Al-Zn5½Mg2½-Cu1½	
<u>AA Alloy Number</u>				
C355.0 Al-Si5MgCu				
		<u>Others</u>		
		Hiduminium 48	Al-Zn4½-Mg2½	
		S.F.1	Al-Zn4Mg2	

TABLE 2. TENSILE DATA FOR SQUEEZE FORMED MATERIAL (CASTING-TYPE ALLOY)S COMPARED WITH CONVENTIONAL PROPERTIES OF CHILL CASTINGS.

ALLOY DESIGN.	APPROXIMATE COMPOSITION	TEMPER COND'N.	MECHANICAL PROPERTIES OF SQUEEZE FORMED MATERIAL			COMPARABLE PROPERTIES OF CONVENTIONALLY CHILL CAST MATERIAL		
			O.2% PS MNm ⁻²	UTS MNm ⁻²	ELONGATION %	O.2% PS MNm ⁻²	UTS MNm ⁻²	ELONGATION %
LM4	Al-5Si-3Cu	M	152	197	5		>160 200	>2 3
LM5	Al-5Mg	M	142	250	14	100 >90 90	>170 230	>5 10
LM13	Al-11Si-Mg-Cu	TF	295	325	3	- 280	>280 290	- 1
LM18	Al-5Si	M	103	187	13	>60 80	>140 150	>4 6
LM25	Al-7Si-Mg	M	124	195	15	>80 90	>160 180	>3 5
		TE	165	235	7	>130 150	>190 220	>2 2
		TF	250	300	10	>220 240	>280 310	>2 3

Temper condition: M = as formed; TE = solution treated and stabilised; TF = solution treated and aged to maximum strength

TABLE 3. TENSILE DATA FOR SQUEEZE FORMED MATERIAL (FORGING TYPE ALLOYS) COMPARED WITH CONVENTIONAL PROPERTIES OF FORGED MATERIAL.

ALLOY DESIGN.	APPROXIMATE COMPOSITION	TEMPER COND'N.	MECHANICAL PROPERTIES OF SQUEEZE FORMED MATERIAL			COMPARABLE PROPERTIES OF CONVENTIONALLY FORGED MATERIALS			
			O.2% PS MNm ⁻²	UTS MNm ⁻²	ELONGATION %		O.2% PS MNm ⁻²	UTS MNm ⁻²	ELONGATION %
AA 2014	Al-4.5Cu-Si-Mg-Mn	T6	465	489	4	Die Forgings (Long.) Minimum properties (Trans.) Typical long. properties	>379 >372 414	>434 >434 483	>6 >2 13
AA 2024	Al-4.5Cu-Mg-Mn	T4	310	445	10	Plate - Minimum properties Typical long. properties	>276 324	>427 469	>12 20
AA 6061	Al-lMg-lSi-O.5Cu-Mn	T6	325	335	8	Die Forgings (Long.) Minimum properties (Trans.) Typical long. properties	>241 >241 276	>262 >262 310	>7 >5 12
AA 6066	Al-lMg-1.5Si	T6	385	405	5	Die Forgings (Long.) Minimum properties Typical long. properties	>310 .. 359	>345 .. 393	>8 .. 12
AA 6082	Al-lMg-lSi-lCu-Mn	T6	260	285	7	Forging stock and forgings Typical long. properties	255 ..	295 ..	18 ..
AA7075	Al-5Zn-2Mg-Cu	T6	525	565	6	Die Forgings (Long.) Minimum properties (Trans.) Typical long. properties	>427 >414 503	>503 >483 572	>7 >2 11
SF1	Al-4Zn-2Mg	T73	415	455	4	Die Forgings (Long.) Minimum properties (Trans.)	>379 >359	>441 >421	>7 >2
		Non Std. T6/T73	335	385	10	Forgings (Long.) Minimum properties (Trans.) Typical long. properties	>330 >310 350	>385 >370 400	>8 3 10
SF3	Al-5Zn-lMg	Non Std. T6/T73	340	370	13	Plate - Minimum properties Typical long. transverse Properties.	>260 300	>320 360	>8 12

Temper condition: T6 = solution treated and aged to maximum strength; T73 = solution treated, doubled aged to maximise corrosion resistance; T6/T73 = heat treated; modified to maximise stress corrosion resistance in these alloys.

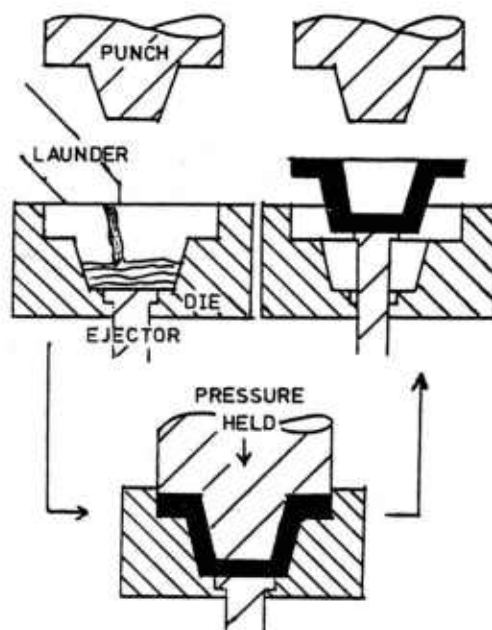


FIGURE 1. Representation of Squeeze Forming Process: Backward Metal Extrusion.



FIGURE 2. Tank wheel made in high strength AA 7075 type alloy. Wheels of up to 34 kg have been formed. Note the soundness in the component section shown.

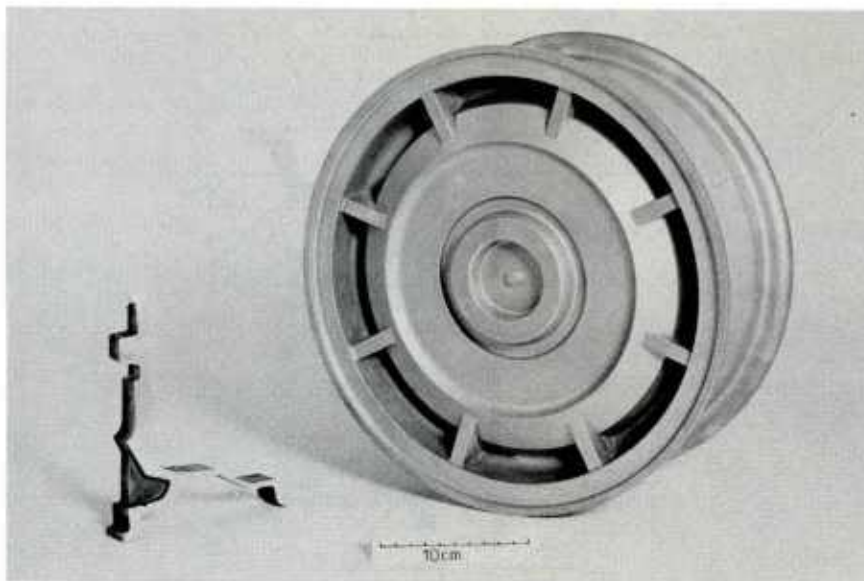


FIGURE 3. Prototype car wheel made by Squeeze Forming, to illustrate the undercut form capability. Note the complex cross-section, thickness ranging from 2.5 mm to 24 mm. Formed in LM25 alloy.

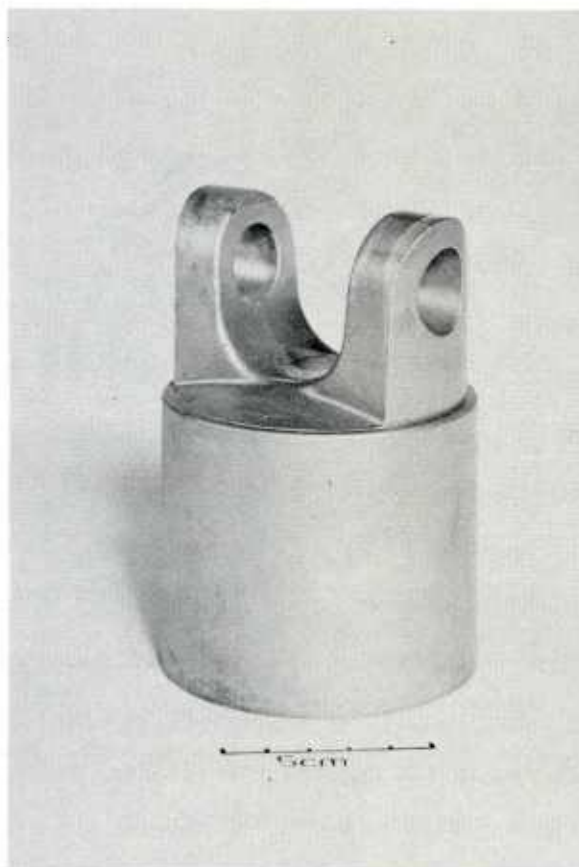


FIGURE 4. Prototype Hooks Joint Component. This illustrates the use of sliding cores for lateral through-holes. Made successfully in a range of casting and forging alloys. Component weight: 0.9 kgs.

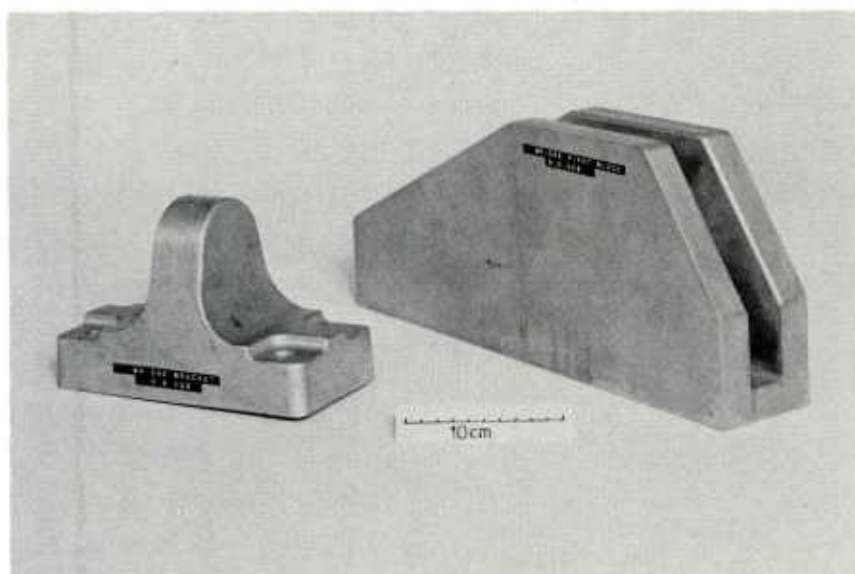


FIGURE 5. Two rectangular form components, made in a weldable Al4Zn2Mg alloy of relatively high strength, which forms part of a prototype military bridge. The smaller bracket component has been made in a variety of alloy systems for material evaluation purposes.

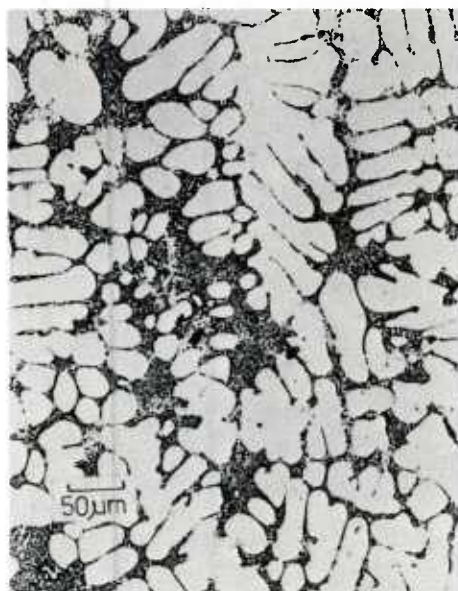


FIGURE 6. Photomicrograph of Squeeze Formed LM25 alloy sample. As formed. Etched.

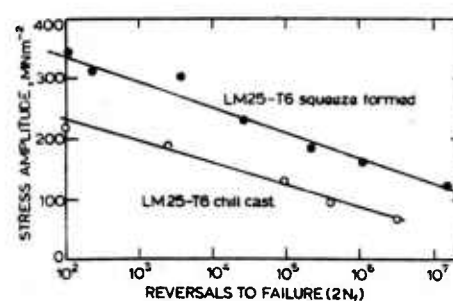


FIGURE 7. Fatigue data for casting alloy LM25-T6; squeeze formed and conventionally cast conditions.



FIGURE 8. Photomicrograph of a squeeze formed AA 6066 alloy sample. As formed. Etched.

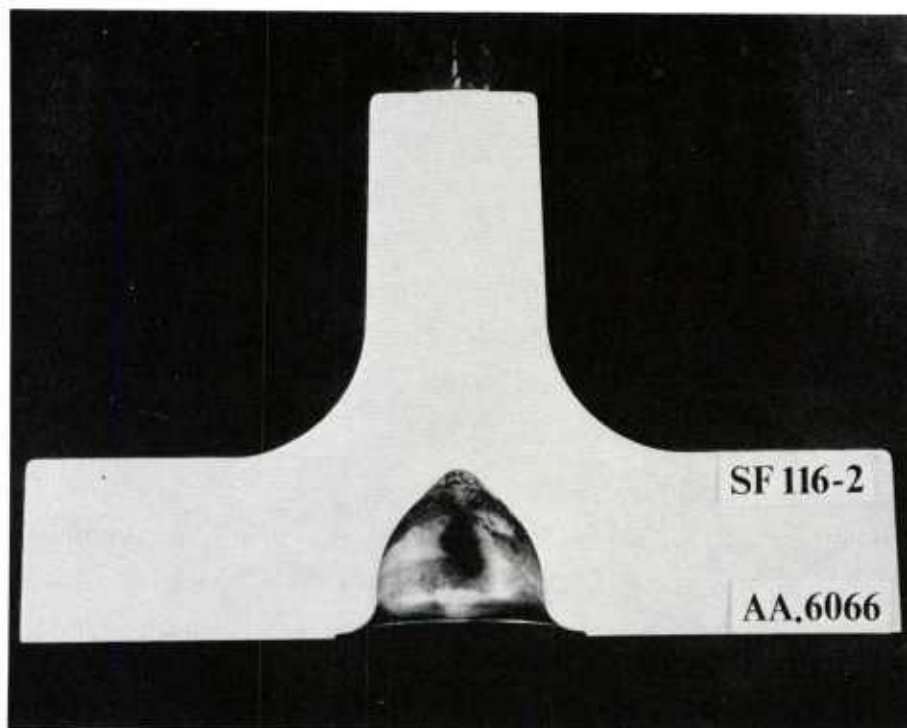


FIGURE 9. Etched macrostructure of longitudinal half section of a bracket component. As formed. Alloy AA 6066.

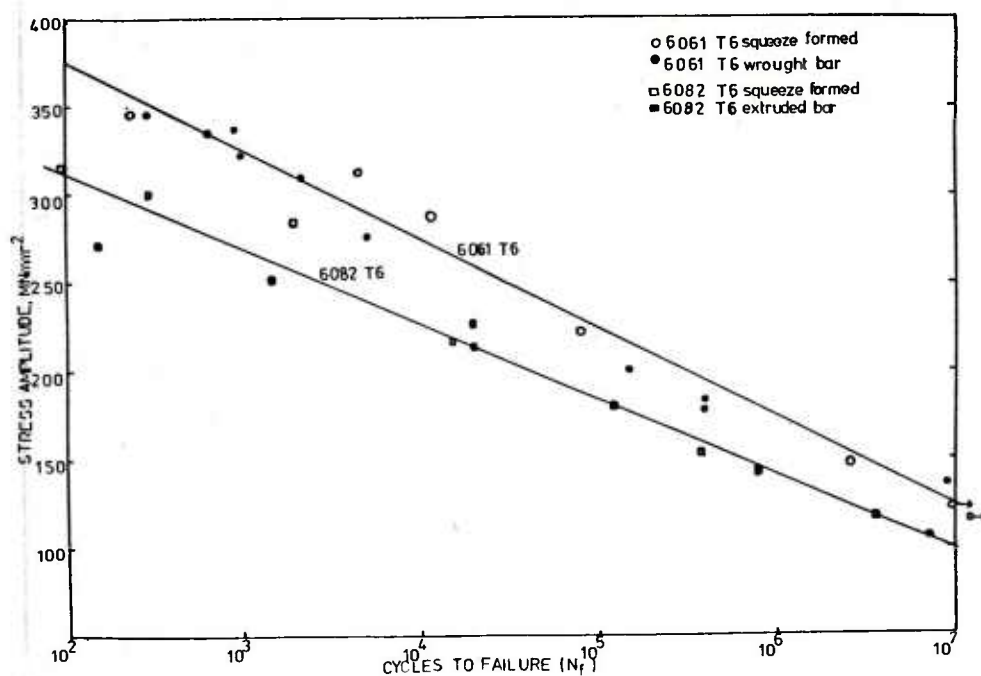


FIGURE 10. Fatigue data for two "forging-type" alloys: squeeze formed and conventionally worked material.

DERNIERS DEVELOPPEMENTS DE LA COULEE EN SABLE SOUS BASSE PRESSION ADAPTES
A LA REALISATION DE GRANDES PIECES DE STRUCTURES AERONAUTIQUES

par
GEORGES BROIHANNE
Ingénieur
MESSIER FONDERIE D'ARUDY
ARUDY
64260
FRANCE

RESUME -

La coulée en sable sous basse pression développée par la Société MESSIER FONDERIE D'ARUDY pour des pièces de grandes dimensions doit permettre d'envisager maintenant la réalisation en fonderie, d'ensembles structuraux monoblocs conçus auparavant par assemblage des tôles ou de pièces usinées.

Ce mode de coulée offre en effet des possibilités supérieures à la coulée classique par gravité :

- remplissage de toiles fines sur de grandes surfaces,
- santé métallurgique accrue même pour des pièces complexes,
- parfaite reproductibilité des conditions de coulée,
- possibilité de couler des pièces complexes en alliages à hautes caractéristiques

La conception en fonderie de telles pièces se heurte à l'heure actuelle dans les Bureaux d'Etudes :

- au "Casting factor"
- au manque de résultats en tenue en fatigue des pièces moulées,
- à la nécessité de concertation dès le stade de l'avant projet, avec un petit nombre de fondeurs qualifiés pour optimiser coût et poids.

1)- SCHEMA CLASSIQUE DE LA COULEE SOUS BASSE PRESSION -

1.1.- Une machine à couler sous basse pression se compose (voir schéma n° 1) :

- d'un four de maintien étanche (a) soumis à une surpression interne de l'ordre de 0,2 à 1,5 bar contenant un creuset rempli de métal liquide,
- d'un dispositif de remplissage composé d'un tube plongeur (b) en fonte et d'une buse d'injection (c) assurant le transfert du métal liquide du creuset vers le moule,
- d'un dispositif pneumatique (d) de mise en pression du four étanche au moyen d'air ou d'un gaz neutre,
- d'une superstructure (e) supportant le moule et comportant un ou plusieurs orifices de remplissage.

1.2.- Les différentes étapes de la coulée sont les suivantes (voir schéma n° 2) :

- Mise sous pression progressive du four permettant de faire monter le métal dans le tube,
puis dans la pièce (à partir du point A) avec une vitesse ascensionnelle en relation directe avec cette mise en pression,
- application d'une surpression dès la fin du remplissage du moule (à partir du point B),
- maintien de cette surpression pendant une durée au moins égale à la solidification de la pièce (jusqu'au point C),
- relâchement de la pression du four, ce qui a pour effet de faire redescendre dans le creuset le métal non solidifié dans le tube et la buse de coulée.

1.3.- Il est important de noter :

- que le remplissage du moule doit être non turbulent pour éviter la formation d'oxydes ou de soufflures dans les pièces,
- que le moule doit comporter des orifices d'évacuation d'air assurant un bon remplissage par le métal en évitant toutefois les fuites de métal lors de l'application de la surpression,
- que la solidification doit débuter dans la pièce sur les parties les plus éloignées des amenées du métal, se produire dans la pièce de proche en proche jusqu'à ces amenées, et se terminer enfin au niveau des buses d'injection qui seront le siège de la contraction de solidification.

Cette condition (solidification dirigée) permet d'assurer la mise en pression constante du métal de l'empreinte par les amenées du métal qui jouent ainsi le rôle de masselottes utilisées dans la coulée par gravité.

.../...

II)- PERFECTIONNEMENTS APPORTES POUR SATISFAIRE A LA REALISATION DE PIECES AERONAUTIQUES

2.1.- Les machines à couler sous basse pression ont été conçues et réalisées depuis une quinzaine d'année pour la coulée en moules métalliques de pièces de qualité standard :

- roues et culasses d'automobiles,
- carcasses de moteurs électriques,
- carters d'embrayage, etc...

La coulée sous basse pression se justifiait essentiellement :

- par son intérêt économique (réduction de la masse du système de coulée),
- par son automatisé permettant la réalisation de grosses pièces et l'amélioration des conditions de travail.

2.2.- La complexité des pièces aéronautiques, leurs faibles séries et leurs qualités métallurgiques sont souvent incompatibles avec la coulée en coquille.

Les amenées du métal sont en effet d'autant plus nombreuses que la qualité demandée est grande, (car elles jouent le rôle de masselottage) et leur démoulage est souvent quasi impossible en moule permanent (coquille).

C'est pourquoi MESSIER FONDERIE D'ARUDY a développé la coulée en sable sous basse pression pour satisfaire à toutes ces exigences.

2.3.- Le développement de ce procédé pour la réalisation de pièces aéronautiques a conduit :

- à l'amélioration des machines existantes en vue d'obtenir une vitesse de remplissage programmable et reproductible pour chaque type de pièce (systèmes de régulation),
- à l'adaptation de ces machines à la coulée de moules sables pouvant peser plusieurs tonnes,
- à définir des règles de conception des systèmes d'amenée de métal dans l'empreinte (sections des attaques de coulée en fonction des épaisseurs de pièces, position et forme des refroidisseurs métalliques inclus dans les moules sable, systèmes de filtrage des oxydes, systèmes d'évacuation de l'air etc...)
- à définir des conditions de préparation des moules avant la coulée (induction des moules, préchauffage, etc...).

2.4.- MESSIER FONDERIE D'ARUDY s'oriente de plus en plus vers les moules composites sable-céramique-parties métalliques :

- le sable est utilisé dans les zones d'amenée du métal ainsi que dans les zones non désignées de la pièce en raison de son coût peu élevé,
- la céramique est utilisée dans les parties de la pièce pour lesquelles un bon état de surface ($R_a = 6,3 \mu$) est demandé ainsi que dans les zones où des formes indéformables de la pièce sont obtenues par des parties de modèle fusible,
- les parties métalliques (coquilles ou refroidisseurs) sont utilisées dans les zones critiques des pièces pour lesquelles de hautes caractéristiques sont demandées,
- des inserts métalliques, même très complexes (tubulures de refroidissement) peuvent être noyés dans le métal au moment de la coulée.

III)- CONSEQUENCES DES PERFECTIONNEMENTS APPORTES A LA COULEE BASSE PRESSION -

3.1.- Grande reproductibilité des conditions de coulée :

- température de coulée parfaitement maîtrisée (régulation du four),
- vitesse de remplissage parfaitement maîtrisée (régulation du débit d'admission de gaz dans le four),
- surpression après remplissage parfaitement maîtrisée (par le même système de régulation).

3.2.- Gradient thermique facile à diriger :

Dans un moule isolant (sable ou céramique), il est plus facile de maintenir liquides, le plus longtemps possible, les attaques de coulée (jouant le rôle de masselottage) tandis que la solidification de la pièce peut être accélérée par l'utilisation de refroidisseurs métalliques.

3.3.- Grande surpression d'alimentation :

Cette surpression appliquée par les attaques de coulée sur le métal liquide de la pièce dès la fin du remplissage est de l'ordre de 300 à 500 mbar, ce qui correspondrait à l'effet de masselotte de 1,6 à 2,5m de hauteur.

Cette grande valeur améliore considérablement la compacité des pièces. Elle est rendue possible par un revêtement appliqué sur les moules empêchant la pénétration du métal dans le sable.

3.4.- Possibilité de couler des alliages à hautes caractéristiques :

- Certains alliages au Cu, Zn, Ag présentant sur éprouvettes coulées de très hautes propriétés mécaniques qu'il est très difficile d'obtenir sur pièces réelles en raison de leurs difficultés d'alimentation par la technique classique de coulée par gravité. Les propriétés mécaniques sur pièces réelles sont alors affectées par le faible niveau de santé interne, faisant perdre à ces alliages leur intérêt au profit d'alliages classiques (AS7G06 ou A357) plus faciles à couler.

- La coulée sous basse pression a permis l'utilisation de ces alliages à très hautes caractéristiques, la suppression d'alimentation élevée permettant garantir la santé interne et de maintenir ce niveau de propriétés sur pièces réelles.

IV)- APPLICATION A LA REALISATION DE PIECES DE STRUCTURES D'AVIONS FINES, DE FORMES COMPLEXES & DE GRANDES DIMENSIONS -

4.1.- La reproductibilité des conditions de coulée, la facilité de diriger le gradient thermique et la grande valeur de la surpression appliquée au métal pendant la solidification ont permis :

- a)- l'obtention de voiles minces sur de grandes surfaces (par exemple 2,5mm \pm 0,5 pour des moules sable de 3m de long et 1,5 à 2mm pour des moules ou parties de moules céramique),
- b)- d'excellentes caractéristiques mécaniques rendues possibles par l'emploi de refroidisseurs métalliques inclus dans les parties de moule sable ou céramique et accélérant localement la vitesse de solidification,
- c)- une excellente santé métallurgique même sur des alliages difficiles à très hautes caractéristiques mécaniques.

4.2.- Cependant tous avantages n'ont été exploités que très partiellement :

En effet les constructeurs d'avions de cellules ou de moteurs se heurtent encore à un certain nombre de difficultés :

- a)- Casting factor : Ce coefficient de sécurité pour le dimensionnement est imposé par une réglementation américaine très ancienne (FAR 25) à tout concepteur de pièce coulée, ce qui conduit à l'alourdir et à réduire son intérêt par rapport à une pièce remplissant la même fonction et obtenue par une autre technique de mise en forme,
- b)- Les essais grandeurs : ces essais statiques ou de fatigue sur pièces réelles sont entrepris à l'heure actuelle par quelques sociétés qui, conscientes de l'intérêt économique de la solution fonderie, veulent homologuer un petit nombre de fondeurs de qualité pour la réalisation de pièces structurales peu sollicitées. La multiplication de tels essais (bien que fort onéreux) devrait permettre de mieux évaluer le comportement des pièces en utilisant (ce que des essais destructifs sur éprouvettes sont impuissants à traduire) et conduire à la réduction du casting factor),
- c)- Le manque de résultats concernant la corrélation entre la tenue en fatigue et :
 - l'état de surface des pièces de fonderie,
 - la santé métallurgique,
 - l'allongement à rupture,

Des essais sont également entrepris sur des grands nombres d'éprouvettes représentant des parties travaillantes de pièces (raccordement de nervures, raccordement de toiles, brides, etc...) ou des petites pièces pour mieux apporter aux concepteurs les éléments qui permettraient :

- de réduire le casting factor,
- de limiter les essais grandeurs.

V)- CONCLUSION -

La fonderie se présente comme le moyen de mise en forme qui permet le mieux l'économie de matière première.

Elle peut, dans un proche avenir, espérer apporter des solutions à la réalisation de structures monoblocs obtenues auparavant :

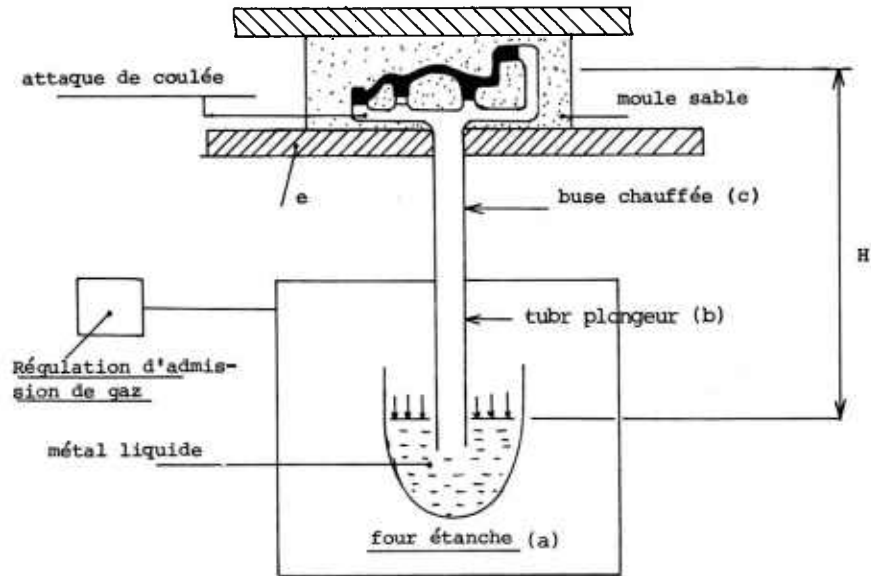
- par usinage dans la masse,
- par mécano-assemblage de tôles ou pièces usinées,
- par matriçage puis usinage,

dans la mesure où il est possible d'atteindre des épaisseurs fines et une grande fiabilité sur le plan métallurgique.

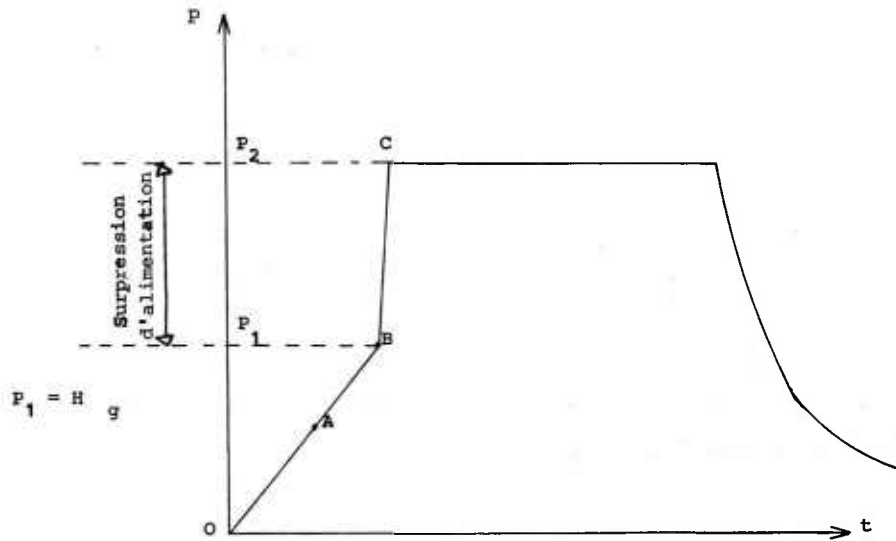
Malgré l'avantage intrinsèque des matériaux corroyés sur les matériaux coulés, il est d'ores et déjà possible de concevoir des pièces coulées plus rigides et moins lourdes qu'un assemblage de tôles ou de pièces usinées remplissant la même fonction.

Une concertation entre les Bureaux d'Etudes et la Fonderie est une absolue nécessité dès le stade de l'avant projet pour arriver à ce résultat et ainsi optimiser coût et poids.

Les pièces décrites en annexe sont le fruit de cette collaboration.

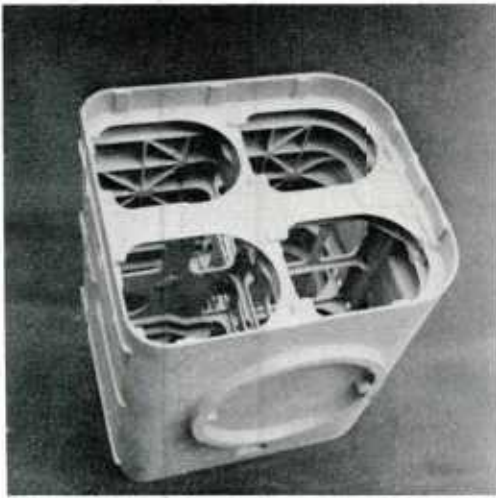


SCHEMA n° 1

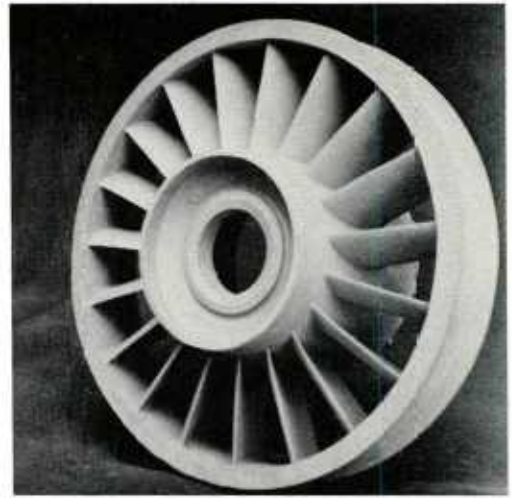


SCHEMA n° 2

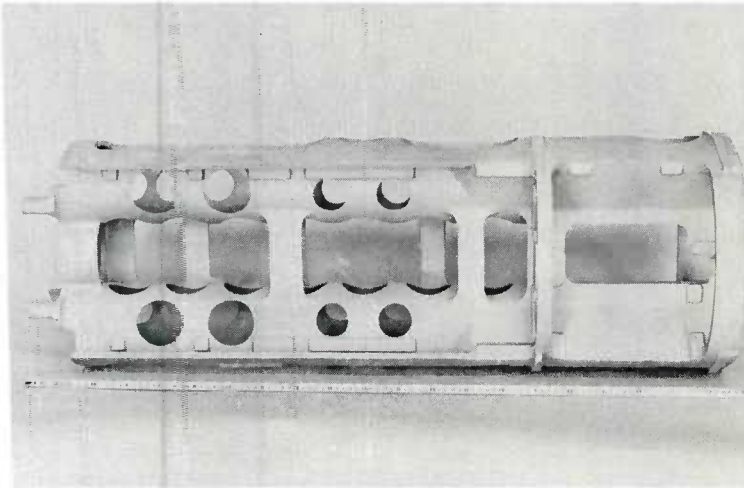
CYCLE DE PRESSION DANS L'ENCEINTE DU FOUR POUR CHAQUE COULEE



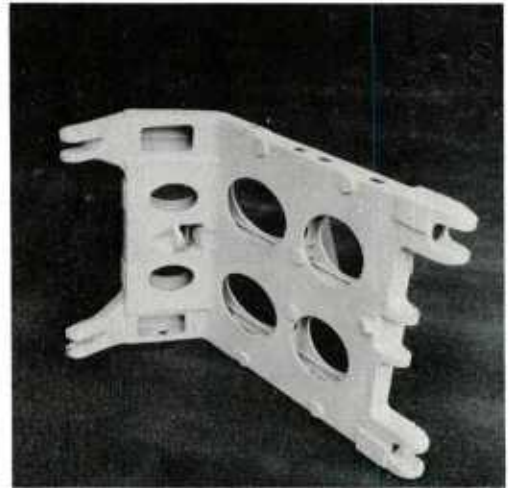
Support de 4 missiles HOT en AS7G06 (A 357-0)
coulé sous basse pression - Poids : 23,5Kg -
Dimensions : 550 x 550 x 580mm -
Toiles épaisseur : 3mm
Caractéristiques mécaniques en zones désignées :
R > 280 Mpa EO.2 > 220 Mpa A > 3%



Redresseur d'entrée d'air pour moteur ASTAFAN
en AS7G06 (A 357-0) coulé sous basse pression-
Dimensions : Ø 700 - H: 250mm - Poids : 26,5Kg
2 tubes inserts dans chaque aube
Caractéristiques mécaniques en zones désignées:
R > 280 Mpa EO.2 > 220 MPa A > 3%



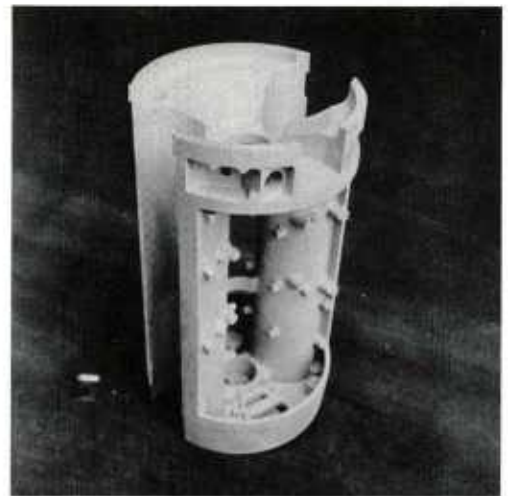
Support de missile KORMORAN en AS7G06 (A 357-0)
coulé sous basse pression.
Dimensions : Ø 350mm - H : 1050mm -
Toiles épais. 3,5mm - Poids : 20 Kg -
Caractéristiques mécaniques en zones désignées:
R > 280 MPa EO.2 > 220 MPa A > 3%



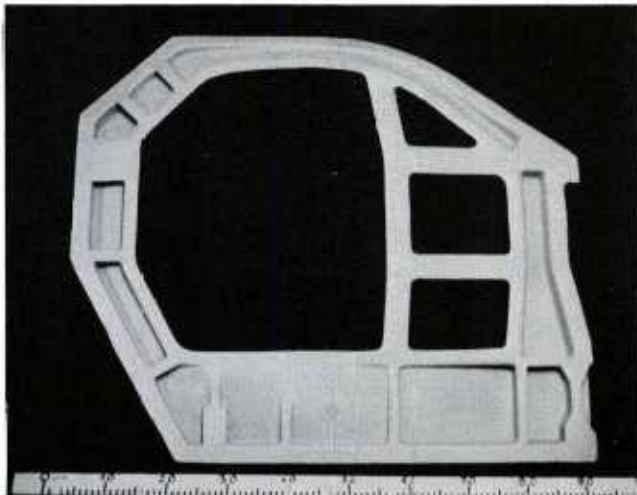
Bras de Porte de l'AIRBUS A 200 coulé en
sable en AS7G06 (A 357-0) sous B.Pression -
Dimensions : 600x500x350mm - Poids : 10Kg -
Epaisseurs de toiles : 3mm -
Caractéristiques mécaniques en zones désignées:
R > 280 MPa EO.2 > 220 MPa A > 3%



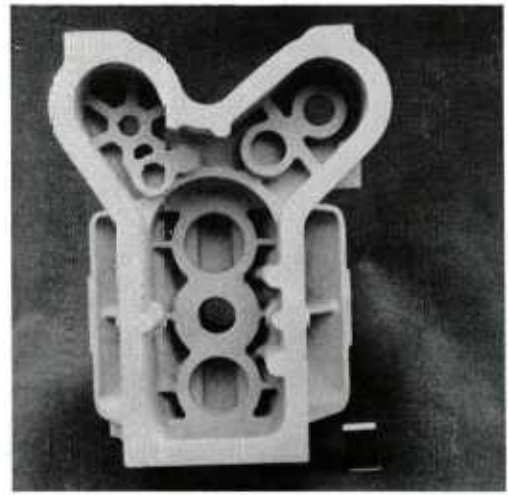
Ossature de Missile AM 39 : Case AV coulée
en sable sous basse pression en AS7G06
(A 357-0) . Poids : 15Kg
Dimensions : \varnothing 350 mm x 730mm
Caractéristiques mécaniques en zones désignées :
R $>$ 280 MPa EO.2 $>$ 220 MPa A $>$ 3%



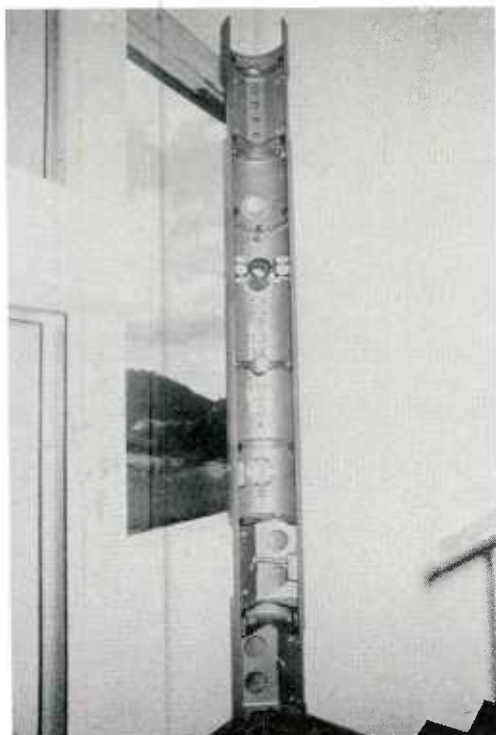
Ossature de Missile AM 39 : Case AR coulée
en sable sous basse pression en AS7G05
(A 357-0) - Poids : 10,2 Kg -
Epais. de toiles après usinage des tuyères: 1,7mm
Caractéristiques mécaniques en zones désignées
R $>$ 280 MPa EO.2 $>$ 220 MPa A $>$ 3%



Ossature de Trappe Mir 111 en AS7G06 (A 357-0)
coulée en sable sous basse pression - Poids: 10,5Kg
Dimensions : 1000 x 850 x 80mm
Toiles épaisseurs : 4mm - Bossages épais. 40mm-
Caractéristiques mécaniques en zones désignées:
R $>$ 280 MPa EO.2 $>$ 220 MPa A $>$ 3%



Carter d'entrée pour moteur ASTAZOU coulé en
AS7G05 (A 357-0) sous basse pression.
Dimensions : 470 x 260 x 360mm
Poids : 14,500 Kg
Caractéristiques mécaniques en zones désignées:
R $>$ 280 MPa EO.2 $>$ 220 MPa A $>$ 3%



Réservoir Pendulaire de Kérosène

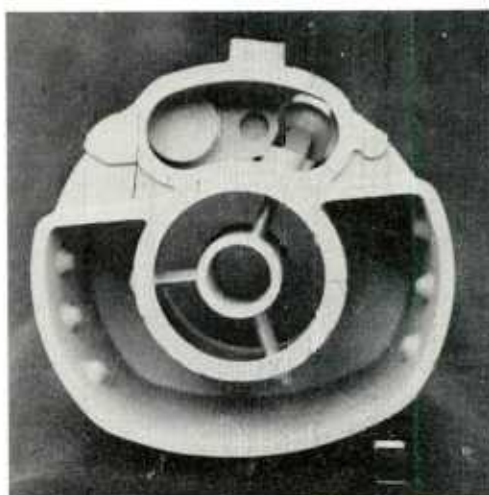
Coulé en 3 éléments en sable sous basse pression
alliage : AS7G06 (A 357-0)

longueur totale : 4020mm - Diamètre : 417mm -

Poids de l'ensemble à l'état brut : 289 Kg

Caractéristiques mécaniques mini en zones désignées :

R > 280 MPa EO.2 > 220 MPa A > 3%



Carter d'entrée pour moteur MAKILA coulé en
AS7G06 (A 357-0) sous basse pression.

Dimensions : \varnothing 550 mm - H : 260 mm

Poids : 16 Kg

Caractéristiques mécaniques mini en zones désignées

R > 280 MPa EO.2 > 220 MPa A > 3%



Roue axiale pour moteur ARBIZON 1V en AU4Z3G coulée en coquille
sous basse pression avec noyaux céramique et empreintes de palas
obtenues par cire perdue.

Dimensions : \varnothing 237 mm - H : 180 mm - Poids : 4 Kg -

Caractéristiques mécaniques mini en zones désignées :

R > 380 MPa EO.2 > 320 MPa A > 3%

New Developments in Aluminium and Titanium investment castings

Dr. Günther Wedeking - Titan-Aluminium-Feinguß GmbH, Postfach 280, 5780 Bestwig

Continuing increase in the requirement of improved technological properties of castings result, in many cases, in superseding conventional casting processes by special technologies. This general development naturally includes the investment casting process of light metal alloy castings.

Aluminium and Titanium are most important basic materials in modern aircraft construction. What contribution can be made by aluminium investment castings to the manufacture of aircraft units and what can be expected of them.

Integral construction is one of the features of modern aircraft construction. This involves limiting the expensive assembly of individual parts to a minimum. In this respect investment casting has proved to be an especially efficient moulding process as it combines considerable cost savings in material, assembly and machining with the unsurpassed degree of freedom it gives to the designer of the individual casting. On the other hand the investment casting process has to compete with other moulding processes in respect of the technological aspects of a component. Of these, tolerances, achievable dimensions and wall thicknesses of a component and, above all, the strength of the material are essential.

1. Achievable component sizes and tolerances

In comparison to other casting processes the tolerances obtainable in investment casting are excellent and represent more a question of tooling expense than a problem.

Since its introduction continual demands have been made on the light metal investment casting process with regard to the size of component required of it. This is a trend which apparently remains constant. The possibility, offered by investment casting, of producing complex components integrally as a single casting is being increasingly exploited. This exploitation is in line with the progress made by foundry technology in obtaining higher mechanical parameters and to the increasing adoption of integral construction as an economic means of production. Component sizes at present obtainable depend to a great extent on the capacity of the individual investment casting foundry. Formerly handling of a standard cluster presented personnel with no great problems. In the meantime, however, it has become so large and heavy that handling has to be carried out by manipulators. This has meant increasing the strength of the ceramic both to support the load of the cluster itself and also to absorb the metallostatic casting pressure. The manufacturers of investment castings have come to terms with increasing component sizes and will have to continue making adjustments. One metre would be a typical investment casting dimension at present.

2. Mechanical properties and attainable wall thicknesses

The contingencies of the process itself, namely the pouring of molten metal into a heated ceramic shell and the problem of controlling the cooling of the casting or of the shell during solidification meant that a development period was required before aluminium investment castings could achieve the mechanical properties which are, today, more or less taken for granted in other casting processes, e.g. sand casting. However, the values shown in table 1a can be considered as representing thin walled investment castings as they are currently required for structural parts in aircraft construction. Special casting techniques enable values shown in table 1b to be achieved.

What processes and assumptions have enabled us to reach this stage?

For many years it has been an established fact that the fineness of the metallurgical structure has a decisive influence on the properties of a casting, whether produced by investment or other casting processes. An indication of structural fineness is given by the grain size. Dendrite arm spacing, however, is the decisive criterion. A dendrite belongs to the solidification morphology of most cast metals and can be described as a three dimensional tree-like formation with lateral arms that can be seen in two dimensions, for example, in fig. 1. A variety of investigations (2,3) succeeded in proving that dendrite arm spacing is ideally suited to establishing a correlation between the microstructure of a casting alloy and the mechanical properties obtained. This is especially the case with aluminium-silicon alloys. Fig. 2 shows the dependence of tensile strength, proof stress and elongation values on dendrite arm spacing, and can be taken as representative of many experiments which have been carried out in this field. This recognition of the dependence of the mechanical properties on dendrite arm spacing has even led to the development of processes based on the direct indication given by dendrite arm spacing of mechanical properties. In foundry practice this process is of unusual interest as a non-destructive testing method.

Dendrite arm spacing has an even deeper significance:

Small dendrite arm spacing linked with the heat treatment of castings leads to short diffusion paths. That is, the solution treatment and the age-hardening have to be carried out in conjunction with dendrite arm spacing. This requires a broader spectrum of temperatures and times than the relevant specifications at present allow.

Fig. 3 shows the effect of a special solution heat-treatment on the microstructure of a casting in A 357: the modification of the structure is significant and leads to excellent ductility while maintaining strength.

The dendrite arm spacing itself is dependent on the so-called local solidification time. This is the time taken for a volumetric element of molten metal to commence solidification and to complete it. The cooling rate, which is considerably simpler, can be used instead of local solidification time (Fig. 4) and rapid cooling equally good mechanical properties can be achieved.

There are two decisive factors influencing local solidification time:

- a) the wall thickness of the casting
- b) the heat extraction rate during solidification

a) Wall thickness

It has been known for a long time that the wall thickness of a casting has a strong influence on the obtainable mechanical properties because it determines the local solidification rate. A rule of thumb would be that the solidification rate increases as the square of the wall thickness, i.e. if a given casting wall thickness is doubled, the solidification rate quadruples.

The dendrite arm spacing and the mechanical properties are closely linked with this. This familiar fact gives ground for thought because in a casting possessing various wall thicknesses, areas with thick walls will have lower strength than areas with thin walls, unless special measures are taken. These facts have their origin in basic physical phenomena and every designer of castings must be familiar with them. The desire to achieve an optimum relationship of wall thicknesses is understandable but can lead to difficulties in extreme cases.

Where the difference in wall thickness is not too extreme the investment casting manufacturer can solve the problem by measures for controlling the cooling process. Apart from this the modern aircraft industry is showing a welcome tendency to take these findings into account in their design and processing. Those areas of a casting where heat-loss is obstructed, the so-called "hot spots", have the same effect as large wall thicknesses. The same can be said for the zones of a casting situated near gates or feeders, where excessive heat is produced by the molten metal flowing into the mould cavity. Experienced material testers have good reasons to avoid taking test specimens from these areas. It is, of course, much more advantageous to take the basic principles of heat-loss into account when designing the gate and riser systems. This means that the foundryman must be acquainted not only with the stressed areas but also with the function of the casting.

b) The heat equilibrium of the solidification process

Before and during the solidification of poured metal and superheat and the solidification heat must be given off to the shell and the surroundings. Obviously rapid heat-loss depends on as little heat as possible being put into the system, i.e. the metal should be poured with as little super-heat as possible.

The cooling rate of the metal in the mould is primarily determined by the thermal properties of the metal itself, but also by the surrounding ceramic shell which, by its very nature, acts rather as an insulating medium. The solidification heat from the metal conducted into the ceramic shell is clearly proportional to that part of the metal which has solidified in the area under observation. The rate of this heat transfer determines the fineness of the structure of the casting. For this reason the investment casting manufacturer must strive to design and use the ceramic shell in such a way that it acts as a directly available heat sink. Here it is of great importance to choose suitable ceramic materials, the thermal properties of which can vary greatly. The shell temperature should also be kept as low as possible when pouring has taken place. In this latter case the temperature distribution of the shell takes place as shown in simplified form in Fig.5.

If the ceramic shell - e.g. in the case of thin-walled components - absorbs the solidification heat without increasing its outer temperature, the surroundings are of no further importance in the solidification process.

At this point problems arise in the investment casting foundry. The need to pour the metal as cold as possible and to remove the heat as quickly as possible clashes with the obvious necessity to fill the mould completely. In order to solve this problem ways must be found of achieving a complete casting with good mechanical properties taking into account the three variables in foundry practice namely: temperature of the melt, temperature of the ceramic mould and mould fill rate.

3. Modern Foundry Practice

For this purpose special foundry processes have been developed, tested and put into practice

Of these the most important are:

a) Pouring under vacuum

The conventionally treated and degassed melt is poured into the mould under vacuum. By comparison with normal pouring under atmospheric conditions this process permits a higher cavity fill rate and therefore a lower pouring temperature. However, if solidification commences under vacuum the danger exists, even, in the case of a well-degassed melt, that the precipitation of hydrogen in the casting structure becomes unavoidable. The effect of this on casting properties are well known.

b) Melting and casting under vacuum

This process avoids the precipitation of elementary hydrogen in the casting structure because of the excellent degassing effect it has on the melt. The good mould fill rate and the low pouring temperatures create castings with excellent mechanical properties. The high metallurgical purity of the melt should also be mentioned in this context.

c) Casting under low pressure

In this process the creation of a differential pressure between the melt compartment and the ceramic mould forces the metal upwards into the mould. This process can take place under various basic pressures; it is only the differential pressure which is important for filling the mould. The advantage of this method lies in the wide range of mould fill rates which it offers in the non turbulent rising metal and under could pouring conditions. Fig. 6 shows a typical aircraft structural part which is well suited to this casting process while Fig. 7 shows the typical microstructure obtained and the typical mechanical properties. The nominal wall thickness is 1,6 mm.

4. Solidification with cooling elements

In order to obtain a good casting structure with good mechanical properties cooling elements can be used in the mould to induce increased solidification rates in localized areas. Cooling elements are used especially in zones with a drastic increase in wall thickness in components whose walls are already thick, e.g. compressor impellers for turbochargers. Another case would be the area of a casting where the melt enters the mould cavity (gate) which receives additional heat by contact with the metal stream. These cooling elements can be made of various materials and be equipped with secondary cooling by a water circulation system. In this process, however, one must not lose sight of the fact that the mechanical properties obtained in thick walled zones decrease with increasing distance from the "quench surface". This is unavoidable in view of the laws of heat conduction during a solidification process and can be easily demonstrated.

In recent years, better casting alloys with improved strength have been developed. Such alloys, based on the binary system Al-Cu known internationally under the names K01 or Avior, have been introduced into foundry practice.

These alloys possess a broad solidification range and their tendency to micro-segregation, micro-porosity and hot tearing create problems in casting. It has been found that it is, in practice, difficult to obtain sound castings in these alloys without using the principle of controlled solidification.

Fig. 8 shows the process of controlled solidification with secondary cooling using the example of a thick walled compressor impeller. The plate surface rests on a water-cooled copper chill. In this position pouring takes place. Because of the unilaterally controlled heat extraction it is possible to locate the riser on what in the normal foundry sense is the "wrong" side of the casting.

Fig. 9 shows the mechanical properties of test specimens cut from the casting at various distances from the chill. The alloy is K01. The mechanical properties decrease with increasing distance from the cooling surface or, to put it another way as the solidification rate decreases.

Based on the principles of heat extraction during solidification the modern aluminium investment casting industry produces castings which offer the design advantages of the lost wax process as well as giving cast structures with excellent mechanical properties. Having mastered the technology of casting a good basis has been established for improvement of casting qualities by means of adjustment of metallurgical parameters, such as melt analysis and treatment, and, equally important, heat-treatment. It is fortunate that the demand for thin walled high strength components matches the basic principles of melting, pouring, and solidification.

The history of titanium investment casting is short enough to state that the process is still in its development phase. This consists of the development of suitable melting technology and of mould material systems which resist the metallurgical attack of molten titanium.

To date we know of no moulding material system for titanium investment castings which would not react to some extent with the solidifying metal. In this case "react" should be understood as meaning that certain elements from the mould material diffuse into the surface of the titanium casting during solidification. This causes the casting skin to become brittle. This condition of the casting skin can be demonstrated quite simply by measuring the micro hardness and has by its nature a strong influence on the fatigue properties of the cast material (Fig. 10).

Titanium is characterized by a high shrinkage (approx. 2,5 %) and for this reason tends to form shrinkage cavities. In spite of counter measures taken in the casting technique it is impossible to produce complex castings which are not completely free of defects. Micro-shrinkage is often present, giving rise to sharp edged defects which also have a negative influence on the mechanical properties attainable.

The effect of the two defects mentioned can be eliminated by special processes in the investment casting.

The casting skin is removed chemically and the corresponding loss of wall thickness taken into account in designing the casting and wax injection tool.

Today the isostatic compression process (HIP) has become an indispensable element in the production of titanium investment casting. HIP permits a safe, simple and economic "healing" of structural defects, leaving no trace afterwards.

Tests have shown that both processes influence the fatigue properties of cast titanium (Fig. 11).

By this means, cast titanium has found new applications which not only permit static loading but also dynamic loading to a degree which had not hitherto been attained.

References

1. Mietrach, D.
Aluminium 57 (1981), S. 416
2. Oswalt, K.J. and M.S. Misra
Trans. AFS 88 (1980), S.845 - 862
3. Spear, R.E. and Gardener, G.R.
Trans. AFS 71 (1963), S. 209

Table 1 a : Mechanical properties: required

<u>Alloy</u>	<u>Spec.</u>	<u>YS MPa</u>	<u>U S MPa</u>	<u>El %</u>
K01	AMS 4228	345	414	5
A 357	prelim.Spec	250	310	5

Table 1 b : Typical (castings)

<u>Alloy</u>	<u>YS MPa</u>	<u>U S MPa</u>	<u>El %</u>
K01	380	450	5
A 357	260	350	5

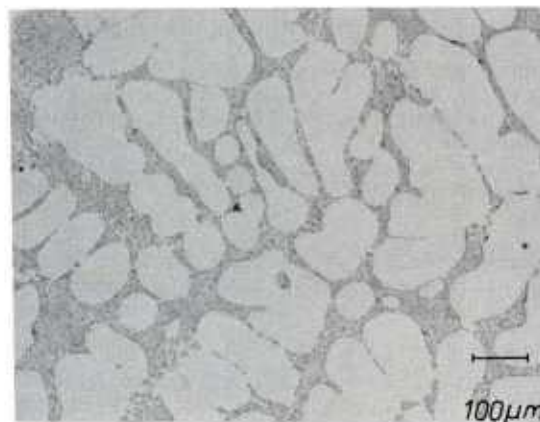


Fig. 1 : Typical solidification morphology (Dendrites)
A 357 (Al-7% Si - 0,6 % Mg), as cast.

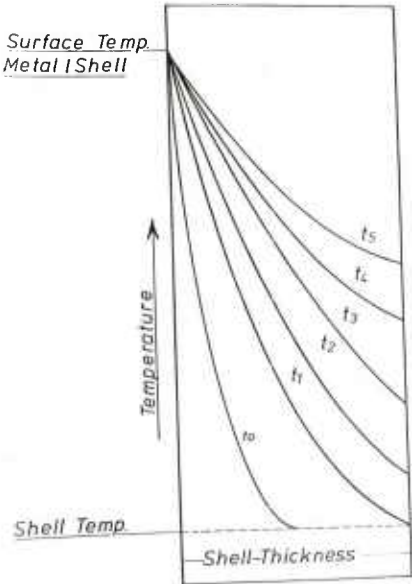


Fig. 5 : TEMperature distribution in the shell after pouring

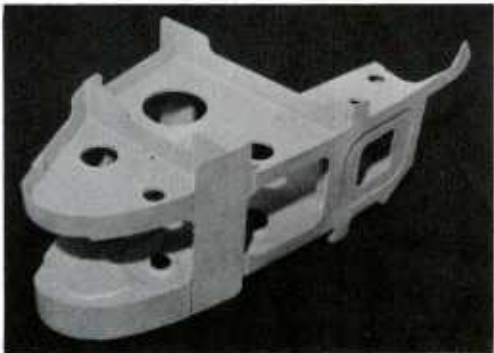
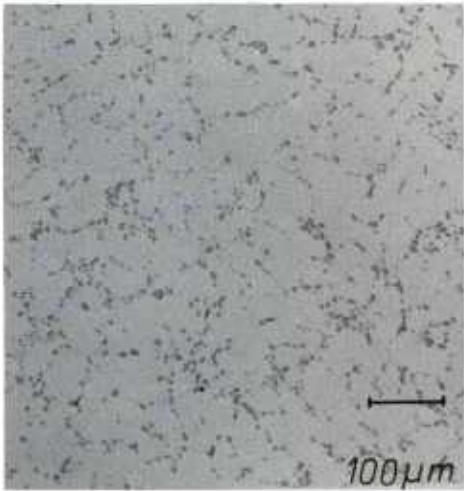


Fig. 6 : Typical aircraft casting in A 357



<u>YS MPa</u>	<u>US MPa</u>	<u>El %</u>
362	258	9.3

Fig. 7 : Microstructure and strength properties in the casting of Fig. 6

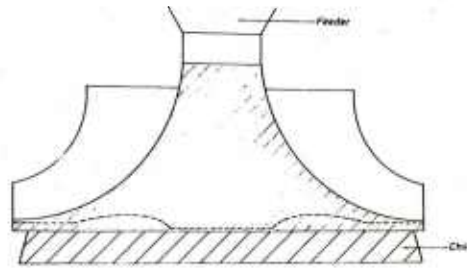


Fig. 8 : Controlled solidification of an Impeller

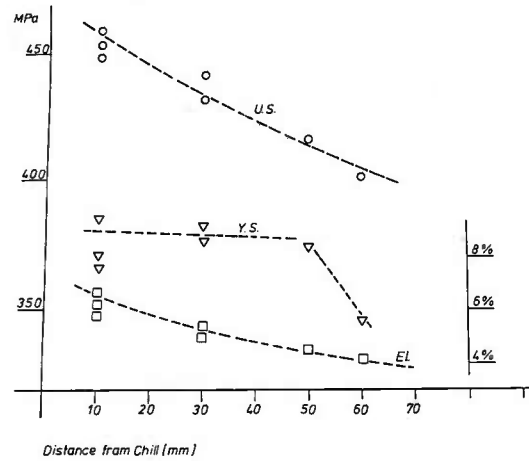


Fig. 9 : Strength properties of test bars, cut from the casting of Fig. 8 at various distances from the chill.

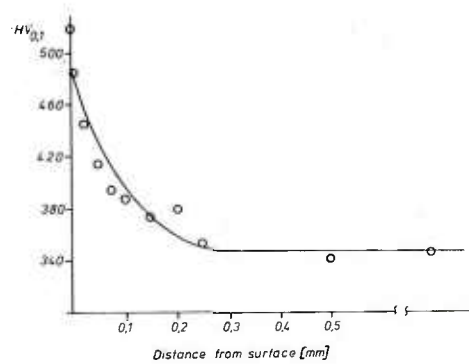


Fig. 10 : Micro-Hardness of casting-skin (TiAl6V4)

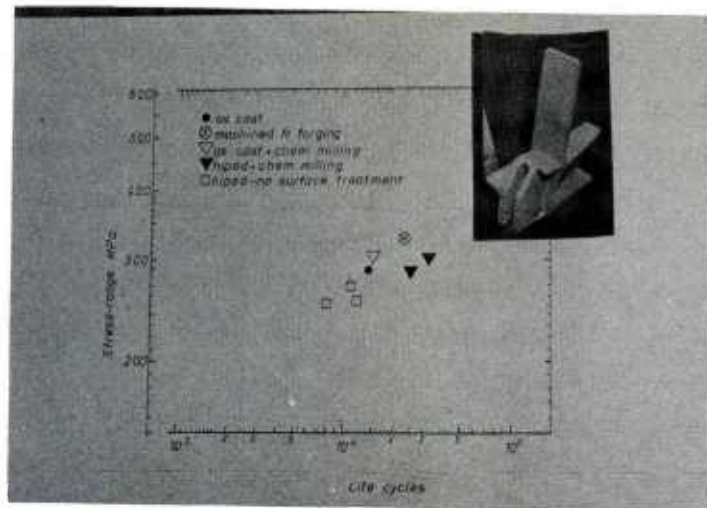


Fig. 11 : Fatigue strength behaviour of brackets
(Ti Al 6V4 investment casting)

SESSION II

RESUME DES DISCUSSIONS

par

M.Dupont

La fonderie des alliages légers constituait le thème dominant de cette session avec trois conférences, celles de MM.Williams (procédé squeeze forming), Broihanne (coulée basse pression) et Wedeking. Les deux autres conférences (MM.Apelian et Van Houten) concernaient plus particulièrement le processus de solidification, respectivement contrôle de la structure de fonderie et modélisation du processus.

MM.Broihanne et Wedeking ont traité de procédés utilisés industriellement, respectivement par Messier Fonderie d'Arudy et Tital, et en ont présenté les derniers développements. Les discussions ont notamment permis d'attirer l'attention sur l'intérêt que présente la coulée Basse Pression dans le cas des alliages — tels les alliages au Cu — ayant tendance à criquer lors du refroidissement. L'amélioration par rapport à la coulée classique, par gravité, s'explique par une meilleure alimentation du moule pendant la solidification. L'application du procédé aux alliages de Magnésium a également été évoquée. Les difficultés rencontrées ne sont pas d'ordre métallurgique; elles relèvent de la sécurité des personnels, des dangers d'explosion existent en effet, notamment dans le cas des moules en sables en raison de leur porosité. L'application aux alliages de magnésium dépend donc de l'amélioration des machines et des installations de coulée.

Le "squeeze forming" présenté par M.Williams est lui un procédé en cours de développement, intermédiaire entre le moulage et le forgeage, applicable aux alliages traditionnels de fonderie mais aussi aux alliages à haute résistance tels le 7015, un aspect séduisant de cette technique. Cette conférence a donné lieu à de nombreuses questions relatives, pour la plupart, aux possibilités d'utilisation industrielle du procédé. La nécessité de créer des outillages qui peuvent s'avérer très onéreux dans le cas de certaines pièces, leur durée de vie — M.Williams a avancé le chiffre de 50 000 pièces réalisables avec la même matrice — le cycle de fabrication très court laissent penser que ce procédé est bien adapté aux séries importantes. En matière de spécifications et notamment de caractéristiques minimum garanties, la question est posée en terme de référence aux pièces moulées ou aux pièces forgées; le deuxième terme de l'alternative paraît, s'il peut être retenu, plus favorable au développement du procédé.

M.Van Houten a développé à l'attention des spécialistes présents, les résultats d'une étude de simulation numérique de la solidification dans le cas de formes simples. Il faudra suivre avec attention le passage aux pièces de formes complexes

Enfin, M.Apelian, au cours d'un exposé particulièrement dense, a présenté trois procédés permettant de contrôler la structure de fonderie; d'une part le "rhéocasting" et la "solidification — diffusion" applicables aux pièces moulées, d'autre part le procédé de fusion contrôlée Vader qui permet d'obtenir des lingots de superalliages dotés d'une structure fine et équiaxe, matriçable directement.

La discussion a permis de préciser les points suivants:

- le "thixoforging" (forgeage d'une boue métallique obtenue par rhéocasting) et le "squeeze forming" présentent certaines analogies, cependant les conditions d'utilisation des outillages, vitesse de fermeture et température, sont semble-t-il très différentes.
- dans le procédé de "solidification — diffusion", des contraintes existent quant à la taille et la répartition des particules solides mais c'est leur composition chimique ainsi que celle de la phase liquide qui sont prépondérantes.
- le procédé Vader n'est pas limité aux lingots, il paraît possible d'obtenir des ébauches préformées — ébauches de disques de turbines par exemple — et ainsi de réduire au minimum les opérations de matriçage.

AN EVALUATION OF VACUUM CENTRIFUGED TITANIUM CASTINGS FOR HELICOPTER COMPONENTS

L.J. Maidment and H. Paweletz

Helicopter & Transport Division, Messerschmitt-Bölkow-Blohm GmbH,
8 München 80, w.-GermanyAbstract

The applicability of centrifugally cast Titanium (Ti6Al4V) for the manufacture of a critical helicopter component - a rotor head - has been investigated. The economic aspects have also been taken into consideration. The results of the present investigation can be summarised as follows:

- the endurance limit of cast Titanium is approximately 63 % that of the wrought alloy. An acceptable component fatigue life could, conceivably, be obtained by incorporating minor design modifications.
- a 15 % reduction in the machining costs was achieved. This factor alone does not make casting a viable economic alternative to forging especially in view of the almost identical price for the forged and cast rotor head blank.

However, improvements in the centrifugal casting technique leading to enhanced micro-structural and mechanical material properties, would certainly play a decisive role in extending the application of cast Titanium in the Aerospace industry.

1. Introduction

A full scale investigation of a centrifugally cast Titanium alloy (Ti6Al4V), has been carried out at MBB's Helicopter Division with two objectives in mind:

- a saving in raw material made possible by casting parts with near net dimensions. In view of the continuing shortage of Titanium on the world market, this is particularly significant for components with a high forged blank to finished part weight ratio. A substantial reduction in the price of the cast blank as compared with the corresponding forging was anticipated.
- a reduction in the machining costs, contributing to an overall decrease in the price of the part.

The present investigation was carried out in two stages. The mechanical properties - static and dynamic strength, fracture toughness and crack propagation characteristics - of vacuum centrifuged Ti6Al4V were determined on coupons machined from centrifugally cast experimental components. In order to assess the suitability of this material for dynamically stressed parts, cast rotor heads were subjected to flight simulation tests. The experimental components and rotor heads, manufactured by the rammed graphite process, were supplied by Titech International/Pomona, USA.

2. Experimental Programme

Coupons for the determination of the mechanical properties were machined from centrifugally cast experimental components (Fig.1).

2.1 Material

The chemical composition of the cast alloy is tabulated below:

Element Wt. % Alloy	Al	V	Fe	C	O ₂	N ₂	H ₂	Ti
Ti6Al4V	6.23	3.90	0.13	0.015	0.15	0.017	0.0037	Remainder

Table 1 Chemical composition [1]

2.2 Mechanical Properties2.2.1 Static

Flat, unnotched coupons were taken randomly from various parts of the component (cylinder jacket, rib and cover plate) in order to eliminate possible effects of the location of the test coupon on the strength. The average strength values are tabulated below:

Property Alloy	$R_{p0.2}$ (N/mm ²)	R_m (N/mm ²)	A (%)	Z (%)
Ti6Al4V (Cast/annealed 730°C/2h)	890	940	7	11

Table 2 Static Strength [1]

2.2.2 Notched stress Rupture

The notch sensitivity of the as-cast alloy was evaluated. A cylindrical test coupon with specified notch geometry in accordance with the German Aerospace Specification LN 9047 is subjected to a static stress of 1160 N/mm². A minimum crack free period of 5 hours is specified. Three as-cast alloy specimens were tested. After 15 hours no cracks were detected at which point the tests were discontinued.

2.2.3 Dynamic

Flat notched ($\alpha K = 2.5$) coupons were axially loaded ($A = 0.9$). S/N curves were established for the as-cast as well as various heat treat conditions. The endurance limit are tabulated below:

Property Condition	Endurance limit $> 3 \cdot 10^7$ cycles σ_D (N/mm ²)
As cast	approx. 80
Vac. Annealed (730°C/2h)	" 80
HIP (920°C/3h/1500 bar)	" 85
Solution treated (920°C/3h/rapid Argon cool)	" 80

Survival probability = 50 %
Statistical confidence = 50 %

Table 3 Endurance limits [2]

Due to the large inherent scatter of values in the individual S/N curves, there was no significant difference in the endurance limit between the as cast and heat treat conditions. A resultant S/N curve using all the experimentally determined load/cycle value was established and compared with a computed fatigue S/N curve for wrought alloy coupons with the same notch factor (Fig.2). The endurance limit for the cast alloy was found to be approximately 63 % of the corresponding value for the wrought alloy ($\sigma_{Dcast} = 87$ N/mm²; $\sigma_{Dwrought} = 138$ N/mm²). The lower fatigue strength of cast Ti6Al4V with respect to the corresponding wrought alloy is essentially due to a basket weave microstructure of similarly oriented, low shear strength α -platelets which promote early crack initiation [3]. Lenticular grain boundary α outlines prior β -phase grains. The high scatter in the fatigue results is also due to microstructural defects e.g. pores and inclusions. A typical microstructure of annealed cast Ti6Al4V is illustrated in Fig. 3. Gas induced pores are visible.

2.2.4 Fracture toughness

Fracture toughness measurements were carried out on annealed cast CT coupons machined from the ribs and cover plate of one component. Due to insufficient specimen thickness, K_{IC} instead of K_{Ic} values were determined. The average value of 10 measurements together with the corresponding value for annealed wrought Ti6Al4V is tabulated below.

Property Alloy	K_{IC} (N . mm ^{-3/2})
Ti6Al4V Annealed cast	2271
Annealed wrought	1950

Table 4 Fracture toughness [4]

The variation coefficient, $V = s/K_c$ (1)
a measure of the scatter was 0.07 which is normal.

2.2.5 Crack propagation

Nine test coupons of annealed cast Ti6Al4V were subjected to one-step loading - max. load = 7000 N ; $R = 0.1$; freq. = 130 Hz - on a 20 KN Amsler pulsator. The scatter, $T_{N90} : T_{N10} = 1 : 2.18$ (Fig.4), is relatively high when compared to a corresponding ratio 1 : 1.3 for the annealed wrought alloy. The crack propagation velocity, dl/dN was computed using the HSB FORTRAN programme (Fig.5). The values of constants C and n of the Forman Equation

$$\frac{dl}{dN} = \frac{C (\Delta K^n - \Delta K_o^n)}{(1-R) K_c - \Delta K} \quad (2)$$

were found to be: $C = 4.38 \cdot 10^{-7}$
 $n = 2.07$

The minimum value of the crack propagation stress factor, ΔK_o was 200 N . mm^{-3/2} and is roughly the same as the value for the annealed wrought alloy ($\Delta K_o = 208$ N . mm^{-3/2}; $R = 0.2$).

3. Rotor Head Testing

The normally forged rotor head of the MBB Bo 105 helicopter was selected as a prototype casting component in view of the potential saving in the amount of raw material used (wt. of forged blank = 77 kg; wt. of finished part = 18 kg) and a reduction in the machining costs. Three vacuum centrifuged rotor head blanks with a 5 mm overall metal stock (wt. of cast blank = 29 kg) were supplied by Titech International (Fig.6). After machining, the final dimensions being the same as for the forged head, two rotor heads were shot peened all over - the boreholes were masked prior to peening - in order to investigate the effect, if any, of shot peening on the fatigue life of the part (Fig.7). The peening parameters were similar to those established in previous work carried out at the Helicopter Division [5][6].

The cast rotor heads were dynamically stressed in a manner identical to that for evaluating the forged counter part. The test set-up is illustrated in Fig.8

The 4 arms of the rotor head, mounted on the main rotor shaft flange, were subjected to mutually opposing flapwise and synonymous chordwise bending moments of equal magnitude. The application of force of each of the 4 loading cylinders was 45° to the horizontal. Each pair of diametrically opposite cylinders was activated simultaneously, thereby subjecting the rotor head to a rotatory bending motion. This was adjusted to achieve a bending couple, M_m of 1600 kp . m (approx. 15700 N . m). The applied frequency was 1 Hz. Two rotor heads, one of which was shot peened, were tested to fracture. The fatigue life of both heads is plotted in an S/N curve (Fig.9), which includes the values of previously tested forged rotor heads. The crack initiation site in one cast head was one of the tapped blind holes, an area of maximum stress concentration. In the second case, the crack started out from a surface shrinkage fault (Fig. 10) in one of the arms of the rotor head. The crack was transcrystalline (Fig. 11).

4. Conclusions

The cast rotor head offers two advantages:

- a significant saving in raw material, almost 50 kg, although at the present time this factor does not make it cheaper than the forged component. Based on current quotations for production runs, forged and cast rotor head blanks cost roughly the same. The cast blanks for the present investigation were ordered in mid-1978. At that time, the forged rotor head blank was 8 % more expensive than its cast counter part.
- a reduction in machining time from the cast blank to the finished part of approx. 30 % relative to the forging. This decreases the machining costs by roughly 15 %.

Despite the inherently lower fatigue strength of cast Titanium, leading to a reduced crack free fatigue life for the cast head at the high stress level used during testing - operational flight stresses are considerably lower - the vacuum centrifuged rotor head, like its forged counterpart, incorporates essential fail safe characteristics such as a relatively low crack propagation rate and a large critical crack length. Furthermore,

oil seepage through incipient cracks in the rotor head under service conditions would simplify crack detection. The fatigue life of the cast head could be increased by incorporating minor structural changes e.g. using through bores to connect the head and rotor shaft flange. This would reduce the high stress concentration associated with tapped blind holes. In order to obtain a straight comparison of the fatigue life of the cast and forged version of a dimensionally and structurally identical component, design modifications were not carried out.

On the other hand, stringent acceptance procedures for the cast head would have to be established in connection with the definition of allowable microstructural parameters - grain size and morphology, size and distribution of internal defects such as pores and inclusions. Repair welding, especially in critical areas would have to be severely curtailed if not ruled out. These could lead to a higher rejection rate and an increased unit price for the cast rotor head, in order to guarantee an acceptable standard of reproducibility. Furthermore, a limitation of the operational life of the rotor head and/or crack testing at regular intervals may have to be taken into consideration. The forged head has an indefinite operational life and is not subjected to crack testing during service.

Summing up, the large scale use of cast rotor heads can only be justified in the face of significant economic advantages vis à vis the forged component. A necessary precondition is an acceptable strength level. At present, the only tangible advantage is a moderate reduction in the machining costs. This factor alone does not make casting an economical alternative to forging, in view of the cost intensive acceptance and inspection procedures outlined above.

5. References

- [1.] R. Mayer and E. Bilgram: " Ermittlung der statischen und dynamischen Kenndaten von Schleudergußteilen aus Ti6Al4V " (MBB/TN-BT26-20/79).
- [2.] H. Paweletz: " Schwingfestigkeit von Flachzugproben ($\alpha_K = 2.5$) aus Titan-Schleuderguß (MBB/TN-DE131-14/79).
- [3.] D. Eylon and B. Strobe: " Fatigue crack initiation in Ti6wt.%Al-4wt.%V castings", Journal of Materials Science 14 (1979) pp 345-363.
- [4.] U. Kurth: " Untersuchung des Rißfortschritts- und Bruchzähigkeitsverhaltens von Ti6Al4V gegläht " (IABG/B-TF-948).
- [5.] L.J. Maidment: "Kugelstrahlen von Ti6Al4V " (MBB/TN-DS41-5/77).
- [6.] S. Walter: " Untersuchung zur Qualifizierung des Kugelstrahlverfahrens für Bo 105-Rotorstern aus Titan-Schleuderguß " (MBB/TN-DE422-2/79)

6. Acknowledgements

- The fracture toughness and crack propagation measurements were carried out under supervision of Mr. Ulrich Kurth of the IABG.
- The mechanical testing and metallography were done at MBB's Central Research Laboratories by Mr. Reinhold Mayer, Miss Anneliese Ettingshausen and Mrs. Erika Bilgram.
- Mr. Siegfried Walter supervised the shot peening of the rotor heads at the Helicopter Division's manufacturing facilities in Donauwörth.
- The rotor heads were tested at the Helicopter Divisions test facilities under the supervision of Mr. Günther Hund and Mr. Othmar Gross.
- The authors would also like to thank Mr. Emil Weiland, Director of Engineering at the Helicopter Division, for his advice and support throughout the programme and for permission to present this paper.

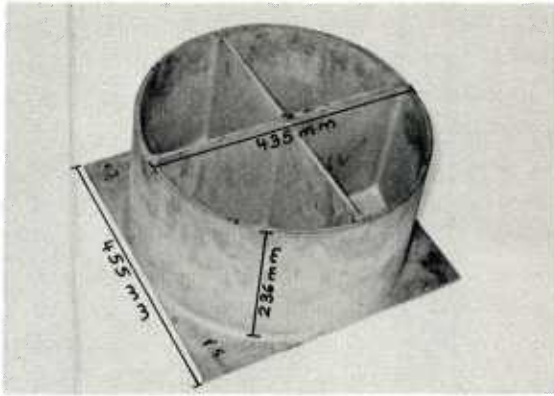


Fig. 1
Vacuum centrifuged
experimental component

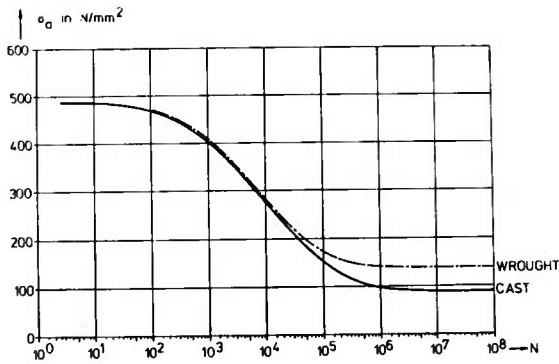


Fig. 2
S/N curve: Cast vs wrought Ti6Al4V



Fig. 3
Annealed cast Ti6Al4V
(Mag. 50:1)

WERKSTOFF : Ti AL6 V4 6055
TEMPERATUR : RT

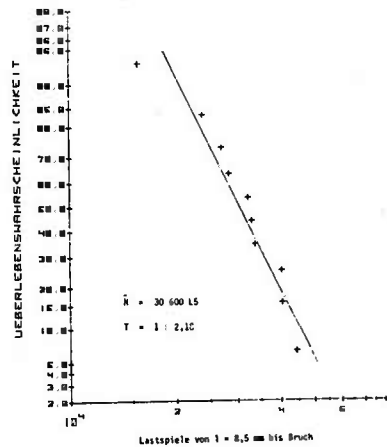


Fig. 4
Scatter in crack propagation values

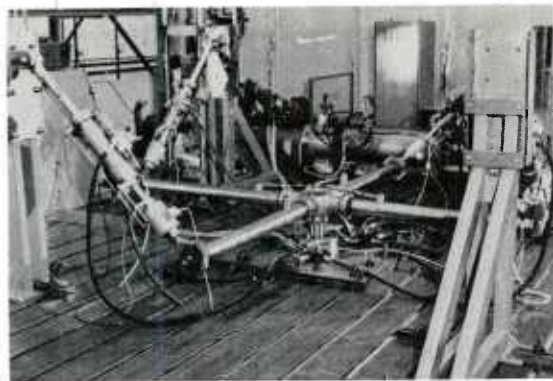


Fig. 8

Rotor head test stand

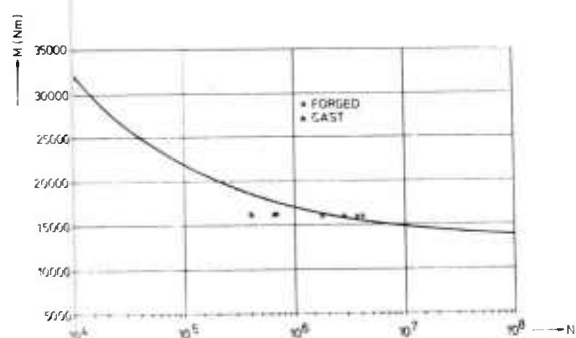


Fig. 9

Fatigue life: forged and cast heads

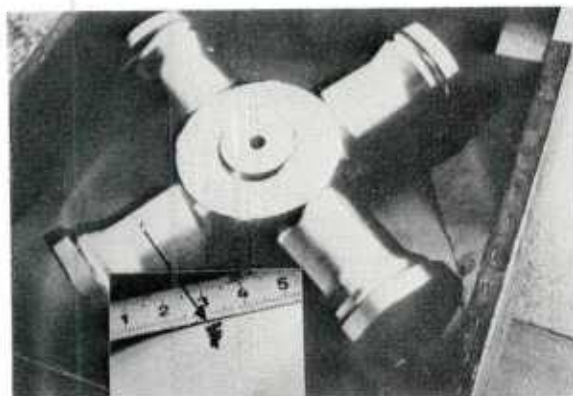


Fig. 10

Surface shrinkage fault as crack initiation site



Fig. 11

Transcrystalline crack path
(Mag. 12:1)

Grain Refinement of Cast Nickel-Base Superalloys And Its Effect on Properties

by

A.F. Denzine, Graduate Student; T.A. Kolakowski,
Graduate Student and J.F. Wallace, Republic Steel
Professor and Chairman, Department of Metallurgy
and Materials Science, Case Western Reserve
University, Cleveland, Ohio, USA 44106.

SUMMARY

This investigation studies the influence of refinement of the cast grains on the mechanical properties of nickel base superalloys (713LC, MAR-M-246 and C103). The purpose was to improve the service life of T-63 rotors which now have their service life limited by fatigue in the rim sections. The rotor is presently produced from MAR-M-246 by a vacuum investment casting process. The conventional casting techniques employed in its manufacture result in large columnar grains which cause an anisotropic fatigue behavior.

The grain refining technique developed consisted of adding 0.12B to the melt and establishing the proper time-temperature cycles so that substrates for effective heterogeneous nucleation were available for grain refinement of the different section sizes in the T-63 rotor. The mechanical properties investigated included tensile properties, low-cycle fatigue resistance, combined fatigue-creep lives, thermal fatigue and oxidation properties, and stress rupture behavior were determined for the unrefined, fine columnar, and refined equiaxed structures of the three test alloys. The grain refinement improved the low-cycle fatigue performance of 713LC and MAR-M-246 alloys; the fatigue behavior of C103 was not affected. Grain refinement increased the yield strength and decreased the tensile strength of 713LC and MAR-M-246. The strength of C103 was decreased.

INTRODUCTION

Gas turbines are now used in a variety of aircraft, marine, industrial and vehicular applications as well as high performance military aircraft. Since the early 1960's a trend of rapidly rising turbine inlet temperatures has occurred (1) because of the increase in efficiency (2). The growing demands of advancing gas turbine engine technology have, since the early 1940's, required the development of high strength heat-resistant materials. To keep pace with the increasing temperature in recent years, improved technology has led to the development of alloys capable of higher strengths at these elevated temperatures. These approaches have included directionally solidified alloys and eutectics, superalloy powder metallurgy, dispersion strengthening, and processing improvements. However, the disparity which exists between alloy capability and the rise in inlet temperature has not been offset completely by advancements in component cooling concepts, so a need for improved materials remains.

A. Service Considerations

While the high temperature capability of an alloy is most commonly expressed in terms of a temperature to produce rupture in 100 hours at a given stress, several additional properties must be considered. The choice of which properties are most critical depends on the location in the gas turbine under consideration. This study will be restricted to the hot section of the gas turbine engine, with emphasis on improving the properties of the turbine rotor.

A rotor is customarily divided into three general areas; the hub, the rim, and the blades. As shown in Figure 1, the hub section is located near the axis of the disc. In the hub section, operating temperatures are low or approximately 500°F (278°C), but stresses from centrifugal loads are high. High tensile strength and good low-cycle fatigue resistance are primary requirements in the hub section. The rim section is the outer region of the disc in the area of blade attachment. In this region temperatures of 1400°F (760°C) add hot corrosion resistance to the fatigue and tensile requirements. In the blade section, where operating temperatures are the highest, up to 1800°F (980°C), stress rupture life is of primary importance. The blade root is subjected to temperatures of 1400-1600°F (760-870°C) and stresses of 40,000 to 80,000 psi (3) (276-552 MPa) and requires strength, creep ductility and low-cycle fatigue strength. Steep thermal gradients of 500°F (278°C) along a blade span in normal engine operation add to the combination of fatigue and creep. Since these parts are in contact with high-temperature combustion products of high oxygen content, good oxidation resistance is mandatory. Resistance to surface degradation by hot corrosion (oxidation in combination with sodium, sulfur, vanadium, and other fuel or air contaminants) is also an important requirement.

All three sections of the rotor are subjected to mechanically and thermally induced cyclic strain. The mechanical strains have a high mean strain (from the centrifugal loading) with a low alternating strain from vibrations of the spinning rotor. The frequency of the cyclic strain in the hub and rim depends upon rotational speed, while the blade and blade root experience higher frequencies from airfoil twist and bending.

The thermally induced cyclic strain arises during acceleration and deceleration of the turbine. During acceleration, turbine blade leading and trailing edges heat up faster and expand more than the cooler midchord region. This nonuniform heating results in internal stresses which are compressive in the hotter regions and tensile in the cooler regions. Following acceleration is an equilibrium period

during which a nearly uniform temperature is present across the blade. On deceleration, the leading and trailing edges cool more rapidly than the center region resulting in tensile stresses in the cooler edges and compression in the hotter center. This sequence is shown schematically in Figure 2 (4). By a similar mechanism, the rim is subjected to thermal cyclic strain when the engine is started and stopped.

In the preceding discussion, the service requirements were treated for the general case of a gas turbine rotor. In this study, a particular gas turbine rotor will be examined. The rotor (Figure 3) is designed for use in the small T-63 gas turbine. Currently, the T-63 first stage turbine rotor is being replaced after 1000 hours of service because of the appearance of thermal fatigue cracks in the rim section as indicated by arrows in Figure 1. It is desired to improve the fatigue properties and extend the service life to 2000 hours or more. The T-63 rotor achieves a temperature of approximately 1400°F (760°C) at the rim, the blades encounter about 1800°F (900°C). The temperature decreases when moving toward the axis to no more than 500°F (260°C) in the hub section.

B. Rotor Manufacture: Alloys and Processes

The T-63 rotor is currently being produced as an integral wheel (blades and disc are a single piece) using a vacuum investment casting process. Several nickel base superalloys are used to produce the rotors: 713C, 713LC and MAR-M-246. Considerable nickel-base superalloy development has been conducted including various additions of elements (5-9), control of grain orientation (10-13) and directionally solidified eutectics (14).

The main emphasis of alloy and process development has been to improve the stress-rupture properties and thermal fatigue resistance in blade sections. For the T-63 rotor under consideration in this study, failure was not occurring from a stress rupture or thermal fatigue condition in the blades but from combined thermal and mechanical fatigue in the rim and hub. This situation occurs because the conditions of use of the T-63 rotor are such that the fatigue properties in the rim are more critical than the stress rupture properties in the blades. The nickel base alloys are used in fatigue applications because their endurance limit is maintained at elevated temperatures although some problems with their fatigue behavior do occur (15). The fatigue behavior is a consequence of the planar slip mode which is operative to approximately 1400°F (760°C). Fatigue life is then governed by the fast crack propagation rates along planar slip bands and through carbide phases. Therefore, to attain the ultimate in fatigue properties, structural heterogeneities should be eliminated and slip dispersed.

The approach toward improving stress-rupture properties has been to control the solidification behavior to minimize the grain boundary material oriented normal to the major stress direction; the extreme example of this is single crystals. Solidification control can also be used to improve fatigue properties by the production of a uniform, fine equiaxed grain size. Improved low-cycle fatigue resistance with a reduction in grain size has been obtained in work involving wrought nickel-base superalloys (1,16,17). A similar increase in tensile properties occurs with inoculated and refined cast alloys (18).

A homogeneous fine equiaxed structure has the considerable advantage of providing uniform properties in all directions compared to the greater variation in the anisotropic properties of a columnar grained material. Also, the fine grains tend to disperse slip and to minimize the effects of segregation and structural heterogeneities by reducing their degree and extent.

C. Solidification and Grain Refinement Principles

The parameters which must be controlled to refine the cast structure can be deduced from known principles of solidification. These principles of solidification are widely known and are only mentioned here. The two step processes that have to be controlled are nucleation and growth. Nucleation may be difficult even though commercial alloys all solidify by heterogeneous nucleation. Growth requires a consideration of constitutional supercooling (19-20). Refinement of the as-cast structure requires that nucleation occur at a large number of sites and that extensive growth of crystals be avoided. It follows that grain refinement necessitates both ease of nucleation and inhibition of the continued growth of crystallites in the melt. Effective nucleation can be influenced by a number of means including chilling, thermal cycling, mechanical vibration (19-25), rotation of the mold (10,26) and natural convection (27).

Inoculation, or the addition of stable substrates for heterogeneous nucleation, has been one of the more effective techniques for grain refinement when utilized along with constitutional supercooling. Inoculation generally refers to the addition of a substance to the melt which provides finely distributed particles on which nucleation of the parent solid can readily occur. These substances may be added to the crucible before melting, to the melt itself, or in the form of a prime-coat on the mold. The mechanism by which inoculants reduce the work of nucleation (and thus the critical nucleus size) can be rationalized in terms of interfacial energies (28). The interfacial energy between the substrate and the nucleus is substantially less than between the liquid and nucleus. This fact plus the ability of rough surfaces on substrates to lower the number of atoms required to provide a stable nucleus and to reduce the surface area in contact with the liquid account for the lower interfacial energy for nucleation attained by inoculation.

The criteria that an inoculant must possess to perform as a stable substrate for heterogeneous nucleation (19,22,28) include: epitaxy between the crystal structure of the parent solid; stability of the particle; similar density; good dispersion of fine particles; clean surfaces and a rough surface. In addition to the presence of effective substrates, constitutional supercooling is necessary along with suitable thermal gradients for grain refinement to occur. These principles have been used successfully to refine a considerable range of alloys (19,22,29-31). Inoculation of the solidifying metal by additions to the mold is also a feasible technique, such as adding CoO to the prime coat of investment castings. This latter technique results in a fine columnar structure.

D. Objectives

The present work was undertaken with the following specific objectives.

1. Develop a technique for structure control of cast rotor rim, hub, and blade sections.
2. Test the effect of structural control on properties, using a combination of tensile, low-cycle fatigue, combined fatigue-creep, thermal fatigue-corrosion, and stress rupture tests.
3. Adapt the technique to a production facility for limited production of rotors with controlled structure and properties.

EXPERIMENTAL PROCEDURES

A. Alloy Selection

The three alloys chosen for use in this study were 713LC, MAR-M-246, and C103 with their compositions listed in Table I. These alloys were selected since they are of current interest, have the necessary strength and corrosion resistance and provide a range of alloys to insure wide application of the grain refining techniques developed. The 713LC has been used for production turbine components, is the least expensive and is considered easy to cast (23). MAR-M-246 has higher strength and reduced ductility up to 1800°F (980°C) compared to 713LC (32-33). C103 is newer and contains 1% hafnium to increase transverse ductility and improve hot corrosion resistance.

B. Investment Mold Design

Investment molds were designed to simulate the thermal processing of the hub, rim, and blade sections of the T-63 rotor. These molds permitted the development of structure control techniques separately on each of the three section before using the rotor molds. The most important parameter to be controlled is solidification time, which is proportional to $(V)^2/(SA)^2$ (V =casting volume, SA =surface area of casting), which therefore varies for the hub, rim, and blade sections. The molds are designed such that sound castings can be produced. The molds taper inward from the top to the bottom to insure proper feeding and are adequately risered. The dimensions were also limited by the capacity of the furnace and mold heater available.

The design of the investment cast molds used to simulate the hub and rim sections are shown in Figures 4 and 5 respectively, based on the dimensions in Figure 3. The molds were produced at a commercial plant supplying the turbine component industry, using seven layers of zircon flour slurry. Half of the molds had a CoO prime coat. The specimens used in tensile, fatigue, and combined creep-fatigue tests were machined from hub and rim molds. The thermal fatigue-oxidation specimens and tubular stress rupture specimens were cast in clusters with six specimens arranged under a riser on each mold as shown later.

The design of the two types of rotor molds employed in this study was identical to that commonly used in the industry. Flat stress rupture paddles were cast in place of blades on a seven and one half inch diameter rotor. This type of casting permitted the evaluation of the stress rupture properties of the alloys with grain morphologies which simulate the structures obtained in integrally cast rotor blades. The T-63 rotor mold used to cast final rotors was the DD 536-A mold cast by Austenal Division of Howmet Corporation, La Porte, Indiana. The rotor molds were made of seven to nine layers of zircon flour slurry and had a prime coat of CoO.

C. Casting Technique

All of the experimental, simulated section castings were produced in a small experimental vacuum induction furnace; the rotor castings were made in the production unit (Austenal Division of Howmet Corporation). For heats from the small furnace, the charge (remelt stock plus additions) is melted in a stabilized zirconia crucible which is placed within a graphite susceptor. Power is supplied by a 275 KVA, 960 cycle motor-generator set with appropriate controls. The six pound charge is melted in approximately fifteen minutes and can then be poured by tipping the furnace toward the mold positioned in the mold preheating oven.

For a typical heat, the technique used is as follows. After loading the charge, the furnace is evacuated to a pressure of 10-25 microns (during the production casting of rotors, a vacuum of 8-20 microns is used (23)) requiring a pump down time to 8-12 hours using a mechanical roughing pump. The mold preheating oven is started and controlled to $\pm 15^\circ\text{F}$ (8°C). The charge is then heated, and as melting begins the furnace is back-filled with $\frac{1}{2}$ atmosphere of argon to prevent the loss of high vapor pressure elements and reduce bubbling at the surface of the melt. The superheat is measured within $\pm 25^\circ\text{F}$ (14°C) using a Pt-Pt 10%Rh immersion thermocouple. When the desired superheat is achieved, the furnace is poured in approximately one second. The vacuum is then broken, and an exothermic "hot-top" compound is placed on top of the riser to assure soundness and avoid nucleation from particles falling from the top surface. The mold preheating oven is then turned off and the casting allowed to cool in the furnace.

Several hub and rim castings and all of the rotor castings were produced on the production melting unit at Howmet. The furnace is rated at 90KW and operates at 3000 cycles per second. A fourteen pound charge can be melted in approximately five minutes. After melting and following the selected thermal superheating and thermal cycling, the interlock between the melt chamber and the mold chamber is opened and the molten charge is poured into a preheated mold. The interlock is then closed and the vacuum is broken in the mold chamber only.

Before proceeding with the development of a grain refinement technique, the values of mold preheat temperature and melt superheat temperature were established. A matrix of heats was produced with mold preheat temperature varying from 1500°F to 1900°F (815 to 1038°C) and melt superheat varying from 200°F to 350°F (110 to 195°C). The combination of a 1650°F (900°C) mold and a 250°F (120°C) superheat was selected for use as baseline conditions. This selection was based on the as-cast structure which produced an average grain size (coarse columnar morphology) and secondary dendrite arm spacing that was similar to those for the T-63 rotor produced on a commercial basis. This combination of mold temperature and superheat also results in the best as-cast mechanical properties (33).

With a casting process established for the production of baseline heats, a series of variations from the basic technique were evaluated in terms of their effect on control of grain size and morphology. A detailed description of the techniques used and their effect on the microstructure are provided in the Results and Discussion section since these techniques have to be discussed in terms of the resulting structures. In brief, the hub and rim molds were altered, using a CoO prime coat to produce fine columnar grains. The alloy compositions were changed by the addition of small amounts of cerium, calcium cyanamide, nickel-boron powder, boron and zirconium to the melt. The maximum melt temperature was carefully controlled to insure the production of the proper substrates. Thermal cycling techniques with pouring temperatures as low as 50°F (10°C) were also employed. The end result was the attainment of coarse columnar, fine columnar, and fine equiaxed structures depending on the casting technique employed. These techniques were applied to the production of hub, rim and blade sections and later to the production of rotors.

D. Mechanical Testing

The schedule of mechanical testing is summarized in Table II. Hub and rim sections were subjected to tensile and low cycle fatigue tests (strain controlled) at temperatures consistent with in-service operating temperature (room temperature, 1000°F (538°C), 1400°F (760°C) for rim specimens; room temperature and 500°F (260°C) for hub specimens).

A threaded end hourglass specimen (Figure 6) was designed for use in the tensile, strain cycle fatigue and fatigue-creep tests at room and elevated temperature. The design is similar to that used in previous studies (34-36). Specimen dimensions were limited by the dimensions of the casting to a maximum length of 2.750" (7 cm) and maximum diameter at the thread of 0.500" (1.27 cm) with a minimum diameter of 0.250" (.635 cm). The stress concentration factor from this shape was calculated to be 1.027 at the outside diameter. The hourglass geometry of the gage section was chosen after consideration of the advantages and disadvantages of that design (34). The advantages are: controlling and measuring the strain at the fracture cross-section; utilization of large compressive strains without buckling; a limited length over which the temperature has to be controlled closely; reducing the significant test section; and ready location of the diametral strain sensors with allowance for their accurate measurement.

Mechanical fatigue and tensile tests were performed on an M.T.S. closed loop servo-hydraulic testing facility. The movement of the axial ram was controlled by diametral strain measured by the movement of two quartz rods located across the diameter of the specimen. This strain was then converted electronically into axial strain fed into the PDP-11 computer of the M.T.S. unit. Conversion of diametral strain to axial strain required an input of Poisson's ratio or Young's modulus into the plastic strain computer. These values were obtained for each material at each grain size on a Baldwin machine which can be calibrated directly using hanging weights for load calibration and a rod of known taper driven through a U-type strain gage for strain calibration.

For high temperature testing, heat was supplied from a double wound induction coil. The temperature was controlled to $\pm 9^\circ\text{F}$ (5°C) by a thermocouple located directly beneath the coil near the top of the hourglass. A second thermocouple was attached at the minimum diameter, between the two quartz rods.

Axial alignment of the load cell, specimen, and ram was achieved through the use of a Wood's metal grip at the bottom of the specimen. After the specimen was inserted, the grip was heated until the Wood's metal became molten. The specimen was then free to float and axially align itself when a small load was applied; the Wood's metal was then allowed to solidify and, thereby, properly located the specimen.

The mechanical fatigue tests were conducted in a strain control mode, with a zero mean strain. To determine the strain levels for the tests, the shape of the ϵ vs. N curve was estimated first. This was accomplished by using the data from a monotonic tensile test, a single strain controlled fatigue test, and an incremental step test (36).

Selection of a suitable cyclic frequency was based on the capabilities of the testing system, which is usually limited by the dynamic characteristics of the extensometer. Frequencies are limited to those levels which do not disrupt isothermal conditions because of adiabatic heating. Further, poor hysteresis records result when the X-Y recorder is driven excessively fast. For these tests, the cyclic frequency was varied from 0.3 Hz to 0.5 Hz depending on the strain range. At higher strain amplitudes, a lower frequency was used to maintain a nearly constant strain rate for all strain ranges. The cyclic frequency selected is within the range used in previous studies (36) where no significant difference in fatigue life was observed for frequencies of 0.1 to 10 Hz.

A one-channel block program was used to produce the fatigue-creep cycle. The load was applied as a sinusoidal wave function with respect to time and began the first cycle in the third quadrant or compression direction from the zero stress and strain origin. The first channel block program cycled the specimen through the third, fourth and first quadrants of the sine function or from zero strain to maximum compression to zero strain to maximum tension. At this point the computer held the specimen at the maximum tensile strain for 90 seconds. After completion of the hold time, a second channel block program returned the specimen to zero strain. After a few cycles, a stabilized hysteresis loop was

generated. Apart from the 90 second hold time, the cycle was completed in 0.5 seconds.

The tensile hold time of 90 seconds was chosen to produce significant stress relaxation in each cycle while allowing the tests to be completed in a reasonable length of time. Comparing the test frequency of the present study, .01 Hz, to earlier (37,38,39) strain range partitioning results, indicates the creep component of the cycle, $\Delta\epsilon_{cc}$ as approximately 10%. The half-cycle strain ranges investigated were 0.3 to 0.6% which produced failure within 1 to 10^4 cycles. These ranges were comparable to those used to establish the conventional low-cycle fatigue data.

The thermal fatigue performance of simulated blade specimens was evaluated using the specimen shown in Figure 7. Testing was conducted on the thermal fatigue facility at NASA Lewis Research Center. This type of equipment is typically used to simulate the environment of a jet engine and is widely used in the evaluation of turbine alloys. The paddle specimens were quickly heated in the blast of a jet burning a mixture of Jet-A grade jet fuel and air to a temperature of 1800°F (980°C) at Mach 0.3 and then quickly cooled to 1000°F in an air blast at Mach 0.7. To assure uniform heating, the sample holder was rotated in the blast at 450 rpm. All specimens were weighed before testing and were weighed and inspected at ten hour intervals. The test temperature was monitored using an optical pyrometer which was calibrated by placing a thermocouple on a dummy specimen. The test cycle had a duration of 2.5 minutes, with two minutes heating and 30 seconds cooling. A total of 2400 cycles was run in the 100 hour test duration. This technique is similar to that used by other investigators (14).

Both tabular and flat specimen stress rupture tests were performed on Satec Model LD creep units. The tubular specimens illustrated in Figure 8 were tested in air at 1800°F $\pm 3^\circ\text{F}$ (980°F $\pm 1.7^\circ\text{C}$). Temperatures were controlled with chromel-alumel thermocouples. Tests were made at constant load with initial stress levels of 17.62 to 38.18 ksi (121.5 to 263.3 MPa) for tubular specimens and 20.00 ksi (137.9 MPa) for flat specimens.

Specimen strain was measured for selected stress levels by monitoring load train motion with a LVDT with the output measured on a chart recorder. This provided a record of axial displacement vs. time. Minimum creep rates were calculated from the slope of the straight section of the creep curve which followed the primary creep portion. All specimens were tested to failure and elongations to failure were measured with dividers and a ruler.

E. Microstructural Analysis

A major portion of the microstructural examination of castings and test specimens was performed using light microscopy and standard metallographic techniques. The etchant had the following composition: 150 ml methanol, 50 ml HCl, and 2.5 grams CuCl_2 . The grain size and shape, gamma prime size and distribution, grain boundary morphology and the morphology of carbides, borides and other phases were evaluated.

The light microscopy study was augmented by the electron microprobe which was used to investigate the partitioning of alloying elements. A Materials Analysis Company Model 400 S microprobe was employed in this study. The three spectrometer system was operated at 20 KeV using $\text{K}\alpha_1$ radiation.

RESULTS AND DISCUSSION

A. Structure Control of Superalloy Castings

As described in Experimental Procedures, a mold preheat temperature of 1650°F (900°C) in combination with a superheat of 250°F (140°C) was selected for use in the production of baseline heats of the three alloys. This selection provides a coarse columnar grain structure similar to that present in the T-63 rotor produced on a commercial basis. The macrostructure of a baseline heat of 713LC also has a coarse columnar structure and grains up to 0.5" (1.25 cm) diameter. A nearly identical structure is obtained from baseline heats of MAR-M-246 and C103 with a slight increase in maximum grain size for hub molds compared to rim molds.

To obtain a fine columnar structure, an investment mold inoculated with a prime coat of cobaltous oxide (CoO) was employed. Using alloy 713LC and thermal conditions identical to those for a baseline heat, a fine columnar structure was produced. As the molten metal comes into contact with the mold wall, the CoO is reduced to Co which acts as a substrate for nucleation at the surface. A similar result was obtained for MAR-M-246 and C103 cast in inoculated rim molds.

To obtain a fine equiaxed structure requires that nucleation occur at a large number of sites. As discussed in the Introduction, inoculation together with constitutional supercooling has been found to be the most effective technique for grain refinement. Ti, Zr, B and C are the most widely used inoculants and the solute segregation at the solid-liquid interface provided by the solute elements present in the alloy. For the alloys under consideration, titanium and carbon contents are closely controlled to allow the formation of a suitable proportion of gamma prime and carbides for optimum mechanical properties but sufficient latitude is available for additions of these elements as inoculants without major microstructural changes. Using an inoculated mold preheated to 1600°F (870°C) additions of 0.1 wt. % Zr (in sponge form) and 0.1 wt. % B (elemental powder wrapped in nickel foil packets) were made to a crucible charged with 713LC.

To obtain refinement, suitable substrates must be formed in the melt. The Ti-B-C ternary phase diagram (Figure 10) (40) serves only to approximate solid state transformation temperature in certain highly segregated regions of the Ni rich systems being considered. It is apparent from Figure 10 that the melt must be heated to temperatures above the 1510°C (2750°F) isotherm (shaded or cross hatched) to form TiB and TiC. Melt temperatures in excess of the similarly shaded 2160°C (3920°F) isotherm are

required to form TiB_2 . Based on this approximation, the melt temperature was established in the range of 2850°F-2900°F (1565-1595°C) since higher temperatures are regarded as extremely detrimental to crucible life and significantly lower temperatures probably would not permit the formation of TiB and TiC . After this temperature range is achieved, the charge is allowed to cool in the crucible for 10-25 minutes (until solidification has progressed sufficiently to freeze the top metal completely over) to provide substrates of TiC and TiB . The charge is then reheated and poured quickly with a 50-100°F superheat. This freezing and remelting has the advantage of facilitating temperature control on the pour temperature. When this thermal cycling technique was performed on 713LC without any added boron or zirconium, no effect was observed on the grain macrostructure. However, when 0.1%B and 0.1%Zr were added to the charge and the thermal cycle was performed, grain refinement was obtained.

The macrostructure resulting from this casting technique is a fine equiaxed structure with a grain size of ASTM #3. The same technique was then applied to the larger hub mold, resulting in a fine equiaxed structure with a thin columnar region at the surface and a grain size of ASTM #2. This technique was applied to alloy MAR-M-246 hub and rim molds to obtain even finer equiaxed structures with equiaxed grain sizes of ASTM #4 and ASTM #3.5 for the rim and hub sections, respectively. The additional refinement in this alloy compared to that of 713LC is attributed to the higher carbon and refractory metal content of MAR-M-246.

The application of the previously described technique proved unsuccessful with rim sections of alloy C103. A coarse columnar structure was produced. In alloy C103 the most significant alloying addition (compared to 713LC and MAR-M-246) is 1% hafnium. Since the existing grain refinement theory is based on the formation of titanium and zirconium borides and carbides in the melt (which then act as substrates for heterogeneous nucleation), it is significant that a higher negative free energy of formation exists for hafnium borides and carbides than for the titanium and zirconium counterparts (41). The hafnium in the alloy would be expected to react preferentially with the boron and carbon, reducing the amount available to the titanium and zirconium. The hafnium borides and carbides apparently do not act as effective substrates for reasons that will be discussed later.

To verify the presence of hafnium as the source of the problem, a heat was made using alloy MAR-M-246 and a 1% addition of hafnium. The casting technique employed was that which previously produced refinement in MAR-M-246. Instead of the previous fine grained equiaxed structure, coarse equiaxed grains result with a region of fine columnar grains at the surface.

A comparison of the Ti-Zr-B and Ti-Hf-B (40) ternary phase diagrams (again only serving as approximations in a highly alloyed, Ni-rich system) in Figures 11a and 11b indicates that the titanium and zirconium borides begin to form upon cooling from temperatures above the 1445°C (2635°F) minimum shown in Figure 11a. However, the hafnium borides can begin to form upon cooling from temperatures above about 1540°C (2804°F) as shown in Figure 11a. Therefore, heating to the intermediate temperature range between 2635°F and 2804°F (1445 and 1540°C) is designed to result in the formation of effective substrates of titanium or zirconium borides with a minimal loss of substrates from the presence of hafnium because the boron is not tied up as hafnium borides that apparently fail to serve as substrates.

Using boron and zirconium as inoculants and a cobaltous oxide coated rim mold, a C103 heat was made by heating to approximately 2660°F (1460°C), cooling and then pouring with a 50°F superheat. The casting surface was composed of fine columnar grains because of the action of the mold inoculant and the body of the casting was equiaxed with an average grain diameter of 0.07". While this structure is not as fine grained as those of 713LC or MAR-M-246, it represents a significant improvement compared to previous attempts with C103 in this investigation. A second heat was made under the same conditions with the maximum temperature increased to the upper limit (2804°F) (1540°C) suggested by the phase diagram approximations. The structure was wholly equiaxed, with an average grain diameter of 0.004" (ASTM #3.5). The same technique was then applied to an inoculated hub mold and the structure was wholly equiaxed with an average grain diameter of 0.005" (ASTM #3).

B. Production of Test Castings and Rotors

The grain refinement technique utilized on the simulated mold section castings employed alloying additions of 0.1%B plus 0.1%Zr and a thermal cycling between 2800°F (1538°C) for 713LC and MAR-M-246 or 2635 to 2804°F (1445-1540°C) for C103 and the melting temperature of the various alloys. After this cycling a low pouring temperature with 50 to 80°F superheat and low mold temperature of 1650°F (900°C) was utilized. In addition, the melt chamber was back-filled with $\frac{1}{2}$ atmosphere of argon after melting had started. During the production casting of integrally cast rotors in a commercial melting unit, these alloying additions and thermal cycling can be readily accomplished but the low pouring and mold temperatures and argon back-fill would interfere with filling the thin blade sections of the rotor. Zirconium additions could lead to hot tearing problems.

Since MAR-M-246 alloy is now used for production rotors, this composition was the one investigated. Two experimental heats of MAR-M-246 were cast from the small size furnace into rim molds to determine whether the zirconium addition and argon back-fill were necessary to grain refine in the experimental furnace. The results showed that grain refinement was obtained without zirconium additions with only 0.1%B added. However, the argon back-fill proved to be necessary in this laboratory furnace. These results indicate that titanium borides are the primary substrates for heterogeneous nucleation of the nickel solid solution phase. Poor vacuum conditions once melting begins (pressure approximately 200 microns and an excessively high leak rate) in the small size experimental furnace may have contaminated the surface of these substrates without argon back-fill. A $\frac{1}{2}$ atmosphere back-fill reduces the leak rate of outside air to a very low level and minimizes the available oxygen for substrate contamination. The production melting unit was capable of much better vacuum conditions (less than one micron and very low leak rates). An argon back-fill was later proven to be unnecessary for grain refinement on this unit.

The tubular stress rupture specimens were cast on the laboratory casting facility. An argon back-fill was used, 0.1%B was added and thermal cycling was employed in grain refined heats. Problems with

filling the long, thin tubular specimens made higher pouring and mold temperatures necessary. Mold temperature was held at 1900°F (1038°C) baseline heats were poured with 250°F (140°C) superheat and refined heats were poured with 150°F (83°C) superheat. The baseline heats had long columnar grains oriented perpendicular to the specimen axis which often extended across the entire tubular cross-section. The refined heats exhibited an equiaxed structure with grain diameters of approximately 0.005-0.010 inch (.125-.255 mm). These equiaxed grains are slightly larger than the 0.004 inch (.10 mm) diameter grains obtained previously in rim molds because of the higher pour and mold temperatures that were needed to fill the thin tubular specimen molds.

The remainder of the casting work was conducted on the production facility at Austenal Division of Howmet Corporation, La Porte, Indiana using MAR-M-246. Two series of hub and rim molds (Heats 1-10 and Heats 11-16) were cast to establish an optimum refinement technique. Tables III and IV summarize the preliminary results of these heats. The temperatures referred to in these two tables were obtained with an optical pyrometer. A check of the melting temperature of MAR-M-246 using the optical pyrometer showed the alloy to melt at 2250°F (1232°C). Previous experience with MAR-M-246 on the experimental furnace using an immersion thermocouple indicated that the alloy melts at approximately 2350°F (1288°C). This discrepancy caused the reported temperatures in Tables III and IV to be somewhat low. In addition the time required to reach the maximum temperature of the thermal cycle was not controlled or even measured in these heats while it had been consistently 20 minutes in heats made on the experimental facility. The lack of cycle time and temperature control were responsible for the inconsistent success in grain refining MAR-M-246 in these preliminary production heats.

Only Heats #3 and #10 showed a wholly equiaxed structure. However, this series of heats provided considerable useful information. Heat #3 demonstrated again that grain refinement could be obtained without a zirconium but not without a boron addition. Heat #10 confirmed that refinement was possible without an argon back-fill and that only a boron addition and proper time and temperature control of the thermal cycle were necessary. Based on these results, the formation of titanium borides to act as potent substrates for heterogeneous nucleation appears to be dependent on both time and temperature. These two parameters were carefully controlled in subsequent production heats to duplicate the conditions used successfully on the experimental casting facility. This duplication required that the maximum temperature of the thermal cycle was reached in approximately twenty minutes.

The next series of heats employed MAR-M-246 cast in T-63 rotor molds. Table V shows the results of the six heats. The first rotor (serial number J 311) was cast as a control sample. Conventional production techniques of Austenal Division of Howmet were used to obtain a coarse columnar structure. The other five rotors were grain refined by the following modified technique.

- a. Add 0.1%B (powder wrapped in Ni foil) to the charge.
- b. Thermal cycle to melting temperature plus 375-450°F (210-250°C) in approximately 20 minutes.
- c. Cool the melt until partial solidification had occurred.
- d. Reheat and pour with 10-25°F (6-14°C) superheat into an 1800°F (980°C) mold.

This technique resulted in a consistent fine equiaxed structure with an approximate grain diameter of 0.004 inch and is the recommended refinement technique. The low pour and mold temperatures caused incomplete fill in the blade sections of the rotors. Three additional grain refined MAR-M-246, T-63 rotors were poured into 2100°F (1149°C) molds at superheats of +20, +50 and +100°F (11, 28 and 25°C) (not listed in Table V). The rotors poured at +20°F (11°C) and +50°F (28°C) superheat also failed to fill in the blade sections properly. However, the rotor poured at +100°F (55°C) superheat was completely filled. The grain structure remained wholly equiaxed with an average grain diameter of 0.004-0.006 inch (.10-.15 mm).

The 7½ inch (19 cm) diameter test rotors with stress rupture paddles in place of blades were also cast with MAR-M-246 in 2100°F (1149°C) molds at the production facility. A baseline (columnar) rotor was cast using conventional practice. The macrostructure in the paddle is identical to that of a conventionally cast T-63 rotor blade. A refined (equiaxed) test rotor was cast using the modified grain refinement technique and a superheat of +100°F (55°C). The refined structure in the stress rupture paddles is identical to that observed in grain refined T-63 rotor blades.

C. Microstructural Analysis

Analysis of the microstructure showed that the grain refinement technique used for 713LC produces a carbide and boride network at the equiaxed grain boundaries. The other features of the structure such as the γ' phase (Ni_3AlTi) and blocky MC and elongated M_{23}C_6 carbides were not affected. A similar behavior occurred in the MAR-M-246 alloy except that more MC carbides were present. Grain refinement affects the structure of C103 differently. The grain boundary carbides still occur but volume fraction of $\gamma-\gamma'$ eutectic has increased and the number of angular carbides within the grains has decreased.

The electron microprobe analysis on the grain refined rim sections showed the partitioning of the major elements. In 713LC and MAR-M-246, the carbides are depleted of nickel and titanium-rich MC carbides and chromium, molybdenum and tungsten-rich M_{23}C_6 carbides are present. In alloy C103, the hafnium is partitioned to the $\gamma-\gamma'$ eutectic phase compared to the matrix and is also concentrated in the angular primary carbides characteristic of hafnium-modified alloys. These results indicate the reasons for the difficulty experienced with grain refining the hafnium-modified alloys.

D. Mechanical Testing

1. Tensile Tests

The influence of anisotropy on tensile properties was studied by a series of tests to relate the stresses and strains in "hard" and "soft" grains to the "hard" or "soft" orientation for controlling

the test. The terms "hard" and "soft" refer to regions of high and low modulus of elasticity, respectively. To obtain an axial strain $\epsilon = (e_d/v)$, using subscripts S = soft, H = hard, d = diametral, ν = Poisson's ratio, and E = elastic modulus, the following table is generated:

EXTENSOMETER CONTROLLING IN SOFT ORIENTATION

	"Soft" Grain			"Hard" Grain		
Axial Strain	$\frac{1}{\nu_S}$	e_d		$\frac{1}{\nu_S}$	e_d	$\frac{E_{dS}}{E_{dH}}$
Axial Stress	$\frac{1}{\nu_S}$	e_d	E_{dS}	$\frac{1}{\nu_S}$	e_d	$\frac{E_{dS}}{E_{dH}} E_{dH}$

EXTENSOMETER CONTROLLING IN HARD ORIENTATION

Axial Strain	$\frac{1}{\nu_H}$	e_d	$\frac{E_{dH}}{E_{dS}}$	$\frac{1}{\nu_H}$	e_d	E_{dH}
Axial Stress	$\frac{1}{\nu_H}$	e_d	$\frac{E_{dH}}{E_{dS}} E_{dS}$	$\frac{1}{\nu_H}$	e_d	

From these relations, the maximum stress is equal in hard and soft grains when controlling in the hard orientation. The maximum strain occurs in the soft grains when controlling in the hard direction. It would then be predicted that failure would initiate in the soft grains with the test controlled in the hard orientation. This behavior was confirmed by conducting a pair of fatigue tests on samples from the same heat, with nearly equal anisotropy, positioning one sample in the hard orientation and one in the soft orientation. The specimen tested in the soft orientation had nearly double the fatigue life of its counterpart.

The orientation used to control fatigue and tensile tests of coarse grained samples exerts a significant effect on the results and has to be selected prior to testing. Using the hard orientation results in conservative estimates which may not accurately reflect the properties of a larger section. Using the soft orientation results in a consistently optimistic performance. The use of an "average" orientation has been chosen since the results will be somewhat conservative but will still reflect the scatter characteristic of the coarse grained material. It may be difficult to locate an average orientation since the properties may change discontinuously when moving from a hard to a soft grain. In such cases, the hard orientation is chosen as the test direction as a conservative measure.

The tensile test results of rim and hub molds are summarized in Tables VI and VII respectively. This data represents specimens from rim molds which were tested at room temperature, 1000°F (528°C) and 1400°F (760°C) with baseline and refined grain morphologies. Columnar grained specimens were tested at room temperature only since the properties were inferior. Also included in these tables are data from hub mold specimens tested at room temperature and 500°F (260°C) (baseline and refined). The tabulated data represents the average of a minimum of two tests unless otherwise indicated.

The yield strength and tensile strength of all three alloys are generally insensitive to increasing test temperature. The yield strength of baseline heats increases from about 110 ksi (260 MPa) for 713LC to 125 ksi (832 MPa) for MAR-M-246 and 130 ksi (897 MPa) for C103. Grain refinement results in an increase in yield strength of 713LC to 120 ksi (828 MPa) and MAR-M-246 to 135 ksi (931 MPa) with a slight decrease in tensile strength for these alloys. The yield strength of C103 decreases to 128 ksi (883 MPa) and tensile strength also is lowered as a result of grain refinement. The fine columnar grained structures are lower in both tensile and yield strengths compared to their baseline and refined counterparts. The ductility of the three alloys decreases at temperatures above 1200°F (650°C). Alloy 713LC has considerably greater ductility (12% elongation) than MAR-M-246 at 5% and C103 at 6% in both the baseline and refined states because of the relatively small volume fraction of carbides in this low carbon alloy. Grain refinement results in a small decrease in ductility for these alloys at these test temperatures which is attributed to the increase in brittle constituents such as networks of borides and altered carbide morphologies. The columnar grained castings have greater ductility than refined castings but less than baseline castings because the columnar grain boundaries are aligned normal to the major stress axis but do not contain the boride and altered carbides present in the grain refined structure.

The modulus of elasticity and Poisson's ratio as determined by conventional methods are summarized in Table VIII. Poisson's ratio is .316 for the three alloys; the elastic modulus at room temperature increases from 29.7×10^6 psi (20.5×10^5 MPa) for 713LC to 31.53×10^6 psi (21.74×10^5 MPa) for MAR-M-246 and 32.11×10^6 psi (22.15×10^5 MPa) for C103. The modulus of elasticity of the three alloys decreases at 1400°F (760°C) with the average decrease from about 31×10^6 psi (20.4×10^5 MPa) at room temperature to about 24×10^6 psi (16.55×10^5 MPa) at 1400°F (760°C).

2. Low Cycle Fatigue Tests

Room temperature strain-life curves of rim mold specimens are shown in Figure 12. Several trends are apparent as described below.

1. The baseline material shows considerably greater scatter than the columnar or refined materials as a result of the anisotropy effects. An accurate assessment of the limits of the scatter band requires testing a greater number of specimens; these limits of the scatter band are essential to designers since the lower limit must be employed in the design.

2. The baseline properties of the alloys are superior in performance to their fine grained columnar counterparts because of the orientation of the fine columnar grains with their major axes normal to the tensile axis of the specimen.

3. For alloys 713LC and MAR-M-246, the slopes of the fatigue curves follow the relation (42)

$$(2N_f)^x \Delta\epsilon_T = K$$

with K varying from 0.032 for 713LC columnar to 0.07 for MAR-M-246 refined and $x = 0.24$. Alloy C103 has a considerably shallower slope and does not conform to this behavior.

4. The performance of baseline MAR-M-246 and baseline 713LC is nearly identical. Columnar grained MAR-M-246 has a distinct advantage over columnar 713LC.

5. The fatigue performance of refined 713LC and MAR-M-246 is superior to their respective columnar or baseline grain structures. At a strain amplitude of 0.003, refined MAR-M-246 has a factor of four increase in cycles to failure compared to baseline MAR-M-246. Refined 713LC has fatigue life increased 1.8 times that of baseline 713LC at the same strain amplitude.

6. The shallow slope of the 3 strain-life curves for C103 indicates that this alloy is extremely sensitive to small changes in grain morphology, with columnar, baseline and refined data falling on nearly the same line.

The poor strength behavior of the columnar grained alloy in room temperature fatigue and room and elevated temperature tensile tests predicates the elimination of this grain morphology in future testing. Emphasis is, therefore, focused on the performance of baseline and refined material.

The 1000°F (538°C) fatigue performance of rim mold material is shown in Figure 13. The relative positions of the fatigue curves are unchanged with respect to the room temperature data. The slopes of the 713LC and MAR-M-246 baseline curves have decreased somewhat with the following parameters; $x = 0.224$ for MAR-M-246 and 713LC refined, and $x = 0.21$ for MAR-M-246 and 713LC baseline (coarse columnar).

This slope change can be rationalized in terms of the variation in ductility with temperature for the materials tested. At 1000°F (538°C), the elongation of 713LC baseline has decreased from 15% to 12%, with MAR-M-246 baseline dropping from 8.7% to 5.0%. Refined 713LC, refined MAR-M-246, and C103 baseline and refined show a much smaller decrease in ductility over the same temperature range. The mechanism by which this decrease in ductility affects the slope of the fatigue curve can be explained in terms of the elastic and plastic strain contributions to the total strain life-curve. At low strain amplitudes the fatigue performance is dependent mainly upon the strength of the material since the straining is almost totally elastic. At higher strain amplitudes, the dominance of the elastic factor is reduced as the amount of plastic straining increases. The importance of material ductility, as reflected by the fatigue ductility exponent and coefficient, increases with increasing plastic strain. Therefore, the reduced ductility present at 1000°F (538°C) results in decreased high strain fatigue life with low strain fatigue life unaffected, thereby reducing the slope of the fatigue curve.

The fatigue curves for rim material tested at 1400°F (760°C) are shown in Figure 14. Several significant features are apparent in this figure.

1. The performance of refined MAR-M-246 and refined 713LC is superior to that of baseline heats of those materials.

2. The slopes of all six fatigue curves are reduced compared to the 1000°F (538°C) data. This is again the result of a ductility loss, with the minimum in the ductility versus temperature curve (Table VI) occurring at 1400°F (760°C). The reduced slopes have the parameters $x = 0.20$ for 713LC and $x = 0.18$ for MAR-M-246.

3. At high strain amplitudes, 713LC has considerably better fatigue life than MAR-M-246 or C103. This is attributed to the ductility of 713LC which, at 1400°F (760°C), is three times that of MAR-M-246 or C103. At lower temperatures 713LC had nearly double the ductility of MAR-M-246, but the strength advantage of MAR-M-246 was sufficient to compensate for its inferior ductility.

4. At low strain levels MAR-M-246 has the superior fatigue life. Since the straining is elastic in this region, the strength of MAR-M-246 dominates.

5. At low strain levels, the fatigue life of MAR-M-246 and C103 is superior (at 1400°F (760°C)) to that at room temperature. At 1400°F (760°C), the decrease in the modulus of elasticity (Table VIII) results in less stress required to achieve a given strain. Since the fatigue test is being conducted in a strain control mode, specimens at the same strain level are subject to less stress at 1400°F (760°C) than at room temperature. While the modulus decreases with temperature, the yield strengths of these alloys are essentially constant up to 1400°F (760°C) (Table VI). Therefore, under wholly elastic strain conditions, fatigue life at 1400°F (760°C) will be superior to that at room temperature.

Room temperature strain-life curves of hub mold specimens are shown in Figure 15. The data has very close agreement with that of room temperature rim molds. For MAR-M-246 and 713LC, refined specimens have superior fatigue performance compared to their baseline counterparts. The fatigue parameters for room temperature hub mold specimens are $X = 0.24$ and $K = 0.072$ for MAR-M-246 refined and $K = 0.051$ for 713LC baseline. Again, C103 has a much shallower slope of the $\Delta\epsilon_T/2$ vs. $2N_f$ curve than 713LC or MAR-M-246.

The 500°F (260°C) fatigue performance of hub mold material is shown in Figure 16. At this low test temperature, the fatigue curves are nearly identical to those at room temperature. This is the expected

result since no significant changes occur in tensile properties at 500°F (260°C) compared to room temperature as shown by the data in Tables VI and VII.

The fatigue curves for each of the alloys at various test temperatures and grain morphologies are shown in Figures 17, 18 and 19 for 713LC, MAR-M-246, and C103 respectively. For 713LC (Figure 17), the decrease in slope of the fatigue curves with increasing test temperature is apparent for both baseline and refined materials. Baseline material is more susceptible to the slope change as it experiences a greater decrease in ductility with increasing temperature.

The behavior of MAR-M-246 is significantly different as shown in Figure 18. The slopes of the fatigue curves decrease with increasing temperature. However, the baseline and refined curves, at a given temperature, remain nearly parallel. The high temperature, low strain behavior of MAR-M-246 is interesting since the reversals to failure exceed those for room temperature specimens at the same strain amplitude.

C103 has the unique characteristic of being insensitive to changes in test temperature or grain morphology (Figure 19) with extreme sensitivity to changes in strain amplitude. At low strain amplitudes this material is comparable to the other alloys in terms of fatigue life but at strain amplitudes in excess of 0.004.

3. Combined Fatigue-Creep Tests

The results of the fatigue-creep tests conducted at 1400°F (760°C) for the three alloys are contained in Figure 20, 21 and 22. In general, several trends are evident.

1. The slopes of the fatigue-creep curves are steeper than the conventional fatigue data. This indicates that the hold-time reduces the cycles to failure at lower strain amplitudes - higher life values. The creep damage is most evident in the high-cycle region at the longer test times. An exception to this was refined 713LC.

2. Both 713LC and MAR-M-246 demonstrate significantly longer lives in the refined than baseline condition in the fatigue-creep test. C103 shows only very limited effect of the grain morphology on fatigue-creep behavior. The data for the refined alloy indicates slightly better fatigue-creep behavior. This is in agreement with earlier fatigue tests which showed C103 is insensitive to test temperature and grain size.

3. The fatigue creep data at shorter lives and high strain amplitudes are generally similar to conventional fatigue properties for MAR-M-246 and have longer lives than conventional fatigue for baseline 713LC and C103.

In the conventionally cast baseline condition both 713LC and MAR-M-246 undergo a reduction in life with the hold times test at long lives compared to the standard fatigue data. At about 10^3 reversals, the life is reduced by a factor of 2.5 for both alloys. This is comparable to the reduction by a factor of 5 reported for MAR-M-200 columnar grained material tested in tension-tension at 1400°F (760°C) (43). This data for Reference 43 was obtained using a test frequency of 0.033 cps and this reduction factor was cited near 10^3 reversals. This reduction of 5 in life is comparable to the present work since the test temperature of 1400°F (760°C) is low and the amount of life reduction is not excessive. At a higher temperature of 1700°F (925°C), the same reference reports a reduction in life of two orders of magnitude.

The influence of grain morphology on the hold time test properties is evident in Figure 20 through 22. The fatigue-creep properties of refined 713LC and MAR-M-246 were improved over the baseline condition, indicating that the fine grains were not detrimental to creep at this temperature. A similar effect for creep in nickel-base superalloys has been reported elsewhere (44,45). The grain boundaries of the refined alloys contain greater amounts of discontinuous carbide and boride phases because of the addition of boron and zirconium during refinement. These phases improve creep properties by inhibiting grain boundary sliding; however, grain boundary sliding would not be expected at 1400°F (760°C).

Although the literature indicates that hold times reduce the number of cycles to failure, the equivalent performance of MAR-M-246 and improved life of 713LC and C103 at high strain amplitudes (life less than 3×10^2 reversals) is not too surprising based on analysis of other work (46). To determine whether strain-aging did account for the greater life in the low-cycle region, the highest strain amplitude hysteresis loops for baseline and refined 713LC were examined. It was expected that strain-aging would cause an increase in the modulus between the initial and final stabilized cycles and be most apparent in baseline 713LC. No significant change in modulus was observed; however, the width of the loops tended to decrease after a few cycles, indicating less inelastic strain or an increase in yield strength. Another approach was tried by comparing the hardness of the fractured specimens in the heated test section to that of the unheated, essentially unstrained, threaded portion for both short and long life specimens. The results indicated that the greatest increase in hardness in the heated test section from strain-aging occurred with 713LC. This difference in hardness usually decreased with increasing test time, indicating that the greatest effect should occur after a few cycles. Both 713LC and C103 indicated a larger increase in hardness than the slight increase for MAR-M-246. This is consistent with the observed hold time results since these indicated that MAR-M-246 maintained equivalent life compared to conventional fatigue whereas baseline 713LC and C103 demonstrated an improvement at less than 10^3 reversals.

A summary of the results of the hold time tests for each of the alloys in the refined condition is shown in Figure 23. These data illustrate that refined 713LC has substantially higher life at all strain amplitudes compared to MAR-M-246 and C103. At a strain amplitude of 0.004, the life of 713LC is greater by a factor of 7 than for MAR-M-246 and C103. This improvement is attributed to the greater ductility of 713LC at 1400°F (760°C) indicated by the tensile test results in Table VI and VII. This higher ductility allows the alloy to absorb the effects of creep damage. In addition the higher strain-aging

response of this alloy imparts strength during cycling.

4. Thermal Fatigue and Corrosion Testing

Thermal fatigue testing of baseline and refined blade specimens of the three alloys was performed on a burner rig with air velocity of Mach 0.3. The samples were cycled between 1800°F (980°C) and 1000°F (538°C) with 2400 cycles accumulated during the 100 hour test duration. Examination of the specimens revealed that none formed thermal fatigue cracks during the test. This specimen is similar to a blade shape and does not have a shape that produces severe thermal gradients with high thermal stresses.

The test was interrupted periodically and the specimens were examined for cracks and were reweighed to measure the corrosion rate. A plot of the weight change versus exposure time is shown in Figure 24. All of the specimens gained weight in the first 10-20 hours as oxide layers built upon the specimen surface. After reaching a maximum, the weight began to decrease as surface scale was removed by the gas flow. From this figure, several conclusions can be drawn:

1. After exposure times of 30 to 70 hours depending on the alloy, the rate of weight loss approaches a 'steady state' value where the formation and loss of oxide scales are at equal rates.
2. Grain refinement produces an increase in weight loss for MAR-M-246 and C103, with refined and baseline 713LC nearly equal.
3. The rate of weight loss is significantly greater for C103 than for the other alloys.

The scaling of oxide layers was confined mainly to the leading edge of the blade in the region of gas impingement. A study of the corroded layers at the leading edge of a 713LC baseline specimen was conducted at the point of maximum test temperature in the center along the length of the blade. The principal features are an oxidized layer 0.001 inch (0.0254 mm) thick with a depleted zone beneath it. The gamma prime in the alloy appears to have coarsened somewhat from the high temperature exposure.

A grain refined thermal fatigue specimen of alloy 713LC was also studied. The scaling was confined to the curved edge of the blade and did not extend to the face of the blade whereas the scaling of the baseline specimen does occur on the face. The corroded layer was thicker (0.002 inch (.0508 mm) maximum) at some locations on the refined specimen and the depleted zone and coarsened gamma prime were similar to those of the baseline specimen.

An electron microprobe study of this surface layer was performed. The layer is heavily concentrated with Cr and Ni with some concentration to Ti and Al. A region of chromium depletion is apparent, with evidence of some aluminum depletion at the metal-scale interface. No appreciable concentration of sulfur is visible in the base metal or scale.

Baseline MAR-M-246 is little affected by thermal fatigue exposure. Only a shallow discontinuous scale forms on this alloy. A shallow scale is also present on the refined samples with increased loss of material at the leading edge. The microstructure has the characteristic coarsened gamma prime, but does not show any evidence of the formation of sigma or other embrittling phases commonly formed after high temperature exposure. Electron microprobe analysis of this scale on MAR-M-246 indicates a heavy concentration of nickel and chromium in the surface layer in addition to a build-up of aluminum and titanium. A thin (0.0005 inch (.127 mm)) layer at the metal-scale interface is depleted in chromium and aluminum. No significant sulfur concentration is present in the scale. The microprobe results obtained for 713LC and MAR-M-246 are consistent with those reported in the literature (47-49). In thermal fatigue tests involving higher temperatures, longer durations and exposure to sea salts, sulfur played a more dominant role.

Severe corrosion was apparent on the C103 baseline specimens that were tested. The corrosive attack extends over half of the face of the blade with some damage at the trailing edge. This condition deteriorates with the refined C103 sample where the majority of the blade surface is affected. A relatively shallow surface scale was present which overlies a prominent depleted zone. The surface layers were rich in Ni, Cr and Ti, with no visible depletion of Al.

5. Stress Rupture Tests

The results of the as-cast, tubular stress rupture tests are listed in Table IX; the stress versus life curves are summarized in Figure 25. At high stress levels and lives of less than about 15 hours, the refined 713LC has longer stress rupture life than the baseline alloy. However, at lower stress levels the curves cross with baseline rupture lives longer than refined. The elongations to failure of both the refined and baseline alloy exhibit a maximum (Table IX) at approximately 23.0-25.0 ksi (158.6 - 172.4 MPa). At higher stress levels the refined elongations are greater than the baseline elongations; at lower stress levels (where the baseline lives are superior) the baseline elongations exceed the refined elongations. At these low stress levels (20.56 ksi (141.8 MPa)), the minimum creep rate of the refined 713LC is approximately three times that of the baseline 713LC. This faster creep rate and reduced ductility at low stress levels are responsible for the crossing of the stress versus time to rupture curves in baseline and refined 713LC.

At high stress levels, the refined MAR-M-246 shows significantly longer stress rupture lives than the baseline material. Two curves converge at about 110 hours and 26.5 ksi. However, they do not cross over as in the case of 713LC. The elongations listed in Table VIII do not show the sharp maximum seen in 713LC. The elongations of the refined MAR-M-246 are greater at higher stress levels than the baseline alloy and they converge at lower stress levels along with the time to rupture. The minimum creep rate of the refined MAR-M-246 at 30.0 ksi (206.9 MPa) is approximately three times that of baseline MAR-M-246. The flat stress rupture specimen tests performed on refined and baseline MAR-M-246 were con-

ducted at a lower stress level (20.0 ksi (137.9 MPa)) and a higher temperature. The results of these tests are discussed later in this section of the report.

The stress rupture behavior of baseline and refined C103 are similar to those obtained with MAR-M-246 but the curves are generally lower and converge at about 110 hours and 20.5 ksi (141.4 MPa). Considerably more scatter is evident in the data for the C103 alloy. The elongations of the refined material are significantly higher at all stress levels than the baseline material. As was the case with MAR-M-246, no maximum in elongation is observed over the stress range tested. The minimum creep rate (at 30.0 ksi (206.9 MPa)) of refined C103 is about three times that of baseline C103. The minimum creep rates of both the baseline and refined C103 are approximately one half of the baseline and refined minimum creep rates of MAR-M-246 at the same stress level. This behavior is attributed to the convoluted, interlocking grain boundaries in alloy C103.

Figure 25 is a summary of the 1800°F (980°C) tubular stress rupture life results. Alloy MAR-M-246 is clearly superior to the other two alloys; C103 has similar stress rupture properties to 713LC at the higher stress levels but is superior to 713LC at the lower stress levels. Based on these results and those observed earlier, MAR-M-246 in the refined condition appears to be the best material for rotor production and was selected. MAR-M-246 is presently being used for the production of T-63 rotors. The casting of grain refined MAR-M-246 rotors has already been discussed in a previous section of this report.

Although the creep strength expressed in terms of minimum creep rate of baseline material is higher than that of refined material in all three test alloys, the times to rupture of the refined alloys are longer than baseline alloys at relatively high stress levels. This effect has already been attributed to the increased creep ductility of the refined material at these stress levels. The grain structure of the baseline tubular stress rupture specimens was columnar with the long axis of the grains oriented perpendicular to the specimen and principal stress axis. The refined specimens had equiaxed grains with grain diameters of 0.005-0.010 inch (.127-.254 mm). These structures are similar to those observed in the critical zone of stress rupture in baseline and refined turbine rotor blades. The location of this critical zone is demonstrated in Figure 26 (50).

The importance of grain boundaries that are perpendicular to crack growth direction (and thus parallel to the stress axis) in the enhancement of rupture life is implicit in the work on directionally solidified cast superalloys and elongated grain, dispersion hardened structures. Columnar grains which are oriented perpendicular to the major stress axis produce lower rupture lives and creep ductility in superalloys when compared to columnar grains oriented parallel to the stress axis in directionally solidified or equiaxed structures (11). The results obtained in this study support this theory despite the increased grain boundary area of the refined alloys over the baseline alloys. This increased grain boundary area causes a higher creep rate by a factor of approximately three because of enhanced diffusional creep. Despite the enhanced diffusional creep, the detrimental effects of unfavorably oriented columnar grain boundaries on rupture life and creep ductility make equiaxed grains superior at high stress levels.

In addition to the grain boundary orientation effects discussed above, the increased boron level in the refined alloys is considered to have influenced their creep properties. Trace additions of boron, zirconium and magnesium to superalloys can increase life 13 times, elongation 7 times, rupture stress 1.9 times and n , stress dependence of creep rate, from 2.4 to 9.0 (51). Although each of the three test alloys contain base levels of 0.005-0.020% boron, the refinement technique adds 0.100% or approximately a tenfold increase. This added boron both forms substrates for heterogeneous nucleation and boron segregates at the grain boundaries. The skeletal grain boundary borides found in grain refined 713LC support this theory.

While some mechanisms to explain the boron effect on stress rupture properties in nickel base superalloys have been offered (51,52), considerable differences of opinion still exist. Most hypotheses hinge on the unusual size of the boron atom (about three-fourths the size of the usual substitutional elements, Fe, Cr, Co, Ni, Mn and V, but somewhat larger than the interstitials H, C and N). Boron atoms segregate to grain boundaries where, because of their odd size, they are accommodated by natural lattice imperfections or holes which result from orientation differences between neighboring grains. The obvious result is that boron slows down diffusion through the grain boundaries.

Since boron atoms in the grain boundaries block short-circuit diffusional paths, they can be expected to disrupt normal grain boundary precipitation kinetics. This leads to the development of discontinuous rather than continuous grain boundary precipitates in several alloys. Also boron has been shown to retard the formation of depleted grain boundaries (carbides surrounded with an all γ or all γ' zone). These depleted zones can develop on boundaries transverse to stress during creep and cause reduced life and ductility. In γ' - free alloys, boron slows down carbide precipitation in grain boundaries and shunts carbon into the grains (53,54). The one general mechanism that is consistent with the above observations is that boron retards grain boundary diffusion.

The tubular stress rupture tests discussed above served largely as a screening test to determine which of the three alloys was most suitable for rotor production. The decision to cast refined MAR-M-246 rotors was based on the significant improvement in low cycle fatigue properties that this alloy displayed upon refinement and its superior stress rupture properties (Figure 25). The converging of refined and baseline MAR-M-246 stress rupture curves at low stress levels suggested that under extreme creep conditions (high temperatures and low stresses) the refined alloy might sacrifice too much in stress rupture properties to be acceptable for rotor production. Flat stress rupture paddles cast in place of rotor blades on baseline and refined MAR-M-246 test rotors were tested to determine whether this was the case.

Stress rupture tests were run at 20 ksi (137.9 MPa) and 1850°F (1010°C) and the results on flat baseline and refined MAR-M-246 paddle specimens are shown in Table X. The average life of the baseline specimens (88.4 hours) is longer than that of the refined specimens (68.7 hours). Refined creep elongations were greater than baseline elongations. Minimum creep rates of refined alloy were approximately

twice the minimum creep rates of baseline alloy.

Based on these results, it appears that under conditions of very high temperatures and relatively low stress levels, refined stress rupture properties in MAR-M-246 rotors are slightly inferior to baseline properties. The enhanced diffusional creep which results from increased grain boundary area in the refined alloy has overcome the grain boundary orientation and boron effects which caused improved stress rupture properties in refined alloy at lower temperatures and higher stress levels. It should be noted however, that the severe creep conditions employed in these tests are not representative of conditions in the critical zone for stress rupture in a turbine rotor blade shown in Figure 26. In the T-63 rotor the maximum blade temperature is about 1800°F (980°C) (at the blade tip) and the rim operates at about 1400°F (760°C); the critical zone probably experiences temperatures of approximately 1500-1700°F (815-925°C). Bearing this in mind, the stress rupture properties of a refined MAR-M-246 rotor could be as good as baseline MAR-M-246 rotor stress rupture properties under service conditions. Also it has already been shown that the fatigue properties of the refined alloy are superior to the fatigue properties of the baseline alloy. The complex loading and temperature distribution conditions in an integrally cast rotor suggest that the refined alloy may well have overall advantages. The final evaluation of refined versus baseline rotor performance obviously requires service testing.

CONCLUSIONS

This investigation was conducted to determine the influence of grain refinement and microstructural control on the significant properties of nickel-base superalloys for use in integrally cast turbine rotors such as the T-63 commercial rotor produced in investment molds. The alloys selected were 713LC, MAR-M-246, and C103 and the properties studied were tensile at room temperature to 1400°F (760°C), low cycle, strain controlled mechanical fatigue at room temperature to 1400°F (760°C), combined fatigue-creep at 1400°F (760°C), stress rupture at 1800 and 1850°F (980 and 1010°C) in air, thermal fatigue, and hot oxidation resistance. This investigation yielded the following conclusions:

1. A grain refinement technique was developed to attain a fine equiaxed grain structure compared to the conventional commercial coarse columnar grains throughout the various sections of the integrally cast rotors. T-63 rotors of good quality were successfully cast with this fine structure throughout. The technique consists of adding 0.1% boron powder wrapped in nickel foil to the charge followed by thermal cycling the melt. This cycling was to raise the temperature of 713LC and MAR-M-246 molten alloys to over slightly 2800°F (1538°C) and to between 2635 and 2804°F (1445 and 1540°C) for C103 in approximately twenty minutes followed by cooling the melt until partial solidification has occurred. The alloy is then reheated and poured into an 1800-2100°F (980-1150°C) mold with about a 100°F (55°C) superheat. Refinement is attributed to the formation of titanium borides which act as stable substrates for heterogeneous nucleation.
2. Grain refinement produced an increase of 10 ksi (69 MPa) in the yield strength of 713LC and MAR-M-246 with a slight decrease in tensile strength. Both the yield and tensile strengths of C103 decrease following grain refinement. Grain refinement also resulted in a small decrease in the ductility of each alloy at the given test temperature.
3. Grain refinement produced an increase in low cycle, strain controlled fatigue life by a factor of 2-4 compared to baseline material for alloys 713LC and MAR-M-246. These improved properties could potentially be used to improve service life. Baseline specimens exhibit considerable scatter because of anisotropy. Fine columnar castings are decidedly inferior to baseline or refined castings. As the test temperature increases, the slopes of the strain-life curves decrease as a result of the lower ductility at elevated temperatures. At low strain amplitudes, fatigue life increases with increasing temperature. The fatigue performance of C103 is insensitive to changes in test temperature and grain morphology, but it is extremely sensitive to strain amplitude.
4. The cycles to failure during the fatigue-creep test which contained a 90 second hold time in the fatigue cycle are significantly longer for 713LC and MAR-M-246 with a grain refined, fine equiaxed compared to coarse grained columnar structure. Comparison of each of the refined alloys in the hold time test showed 713LC was superior in life to MAR-M-246 or C103 by a factor of 7 at 10^3 reversals. Alloy C103 shows only a very slight improvement in fatigue-creep behavior resulting from refinement.
5. The 1800°F (980°C) stress rupture tests conducted on coarse grained columnar and fine equiaxed nickel-base superalloys indicated that grain refinement produced slightly better stress rupture properties at high stress levels than coarse columnar structures with the long grain axis oriented perpendicular to the stress axis. At stress levels greater than about 23.0 ksi (159 MPa) and lives of less than about 15 hours, grain refined 713LC has longer stress rupture lives than the coarse columnar alloy. However, at lower stress levels, the curves cross over and the rupture lives are longer for the coarse columnar than fine equiaxed grains. At high stress levels grain refined MAR-M-246 and C103 have longer rupture lives than the baseline alloys; the behavior of the two structures converge at a life of about 110 hours and a stress of 26.5 ksi (183 MPa) for MAR-M-246 and 20.5 ksi (141 MPa) for C103. The stress rupture properties of MAR-M-246 in the as-cast condition are superior to those of the other two alloys at 1800°F (980°C). The superior rupture lives of refined alloys over baseline alloys (at high stress levels) are attributed to the higher level of boron in the refined alloys and to grain boundary orientation effects.
6. At a higher temperature of 1850°F (1010°C) and lower stress level of 20.0 ksi (138 MPa) the stress rupture properties of large columnar grained MAR-M-246 was slightly longer at 88.4 hours compared to 68.7 hours for fine grained equiaxed MAR-M-246. The minimum creep rates of the refined alloy were approximately twice the minimum creep rates of the coarse columnar MAR-M-246; creep elongations of the refined structure were 9.5% compared to 5.9% for the coarse columnar structure.

7. Conventional thermal fatigue in a burner rig did not produce thermal fatigue cracks in baseline or refined specimens of the three test alloys. The oxidation rate (as measured by weight change) was increased for grain refined samples of C103 and MAR-M-246 but the same for 713LC.

8. The structural control technique was proven by adapting it to a production facility for limited production of rotors with controlled structure and properties.

ACKNOWLEDGEMENTS

The project was supported by AMMRC at Case Western Reserve University as a part of the U.S. Army Aviation Systems Command Manufacturing Technology Program. Appreciation is expressed by the authors to: Robert French and Perry Smoot of AMMRC, E. Scott Nichols of Allison Division of Detroit Diesel, W.M. Garcia and R. Ranson of Austenal Division of Howe Met., R.L. Ashbrook and J. Johnson of NASA Lewis Research Center for their contributions.

REFERENCES

1. Merrick, H.F., Maxwell, D.H., Gibson, R.C., "Fatigue in the Design of High-Temperature Alloys", Fatigue at Elevated Temperatures, ASTM STP520, American Society for Testing and Materials, 1973.
2. De Corso, S.M., Harrisons, D.E., "Ceramics in Industrial Gas Turbines", ASME Report 72-GT-04, 1972.
3. Fawley, R.W., "Superalloy Progress", The Superalloys, Wiley and Sons, 1972.
4. Varin, J.D., "Microstructures and Properties of Superalloys", The Superalloys, Wiley and Sons, 1972.
5. Dahl, J.M., Danesi, W.F., Dunn, R.G., "The Partitioning of Refractory Metal Elements in Hafnium-Modified Cast Nickel-Base Superalloys", Metallurgical Transactions, Vol. 4, 1973.
6. Kotval, D.S., Venables, J.D., Calder, R.W., "The Role of Hafnium in Modifying the Microstructure of Cast Nickel-Base Superalloys", Metallurgical Transactions, Vol. 3, 1972.
7. Duhl, D.N., Sullivan, C.P., "Some Effects of Hafnium Additions on the Mechanical Properties of a Columnar-Grained Nickel-Base Superalloy", Journal of Metals, July, 1971.
8. Duhl, D.N., Erickson, J.S., Sullivan, C.P., "Advances in Directional Solidification Spur Usage in Turbine Airfoil Shapes", Metal Progress, March, 1973.
9. Sell, M., Sullivan, C.P., Ver Snyder, F.L., "Unidirectionally Solidified Superalloys", Superalloy Conference, 1972.
10. Cole, G.S., Cremiso, R.S., "Solidification and Structure Control in Superalloys", The Superalloys, Wiley and Sons, 1972.
11. VerSnyder, F.L., Guard, R.W., "Directional Grain Structures for High Temperature Strength", Transactions of the ASM, Vol. 52, 1960.
12. Piearcy, B.M., VerSnyder, F.L., "A Breakthrough in Making Turbine Components---Directional Solidification and Single Crystals", Metal Progress, November, 1966.
13. VerSnyder, F.L., et al, "Directional Solidification in the Precision Casting of Gas-Turbine Parts", Trans. Am. Found. Soc., 1967.
14. Dunlevey, F.M., Wallace, J.F., "The Effect of Thermal Cycling on the Structure and Properties of a Co, Cr, Ni-Ta-C. Directionally Solidified Eutectic Alloy", Met. Trans., Vol. 5, June 1974, p. 1351.
15. Gell, M., Leverant, G.R., "Ordered Alloys: Structural Application and Physical Metallurgy", Claiter's Publishing, 1970.
16. Muzyka, D.R., "The Metallurgy of Nickel-Iron Alloys", The Superalloy, Wiley and Sons, 1972.
17. Tien, J.K., "On the Celestial Limits of Nickel-Base Superalloys", Super-Alloys--Processing, Proceedings of the Second International Conference, 1972.
18. Hockin, J., Taylor, W., "Factors Affecting the Mechanical Properties of Cast Nickel-Base Superalloys", Proceedings of the Second World Conference on Investment Casting, June 1969.
19. Form, G.W. et al, "Grain Refinement of Cast Metals, presented at the 27th International Foundry Congress, Zurich, 1960.
20. Chalmers, B., Principles of Solidification, John Wiley and Sons, 1964.
21. Chalmers, B., "Shapes and Sizes of Grains in Castings", Solidification, ASM, 1971.

22. Wallace, J.F., "Grain Refinement of Steels", *Journal of Metals*, 1963.
23. Private Communication, W. Garcia, Chief Metallurgist, Austenal Division of Howmet Corporation, April 23, 1975.
24. Freedman, A.H., Wallace, J.F., "The Influence of Vibration During Solidification of Castings", *A.F.S. Transactions*, Vol. 65, 1957.
25. Garlick, R.G., Wallace, J.F., "Grain Refinement of Solidifying Metals by Vibration", *Modern Castings*, June 1959.
26. Bolling, G.F., "Manipulation of Structure and Properties", Solidification, ASM, 1971.
27. Smith, C.L., et al, "A Survey of Solidification and Casting Literature up to Mid 1969", *Scripta Met.*, Vol. 4, 1970.
28. Turnbull, G.K., et al, "Grain Refinement of Steel Castings and Weld Deposits", *AFS Transactions*, Vol. 69, 1961.
29. Wilson, F.F., et al, "Grain Refinement of Steel Castings", *Journal of Metals*, June, 1967.
30. Jackson, W.J., Hall, T., "Grain Refinement in Cast Austenitic Steels", The Solidification of Metals, 1967.
31. Tarshis, L.A., et al, "Experiments on the Solidification Structure of Alloy Castings", *Metallurgical Transactions*, September, 1971.
32. Letter from N. Paulucci, Metallurgical Engineer, Sherwood Refractories, Inc., Cleveland, Ohio, dated May 31, 1974.
33. International Nickel, "Alloy 713LC, Preliminary Data", July, 1964.
34. Slot, T., Stentz, R.H., Berling, J.T., "Controlled Strain Testing Procedures" in Manual on Low Cycle Fatigue Testings, ASTM, STP #465, 1969.
35. Private Communication, G. Halford, Metallurgist, NASA, Lewis Research Center, January, 1975.
36. Raske, D.T., Morrow, J., "Mechanics of Materials in Low Cycle Fatigue Testings", in Manual on Low Cycle Fatigue Testing, ASTM, STP #465, 1969.
37. Manson, S.S., "The Challenge to Unify Treatment of High Temperature Fatigue - A Partisan Proposal Based on Strainrage Partitioning", Fatigue at Elevated Temperatures, ASTM, STP #520, 1973.
38. Krempl, E., Wundt, B.M., "Hold-Time Effects in High Temperature Low-Cycle Fatigue - A literature Survey and Interpretive Report", ASTM STP #489, 1971.
39. Solomon, H.D., Coffin, L.F. Jr., "Effects of Frequency and Environment on Fatigue Crack Growth in A-286 at 1100°F", Fatigue at Elevated Temperatures, ASTM, STP #520, 1973.
40. Rudy, E., "Compendium of Phase Diagram Data-Part V", AFML-TR-65-2, Wright-Patterson AFB, Ohio.
41. Aronsson, B., *Die Verfestigung Von Stahl*, Institut for Metallforskning, Stockholm, Sweden, 1969.
42. Gell, M., Leverant, G.R., "The Fatigue of the Nickel-Base Alloy, MAR-M-246, in Single Crystal and Dolumnar Grained Forms at Room Temperature", *Trans. Metl. Soc. AIME*, September, 1968.
43. Leverant, G.R., Gell, M., "The Elevated Temperature Fatigue of Nickel-Base Superalloy, MAR-M-200, in Conventionally-Cast and Directionally-Solidified Forms", *Met. Trans.*, June, 1969.
44. Leverant, G.R. Duhl, D.N., "The Effect of Stress and Temperature on the Extent of Primary Creep in Directionally Solidified Nickel-Base Superalloys", *Metallurgical Transactions*, Vol. 2, March, 1971.
45. Leverant, G.R., Kear, G.H., "The Mechanism of Creep in Gamma Prime Precipitation-Hardened Nickel-Base Alloys at Intermediate Temperatures", *Metallurgical Transactions*, Volume 1, February, 1970.
46. Coffin, L.F. Jr., "The Effect of Frequency on the Cyclic Strain and Low Cycle Fatigue Behavior of Cast Udimet 500 at Elevated Temperature", *Metallurgical Transactions*, Volume 2, November, 1971.
47. Belcher, P.R., et al, "Black Plague Corrosion of Aircraft Turbine Blades", Hot Corrosion Problems Associated With Gas Turbines, ASTM SRP 421, 1967.
48. Hamilton, P.F., et al, "Nickel-Base Alloys and Their Relationship to Hot Corrosive Environments", Hot Corrosion Problems Associated With Gas Turbines, ASTM STP 431, 1967.
49. Wall, F.J. Michael, S.T., "Effect of Sulfate Salts on Corrosion Resistance of Gas Turbine Alloys", Hot Corrosion Problems Associated With Gas Turbines, ASTM SRP 421, 1967.
50. Glenn, R.J.E., et al, "Materials For Gas Turbines", *International Metallurgical Reviews*, Vol. 20, Review 193, 1975, pp. 3-19.

51. Decker, R.F., "Strengthening Mechanisms in Nickel-Base Superalloys", International Nickel Corporation, Presented at Steel Strengthening Mechanisms Symposium, Switzerland, May 1969.
52. Brown, J.T., and Bulina, J., "W545- A New Higher-Temperature Turbine Disk Alloy", High Temperature Materials, 1957.
53. Hull, F.C., Stickler, R., "Effects of Nitrogen, Boron, Zirconium and Vanadium on the Microstructure, Tensile and Creep Properties of a Chromium-Nickel-Manganese-Molybdenum Stainless Steel", Joint International Conference on Creep, The Institute of Mechanical Engineers, London, 1963.
54. Crussard, C., et al, "The Influence of Boron in Austenitic Alloys", Joint International Conference on Creep, The Institute of Mechanical Engineers, London, 1963.

TABLE I

Composition of Alloys

<u>Element</u>	<u>713 LC</u>	<u>Mar-M-246</u>	<u>C-103</u>
Carbon	0.03 - 0.07	0.15	0.14 - 0.18
Chromium	11.00 - 13.00	9.00	11.2 - 11.8
Molybdenum	3.80 - 5.20	2.50	1.75 - 2.25
Niobium			
Tantalum	1.50 - 2.50	1.50	4.80 - 5.20
Aluminum	5.50 - 6.50	5.5	3.30 - 3.70
Titanium	0.40 - 1.00	1.5	3.80 - 4.20
Boron	0.005 - 0.015	0.015	0.010 - 0.020
Zirconium	0.05 - 0.15	0.05	0.05 - 0.12
Silicon	0.05 max.	0.05	0.30 max.
Manganese	0.50 max.	0.10	0.20 max.
Iron	0.50 max.	0.15	0.50 max.
Copper	0.50 max.	LAP*	LAP*
Sulfur	0.015 max.	LAP*	0.015 max.
Cobalt	-	10.0	8.0 - 9.0
Tungsten	-	10.0	4.8 - 5.2
Hafnium	-	-	0.80 - 1.202
Nickel	Balance	Balance	Balance

* Low as Possible

TABLE II
Schedule of Mechanical Tests

TEST REQUIREMENTS

<u>Type of Test</u>	<u>Section</u>	<u>Temp. °F (°C)</u>
1. Tensile	HUB	Room, 500 (260)
2. Tensile	RIM	Room, 1000,1400 (538,760)
3. Fatigue, Mech. ⁽¹⁾	HUB	Room, 500 (260)
4. Fatigue, Mech.	RIM	Room, 1000,1400 ⁽³⁾ (538,760)
5. Fatigue, Thermal	BLADE	1800°F ⁽²⁾ (980)
6. Fatigue-Creep	RIM	1400°F (760)
7. Stress Rupture	TUBULAR	1800°F (980)
8. Stress Rupture	BLADE	1850°F (1010)

NOTES

(1) Strain controlled test.

(2) Cyclically heated rapidly to 1800°F (980°C), cool rapidly to 1000°F (538°C), observe crack pattern at various intervals.

(3) Screening test.

TABLE III

Summary of First Series of Heats made on Production Facilities

HEAT NO.	1	2	3	4	5	6	7	8	9	10
MOLD*	Hub	Rim	Hub	Rim	Hub	Rim	Hub	Rim	Hub	Rim
ARGON	Yes	Yes	Yes	Yes	Yes	Yes	Yes	No	No	No
BORON	Yes	Yes	Yes	Yes	Yes	Yes	Yes	No	Yes	Yes
ZIRCONIUM	Yes	Yes	No	No	No	No	No	No	Yes	No
SUPERHEAT-°F**	50	50	50	100	200*	200*	100	100	100	100
THERMAL CYCLE** (2800°F, Freeze)	Yes	Yes	Yes	Yes	Yes	Yes	Yes	No	Yes	Yes
TYPE OF GRAINS	Columnar And Equiaxed	Columnar And Equiaxed	Equiaxed	Columnar And Equiaxed	Columnar And Equiaxed	Columnar And Equiaxed	Columnar	Columnar And Equiaxed	Columnar	Equiaxed
SIZE OF GRAINS (In.)	.250 And .060	.060 And .045	.004	.200 And .125	.350 And .125	.250	.200	.125 And .060	.375	.006
COMMENTS	Mold*** Didn't Fill	-	-	-	-	-	-	Mold*** Didn't Fill	-	Mold*** Didn't Fill

*** Mold Did Not Fill Because Of A Miss-Pour Or The Mold Tipped Over.

** Temperatures measured with optical pyrometer.

* Mold Temp = 1800°F (oven temperature).

TABLE IV

Summary of Second Series of Heats made on Production Facilities

HEAT NO.	11	12	13	14	15	16
MOLD*	Hub	Rim	Hub	Rim	Hub	Rim
ARGON	No	No	No	Yes	Yes	Yes
BORON	Yes	Yes	No	Yes	Yes	No
ZIRCONIUM	No	No	No	No	No	No
SUPERHEAT (°F)**	100	100	100	100	100	100
THERMAL CYCLE** (2900°F, Freeze)	Yes	Yes	Yes	Yes	Yes	Yes
TYPE OF GRAINS	Columnar And Equiaxed	Columnar And Equiaxed	Columnar And Equiaxed	Columnar	Columnar And Equiaxed	Columnar
SIZE OF GRAINS (In.)	.250 And .250	.100 And .060	.250 And .250	.250	.250 And .200	.250
COMMENTS	-	-		-	-	Cold Mold

* Mold Temp = 2000°F(oven temperature).

** Temperatures measured with optical pyrometer.

TABLE V

Summary of Heats for Production Facility Cast T-63 Rotors

SERIAL NO.	J311	J269	J314	J301	J291	J289
ADDITION	NONE	B	B	B	B	B
THERMAL CYCLE	NO	YES	YES	YES	YES	YES
MAXIMUM TEMP. (°F)*	+300	+400	+400	+400	+450	+375
POURING SUPERHEAT * (°F)	+300	+10	+25	+15	+15	+25
TYPE OF GRAINS	Columnar	Equiaxed	Equiaxed	Equiaxed	Equiaxed	Equiaxed
APPROXIMATE SIZE OF GRAINS (In.)	.250"	.004"	.004"	.004"	.004"	.004"

* TEMPERATURES REFER TO HOW HIGH ABOVE THE EXPERIMENTALLY ESTABLISHED MELTING TEMPERATURE THE ALLOY WAS.

TABLE VI

Tensile Data — Rim Molds			
Alloy	Grain	Temperature °F	0.2% Yield Strength
713 LC	Base ¹	R.T.	110,000
*713 LC	Base	1000	112,000
713 LC	Base	1400	113,200
713 LC	Ref. ²	R.T.	120,000
*713 LC	Ref.	1000	122,000
713 LC	Ref.	1400	118,600
Mar M 246	Base	R.T.	124,000
*Mar M 246	Base	1000	125,300
Mar M 246	Base	1400	124,100
Mar M 246	Ref.	R.T.	138,100
*Mar M 246	Ref.	1000	134,600
Mar M 246	Ref.	1400	131,200
C103	Base	R.T.	133,400
*C103	Base	1000	131,700
C103	Base	1400	129,900
*C103	Ref.	R.T.	127,900
C103	Ref.	1000	127,400
*C103	Ref.	1400	127,800
*713 LC	Col. ³	R.T.	108,600
*Mar M 246	Col.	R.T.	123,000
*C103	Col.	R.T.	127,600
Tensile Strength			
Elongation %			
713 LC	Base ¹	R.T.	15.0
*713 LC	Base	1000	12.0
713 LC	Base	1400	10.2
713 LC	Ref. ²	R.T.	12.0
*713 LC	Ref.	1000	11.8
713 LC	Ref.	1400	9.6
Mar M 246	Base	R.T.	8.7
*Mar M 246	Base	1000	5.0
Mar M 246	Base	1400	3.0
Mar M 246	Ref.	R.T.	5.4
*Mar M 246	Ref.	1000	5.0
Mar M 246	Ref.	1400	3.0
C103	Base	R.T.	6.0
*C103	Base	1000	6.1
C103	Base	1400	3.4
*C103	Ref.	R.T.	5.9
C103	Ref.	1000	5.4
*C103	Ref.	1400	3.0
*713 LC	Col. ³	R.T.	10.8
*Mar M 246	Col.	R.T.	6.6
*C103	Col.	R.T.	8.0

¹Baseline Heat.²Refined Heat.³Columnar Heat.

* Single Test.

1000°F = 538°C

1400°F = 760°C

1 MPa = 145 psi

TABLE VII

Tensile Data — Hub Molds			
Alloy	Grain	Temperature °F	0.2% Yield Strength
713 LC	Base ¹	R.T.	108,800
713 LC	Base	500	109,000
713 LC	Ref. ²	R.T.	119,600
*713 LC	Ref.	500	120,200
Mar M 246	Base	R.T.	125,100
Mar M 246	Base	500	126,000
Mar M 246	Ref.	R.T.	137,600
*Mar M 246	Ref.	500	137,500
C103	Base	R.T.	130,400
C103	Base	500	131,500
C103	Ref.	R.T.	128,200
*C103	Ref.	500	127,900
Tensile Strength			
Elongation %			
713 LC	Base ¹	R.T.	14.0
713 LC	Base	500	12.8
713 LC	Ref. ²	R.T.	11.7
*713 LC	Ref.	500	11.6
Mar M 246	Base	R.T.	5.2
Mar M 246	Base	500	5.0
Mar M 246	Ref.	R.T.	5.0
*Mar M 246	Ref.	500	5.0
C103	Base	R.T.	7.0
C103	Base	500	6.3
C103	Ref.	R.T.	6.4
*C103	Ref.	500	6.0

¹Baseline Heat.²Refined Heat.

* Single Test.

500°F = 260°C

1 MPa = 145 psi

TABLE IX
Results of as Cast, Tubular Stress Rupture
Tests Conducted at 1800°F (980°C) in Air

ALLOY	GRAIN STRUCTURE	σ (ksi.)	LIFE (HR.)	% ELONG.	MINIMUM CREEP RATE (IN./IN./HR.)
713LC	Baseline	35.25	0.3	1.8	3.08×10^{-4}
		30.00	2.1	3.4	
		26.43	3.2	4.7	
		23.50	10.8	7.4	
		20.56	47.6	5.6	
		17.62	134.1	4.8	
713LC	Refined	30.00	0.4	2.1	8.62×10^{-4}
		30.00	3.0	4.2	
		26.43	6.1	8.7	
		23.50	13.5	5.5	
		20.56	25.3	4.5	
		17.62	72.7	3.2	
MAR-M 246	Baseline	38.18	5.4	2.4	1.23×10^{-4}
		35.25	10.1	2.9	
		30.00	25.0	2.4	
		30.00	41.0	3.1	
		26.43	119.6	4.8	
		26.43	112.6	3.6	
MAR-M 246	Refined	38.18	7.0	3.9	4.50×10^{-4}
		35.25	12.8	5.7	
		30.00	28.2	5.0	
		30.00	53.2	4.6	
		26.43	120.0	4.7	
		26.43	96.6	3.8	
C-103	Baseline	35.25	1.8	2.0	9.85×10^{-5}
		30.00	0.3	0.0	
		30.00	1.5	1.2	
		26.43	19.1	1.6	
		23.50	29.6	1.4	
		20.56	139.6	2.1	
C-103	Refined	35.25	2.7	6.1	2.56×10^{-4}
		30.00	4.7	5.7	
		30.00	12.2	4.9	
		26.43	41.7	4.1	
		23.50	57.2	3.6	
		20.56	138.2	4.1	

1 MPa = .145 ksi

TABLE VIII

Alloy	Grain	Temperature °F	Elastic Constants		
			E_{long} (x 10^6 psi)**	E_{diam} (x 10^6 psi)*	ν
713 LC	Ref.	R.T.	29.7	94.0	0.316
713 LC	Ref.	500°F	28.0	88.6	
713 LC	Ref.	1000°F	25.0	79.1	
713 LC	Ref.	1400°F	22.2	70.3	
Mar M 246	Ref.	R.T.	31.53	100.0	0.3155
Mar M 246	Ref.	500°F	29.1	92.2	
Mar M 246	Ref.	1000°F	26.5	84.0	
Mar M 246	Ref.	1400°F	24.3	77.0	
C103	Ref.	R.T.	32.11	101.6	0.316
C103	Ref.	500°F	30.0	94.9	
C103	Ref.	1000°F	27.2	86.1	
C103	Ref.	1400°F	25.0	79.1	

*Measured

500°F = 260°C

**Calculated

1000°F = 538°C

1400°F = 760°C

1 MPa = 145 psi

TABLE X

Results of Baseline and Refined MAR-M 246 Flat Stress Rupture
Tests Conducted at 1850°F (1010°C) and 20.0 KSI (138 MPa) in Air

<u>GRAIN STRUCTURE</u>	<u>LIFE (HR.)</u>	<u>% ELONG.</u>	<u>MINIMUM CREEP RATE (IN./IN./HR.)</u>
Baseline*	62.8	5.2	7.35×10^{-4}
Baseline	124.0	7.3	5.60×10^{-4}
Baseline	59.5	5.1	7.36×10^{-4}
Baseline	71.4	5.9	6.57×10^{-4}
Baseline	98.7	5.2	5.13×10^{-4}
Refined	112.5	13.0	1.09×10^{-3}
Refined *	29.4	5.6	1.84×10^{-3}
Refined	72.9	9.8	1.35×10^{-3}
Refined	50.7	7.8	1.36×10^{-3}
Refined	38.5	7.5	1.68×10^{-3}
Average Baseline**	88.4	5.9	6.17×10^{-4}
Average Refined **	68.7	9.5	1.37×10^{-3}

* Broke In Grip - Invalid Test

** Average of Four Valid Tests

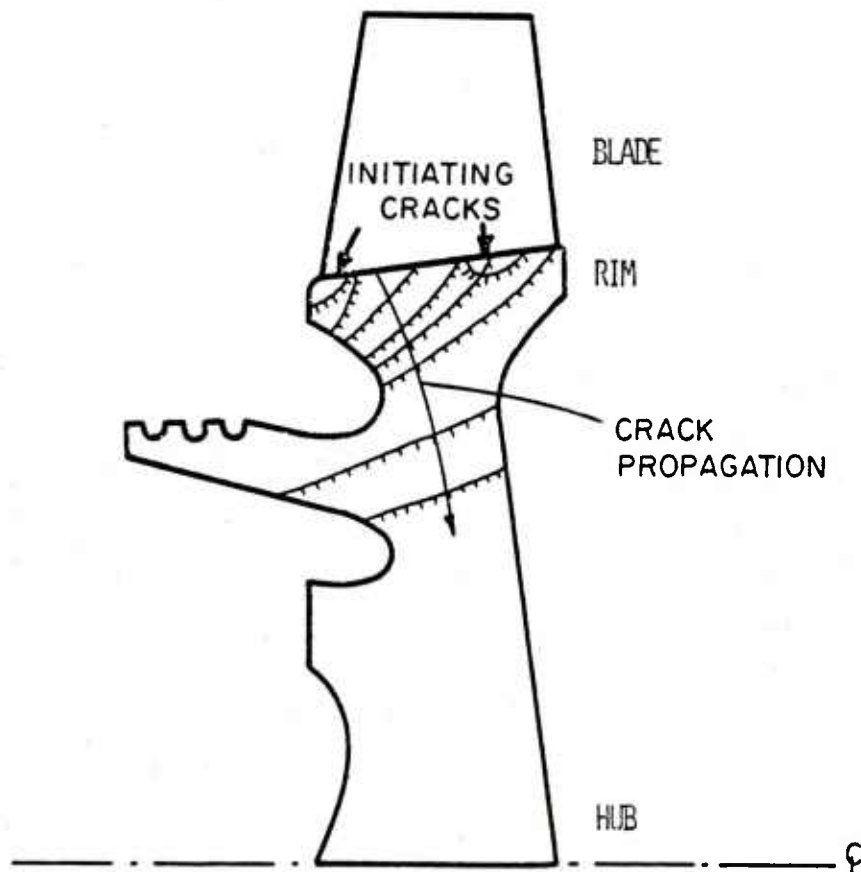


Fig.1 Schematic cross section of turbine rotor showing hub, rim, and blade areas, indicating initiating cracks

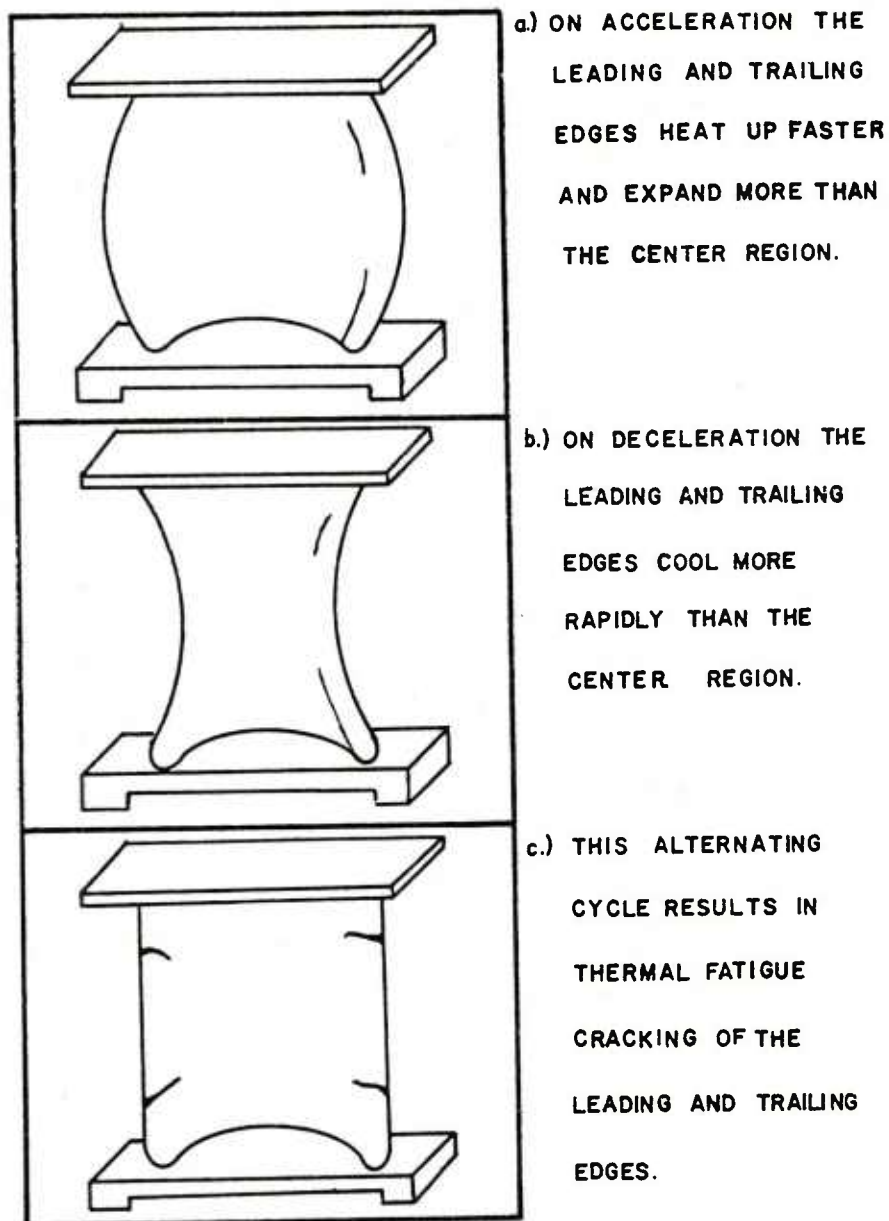
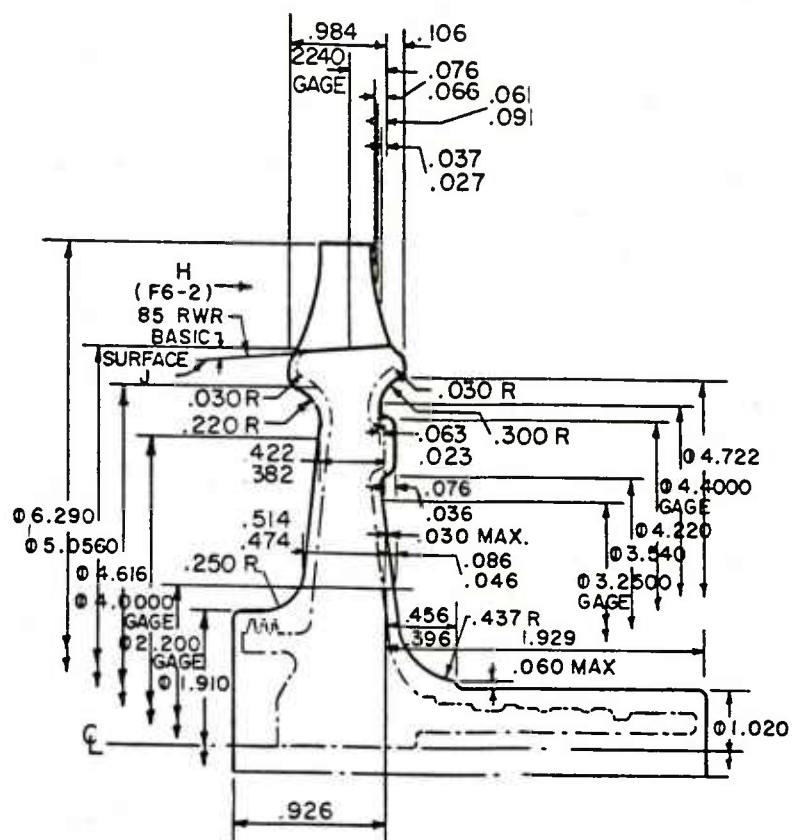
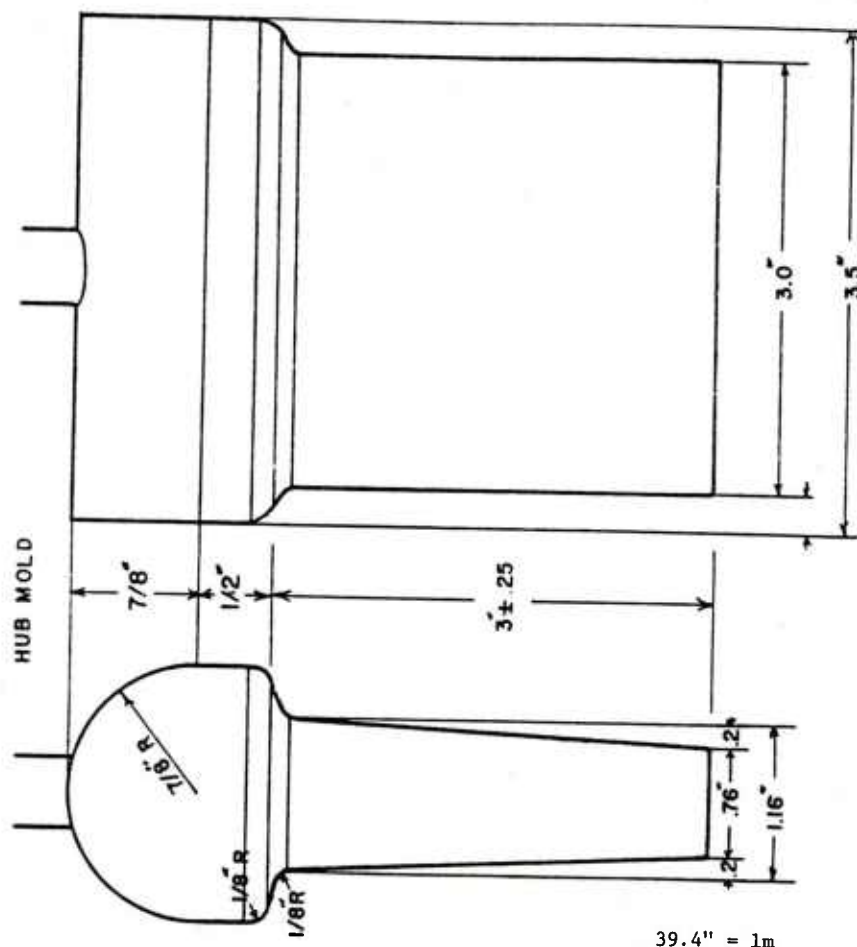


Fig.2 Sequence of events leading to the development of thermal fatigue cracks in gas turbine blades



39.4" = 1m

Fig.3 Drawing of the first stage turbine rotor for the T-63 engine



39.4" = 1m

Fig.4 Casting used to simulate hub section of T-63 rotor

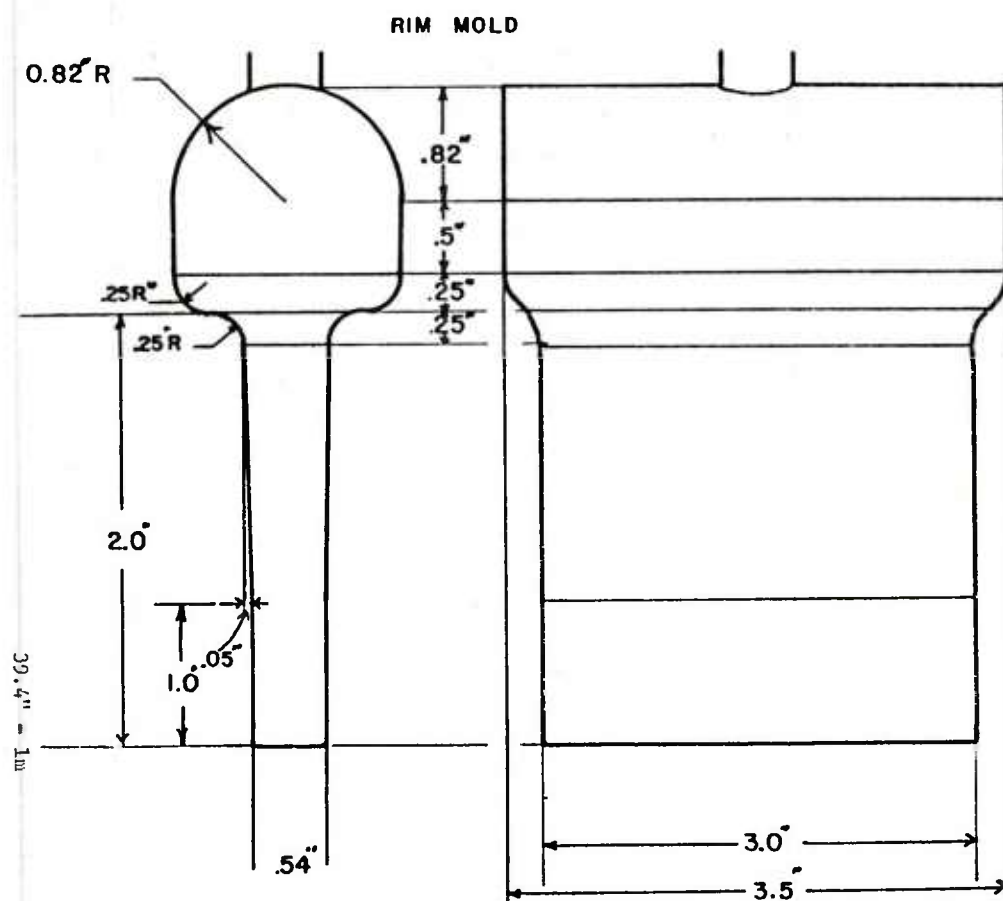
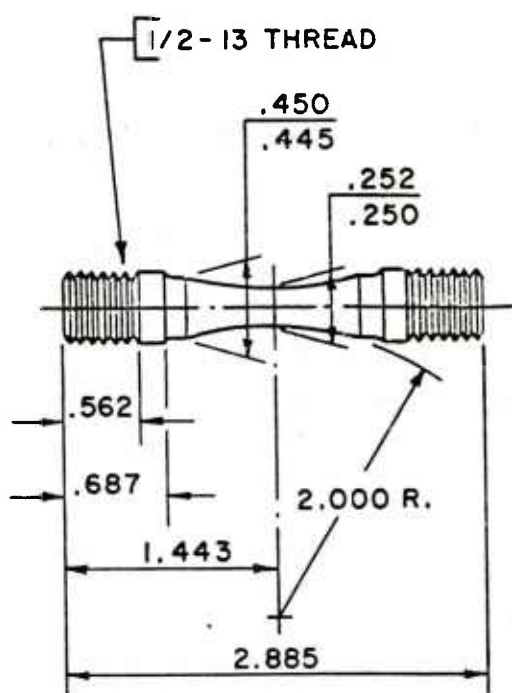


Fig.5 Casting used to simulate rim section of T-63 rotor



39.4" = 1m

Fig.6 Threaded end hourglass specimen for tensile, low cycle fatigue, and fatigue-creep testing

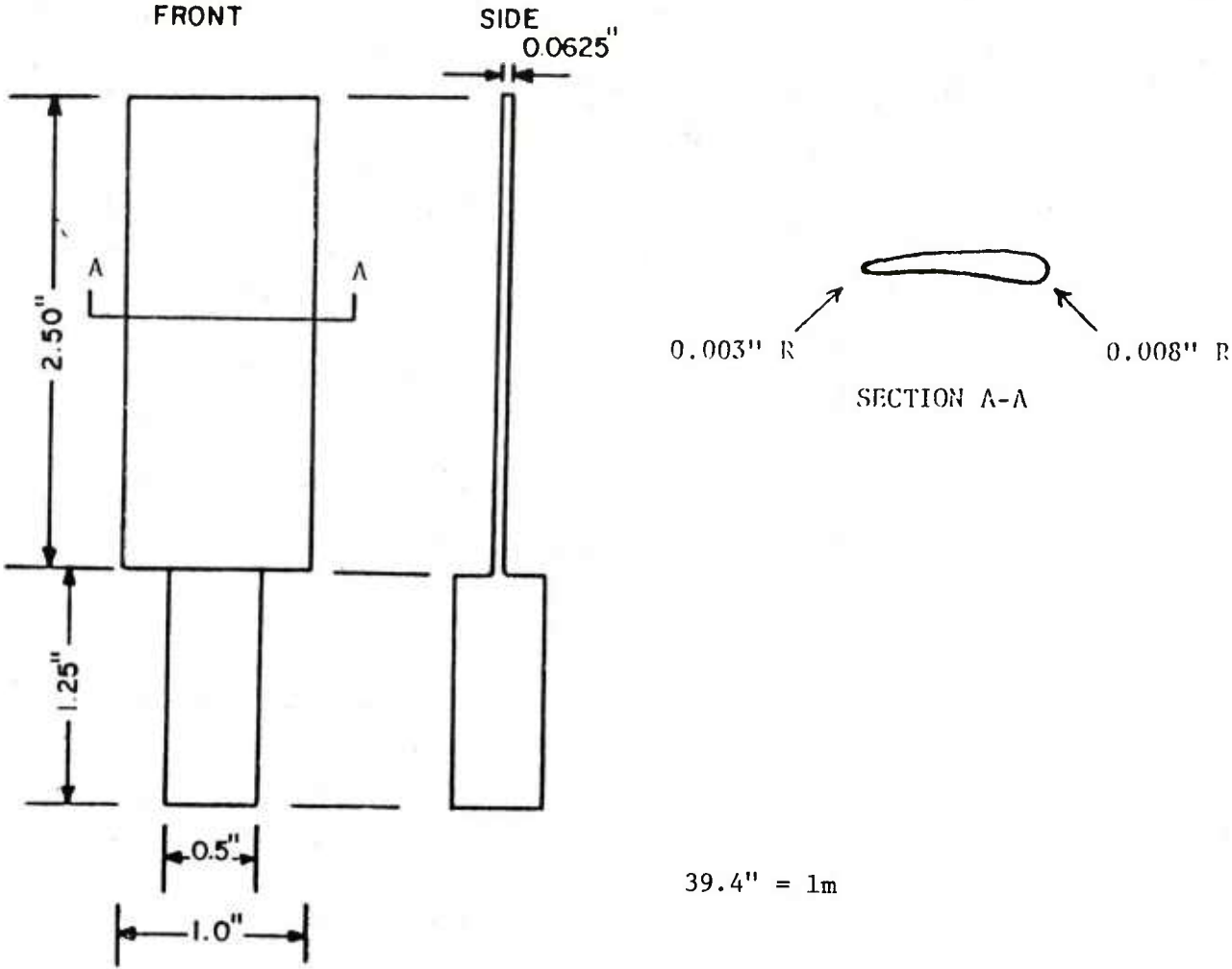


Fig.7 Simulated airfoil specimen used in thermal fatigue testing

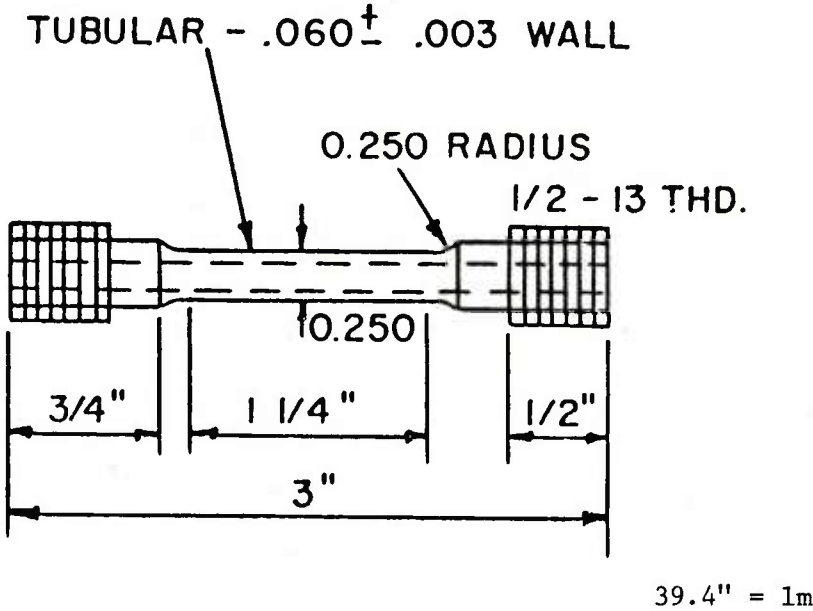
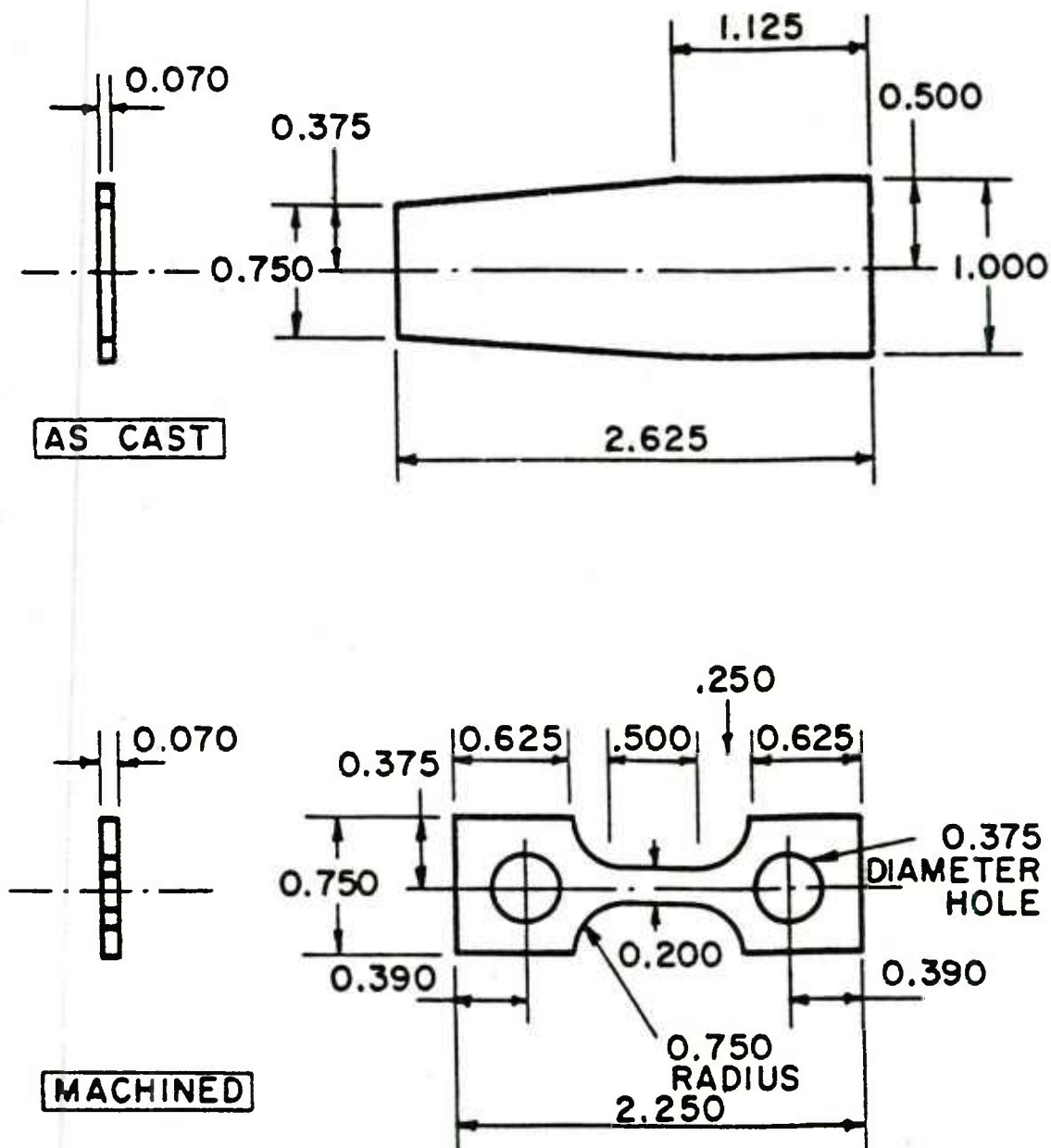


Fig.8 Cast to size tubular stress rupture specimen



39.4" = 1m

Fig.9 Flat stress rupture specimen, as cast and machined to final shape

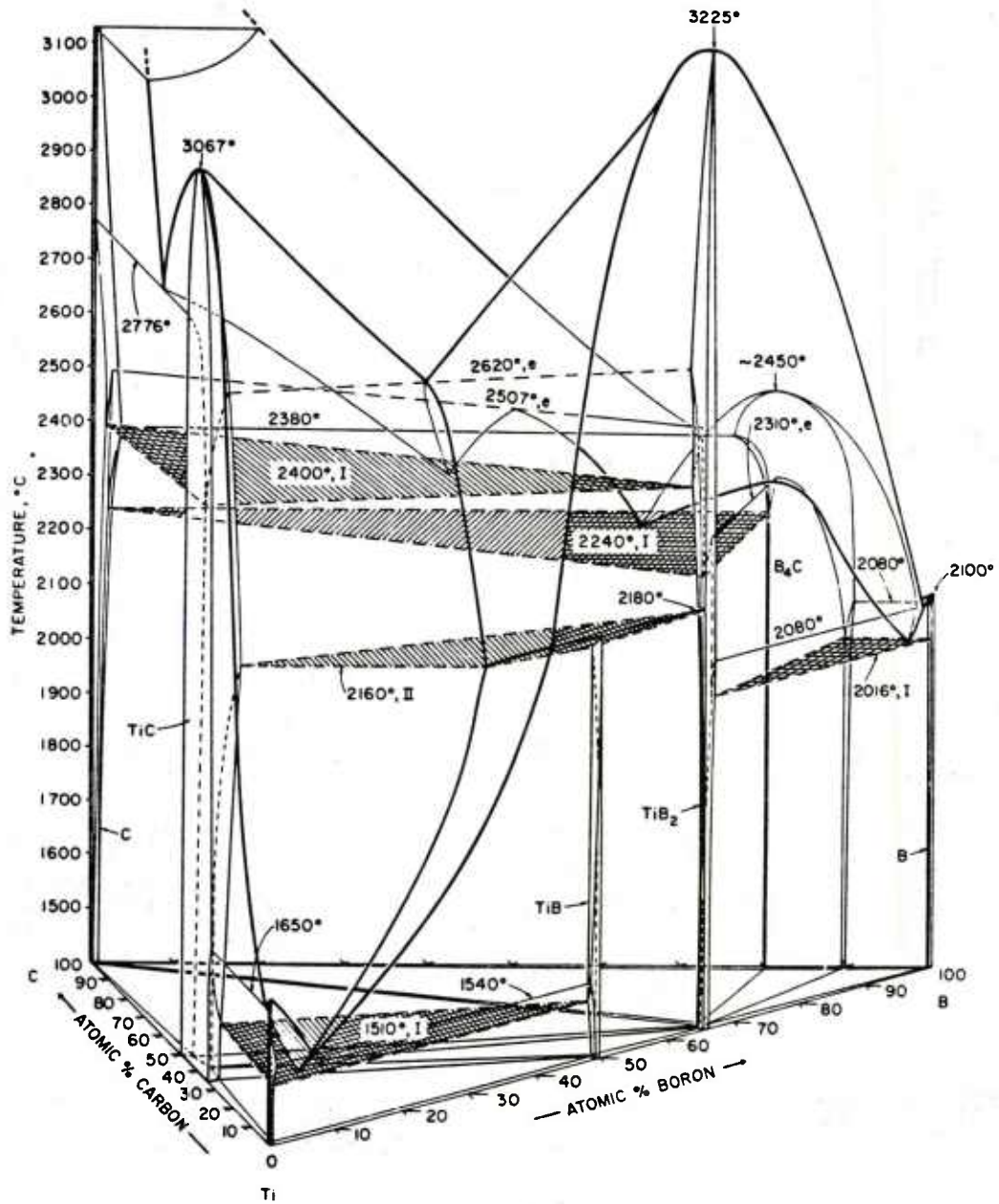


Fig.10 Isometric view of the Ti-B-C system

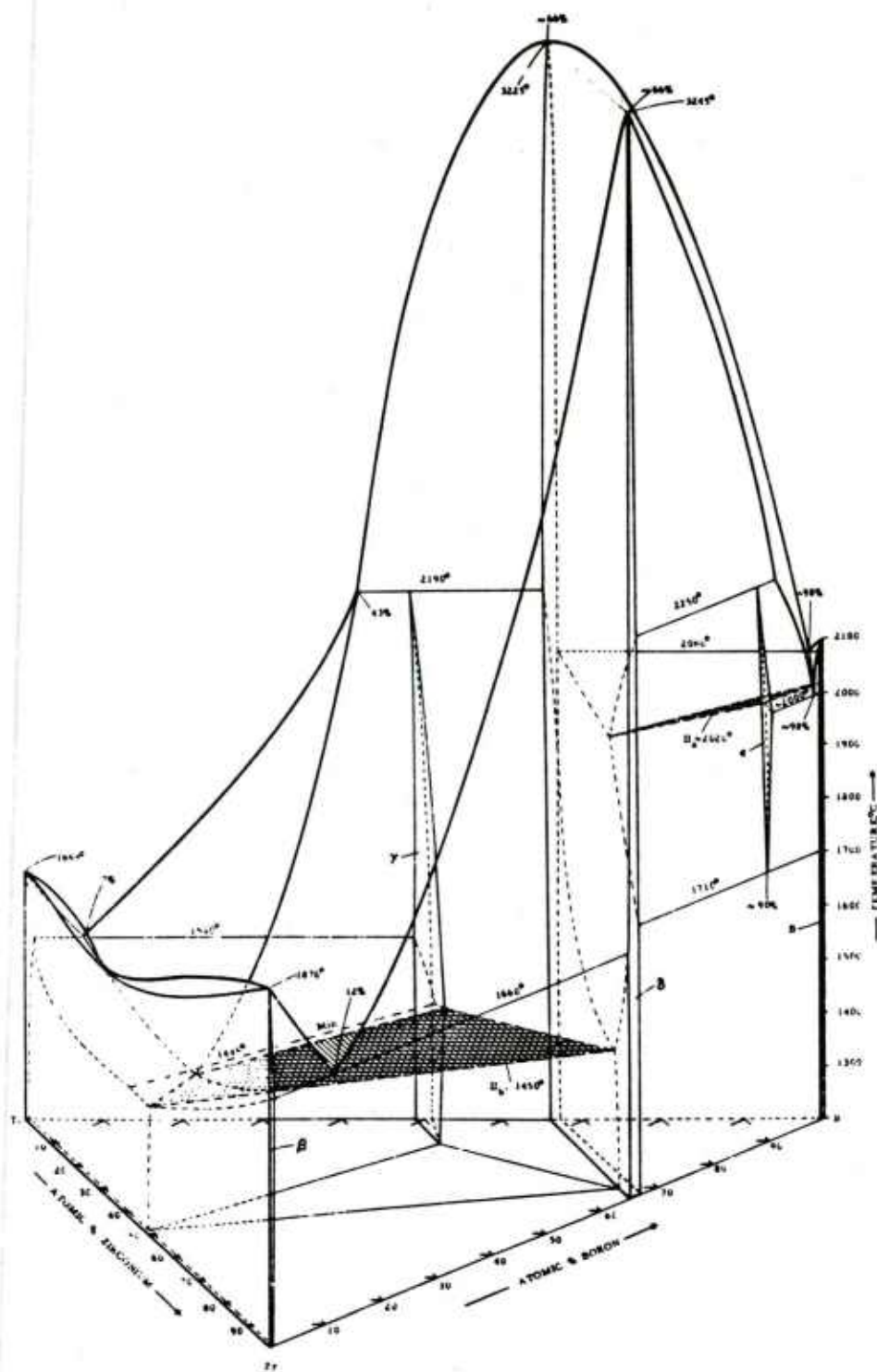


Fig.11(a) Isometric view of the Ti-Zr-B system

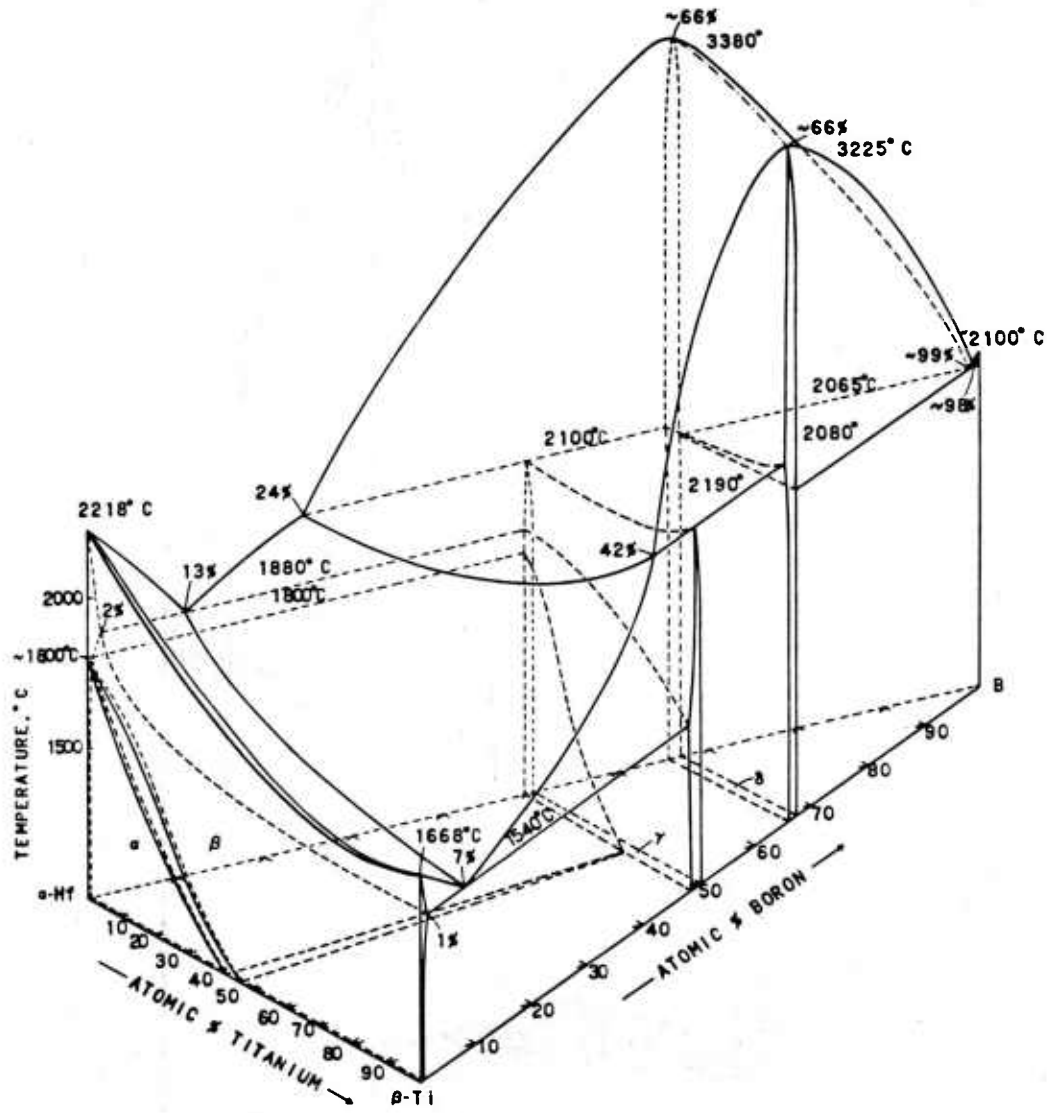


Fig.11(b) Isometric view of the Ti-Hf-B system

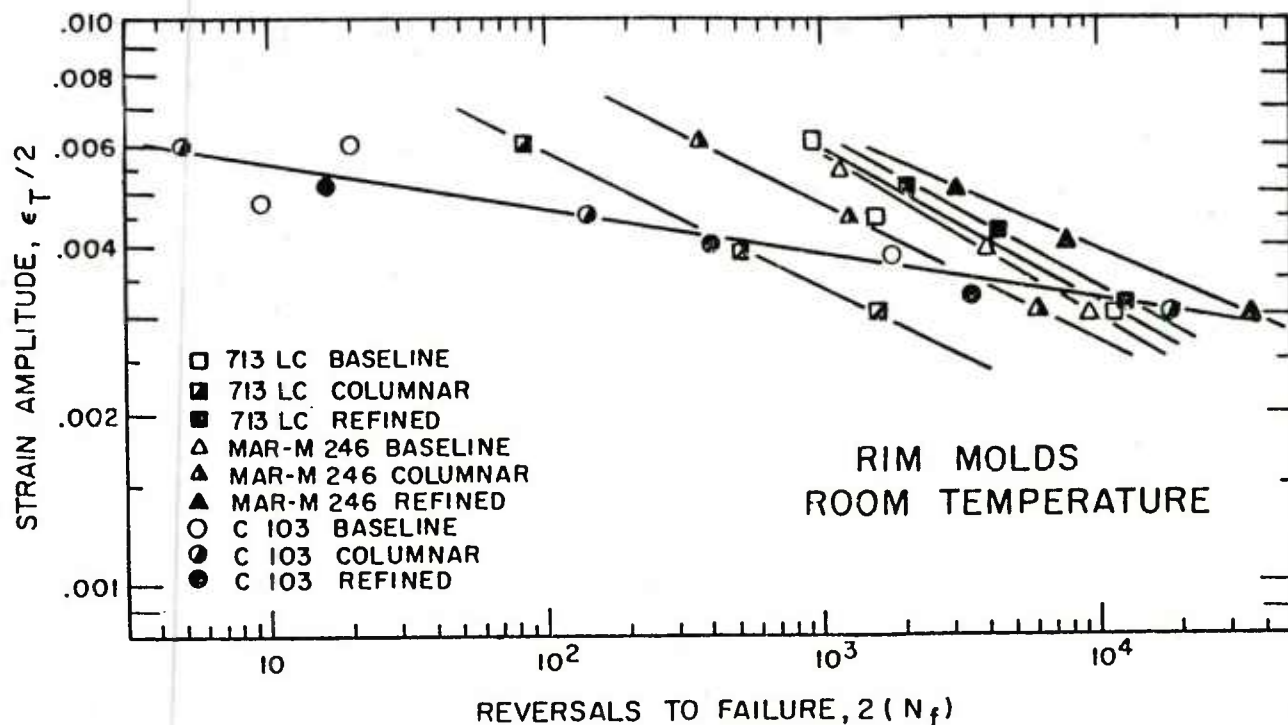


Fig.12 Room temperature low cycle fatigue behavior of specimens from the mold simulating the rim of the rotor

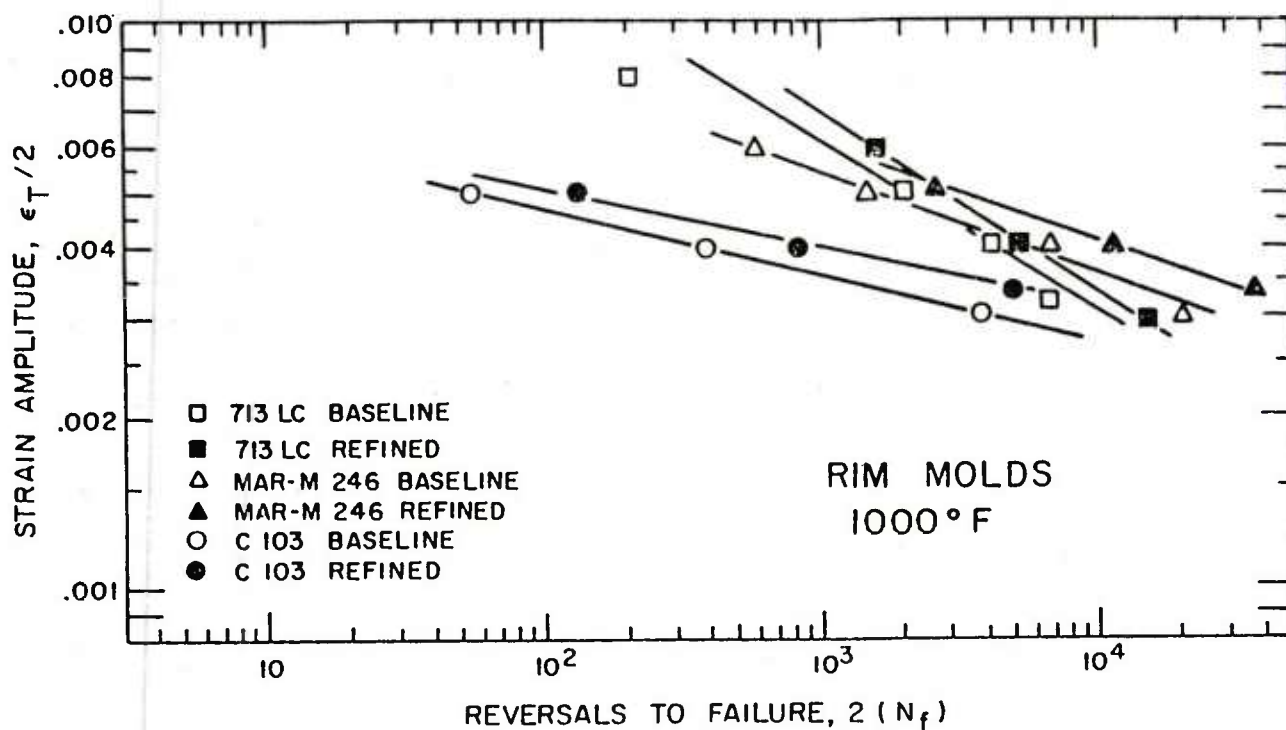


Fig.13 Low cycle fatigue behavior at 1000°F for rim mold specimens

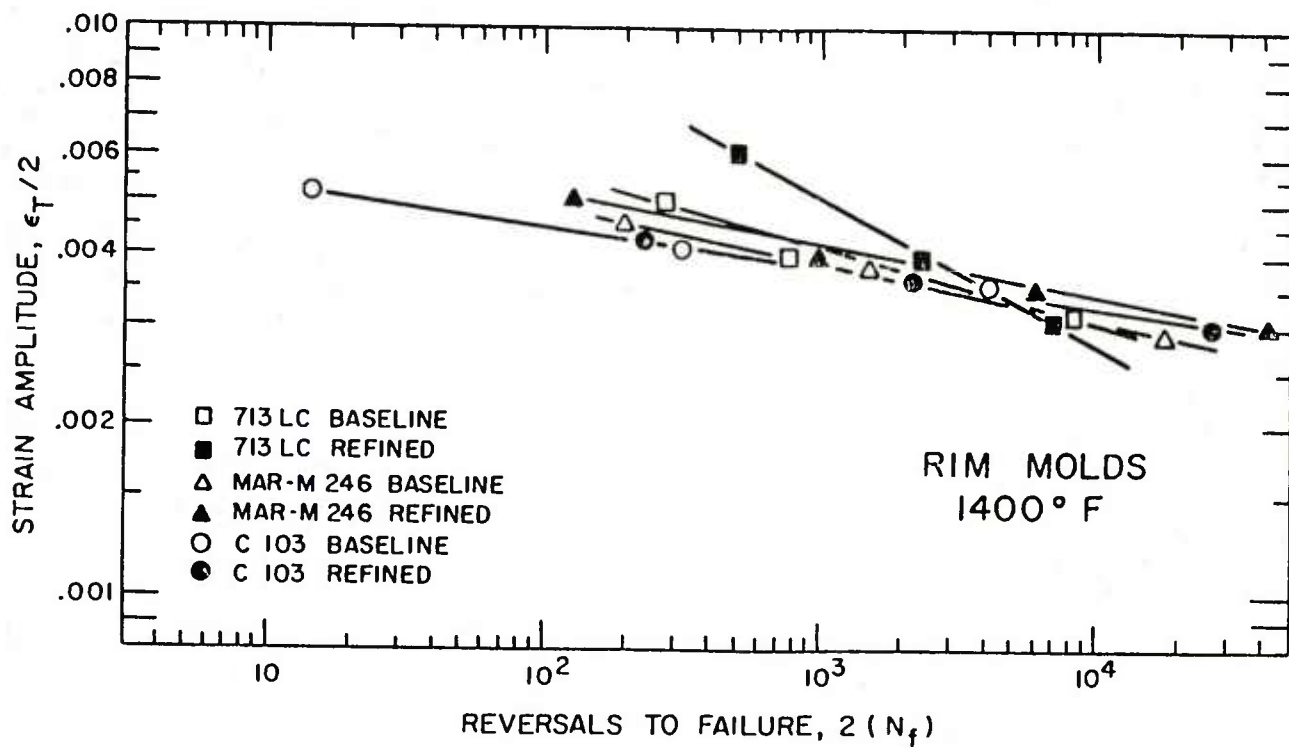


Fig.14 Low cycle fatigue behavior at 1400°F for rim mold specimens

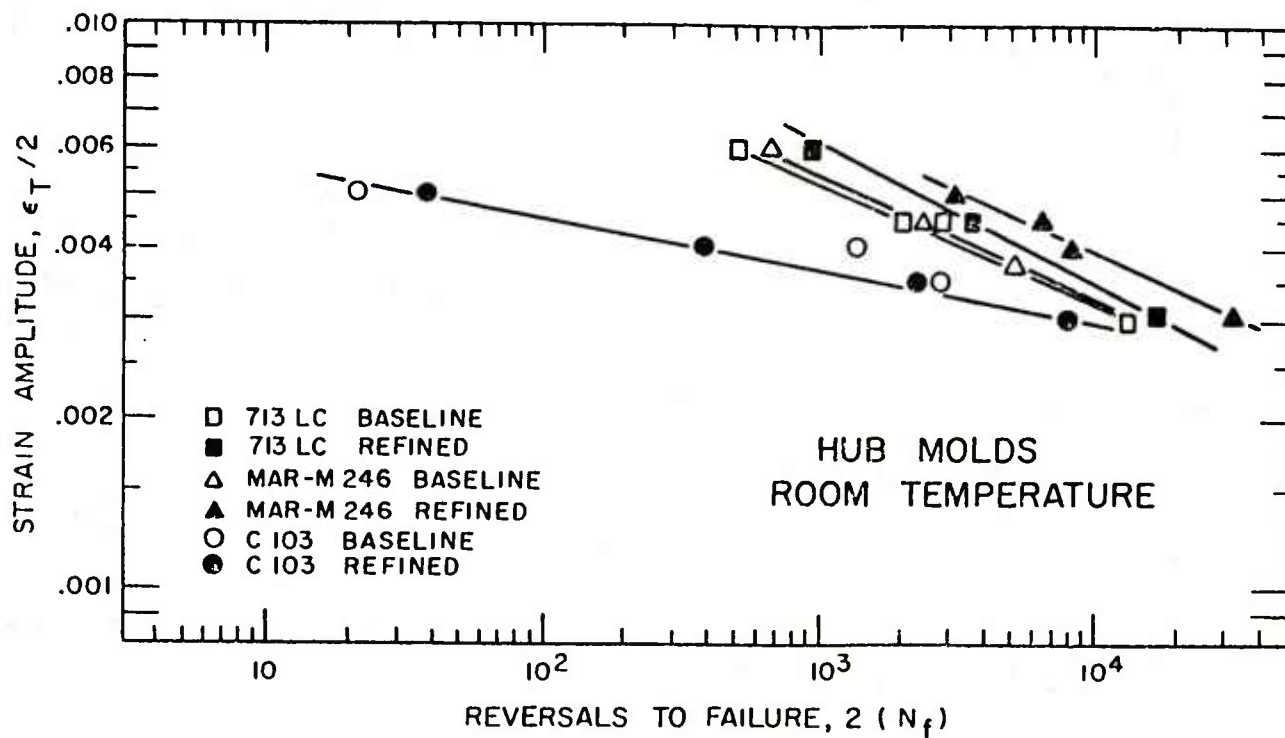


Fig.15 Room temperature low cycle fatigue behavior of specimens from the mold simulating the hub of the rotor

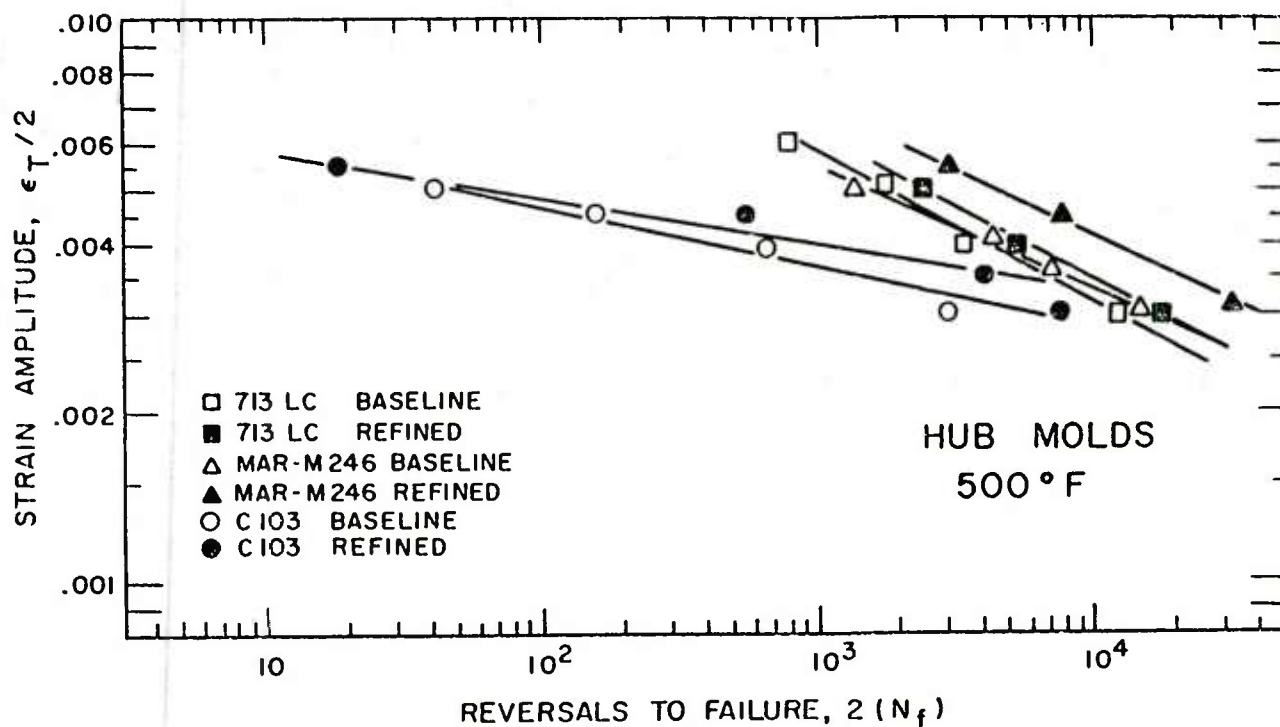


Fig.16 Low cycle fatigue behavior at 500°F for hub mold specimens

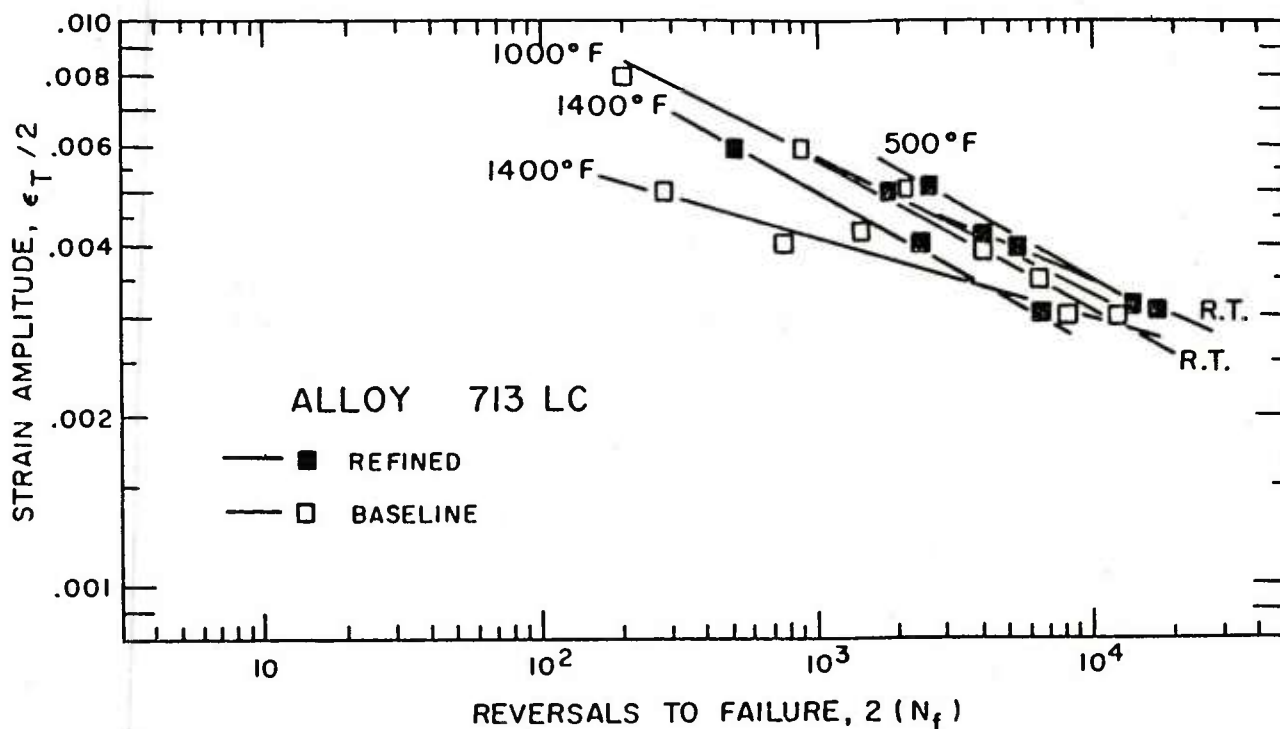


Fig.17 Low cycle fatigue curves for 713 LC in the baseline, coarse columnar and refined, fine grained equiaxed conditions

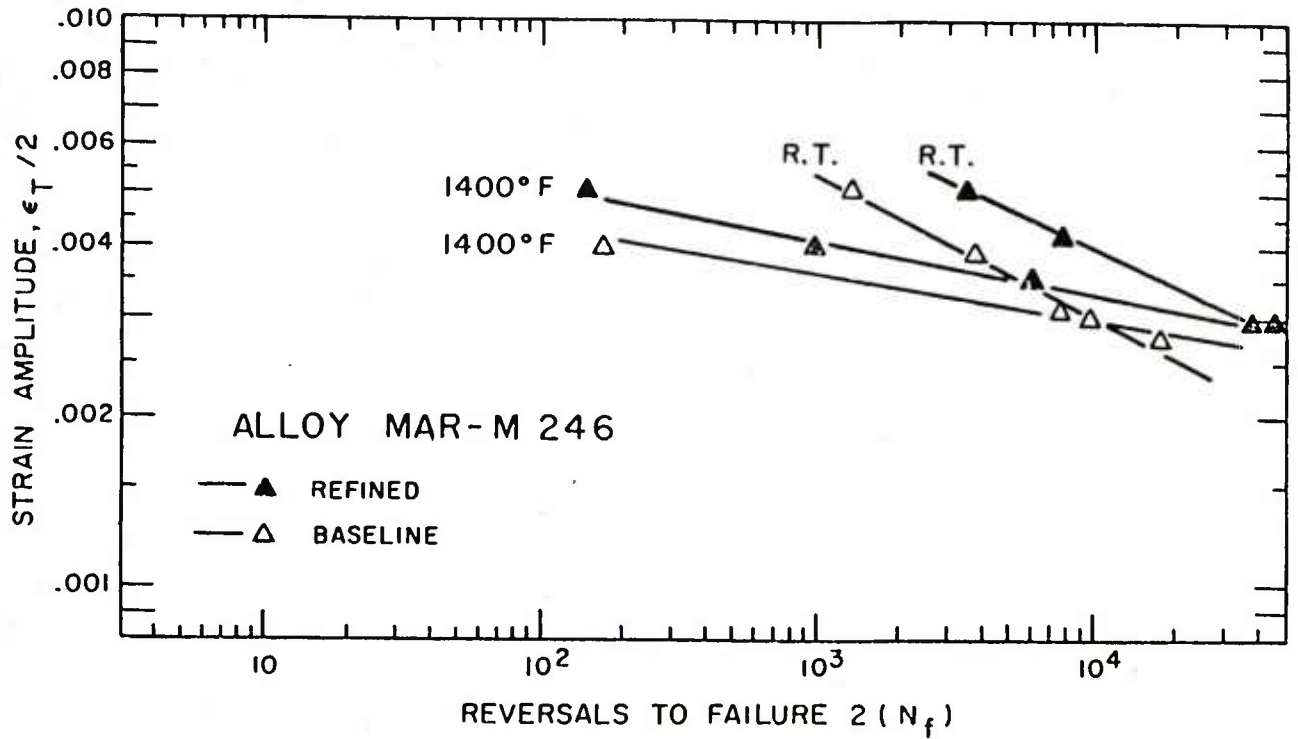


Fig.18 Low cycle fatigue curves for MAR-M 246 in the baseline, coarse columnar and refined, fine grained equiaxed condition

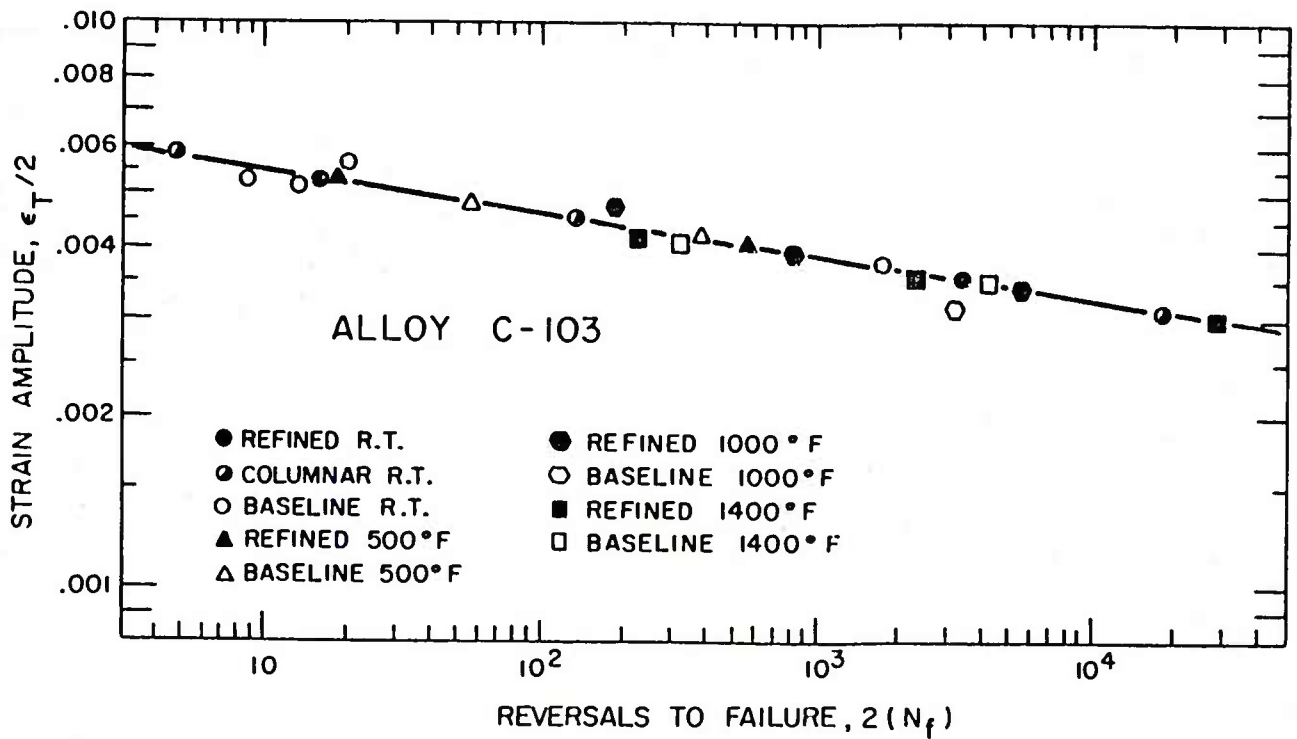


Fig.19 Low cycle fatigue curves for C 103 in the coarse columnar (baseline), fine columnar, and fine grained equiaxed condition

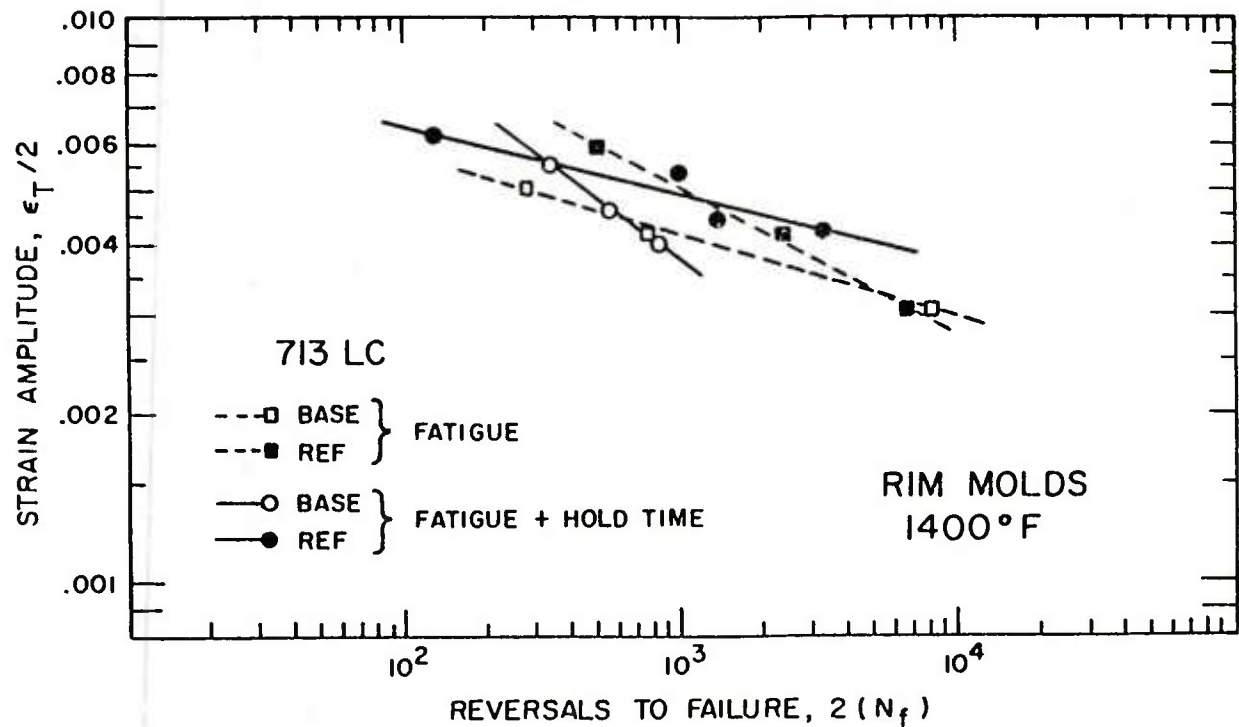


Fig.20 Effects of 90 second hold time on 1400°F fatigue properties of baseline and refined 713 LC

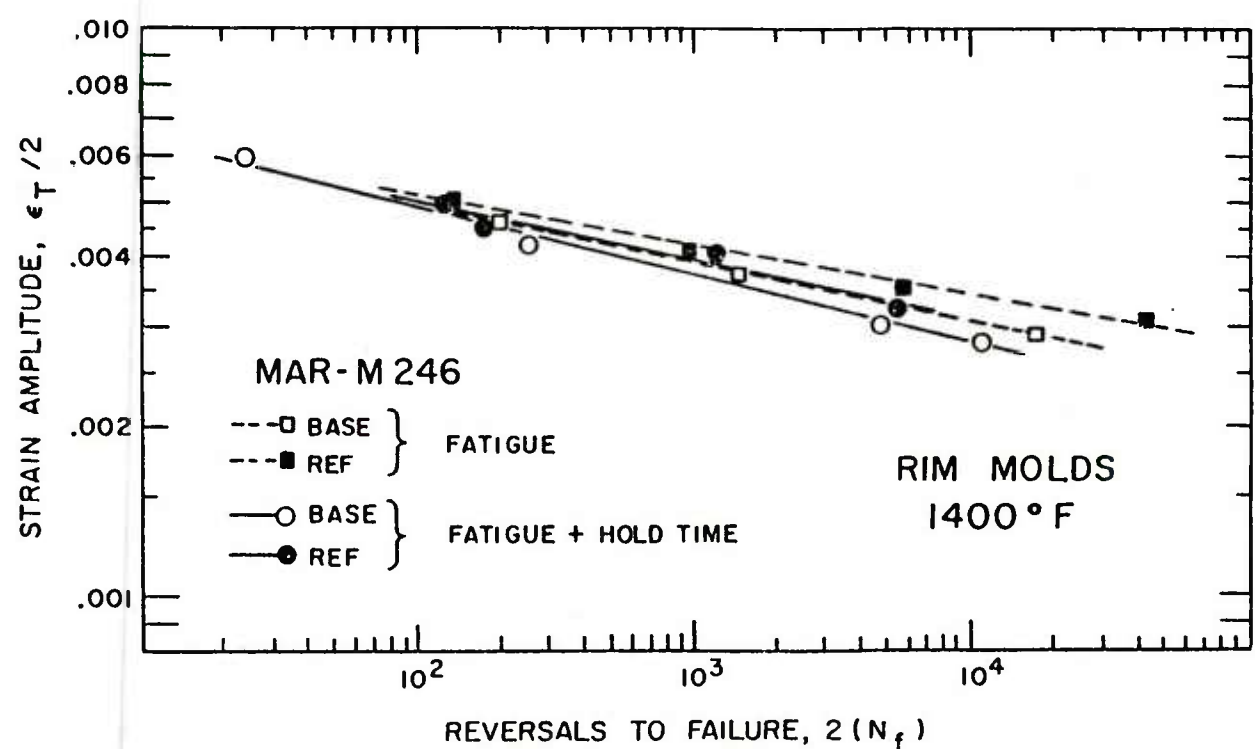


Fig.21 Effects of 90 second hold time on 1400°F fatigue properties of baseline and refined MAR-M 246

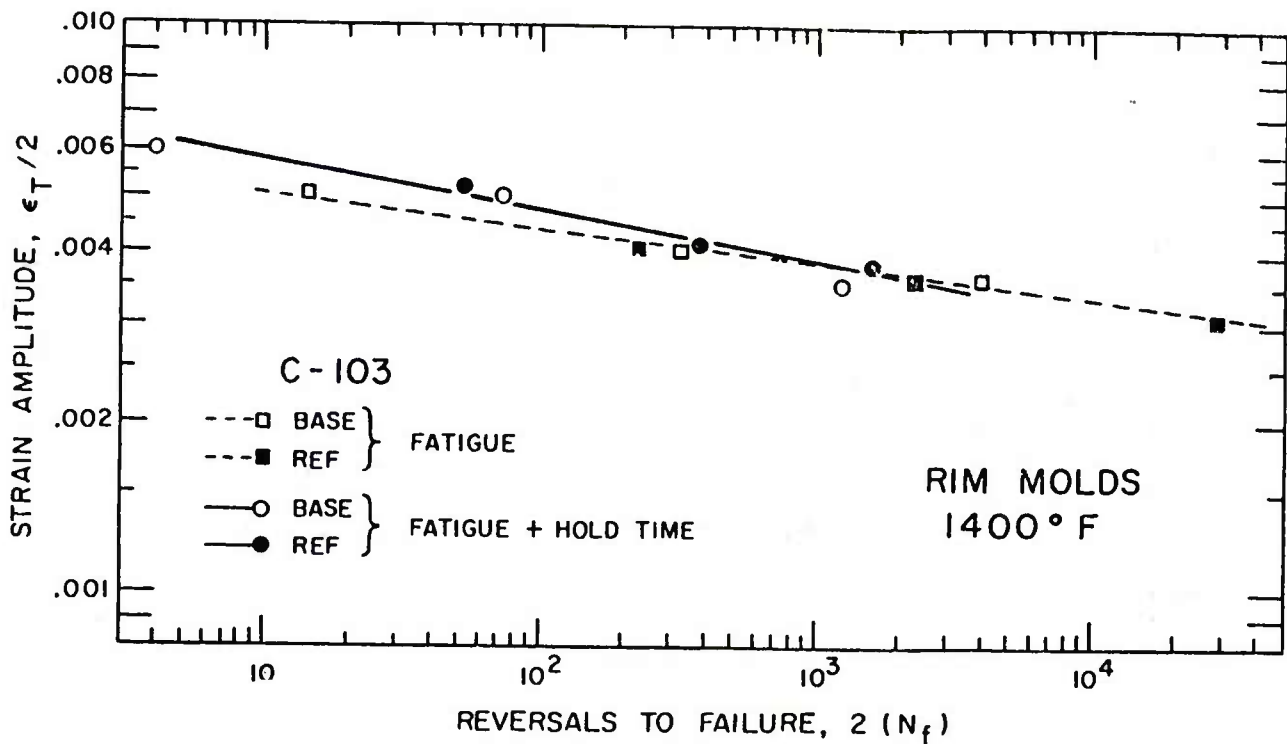


Fig.22 Effects of 90 second hold time on 1400°F fatigue properties of baseline and refined C 103

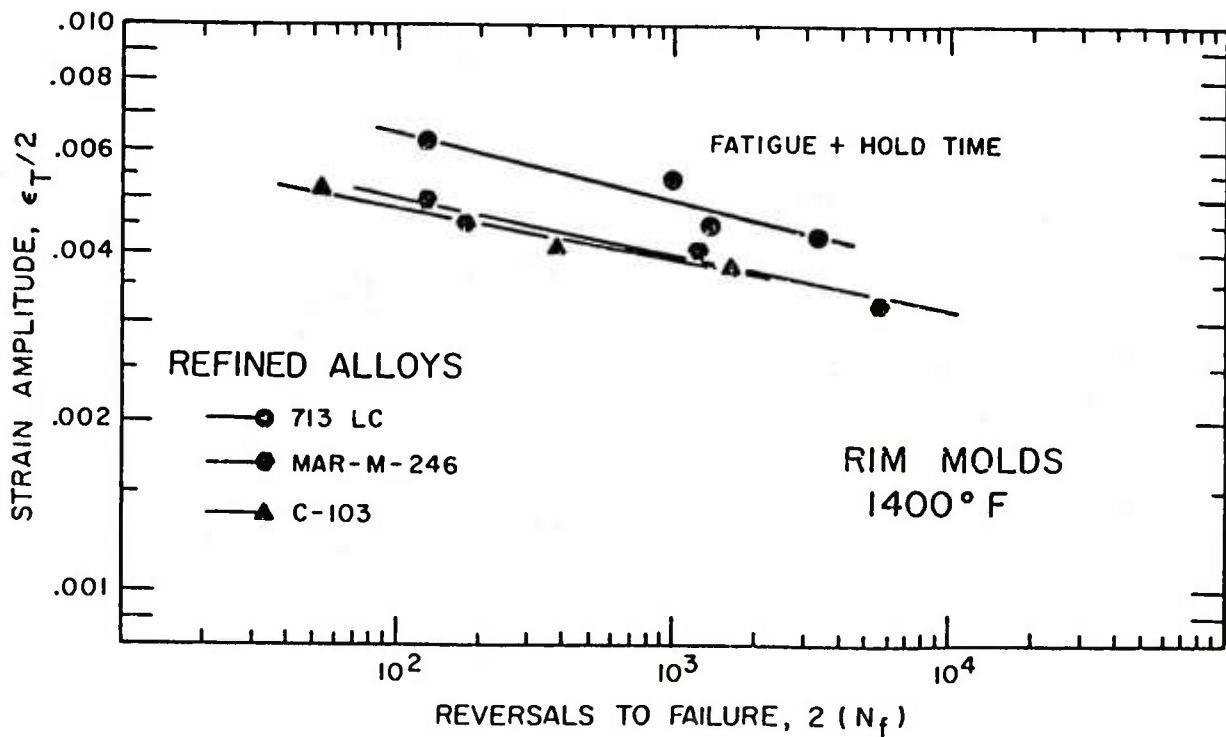


Fig.23 Summary of fatigue-creep properties of 713 LC, MAR-M 246 and C 103 in the grain refined condition

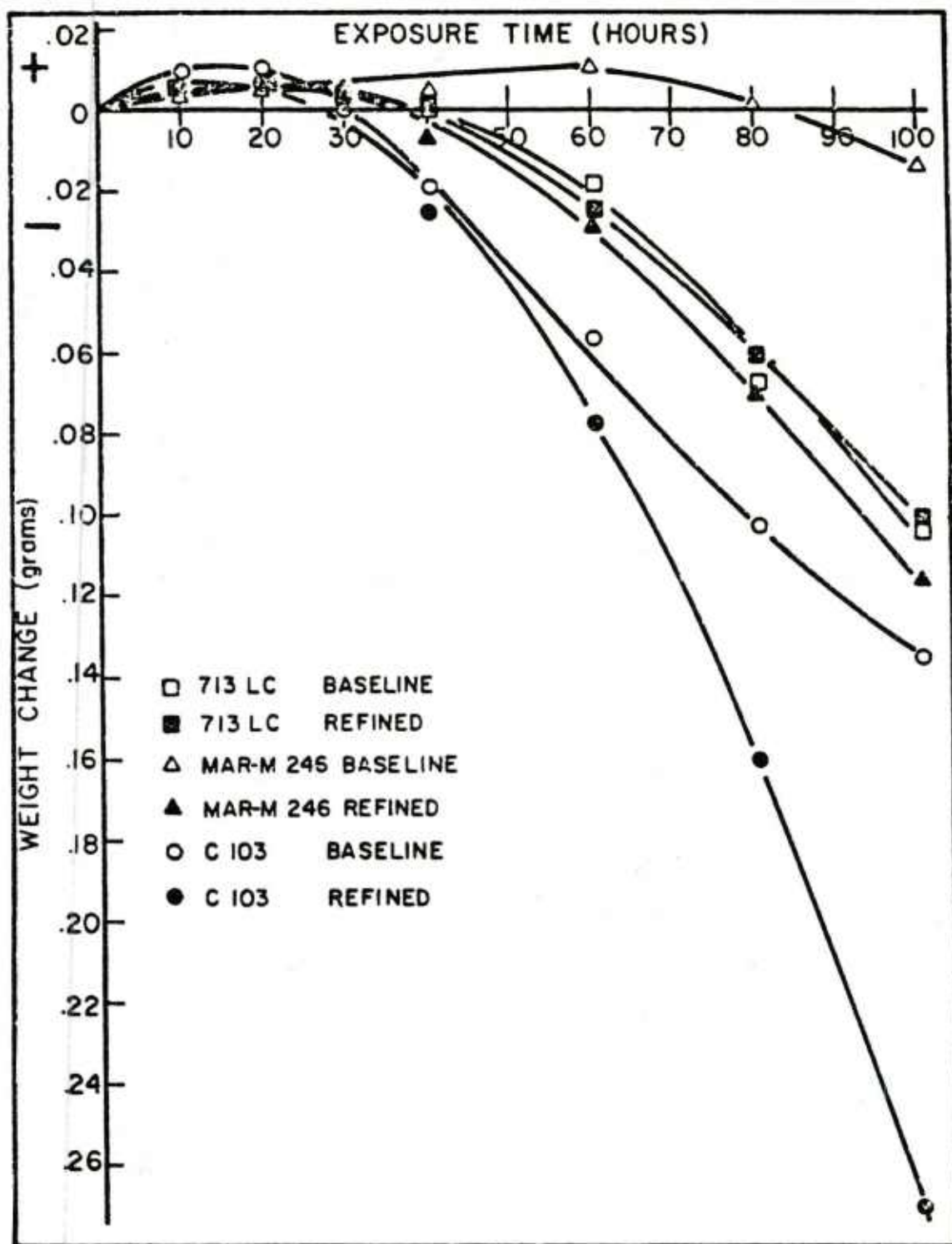


Fig.24 Weight change versus exposure time for thermal fatigue specimens tested in a burner rig at Mach 0.3

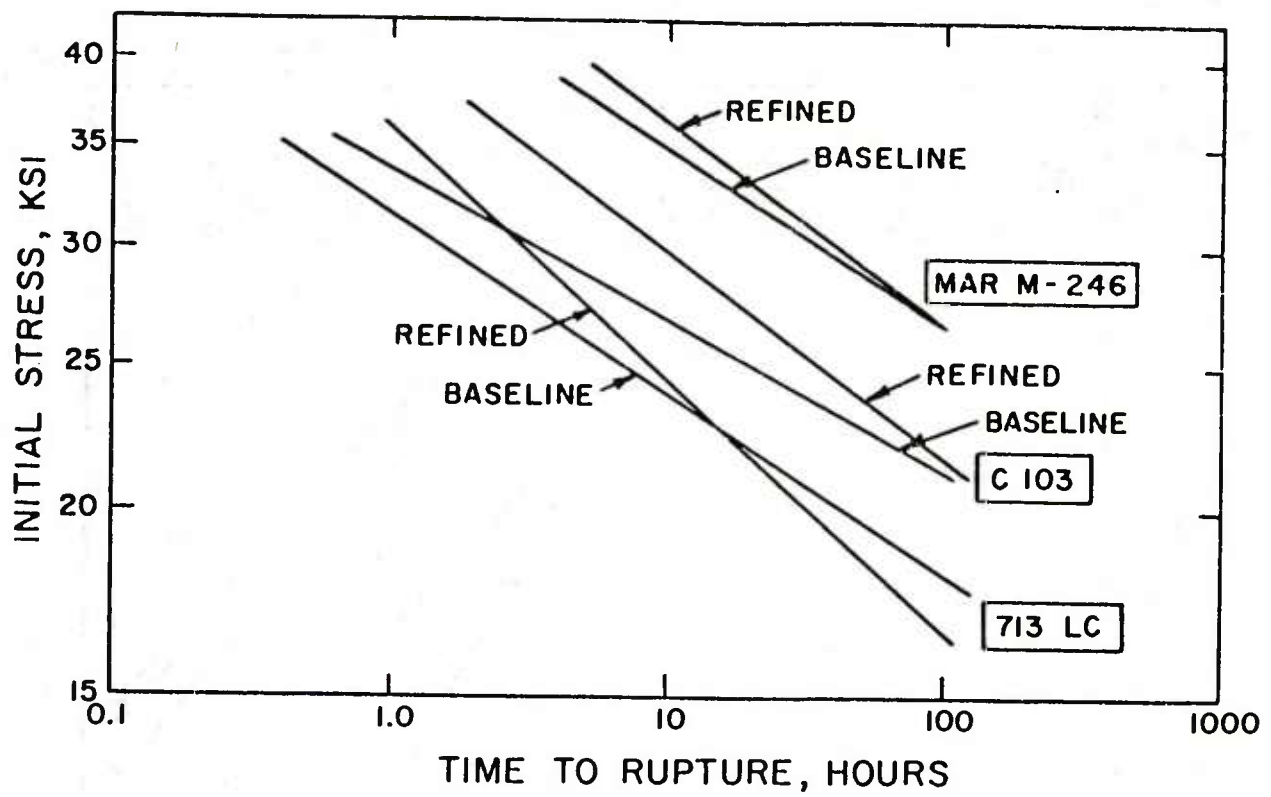


Fig.25 Summary of stress rupture curves for as cast tubular specimens tested in air at 1800°F

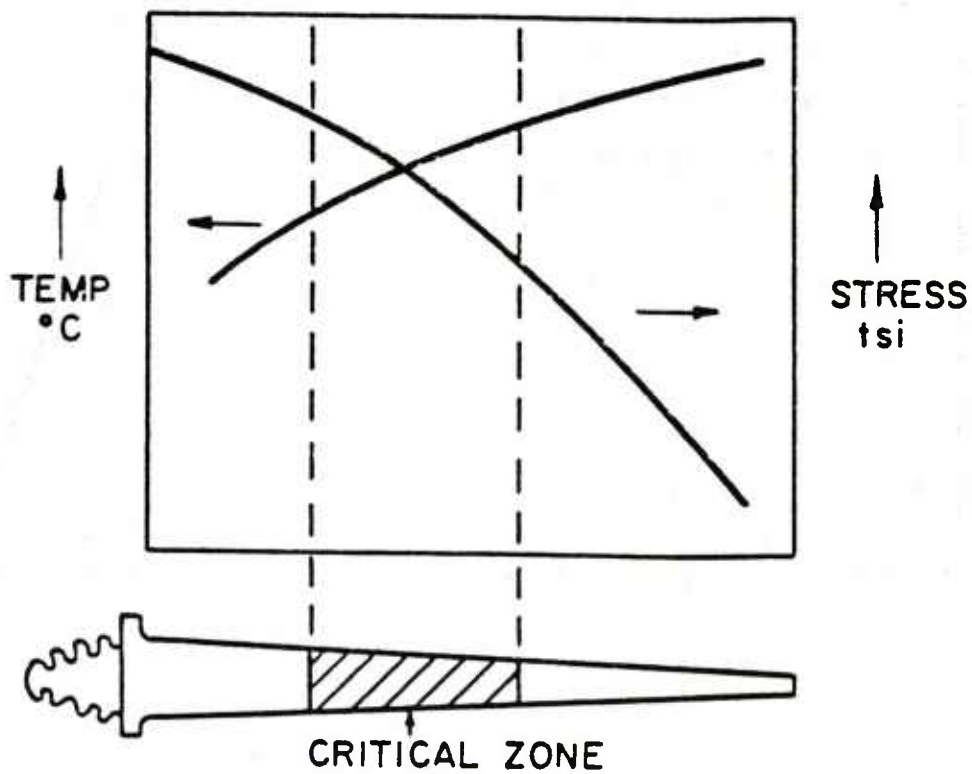


Fig.26 Stress-temperature distribution along blade aerofoil (Reference 30)

CAST TITANIUM COMPONENTS FOR ROTATING GAS TURBINE APPLICATIONS

Bruce A. Ewing
 Detroit Diesel Allison
 Division of General Motors Corporation

ABSTRACT

Investment cast titanium compressor impellers and integrally bladed rotor components offer the potential for significant cost reduction in gas turbine design. Cast titanium development activities at Detroit Diesel Allison (DDA) are discussed, and examples of rotating components with accompanying dimensional and mechanical property data are presented. Future trends and needs in this technology area are also discussed.

I. INTRODUCTION

There exists a growing concern for cost effectiveness in gas turbine design and, as a result, there has been an increased interest in processing techniques that offer the potential for producing near-net-shape components. In terms of compressor applications, the investment casting of titanium alloys offers an excellent opportunity to realize substantial cost savings compared with conventionally machined wrought products. Consequently, activity in this area has expanded significantly. However, the bulk of this effort has been directed toward static compressor applications, such as cases, stators, and housings. More recently, interest in titanium alloy castings has advanced into dynamic application areas such as impellers and integral wheels. It is in these areas that the net or near-net-shape making capability afforded by investment casting exhibits the greatest potential for reducing procurement costs in high-performance gas turbine designs.

For the past several years, DDA has been actively involved in the evaluation and development of titanium investment castings for rotating compressor applications. This work represents an important element in DDA's efforts to produce the most cost effective turbine engine designs possible. Emphasis is currently on high-performance impeller components in the Allison 250-C28B/C30 and the future 280-C1 turbine designs, cross sections of which are shown in Figures 1 and 2.

The potential of the investment casting process to produce high quality, near-net-shape rotating components that meet stringent dimensional criteria is the major incentive for pursuing castings as a substitute for forgings that require extensive and costly machining. A graphic example of the amount of machining required to produce a sophisticated impeller configuration from a forging is shown in Figure 3. In this case, the impeller is a 250-C28 configuration in the Ti-6Al-4V (Ti-64) alloy. For comparison, the advantages of an investment casting over a forging are dramatically presented in Figure 4. As shown, the airfoils require tip contouring and the shafts and backplate require only limited machining to make the casting ready for assembly into the engine. Cost studies conducted on this configuration indicate a savings of approximately 40% is possible with an investment casting versus the forging. On the basis of cost benefit studies performed recently by DDA using an analytical model developed for the NASA General Aviation Turbine Engine (GATE) program, this savings translates into over \$60 million for two important mission/vehicle configurations. If potential military requirements are added, and the application spectrum is expanded to one worldwide in nature, a huge potential life-cycle savings is indicated.

Although significantly reduced acquisition and life-cycle costs provide the incentive for utilizing titanium castings in compressor designs, it is important to point out that the component design must recognize the mechanical capabilities of the casting versus its wrought counterpart. Specifically, for the Ti-64 alloy, low-cycle fatigue (LCF) and high-cycle fatigue (HCF) lives can be significantly reduced. These reductions, however, need not limit the utilization of castings, if the stress/temperature environment of the impeller and the property capabilities of the casting are understood and properly matched. For example, in the early 250-C28 impeller design (Figure 4), the hub is solid and, as a result, maximum operating stresses are moderate. With a modest redesign of the impeller backface, operating stresses were reduced to a level consistent with the low-cycle fatigue capabilities of cast Ti-64.

In higher performance compressor applications, however, such as the DDA advanced technology 280-C1 turboshaft engine, the impellers are hollow to accommodate shafting. As a result, bore stresses are significantly increased over comparable stresses in solid impeller designs. In addition to the unique stress problems imposed by hollow bore impeller designs, the operating temperatures in the later stages of the compressor tend to increase significantly due to pressure rises and soak-back from the turbine. As a result, the fatigue environment in which a titanium casting must perform in advanced applications can be further aggravated. Matching alloys and processing techniques to these types of applications is a major challenge, as the substitution of titanium investment castings for machined wrought components must be made without sacrificing design life, reliability, or engine performance.

II. EARLY DDA CAST TITANIUM FEASIBILITY STUDIES AIMED AT ROTATING APPLICATIONS

Consideration of castings for man-rated rotating compressor applications has, until recently, suffered because the high melting point and extremely reactive nature of titanium alloys make it difficult to cast high integrity/close tolerance shapes. In addition, there is strong concern in the industry about the inherently lower fatigue capability observed in the cast forms, as opposed to the wrought forms, of a given alloy.

To overcome potential fill, soundness, and surface quality problems in the investment casting of high-performance titanium compressor impellers, OOA conceived a processing approach designed to preclude the obvious fill and reactivity problems associated with the conventional casting of components.

This approach involves casting a component with airfoils uniformly oversized to ensure total fill; hot isostatic pressing (HIP) to eliminate microshrinkage or porosity; and subsequent chem milling to eliminate surface contamination that might be present either from casting or HIP and to bring oversized surfaces into final tolerance. Working closely with Precision Castparts Corporation (PCC) of Portland, Oregon, controlled casting experiments were conducted with the Ti-64 alloy, utilizing OOA-supplied tooling based upon an advanced high-pressure ratio impeller design that was a precursor to the Model 250-C28 design. Of major concern was the amount of additional airfoil stock that would be required to effect fill with the proprietary PCC shell system. To evaluate thickness additions as a variable on fill characteristics, inserts with varying thickness increases of 0.64 mm (0.025 in.), 0.89 mm (0.035 in.), and 1.14 mm (0.045 in.) in airfoil regions were built into low-cost plastic tooling. Utilizing this tooling, impeller patterns representative of airfoils of different thicknesses were produced.

To produce molds, investment techniques similar to those used for superalloys were employed. Utilizing skull melting techniques, castings were manufactured as shown in Figure 5. Subsequently, the castings that were fully processed through HIP and chem mill operations were evaluated for overall surface/fill quality, HIP densification characteristics, dimensional integrity, and chem mill response. Complementary effort were evaluations of tensile and LCF/HCF characteristics.

The results indicated that satisfactory fill was achieved for all thickness increases, that fully dense structures could be achieved, and that chem milling could be accurately performed. Based upon these results and mechanical property evaluations, a scale-up of the effort was undertaken to include the manufacturing of tooling for the casting of full-scale 250-C28 impellers suitable for rig and engine evaluation.

III. FIRST-GENERATION IMPELLER QUALIFICATION EFFORTS

Utilizing full-scale 250-C28 tooling, PCC produced several impellers in the Ti-64 alloy.

The airfoil patterns used for the impellers were made from plastic and contained a 0.64 mm (0.025 in.) uniform stock addition to each airfoil surface to ensure fill. A typical sequence for the fabrication of plastic impeller assembly patterns is shown in Figure 6.

Following investing of the patterns and casting, in which the alloy was melted by skull techniques, the impellers with oversize airfoils were hot isostatically pressed. Initial castings were processed using HIP at 843°C (1550°F) for 2 hr and 103.4 MPa (15 ksi). However, because of concern that these parameters might not eliminate all potential porosity, later impellers were processed using HIP at 899°C (1650°F) for 2 hr and 103.4 MPa (15 ksi). The castings were then chem milled to final airfoil tolerance.

Visual Nondestructive Evaluation (NDE) Quality

Overall quality of the first impeller castings was judged excellent as total fill was realized on all surfaces, and the chem milled surfaces were free of mold metal reaction. In almost all cases, however, varying degrees of welding were performed by PCC in airfoil and hub locations to repair small laps and pits. Overall visual quality of the impellers was impressive. Subsequent X-ray and dye penetrant review of the castings indicated good conformance to drawing requirements.

Dimensional Inspection Results

As shown in Table I, initial results for the first 250-C28 impellers inspected were very promising and, with the general exception of certain throat, hub, and airfoil contour dimensions, the impellers revealed excellent conformance to drawing requirements. Further dimensional inspection work completed on additional impellers produced results that basically followed those obtained for the first impellers, showing that blueprint requirements for airfoil thickness were consistently met. Throat dimensions, however, consistently failed to meet blueprint requirements, as they were tight and inconsistent from one impeller to the other. With respect to airfoil contours, basic shapes were displaced when compared with drawing requirements, reflecting a droop at the leading edge where the condition was the most severe. However, overall airfoil contours were similar, suggesting that the airfoil segments were not registering one to the other.

To establish the cause for the dimensional problems, a review of the impeller tool and its relationship to the pattern assembly was conducted. As a result, it was found that an interference existed between the booking surfaces of airfoil segments, causing irregular displacements in positions. This finding tended to explain the problems with both the throat openings and the airfoil droop. Although the quality of the tool used for these first-generation castings was less than optimum, it was possible, by paying very close attention to assembly detail, to obtain castings with a high degree of dimensional integrity. Despite the tooling problems, enough was learned through these experiences to provide confidence that the basic processing concept was capable of achieving dimensional characteristics of the type required for a modern, high-performance impeller application.

Mechanical Property Evaluations

Substantial impact, tensile, and LCF testing was conducted on specimens machined from fully processed Ti-64 impeller castings in the As-HIP condition. Typical tensile and impact results from this effort are presented in Figures 7 and 8. As is indicated, impact strengths are comparable, but ultimate tensile strengths are degraded approximately 20% compared with the wrought Ti-64. Smooth and notched LCF data for specimens machined from cast Ti-64 impellers are presented in Figures 9 and 10. In comparison to wrought Ti-64 LCF capability, a loss in strength is indicated. Specifically, on a typical basis, cycles to failure for a given strain range are reduced on the order of one half.

In the area of HCF testing, impellers were bench tested to assess the in situ fatigue capabilities of 250-C28 impeller airfoils. In this testing, the airfoils were strain-gage instrumented and then excited by an air siren. By controlling vane deflection, stresses were controlled and endurance limits established. As is shown by Figure 12, the HCF capabilities of the cast airfoils were reduced approximately 25% compared with the wrought airfoils tested in equivalent conditions.

Overall, the results of mechanical property testing performed on Ti-64 impeller castings have shown a reduction in strength capability compared with the wrought counterparts. However, the potential exists to utilize castings in selected designs and still maintain an adequate level of reliability and durability, provided the stress/temperature environment unique to the impeller design and the mechanical property capability of the casting are well understood.

Component/Engine Testing

Component/engine testing of early 250-C28 impellers included both cyclic spin testing (LCF) and engine testing. Details of this testing follow.

Cyclic Spin Testing

Two ambient temperature cyclic spin tests were successfully completed by DDA on fully machined impellers. In this testing, the impellers were cycled from a simulated idle speed to maximum speed plus 18% to compensate for temperature and back-to-idle speed. Dwell times at maximum speed were periodically applied to simulate hold times.

The first impeller was tested at stress levels in excess of those developed during engine operation so that it would fail in a reasonable period of time. This was accomplished by machining the backplate to a modified configuration. After failure occurred at 12,006 cycles, the failure origin was determined to be at the radius of the balance ring as predicted by a stress analysis. Careful metallurgical review followed, and the test results were considered very encouraging.

To verify the long-term integrity of the design that was developed specifically for a casting, the second impeller was machined to an engine configuration and tested to simulated engine test stress levels. This casting was successfully retired after 45,000 cycles. As with the first test, the results were highly encouraging.

Engine Testing

One of the impellers (Figure 12) produced from the 250-C28 tool was satisfactorily engine tested in a 250-C28 engine. The results indicated attractive engine performance compared with that predicted for a wrought impeller. Overall, the performance results for this test program were considered promising.

IV. SECOND-GENERATION COMPONENT DEVELOPMENT

The work conducted on 250-C28 impellers provided confidence that cast titanium components could be developed for rotating applications. It was clear, however, that the use of the Ti-64 alloy would be restricted only to those applications in which the stress and temperature environment could accommodate the relatively reduced fatigue capabilities of the cast form of the alloy.

Consequently, efforts were undertaken at DDA to evaluate alternative alloys and processing concepts that could lead to the cost effective utilization of cast titanium in advanced, high-performance applications. Of particular interest were hollow bore impellers and integrally bladed fan rotors for existing and derivative advanced technology designs. Two general approaches involving advanced alloys and dual-property fabrication concepts are being pursued.

Advanced Alloys

Full-scale Model 250 impellers have been produced and evaluated in each of the following alloys:

- o Ti-6Al-2V-4Zr-6Mo (Ti-6246)
- o Ti-6Al-2V-2Zr-2Mo-2Cr-0.25Si (Ti-62222S)
- o Ti-6Al-2V-4Zr-2Mo (Ti-6242)
- o Ti-2.6Al-1.3V-7Sn-2Zr (Transage 175)

In addition, Ti-6246 alloy second-stage 280-C1 impellers and Transage 175 integrally bladed fan rotors have been produced. This work has been conducted under both in-house and U.S. Army/Air Force sponsorship and is ongoing. Much work remains to be done with these alloys and configurations; however, at this point it can be noted that very attractive levels of both temperature capability and fatigue strength have been demonstrated. The Ti-6246 and Transage 175 alloys, in particular, appear to offer the best potential for utilization in next-generation designs.

With respect to the Ti-6246 alloy, elevated temperature creep resistance, which is competitive with wrought Ti-6246, has been demonstrated. In addition, a twofold advantage in fracture toughness has been measured for the casting over the conventionally processed forgings. In terms of fatigue capability, the results of tests run on specimens machined from cast Ti-6246 impellers indicate a two- to threefold improvement over cast Ti-64 in LCF life capability for a given strain range. In HCF capabilities, the extrapolated stress for 10^7 cycles for Ti-6246 was improved 10%-15% over Ti-64. From a weld-repair standpoint, however, the Ti-6246 alloy is not as readily weld repairable as Ti-64. Therefore, additional work is required in this area to minimize the incidence of weld and heat affected zone cracking that has been observed in heavy sections of impeller castings.

Excellent castability and weld repair characteristics in combination with outstanding mechanical properties have been developed with the moderate temperature Transage 175 alloy, a development of the Lockheed

Missiles and Space Company. In the case of work that has been directed at integrally bladed, high-bypass fan rotors (Figure 13), tensile properties competitive with wrought 17-4PH have been realized. As fan blades are particularly vulnerable to foreign object damage this level of strength is of particular interest to designers. From an LCF and HCF standpoint, work completed to date indicates a fatigue parity with wrought Ti-64. This is a major accomplishment and could lead to the introduction of titanium castings into a number of critical fatigue-limited applications currently requiring wrought titanium.

Dual-Property Components

DDA experience with dual-property components has been extensive, involving HIP bonding of both superalloy and titanium details for small gas turbine wheels and impellers. Interest in the dual-property concept stems from an ability to selectively locate materials in specific component areas in which specialized properties are required to achieve high performance. In the case of titanium impellers with highly stressed LCF-limited bores, the concept is ideally suited, as it provides the potential for combining wrought, fatigue-resistant hubs with cost effective near-net-shape cast airfoils.

To demonstrate feasibility of the concept in DDA designs, a cavity for acceptance of a wrought Ti-64 hub was machined into a Ti-64 impeller casting in a 250-C28 configuration. A photograph showing the machined cavity is shown in Figure 14. In designing the bond line geometry, the wrought portion of the joint was intentionally located in a region in which it would be preferentially exposed to the highly stressed areas in the backplate as well as in the hub and, at the same time, provide suitable material for specimen testing across the bond joint. The machined shell and hub details are shown in Figure 15.

To prepare the details for assembly, thorough cleansing was required to remove any residual film. To effect assembly, the cast shell was heated to 204°C (400°F) and the plug was cooled by immersing it in liquid nitrogen. The hub was then inserted into the casting and the assembly temperature was allowed to equalize; this resulted in a tight fit between details.

To effect bonding of the cast and wrought surfaces through HIP techniques, it was necessary to evacuate and seal the joint interface. To accomplish this, the exposed top seam was completely laser tack-welded (Figure 16), and all but a short segment on the bottom seam was laser welded. The assembly was then placed in an evacuated chamber, and final closure of the bottom seam was performed with an electron beam (EB) weld as shown in Figure 17.

To evaluate the effect of HIP bonding on the integrity of the bond, the impeller was sectioned, polished, and etched. Selective microevaluation of the bond joint displayed excellent diffusion of the detail surfaces with no discernible evidence of voids or deleterious structure at the bond interface. Figure 18 shows an etched macroslice of the bonded impeller with selected photomicrographs of representative areas of the bond joint.

Tensile specimens were machined from the bond-joint region, centering the joint in the reduced gage section of the specimen. Ultimate tensile strengths of the specimens were determined and are listed in Table II. All of the failures were at levels comparable to the weaker cast material, demonstrating 100% joint efficiency.

These results were considered significant, as they represented one of the first-known demonstrations of the dual-property concept involving titanium impellers. A major benefit was that it served to illustrate the combined advantages of near-net-shape airfoils and wrought fatigue resistance in critical hub locations. Much work remains to be done in this area. However, the experiment showed the excellent cost effective potential that exists for dual-property impeller designs in advanced applications.

V. FUTURE NEEDS

Over the past five years, much progress has been made toward gaining the confidence of the gas turbine community relative to the use of titanium castings. An example of this is the Pratt and Whitney (P & W) F100 engine, which uses a wide variety of titanium castings for static structural applications. The growing acceptance of titanium castings is largely due to the growing use of HIP to maximize internal soundness, the advances made in molding systems, and the cost pressures that dictate the minimization of machining and the simplification of fabrication processes. Future acceptance and increased use of titanium castings, however, will require improvements in a number of technical and nontechnical areas.

Producibility Demonstrations

The transition to the use of rotating components has been painfully slow due to the high costs and the technical risks involved in qualifying rotating hardware. This is particularly true in the case of retrofit operations in which castings are potential substitutes for more expensive forgings, which have performed satisfactorily and are a known quantity. In new designs, for which tradition is yet to be established, the opportunities are greatest. However, budgets are oftentimes severely limited, and future production requirements are uncertain.

As a result, it is frequently necessary to conduct component development programs at a level that precludes the large-scale manufacturing volume ultimately required to firmly establish yields, generate the required data base for design validation, perform extensive component/engine testing, and work out the problems that invariably develop when attempting to introduce new technology. Consequently, relatively high levels of funding beyond those identified, and which lead to extensive producibility and component/engine test demonstrations, must be allocated if titanium castings are to find their way into rotating applications. Product quality in this day and age is serious business and to prevent surprises and potential liability, in-depth component characterization must be performed.

Process Control

Any time the subject of technology acceptance is discussed, quality assurance and process control must be included. This is particularly true with near-net-shape components that operate in severe stress/temperature environments. The problem of inspecting a near-net-shape impeller is at best difficult.

X-ray and fluorescent penetrant inspection techniques are ultimately the most effective NDE tools available and, in the case of relatively small components, may be very effective. In larger components, like the 250-C28 impeller, the most critically stressed hub portion of the impeller is generally the most difficult to inspect, even with the availability of high-energy X-ray and neutron radiographic devices.

As a result, the need for exacting process control becomes extremely important. Unfortunately, however, success in the titanium casting business is often keyed to a proprietary shell system or technique, which makes control difficult. If the vendor does not understand how critical it is to maintain parameter control and documentation, difficulties are likely to arise that could lead to serious consequences. To offset these possibilities, it is recommended that coding systems be developed for proprietary components in the casting system. By establishing ranges and monitoring frequently, it will be possible to prove that key elements in a proprietary process have not changed, and that consistent performance can be expected.

Development of Alternate Sources

A high technology base is a prerequisite for companies wishing to participate in the casting of complex rotating titanium components. The number of casting vendors currently capable of participating in this technology area is severely limited, and experience has taught that competition yields an improved product. Therefore, another need that must be addressed in the future is multiple source encouragement and development. Briefly stated, it is imperative that the potential of titanium castings be recognized by both engine manufacturers and casting suppliers and that further commitment to titanium casting be made on the part of casting suppliers to stimulate development for its future use and to satisfy the long-range needs of both industry and government.

VI. CONCLUSIONS AND RECOMMENDATIONS

1. Investment cast titanium compressor components offer the potential for significant acquisition cost savings as substitutes for machined forgings in current and future weapon systems. Impellers, integrally bladed fan rotors, and integrally bladed axial compressor rotors are the most promising components in small engine designs. Fan and compressor blades are the best candidates for large engine designs.
2. The state of the art for sophisticated net-shape titanium castings has increased substantially over the last several years in the areas of dimensional control and structural integrity, evidenced by the static and rotating components either in production or under development for future applications.
3. New alloys and processing concepts offer the potential for obviating many of the concerns designers have traditionally held for the fatigue performance of cast components in rotating applications.
4. Producibility/reliability characteristics of sophisticated net-shape rotating components are relatively unknown. High development costs, technical complexities, and the critical nature of applications have tended to restrict exploitation.
5. The market potential for the utilization of titanium castings as substitutes for forgings is significant. It is recommended that government agencies and industrial suppliers review their strategies concerning their involvement with the development of titanium castings to accelerate the implementation of this cost saving technology into current and next-generation weapons systems.

ACKNOWLEDGMENTS

Precision Castparts Corporation of Portland, Oregon, has supplied the basic technical expertise that now makes it possible to seriously consider utilization of dimensionally complex near-net shapes in rotating gas turbine design. Their cooperation and participation in various DDA programs is acknowledged and appreciated. In the area of new alloy developments, Dr. Frank Crossley of the Lockheed Missiles and Space Company, Sunnyvale, California, has provided strong support and guidance in adapting the Transage 175 alloy to cast rotating applications. Acknowledgment is therefore given to this cooperation.

Acknowledgment is also given to Mr. Mike Galvas of the U.S. Army Applied Technology Laboratory, Ft. Eustis, Virginia, and to Mr. Carl Lombard, formerly of the U.S. Air Force, Wright Aeronautical Laboratories, Dayton, Ohio, for their pioneering manufacturing technology sponsorship in the rotating cast titanium area.

Acknowledgment is also due several DDA personnel who, through their efforts, have substantially contributed to DDA's position in the cast titanium application area. Deserving of special recognition are Mr. Brian King, Dr. Mehmet Doner, Dr. Amiya Chakrabarti, Mr. Wayne Hepfer, Mr. Ken Green, and Mr. Randy Kanaby.

Table I.
Summary inspection results for Model 250-C28 impeller castings.

	Throat measurements*				
	AU (main vane), in. (cm)			AW (splitter), in. (cm)	
	Section BB**	Section DD	Section FF	Section DD	Section FF
Print requirement	0.3883 (0.9863)	0.4907 (1.2464)	0.5551 (1.4100)	0.3304 (0.8392)	0.4483 (1.1387)
Avg of 15 vanes	0.3865 (0.9817)	0.4841 (1.2296)	0.5487 (1.3937)	0.3329 (0.8456)	0.4476 (1.1369)
Std deviation	0.0029 (0.0074)	0.0047 (0.0119)	0.0067 (0.0170)	0.0014 (0.0036)	0.0097 (0.0246)

Blade thickness measurements (main vane), in. (cm)				
Location***	Section AA	Section CC	Section FF	
Q dimension Blueprint	0.020+0.005 (0.051+0.013)	0.017+0.005 (0.043+0.013)	0.010+0.003 (0.025+0.008)	
Avg 15 vanes	0.0196 (0.0498)	0.0173 (0.0439)	0.0135 (0.0343)	
Std deviation	0.0007 (0.0018)	0.0011 (0.0028)	0.0009 (0.0023)	
T dimension Blueprint	0.046+0.005 (0.117+0.013)	0.040+0.005 (0.102+0.013)	0.025+0.005 (0.064+0.013)	
Avg 5 vanes	0.0470 (0.1194)	0.0428 (0.1087)	0.0258 (0.0655)	
Std deviation	0.0010 (0.0025)	0.0017 (0.0043)	0.0011 (0.0028)	
U-dimension Blueprint	---	0.097+0.005 (0.246+0.013)	0.043+0.005 (0.109+0.013)	
Avg 5 vanes	---	0.0890 (0.2261)	0.0450 (0.1143)	
Std deviation	---	0.0015 (0.0038)	0.0025 (0.0064)	

*Throats may vary ± 0.007 in. (0.018 cm) on individual vanes. On an average basis, throats may vary ± 0.005 in. (0.013 cm).

**AA FF: Section increments starting at impeller hub and progressing to vane tip

***Q T: Tip-to-hub airfoil locations

Table II.
Room temperature tensile results for joint specimens machined from a dual-property Ti-64 impeller.*

Specimen type	UTS-MPa (ksi)
Typical parent metal cast Ti-64	896.2 (130.0)
Butt No. 1	899.0 (130.4)
Butt No. 2	930.7 (135.0)
Butt No. 3	885.8 (128.5)

*Cast airfoil shell-wrought hub

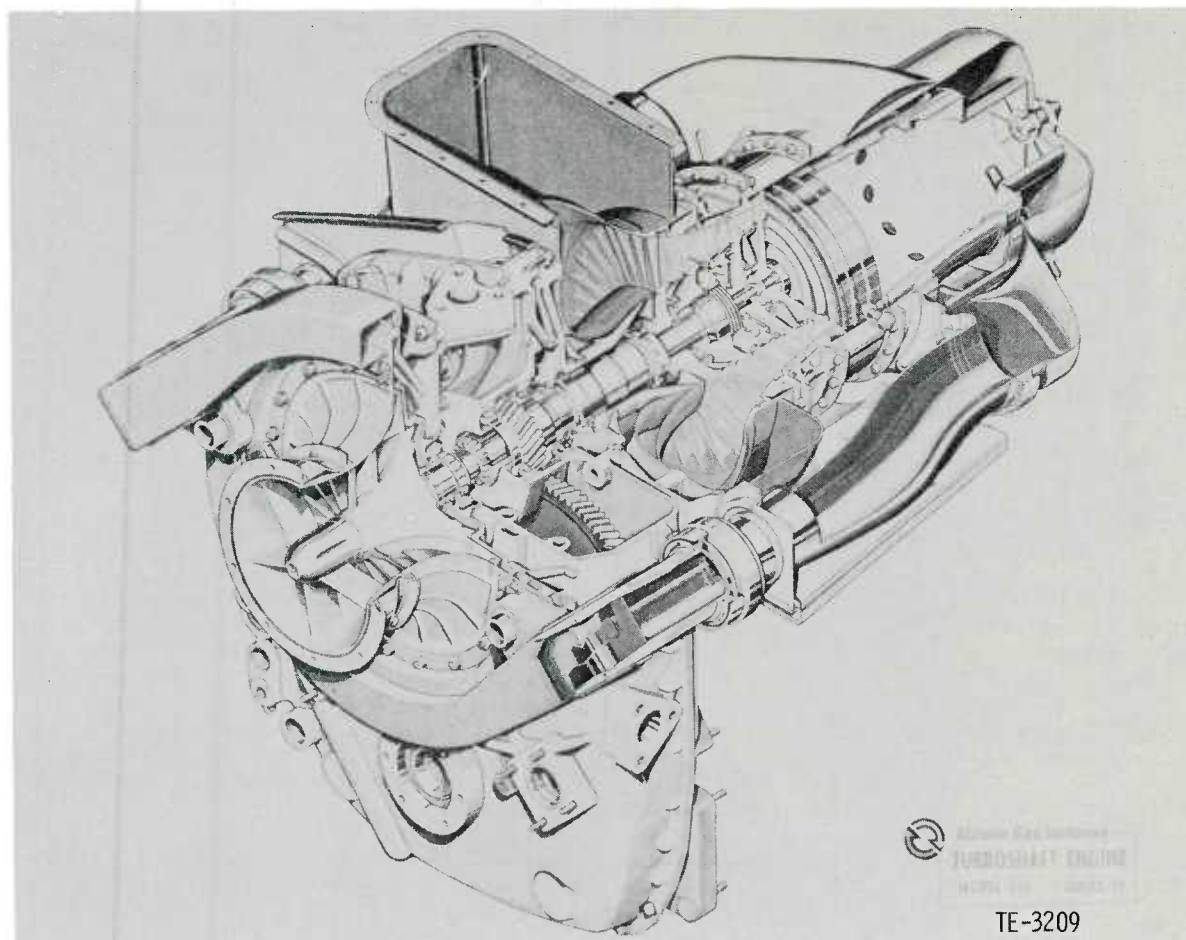


Figure 1. Cutaway of the 250-C30 turboshaft engine.

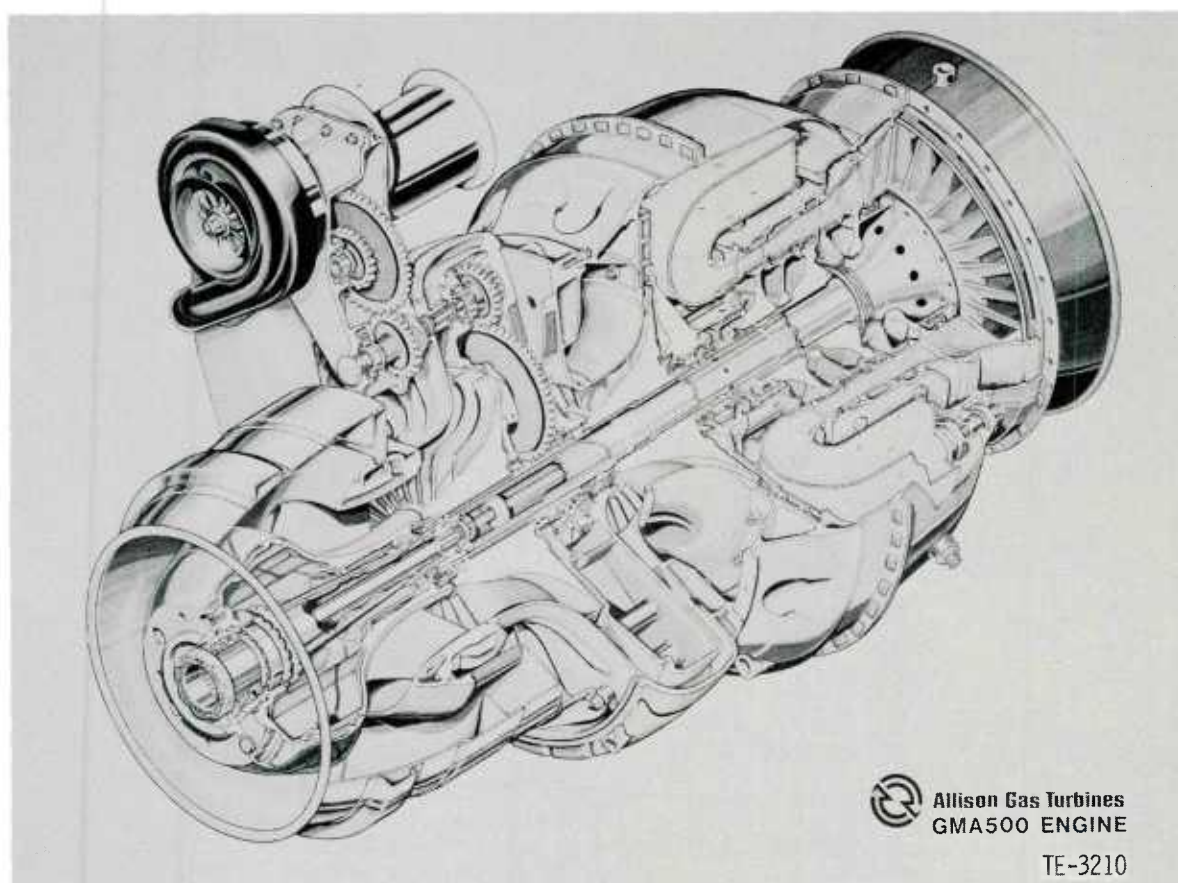


Figure 2. Cutaway of the 280-C1 turboshaft engine.

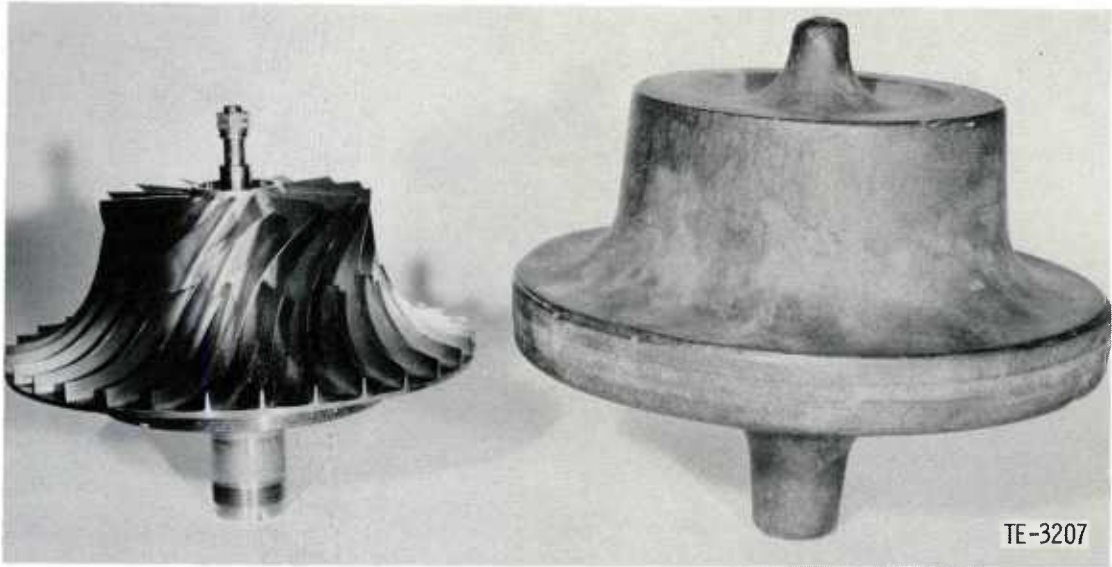


Figure 3. 250-C28 impeller forging before and after machining to final configuration.

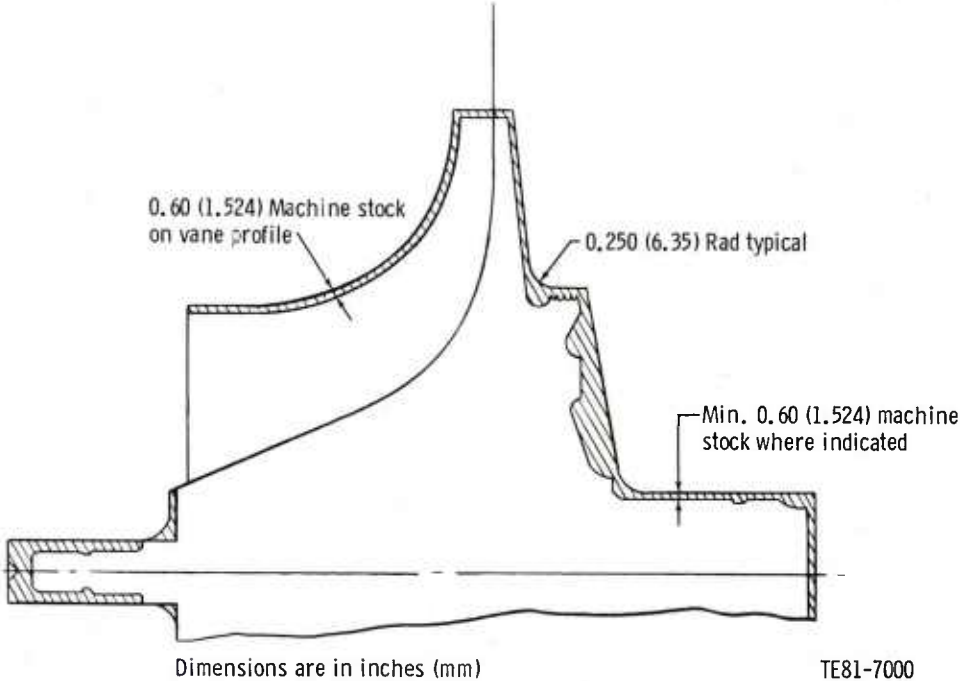
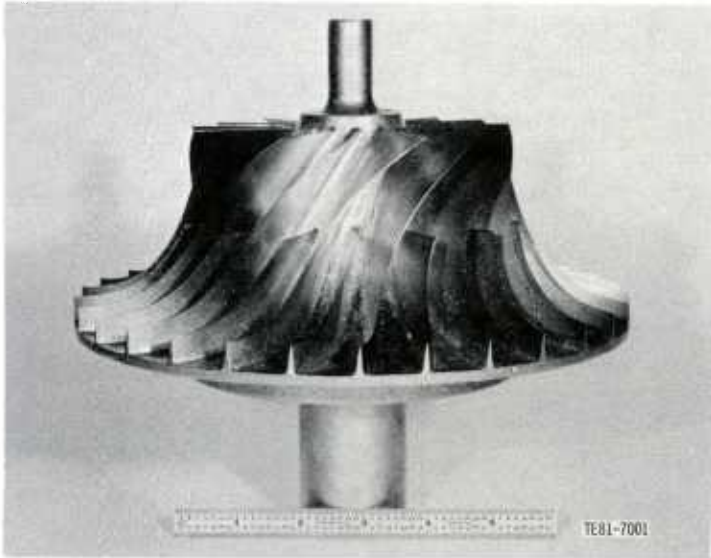


Figure 4. As-received PCC-supplied 250-C28 casting (top) and schematic (bottom) showing areas that require DDA machining for conversion into a finished component.

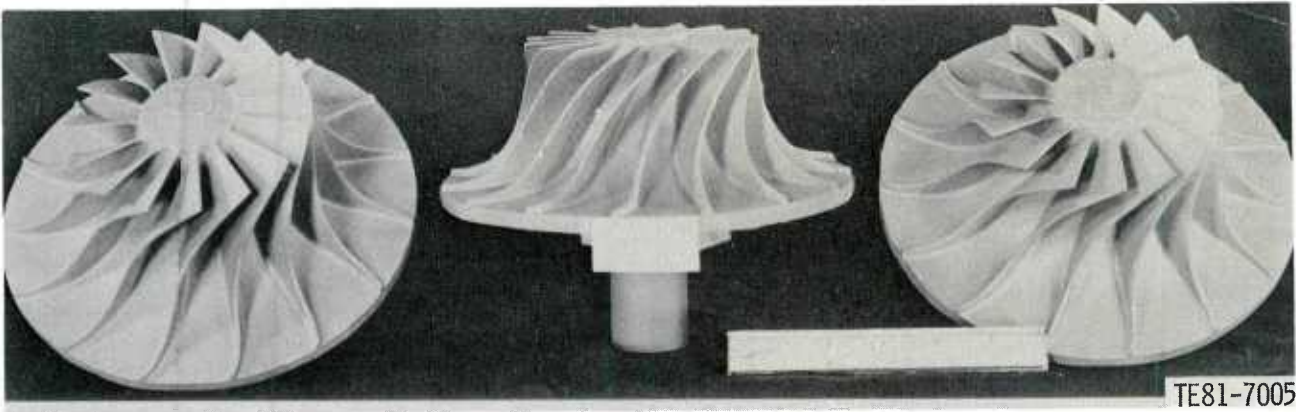


Figure 5. Simulated 250-C28 impeller castings.

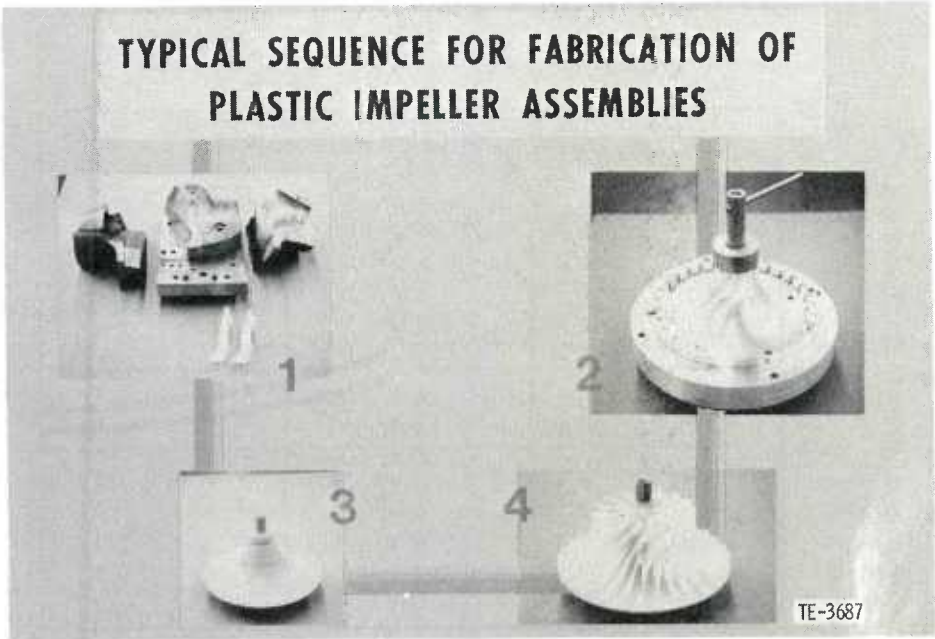


Figure 6. Typical sequence for fabrication of plastic impeller assemblies.

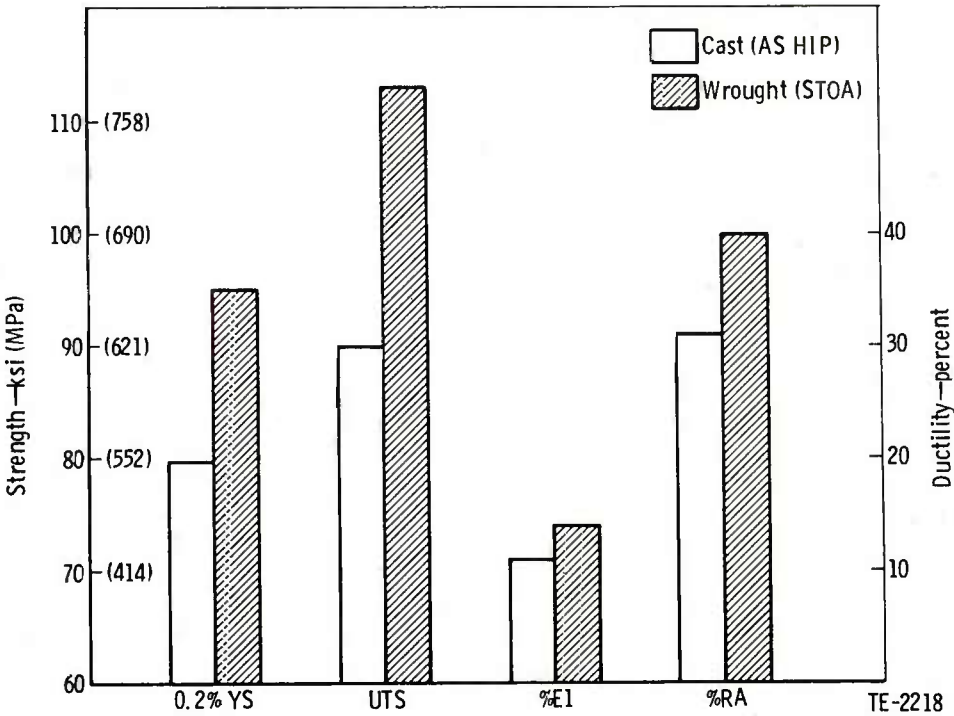


Figure 7. Relative tensile capabilities at 204°C (400°F) of full-scale Ti-64 cast and wrought Model 250 Series impellers.

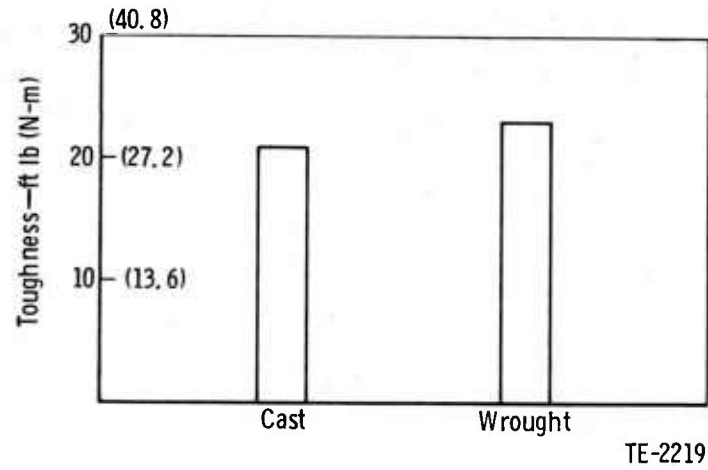


Figure 8. Relative room temperature Charpy V notch impact resistance of cast and wrought Ti-64.

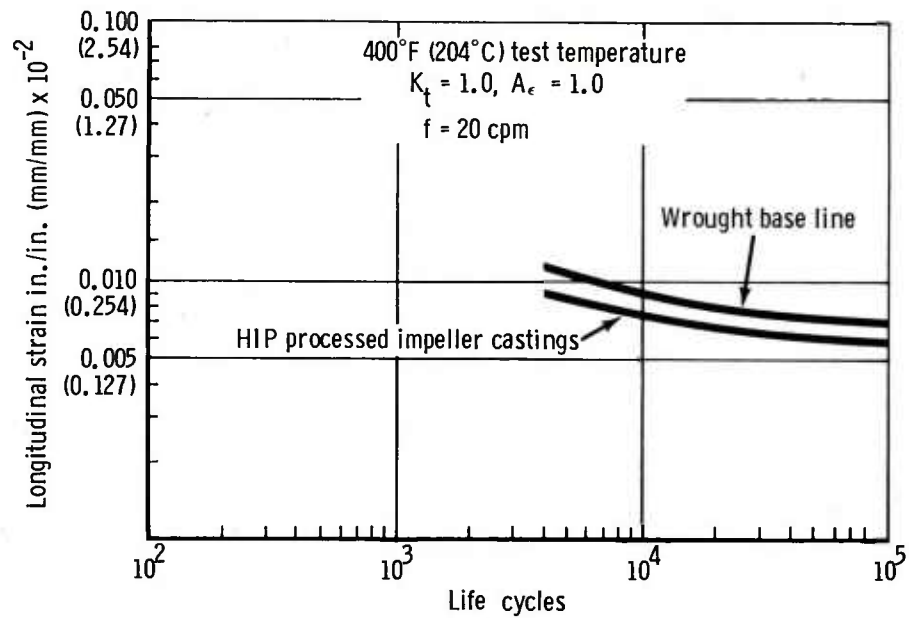


Figure 9. Smooth bar LCF results for cast and wrought Ti-64 at 204°C (400°F).

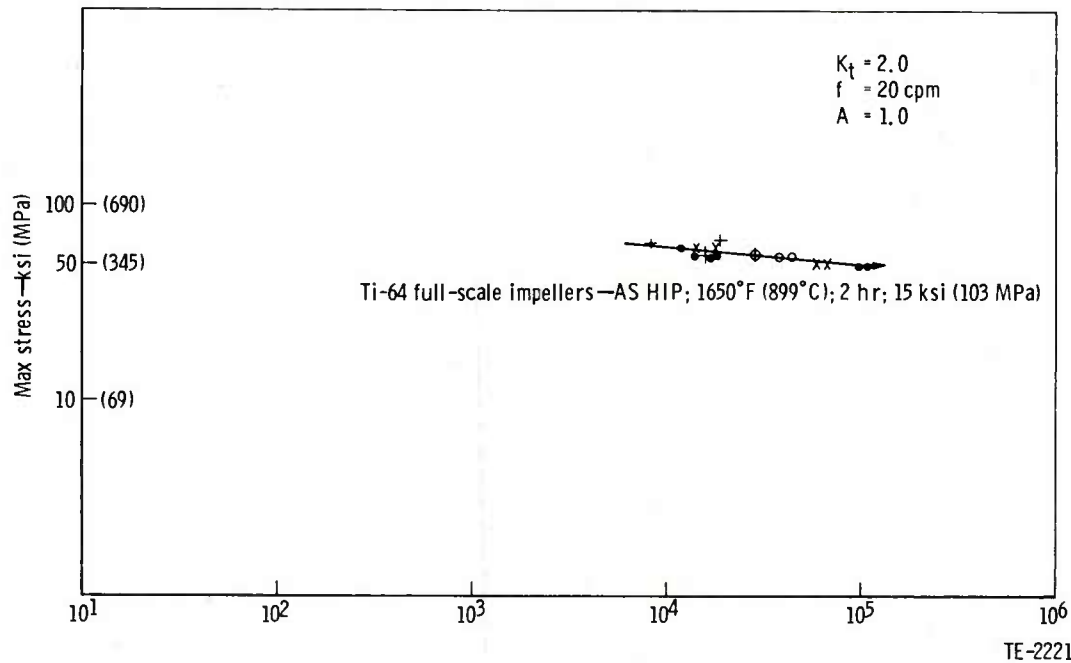


Figure 10. Notched bar LCF results for cast Ti-64 at 204°C (400°F).

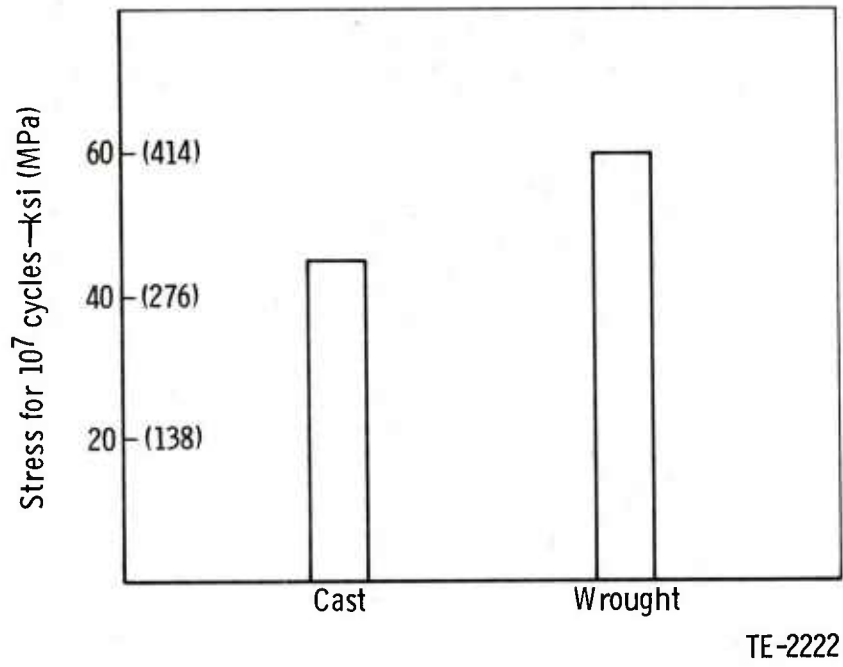


Figure 11. In situ HCF results for Ti-64 Model 250 impeller airfoils.

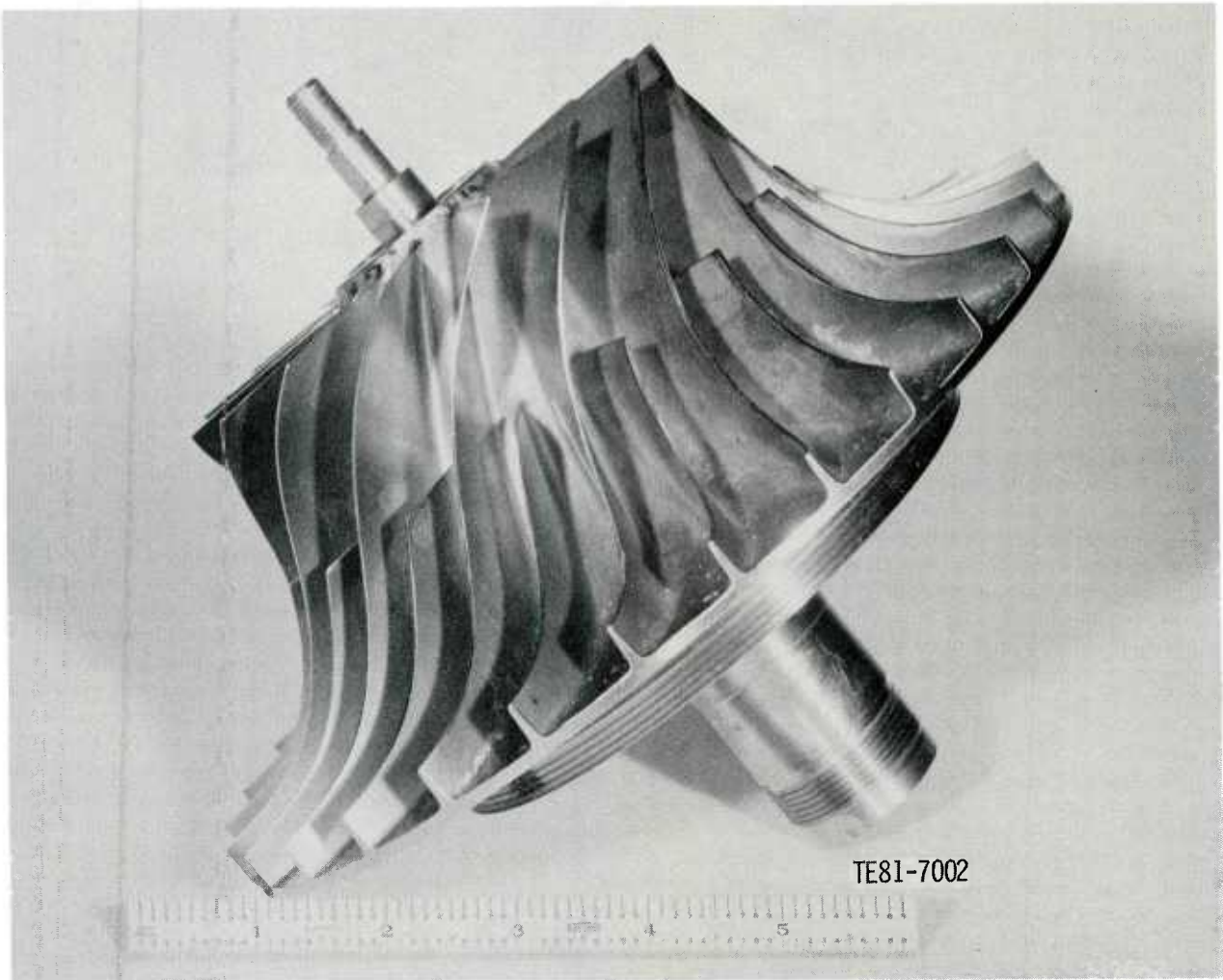


Figure 12. Model 250-C28 cast Ti-64 engine test impeller.

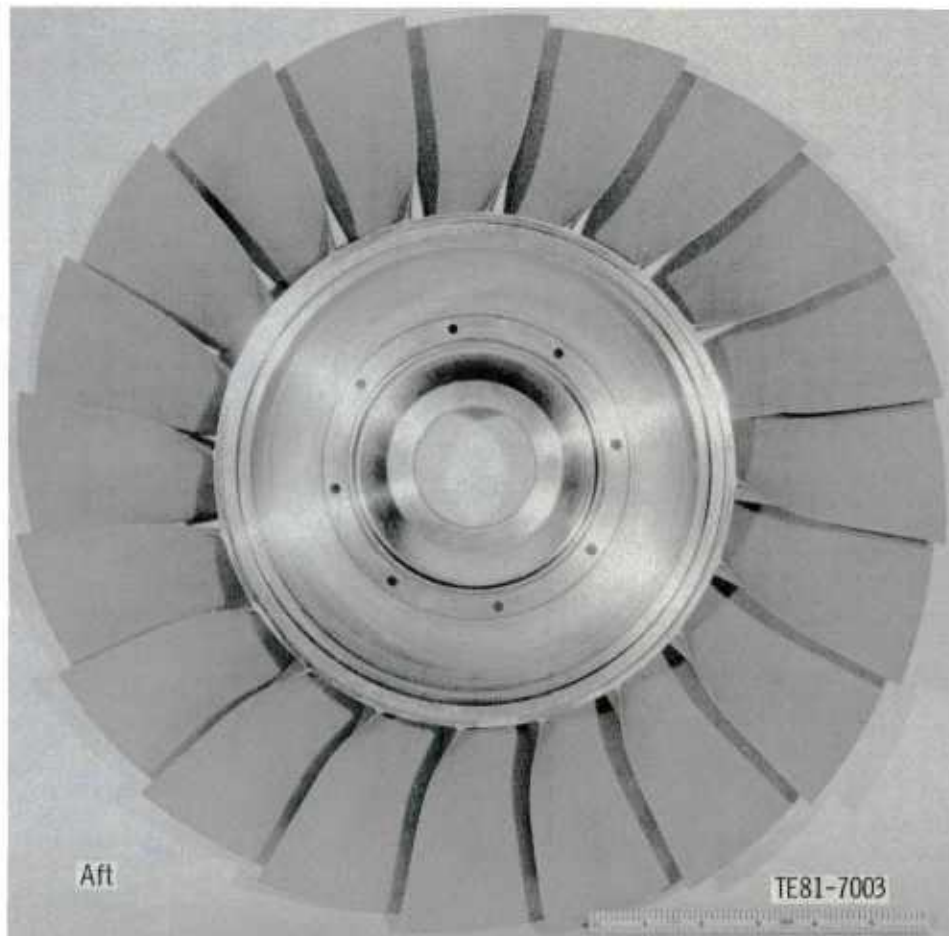
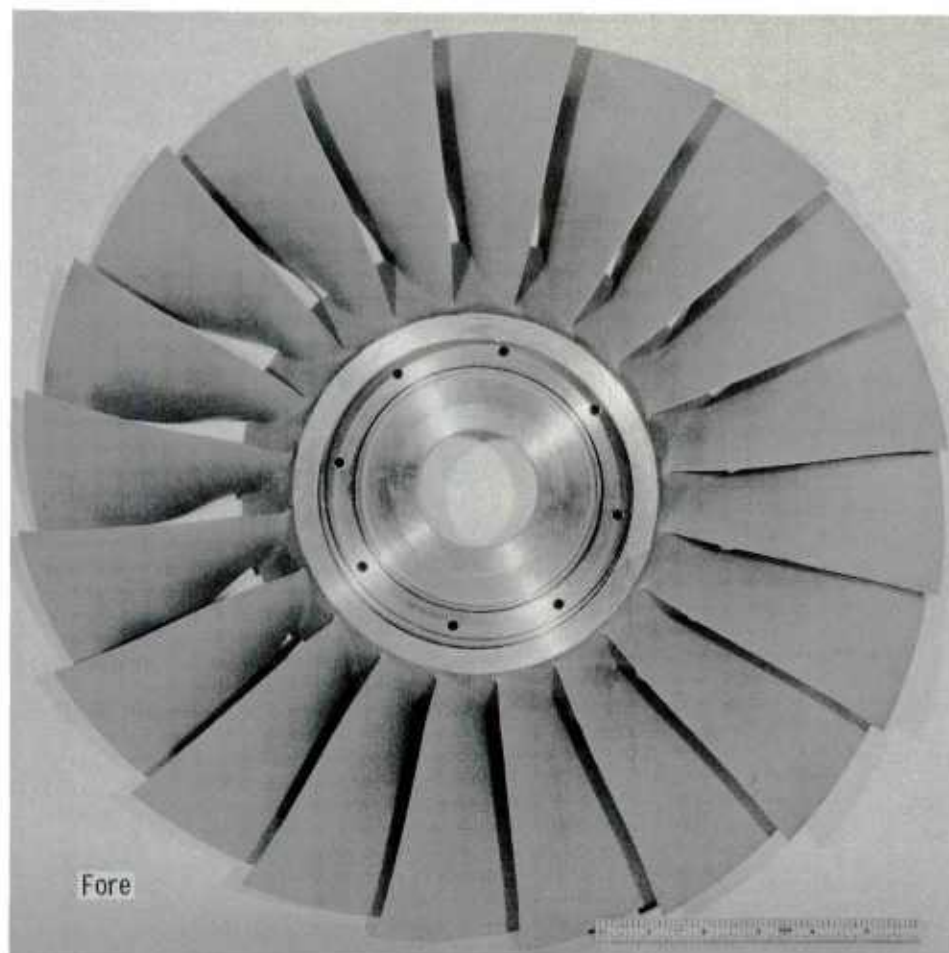


Figure 13. Investment cast integrally bladed high-bypass fan rotor in the Transage 175 alloy.



Figure 14. Cast airfoil shell with machined cavity.

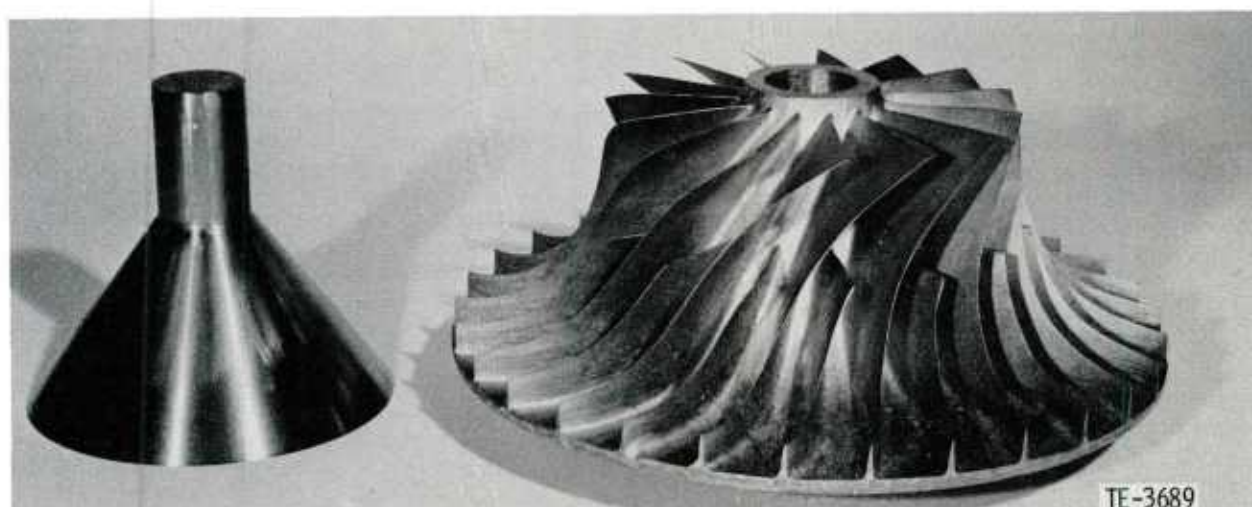


Figure 15. Cast airfoil shell with match-machined wrought hub.

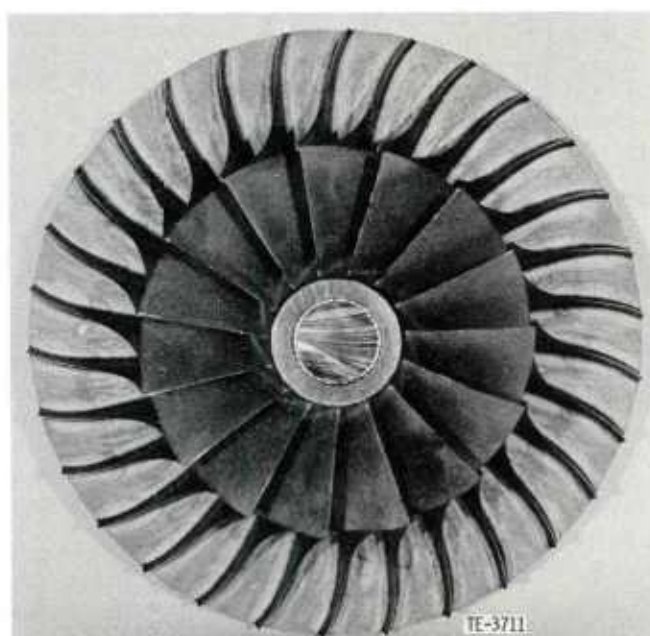


Figure 16. Hub/shell assembly with laser-welded seam.

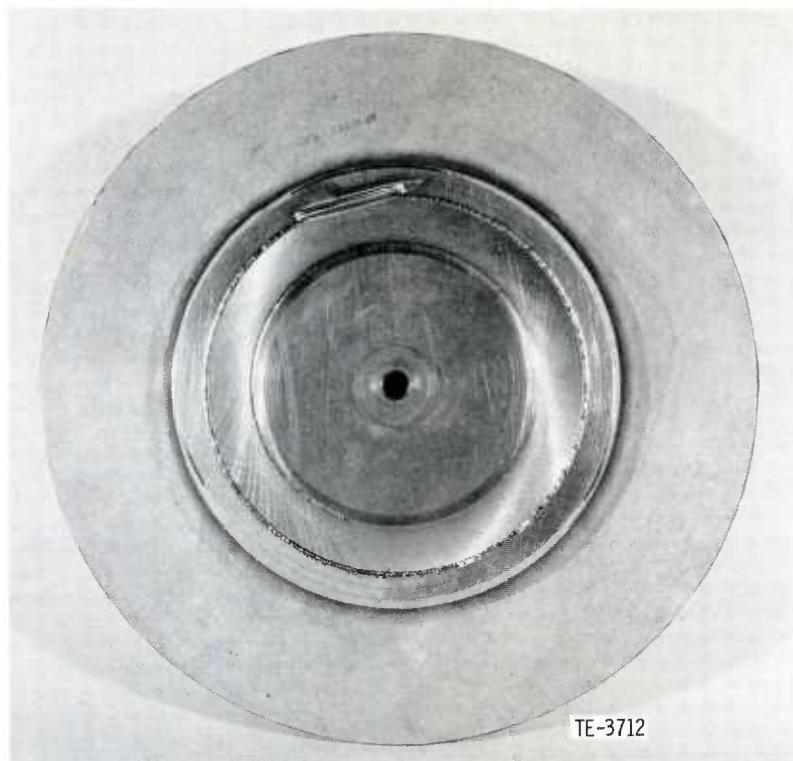


Figure 17. Hub/shell assembly with laser-welded seam and final EB-welded closure.

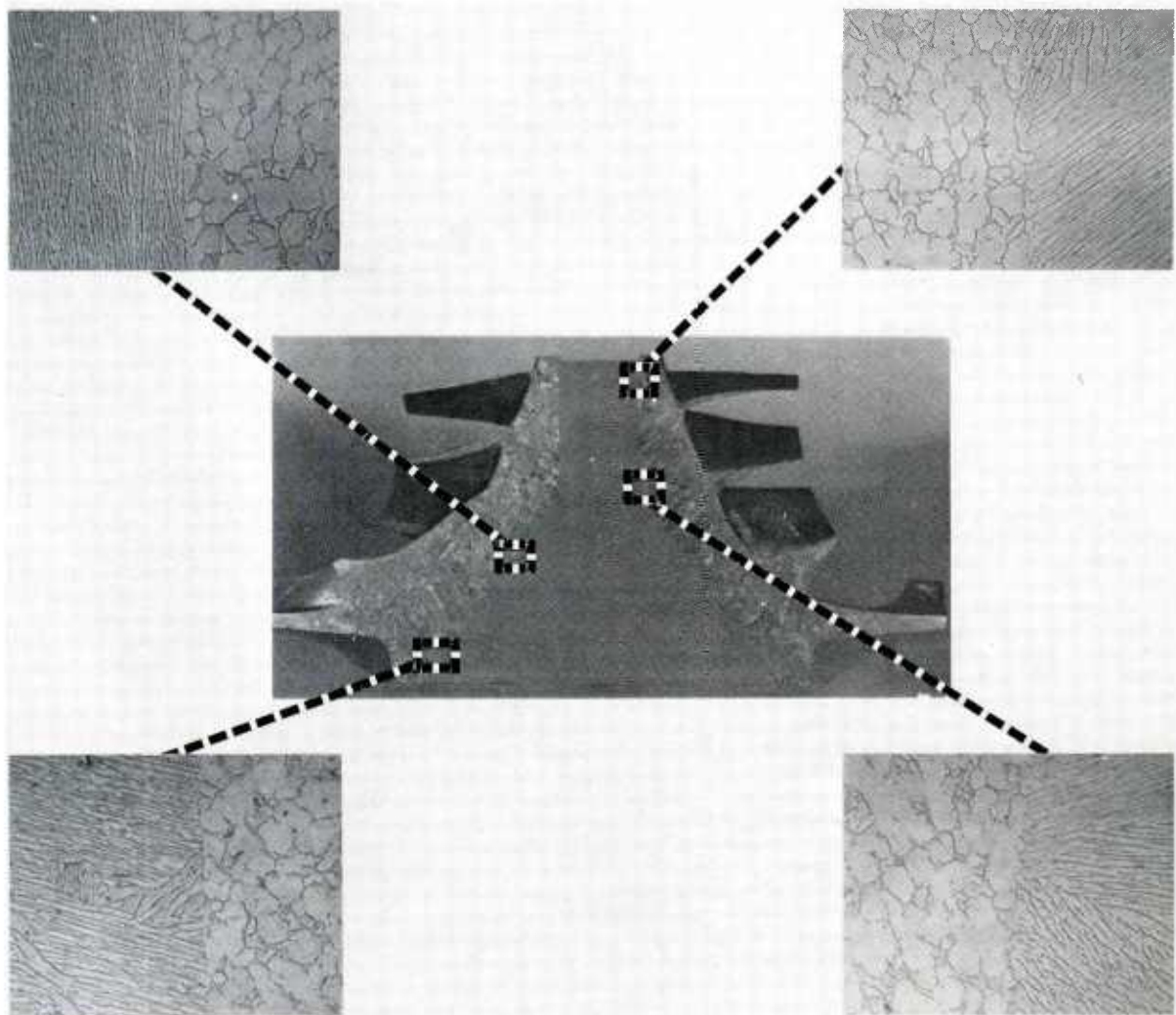


Figure 18. Bonded impeller cross section showing selected photomicrographs of the bond joint.

RÉALISATION DE PIÈCES CRITIQUES EN FONDERIE DE PRÉCISION

par
M. BRUN, G. VANDENDRIESSCHE, D. FOURNIER, M. MEURTIN
TURBOMECA
BORDES
64320
BIZANOS
France

INTRODUCTION

Dans une petite turbomachine, la part des pièces réalisée en cire perdue s'est considérablement accrue ces dernières années (voir tableau n° 1). Cette évolution significative a atteint non seulement tous types de matériaux (aciers, superalliages, titane, aluminium etc...) mais tous types de produits. Dans ce cadre, le phénomène récent le plus remarquable est l'extension de cette technologie dans les applications pour pièce tournante, à savoir les roues de turbine et les roues de compresseur.

Nous examinerons dans ce qui suit les raisons d'un tel choix, les problèmes posés par l'emploi de ce procédé pour des éléments mobiles fortement sollicités et analyserons les résultats obtenus sur quelques exemples concrets.

1. ROUES DE TURBINE COULEES MONOBLOC

La recherche de l'accroissement des températures d'entrée turbine a amené les constructeurs à faire un large appel aux superalliages de fonderie pour les pales de turbine. Or, pour les petites turbomachines, la taille des ensembles tournants et le nombre d'aubes se prêtent mal à une construction du type disque et pales séparées ; celle-ci, outre son coût de fabrication élevé, entraînerait la réalisation de très petites pales difficilement accrochables sur moyeu. L'alliance entre la conception « monobloc » et l'utilisation pour les pales d'alliages à haute tenue en fluage a donc conduit les constructeurs à examiner les perspectives offertes par la cire perdue aux roues de turbine en superalliages.

S'agissant avant tout d'une pièce à haute intégrité dont l'éclatement peut avoir des conséquences catastrophiques, l'objectif visé était non seulement l'obtention de caractéristiques mécaniques suffisantes dans la zone du moyeu, mais la garantie d'un niveau de qualité et de fiabilité satisfaisant. Cette dernière considération a été ici l'élément fondamental dictant le choix de l'alliage, de la forme de la pièce et des conditions de fabrication et de contrôle. Nous montrerons, sur un exemple concret, que le faisceau des propriétés mécaniques issu de cette technologie demeure tout à fait attractif et tenterons de remettre en cause les idées communément admises sur les pièces de forge et les pièces de fonderie.

1.1. Les facteurs de qualité

Les reproches traditionnels formulés à l'encontre des pièces de fonderie sont au plan de la qualité : l'importance des défauts, le manque de reproductibilité et la difficulté d'exercer un contrôle efficace. Nous examinerons dans le cadre de cette application comment ces problèmes ont été abordés.

1.1.1. Minimiser les défauts

Nous citerons les défauts essentiels.

- Malvenues :

Elles sont dues à des zones non alimentées en métal liquide ; elles concernent essentiellement les pales. Une température de coulée élevée, un moule chaud, une pression d'alimentation correcte, une géométrie de pales favorable (faible largeur, une épaisseur de paroi suffisante), etc... sont des facteurs positifs permettant d'éviter ou de diminuer ces anomalies.

- Déformations :

Celles-ci, liées à la déformation du moule, dépendent essentiellement de la géométrie de ce dernier. Un voile mince et de grand diamètre est défavorable.

- Défaut de cristallisation (voir photo 1)

Il correspond généralement à un avancement convergent des différents fronts de solidification emprisonnant dans la pièce une masse de métal liquide, qui en se solidifiant, donne une zone à structure fine, avec une forte hétérogénéité de composition et à microretassures. Un bon masselottage avec un cône d'alimentation sans étranglement, des conditions de coulée adaptées doivent donc être recherchées.

Nota : la maîtrise de la taille du grain est parfois également difficile dans les pièces de forge (voir photos 2 et 3).

- Criques à chaud

La sensibilité à ce défaut varie d'un alliage à l'autre. Elle est exacerbée par des changements brutaux de section.

- Microretassures et microporosités

La tendance à la microretassure dépend fortement de la nuance. Par exemple les additions de Hf en quantité modérée (1 à 2 %) donnent lieu à la formation d'un eutectique $\gamma-\gamma'$ à bas point de fusion par rapport à la matrice et ayant une bonne pénétration dans l'espace interdendritique (1), (2). C'est le cas des nuances Mar M 004 et Mar M 247 1c.

Elle est diminuée par une température de coulée élevée.

Elle peut être influencée par la géométrie de la pièce. Par exemple des gorges profondes de faibles rayons peuvent provoquer un foyer chaud retardant la solidification et entraînant localement des retassures.

La Compaction Isostatique à Chaud (CIC) offre une solution décisive ; cependant outre son coût, l'utilisation de ce procédé nécessite une mise au point particulière qui s'avère parfois délicate. L'obtention de pièces à faible niveau de retassure sans CIC reste un objectif fondamental.

- Inclusions

Elles ont pour origine le contact entre le métal liquide et les enveloppes réfractaires (spinelle, Zr O₂, etc...). Il peut s'agir soit d'une réaction chimique au cours de l'élaboration ou de la refusion, soit d'une simple action mécanique. Les alliages à forte teneur en éléments facilement oxydables (Ti, Al, Hf, etc...) ont une forte réactivité.

En outre une température de coulée élevée accroît les risques de formation d'inclusions. Une analyse systématique sur pièces nous a montré que celles-ci proviennent en général à égalité de l'élaborateur et du fondeur.

Les éléments de solution pour résoudre ce problème sont :

- . une surveillance sévère des revêtements de four, des creusets et des parois internes des carapaces.
- . une procédure de fonderie soignée :
 - . propreté des jets
 - . surveillance de la propreté de la surface du bain
 - . technique spéciale de fusion et de versement
- . la filtration du métal liquide après l'élaboration et parfois même après la refusion.

Ces inclusions, généralement de faible taille (<0,1 mm) peuvent se localiser en profondeur ou près de la surface. Cependant leur masse volumique étant plus faible que la matrice, un mécanisme de décantation s'opère lors de la fusion et de la solidification. Ceci a été clairement mis en évidence lors de nos tentatives d'inoculation artificielle d'oxydes divers. La densité de ces défauts, et c'est un fait expérimental, est donc sensiblement plus élevée près de la surface de la pièce située du côté de l'attaque de coulée et sur les pales. En surface, elles sont souvent associées à une retassure générant des indications lors du contrôle par ressuage (voir photo 4 et 5). Il est donc conseillé de prévoir un usinage superficiel au moins pour les zones contraintes situées sur la face supérieure.

Nota : Ce type de défauts affecte également les pièces de forge en superalliages. Il arrive même que les conditions de refusion à l'électrode consommable entraînent un rassemblement local des inclusions en nappes plus ou moins étendues et non nécessairement associées à des fissures ; elles sont alors parfois difficiles à détecter lors du contrôle ultrasons et peuvent conduire à des ruptures catastrophiques (voir photos 6 et 7).

1.1.2. Garantir la reproductibilité

Les observations précédentes fournissent des éléments du choix des conditions opératoires. L'optimisation de celles-ci permettant une reproductibilité satisfaisante, ne peut se faire qu'à travers l'examen comparé des résultats de dissection (macro et microstructure, propriétés mécaniques) obtenus sur pièces

- réalisées en faisant varier légèrement les conditions opératoires
- fabriquées à partir de différentes coulées mère
- appartenant à un même lot de fabrication.

L'ensemble des résultats des contrôles effectués et de ceux issus de l'expérimentation au banc d'essai et sur machine de vol, constitue une sanction de la gamme utilisée.

Toutes les études que nous avons effectuées et l'expérience accumulée sur plusieurs milliers de roues, nous ont démontré que la température de coulée est un paramètre primordial ; la température du moule joue un rôle plus modeste, sauf si le moyeu est mince.

La solidification induit des contraintes résiduelles d'importance variable et de maîtrise délicate. Il est donc recommandé d'appliquer un traitement de détente.

1.1.3. Assurer un contrôle efficace

La méthode consiste à effectuer un contrôle destructif complet sur une pièce par campagne de coulée et un contrôle non destructif individuel le plus performant possible.

- Contrôle destructif :

Il comprend après les examens non destructifs habituels :

- . un examen macrographique superficiel,
- . un examen macro et microstructural sur coupe (contrôle de la microretassure, de la propreté, de la cristallisation),
- . une caractérisation mécanique limitée généralement aux essais de traction et de fluage.

- Contrôle non destructif sur pièce brute ,

Il comprend :

. Un examen radiographique : avec les foyers conventionnels, la résolution est environ de 5 % du chemin parcouru dans la matière par les RX. Une telle méthode est donc peu adaptée au contrôle du moyeu pour lequel sa capacité de détection est limitée aux gros défauts. En revanche, elle est plus appropriée à celui de la zone des pales où il est possible de détecter des défauts (porosités ou inclusions peu denses) de l'ordre de 3/10 mm. L'introduction de la radiographie à micro foyer (taille inférieure au 1/10 mm) associée à la technique de l'agrandissement peut permettre de descendre cette limite, à cet endroit, à 5/100 mm et d'effectuer un contrôle complémentaire de la cristallisation par emploi des phénomènes de diffraction.

. Un examen par ressuage : il n'autorise que la détection des retassures ou discontinuités superficielles. Si la gamme dite à « haute sensibilité » fournit des indications pour des défauts de taille très réduite (souvent < 1/100 mm) la corrélation de celles-ci avec la dimension réelle des anomalies reste délicate. Cette méthode donne donc avant tout une appréciation sur la qualité générale du produit.

. Contrôle de la retassure et de la macrostructure de la zone centrale située face à la masselotte (ou sur rehausse). Le critère à imposer est issu de l'expérience acquise sur l'élément concerné. Cet examen est un facteur de garantie de reproductibilité du procédé de fabrication.

. Contrôle de la retassure et de la macrostructure sur carotte prélevée au centre de la roue. Cette méthode est très efficace pour déceler les défauts de cristallisation. Par contre, un tel prélèvement n'est pas toujours autorisé par le dessin de pièce finie.

. Contrôle par ultrasons

Le manque d'efficacité du contrôle radiographique, les risques divers d'anomalies dans le moyeu et en particulier ceux relatifs aux défauts de cristallisation surtout lorsque tout prélèvement central est impossible, nous ont incité à développer une méthode de contrôle sondant le volume de cette partie critique de la pièce.

Compte tenu de la structure grossière et fortement orientée issue de nos conditions opératoires particulières (photo n° 8) et sur la base de travaux analogues (3-4-5-6-7) nous avons étudié le problème général de la propagation des ondes ultrasonores dans un matériau élastique anisotrope et plus spécialement dans les monocristaux dendritiques de superalliages à base de Nickel. Nous avons cherché à appliquer les résultats de cette analyse aux moyeux des roues coulées considérés comme une juxtaposition de cristaux séparés par des joints. Nous avons ainsi montré que l'atténuation et la déviation du faisceau ultrasonore passent par un minimum significatif lorsque l'axe de ce dernier forme avec l'axe des dendrites primaires un angle de 45° (photo n° 9).

Selon cette orientation la valeur de l'atténuation est alors de 0,5 à 1 dB/cm au lieu de 4 dB/cm pour toutes les autres directions. Elle est alors comparable à celle couramment mesurée sur la plupart des alliages de forges.

Nous en avons déduit deux applications pratiques :

. Contrôle de la structure de solidification

Il est fondé sur la variation importante d'atténuation entre les différentes structures (basaltique et équiaxe) d'une onde longitudinale se propageant dans la matière avec un angle de 45° par rapport à l'axe de la roue (photos 10 et 11). Le principe de sondage issu de cette remarque est indiqué sur le schéma n° 1. Il impose cependant des contraintes sur le plan du brut apte au contrôle ultrasons.

Nota : Nous avons également observé qu'une zone équiaxe donne lieu à une variation sensible de l'atténuation lors d'un sondage axial par contact. Cependant, cette méthode, bien que rapide et permettant l'examen d'un grand volume de matière, ne différencie pas suffisamment les structures à gros grains de celles à grains fins.

. Contrôle des défauts

La technique utilisée est indiquée sur le schéma n° 2. Le choix d'une seule direction de sondage, imposée par les considérations précédentes est confortée par la remarque suivante : en raison du mécanisme de leur formation, les défauts éventuels présentent une relative isotropie et offrent donc une surface réfléchive, parfois faible mais généralement multidirectionnelle. Par opposition les éléments réalisés par forgeage, par le champ de déformation appliqué, contiennent des défauts le plus souvent planaires et de surfaces plus réfléchissantes, mais dont la détection est fortement liée à l'orientation principale de ces surfaces par rapport à l'axe d'observation.

Le niveau de détection correspondant est celui d'un trou à fond plat de \varnothing 0,5 mm à 18 mm de profondeur et de \varnothing 1 mm à 32 mm de profondeur. C'est celui habituellement imposé dans le contrôle des pièces de forge. Il est en accord avec la taille critique de défaut autorisé par les caractéristiques de propagation de cet alliage et les conditions de sollicitation en service.

. Contrôle non destructif sur pièce finie :

Il comporte :

- un examen par ressuage selon une gamme à très haute sensibilité,
- un contrôle par courants de Foucault sur la surface interne des alésages. Ce dernier est sensible non seulement aux retassures ou criques, mais dans certains cas aux hétérogénéités locales d'origine métallurgique (inclusions, ségrégations, etc...).

1.2. Propriétés mécaniques et structurales - Examen d'un exemple concret.

1.2.1. Généralités

Les propriétés mécaniques à prendre en considération dans le cas d'une roue de turbine monobloc sont :

- le fluage dans la zone des pales,
- la résistance à l'éclatement du moyeu,
- la tenue à la fatigue oligocyclique du moyeu,
- la fatigue thermique dans la zone de la jante.

Si le fluage conduit à une première sélection de nuances envisageables, les exigences relatives aux caractéristiques de traction et de tenue à la corrosion, ainsi que les impératifs de qualité restreignent généralement le domaine du choix et imposent les conditions de fabrication et de contrôle. La caractérisation complète sur pièces aux plans structural et mécanique et les essais aux bancs partiels et sur moteurs constituent les éléments indispensables de la décision finale.

Or, les propriétés mécaniques des pièces de fonderie étant réputées ne pas être très attractives pour un élément fortement sollicité, une solution roue monobloc peut, à priori, paraître peu prometteuse.

Nous avons choisi d'examiner cette question à travers un exemple concret ; l'alliage utilisé est le Mar M 004, dont la composition est indiquée dans le tableau 2 et qui a une coulabilité et une ductilité en traction supérieure à celles de l'INCO 713.

1.2.2. Propriétés structurales

Les conditions de fabrication sélectionnées conduisent à une structure générale grossière (photos 12-13 et 14). En particulier dans le moyeu le grain est colonnaire ; sa taille est de 1 à 3 cm de long pour un diamètre de 1 cm environ et l'axe des dendrites primaires est voisin de l'axe de la roue. Dans les pales la cristallisation est plus fine. Ces différences structurales s'accompagnent éventuellement d'hétérogénéité de composition et rendent difficile le choix d'une température de mise en solution valable pour toute la pièce.

Nous devons faire cependant les remarques complémentaires suivantes :

- La macrostructure observée dans les pales est favorable à la tenue en fluage.
- Les notions de grains et de joints de grains sont totalement différentes dans une pièce de forge et dans une pièce de fonderie. Dans un cas, le mécanisme de formation est la recristallisation, dans l'autre, la solidification.
- Le joint est ici fortement festonné (photos 15 - 16 et 17). Dans un superalliage de forge, il est souvent constitué de facettes planes.
- La finesse de la structure interdendritique (largeur de l'espace interdendritique et épaisseur des bras de dendrite) est ici un paramètre beaucoup plus important que la taille du grain lui-même. Elle apparaît ici comme relativement remarquable, l'épaisseur des dendrites secondaires étant de l'ordre de $130 \pm 20 \mu\text{m}$.
- L'espace interdendritique est semé d'eutectiques $\gamma-\gamma'$ (50 à $100 \mu\text{m}$) durcissant mais ductile (photos n° 18).
- Les carbures sont polyédriques et non en écriture chinoise à arêtes vives (photos n° 19 et 20).
- La fraction volumique des éléments durcissants γ' est très élevée ($\approx 60\%$). Bien que les gros précipités dominent ($\approx 1 \mu\text{m}$), leur taille peut être très variable (40 \AA à $1 \mu\text{m}$) ; ils sont de type cubique (8) dont les faces sont perpendiculaires aux directions $\langle 100 \rangle$ de la matrice et du précipité (photos 21 et 22). Dans un matériau forgé, la précipitation est beaucoup plus homogène.

1.2.3. Propriétés mécaniques

La bonne tenue au fluage, ne pouvant être remise en cause par la structure obtenue dans la zone des pales, nous nous sommes attachés à caractériser le moyeu vis-à-vis des sollicitations imposées en nous efforçant de tenir compte de l'anisotropie de cette partie de la pièce. Nous présenterons dans ce qui suit, les résultats principaux de cette étude menée avec le Centre des Matériaux de l'Ecole des Mines (8). Les plans de dissection et la géométrie des éprouvettes utilisés sont indiqués sur le schéma n° 4.

1.2.3.1. Traction

Les valeurs de R et de A % dépendent assez fortement de la taille de l'éprouvette (voir tableau 3). Si la limite élastique est indifférente à ce paramètre, l'accroissement du diamètre a pour effet d'augmenter la charge de rupture, de diminuer l'allongement et de réduire la dispersion.

La résistance à l'éclatement de la roue doit donc être supérieure à celle prévue à partir des caractéristiques minimales relevées sur éprouvette de 5 mm de diamètre. Ceci a été confirmé par un essai d'éclatement qui s'est effectué pour une contrainte appréciée à 850 MPa.

Il n'y a pas d'influence significative de la température sur les résultats obtenus entre 20°C et 600°C .

Sur les surfaces de ruptures les traces du squelette dendritique apparaissent nettement à 20°C ; elles s'estompent à 600°C .

1.2.3.2. Propriétés de fatigue oligocyclique (courbes 1 à 3)

. En déformation longitudinale imposée :

- les courbes donnant la contrainte à demie durée de vie en fonction du nombre de cycles à rupture présentent une évolution comparable à celle de l'INCO 718 jusqu'à 10^4 cycles (courbe n° 1). Si les niveaux sont assez différents à température ambiante en relation avec les valeurs respectives des charges de rupture en traction, ils se rapprochent sensiblement à 500°C .
- la représentation habituelle des résultats de fatigue ($\Delta\epsilon_p^{1/2}-N_f$) suppose un matériau isotrope. Elle conduit donc ici à une forte dispersion des résultats. Celle-ci en revanche est fortement réduite si les valeurs obtenues sont rapportées sur une courbe donnant la contrainte équivalente $\frac{E\Delta\epsilon_t}{2}$ en fonction du nombre de cycles à rupture.
- Il n'y a pas d'influence marquée du rapport des déformations totales $R_\epsilon = \epsilon_{t,\text{MIN}}/\epsilon_{t,\text{MAX}}$ sur la durée de vie.
- En déformation plastique constante, l'augmentation de la température de 20 à 600°C , entraîne à une réduction de la durée de vie par un facteur 5 ; elle est toutefois sans action sur la contrainte. Ce rôle de la température, non corrélée aux propriétés de traction, est due soit à l'environnement, soit plus probablement à une modification du mécanisme de déformation.

Le Mar M 004 reste cependant peu sensible à l'effet de température entre 20° et 600°C comparativement à l'INCO 718 pour lequel le passage de 20° à 550°C induit une réduction de durée de vie 10 fois supérieure.

L'analyse détaillée des zones d'amorçage et des surfaces de rupture a permis de dégager les observations générales suivantes :

. Amorçage :

Il est de type cristallographique (photo 23). Il s'effectue sur des plans (111) contenant le système de glissement avec le facteur de Schmid le plus élevé. Il est favorisé par des hétérogénéités cristallines locales : joints de grains, carbures, pores. En revanche, si de grandes étendues de porosités peuvent être néfastes, des petites retassures ($<0,5\%$) ne semblent pas avoir une action significative : ainsi, des fissurations secondaires amorçées sur une microretassure sont parfois rencontrées sur le fût d'éprouvettes de fatigue rompues normalement (photo 24).

. Propagation :

à 20°C : dans le domaine des faibles vitesses au voisinage du seuil (10^{-10} m/cycle), on note des facettes très cristallographiques de type (111) et des rivières de clivage (voir photo 25). Le plan moyen de propagation est d'orientation (001) (photo 26). Lorsque la vitesse croît le faciès de propagation devient plus planaire avec quelques traces de squelette dendritique. Des stries sont décelables à partir de 10^{-6} m/cycles.

à 600°C : le domaine cristallographique est pratiquement inexistant. La propagation s'effectue selon un plan d'orientation (100) marqué par des lignes de clivage parallèle à la direction macroscopique de propagation (photos 27 et 28).

Nous devons souligner un fait remarquable : l'amorçage et la propagation entre 20°C et 600°C sont toujours de type transgranulaires.

1.2.3.3. Résistance à la propagation (courbes 4 et 5)

- Elle est excellente ; par rapport à l'INCO 718, à 600°C elle est du même niveau, à la température ambiante elle lui est supérieure ; elle est en outre moins sensible à l'effet de fréquence.
- Les valeurs du seuil sont pour une vitesse de 10^{-10} m/cycles, égales à $15\text{ MPa}\sqrt{\text{m}}$ à 20°C et $9,2\text{ MPa}\sqrt{\text{m}}$ à 600°C ($R = 0,1$).
- La dispersion des résultats est relativement importante à 20°C , plus faible à 600°C . Elle doit être reliée à des effets d'orientation. La représentation de la loi de fissuration en fonction du K_{max} paraît cependant beaucoup plus rationnelle pour différents niveaux de R , surtout à 600°C .
- le KIC est de l'ordre de 70 à $90\text{ MPa}\sqrt{\text{m}}$.

1.2.3.4. Résistance à la fatigue thermique

Cette caractéristique est à relier à la fatigue oligocyclique. L'intensité des sollicitations sur la jante est fortement diminuée par l'introduction de fentes radiales terminées par des trous.

En conclusion, il nous paraît nécessaire de souligner les points suivants :

Malgré une taille de grain élevée, la microstructure reste relativement fine.

Si les propriétés de traction et de fatigue ne sont pas du niveau des superalliages de forge actuellement utilisés, elles demeurent suffisantes dans un certain nombre de cas.

Si la résistance à l'amorçage est médiocre, elle est plus liée à la cristallographie qu'aux défauts métallurgiques, à condition que la taille de ceux-ci ne soit pas trop élevée.

L'excellente résistance à la propagation des criques demeure le fait le plus remarquable. Si la reproductibilité de la fabrication est satisfaisante, on peut s'attendre à ce que le comportement global d'une telle pièce en utilisation donne lieu à des résultats moins dispersés que ne le laissent prévoir certaines caractéristiques obtenues sur éprouvettes de dissection.

1.3. Considération sur les perspectives d'évolution de la technologie

Les développements de ce procédé doivent avoir pour triple objectif : l'amélioration de la qualité, de la reproductibilité et l'accroissement des caractéristiques mécaniques.

- Amélioration de la qualité :

Des efforts doivent être faits pour diminuer encore le risque d'inclusion.

Utilisation de la compaction isostatique à chaud (CIC). Cette technique est très efficace vis-à-vis de la retassure. Cependant, en fonction de la nuance considérée, elle n'est généralement pas sans action sur certaines propriétés mécaniques ; celles-ci ne sont d'ailleurs pas toujours complètement récupérées par un traitement thermique convenable. Ce procédé nécessite donc une nuance appropriée et des conditions opératoires évitant de préférence l'emploi d'un traitement thermique ultérieur. Cette dernière exigence est liée à la possibilité de pratiquer des vitesses de refroidissement élevées dans l'enceinte de compaction.

- Amélioration de la reproductibilité :

L'automatisation doit s'étendre à tous les stades de la fabrication : constitution des couches, séchage, chargement, versement etc...

La température du métal liquide doit être contrôlée et maîtrisée de façon précise.

- Accroissement des caractéristiques mécaniques :

. La recherche de l'augmentation des propriétés de traction et de fatigue incite à agir sur la structure.

- affiner la microstructure : ceci pourrait être obtenu par une vitesse de solidification plus rapide dans la zone du moyeu.

- affiner le grain : certains fondeurs développent différentes techniques (agitation mécanique, inoculation, etc...) provoquant une polygermination. Elles introduisent inévitablement un niveau de retassures élevé et une forte hétérogénéité chimique qui doivent être éliminés par un cycle thermo mécanique approprié (CIC suivi ou non de traitement thermique). Le choix de la nuance est donc un paramètre fondamental. Les caractéristiques de traction et de fatigue mesurées sur éprouvettes de dissection, issues de roues ainsi réalisées sont réputées être significativement supérieures.

. Amélioration de la résistance à l'amorçage :

Celle-ci peut être obtenue par :

- le développement de procédés conduisant à l'obtention de roues à grains fins. Il convient cependant de s'assurer que la résistance à la propagation des criques ne subit pas une dégradation trop sensible.

- des traitements de surface appropriés. Nous avons engagé une étude sur l'action d'un grenaillage superficiel des zones fortement contraintes.

2. ROUES DE COMPRESSEUR COULEES MONOBLOC

Les résultats convenables obtenus sur les roues de turbine coulées en superalliage nous a incité à examiner les perspectives d'application de la fonderie de précision sur des pièces tournantes de compresseur de forme complexe et dont le coût de fabrication selon la voie conventionnelle (forge + usinage) est relativement élevé.

Nous nous contenterons d'évoquer dans ce qui suit, à titre d'illustration, les résultats les plus significatifs que nous avons obtenus sur des rouets centrifuges en acier et en TA6V.

2.1. Rouet centrifuge en acier 17-4.PH

Une mise au point de la composition chimique a été rendue nécessaire afin d'éliminer les risques de formation de ferrite δ (1).

Si on compare les résultats avec ceux obtenus sur le matériau forgé habituellement utilisé (Z 12 CNDV 12 - 17-4PH).

- les propriétés de traction et de résistance à la propagation des criques (voir courbe n° 6) sont voisines, que le 17-4 PH soit ou non compacté.

- la tenue en fatigue du matériau coulé est fortement influencée par la microretassure qui est sur cet alliage relativement importante et avec ramifications.

- à l'aide du CIC, elle devient d'un niveau comparable à celui mesuré sur le Z 12 CNDV 12 (voir courbe n° 7)

- la résistance à l'amorçage demeure cependant préoccupante et doit être améliorée.

2.2. Rouet centrifuge en TA6V

La réalisation d'une telle pièce (photo n° 29) pose de grosses difficultés dimensionnelles. Lorsque celles-ci sont surmontées, l'introduction d'un traitement thermique particulier permet d'atteindre des niveaux de propriétés tout à fait acceptables et comparables à celle du TA6V standard, hormis l'allongement (voir tableaux n° 4 et 5). La résistance à la propagation des criques est ici encore une qualité de base du produit ($KIC \geq 70 \text{ MPa } \sqrt{\text{m}}$). Les structures obtenues sont indiquées sur les photos 30 à 33.

CONCLUSION

Nous avons pu voir à travers des exemples concrets, les résultats tout à fait remarquables qui peuvent être atteints par cette technologie malgré une structure relativement grossière. Nous avons montré qu'une analyse soignée des défauts prévisionnels, une optimisation en conséquence de la nuance, de la forme des pièces, de la gamme de fabrication et de contrôle associée à une bonne connaissance du comportement du matériau en mécanique de la rupture, peuvent conduire à une fiabilité satisfaisante pour des pièces de haute intégrité.

BIBLIOGRAPHIE

- (1) BRUN M. - FOURNIER D. - VANDENDRIESSCHE G. : Introduction des pièces de fonderie dans les parties tournantes de de turbomachines.
Matériaux et Techniques n° 11 - 12 , Novembre - Décembre 1977
- (2) BACHELET Eric - LESSOULT Gérard , Quality of Castings of Superalloys
- (3) SERABIAN S. : Frequency and grain size dependency of ultrasonic attenuation in polycrystalline materials
British journal of NDT, march 1980
- (4) MUSGRAVE M.P.J. : The propagation of elastic waves in aeolotropic media. - I. General principles
Proc. R. Soc. London
- (5) MUSGRAVE M.M.J. - MILLER G.F. : The propagation of elastic waves in aeolotropic media. III : média of cubic summetry.
Proc. R. Soc. London, 1956, ser A, vol. 235, p 352
- (6) D. KUPPERMAN David - J. REIMAN Karl : Ultrasonic wave propagation and anisotropy in austenitic stainless steel weld metal.
IEEE Transactions on sonics and ultrasonics, vol. su-27, n° 1, January 1980
- (7) WHITAKER J.S. and JESSOP T.J. : Ultrasonic detection and measurement of defects in stainless steel - A literature Survey.
The British Journal of Non destructive Testing, volume 23, n° 6, November 1981
- (8) VINCENT Jean Noël - REMY Luc : Comportement en fatigue d'une roue de turbine coulée monobloc
Centre des Matériaux de l'école des Mines de PARIS - 91 CORBEIL ESSONNE
Rapports DRET - 77/333 et 79/365

REMERCIEMENTS

Nous devons remercier la DRET et le STPA pour l'aide financière que ces organismes nous ont apportée, le Centre des Matériaux de l'Ecole des Mines de Paris pour leur collaboration importante à l'analyse des propriétés des roues de turbine coulées.

TABLEAU 1

ÉVOLUTION PAR MOTEUR DU POURCENTAGE
DES PIÈCES COULÉES PAR RAPPORT AU
NOMBRE TOTAL DE PIÈCES BRUTES

ANNÉE	%
1960	13
1970	21
1975	50

TABLEAU 2

COMPOSITION CHIMIQUE DE MarM004

ELEMENTS	CONCENTRATION %
CARBONE	0,03 0,07
SILICIUM	≦ 0,5
MANGANESE	≦ 0,25
ALUMINIUM	5,5 6,5
BORE	0,005 0,0015
CHROME	11 13
FER	≦ 0,5
HAFNIUM	1,1 1,5
MOLYBDENE	3,8 5,2
NIOBIUM	1,5 2,5
TITANE	0,4 1,0
ZIRCONIUM	0,05 0,15
NICKEL	BASE

TABLEAU 3

Alliage MAR M004

Eprouvettes prélevees dans des roues

Ø mm	R. MPa	R0,2MPa	A%
3	940	735	16,5
τ	99	26	2,6
5	904	741	11,5
τ	67	29	2,2
14	870	732	8,8
τ	31	23	1,4

Influence de la taille de l'éprouvette sur les propriétés de traction à la température ambiante .

TABLEAU 4

TA6V COULÉ

TRACTION A 20° C

ÉTAT	ESSAIS SUR BARREAU					ESSAIS SUR ROUET			
SANS TRAITEMENT THERMIQUE		RMPa	R0,2 MPa	A %			RMPa	R0,2 MPa	A %
		893	831	8,64			894	860	7,40
		883	836	4,94			879	837	7,76
		883	836	6,24			874	836	6,64
		852	811	6,72			898	847	7,20
	MOYENNE	877	828	6,63		MOYENNE	886	845	7,25
REFERENCE TA6VPQ FORGÉ						≥ 930	≥ 830	> 9	
AVEC TRAITEMENT THERMIQUE		992	954	3,20			1041	987	4
		982	949	4,48			1074	1034	3,6
		987	954	5,12			1004	970	4,8
		980	944	5,44			983	939	4
	MOYENNE	985	950	4,56		MOYENNE	1025	982	4

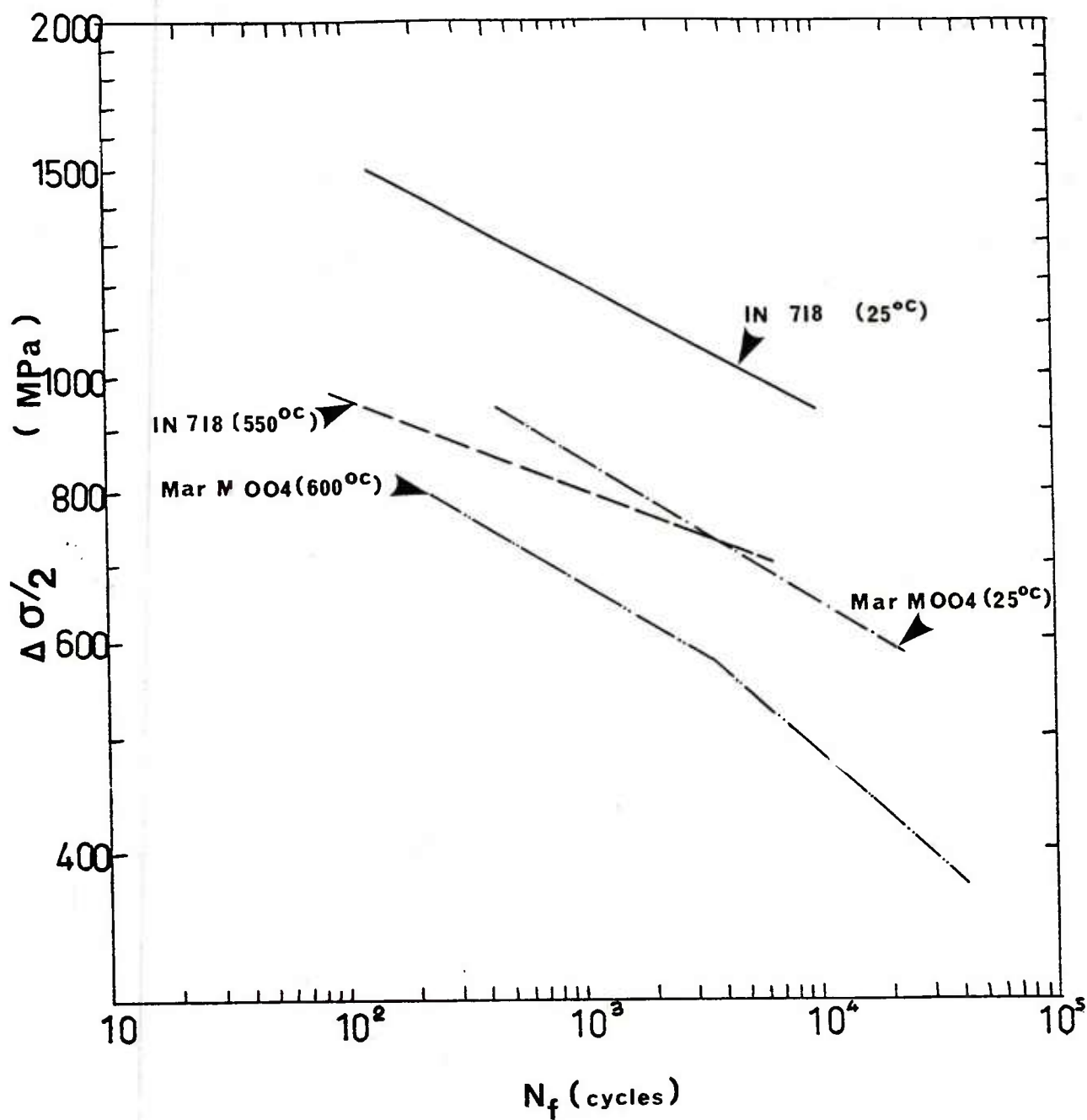
TABLEAU 5

TA6V COULÉ

FATIGUE OLIGOCYCLIQUE A 20° C - 1 Hz - 800 MPa - 0,05 P-P

ESSAI SUR BARREAU				ESSAI SUR ROUET	
ÉTAT		NOMBRE DE CYCLES A RUPTURE			NOMBRE DE CYCLES A RUPTURE
SANS TRAITEMENT THERMIQUE		1870			5970
		3100			2010
		4820			4120
		5740			1420
	MOYENNE	3882		MOYENNE	3380
RÉFÉRENCE TA6VPQ FORGÉ			> 10 000		
AVEC TRAITEMENT THERMIQUE		22350			17510 9560
		11050			12040 15680
		16650			12290 12100
		21070			14110 16960
					7790 18500
					4950
	MOYENNE	17780		MOYENNE	12856

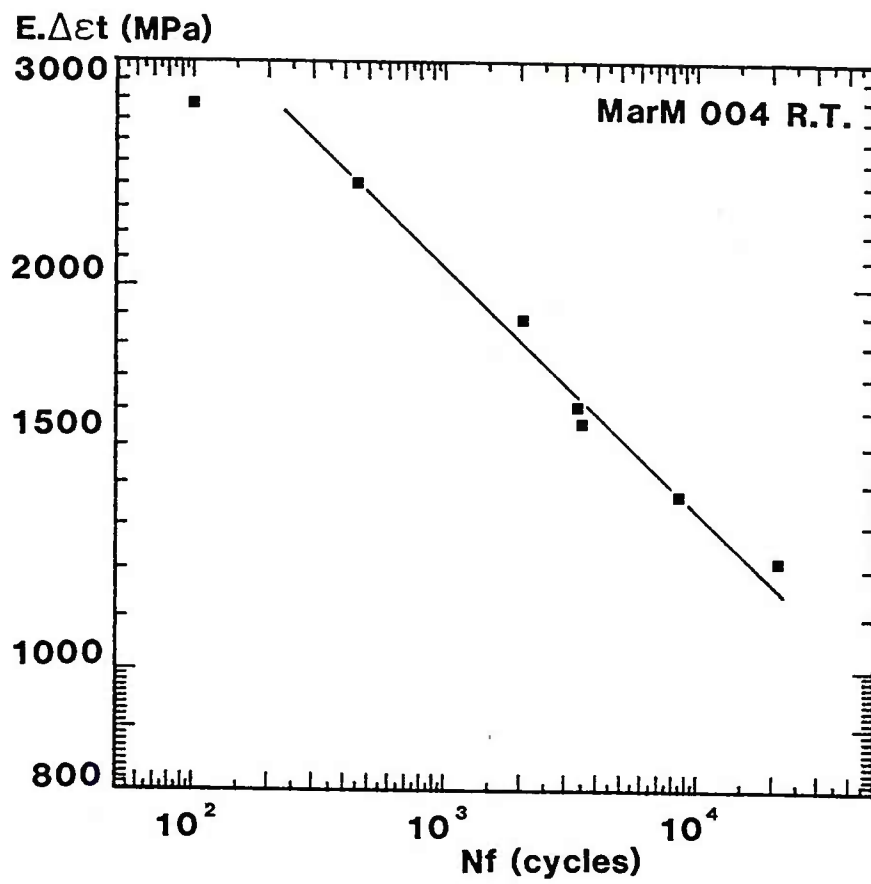
COURBE 1



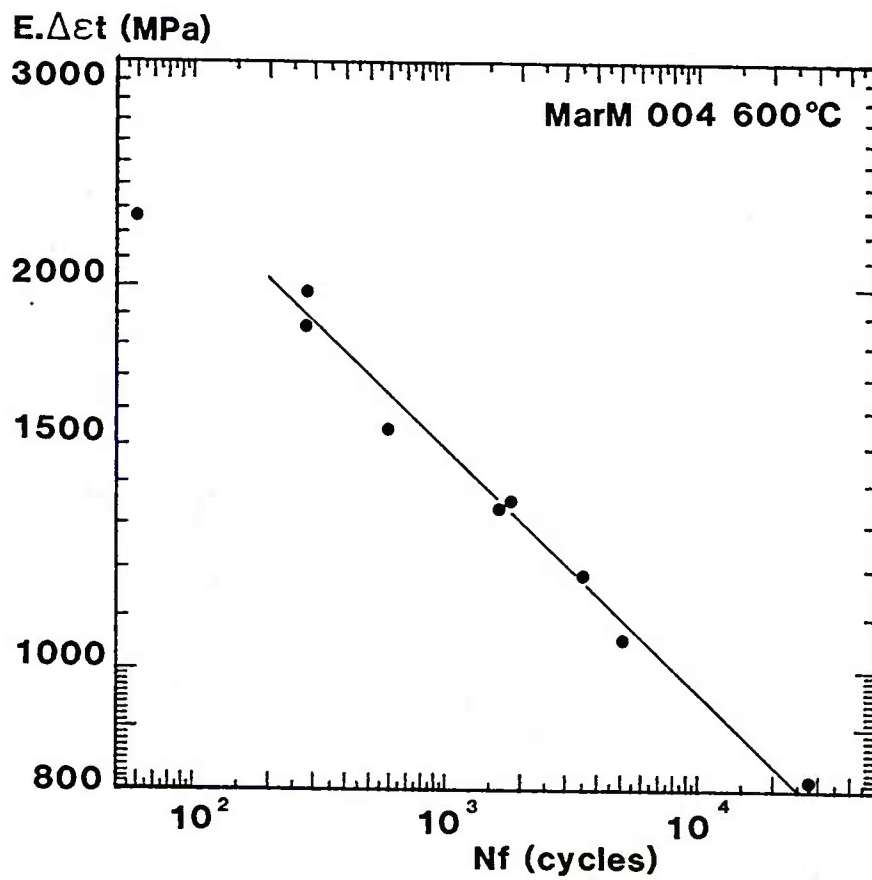
VARIATION DE LA CONTRAINTE A DEMI-DURÉE DE VIE $\Delta\sigma/2$ EN FONCTION
DU NOMBRE DE CYCLES A RUPTURE N_f POUR DIFFÉRENTS MATÉRIAUX

a) MarM004 20°C ; b) MarM004 600°C ;
c) INCO 718 20°C ; d) INCO 718 550°C

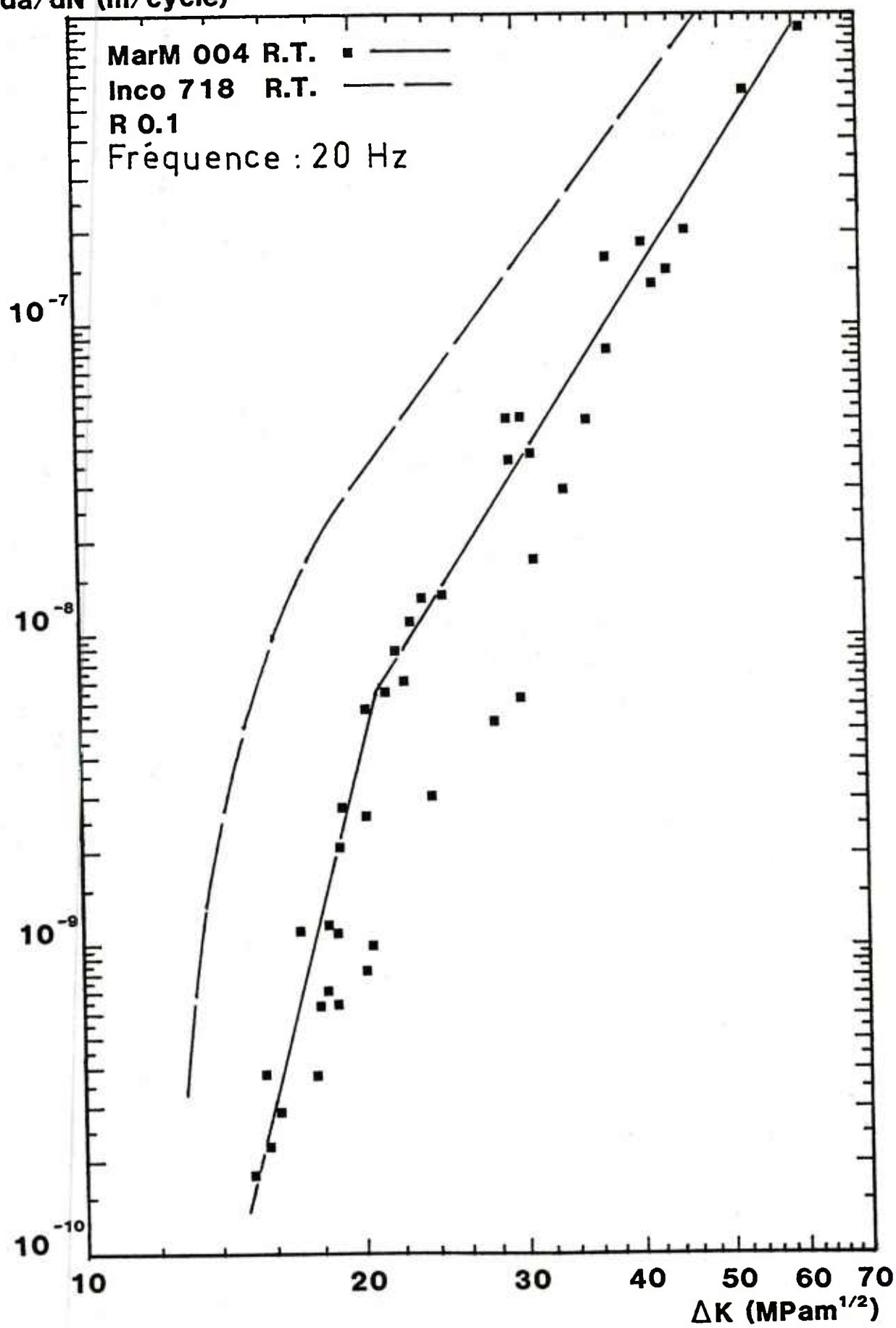
COURBE 2

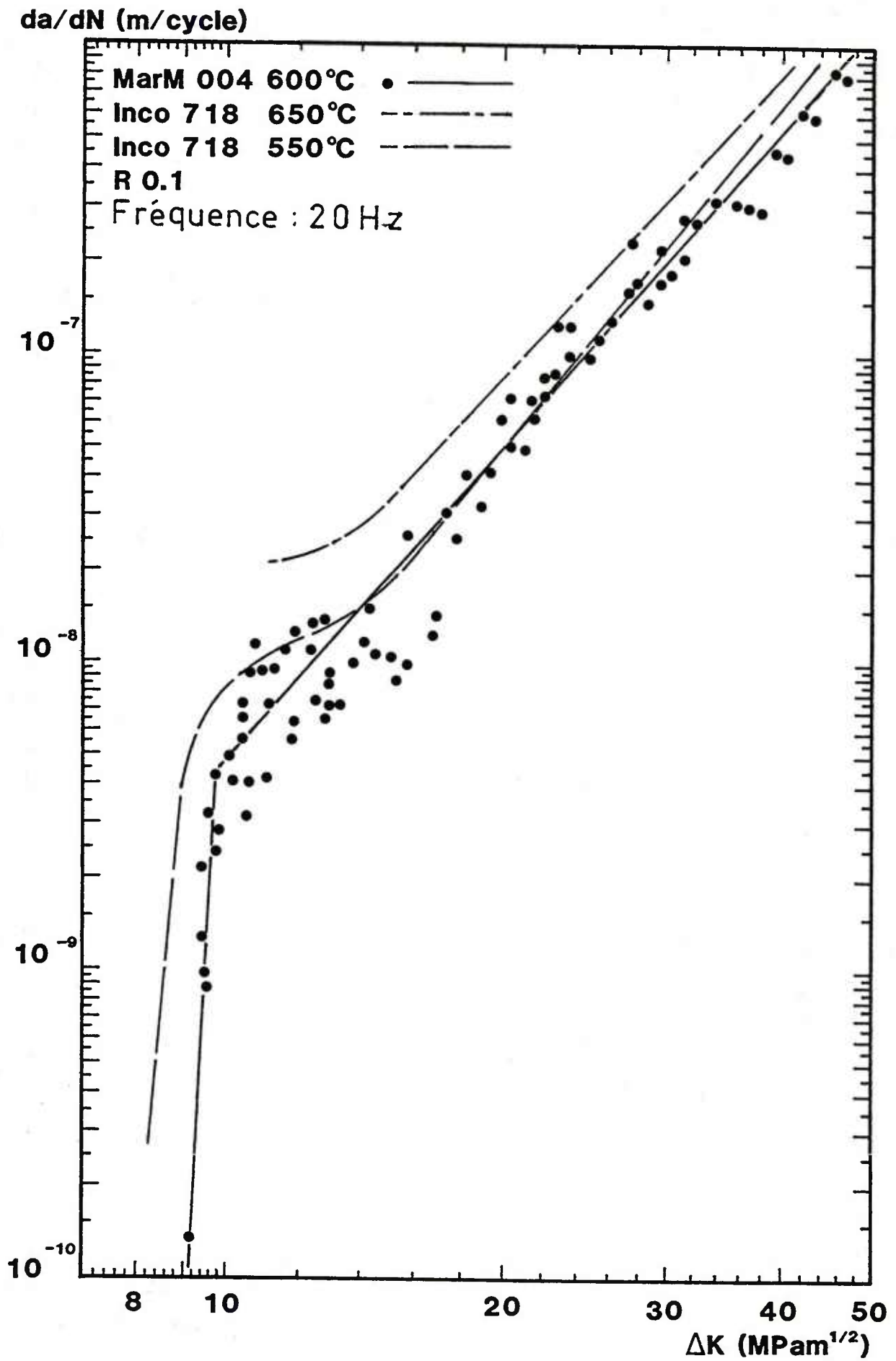


COURBE 3

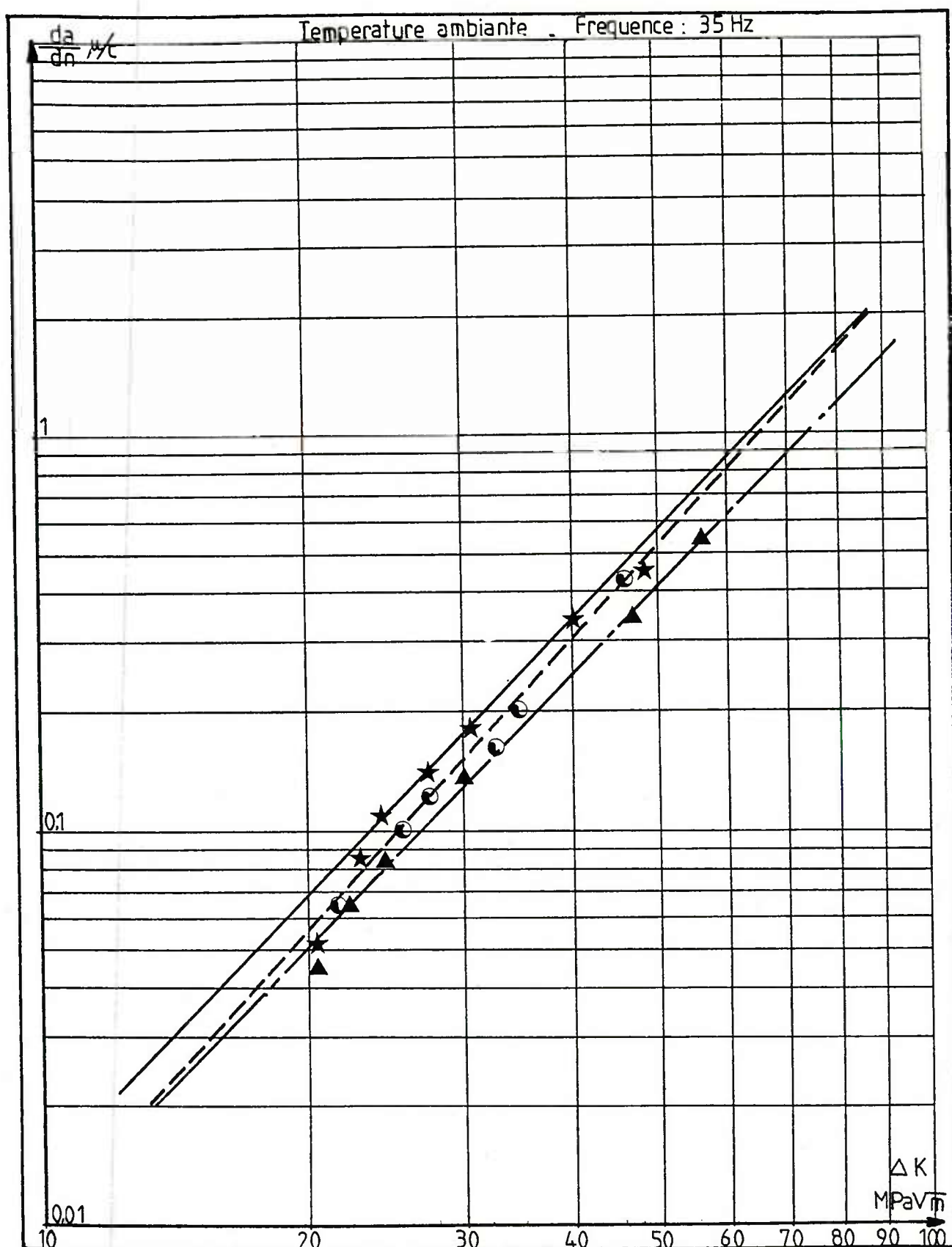


COURBE 4

 da/dN (m/cycle)



COURBE 6

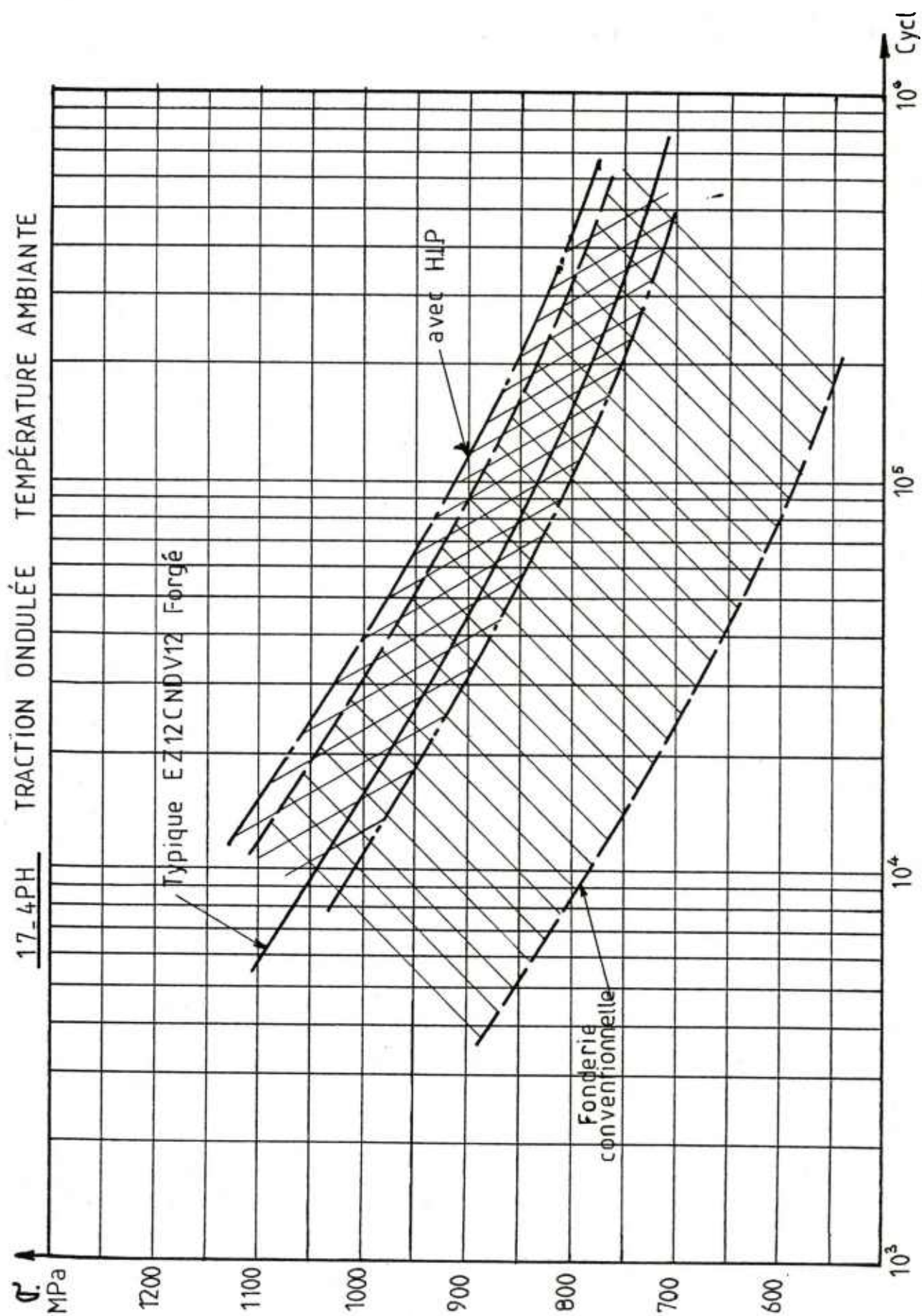


Etude 394 - 17-4 PH_Forgé - Plaque N°1 - Epreuve N°1L ★—★

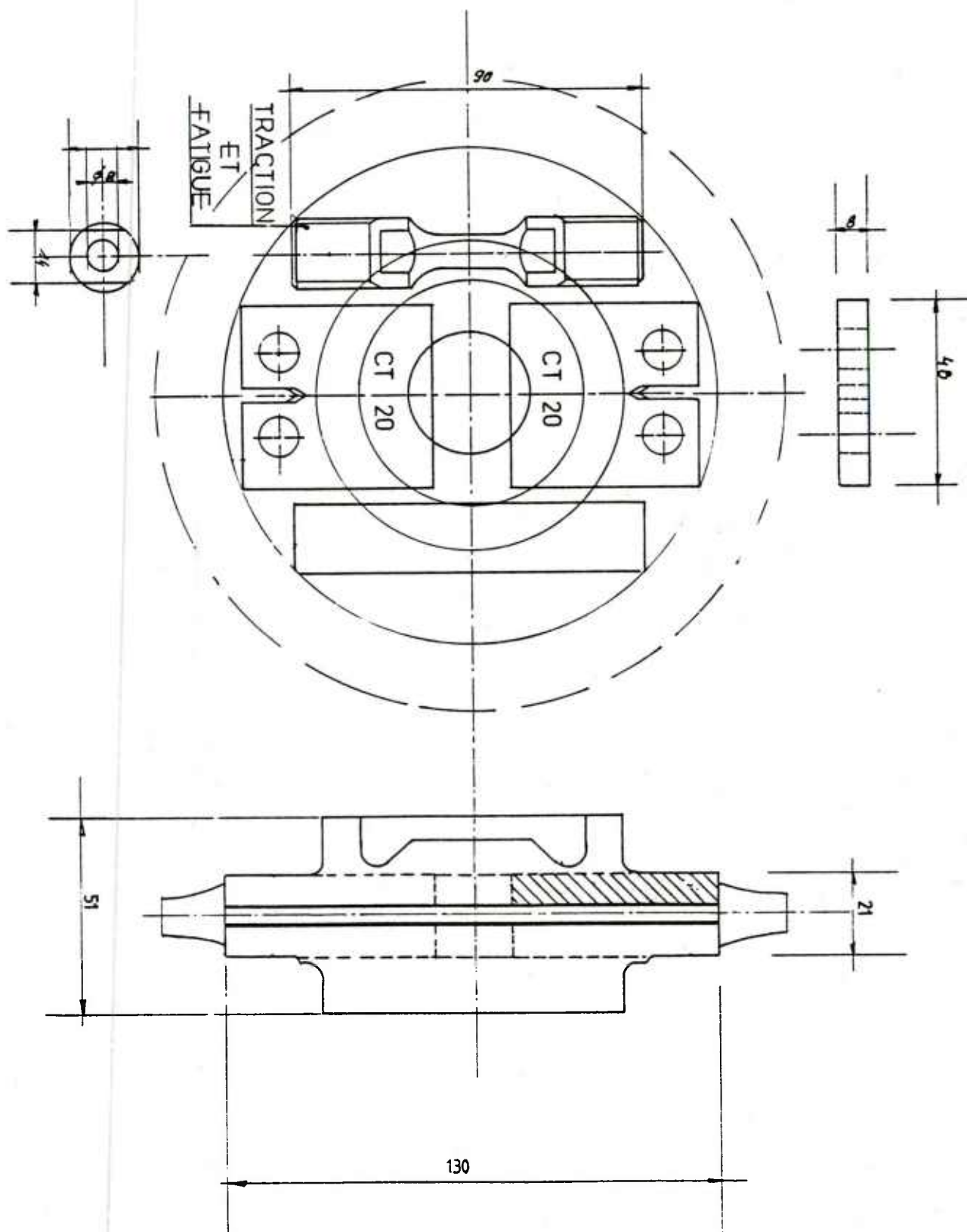
Epreuve N°1T ▲—▲

Etude 541 - 17-4 PH_Coulé

Epreuve N°5 ●—●

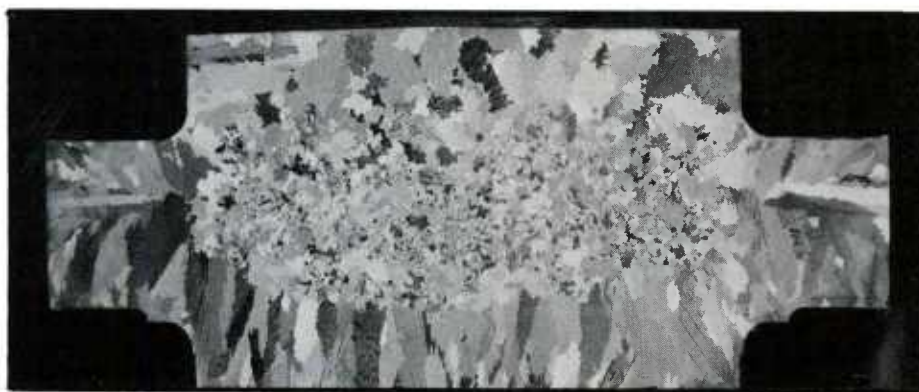


SCHEMA 4



PRELEVEMENT EPROUVETTES

PLANCHE 1

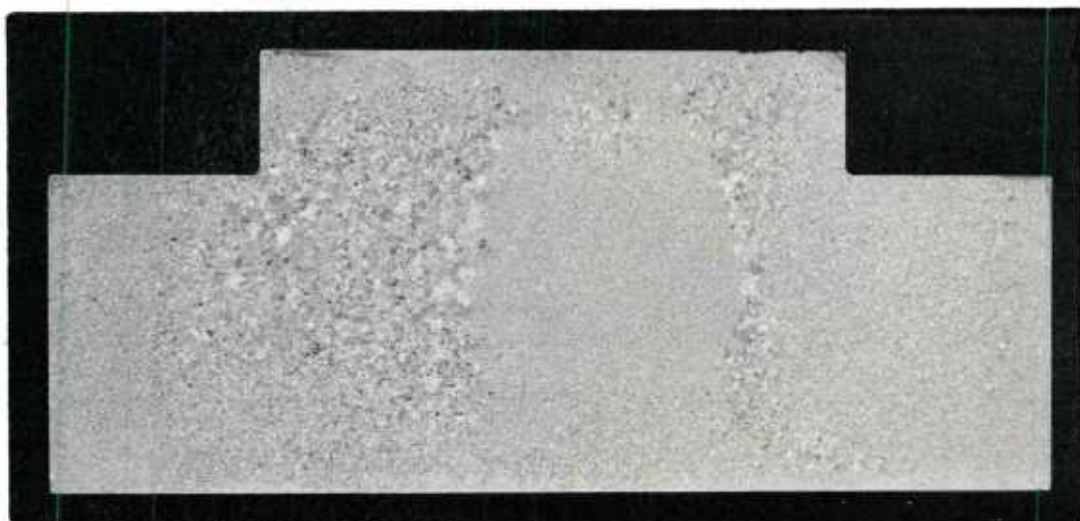


1

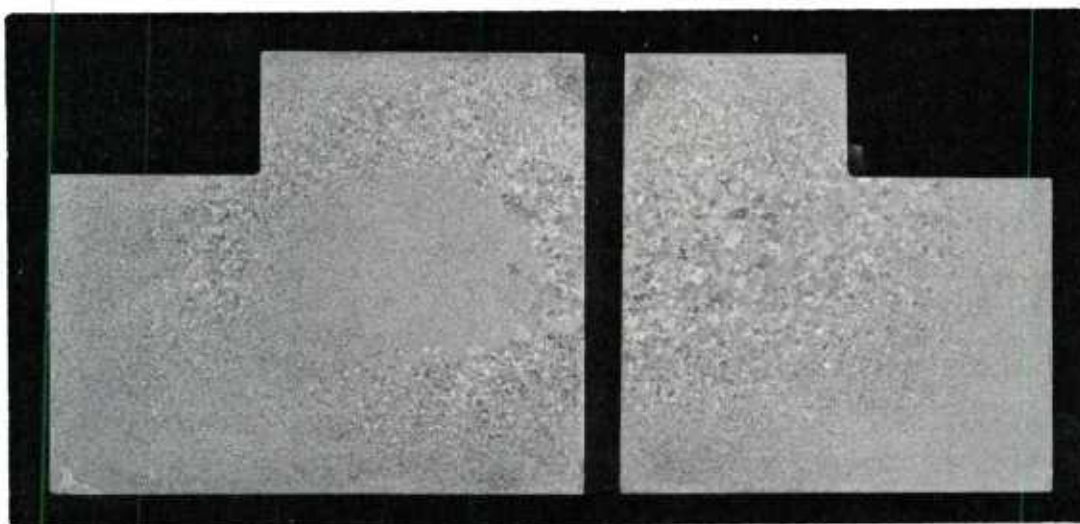
EXEMPLE DE DÉFAUTS DE CRISTALLISATION DANS UNE
ROUE DE TURBINE EN SUPERALLIAGE

PLANCHE 2

EXEMPLES D'HÉTÉROGÉNÉITÉ DE TAILLE DE GRAINS
DANS UNE PIÈCE DE FORGE EN SUPERALLIAGE (U500)



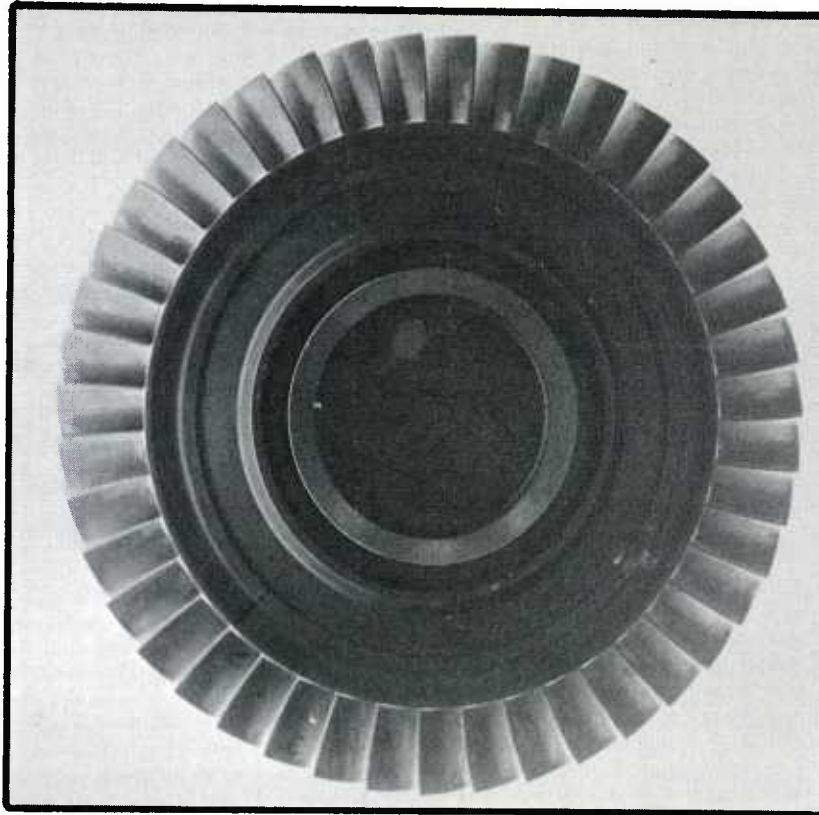
2



3

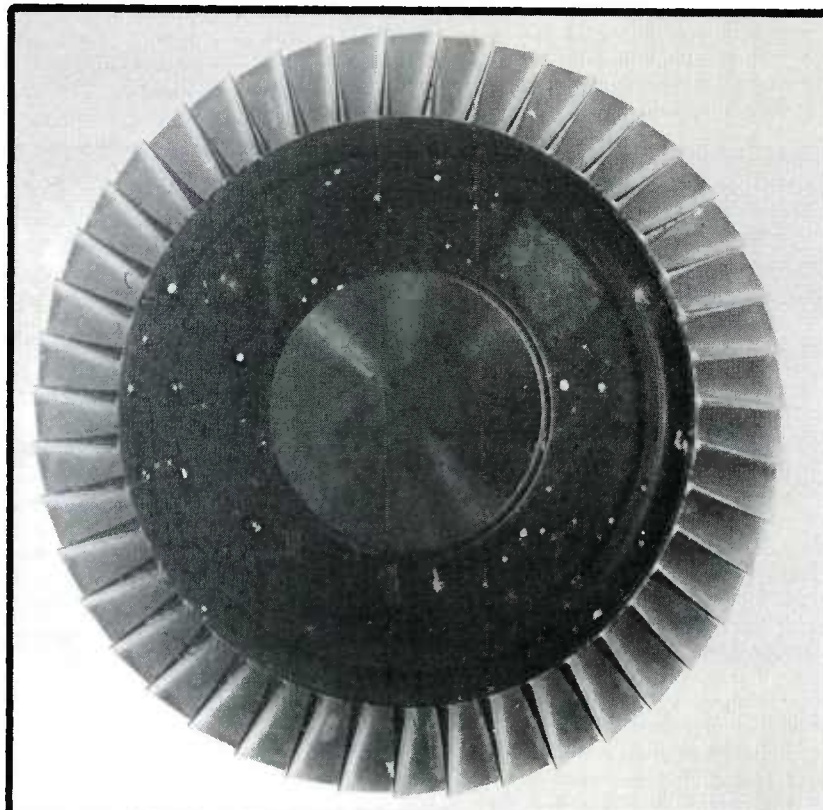
PLANCHE 3

INDICATIONS EN RESSUAGE FLUORESCENT



FACE INFÉRIEURE

4

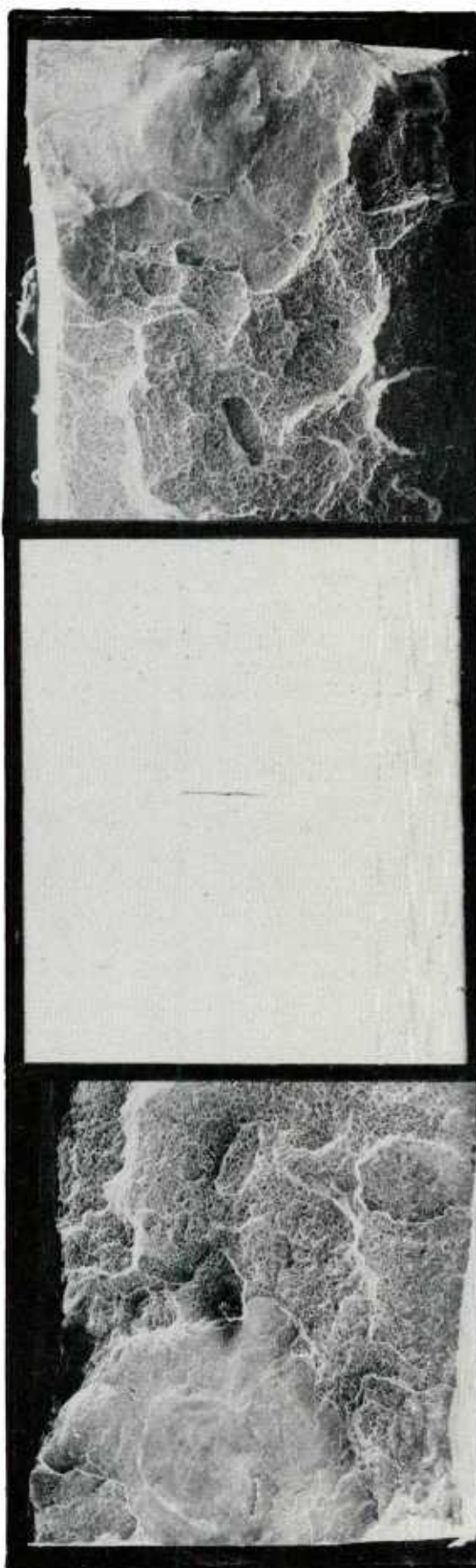


FACE SUPÉRIEURE COTÉ ALIMENTATION

5

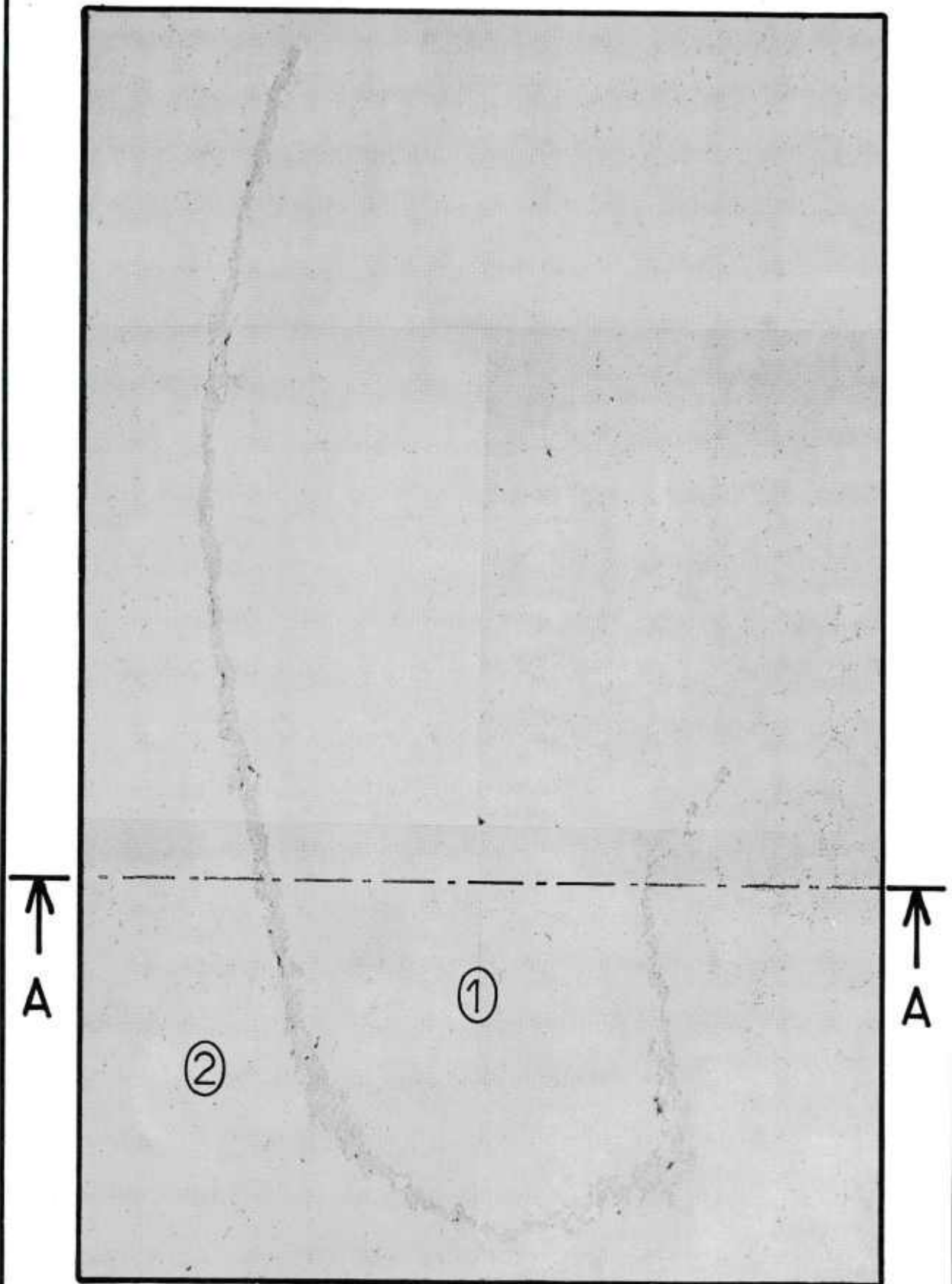
PLANCHE 4

CRIQUE ASSOCIÉE A
UNE INCLUSION DANS
UNE PIECE DE FORGE
EN SUPERALLIAGE



1000 μ

PLANCHE 5



7

IMPORTANTE NAPPE D'INCLUSIONS (50 mm x 2,5 mm)
DANS UNE PIECE DE FORGE EN SUPERALLIAGE

1000 μ

PLANCHE 6



8

MACROGRAPHIE D'UNE ROUE DE TURBINE
COULÉE EN SUPERALLIAGE

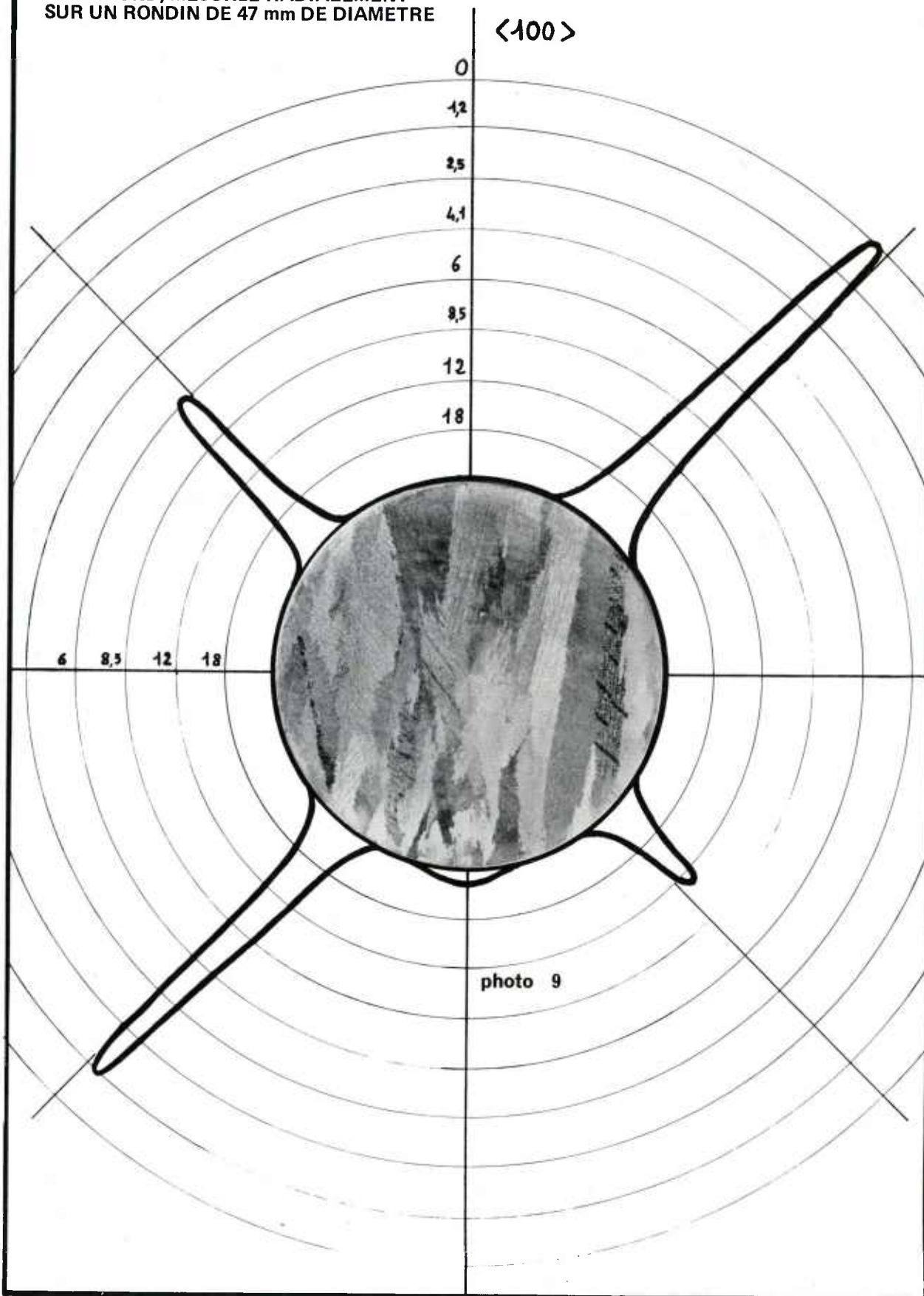
ECHOGRAPHIE

PLANCHE 7

Structure basaltique

HAUTEUR RELATIVE (dB) DE L'ÉCHO
DE FOND, MESURÉE RADIALEMENT
SUR UN RONDIN DE 47 mm DE DIAMÈTRE

<100>

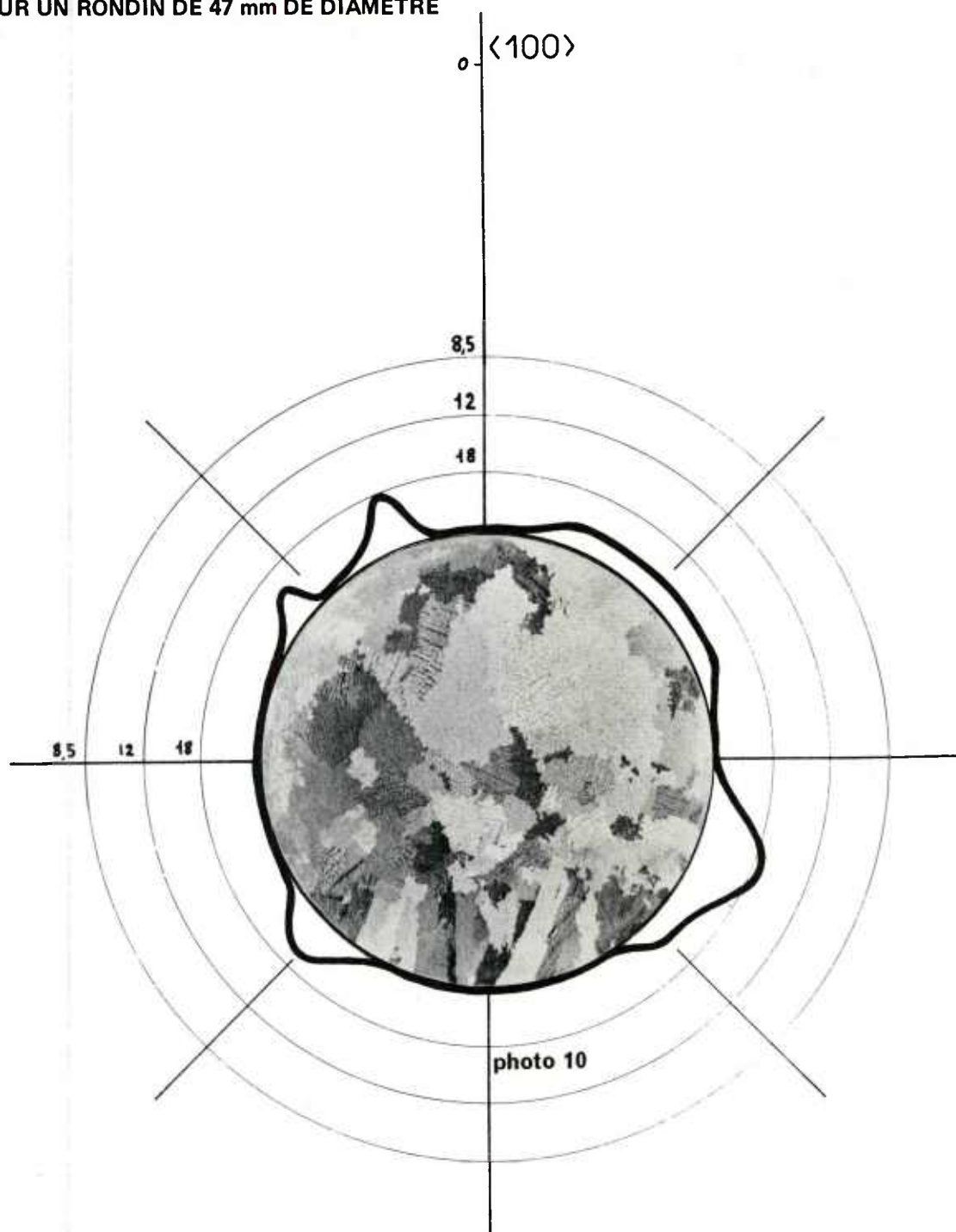


ECHOGRAPHIE

PLANCHE 8

HAUTEUR RELATIVE (dB) DE L'ÉCHO
DE FOND, MESURÉE RADIALEMENT
SUR UN RONDIN DE 47 mm DE DIAMÈTRE

Structure
semi-équiaxe



ECHOGRAPHIE

PLANCHE 9

HAUTEUR RELATIVE (dB) DE L'ÉCHO
DE FOND, MESURÉE RADIALEMENT
SUR UN RONDIN DE 47 mm DE DIAMÈTRE

Structure
entièrement équiaxe

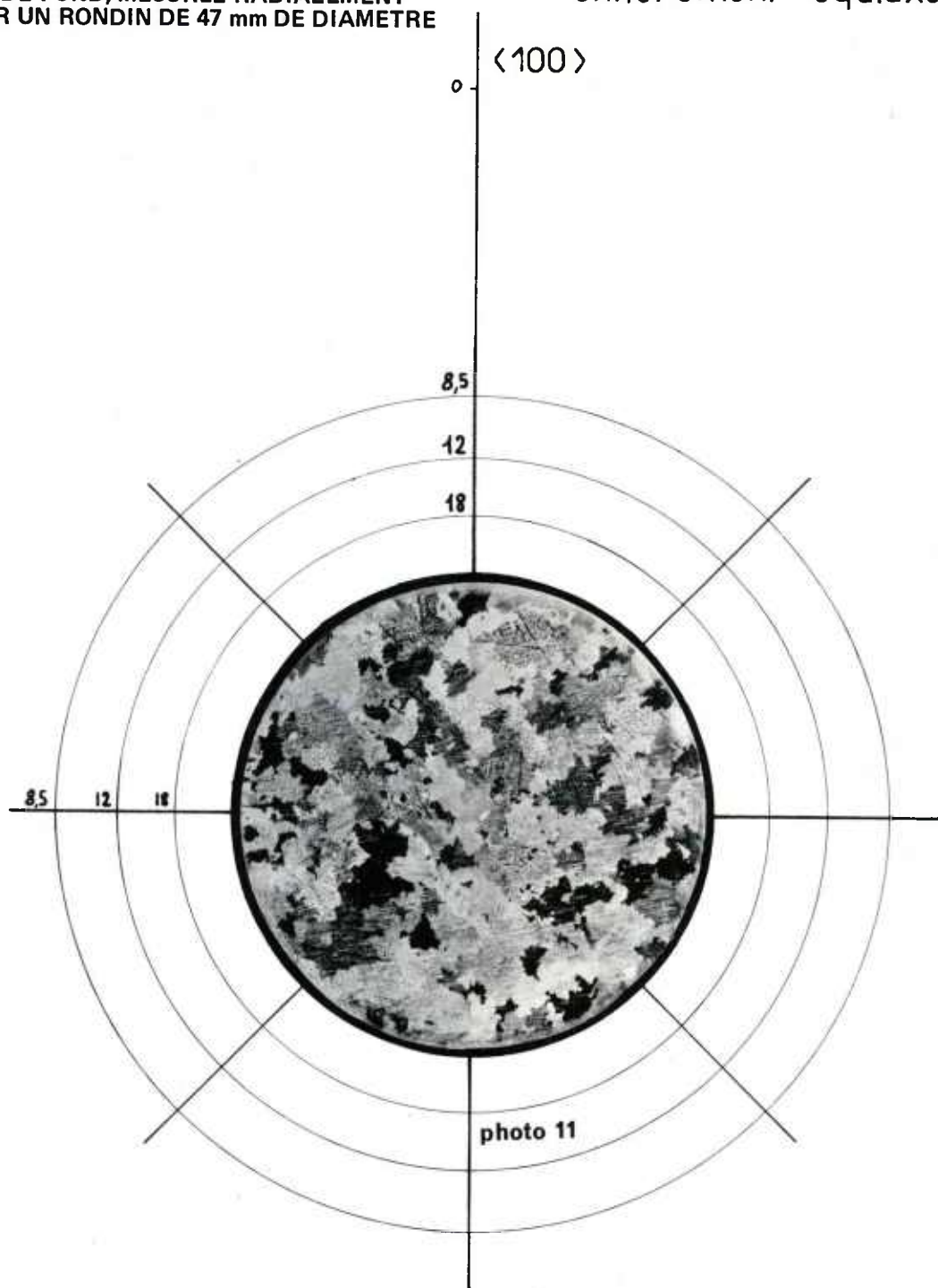
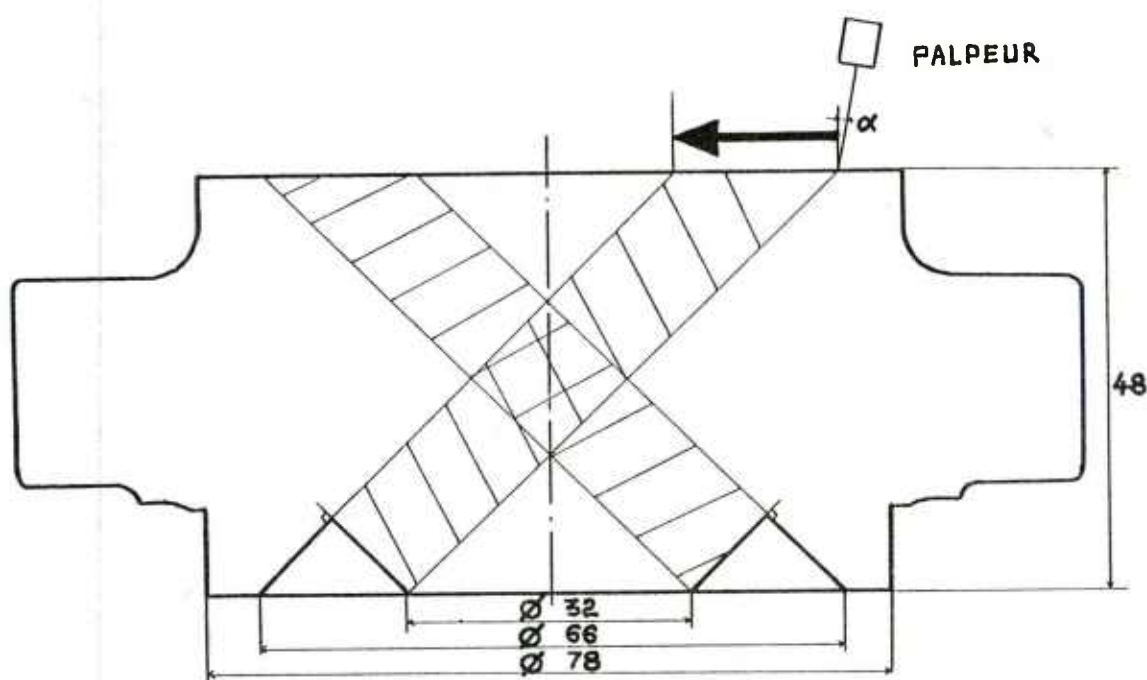



PLANCHE 10



 ZONE
EXPLOREE
 $\alpha = 10^\circ$

SCHEMA 1: CONTROLE
DE LA STRUCTURE

PLANCHE 11

SCHEMA 2: CONTROLE
DES DEFAUTS

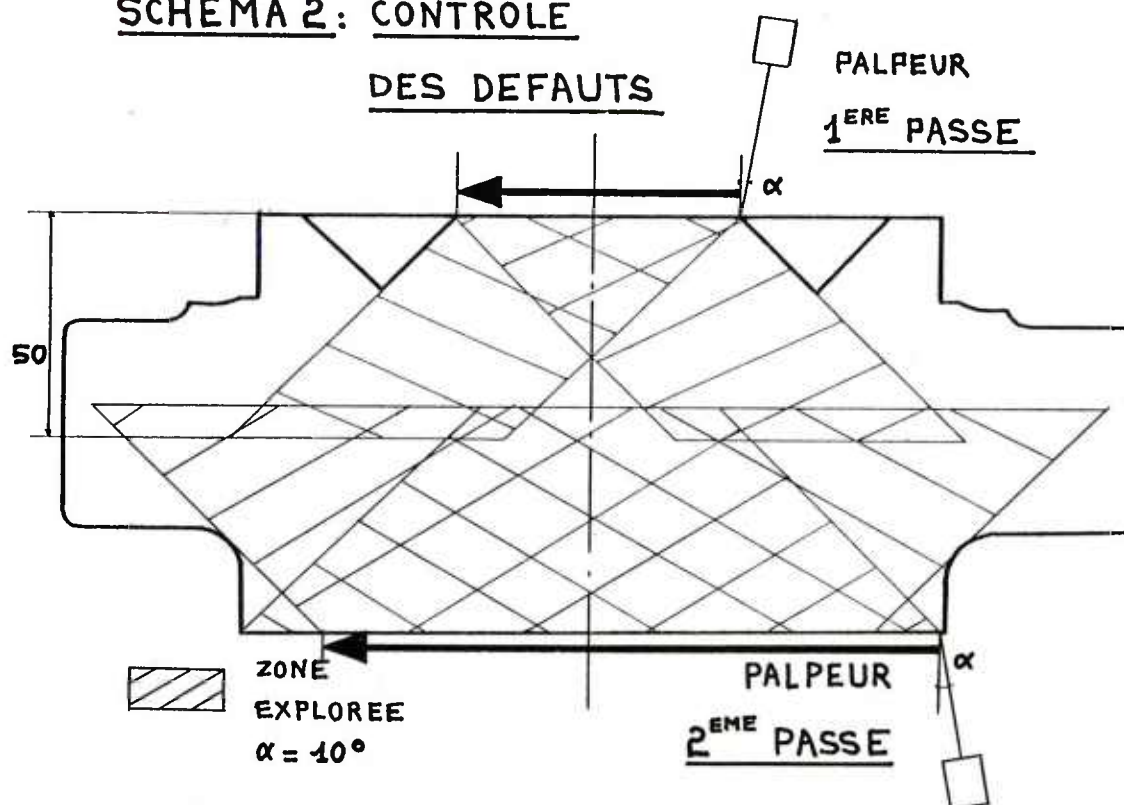
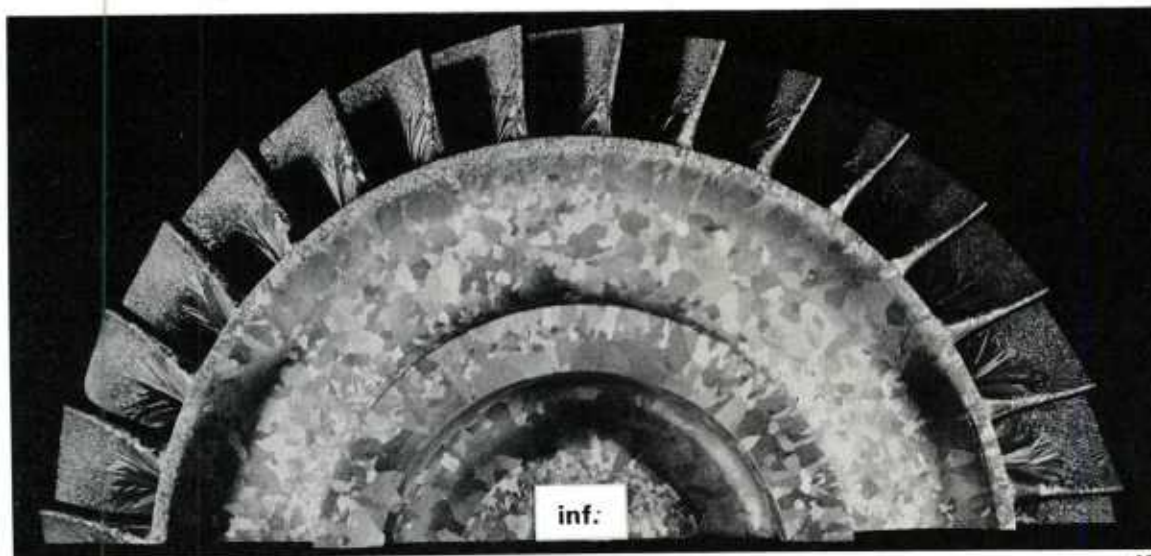
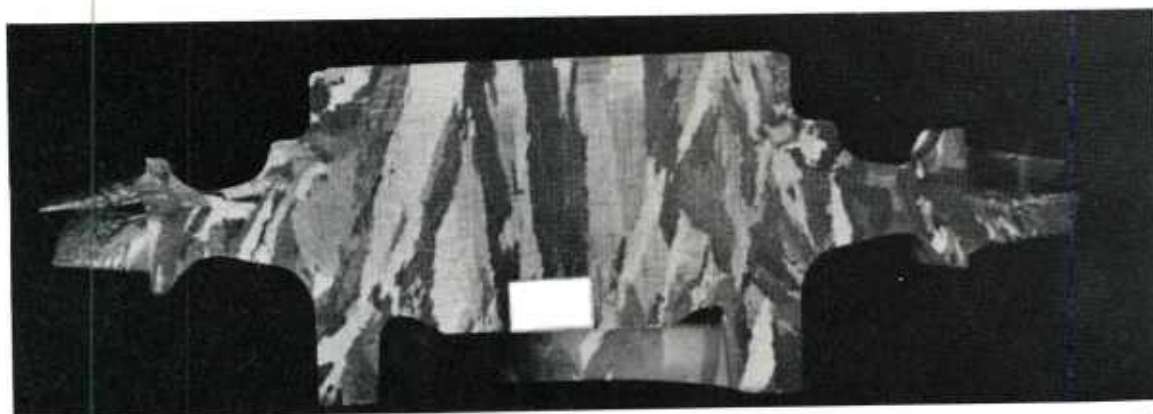


PLANCHE 12

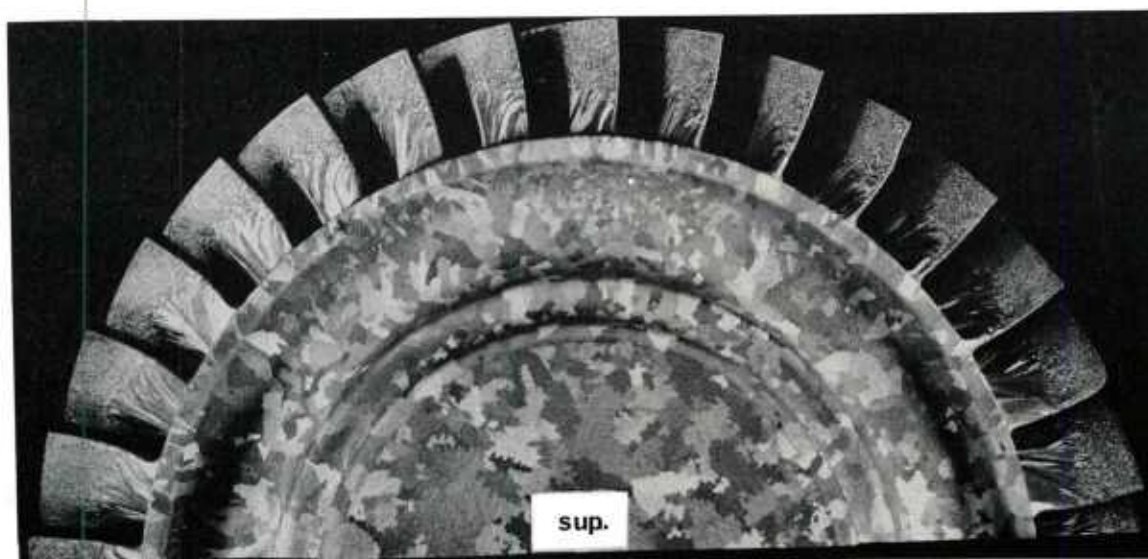
MACROGRAPHIE D'UNE ROUE
DE TURBINE EN MarM004



12

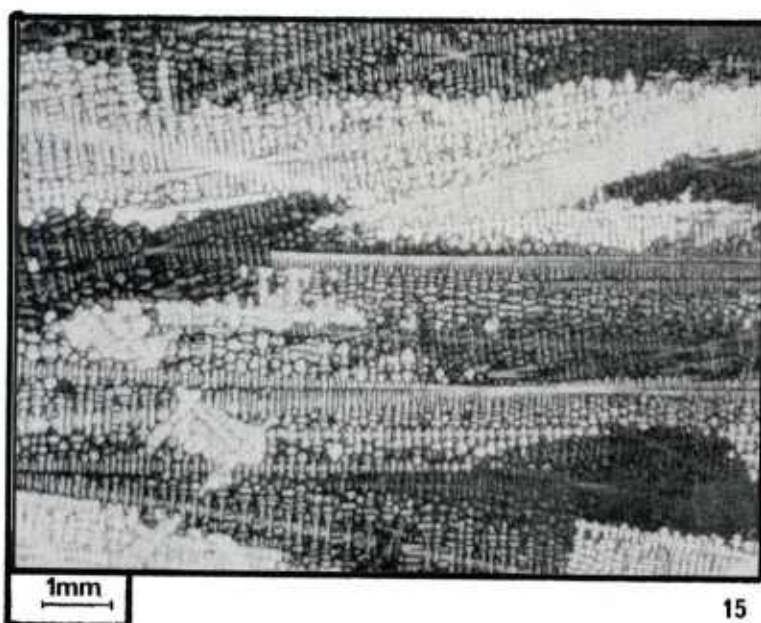


13

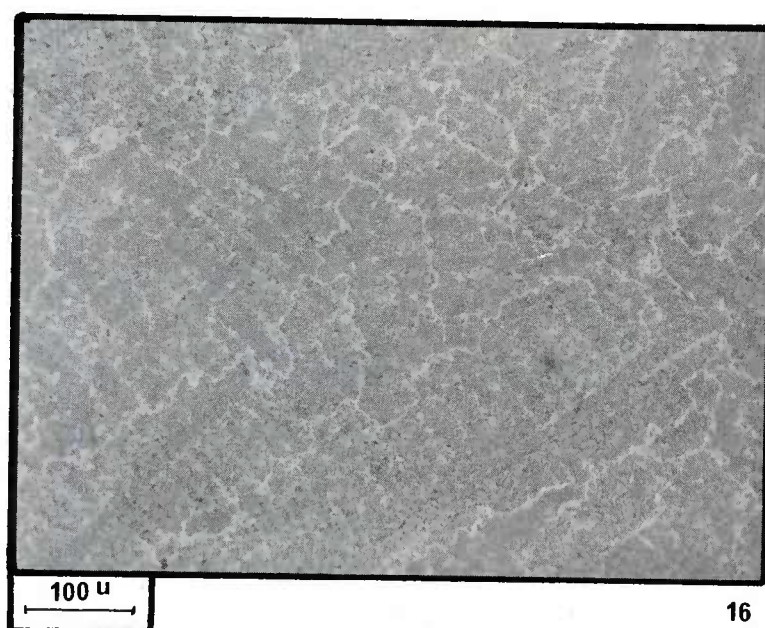


14

PLANCHE 13

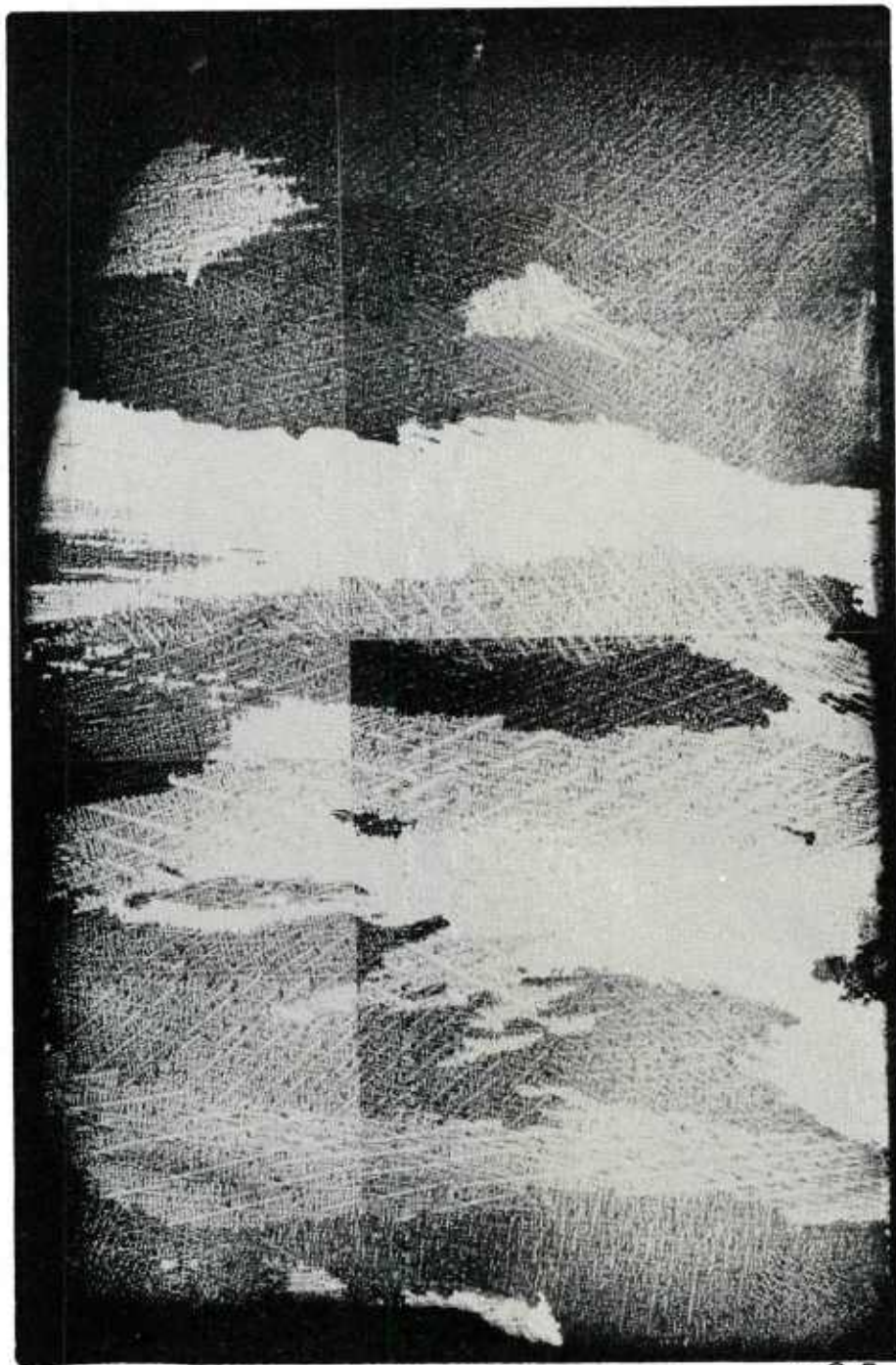


MACROSTRUCTURE DANS LA ZONE DE MOYEU



MICROSTRUCTURE DANS LA ZONE DES PALES

PLANCHE 14

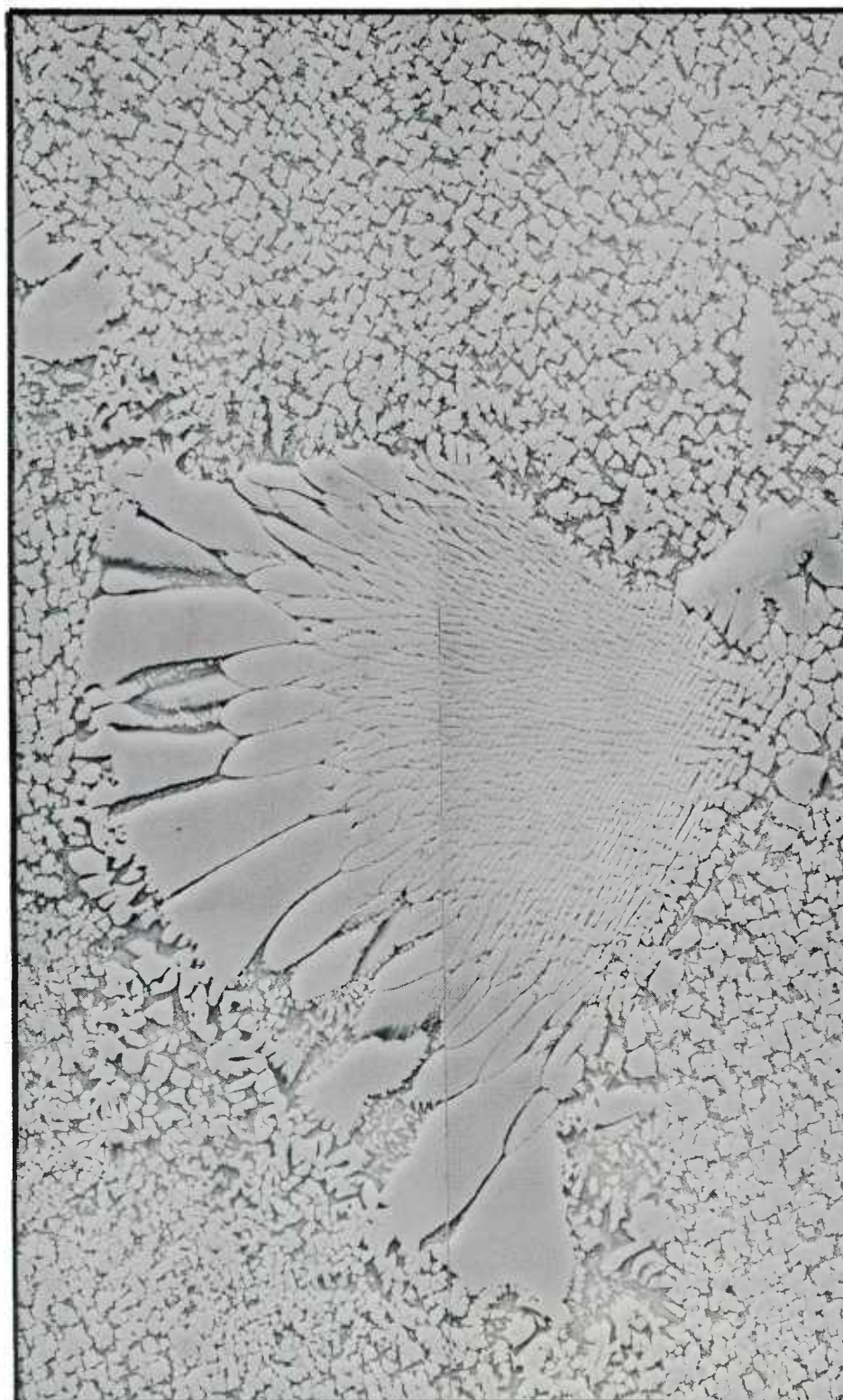


17

x 2,5

MACROSTRUCTURE DANS LA ZONE DU MOYEU

PLANCHE 15



18

PLAGE D'EUTECTIQUE γ/γ' DANS
L'ESPACE INTERDENDRITIQUE

10 μ

PLANCHE 16

MICROSTRUCTURE DANS LE MarM004

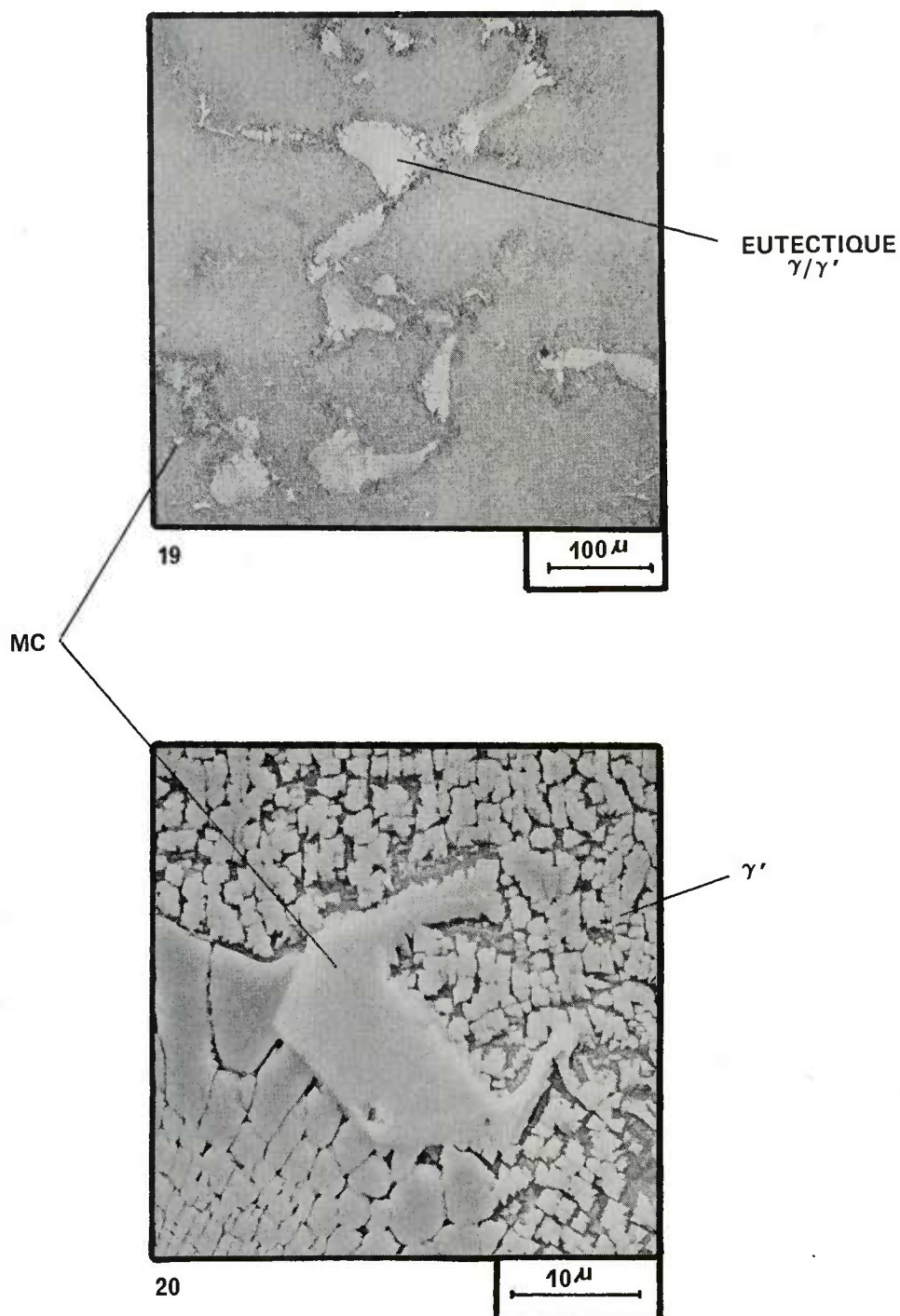


PLANCHE 17

MORPHOLOGIE DES PRÉCIPITÉS γ'

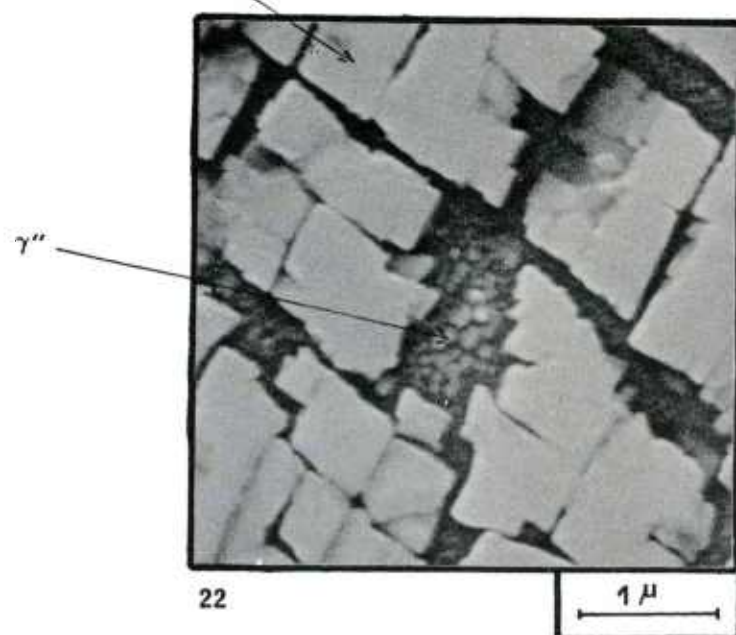
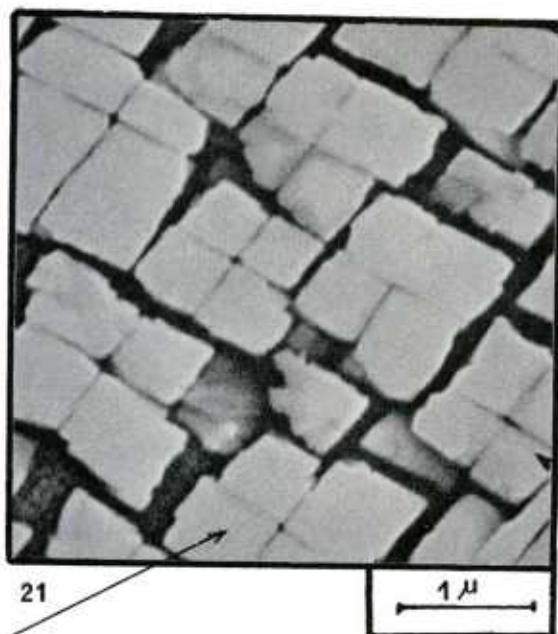
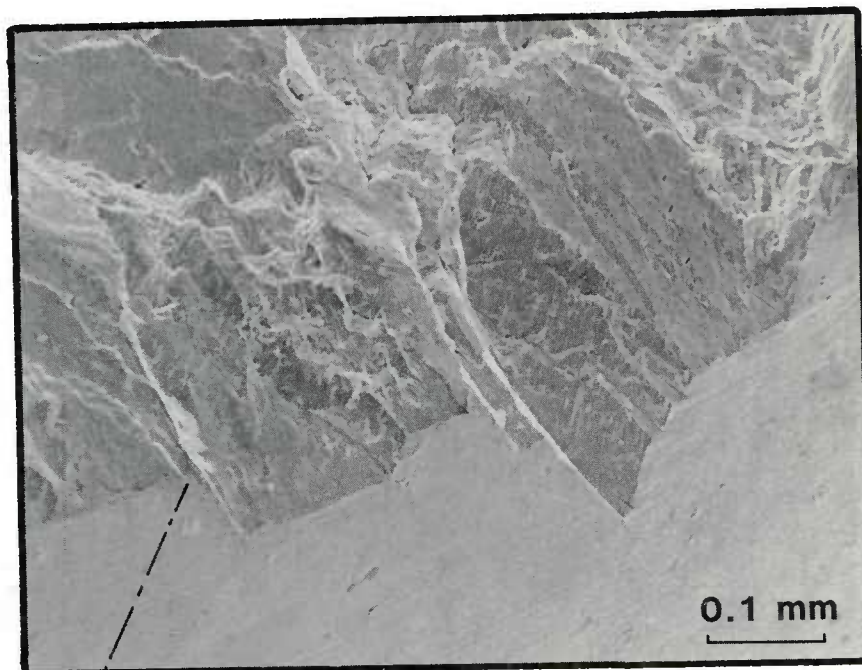
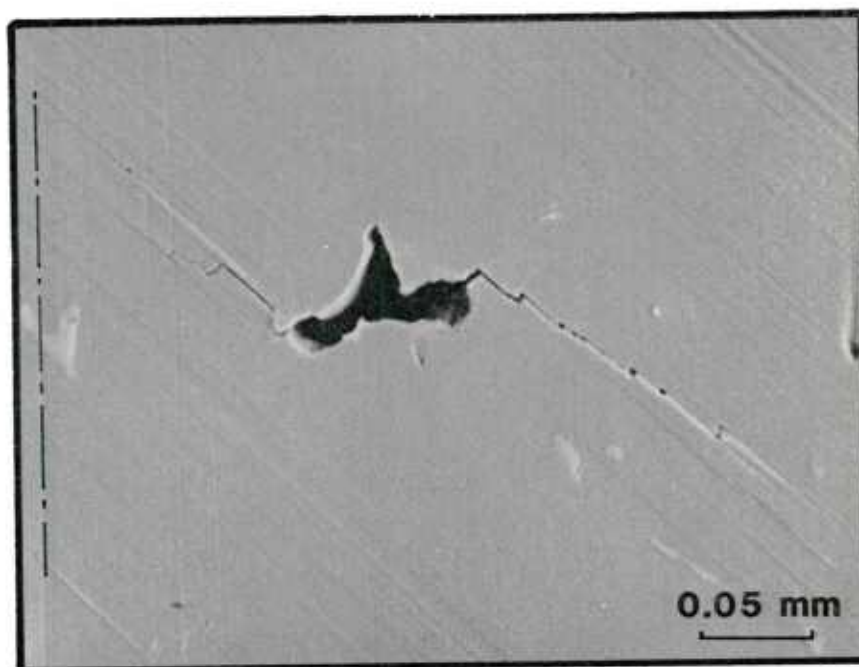


PLANCHE 18



23

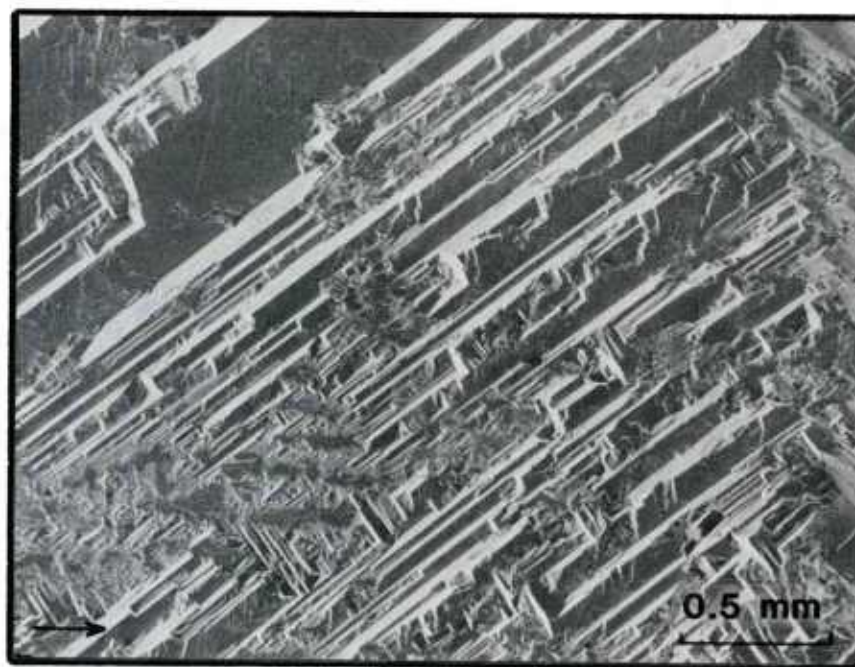
SITE D'AMORÇAGE D'UNE ÉPROUVETTE F.P. CYCLÉE A 600° C ET ROMPUE
 $E \Delta \epsilon_t = 1\,050 \text{ MPa}$ - $N_f = 5\,000 \text{ CYCLES}$
 (AXE = DIRECTION DE SOLLICITATION)



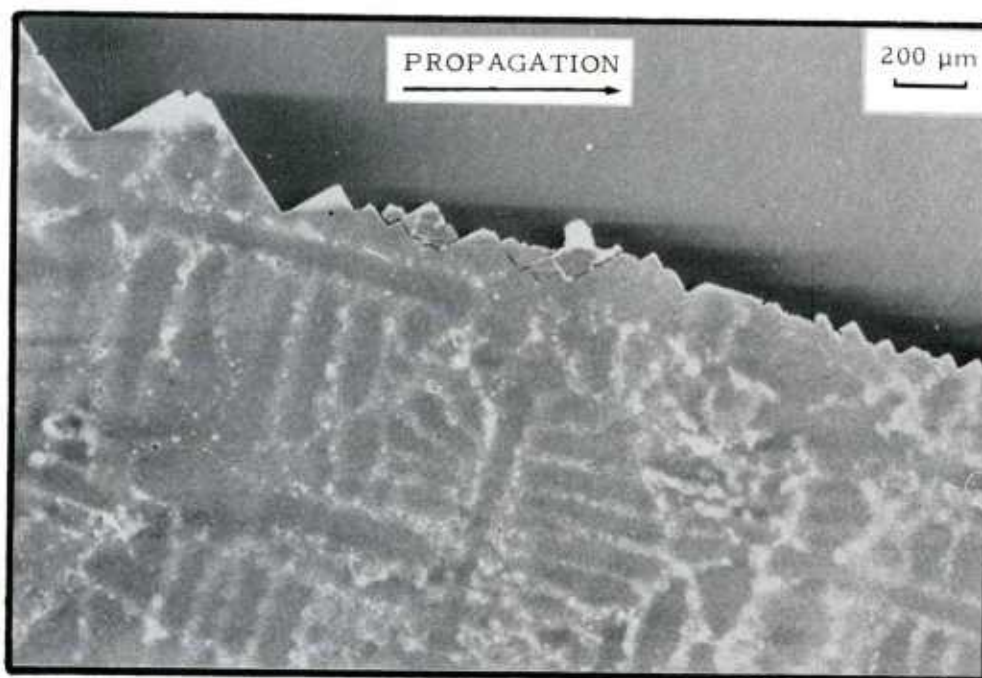
24

AMORÇAGE D'UNE FISSURE SECONDAIRE A PARTIR D'UNE POROSITÉ DÉBOUCHANTE
 MICROGRAPHIE DU FUT D'UNE ÉPROUVETTE CYLINDRIQUE - ESSAI A 20° C
 $E \Delta \epsilon_t = 1876 \text{ MPa}$ - $N_f = 2\,050 \text{ CYCLES}$

PLANCHE 19

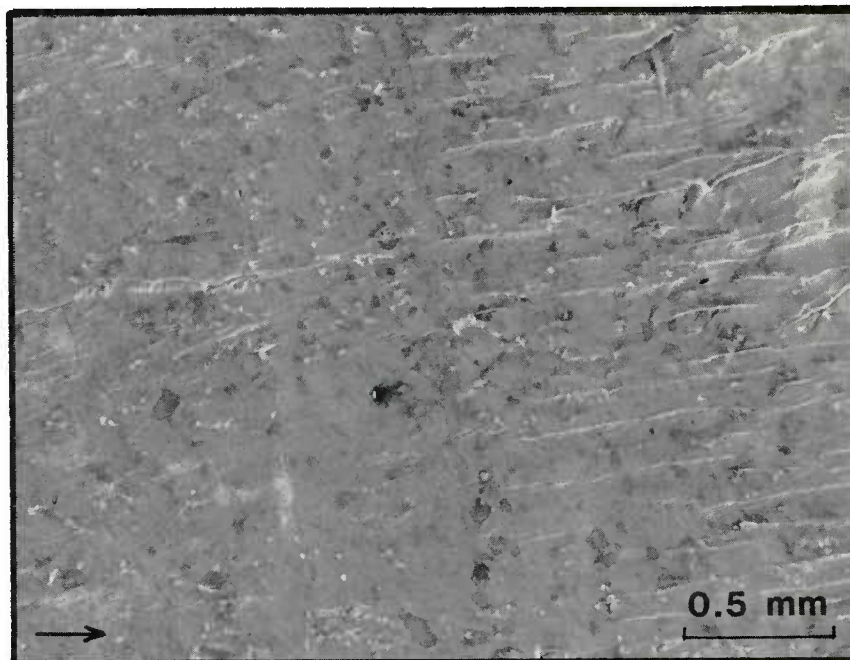


25
 FRACTOGRAPHIE D'UNE ÉPROUVETTE DE FISSURATION
 AUX FAIBLES ΔK , FAIBLES VITESSES A 20° C
 (FLECHE = SENS DE PROPAGATION)



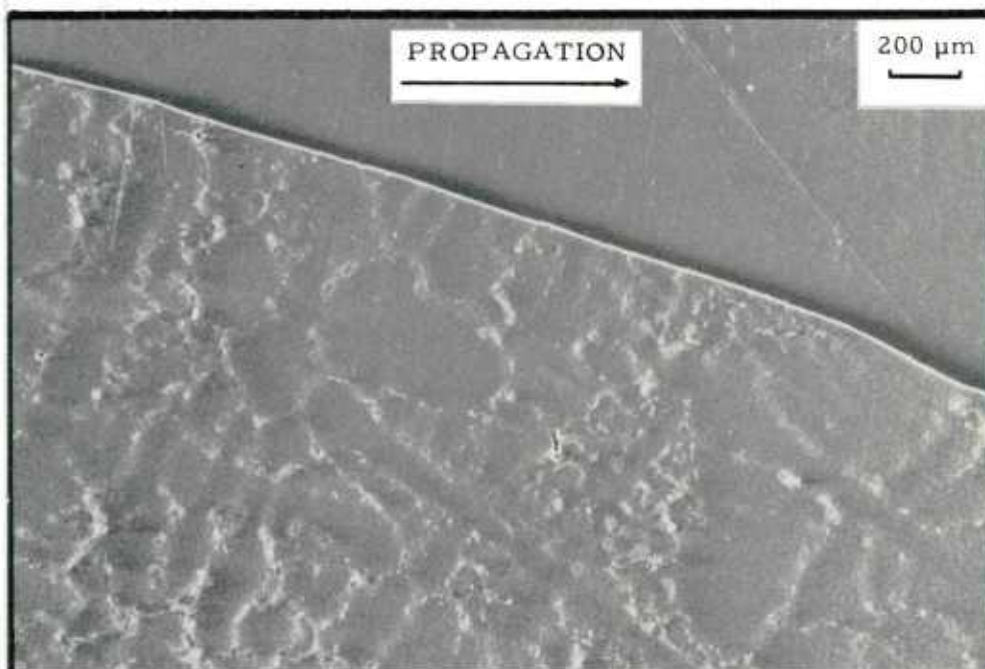
26
 COUPE LONGITUDINALE D'UNE ZONE DE SEUIL DE PROPAGATION,
 ÉTAT ATTAQUÉ. MarM004 ; CT 20 ; 20° C ; R = 0,1

PLANCHE 20



FACTOGRAPHIE D'UNE ÉPROUVETTE DE FISSURATION
AUX FAIBLES ΔK , FAIBLES VITESSES, A 600° C

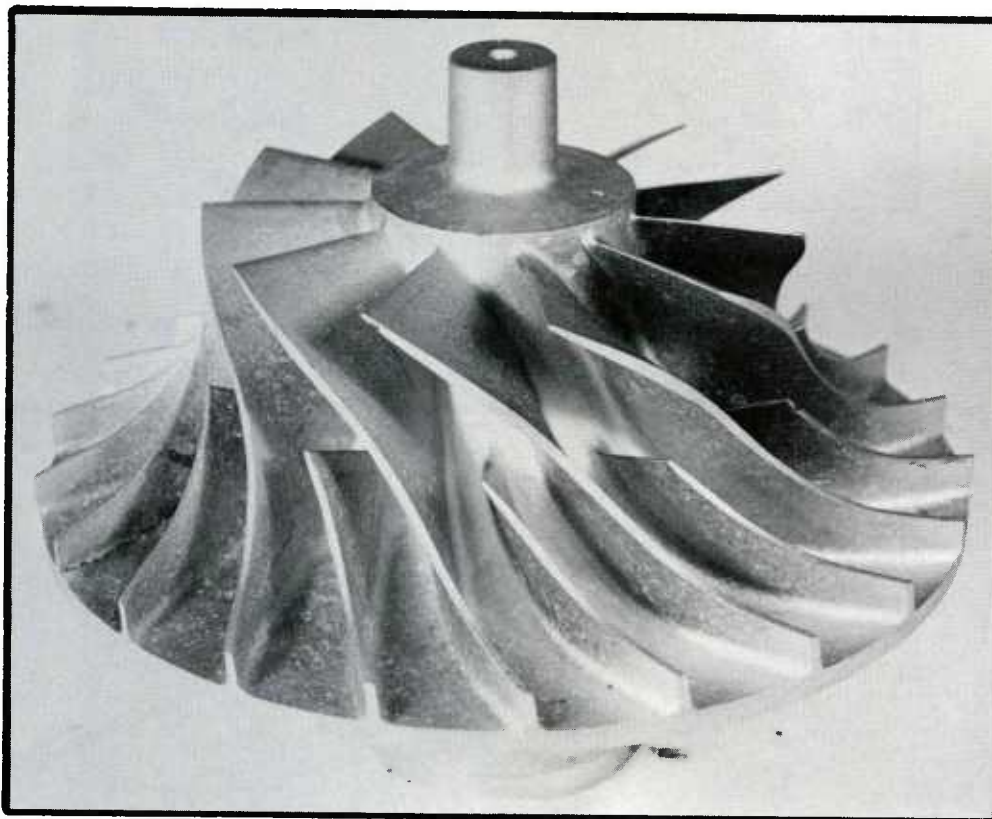
27



COUPE LONGITUDINALE D'UNE ZONE DE SEUIL DE PROPAGATION
ÉTAT ATTAQUÉ. MarM004 ; CT 20 ; 600° C ; R = 0,1

28

PLANCHE 21



ROUET CENTRIFUGE
TA6V COULÉ

PLANCHE 22

TA6V COULÉ

ÉTAT NON TRAITÉ

ÉTAT TRAITÉ



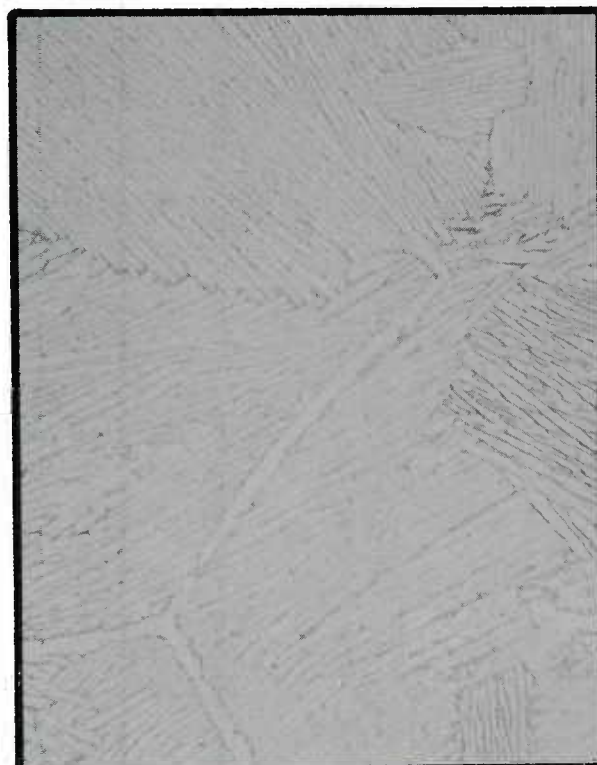
30

100 μ



32

100 μ



31

100 μ



33

100 μ

"ELECTROSLAG CASTING EVALUATION"

A. Mitchell & G. Sidla
University of British Columbia
Vancouver, Canada
V6T 1W5

The electroslag casting process (ESC) is used widely in the USSR for the production of high-quality steel castings. This study was directed towards an examination of ESC's potential applications in North America for the manufacture of near-net-shape castings in alloy steels. We report on the development of a cheap, simple version of the ESC process intended for the manufacture of castings in the weight range from 10 - 1000 Kg. We have demonstrated the application of ESC to the production of a number of cast shapes, such as gears and shafts (SAE 4340) and tubular sections (SAE 4340, D6AC). The study reports on mechanical property investigations for these components and comments on the range of ESC application arising from the conclusions of the work.

The electroslag-remelting process has become an accepted method of producing high quality forgings in a variety of steels and related alloys. At a very early stage in the process's development it was recognized that the technique had the potential to cast not only ingots but also simple shapes. From this recognition stems the electroslag casting (ESC) process, and the product's use in the as-cast condition.

The ESC process is reported to be used widely in the USSR, where the work of the E.O. Paton Institute of Electrical Welding has led to its strong development. There are literature descriptions of the use of ESC products in valves, gears, rolls, and crank-shafts, in casting sizes ranging from a few kilogrammes up to several tonnes.

Accounts of the process are available in the literature and a schematic of the process is shown in Figure 1. The consumable electrode, produced by either rolling or casting, is remelted into a water-cooled crucible resting on a water-cooled baseplate. Electrical connections are made to the electrode and to the baseplate, using a line-frequency transformer as the power supply. Heat for melting is generated by Joule heating of the liquid slag. The melting process causes a progressive solidification in the casting pool and some chemical refining is also observed due to the contact with a highly basic, superheated slag. The result is a directionally solidified casting, free from shrinkage defects, of very uniform composition, and usually possessing isotropic mechanical properties. A continuous, thin shell of solidified slag on the mould surface also provides for a smooth, defect-free casting finish. Advantages claimed for the product are:

- (i) more reproducible mechanical properties
- (ii) freedom from conventional casting defects
- (iii) properties comparable with forged products.

The range of alloys processed by electroslag is very large, covering low-alloy and carbon steels, stainless steels and nickel-base alloys, tool and die steels, and special alloys such as the Inconels, Nimonics, and Hastelloys.

With such a wide range of applications and the advantages claimed, it is germane to ask why the process is not used more widely. The following study addresses this problem.

Experimental Study of ESC

Mould Systems

The major disadvantage of the ESC process in an economic context is that it involves water-cooled copper moulds which represent a very substantial cost barrier. In order to circumvent this problem a study of alternative mould systems for ESC was conducted.

Water cooling is mandatory if the essential features of the process are to be retained, and a brief study of the heat flows involved indicates that only copper and aluminium are potential mould materials. Since the fabrication and inventory costs make copper unattractive, aluminium was considered to be the only viable alternative. Accordingly, a mould was constructed for an ESC gear casting by cast-to-shape aluminium, as shown in Figure 2. The water-channel positions and dimensions were calculated to give a maximum hot-face temperature of 300°C during the ESC process. The gear face against the mould was covered with a thin layer of slag (Figure 3) and was generally of high quality with respect to surface and internal structure. Following the successful design of a gear mould using water-cooled cast aluminium, a mould for the casting of valve bodies using the same principles was also manufactured (Figure 4).

It is clear from this work that water-cooled aluminium can be used as the ESC mould material: further, that the moulds can themselves be cast, if necessary using a steel object as the pattern. This technique has obvious advantages over formed and welded water-cooled copper, and reduces the mould cost in ESC to an industrially acceptable level.

ESC Installation

A second valid criticism of the existing ESC installations is that the melting furnace itself is very costly. This particular problem was tackled by designing and

building an ESC furnace which had the necessary level of capability to make a 1t casting, but was kept to a minimum cost. The installation is shown in Figure 5 and consists of a 250kVA transformer, the electrode and mould assembly, and a control console. It was designed and erected for a capital cost of about \$25000 and occupies a floor area of 10m². It has a maximum production capability of making a 1000 kg casting every 4 h or can melt, for example, a 200 kg casting every 2 h. It is clear from this exercise that the ESC process need not be a capital-intensive one and is a system suitable for castings where added cost must be kept to a marginal amount.

ESC Properties

One of the remarkable differences between ESC material and conventional castings is the absence of large sulphide inclusions. Figure 6 is a photograph of a sulphur print of the ESC gear showing the very low concentration of sulphides; they are extremely fine and uniformly distributed throughout the cross-section. In direct contrast with this, Figure 7 represents a sulphur print of a conventionally cast gear with its typical network of coarse sulphide inclusions. The ESC gear also possesses good structural integrity, as evidenced by Figure 8, which shows a macroetched section of several teeth. Especially noteworthy is the uniformity of grain size throughout the teeth and the matrix.

In order to verify the reports of excellent mechanical properties in ESC steels, mechanical tests were conducted on gears made using aluminium moulds in SAE 4340 steel. The steel was heat treated to HRC 40 (0.2% YS 1.15GNm⁻²; UTS 1.24GNm⁻²; elongation 16.5%) and tested with respect to fracture and fatigue behaviour. The results of fracture testing are shown in Figure 9, where the ESC results for all three test directions in the casting fall within the same scatter band. The air-melt bar results are those for the longitudinal direction at the bar periphery. It was concluded that the ESC material is isotropic and superior to conventionally rolled, or forged, bar. It has, however, probably the same fracture behaviour as forged material of the same sulphur level.

Bend fatigue tests were carried out on samples taken transverse to the ingot growth direction, with the crack-propagation point placed at the tooth root on the casting surface. The results showed an S-N curve very similar to that observed for conventionally forged SAE 4340, except that the fatigue limit was slightly (10%) higher at the high stress levels. This factor again may possibly be attributed to the low sulphur levels in the ESC material.

In respect of aerospace materials we must observe that there are both potential advantages and disadvantages in applying ESC to high-strength steels. Several studies have been made in the general area of manufacturing electroslog parts in the semi-finished shape condition e.g. hollows for ring rolling or extrusion^{18,19}. In general, the material properties have been found to be highly satisfactory after a relatively modest reduction (e.g. area reductions of 2.5/1) for applications such as landing gear, engine parts and motor casings in steels ranging from 4340, 300M to D6AC. Several examples of studies on these steels are available and show the typical ESR improvements in cleanliness and transverse ductility.

The results of two such tests are shown in Tables 2a and 2b. The acceptability of such steels for landing gear requirements is now established and we must now consider the extent to which the excellent properties seen in the ESR forged product can be retained in the heat-treated casting.

Several studies have been carried out with the above aim as the objective. The results are superficially confusing since on the same steel (4330 Mod.) two authors^{20,21} conclude that the cast structure has²⁰ and has not²¹ the equivalent properties of a forging. In order to reconcile these findings it is necessary to consider the strength level investigated. In the study which concluded that the castings were equivalent to forgings, the strength levels were relatively low (160 ksi Y.S.) and in consequence, the ductility was high (25% elongation). The second study utilized a higher-strength temper series (177-200 ksi Y.S.) with ensuing lower ductilities (16-20% elongation). As a result, in spite of the fact that the cast material passed the requirements of the specification (MIL-T-10458D), there was a significant increase in ductility in the forged material at equivalent high strength levels to the casting. This ductility increase is reflected in superior impact, fracture toughness and crack growth resistance properties in the forgings. We have substantiated these results in our studies and have concluded that in the high-strength lower alloy steels (e.g. 4330-4340 - 300M-D6AC) ESC material does not have as good a fracture behaviour as is observed in forgings made from the same material, probably arising from a grain-size effect.

Notwithstanding the above findings, it is clear that ESC material has a role to play in structural applications. It may not represent the ultimate attainable in properties from a given steel composition, but nevertheless provides mechanical properties which are normally superior to airmelt forgings, in a shape and at a cost which represent significant savings over conventional routes. Since sections, including hollows, have been manufactured in wall-thickness down to approximately 20 mm, the potential field of application is quite wide.

A less-well understood aspect of the ESC product lies in the ability of the process to avoid defect structures arising from random large inclusions, or macrosegregation,

particularly banding. The typical ESC inclusion distribution is represented by Figure 10, where it will be seen that there is a zero probability of finding inclusions greater than approximately 10μ in size. From work carried out on the fatigue behaviour²² of 300M and 4340, it appears that this freedom from large inclusions is probably responsible for the reported increase in fatigue-life at intermediate strength levels, as compared with air-melt forgings. In a similar manner, since the ESC castings are free from banding in these steels, we would expect²³ a similar increase in fatigue life. It is difficult to make a quantitative evaluation of these two factors in the potential use of ESC steel, since they will not always reflect into the property values of individual test samples. However, a sufficiently broad statistical evaluation would probably reveal a smaller scatter in properties for ESC components than for conventional forged material, an observation widely reported already for ESR forged material compared with the equivalent airmelt forgings.

Qualification Problems and Economics

One of the root causes of difficulty in the use of ESC appears to be not in the product quality, but in the product qualification under present Code structures. The ESC products is not a casting in the strict sense, since (a) it has not all been fully liquid at the same time and (b) a number of successive castings are not made from the same bulk liquid heat. On the other hand, it is clearly not a forging made from a well characterized portion of a heat.

If each individual ESC component is to be treated as a separate casting, then the cost of testing (by either non-destructive testing or proof-bar methods) would render the process uneconomic. In order for the technique to be viable, it must fall into a Code category where batch qualification is permitted. The precedent for such a treatment already exists, in that aerospace forgings are made from ingots; here, the quality assurance is based primarily on process reproducibility rather than on exhaustive testing at the ingot stage.

The appropriate qualification scheme for ESC components would be to accept them within either of the present forged or cast component categories, relying on the chemical analysis of the electrode stock as the typical analysis and sampling at various batch sizes for product quality. In addition, the ESC installation, being easily automated, could be qualified with respect to the observance of a standard practice. This system would obviate the need for a special qualification category for ESC with its attendant costs.

Examining the probable process cost, an industrial structure may be constructed, as given in Table 1. From this it may be concluded that the ESC process has an approximate cost of \$0.25/kg above that of a conventional casting at the rough-cast stage. When the cost of dressing a conventional casting is taken into account it is likely that ESC will become cost competitive even without considering the inherent better quality of the ESC product.

Conclusions

From the above study it is concluded that:

1. ESC castings are of a high quality and have mechanical properties equal, or superior, to conventional forgings.
2. ESC castings may be made economically with cast aluminium water-cooled moulds in a simple installation.
3. The probable cost of ESC will be readily offset by the advantages of the process.
4. The major barrier to product acceptance lies in eliminating the unnecessary testing which would be required by a strict adherence to present Codes.
5. If the test-qualification barrier can be overcome, the ESC process is an excellent product method for castings in steels and nickel-base alloys in sizes from 100 to 10000kg, in a quality intermediate between airmelt and remelting forgings.

Acknowledgments

The work was carried out under contract with the Department of National Defence. The authors are grateful to Dr. B.F. Peters of the Defence Research Establishment Pacific (DREP) for his advice during the conduct of the research.

References

1. A. Ujiie, S. Sato, and J. Nagata: 'Electroslag refining', 113; 1973, London, The Iron and Steel Institute.
2. B.E. Paton, B.I. Medovar, G.A. Bojko, and I. Kumish: 'Proc. 4th int. symp. on electroslag remelting processes', 1973, 209; 1973, Tokyo, Iron and Steel Institute of Japan.
3. B.E. Paton, B.I. Medovar, and Yu. V. Latash: 'Proc. 5th int. symp. on electroslag remelting processes', (eds. G.K. Bhat and A. Simkovitch), 239; 1974, Pittsburgh, Pa., Mellon Institute.
4. A. Ujiie: 'Proc. 5th int. symp. on electroslag remelting processes', (eds. G.K. Bhat and A. Simkovitch), 251; 1974, Pittsburgh, Pa., Mellon Institute.

References (Cont'd.)

5. B.E. Paton, B.I. Medovar, and Yu. Emelyaneuko: 'Special electrometallurgy', 169; 1972, Kiev, Naukova Dumka.
6. A. Ujile, S. Sato, and J. Nagata: U.S. patent nos. 3683997; 3853914; 3921699; 3834443; 3835916.
7. B.I. Medovar, B.E. Paton, B.I. Maksimovitch, and G.S. Marinski: U.S. patent nos. 3896878; 3878882; 3892271; 3894574.
8. D.M. Longbottom: U.S. patent no. 3902543.
9. A. Mitchell: Mod. Cast., Nov. 1978, 11, 86.
10. M.P. Braun, S. Kokin, and V.K. Sedunov: Prob. Spec. Electrometall., 1975, 2, 42.
11. B.E. Paton, B.I. Medovar, and G.I. Boiko: Fonderie, 1976, 29, 435.
12. E.F. Dobrovskaya, A.A. Plakhutina, and I.A. Mostovoi: Vestn.Mashinostr., 1975, 4, 62.
13. B.I. Medovar: Prob. Spec. Electrometall., 1975, 2, 15.
14. National Materials Advisory Board: 'Electroslag remelting and plasmarc melting', NMAB Publ. 324, 1975, Washington, D.C., National Academy of Sciences.
15. B.I. Medovar, Yu. V. Latash, B.I. Maksimovitch, and L.M. Stupak: 'Electroslag remelting', JPRS Rep. 2217; 1963, Washington D.C., JPRS.
16. Yu. V. Latash and B.I. Medovar: 'Electroslag remelting', NTIS Translation AD730371; 1971, Springfield, Va. U.S. Department of Commerce.
17. B.E. Paton (ed.): 'Electroslag remelting', JPRS Rep. 63220; 1974, Washington, D.C., JPRS.
18. H.J. Klein: J.Vac. Sci. Technol., 1972, 9(b), 1334-1339.
19. L.S. Licht: Proc. ESR Seminar, ASM (Los Angeles Chapt.) Dec. 11, 1979.
20. M. Kadosé et al: Intl. Report, Katsuta Works, Hitachi Ltd., Japan, 1976.
21. H.J. Klein et al: Proc. 5th Intl. Conf. on Vac. Met. & ESR, Munich, 1976, p. 167.
22. M. Wells, J.J. Hauser, I. Perlmutter: Mater/Metalwork Technol. Ser. 1974, 3, 199-224.
23. G. Haour, M. Kornmann: Mem. Stud. Sci. Rev. Metall, 1980, 77, 955-963.

TABLE 1
ECONOMICS OF ESC

Item	Unit	Unit Cost	Cost of ESC casting, \$/kg	
Electrode	500kg	\$0.05/kg	0.05	
Slag	20kg	\$0.5/kg	0.02	
Power	500kWh	\$0.03/kWh	0.03	
				0.10
Manpower and maintenance	5 man h	\$10/man h	0.10	
				0.10
Mould	150%/year	\$2000/mound	0.01	
Furnace	50%/year	\$25000	0.02	
				0.03
				Total Cost 0.23

TABLE 2a

ESR AISI 4340 Data

Jernkontoret (J-K) Microcleanliness Rating -
ASTM E45 Method A

	<u>T</u>	<u>A</u>	<u>H</u>	<u>T</u>	<u>B</u>	<u>H</u>	<u>T</u>	<u>C</u>	<u>H</u>	<u>T</u>	<u>D</u>	<u>H</u>	
Electrode	2.0	1.0	1.0	1.0	1.0	-	-	-	1.5	1.0	.0018"		
ESR Ingot Top	1.5	1.0	1.5	-	-	-	-	1.5	-	-			
ESR Ingot Bottom	1.0	1.0	1.0	-	-	-	-	1.0	-	-			

Chemistry

	<u>C</u>	<u>Mn</u>	<u>S</u>	<u>P</u>	<u>Si</u>	<u>Cr</u>	<u>Ni</u>	<u>Mo</u>
Electrode (Ladle)	.41	.79	.013	.015	.28	.82	1.83	.24
ESR Ingot Top	.40	.78	.003	.014	.21	.82	1.83	.25
ESR Ingot Bottom	.40	.82	.003	.014	.19	.82	1.81	.25

4340 Transverse Tensile Properties
Forged 5 x 5's Normalized at 1650°F for 1 Hour
Austenitized at 1525°F for 1 Hour
Oil Quenched and Tempered for 4 Hours

		Transverse Ultimate Tensile (PSI)	Transverse Yield Strength (PSI)	Transverse Reduction in Area (%)
4340 VP 10 Heat Average		264,900	220,700	19.8
4340 ESR 400°F Temper	T1	273,900	218,700	34.1
	T2	270,700	208,500	34.0
	X1	269,900	210,800	39.2
	X2	272,900	212,600	36.0
	Avg.	271,800	212,600	35.8
4340 ESR 450°F Temper	T1	254,500	224,500	33.1
	T2	254,500	222,500	31.1
	X1	250,500	221,900	42.4
	X2	252,500	223,600	41.5
	Avg.	253,000	223,100	37.0

4340 Transverse vs. Longitudinal
Tensile Properties
Forged 5 x 5's Normalized at 1650°F for 1 Hour
Austenitized at 1525°F for 1 Hour
Oil Quenched and Tempered at 400°F for 4 Hours

	Ultimate Tensile (PSI)	Yield Strength (PSI)	Reduction in Area (%)	Charpy Impact Strength at -40°F (ft.-lbs.)
4340 Electrode Transverse	274,800	223,000	22.5	7
4340 Electrode Longitudinal	274,100	221,000	43.6	11
4340 ESR Transverse	271,800	212,600	35.8	11
4340 ESR Longitudinal	273,300	212,400	48.0	11

TABLE 2b

SPECIFIED AND ACTUAL ESR INGOT
MECHANICAL PROPERTIES IN 300M STEEL

	Ys. Proof N/mm ²	0.2% Stress (ksi)	Tensile N/mm ²	Strength (ksi)	Elongation %	R. of A. %
Min. Specified Transverse	1550	(225)	1900-2100	(275-305)	5	20
Min. Specified	1550	(225)	1900-2100	(275-305)	8	20
ESR Ingot Transverse	1664	(241)	1952	(283)	8	38.1
ESR Ingot Longitudinal	1644	(238)	1937	(281)	11	45.2

FRACTURE TOUGHNESS VALUES DETERMINED
IN ESR 300M STEEL

Test Piece Orientation	Fracture Toughness K _{IC}	
	MNm ^{-3/2}	ksi √in
Longitudinal (XY)	57.3	52.2
	51.9 (Av.)	47.3 (Av.)
	52.4 (54.6)	47.7 (49.8)
	56.9	51.8
Transverse (ZX)	49.0	44.6
	52.7 (Av.)	48.0 (Av.)
	54.4 (52.5)	49.5 (47.8)
	54.0	49.2

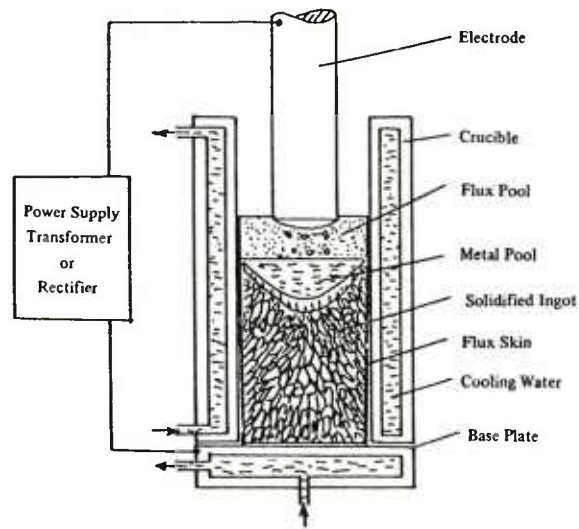


Figure 1: ESC Schematic

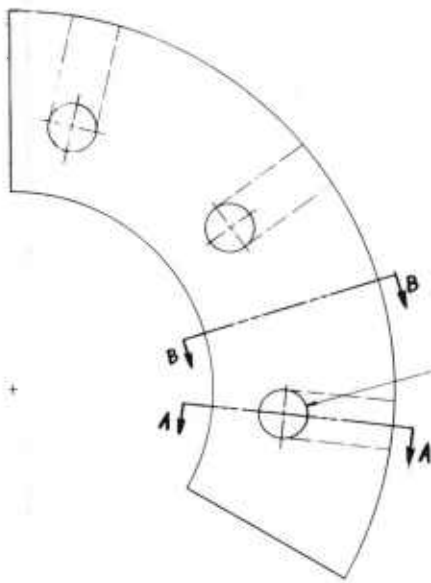


Figure 2: Mold section showing coolant channel.

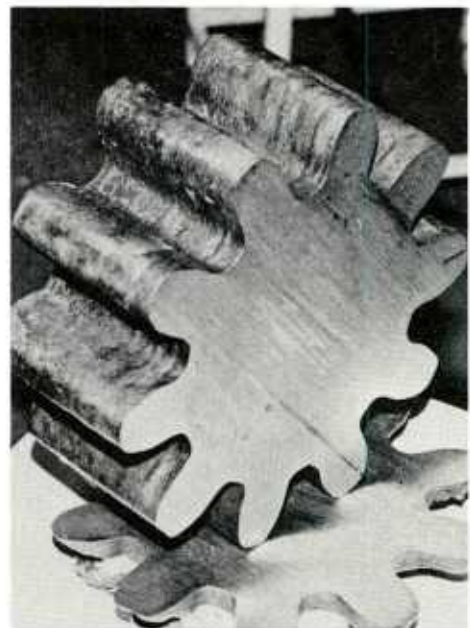


Figure 3: Section of ESC gear casting (200 mm dia.)

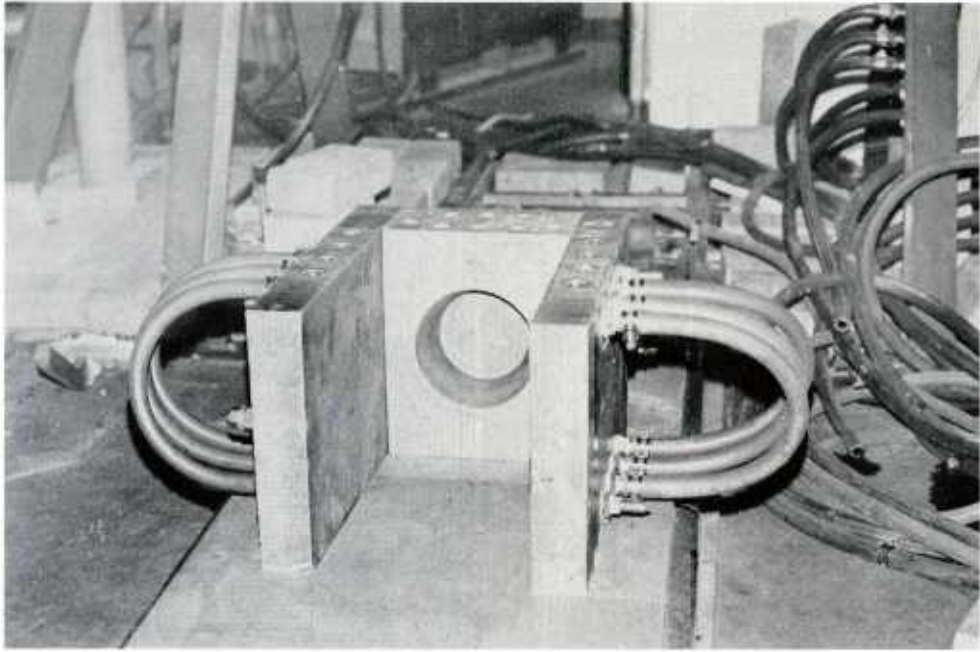


Figure 4: ESC valve mold.

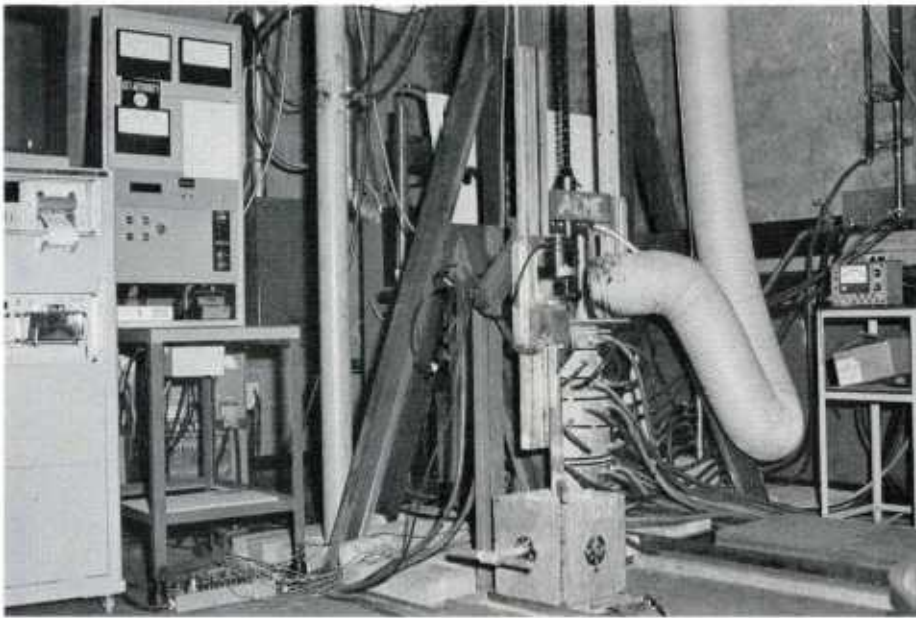


Figure 5: ESC furnace.

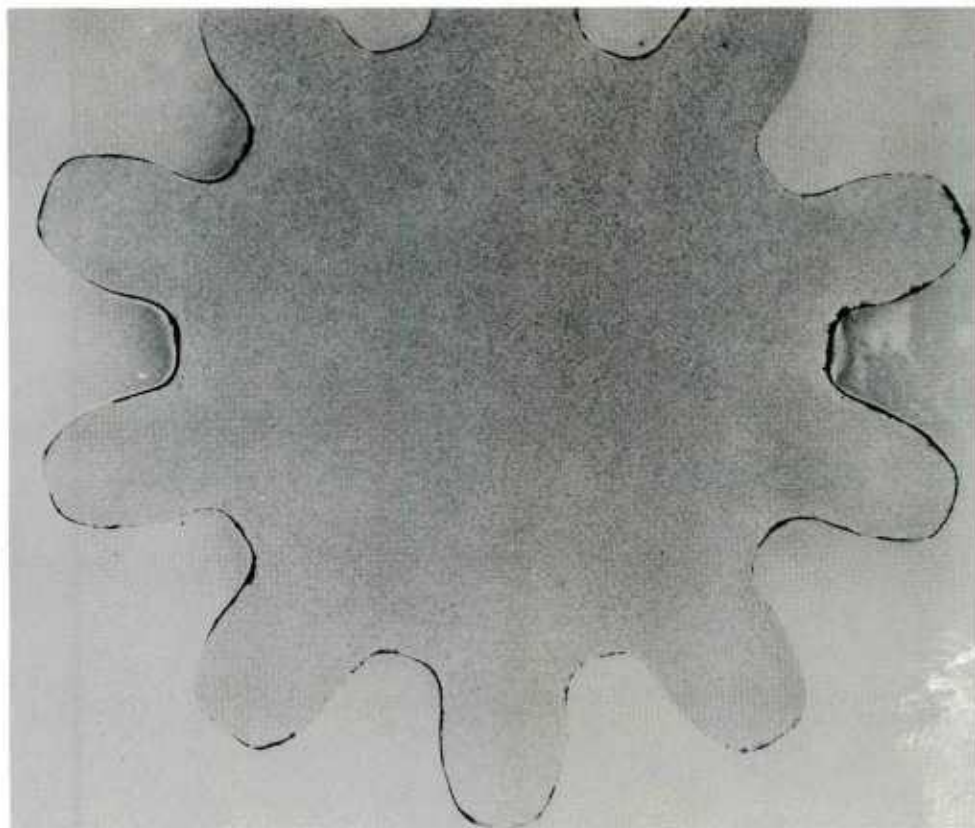


Figure 6: ESC gear, sulphur print (x 1/2).

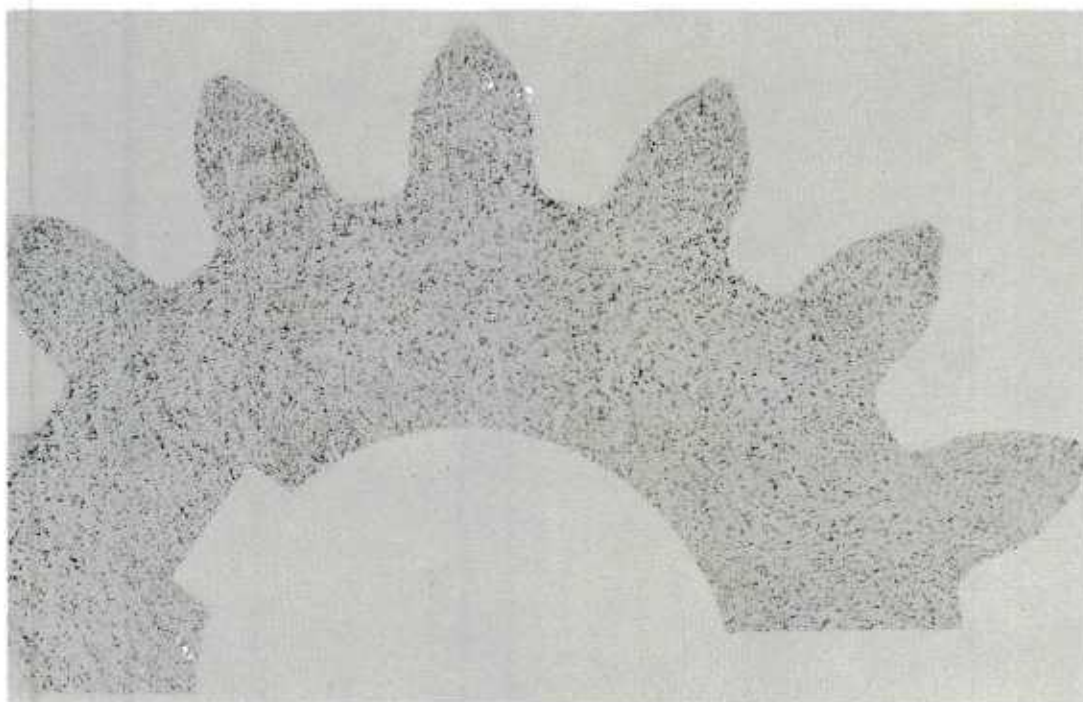


Figure 7: Conventional gear, sulphur print (x 1/2).

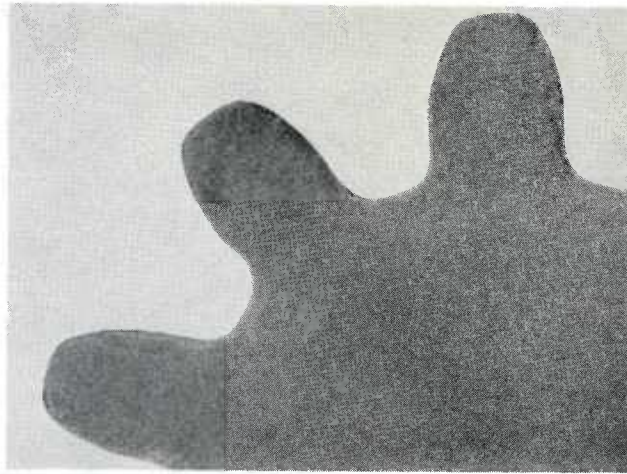


Figure 8: ESC gear, macroetch (x 1/2).

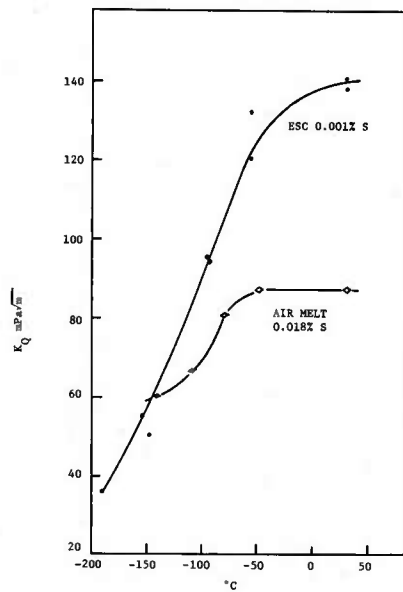


Figure 9: ESC properties, SAE4340 at 40R_c.

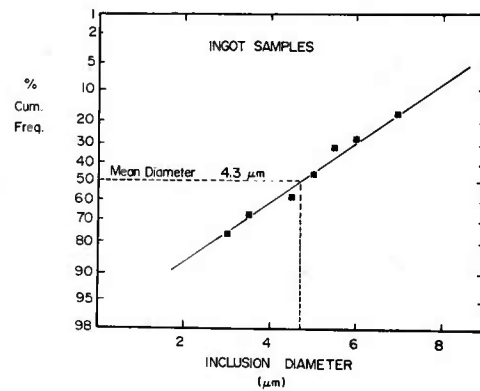


Figure 10: Inclusion distribution, SAE4340 200 mm dia. gear.

SESSION III

DISCUSSION SUMMARY

by

Prof. D. Apelian
(Drexel University)

The *first* paper of Session III titled: "An Evaluation of Vacuum Centrifuged Titanium Castings for Helicopter Components" was presented by L.J. Maidment of Helicopter & Transport Division of Messerschmitt-Bölkow-Blohm of Munich. Questions were raised regarding various aspects of cast versus forged rotorheads.

Finch of British Aerospace raised the question of the geometrical freedom that one enjoys with castings versus machined or forged components where the part geometry must be seriously considered. Mr Maidment answered that the bottom line is really not only technical feasibility but rather technical and *economical* feasibility. For example, Mr Maidment cited that helicopter blade attachments have been considered to be cast; however it has been shown that there is no economic advantage to the casting route. Schutz of IGB clarified that in this work the forgings were not shot peened whereas the castings evaluated were shot peened. Hyde of Westland Helicopters brought to our attention that the manner in which the castings discussed in this paper were processed is significantly different than that presently done in the trade; namely that the castings were not HIPed. Maidment defended his position via two points: (i) HIPing is expensive and if utilized, then cast rotorheads would have been more expensive than the forged rotorheads; (ii) that surface shrinkage pores would not have been affected by HIPing. Finally Mr Hyde commented that "today" all titanium foundries utilize HIPing because in the long run it is cheaper. Duckworth of British Aerospace suggested that ingot make-up and the character of the initial charge in such comparative studies is of paramount importance and should have been accounted for.

The *second* paper of the session was titled "Grain Refinement of Cast Metal-Based Superalloy and its Effect on Properties" and was delivered by Prof. Jack Wallace of Case Western Reserve University, Cleveland, Ohio.

Campbell of Cosworth commented that the results of this work are interesting and truthfully quite surprising. He further stated that "the alloy technologist spends years developing the alloy system and now the solidification technologist comes around and dumps a whole lot of muckings to the melt and expects good mechanical properties!" Campbell raised the issue whether other grain refining methods based on dendrite fragmentation were investigated. Wallace answered that in this work other methods of grain refining such as vibrating the mold and the use of ultrasonics were not carried out, but based on his experience he was concerned that investment molds would not hold up to vibratory manipulation. Wallace agreed with Campbell that with nickel based alloys being an fcc structure one has to be careful; if the optimum is not carried out one can seriously damage properties. Williams of GKN Sancey brought up the issue of grain refining control solely via superheat manipulation thus alleviating the need of grain refining additions. Wallace responded that composition is a key factor here; if the alloy has carbides and borides already present then superheat control alone (that is minimize superheat) will be adequate for grain refining. David Ford of Rolls Royce raised concerns of having boron additions to the melt for grain refining purposes since boron causes incipient melting and also forms embrittling phase which would cause (i) poor high temperature properties, (ii) poor impact properties, and (iii) that the casting would be unHIPable due to the incipient melting point. Wallace responded by saying that HIPing is a crutch for making sound castings and that the ultimate is to make a casting where none of these post casting treatments would be needed. Wallace did agree with Ford that boron additions could be damaging and that one has to be careful; he also confirmed that in the work reported here impact properties were not evaluated.

The *third* paper of the session titled: "Cast Titanium Components for Rotating Gas Turbine Applications" was delivered by Bruce Ewing of Detroit Diesel Allison of Indianapolis, USA. Duckworth of British Aerospace clarified that in Figure seven cast properties are compared to STOA conditions because the forgings were aged. Duckworth asked whether weld repair by the manufacturer is allowed and Ewing confirmed that it was and that the treatment recommended after the closure welds is to stress relief at 1300°F.

The *fourth* paper was titled: "Development of Precision Cast Rotating Parts in Small Turbine Engines" and was presented by Mr Brun of Turbomeca of France. Apelian asked whether any electron beam melting techniques were employed to assess the metal's quality and to evaluate the inclusion character. Brun responded in an affirmative but no details of the inclusion assessment were given.

The *fifth* paper titled "Electroslag Casting Evaluation" was presented by Prof. Alec Mitchell of University of British Columbia, Vancouver, Canada.

Wallace asked as to what are the dimensional limitations of the electroslag remelt process for valves. Mitchell responded by commenting that the limitations of the process are imposed by the progressive nature of the process — i.e., one cannot go from a thick section to a thin section and then back to a thick and so forth simply because of the physical length of the electrode needed, thus there are some limits to section changes. The second limit is imposed by the relative thickness of the electrode and casting section, that is one cannot make thin sections; however three dimensional shapes is not a problem. Mitchell emphasized that in electroslag casting one enjoys precision of mold filling and that the resultant shrinkage is small. Prof. Mitchell reported that 8–10" section valves with 20 thousands of an inch of the designed specs have been made. Duckworth of British Aerospace asked whether precipitation hardening of stainless steels can be made via electroslag technology. Mitchell responded that this poses no problems and that the only limitations to keep in mind is that the product is a casting. If the material's strengthening was designed to be achieved via mechanical working (such as in forgings), then obviously the electroslag process will be deficient in rendering the design property specs. If, however, strengthening is based on alloying, then there is no reason why electroslag technology will not produce a sound product. In addition, fatigue tests on the 4340 gears show that the cast properties are comparable to the forged properties. Duckworth asked whether production facilities exist at the present, and Mitchell answered that there are 2–3 groups (in North America) which are seriously planning to go to production with the process. Lastly, Mitchell commented that in his own laboratory (at the University of British Columbia) he can cast up to 1 ton size steel castings. Dr Ed Wright asked whether any interest has been shown by the gear industry. Mitchell confirmed that one of the first applications is going to be a drive gear for a large ring and that this technology is applicable for helical and bevel gears as well. Mr Bright of the Royal Air Force asked whether the material produced via electroslag technology is different than forged material in terms of stress corrosion sensitivity. Mitchell answered that he would not expect differences in stress corrosion sensitivity.

Finally, John Lee, Deputy Chief Engineer of Westland Helicopters Ltd discussed cast Ti 6AR-4V helicopter stores carriers. Lee reported that a titanium casting has been successfully used in the manufacture of a helicopter stores carrier, which is a stressed class 1 component. The casting is electron beam welded to a wrought titanium component to make the complete assembly.

The main features are:

Suppliers	Dual sourced — USA and Europe
Mould	Rammed graphite
Post Casting Treatment	HIP
Radiographic Standard	ASTM E192 to Table 1
Weight as Cast	21 Kg
Weight Machined	12 Kg (handed item made from 2 handed casting)
Finished Welded Assy.	17 Kg

Initially both foundries experienced considerable difficulties in attaining the required quality — one primarily for dimensions and one primarily for radiographic standard. The problems were such that the part was redesigned in steel (at a weight penalty), but before this started in production both foundries resolved the quality problems, which was helped by the introduction of H.I.P.

Initially the conical part of the assembly was also designed as a casting, but after reassessment it became cheaper to fabricate the cone from two parts machined from bar and E.B. welded together.

The introduction of HIP was found necessary to reduce the extent of weld repair necessary to meet the radiographic standard of acceptance.

Table 2 gives the results of production control tests from integrally cast test pieces and casting cut up tests.

TABLE 1

Radiographic Acceptance Standard

	Acceptance $\frac{1}{8}$ "	Standard $\frac{3}{8}$ "	ASTM E192 $\frac{3}{4}$ "
Gas Holes	5	5	5
Inclusions More Dense	4	4	4
Inclusions Less Dense	5	6	6
Shrinkage Cavity	Nil	2	3
Shrinkage Spongey	5	4	5
Shrinkage Dendritic	4	4	4
Shrinkage Filamentary	Nil	Nil	2
Cracks, Cold Shuts		None Allowed	

TABLE 2

Mechanical Properties

Analysis of Cast Test Bars and Cut Up Results

Specification Requirement of WHMS 422

Integrally Cast Test Bar 900hb KTS 815 0.2% Pr.Str. 5% F1 10% RoFA
Casting Cut Up 880hb KTS 785 0.2% Pr.Str. 5% F1 10% RoFA

			Population of Results (N)	Mean (\bar{x})	Standard Error of Mean of Population (E_1)
Supplier A	Not Hipped	UTS MPa	58	977.103	7.077
		0.2% Proof Stress	58	895.017	6.286
		Elong %	58	6.811	0.205
		Reduct. in Area %	58	13.126	0.683
	Hipped	UTS MPa	89	1017.236	3.683
		0.2% Proof Stress	89	912	2.913
		Elong. %	89	7.673	0.227
		Reduct. in Area %	89	15.530	0.477
Supplier B	Not Hipped	UTS MPa	166	984.265	2.73
		0.2% Proof Stress	166	907.633	2.807
		Elong %	166	7.125	0.125
		Reduct. in Area%	166	14.355	0.262
	Hipped	UTS MPa	71	939.873	2.645
		0.2% Proof Stress	71	838.141	2.751
		Elong %	71	8.723	0.230
		Reduct. in Area %	71	17.079	0.456
Complete Integrated Results of Both Suppliers	Not Hipped	UTS MPa	224	982.411	2.719
		0.2% Proof Stress	224	904.366	2.652
		Elong %	224	7.044	0.107
		Reduct. in Area %	224	14.037	0.263
	Hipped	UTS MPa	160	982.906	3.855
		0.2% Proof Stress	160	879.225	3.548
		Elong %	160	8.138	0.167
		Reduct. in Area %	160	16.218	0.337

A newly developed Process (The GKN+Cosworth Process)
for the
Production of High Integrity Aluminium Alloy Castings.

by

J Campbell, Technical Director, Cosworth Research & Development Ltd, Hylton Road
Worcester, UK.

and

P S A Wilkins, Project Engineer, GKN Contractors Ltd, Ipsley Church Lane, Redditch, UK.

Summary

The process is a high precision, low pressure sand casting technique. It is characterised by an improvement in accuracy over conventional sand castings by a factor of 4 or 5 in external features, and by a factor of approximately 20 times in internally cored features. Very high integrity and good surface finish are routinely obtained in production. The successful application of the process to certain military vehicle and aerospace products is described.

Introduction

In the past designers have tended to discriminate against the use of castings because of one major problem: lack of reliability. This has compounded the disadvantage already suffered by the casting because a larger safety margin has therefore historically been necessary, eroding the weight saving that could otherwise be designed into the component.

The lack of reliability has been commonly experienced in many aspects of the product, including porosity from shrinkage or gas, leading to poor strength or leakage in areas required to be pressure-tight. Other major variabilities include dimensional problems of casting size, distortion, or misplaced cores.

Cosworth have, therefore, developed a substantially new concept for the production of castings. It is an integrated approach designed to eliminate the problems at root source, or to enable them to be controlled within close limits. It has proven during its first few years in operation that it is indeed capable of producing castings of remarkable accuracy and soundness, and is capable of turning out such castings economically, repeatably and reliably, with the minimum of skilled personnel.

The Process

Metal is melted electrically to maximise control, and minimise gas pick-up. It is transferred and held in a large holding furnace where oxides and other non-metallic content can float or sink. Thus nuclei for porosity initiation in the castings are reduced to a minimum. No further nuclei are introduced during casting since this is carried out by pumping the metal uphill, into the mould from underneath.

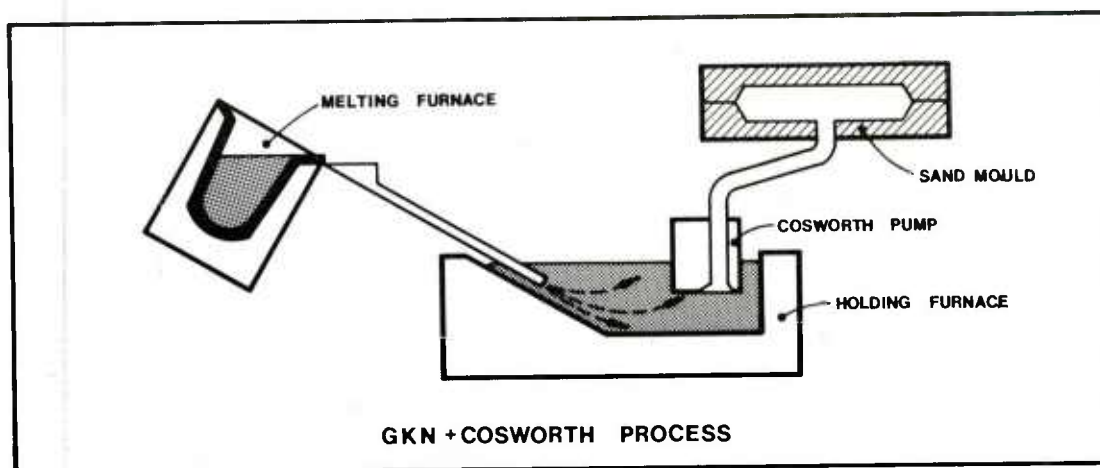


Fig. 1.

Experience has shown that the attainment of turbulence-free filling of moulds is far from easy, and generally not possible with current transfer mechanisms and pumps. Although excellent results have been obtained to date, improvements to the transfer and pumping system are being developed which are expected to yield further breakthroughs in enhanced soundness and strength.

The accuracy of the mould and core assembly is obtained by the use of a room temperature gas hardening process (the SO_2 process) so that the sand shapes are hardened in contact with the pattern prior to stripping. Thermal distortions on dies as in gravity die casting or patternwork as in shell casting, or waxes as in investment casting are thereby eliminated. Also resin tooling can be used, which is relatively quick to make and is often less than half the price of metal tooling.

The accuracy of the casting would still be relatively poor if silica sand were to be used since expansions of up to 1 or 1.5% are to be expected when filling the mould with liquid metal at 700 °C. A low expansion sand is therefore employed. This sand also has a high thermal capacity, correspondingly reducing the temperature which it attains and hence limiting distortion problems to less than 0.05%. Thus, in casting lengths of up to 500 mm, absolute accuracies of better than ± 0.25 mm can be guaranteed and repeatability of ± 0.10 mm can be expected. Dimensions within 200 mm are expected to be repeatable within ± 0.050 mm. Wall thicknesses, defined between an internal core and a mould wall, which are commonly in error by several millimetres in conventional silica sand castings can normally be held to within ± 0.10 mm in a Cosworth casting.

Surface finishes are good compared to conventional sand although, of course, they cannot yet match that of investment castings.

Section thicknesses of 2.4 mm have been produced in castings of overall dimensions up to 200 mm. The limitation here is one of fluidity in cold, high heat capacity moulds. Developments are planned to evaluate how far the thin wall limitation can be extended. Naturally, it is expected that the normal aerospace premium casting expedient of planting ingate/feeders up a vertical thin wall and connected by a slot gate would be equally applicable to the process. Such a move has, so far, been avoided because of the considerable fall in casting yield and the increase in hand finishing which would be necessary. Both these are additional costs.

Examples of castings produced by the Process

Figures 2 - 5 show examples of castings for the military vehicle market. The gearbox casting (figure 3), in particular, is required to be completely free from microporosity in the piston bores. The bores are set in heavy sections up to 40 mm thickness which makes this requirement impossible to meet in the conventional sand casting, despite heavy and extensive chilling. It is met here with only moderate chilling to improve feeding. No feeders were used on the casting. Only six ingates were used as can be seen. Practically no hand work is required elsewhere on the casting.

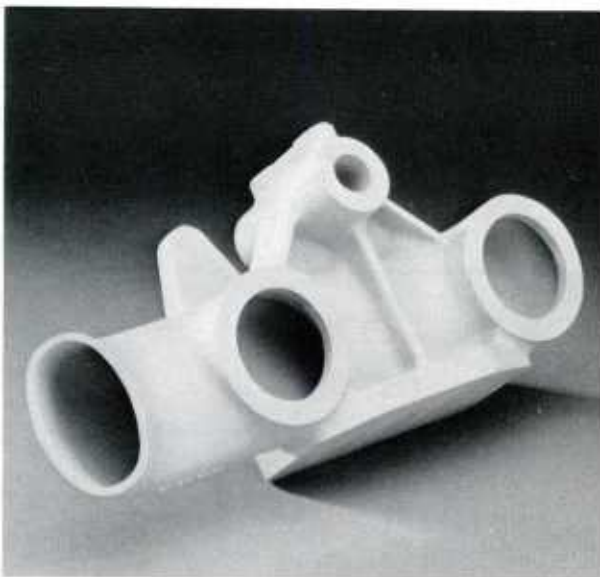


Fig.2. STEERING CONTROL BRACKET



Fig.3. FRONT GEARBOX CASING

The air intake for the Rolls Royce GEM engine is seen in Figure 4. The opportunity was taken to widen the air intake duct up to the limit of the drawing tolerances, by taking advantage of the greater potential accuracy of the process, thus assisting the attainment of maximum performance from the engine. The ingates are concentrated only on the bottom flange of the casting (Figure 5) and no feeders are used elsewhere. Thus again the casting requires minimal hand finishing and so retains its highly repeatable accuracy.

The inhouse chemical specification, corresponding closely to L99 or 357 alloy, is

Element	Si	Mg	Fe	Mn	Cu	Ni	Zn	Pb	Su	Ti
Specification	6.5-7.5	0.45-0.60	0.20	0.10	0.10	0.10	0.10	0.05	0.05	0.20
Typical	7.0	0.54	0.12	0.01	0.01	0.01	0.01	0.00	0.01	0.12

Properties in this casting are required to meet

Ultimate Tensile Strength (UTS)	300 MPa
0.2 % proof stress	240 MPa
Elongation	2.5 %

Over a comparatively short development period of about 6 months, the properties in the bottom flange now routinely achieve

Ultimate Tensile Strength (UTS)	312 MPa
0.2 % proof stress	242 MPa
Elongation	9.8 %

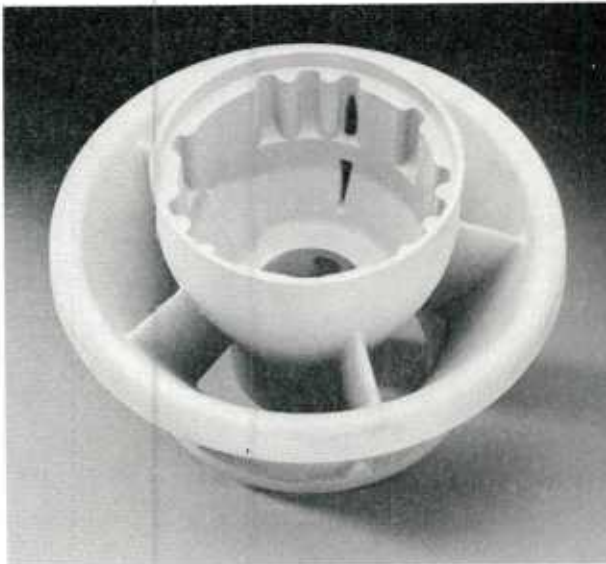


Fig.4. RR GEM AIR INTAKE
(FRONT VIEW)

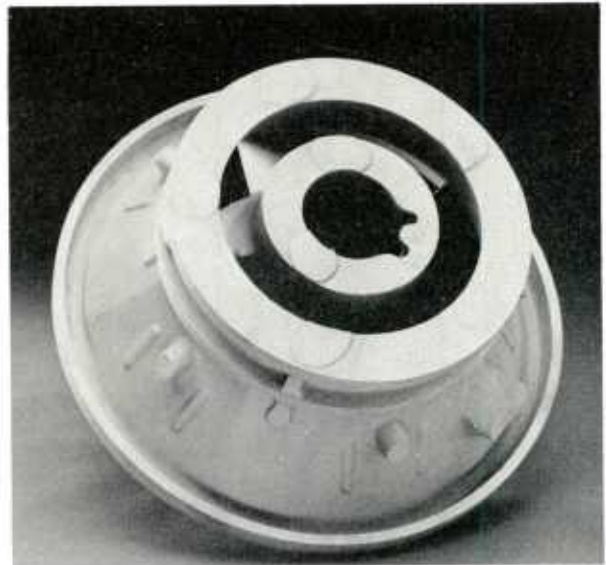


Fig.5. RR GEM AIR INTAKE
(REAR VIEW)

Further engineering improvements to the plant are expected to improve the overall properties within the casting yet further. These castings are routinely produced without any detectable porosity on Xray. In fact the only defect now occasionally seen on an Xray radiograph are isolated minute oxide particles, of maximum size up to approximately 1 mm. Otherwise, most radiographs are routinely absolutely clear.

The Future

It is believed that the benefits of a low turbulence, high accuracy process have been demonstrated to yield castings which are of high soundness, strength and accuracy, and which are closely reproducible in production.

The process is being developed to eliminate turbulence entirely and further benefits to the integrity of isolated bosses and other non-fed areas of castings are expected.

Also, so far, all the achievements to date have been made without the undoubted benefits

of the modification of the silicon eutectic by such elements as sodium or strontium. The same engineering improvements which are designed to reduce turbulence should also enable such additions to be made, with additional benefits to strength and elongation properties. Again, the above properties are achieved despite the use of a polymer quenchant to minimise distortion, and 10% higher properties would be expected with water quenching.

Written Contribution from DR J.CAMPBELL, Cosworth R&D Limited

To clarify an issue which has been repeatedly referred to in the Conference, it is worth defining the important differences between grain size, dendrite arm spacing (DAS) and cell size.

As is well known, a grain is synonymous with a crystal. Thus a raft of parallel dendrites, which might have nucleated and grown from a single source (even though this is often not apparent on a polished planar section) will grow to join together to form a single crystal. The original interdendritic boundaries will ideally be crystallographically invisible, although often, as a result of slight mechanical damage to the raft, will form low angle grain boundaries. As mechanical damage increases, the component parts of the raft will progressively assume the character of separate grains, separated by normal high angle grain boundaries.

The grain size can be controlled by the introduction of heterogeneous nuclei such as titanium and zirconium rich additions to aluminium base alloys, or can be reduced by mechanical fragmentation of the dendrite raft, and possibly of dendrite arms from the main dendrite stem.

It seems, however, that grain refinement by either mechanism will produce only limited benefits in mechanical properties of aluminium alloys (in contrast to other metals such as magnesium where the effect is of primary importance). At the same time the theoretical equations of fluidity¹ can be shown to predict a reduction in fluidity by a factor of 2, principally as a consequence of the reduction in time required to solidify to about 50% solid fraction at the flow tip, at which flow stops, compared to 100% solidification at the entrance of the liquid metal as required in planar front solidification. This reduction in fluidity is experienced by foundrymen. Furthermore, the grain refined material is difficult to feed in sections of intermediate thickness because of the preferential generation of surface-initiated porosity².

Thus the desirability of grain refinement is questionable. The author's foundry is routinely producing high strength 357 alloy with good ductility without resorting to grain refinement.

The reduction of dendrite arm spacing is, however, of undoubted benefit to mechanical properties and the response to heat treatment. For a given alloy, solidifying without undue disturbance, DAS is controlled *only* by local solidification time (or the freezing rate). Perversely, it seems that mechanical efforts to reduce the grain size normally coarsen the DAS³. The good results reported by Cercast for their rotor hubs are therefore all the more surprising.

The silver-containing 201 alloy has a compact, rather irregular dendrite structure, in which the dendrites resemble rosettes (Paper 19-7). These are probably individual grains (although to be certain this would require to be demonstrated by etching, anodic oxidation or other careful metallographic technique). In this case the DAS is not much smaller than the grain size and is not easy to measure separately (it is easy for systems with long straight dendrites where many arms can be counted in a row).

In this system therefore it is convenient to agree to abandon the conventional (and accurate) definitions of grain size and DAS, and use the concept of cell size. This is simply defined in terms of the number of intercepts (irrespective of whether they are grain boundaries or dendrite arm boundaries) measured on a straight line placed at random on the photomicrograph.

This use of the term cell, although useful in this context, is unfortunate in the general context of solidification where it already has two uses:

- (i) It describes a growth mode intermediate between planar and dendritic solidification. It is often observed in the solidification behaviour of nearly planar form. It would be expected to be observable in the eutectic front which in turn follows up the dendrite front in 357 alloys. The intercellular boundaries would constitute deep recesses in this otherwise planar front, and represent the regions where the iron-rich phases would segregate. Methods to control the distribution of these deleterious phases can be based on control of this detailed morphology of the eutectic front.
- (ii) It is used to describe features of cast iron morphology which are volumes containing graphite flakes which appear to have grown from a central nucleus. This region would be better described as a eutectic grain.

To summarise therefore:

- (i) Grain size and/or grain refinement of castings should not be specified by the casting purchaser at this stage. The desirability of grain refinement requires further development and clarification.
- (ii) Dendrite arm spacing (DAS) appears to be a useful parameter for the characterisation of casting quality. In the case of 201 type alloys the use of the concept of cell size (total intercepts on a linear traverse) seems useful, being probably a good approximation to the effective DAS of this system.

1. M.C.Flemings — *Fluidity of Metals*, 30th International Foundry Congress, Prague 1963, pp.61-81.

2. J.Campbell – *The Origin of Porosity in Long Freezing Range Alloys*, British Foundryman, 1969, 62 (4), 147-158.
Feeding Mechanisms in Castings, Cast Metals Res. J, 1969, 5 (1), 1-8.
3. J.Campbell – *Review of the Effects of Vibration During Solidification*, Int. Metall. Rev, 1981, 26 (2), 71-108.

Quality Assurance in Titanium and Aluminium Investment castings

Dr. Christian Liesner - Managing Director - Titan-Aluminium-Feinguss GmbH, 5780 Bestwig

Permanently rising requirements of higher quality of investment casting products as well as new laws with intensified manufacturing liability of producer give the problem of quality assurance an ever increasing importance. Today the presence of an efficient quality assurance system is the basic requirement for approval as supplier for the aircraft and aerospace industry. The integration of the quality assurance department into the company organization as well as its responsibility, jurisdiction and competence are defined in a quality assurance manual. An essential precondition for an efficient quality assurance system is a smooth flow of information between the production areas and quality control department concerned. The main task is to prevent faults accuring, not to investigate or repair faults already in existance. The cost of high quality has to be minimized its purpose or effectivness to be maximized.

Permanently rising demands for higher quality of products as well as new laws with an intensified manufacturing liability give the problem of quality assurance an ever-increasing importance.

The following definition of "Quality" corresponds to the EOQC (European Organisation of Quality Control) and is standardized: "Quality is the accumulation of properties and characteristics of a product which refer to its suitability to comply with stated requirements". It is not possible to inspect quality into a product, quality must be designed into a product. Quality is not an individual property but is the totality of properties which fulfill stated specifications. We find the term: "Fitness for use" in American standards.

As a rule quality only becomes the subject of discussions after a defect has arisen. inspection and testing, the so-called "identification of defects" is no longer sufficient. The decisive approach is prevention of defects. Quality assurance thus seen is for the customer a high guarantee for the quality of the product before purchase. For the manufacturer it means a reduction in risks with extensive economic consequences such as availability, rejection rate and technical life span. This is a manifold and difficult task for the quality assurance.

The development of standards for requirements of quality assurance systems began with MIL-Q-9858 in the USA in 1963, which is known as AQAP/Nato-standard of Bundesamt für Wehrtechnik und Beschaffung (Federal Defence and Procurement Bureau).

Today the presence of an efficient quality assurance system is the basic requirement for approval as supplier for the aircraft and aerospace industries. An independent department quite separate from other production departments must be commissioned to carry out the task of quality assurance. The integration of the quality assurance department into the company organization, as well as its responsibility, jurisdiction and competence are defined in a quality assurance manual.

An essential precondition for an efficient quality assurance system is a smooth flow of information between the production area and quality control department concerned. Without a smoothly functioning information system it is not possible to detect deficiencies at the particular stages of quality assurance which in the last analysis may lead to the failure of the whole system.

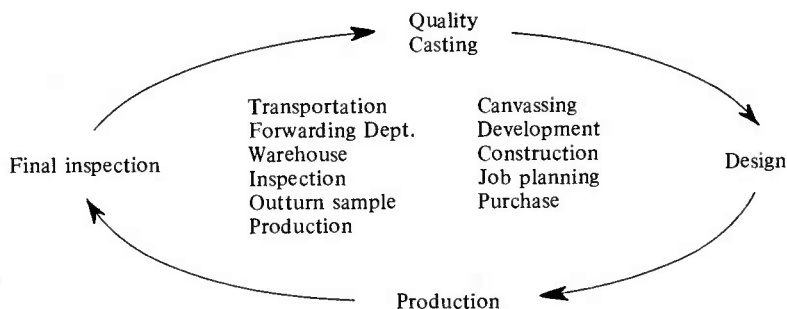


(Fig. 1)

It is possible to show the particular stages of quality assurance in a quality assurance cycle (Fig. 1). The quality of a product depends on design, production and final inspection. Measures which affect quality gear into each other, since the results obtained at each stage of the quality cycle are interdependant. At the centre of the cycle are listed some important levels on demand of the product.

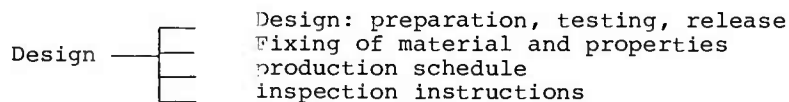
Obviously all quality assurance measures are not necessary in every case, or in their entirety. In order to comply with the requirements of quality and safety of technical products, while giving economic aspects due consideration, every aluminium or titanium investment casting is classified in a safety category, and its quality-degree fixed in

line with the regulation in force for aircraft components (e.g. the regulations of the Bundesamt für Wehrtechnik und Beschaffung). This is the responsibility of the designer in consultation with other related departments (e.g. statics, materials). Safety-Class and quality grade must be shown on the inspection standard, raw casting drawing, inspection report of outturn sample and certificate of conformity.

For a better understanding of the function of our quality assurance system we shall explain the procedure involved for some typical castings.

Fig. 2 shows a titanium casting in alloy TiAl6V4, an alloy which is generally used in the construction of modern aircraft. It is a casting belonging to safety class I, which means that a failure of this casting could mean the crash of the plane and with loss of life.

Fig. 3 shows schematically the phases involved in the design of a titanium casting:



Design:

At the design stage there must be close co-operation between aircraft builder and the casting manufacturer since here the essential characteristics of quality assurance are discussed and established. So a designer is able to make early use of the experiences of the casting manufacturer in order to achieve the best possible design which also takes the attributes of the casting into account.

Production schedule:

After final establishment of design material and material properties, which all serve the purpose of quality improvement or quality assurance, an internal production schedule is drawn up, which defines the production process under consideration of the necessary quality tests, in a way which is readily understandable and repeatable at any time.

Inspection instruction:

Finally after release of drawing and examination of all requirements regarding production, material, heat treatment and special treatments, test instruction is drawn up in which are stated all details of final tests which must be carried out on the finished casting, e.g. extend of inspection as well as the kind, number and position of planned trials.

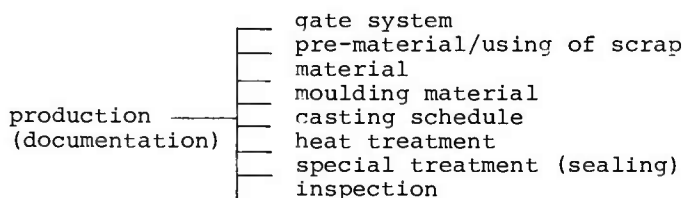
Fig. 4 shows a sketch of the titanium casting shown above, the critical areas are marked with distinguishing marks of quality grades, the locations of test bars for mechanical tests as well as X-Ray beam angles. The manufacturer must check the inspection-instructions and confirm in writing after approval.

After approval of drawings and test instructions, i.e. after completion of design stage for castings, production may start. Before beginning series production the casting manufacturer will provide the customer with three outturn-samples which he believes to be free of defects and have been cast from the same melt.

The outturn samples must be accompanied by the following documents: the inspection report for the outturn samples, the structure, X-Ray films and dimensional report. When the inspection of the outturn samples has been successfully concluded the customer authorizes the beginning of series production by having the test report signed and returning a copy to the casting manufacturer.

At the time of delivery of the outturn sample the production process for castings is laid down in a production plan after consultation between the manufacturer and the customer. Any changes in this production plan must be authorized by the customer. The customer is obliged to treat confidentially any information on production techniques which may be specified in the production plan.

The plan must contain a clear description of the manufacturing process so that this can be repeated at any time as well as the following information:



Especially important in the production process are the melt and casting schedules. An important factor in quality assurance are the narrow tolerances governing the chemical composition and the various alloy elements of the melt. This has the advantage of insuring a uniform chemical composition in the series deliveries which is quite independent of the melt itself. This means that the characteristics of the material which are influenced by the alloying elements can be kept more or less constant. Compliance with the prescribed casting temperatures and mould system temperatures which have a considerable influence on texture and therefore on mechanical properties is decisive. The strict compliance with

QUALITE ET CONTROLE DES PIECES DE FONDERIE DE PRECISION POUR TURBOMACHINES

par

J.Thiery et J.Voeltzel
SNECMA Direction Technique
Route Nationale 7, B.P.81
91003 Evry Cedex, France

Le problème de qualité qui va être examiné concerne les pièces de fonderie de précision des turbo-réacteurs aéronautiques. Il sera volontairement limité aux pièces en aciers et en alliages réfractaires car, malgré les progrès réalisés ces dernières années, la coulée de précision des alliages légers et des alliages de titane reste encore limitée. D'autre part, les problèmes liés à la solidification dirigée et aux monocristaux ne seront pas abordés.

Les principales pièces obtenues par coulée de précision sont :

- pratiquement toutes les aubes de turbine, fixes et mobiles, qu'elles soient pleines ou à refroidissement interne, coulées isolément ou en secteurs,
- des pièces mécaniques diverses et peu critiques des parties chaudes : volets de tuyère, articulations, chapes, leviers... intervenant dans la commande de la tuyère ainsi que dans la fixation des rampes et des obstacles de post-combustion,
- des éléments plus ou moins importants des carters principaux réalisés par mécano-soudure, des supports de palier ainsi que de nombreux bossages soudés ou boulonnés.

Au point de vue matériaux, les aubes de turbine sont réalisées en alliages réfractaires base nickel coulés sous vide (IN 100, Inconel 713, René 77...) ou en alliages base cobalt (HS 31, MAR M 509...). Les pièces mécaniques diverses des parties chaudes sont appelées au 18/8 au niobium, aux alliages base nickel Hastelloy X et C 263 et à l'alliage base cobalt HS 31. Il est à noter que le choix de l'alliage base cobalt HS 31 a souvent été motivé pour sa bonne aptitude au frottement et à l'usure et non pour sa bonne tenue aux hautes températures. Les éléments soudés pour carters principaux sont le plus souvent en acier martensitique à durcissement structural 17/4 PH et en acier austénitique 18/8 au niobium, ou encore pour les carters plus chauds, en alliage austénitique base nickel coulé sous vide Inco 718 ou C 263.

La figure 1 donne la composition chimique, les caractéristiques à froid et la température limite d'emploi des principaux matériaux coulés de précision.

Les figures 2 à 12 présentent un éventail de pièces coulées destiné à illustrer la diversité des problèmes posés aux fondeurs de précision, les aubes mobiles de turbine constituant toutefois les pièces les plus exigeantes compte tenu du niveau élevé des sollicitations thermiques et mécaniques.

Les hautes caractéristiques attendues de ces alliages nécessitent une maîtrise parfaite du procédé de fonderie afin de préserver les qualités potentielles du métal.

En fait, cette recherche de qualité commence avant même de mettre en oeuvre le procédé. Nous essaierons de montrer, en suivant le plan présenté ci-dessous, tout ce qui concourt à l'obtention d'un produit sain aux différents stades de la fabrication :

DIFFERENTS STADES DE RECHERCHE DE LA QUALITE

Matériau de base

Procédé

- . *cire et carapace*
- . *conception du moule*
- . *coulée*

Mise au point de fonderie

- . *dissections*

plan qualité

"procédure de mise au point"

- . *contrôles non destructifs des pièces*

Surveillance de la fabrication

- . *figeage des gammes*
- . *suivi des dérives de fabrication*

1. EXIGENCES DE QUALITE CONCERNANT LE MATERIAU DE BASE

D'une manière générale le fondeur n'est pas autorisé à utiliser lui-même ses chutes pour couler directement de nouvelles pièces. Les chutes, descendants de coulée, pièces rebutées et autres éléments ne peuvent être utilisés que pour constituer de nouvelles coulées-mères avec tout le savoir-faire et les contrôles qui incombent à l'aciériste fournisseur d'alliage. On constate l'abandon progressif de l'approvisionnement du métal de base sous forme de grenaille, si bien que presque toutes les nuances coulées à l'air se présentent, comme les nuances coulées sous vide, sous forme de lingotins.

Les lingotins destinés à la coulée sous vide des aubes de turbine sont actuellement l'objet de cahiers des charges très stricts. Ils sont écroutés à la meule et le tronçonnage est obtenu par une entaille suivie d'une cassure pour éviter l'introduction de crasses ou de grains d'abrasifs dans une éventuelle retassure centrale. Un contrôle de l'homogénéité chimique des différents lingotins de la même coulée-mère est effectué par spectrographie.

En plus de l'analyse des éléments constitutifs de l'alliage, il est demandé aux aciéristes une garantie extrêmement sévère sur les teneurs maximales des éléments nocifs : par exemple pour l'IN 100 :

Bi \leq 1/2 ppm Pb, Ag, Se \leq 5 ppm Sn \leq 25 ppm

Dans certains cas, il est demandé aux aciéristes des analyses très détaillées d'une vingtaine d'éléments avec la possibilité de mesurer des teneurs de 0,1 ppm. Le contrôle des gaz prend de plus en plus d'importance avec un suivi particulier des teneurs en O_2 et en N_2 . En plus de ces contrôles de composition et d'impuretés nocives, on surveille la proportion de crasses pouvant flotter à la surface du bain lors de la fusion. Une grande attention est apportée au cours de la fabrication pour éviter les contacts avec le plomb (en radiographie), le zinc (outillages zingués) et les alliages à bas point de fusion (enrobages Zamac ou Cerrobend).

Pour certains alliages sensibles à l'apparition d'une phase fragilisante au cours du fonctionnement, on complète les exigences sur la teneur individuelle de chaque élément par une exigence supplémentaire entre les teneurs des éléments sensibles de manière à limiter les lacunes électroniques (condition N_V pour éviter l'apparition de la phase σ).

Les aciéristes sont réticents à garantir des caractéristiques mécaniques sur éprouvettes, qu'il s'agisse de grappes d'éprouvettes coulées à la cote ou de grappes de petits barreaux dans lesquels seront prélevées les éprouvettes, car ces caractéristiques dépendent des conditions de mise en oeuvre : surchauffe du métal avant coulée, cinétique de refroidissement avec son incidence sur la taille du grain et la structure métallographique, nature du traitement thermique... D'autre part, les caractéristiques sur ces éprouvettes peuvent être très différentes de celles des pièces à réaliser. Les aciéristes n'ont bien souvent pas les moyens de vérifier les caractéristiques mécaniques dans les conditions de mise en oeuvre des fondeurs et ne contrôlent en fait que la composition chimique de base et les impuretés.

Il est à noter, pour les pièces très difficiles à réaliser, la tendance des fondeurs à sélectionner les coulées mères ; celles qui permettent d'obtenir la pièce envisagée avec un faible pourcentage de rebut sont alors affectées à cette fabrication.

Recyclage des chutes

En principe, tout alliage de fonderie devrait pouvoir être recyclé par l'aciériste tant sous l'aspect coût que pour éviter le gaspillage de matériaux contingentés. Etant donné qu'il faut habituellement fondre de 3 à 6 kg de métal pour obtenir 1 kg d'aube brute de fonderie, on voit l'intérêt qu'il y a à trier soigneusement les chutes en vue de les réutiliser dans de nouvelles coulées-mères.

On a été amené à définir plusieurs classes d'élaboration :

Classe A : métal vierge.	Dans cette classe l'aciériste peut introduire ses propres chutes dans une proportion de 12 %.
Classe B : métal de refusion 50 %.....	La coulée comprend 40 à 60 % de chutes venant de l'aciériste et du fondeur client.
Classe C : métal de refusion 100 %.....	La coulée n'est réalisée qu'à partir des chutes de l'aciériste et du fondeur client.
Classe D : aucune exigence quant à l'origine du métal.	

La classe D est généralement réservée à tous les matériaux coulés à l'air.

Pour les alliages coulés sous vide, la tendance actuelle est d'utiliser le plus possible la classe B avec refusion à 50 % qui permet, compte tenu de la proportion de 40 à 60 % recyclée, d'utiliser une grande partie des chutes non contaminées. Si une pièce ou un alliage est particulièrement exigeant et que l'on craint une dérive des caractéristiques ou des rebuts dus au recyclage, on est conduit à imposer du métal vierge. Il est alors souhaitable d'éponger l'excès de chutes en autorisant pour une pièce facile à couler et relativement peu sollicitée du même alliage, la classe C à 100 % de chutes.

Il y a lieu de préciser que les chutes de fonderie destinées au recyclage doivent être parfaitement identifiées (forme des descendants de coulée différente suivant l'alliage), correctement découpées, ouvertes s'il s'agit d'éléments présentant des cavités et dans toute la mesure du possible exemptes de crasses et de contaminants (utilisation de produits exothermiques non dangereux pour l'alliage).

La qualité du métal recyclé dépend en grande partie du tri et du nettoyage des chutes ; ce problème qui risque d'être l'objet de litiges entre le fondeur et l'aciériste, ne peut être résolu que s'il s'établit entre eux un climat de confiance.

Malgré toutes les précautions prises, il semble que le recyclage soit responsable de certains enrichissements en gaz, en particulier l'azote, et en silicium. Au stage actuel, certains fondeurs estiment que le recyclage ne diminue pas la qualité des pièces, mais rend la mise au point de fonderie plus délicate et moins tolérante.

2. QUALITE AU NIVEAU DU PROCEDE

Dans la technique de fonderie de précision dite "à la cire perdue", le moule utilisé est obtenu par revêtement de céramique d'un assemblage d'un ou plusieurs modèles en cire de la pièce à couler.

Ces modèles sont obtenus par injection de cire dans des moules métalliques de grande précision (figure 13), tenant compte à la fois des caractéristiques dimensionnelles de la pièce et des phénomènes de retrait propres aux cires.

Cet assemblage ou grappe permet de définir et calibrer les attaques de coulée sur la pièce ainsi que les alimentations et la charge de moule ; la figure 14 représente une grappe en cire d'aube de turbine.

Un revêtement de céramique est ensuite effectué par trempés successifs et le moule ainsi préparé est séché puis déciré dans de la cire chaude ou dans un autoclave, le reste de la cire étant brûlé par étuvage à haute température. Ce moule encore appelé carapace est représenté figure 15.

Lors du remplissage du moule par l'alliage liquide, le métal vient occuper l'empreinte laissée par les modèles de cire et donne une grappe métallique à partir de laquelle les pièces moulées seront prélevées (figure 16).

2.1 Qualité au niveau des cires et de la carapace

Cires : De nombreux types de cires sont utilisés pour la réalisation des modèles. Ce sont des cires naturelles ou synthétiques, dérivées de produits pétroliers plus ou moins chargés en composés durcissants ou plastiques ; la cire utilisée pour la réalisation de pièces injectées est généralement vierge ; par contre on recycle les cires servant à l'injection des systèmes d'alimentation. Le choix doit être judicieusement effectué à partir des propriétés de rigidité, de viscosité, de stabilité dimensionnelle et chimique, de l'importance du taux de cendre, etc...

Il faut s'assurer par des contrôles avant utilisation, de la constance des propriétés ci-dessus. Les contrôles sont d'ordre chimique (analyse de composés organiques, taux d'insolubles dans différents réactifs, taux de cendre après combustion) et d'ordre physique (aspect, couleur, absence d'impuretés ségrégées, mesure sous forme de barreaux de la plasticité, de la résistance mécanique et de la constance du retrait).

Carapace : Le moule céramique ou carapace est constitué par une succession de couches recouvrant la grappe de cire (jusqu'à 12 couches). Ces couches composées de particules réfractaires sont déposées au trempé dans des suspensions liquides et par saupoudrage des particules, ce dernier procédé étant de plus en plus remplacé par une immersion en bain fluidisé. Les couches de liquide et de poudre alternent pour créer après séchage une carapace ayant une résistance mécanique suffisante et des propriétés de diffusivité thermique bien adaptées. La prise des couches est réalisée par évaporation et réaction chimique appropriées dépendant du procédé choisi.

De nombreux contrôles sont nécessaires au niveau des réfractaires pour assurer une qualité constante des moules. On procède entre autre, à la vérification de la granulométrie des particules, à la vérification par analyse des constituants (silice, zircone) et des inoculants introduits dans la première couche dont la teneur détermine la germination de l'alliage qui se solidifie à son contact, et à la vérification de la viscosité des bains et de leur pH.

En final, le moule céramique débarrassé de la cire est étuvé plusieurs heures suivant un cycle thermique déterminé, jusqu'à une température d'environ 1100°C afin d'atteindre sa résistance mécanique maximale. Un contrôle global consiste en une pesée de chaque moule. Pour la coulée, le moule est généralement emmaillotté dans une laine de silice ou simplement entouré d'un produit réfractaire concassé suivant le degré de calorifugeage désiré.

2.2 Qualité au niveau de la conception des moules

La qualité des pièces dépend étroitement de la conception des moules. En effet, à ce stade on détermine le mode d'alimentation des pièces (en chute, en source, alimentations secondaires...) ; l'art du fondeur consiste à doser judicieusement ces alimentations pour faciliter la venue des parties minces et à lutter contre les retassures en estimant convenablement le rôle de réchauffe locale que peuvent jouer les alimentations.

Par contre, d'autres impératifs thermiques sont peu compatibles entre eux, par exemple, température modérée et grande vitesse de refroidissement pour éviter le grossissement du grain en même temps que température élevée et refroidissement lent pour limiter les porosités et permettre une bonne venue des toiles minces ; le concepteur disposera alors de bien peu de latitude et devra pour surmonter ces exigences contradictoires utiliser toutes les ressources de son art en se référant constamment à l'expérience acquise. L'absence de microretassure dépendra de la possibilité pour le métal liquide de venir compenser les retraits en cheminant à travers les canaux interdendritiques.

Des études sont effectuées dans le but de simuler par ordinateur la solidification des pièces en fonderie de précision.

Cette approche nécessite en particulier la connaissance précise d'un certain nombre de paramètres : coefficient d'échange thermique et pouvoir émissif entre carapace ou emballage et atmosphère - conductivité et capacité thermique massique pour le métal, la céramique et l'emballage - évolution de la fraction solide du métal en cours de la solidification en fonction de la température - chaleur latente de fusion de l'alliage.

Il doit être ainsi possible d'étudier rapidement en un temps de calcul raisonnable, l'influence, sur la porosité et la grosseur de grain, des paramètres de coulée et de calorifugeage ; on parvient alors à faire l'économie d'essais longs et onéreux.

2.3 Qualité au niveau de la coulée

Au niveau de la coulée, souvent réalisée sous vide, les paramètres à prendre en considération sont essentiellement : la température du moule, le niveau de dégazage (pression statique et dynamique) la surchauffe éventuelle de l'alliage liquide, sa température au moment de la coulée et son homogénéité, enfin la vitesse de coulée.

En plus du contrôle des paramètres ci-dessus, un test de qualité est effectué ; il consiste à déterminer pour chaque coulée - four à induction coupé, bain sans turbulence - le pourcentage de crasse recouvrant le métal liquide avant coulée.

3. MISE AU POINT DE FONDERIE

En règle générale, la mise au point se fait à partir de plusieurs conception de moules et pour diverses conditions de coulée : les moules diffèrent par le mode d'alimentation, la dimension ou le nombre des attaques de coulée, le nombre de pièces par grappe... ; les conditions de coulée comprennent la température de surchauffe, celle du métal au moment de la coulée, la température du moule...

En général, 3 à 4 types de moules suffisent pour obtenir satisfaction ; des améliorations de santé peuvent encore être apportées par modification d'épaisseur de la carapace ou par modification de l'emballage calorifuge.

Dès obtention des pièces conformes à la spécification, une pré-série est lancée ; la technologie retenue et l'appréciation de la qualité des pièces se fait d'une part, en déterminant le taux de rebut sur la pré-série en contrôle non destructif et, d'autre part, en disséquant un certain nombre de pièces afin de bien préciser les propriétés de l'alliage ainsi que la santé interne du métal que les contrôles non destructifs ne caractérisent que de façon limitée.

Deux méthodes sont utilisées par les fondeurs pour garantir dans le temps le respect des spécifications après une mise au point jugée satisfaisante.

- 1 - Le "plan qualité" qui prévoit la dissection d'un petit nombre de pièces à l'origine de la fabrication, suivie de prélèvements systématiques, par exemple de la 10ème, 50ème, 100ème et toutes les 200èmes pièces, pour confirmation du niveau de qualité.
- 2 - De plus en plus, on applique une procédure désignée généralement "Procédure de mise au point" ou "Process Capability Study" chez les anglo-saxons qui se limite aux dissections faites à l'origine de la fabrication, mais sur un nombre de moules et de pièces plus important. Par exemple, coulée de 10 moules avec dissection très approfondie d'une trentaine de pièces.

Quand il s'agit de pièces de haut niveau de qualité telles que les aubes de turbine, ces dissections sont complétées par une caractérisation de la tenue en fatigue vibratoire ou thermique des pièces.

Ensuite, seuls les contrôles non destructifs sont appliqués, des dissections voire des caractérisations en fatigue n'étant reprises qu'en cas de modification de la gamme de fonderie. Cette méthode ne se justifie que si le fondeur apporte un soin extrême à la constance de tous ses paramètres de fabrication.

Malgré ces précautions, il est prudent pour les pièces majeures d'effectuer tous les ans une nouvelle caractérisation approfondie sur pièces.

3.1 Dissection

La dissection permet de vérifier les caractéristiques essentielles de l'alliage telles que résistance à la traction à différentes températures, fluage rupture et fluage allongement, mais elle donne surtout des informations précises sur la structure et la santé métallurgique du métal coulé.

Pour les petites pièces et plus généralement pour les pièces minces qui sont de plus en plus nombreuses, il n'est plus possible de prélever des éprouvettes cylindriques même de taille réduite et l'on doit se contenter, faute de mieux, de mesurer les caractéristiques mécaniques sur des barreaux attenants aux grappes. Un pion est aussi généralement ajouté à la grappe afin de pouvoir facilement s'assurer de la conformité de la composition chimique.

Sur la pièce elle-même, on vérifie la cristallisation, la structure, la répartition des constituants. Enfin, sur 5 à 20 coupes par pièce on chiffre la santé interne (inclusion, ségrégation provenant de l'alliage, du moule ou du creuset, etc...) et surtout le degré de microporosité. Cette dernière mesure est assez souvent responsable du remaniement de la mise au point technologique.

3.2 Contrôles non destructifs

Le tableau ci-après présente un déroulé opératoire qui met en évidence les différents contrôles prévus dans une gamme de fabrication de pièces sollicitées telles que les aubes de turbine.

TABLEAU

Après décochage

Sablage sec
 Attaque poussée (Perchlorure de fer)
 Contrôle macrographique
 Ressuage automatique
 Radiographie
 Traitement thermique (suivant l'alliage)
 Décapage chimique
 Sablage sec
 Polissage (manuel, tonneau, etc...)
 Contrôle visuel et élimination des défauts
 de surface retouchables
 Sablage sec
 Attaque douce (perchlorure de fer)
 Ressuage automatique
 Sablage sec
 Contrôle aspect
 Contrôle dimensionnel

Usinage

Une première attaque acide énergique permet un contrôle macrographique pour s'assurer de la cristallisation correcte de l'alliage (grains basaltiques, gros grains) et révéler les grosses inclusions, gouttes froides, criques, etc...

Directement sur cette attaque un ressuage est effectué ayant pour but d'identifier les pièces qui présentent les inclusions ou des défauts retouchables. La sévérité réelle de la spécification ne sera appliquée qu'à un niveau plus avancé de la pièce.

Vient ensuite le contrôle radiographique qui est responsable du pourcentage de rebut le plus important de l'ensemble des contrôles effectués.

Après préparation fine de la surface, suivie d'un contrôle visuel, d'un sablage et d'une nouvelle attaque plus douce que la première, est effectué le contrôle par ressuage à haute sensibilité avec application de la spécification.

Informations concernant le ressuage

Il n'est pas dans notre intention de présenter une analyse exhaustive de tous les procédés de ressuage utilisés par les motoristes. Nous avons toutefois établi le classement de sensibilité explicité ci-après, qui rend compte des différentes applications.

Sensibilité	Utilisations	Dimension limite des défauts mis en évidence
S1	En inter-opération	0,3 mm
S2	Pièces peu sollicitées	0,2 mm
S3	Utilisé seulement sur pièces usinées	0,1 mm
S4	Pièces sollicitées aubes par exemple	- inférieure à 0,1 mm - 0,5 mm pour criques et défauts linéaires pratiquement sans épaisseur

Les produits de ressuage sont colorés ou fluorescents et l'application se fait au trempé ou par pulvérisation sur pièces avec ou sans potentiel électrostatique.

La dimension limite indiquée dans le tableau ci-dessus correspond au défaut réel. La tache fluorescente observée est normalement de 2 à 5 fois plus importante. En pratique, on ne tient pas compte des taches de ressuage inférieures à 0,3 mm.

Notons que la sensibilité de ces produits est vérifiée systématiquement à l'aide de cales plastiques criquées jointes aux pièces à contrôler et périodiquement au moyen de lames recouvertes d'un dépôt de chrome criqué dans des conditions reproductibles.

Malgré la haute sensibilité des produits de ressuage, l'expérience montre que des défauts linéaires s'apparentant à des criques peuvent ne pas être révélés lorsqu'ils sont oxydés ou fortement comprimés ; c'est le cas en particulier des criques de retrait qui peuvent apparaître au droit des changements de section ou des alimentations insuffisamment rayonnées. Des contrôles par courants de Foucault ou par ressuage sur pièces mises sous tension peuvent alors être utilisés avec succès.

Informations concernant la radiographie

Les contrôles radiographiques des pièces de fonderie de précision font appel à des postes émettant des rayons X à partir de tubes à anodes courtes ou longues adaptées aux pièces à contrôler.

Dans le cas des aubes par exemple, celles-ci sont placées sur des cassettes à écrans de plomb ou dans les cas plus délicats au contact de films à écrans incorporés. Il faut souligner que le contrôle d'une aube complexe peut nécessiter jusqu'à 10 vues différentes et qu'une aube fixe avec ses talons peut exiger 6 vues. Cette technique, bien utilisée, permet la mise en évidence de défauts isolés ayant des dimensions correspondant à une diminution d'épaisseur de la pièce contrôlée d'environ 1 à 2 %.

En fait, compte tenu de leur configuration et de leur aspect habituellement diffus, les microporosités ne sont décelables par rayons X que pour des taux supérieurs, de l'ordre de 3 %, quand ces porosités intéressent l'épaisseur totale ; ces taux peuvent atteindre des valeurs nettement plus élevées, lorsque les porosités n'occupent qu'une faible partie de l'épaisseur.

Comme les limites admissibles de porosités sur coupe en dissection sont souvent pour les aubes de 1 à 3 %, les meilleurs contrôles radiographiques industriels ne permettent pas de garantir la qualité désirée. Seule une mise au point correcte vérifiée par des dissections et un procédé de fabrication soigneusement figé procure cette garantie.

Des recherches sont actuellement entreprises pour améliorer l'efficacité des écrans renforceurs ; certains au plomb à écrans d'antimoine diminuent les rayonnements diffusés et améliorent le contraste par émission d'électrons secondaires.

D'autre part, l'utilisation d'un tube Microfocus permet des agrandissements très importants en éloignant considérablement le film de la pièce. La tache focale est de l'ordre de $15\mu\text{m}$ et l'analyse du film conduit à la détection de fines porosités de diamètre théoriquement inférieur à 0,03 mm. Cette technique n'est utilisée que dans des cas spéciaux.

4. SURVEILLANCE DE LA FABRICATION

a - Gammes figées

Ainsi que nous venons de le souligner à propos de la radiographie, les méthodes de contrôle non destructif sont généralement insuffisantes. Seules les dissections apportent une vue globale de la qualité, dans la mesure où les pièces disséquées, sont représentatives de l'ensemble des pièces fabriquées.

Pour atteindre ce but, le fondeur est astreint à figer la totalité des paramètres importants de son procédé. Ainsi, lorsqu'on considère la fabrication d'une aube de turbine, nous constatons qu'il est nécessaire de figer environ 20 paramètres pour chacune des différentes étapes suivantes :

- injection des cires,
- montage de la grappe,
- confection de la carapace,
- décirage - étuvage,
- emballage - fusion - coulée,
- parachèvement.

Ces figeages sont assortis d'une assurance qualité prévoyant que toute modification doit faire l'objet d'une demande d'accord auprès des méthodes fabrication et du laboratoire. Ce dernier préconise des essais complémentaires s'il le juge utile. De plus, toutes les gammes de fabrication explicitant ces paramètres figés sont déposées et une modification de l'un des paramètres critiques entraîne le changement d'indice de la gamme.

b - Suivi des dérives de fabrication

Malgré toutes ces précautions (mise au point poussée des pièces, figeage du procédé), une dérive accidentelle de la fabrication est toujours possible. Comme le cycle complet d'obtention d'une pièce coulée est de plusieurs semaines, il convient d'être averti aussitôt que possible.

Une méthode couramment appliquée consiste à suivre le taux de rebut au niveau du contrôle radiographique, c'est-à-dire très en amont dans la gamme. Un relevé statistique comportant un niveau d'alerte est journalièrement suivi et dès qu'un lot dépasse ce niveau, un "audit" complet du procédé est effectué.

* Ce pourcentage de porosité représente la moyenne mesurée sur une surface de référence de l'ordre de 1 mm^2 .

5. ORIENTATIONS FUTURES ET TECHNIQUES NOUVELLES LIEES AUX PROBLEMES DE QUALITE

Nous examinerons succinctement les nouvelles orientations en vue d'obtenir des pièces de qualité améliorée ou de performances plus élevées. Nous n'aborderons pas les problèmes délicats de la qualité des pièces destinées à des assemblages soudés et nous nous limiterons au cas particulier des aubes de turbine.

a - Diminution de la sensibilité à la microporosité par action sur les alliages

Plusieurs voies de recherche consistant en de légères modifications de la composition chimique ont été tentées pour réduire la tendance des alliages à former des microporosités diffuses, plus particulièrement dans les zones épaisses. La solution préconisée par MARTIN METALS sur les alliages de la famille MAR M consistant à ajouter 1 à 1,5 % de hafnium et à réduire la teneur en bore et en zirconium apporte une amélioration certaine du point de vue santé et ductilité mais au prix de quelques inconvénients : coût élevé du hafnium, réaction avec le moule et les noyaux, mais aussi pour l'utilisateur une température de solidus abaissée.

Dans la solution adoptée sur les alliages BALDWIN la teneur en carbone est réduite mais celle du bore augmentée dans le but de faciliter l'alimentation entre les dendrites pendant la solidification, les borures se formant plus tard que les carbures. Nous avons vérifié dans le cas de l'alliage B 1914, de caractéristiques voisines de celles de l'IN 100, la très faible tendance à former des microporosités, ce qui constitue un avantage appréciable pour les pièces difficiles.

b - Diminution de la porosité par compression isostatique

Lorsqu'une pièce présente des porosités ou des microporosités internes, il est possible par compactage isostatique à une température très élevée de fermer les porosités non débouchantes ; il y a un effet de soudage par diffusion. Les essais mécaniques montrent que l'influence des porosités est réellement effacée. Cette technique désignée en France par C.I.C (compression isostatique à chaud) et chez les anglo-saxons par H.I.P. (high isostatic pressing) consiste à comprimer la pièce sous une pression d'argon d'environ 100 MPa et à des températures d'environ 30 à 50°C en-dessous du solidus de l'alliage. Cette solution fait appel aux mêmes autoclaves que ceux qui sont mis en place pour la métallurgie des poudres des alliages base nickel.

Bien que ce compactage donne entière satisfaction pour éliminer les porosités internes, il comprend un traitement thermique à très haute température qui peut avoir un effet néfaste sur la structure métallurgique de l'alliage et par là sur ses propriétés mécaniques ; un traitement thermique ultérieur peut éventuellement restaurer la structure. Des dépassements de température avec brûlure sont à craindre si la pièce présente des ségrégations ou des hétérogénéités de composition chimique importantes ou encore si la température de l'autoclave n'est pas parfaitement homogène. Ces observations conduisent à prévoir un contrôle très rigoureux de l'homogénéité de température de l'enceinte de l'autoclave et à surveiller par des examens micrographiques sur pièces les contaminations superficielles. Si l'on rappelle que seules les porosités ne débouchant pas sont effacées, on voit que ce procédé est une solution délicate, à utiliser avec précaution ; au stade actuel, il semble pouvoir être retenu lorsque le constructeur impose des critères de santé que le fondeur ne parvient pas à satisfaire sans compliquer de manière excessive le système d'alimentation de la pièce. On peut dans certains cas utiliser ce procédé pour récupérer des pièces rebutées pour porosités au-delà du standard admissible.

Le haut niveau de température peut accentuer les contaminations superficielles laissées par les céramiques du moule et il est nécessaire d'apporter un soin tout particulier aux opérations de décapage qui précèdent le traitement de compression isostatique.

c - Difficultés de contrôle liées à la réalisation d'aubes creuses

Le développement très important des aubes refroidies par cavités ou canaux nous oblige à signaler les difficultés de contrôle très importantes que l'on rencontre au niveau de la mesure de l'épaisseur des parois des aubes. Bien que dimensionnel, ce problème est actuellement résolu par des mesures magnétiques particulièrement délicates ou par des techniques ultra-sonores dont les performances permettent difficilement de mesurer des épaisseurs de l'ordre de quelques dixièmes de mm avec une précision satisfaisante. Les caractéristiques mécaniques de fluage et de fatigue de ces parois minces, avec leur cristallisation et leurs structures particulières sont, elles aussi, délicates à appréhender.

Notons par ailleurs, les problèmes de contamination interne des aubes, au cours de la coulée, par le noyau et lors du traitement thermique ultérieur par des restes éventuels de noyau ou par le sable introduit au cours des opérations de fabrication.

CONCLUSION

Nous avons essayé de faire ressortir dans cet exposé général, les problèmes qualité rencontrés par le fondeur depuis le choix de l'alliage jusqu'à la réalisation finale de la pièce.

Le point fondamental sur lequel il convient d'insister est la nécessité d'une mise au point très poussée de la procédure de fonderie puis la nécessité du figeage des gammes qui est le plus sûr garant du maintien de la qualité, les opérations de contrôle n'étant destinées qu'à vérifier l'absence de dérive.

Le problème du niveau de qualité à exiger et des processus de contrôle à utiliser est un point particulièrement délicat pour arriver à un compromis prix/performance satisfaisant. La plupart des contrôles non destructifs destinés aux pièces les plus sollicitées sont utilisés à la limite de leurs possibilités et les constructeurs forment le souhait que des progrès soient réalisés dans ce domaine. Ceci n'implique pas qu'il soit souhaitable d'introduire systématiquement des critères plus sévères mais il est utile d'avoir une connaissance précise du niveau de qualité et de pouvoir garantir par des essais non destructifs la constance de cette qualité en production. Par ailleurs, il est nécessaire de développer les études sur la nocivité des défauts, afin de mieux ajuster les exigences de santé aux réels besoins des pièces.

Matière	Composition Chimique Type													Caractéristiques à 20°C		Température maximale d'utilisation
	C	Fe	Cr	Ni	Co	W	Mo	Nb+Ta	Ta	Al	Ti	Ti+Al	Cu	R MPa	R ₀₂ MPa	
18.8 au Nb	0,10	base	18	12				1,2						≥ 440	≥ 200	700°C
17.4 PH	0,05	base	16	4									3	≥ 830	≥ 760	350°C
INCO 718		18	19	base				5						≥ 830	≥ 640	650°C
C 263			20	base	20		6					2,5		≥ 620	≥ 430	850°C
Hastelloy X		18	22	base			9							≥ 440	≥ 240	1100°C
René 77			14,5	base	15		4			4	3			≥ 790	≥ 680	950°C
IN 100			10	base	15					5,5	4,7			≥ 720	≥ 630	1000°C
HS 31			25	11	base	8								≥ 580	≥ 410	1050°C
Mar M 509			24	10	base	7			3,5					≥ 580	≥ 410	1100°C

Fig. 1. - Principaux matériaux de fonderie

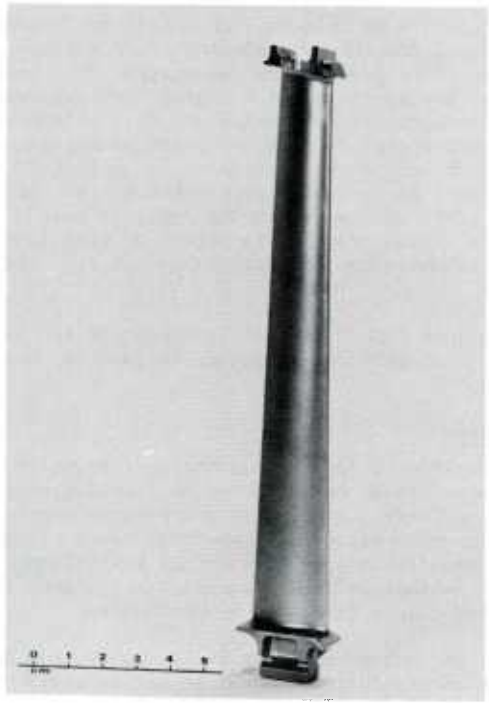


Fig. 2. - Aube mobile de turbine en René 77.

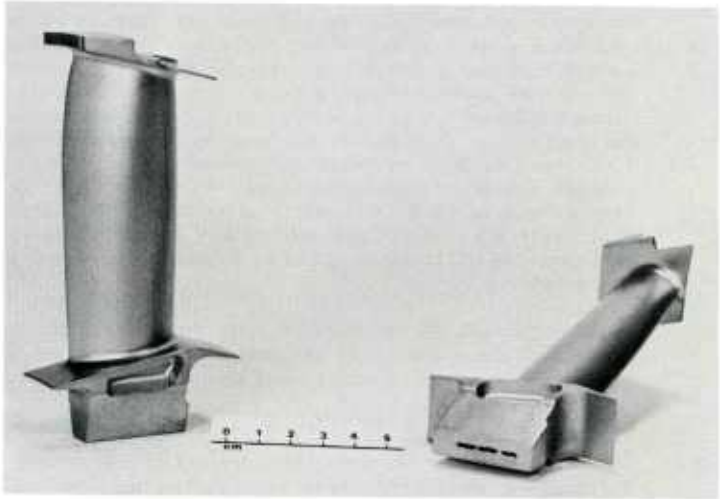


Fig. 3. - Aube mobile de turbine refroidie en IN 100.

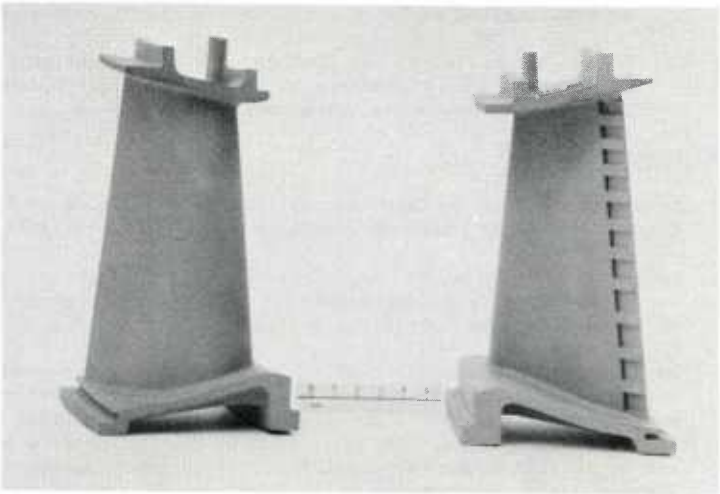


Fig. 4. - Aube fixe refroidie en IN 100.

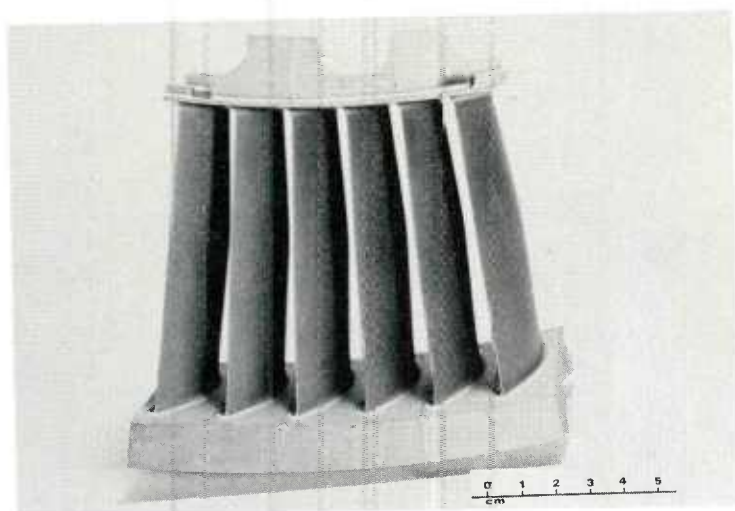


Fig. 5. - Secteur aubes fixes de turbine en René 77.

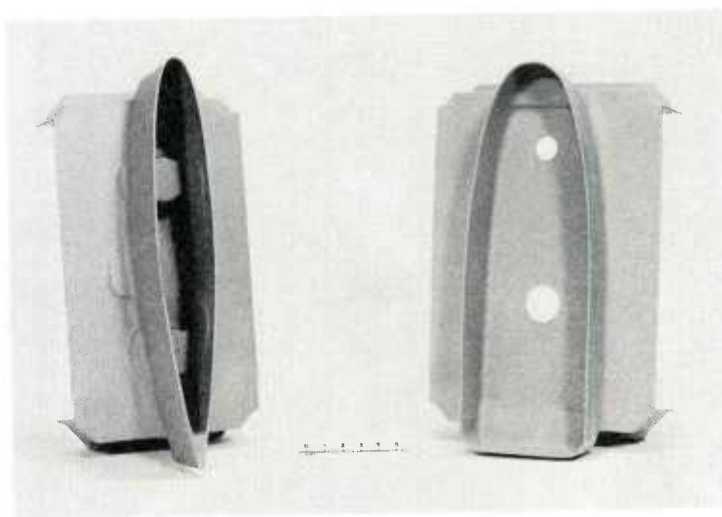


Fig. 6. - Embase bras carter en 17-4 PH.

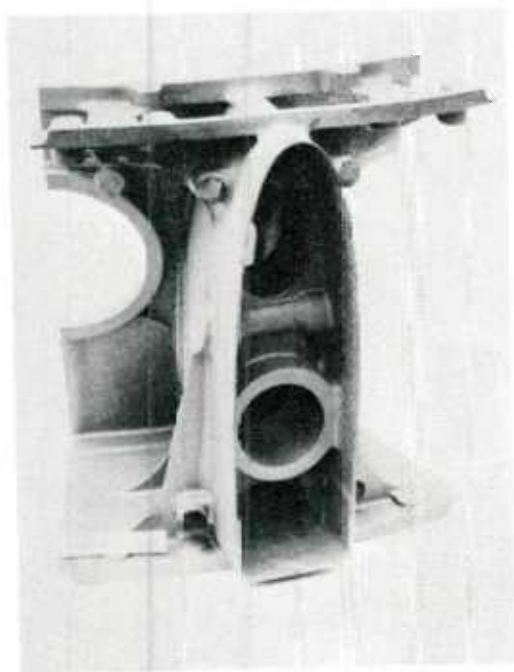


Fig. 7. - Secteur carter en 17-4 PH.

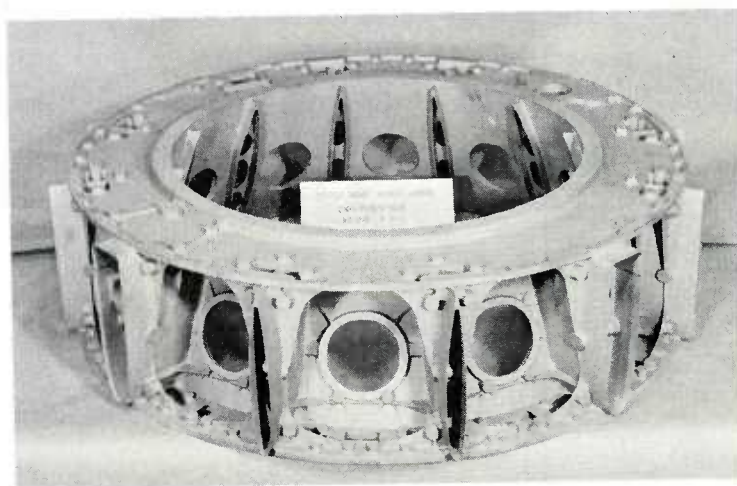


Fig. 8. - Couronne inter-veine en 17-4 PH.

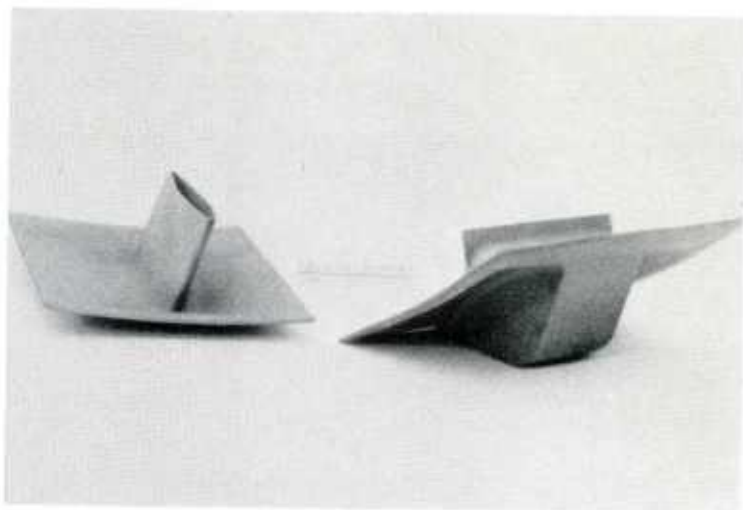


Fig. 9. - Embase bras carter en IN 718.

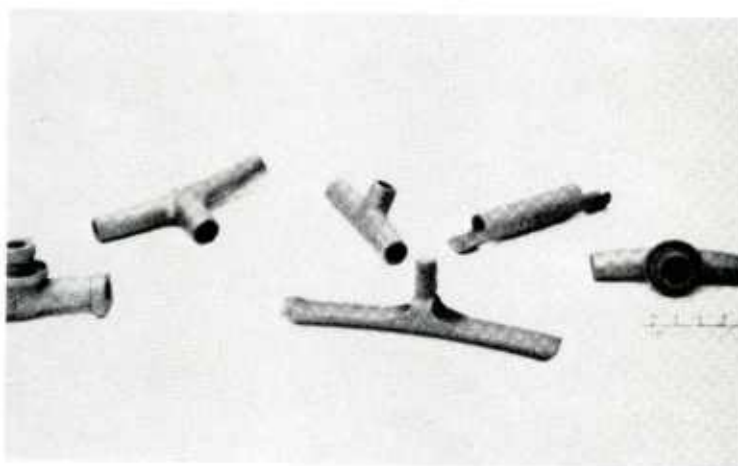


Fig. 10. - Elements de rampe post-combustion en Hastelloy X.

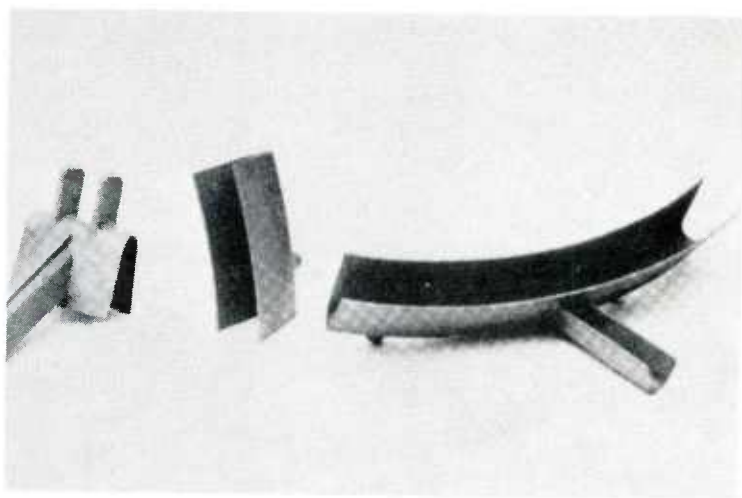


Fig. 11. - Eléments accroche-flamme en HS 31.

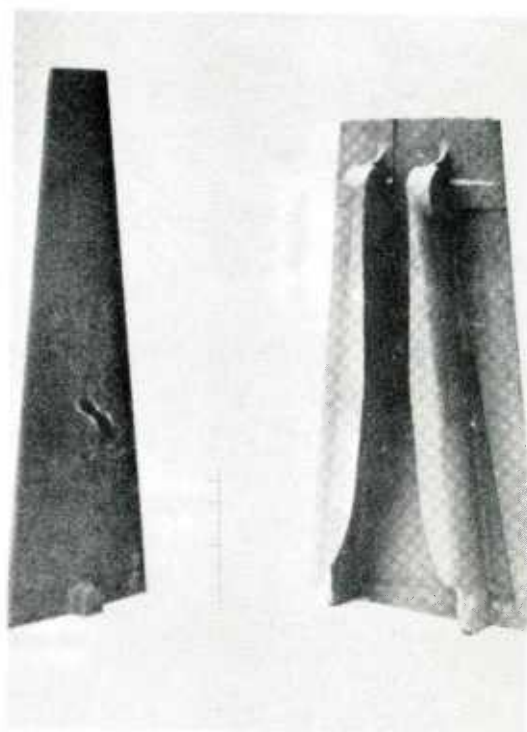


Fig. 12. - Volets de tuyère en HS 31.

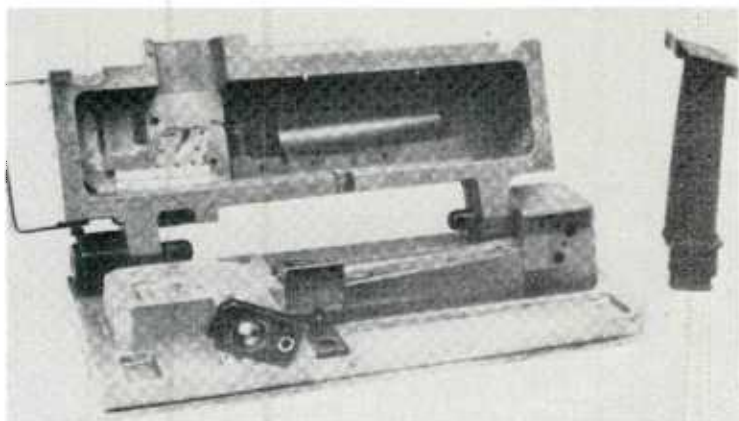


Fig. 13. - Outillage injection de cire pour aube mobile de turbine.

Fig. 14. - Grappe en cire d'aubes fixes avec son système d'alimentation.

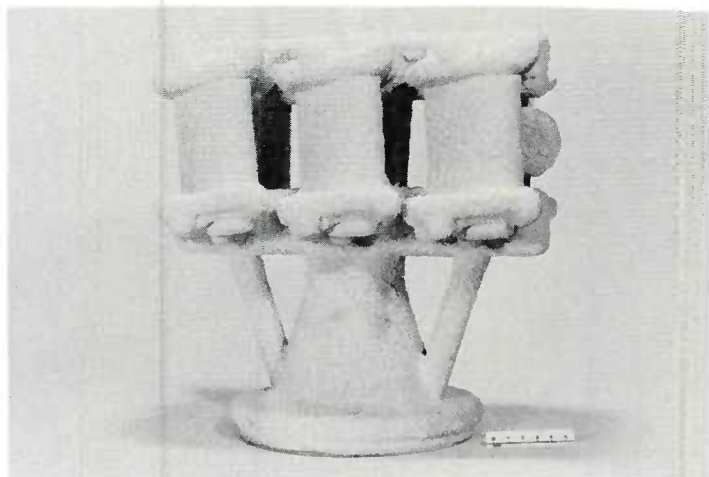
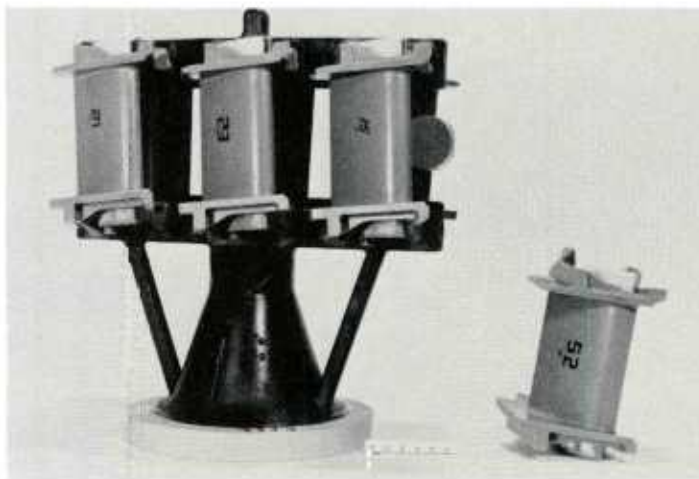
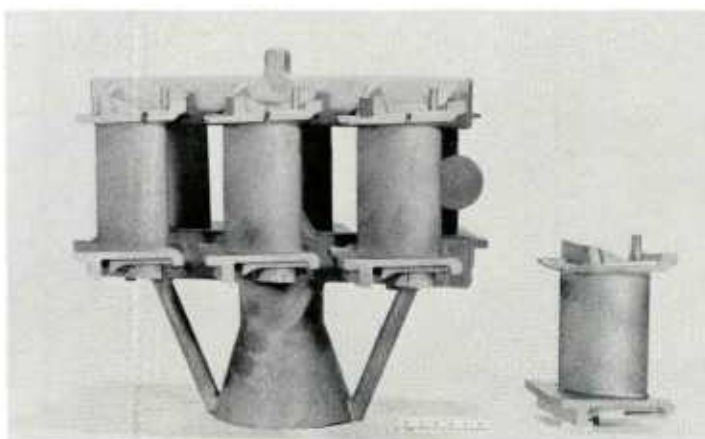


Fig. 15. - Carapace d'une grappe d'aubes fixes.

Fig. 16. - Grappe métallique d'aubes fixes avant découpe.



METALLURGICAL ASPECTS OF QUALITY CONTROL IN THE
PRODUCTION OF PREMIUM QUALITY ALUMINUM INVESTMENT
CASTINGS FOR THE AEROSPACE INDUSTRY.

by
Steve Kennerknecht (B. Eng.)
Chief Metallurgist
Cercast 1979 Inc.,
3905 Industrial Blvd.,
Montreal-North, Quebec
Canada H1H 2Z2

ABSTRACT:

There has been a continuing trend in the Aerospace Fields to overcome the ever increasing manufacturing cost of highly complex and structural components. Following this trend, many of these applications are designed for the investment casting process. The need to combine functions, light weight and strength result in highly complex casting configurations having varying cross sections.

This paper serves to uncover the many metallurgical variables which influence the production of premium quality investment castings. An extensive comprehension of grain refinement, modification, chilling, alloy composition, heat treatment, non destructive testing and basic metallurgy, are essential tools when confronted with a difficult casting problem. What may be impossible for one casting producer may only be a complex problem requiring extensive development for an experienced foundry.

A metallurgical State of the Art in investment casting will be presented , with reference to current developments and innovations in this field.

TABLE OF CONTENTSPAGE NUMBER

1)	<u>MELT AND DEGASSING TECHNIQUES</u>	3
	-Melting Furnaces	
	-Alloy melt treatments	
	-Grain Refinement and Modification	
2)	<u>ALLOY MORPHOLOGY</u>	4
	-Aluminum-Silicon-Magnesium Alloys	
	-Aluminum-Copper-Magnesium Alloys	
3)	<u>GRAIN REFINEMENT</u>	6
	-Introduction	
	-Vibration	
	-Convection	
	-Cooling Rate	
	-Innoculating Agents	
	-Susceptibility to Refinement	
	-Effect of G. S. on Mechanical Properties	
	-G.S. Determination for Problem Solving	
4)	<u>OPTIMIZATION OF CHEMISTRY</u>	14
	-Control of Impurities	
	-Effect of Alloy Concentrations on Mechanical Properties	
5)	<u>MODIFICATION</u>	19
	-Introduction	
	-Acicular Structure	
	-Modified Structure	
	-Sodium Modification	
	-Strontium Modification	
	-Antimony Modification	
	-Effect and Occurance of P	
	-Effect of DAS	
	-Effect on Feeding Distance	
	-Effect on Mechanical Properties	
	-Methods of Determining Modification Before Casting	
	-Developments in Thermal Analysis (Past and Present)	
6)	<u>HEAT TREATMENT</u>	30
	-Introduction	
	-Precipitation in Specific Alloy Systems	
	-Quenching	
	-Sample Determination of Heat Treatment Variables	
7)	<u>RADIOGRAPHY & PENETRANT EXAMINATION</u>	34
	-Eutectic Melting	
	-Segregation	
	-Hot Tearing	
	-Intermetallic Compounds	
8)	<u>FUTURE PROSPECTS</u>	39
	-Vacuum Casting	
	-Hot Isostatic Pressing	
9)	<u>APPENDIX-A</u>	42
	-Macrosegregation	
	-Case Studies	
10)	<u>APPENDIX-B</u>	46
	-Eutectic Melting	
11)	<u>APPENDIX-C</u>	49
	-Selections of Alloys Resistant to Liquid Aluminum	
12)	<u>APPENDIX-D</u>	50
	-Titanium-Boron Hardener Alloy	
13)	<u>BIBLIOGRAPHY & REFERENCES</u>	51

MELT AND DEGASSING TECHNIQUES

Melting Furnaces:

Aluminum alloy is commonly melted in electric, gas-fired or induction, crucible type furnaces. In the electric and gas fired applications, most refractory crucibles are made of carbon bonded silicon carbide or a mixture of clay and graphite. Clay-graphite crucibles are better suited for induction melting applications, where heat is generated within the aluminum charge itself, rather than in the crucible walls.

Each particular type of melting furnace has its own desirable and undesirable characteristics in particular foundry applications. Electric-resistance crucible furnaces are low capacity furnaces due to their slow melt rate; yet offer excellent temperature control in holding furnaces. Coreless induction furnaces are costly due to the expensive electrical apparatus needed, yet the strong stirring produced from the electromagnetic forces may be desired in special applications such as vacuum degassing and elimination of segregation caused by additions of high melting point alloys and elements. In the case of gas fired furnaces, the flame path and exhaust flue must be isolated from the bath surface to discourage hydrogen pick-up from the combustion products. Properly designed gas-fired furnaces offer good melting and holding capabilities with satisfactory efficiency.

Alloy Melt Treatments:

Upon melting of the aluminum alloy to the desired temperature for processing, specialized measures are necessary to remove unwanted oxides, dissolved gases and insoluble ceramic and sludge particles. The control of sludges which may buildup in aluminum alloy melts are controlled by special foundry techniques and are discussed later. Ceramic particles are removed by simple mechanical means, yet gas and oxide control are more technically difficult. Oxide fluxing and degassing procedures complement each other, as gas bubbles are known to adsorb onto the surface of the oxides present in the melt. In fact it is this realization which allows the foundry to develop techniques to control dissolved gas and oxides to an extent suitable for the production of premium quality castings.

Grain Refinement and Modification:

Grain refinement by dispersed particulates of TiB_2 and $TiAl_3$ is adversely affected by degassing techniques employing chlorine based or inert gas fluxing. The vigorous mechanical action and exothermic reaction of gas fluxing, promotes agglomeration of the numerous titanium based particles and thus reduces the total quantity of sites available for grain nucleation.

Melts containing sodium, strontium or antimony for the purpose of alloy modification are not chemically stable during the gas fluxing stage. Chlorine, hexachlorothene and freon are reactive in the melt and combine with these elements to form insoluble compounds which float to the surface of the bath and are removed. Magnesium, as does Na, Sr and Sb are removed from the melt during degassing with chlorine compounds and may thus change the alloy modifying potential. It is for this reason that Mg, Sr, Sb and Na are added in excess of what is needed in the alloy final composition (when using chlorine based degassing agents). Spectrographic analysis or otherwise is thus essential for these melts, after the degassing stage, to ensure correct chemistry controls.

ALLOY MORPHOLOGYA) Aluminium-Silicon-Magnesium Alloys: (356, 357)-Silicon (6.5-7.5%)

Silicon as the main alloying element imparts high fluidity and low shrinkage which result in good castability and weldability. In fact only about 5% of the Silicon in (Al-7%Si-Mg) alloy systems combines with Magnesium to form Mg₂Si precipitates, which are responsible for alloy strengthening.

-Magnesium (0.2-0.7%)

Magnesium and Silicon form a relatively simple alloy structure: the main constituent is Mg₂Si which in the heat treated condition is in solution and to which is due the age hardening after artificial ageing. At room temperature, quantities of magnesium exceeding 0.3% Mg will be present as Mg₂Si. An increase of Magnesium, within the alloy range, results in increased strength at the expense of ductility. Sensitivity to quench rates also increases with Magnesium content. Hardness is also increased with higher Magnesium levels.

-Iron (Max. 0.2%)

Iron is strictly an impurity and causes a severe loss of ductility of the alloy as a result of intermetallic compounds. Premium quality casting alloys are significantly low in iron, and are used for aircraft and aerospace castings requiring high properties. Iron increases somewhat the creep resistance of the alloy at high temperatures, and reduces corrosion resistance unless corrected by Manganese or Chromium.

-Copper (Max. 0.2%)

Copper is present primarily as an impurity in Al-Si-Mg alloys. Copper increases the sensitivity of the alloy to quench rates and decreases creep at high temperatures. Copper is undesirable as it increases corrosion susceptibility by making the surrounding eutectic a less negative potential than the aluminum matrix.

-Manganese (Max. 0.1%)

Additions result in improved strength at high temperatures, increase creep and fatigue resistance and counteract Copper in neutralizing the corrosion susceptibility of the alloy. Manganese is primarily added in alloys of high iron content to increase the ductility. Manganese forms a globular Fe-Mn silicide which is less hindering on mechanical properties than are the sharp needles of primary iron compounds. Manganese increases the quench sensitivity of the alloy. Manganese reduces grain boundary precipitation, thus reducing embrittlement and susceptibility to intergranular corrosion.

-Beryllium (Max. 0.7%)

Beryllium reduces the oxidation of magnesium at high temperatures especially in the molten state. In fact, before foundries used spectrographs for routine chemical analysis, Beryllium was useful in maintaining Magnesium levels of the molten alloy similar to that of the supplied master ingot alloy. Beryllium scavenges iron to some degree, yet has little or no effect on mechanical properties. In fact some reports show that Beryllium coarsens grain size.

-Titanium (Max. 0.2%)

Titanium is added as a grain refiner, usually in conjunction with Boron (Ti/B=5/1). The TiB₂ or TiAl₃ dispersed particulates have lattice spacings similar to that of aluminum, and it is upon these substrates which the primary aluminum dendrites are encouraged to grow.

-Strontium, Sodium, Antimony (Max. 0.05%)

These elements scavenge the phosphorus from the alloy by forming compounds. As phosphorus is the nucleating substrate for primary silicon particles, the lack of free phosphorus will encourage fine distribution of secondary Silicon particles. The resulting 'modification' enhances mechanical properties, particularly the ductility of the alloy.

-Others (Max. 0.05%)

Generally other impurities in small amounts have no significant effect on the alloy. Chromium, Titanium and Zirconium slightly harden the alloy. Nickel increases the chance of corrosion pitting. Chromium and Zinc raise the re-crystallization temperature of the alloy. Chromium increases quench sensitivity and reduces grain boundary precipitation. Cadmium and Silver retard zone formation and reduce natural ageing.

B) Aluminum-Copper-Magnesium Alloys: (201, 202, 204 etc., D25Z)

-Copper (4.0-5.2%)

The best combination of strength and ductility is obtained when copper content is close to the solubility limit (5%Cu) and the alloy is heat treated so the copper is distributed in Guinier Preston (G.P.) zones. When copper exceeds 5%, commercial heat treatment cannot dissolve it and the network of eutectics does not break up. As a result the strength is increased but the ductility is significantly reduced. Lower copper contents, unless compensated by Magnesium, produce lower strength and better ductility. CuAl_2 and $\text{Cu}_2\text{Mg}_8\text{Si}_6\text{Al}_5$ precipitates contribute most to strength in the dispersed heat treated condition. In Al-Cu alloys, the Copper dispersed in the Aluminium oxide, on the skin of the casting, prevents complete passivation which normally protects aluminum and its alloys. As a result Al-Cu alloys are prone to corrosion, particularly stress corrosion cracking (SCC).

-Magnesium (0.15-0.55%)

Magnesium increases the strength and hardness of Al-Cu castings with a decrease in ductility. Strength at high temperature and creep resistance are improved with Magnesium especially if Silicon is low. Magnesium free alloys produce adequate tensile strength, however yield strength depends largely on Magnesium concentration. Highest strengths are obtained with high Magnesium levels, however $\text{Mg} > 0.35\%$ lowers the equilibrium eutectic temperature, and promotes eutectic melting at heat treat temperatures near 535°C (995°F). Therefore Magnesium levels should be held $\leq 0.35\%$.

-Iron and Silicon (Max. 0.15% and Max. 0.1%)

Iron and Silicon are maintained as low as possible to retain high tensile properties. Iron causes an embrittling effect as a result of iron bearing compounds, and reduces the solubility of copper in the matrix upon heat treating. Silicon reduces high temperature strength and creep resistance.

-Manganese (Max. 0.5%)

Manganese has a slight strengthening effect because of its solubility and the fact that it reduces the embrittling effect of iron. This is possible, as the globular Fe-Mn compounds have a more favorable configuration than the acicular shape of primary iron compounds. However when Iron and Manganese content is too high, the resulting primary crystals reduce ductility and fatigue resistance of the alloy. Manganese however reduces the response to ageing and delays the development of full strength potential of the alloy. The major contribution of Manganese to Al-Cu alloys is its ability to form compounds which pin the grain boundary areas, and thus eliminate grain growth during solution heat treatment up to 538°C (1000°F).

-Silver (Max. 1.2%)

Silver is added to Al-Cu alloys primarily to improve the alloys resistance to stress corrosion cracking. Silver additions also improve tensile properties by increasing the alloys ageing response.

-Zinc (Max. 0.05%)

Zinc is either an impurity or a major alloying element (2.5-3.0% in alloys 249 and D25Z). Zinc increases strength but reduces ductility. At low temperature and low concentration, the effect is not too pronounced - at higher temperatures zinc reduces appreciably strength and creep resistance.

-Titanium (0.15-0.35%)

Titanium or Titanium and Boron is added as a grain refiner, and is very effective in reducing grain size. Grain refining results in a better dispersion of insoluble constituents, porosity and nonmetallic inclusions. Also as a result, heat treatment effects are considerably improved.

-Others (Max. 0.05%)

Nickel reduces the iron embrittling effect as does Manganese and increases high temperature properties. Mn-Ni compounds however, reduce room temperature properties. Lithium acts like Magnesium: It increases tensile strength and reduces ductility. Tin lowers strength and ductility of the alloy. Chromium increases high temperature properties only. Most other alloying elements have no beneficial effects on Al-Cu alloys.

GRAIN REFINEMENT

The effect of grain size on mechanical properties result primarily from changes in distribution of porosity, inclusions and microsegregate. In addition, a finer distribution of eutectic material is beneficial in heat treatment and helps speed the distribution of strengthening precipitates. In most alloy systems, preferred fracture paths are through the brittle eutectics found at the grain boundary. Coarser grain and hence coarser grain boundary are structurally less sound than fine grain boundary, and result in lower mechanical properties. A microscopic examination of large and small grain size found in investment castings is depicted in figure A below.

In recent years, it has come to be recognized, that dendrite arm spacing of cast structures usually correlates far better with mechanical properties than does grain size. In practice, one of the most important technical aspects of casting, is the control of nucleation and hence grain size. Most commonly, control is exerted by the use of nucleating agents, natural and forced convection, chilling and controlled cooling, and vibration.



A356 ALLOY:

Dendrite Arm
Spacing (DAS)=
50 um.

50X



A356 ALLOY:

DAS= 150 um.

50X

Comparison of large and small grain size

Fig.A

Vibration:

The introduction of vibration to an undercooled liquid alloy will stimulate nucleation. It is theorized that a pulse of significant intensity causes nucleation to begin by pressure resulting from the collapse of a void formed by cavitation. The large pressure wave would then activate nuclei that would otherwise be inactive at said temperature.

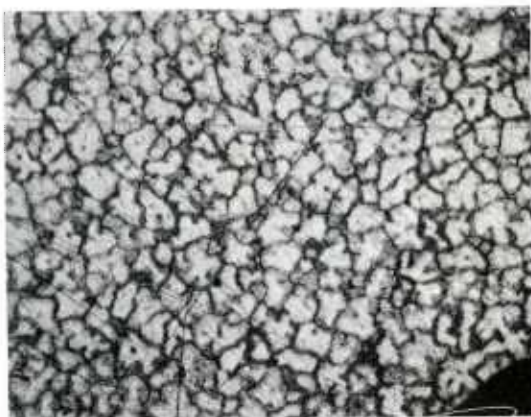
Many attempts have been made to apply these ideas to the grain refinement of commercial castings by mechanical, sonic and ultrasonic means during solidification. However it is now understood that such vibration causes convection in commercial alloys which results in grain refinement by a grain-multiplication mechanism. Testing at Cercast with alloys susceptible to grain refinement has shown that vibration caused only a minimal decrease in grain size and DAS of test castings.

Convection:

Convection has a strong effect on the grain size of cast alloy. In fact the suppression of convection in zero gravity environments produces castings of unusually large grain size.

Natural convection caused by thermal and density variations are present in most castings and aid in the dissipation of superheat. In addition, convection and thermal variations thus produced aid in breaking and melting off of dendrite arms and carry them into bulk liquid, where they may nucleate new grains.

Enhanced convection by rotational, oscillating, stirring or electromagnetic methods are being used commercially with mixed successes. Proper use of enhanced convection produces significant improvement in cast grain size, particularly in heavy sections where the slow cooling rate and lack of nucleation sites produce large grains. Experiments by Cercast on heavy section turbocharger wheels has yielded a >50% drop in DAS as a result of mold oscillating and electromagnetic stirring techniques (see Fig.B). These techniques are not foolproof however and may result in macrosegregation problems as a result of the disturbed solidification pattern.

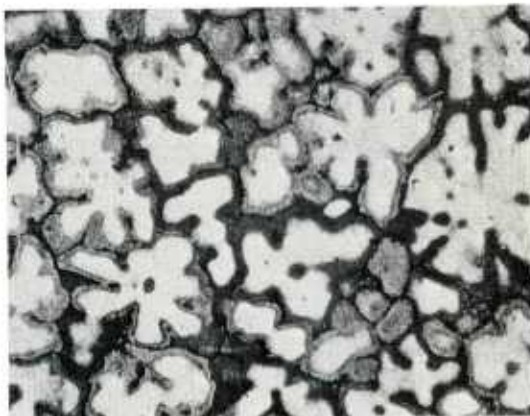


201 ALLOY

(as cast)

Grain size = 100 um.

50X



201 ALLOY:

(as cast)

Grain size = 300 um.

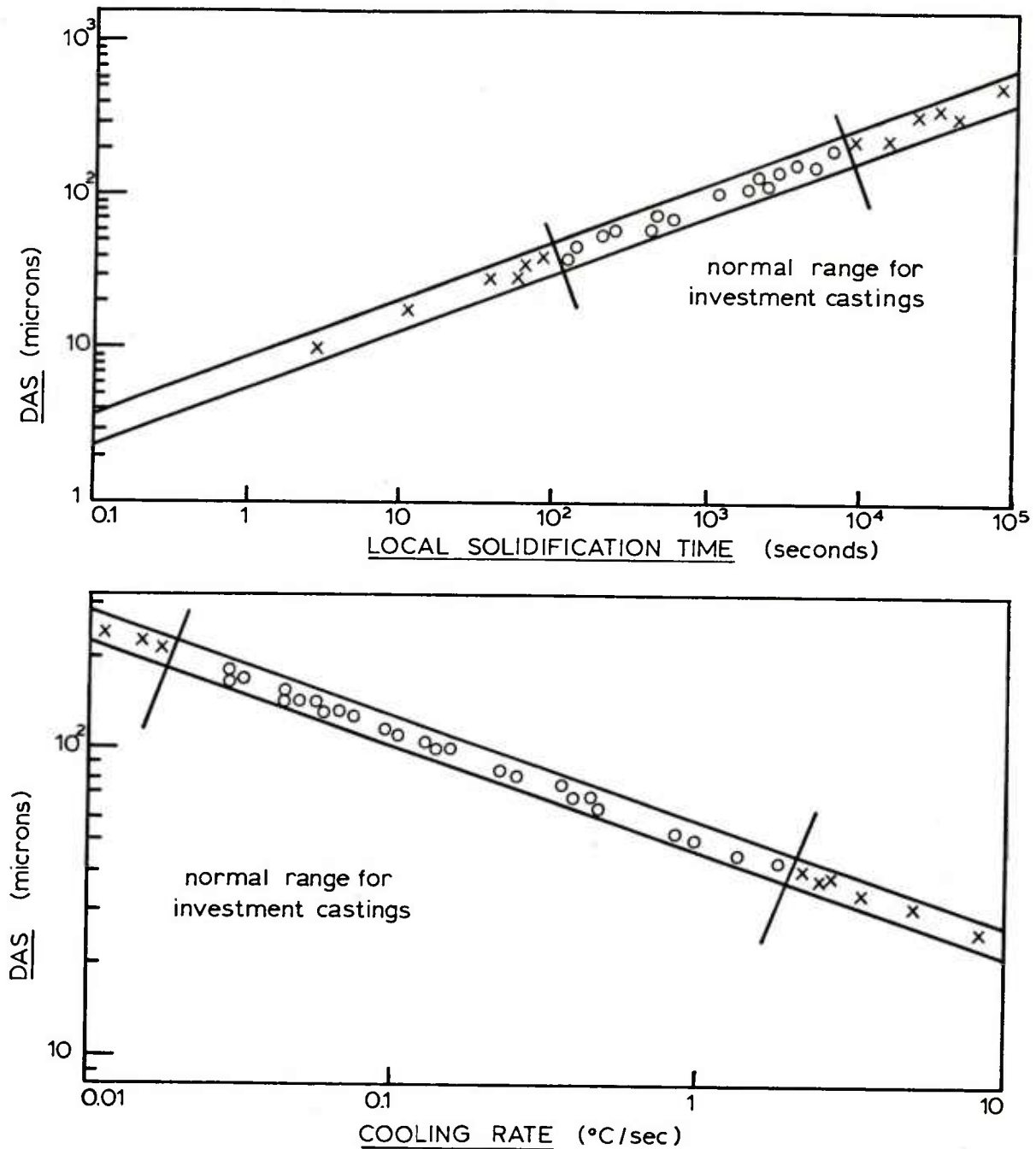
50X

Effect of grain size reduction of cast 201 turbocharger wheel by specialized techniques.

Fig. B

Cooling Rates:

Local solidification time as related to freezing rate of a casting, has a very large effect on grain size and DAS as shown in the following graph (Fig. C).



Effect of cooling rate and local solidification time on cast grain size. Fig. C

Dendrite morphology in most casting situations remains largely unchanged over large ranges of cooling rates, yet it becomes finer as heat is extracted at a greater rate.

In the initial stage of solidification, the growing dendrite is able to branch sufficiently to reduce supercooling (their driving force) to a very low value. However, as local solidification times increase, a coarsening process takes place, whereby initially formed arms become unstable and melt while others continue to grow. The resultant scavenging and fattening of dendrites is a result of the driving force in reducing the surface energy of the dendrites. Consequently, local dendrite arm spacing increases and the final eutectic material is gathered in coarse networks. As a result, final alloy properties will be adversely affected with respect to mechanical strengthening and ductility.

Although substantial benefits are possible by raising the cooling rate of a casting, the foundry is limited in its means to do so. Some factors which limit the cooling rate of investment castings are:

- 1) Both mold and metal temperatures may have to be raised in castings with thin sections for shrinkage feeding considerations.
- 2) Limitations on thermal conductivity of mold materials.
- 3) Limitations on natural or forced air convection to cool the mold surface.
- 4) Necessity of hot mold temperatures to fill thin sections may cause problems in heavier sections.
- 5) Limitations with respect to placement and complexity of metal and graphite chills for reasons of directional solidification.
- 6) Self radiation of adjacent mold surfaces prevents rapid cooling of these areas in the high temperature range.
- 7) Location and concentration of gates and risers cause hot spots within the casting and limit practical cooling rates.
- 8) High superheat needed to prevent segregation of high melting point elements in some casting alloys, discourage rapid cooling.

Inoculating Agents:

As large undercooling producing fine grain size by homogeneous nucleation is not possible in commercial heterogeneous casting alloys, inoculating agents are often added to the molten alloy. Control of grain size by the use of 'grain refiners' are commercially very popular but perhaps the least understood of all methods.

The nature of heterogeneous nucleation and its relation to inoculant effectiveness has been reviewed by many authors. A brief summary of inoculant effectiveness in molten aluminum alloys is shown below in Fig. D.₇

Compounds used to study the Heterogeneous Nucleation of Aluminum from its melt

<u>Compound</u>	<u>Nucleating Effect</u>
VC	strong
TiC	strong
TiB ₂	strong
TiAl ₃	strong
AlB ₂	strong
ZrC	strong
NbC	strong
W ₂ C	strong
Cr ₃ C ₂	weak or nil
Mn ₃ C	weak or nil
Fe ₃ C	weak or nil

Fig. D

Based on classical heterogeneous nucleation theory, the general characteristics of a good grain refiner can be stated simply. The refiner should be one that produces a small contact angle between the nucleating particle and the growing solid. This implies a high surface energy between particle and melt and a low surface energy between solid and particle. The surface energy between solid and particle should decrease with decreasing lattice mismatch between particle and solid. In addition to this criteria, a successful nucleating agent should be as stable as possible in the molten metal, possess a maximum of surface area, and have optimum surface character (perhaps be rough or pitted).

Titanium-Boron Alloys:

Titanium-Boron (5%Ti-1%B) master alloys have been accepted commercially as an optimum agent for grain refinement. The resulting TiB₂ and TiAl₃ particles act as excellent nucleation sites for grain multiplication and are reasonably stable in the melt. For more information regarding the master alloy, see appendix D.

Refinement Mechanism:

Upon addition of grain refiner to the aluminum bath, all constituents melt and dissolve except the fine TiB_2 particulates which disperse into the melt. Upon cooling of the melt, during casting and solidification, a grain of TiAl_3 is nucleated preferentially on each stable TiB_2 particulate. The TiAl_3 substrate thus formed has a crystal structure closely resembling pure aluminum, and hence nucleates the growth of a dendrite. The only requirement for grain refinement is that TiAl_3 be present and active as a nucleant before other impurities can nucleate.

Grain Refining Curve:

According to Pearson¹³, the grain refining curve is a combined effect of two distinct variables. Curve AOB is the consequence of two different time dependent processes of opposing effect, namely on one hand, and improvement in the 'conditioning' of the nucleant particles during the "contact time" and on the other a progressive decrease in effective nucleant particles in the melt during "fade", as indicated by the lines AA' and B'B respectively (see Fig. E). Line B'B is a result of TiB_2 particle coalescence and settlement (appendix D) and line AA' is a result of TiB_2 dispersion in the melt due to thermal diffusion and mechanical mixing.

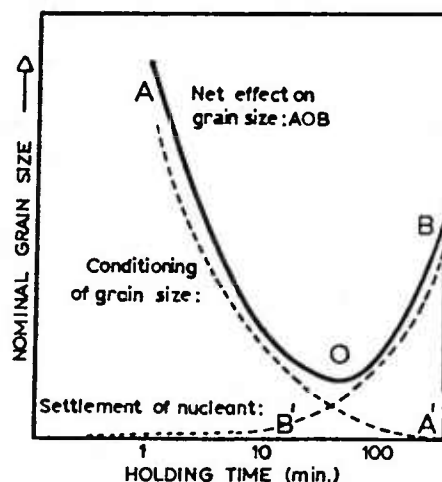


Fig. E

Figure F below, summarizes some of the grain refining data collected by Cercast for alloy 201. As anticipated, initial inoculations of grain refiner required a conditioning period, whereby the TiB_2 particulates are mechanically dispersed, to produce optimum nucleating conditions within the test mold. After the optimum holding time was exceeded, further holding allowed TiB_2 particle coalescence and precipitation, and thus reduced the number of available sites for particle nucleation. Holding times of between 1 minute to 10 minutes are recommended for this particular alloy, with additions of between 0.01% and 0.02% Ti (utilizing the 5:1 Ti/B master alloy). As a result, ladle additions were implemented for the 201 alloy utilizing controlled holding times between inoculation and casting.

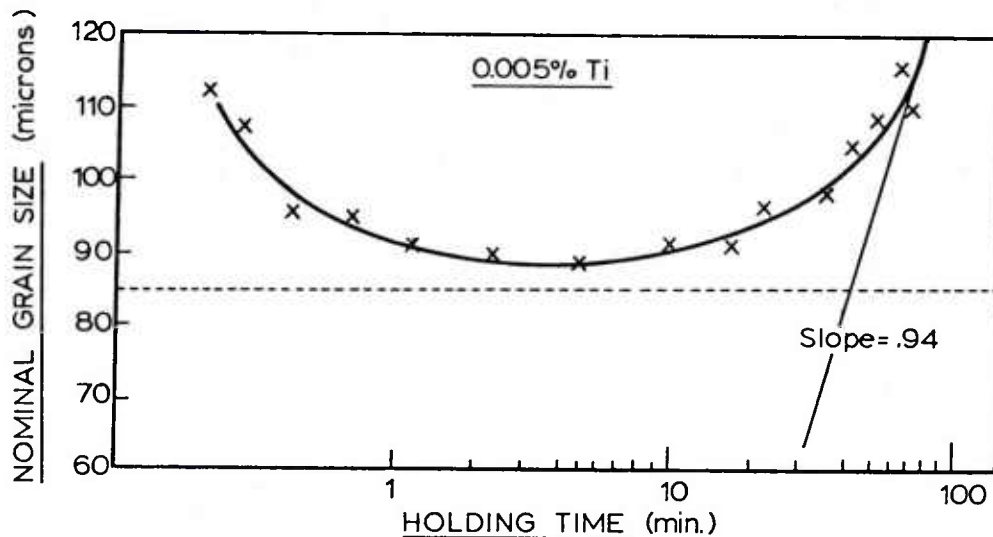


Fig. F

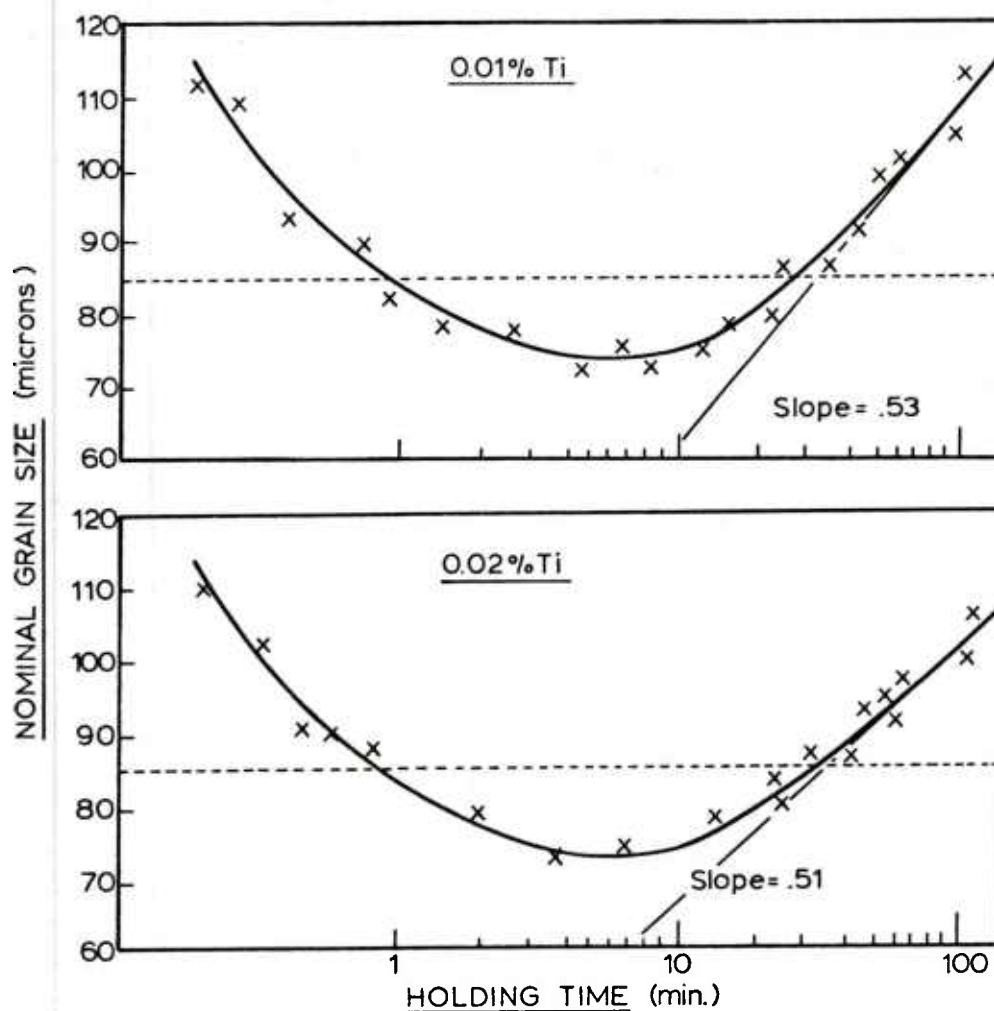


Fig. F

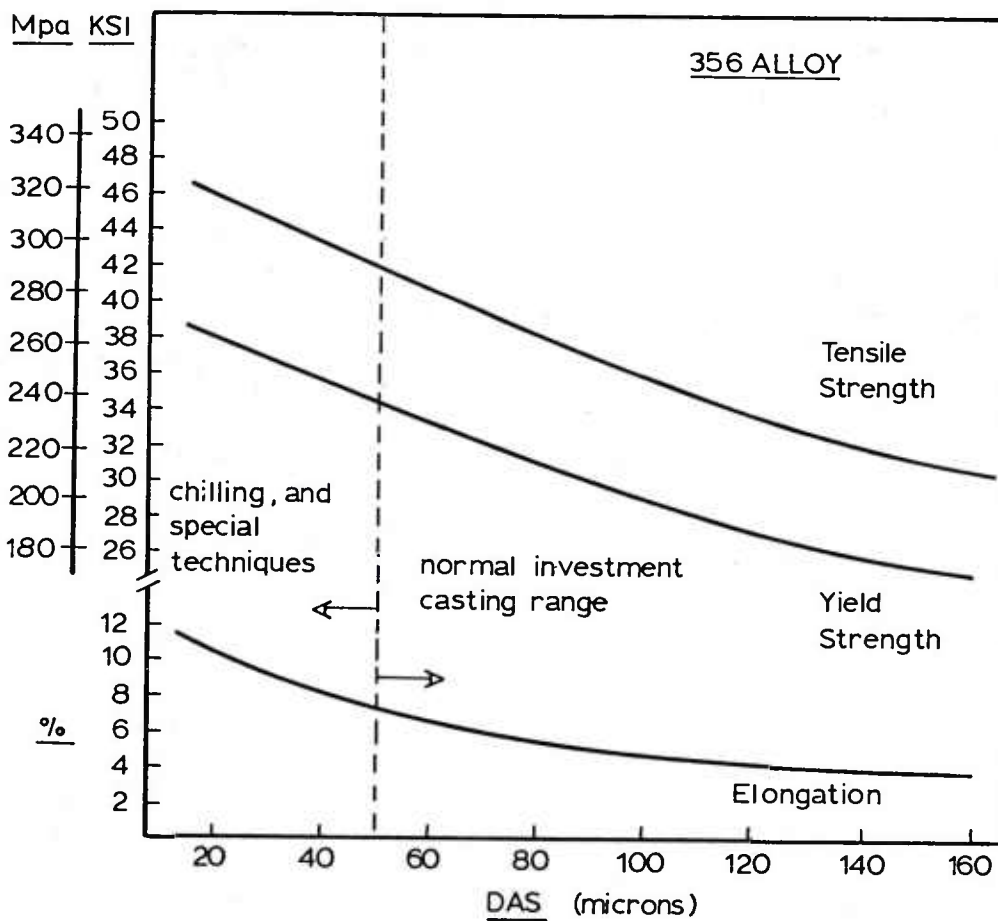
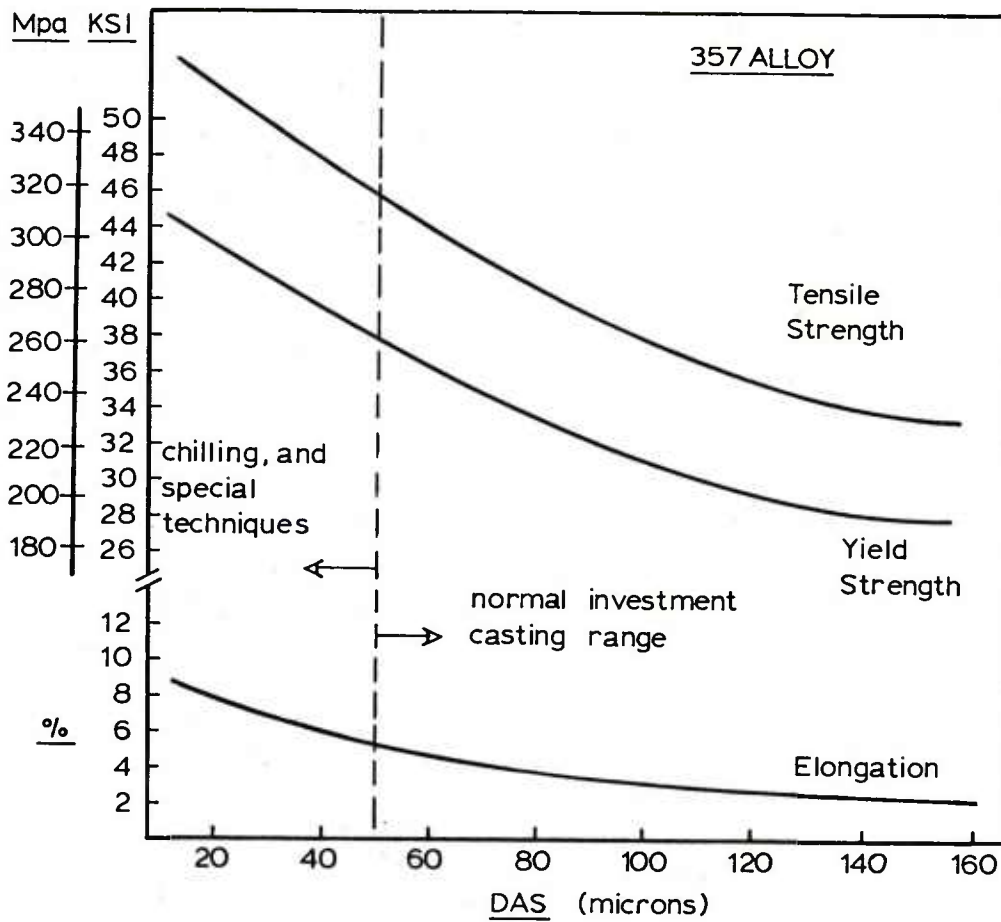
Susceptibility to Refinement:

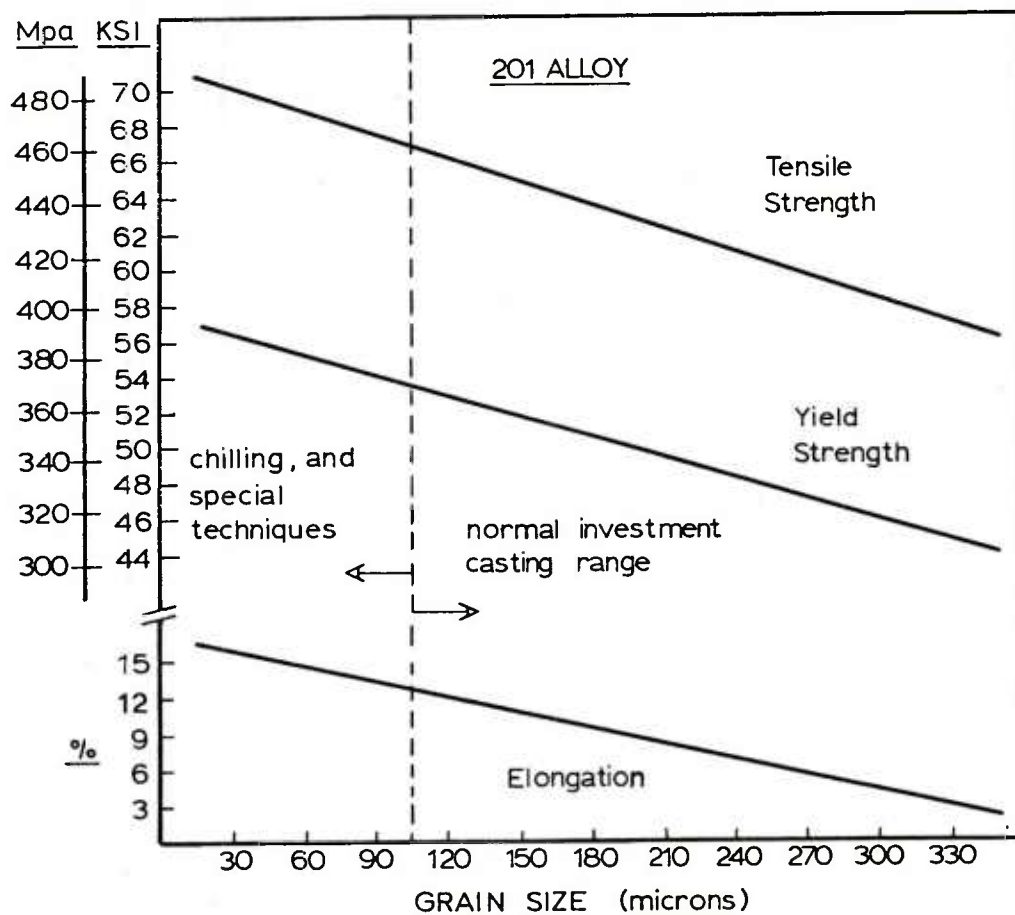
Aluminum silicon pre-alloyed ingot alloys distributed from the producer, contain adequate amounts of Titanium based grain refiner for most casting applications. By experience, these alloys have shown little response with respect to additional refinement susceptibility. Batch additions of refiner to the holding furnace at the onset of casting is usually sufficient, as the refining effect deteriorates very slowly.

High property, high integrity aluminum copper alloys are very susceptible to grain refinement, and require optimum nucleating conditions to prevent hot tearing and large grain size. Properly timed efficient ladle additions of grain refiner are preferred over batch furnace additions and produce the optimum nucleation effect without supersaturating the melt with excess Titanium. The nucleation effect resulting from dispersed TiB₂ particulates in this alloy system, is short lived, due in part to the relatively high holding temperatures required to prevent segregation of high melting point elements (Copper and Silver) upon casting.

Effect of Grain Size on Mechanical Properties:

Fig. G, H, I, represent the effect of grain size on mechanical properties, for the three most popular casting alloys used for aerospace applications (356, 357 and 201). The values presented serve only to show the grain size effect and may vary depending on the chemistry, density, radiographic quality and heat treatment of the particular casting.





201 ALLOY T7

Fig. I

Grain Size Determination for Problem Solving:

A basic check for casting section strength may be performed by a grain size investigation of suspect areas. Barring variations in radiographic quality, areas with large grain size will be weakest, irrespective of melt chemistry and heat treatment variables. Chilling fixtures, grain refinement, heat treatment and melt chemistry may then be optimized, to reduce grain size and bring the area to desired mechanical properties.

As heat treatment response depends on grain size, critical casting areas should be investigated. Large grain sections having a coarser eutectic, will age faster than castings having smaller grain size. Coarse grain areas may fully age in two hours, where as fine grain areas achieve optimum properties at perhaps ten hours of artificial ageing.

The determination of grain size will also help the foundry in deciding whether chilling is necessary and how severe such chills have to be in order to achieve a grain size which, when heat treated, will result in desired properties.

The same method may be used for optimization of gate and riser placement. As a localized section having large grain size cannot be gated and chilled simultaneously, the foundry may choose to move the gate to an adjacent area thus reducing the hot spot which results in a large grain size.

If an area exhibiting large grain size cannot be chilled sufficiently due to configuration problems, or a high mold/metal temperature is necessary to accommodate thin sections in the casting, the foundry may then decide to use modification (Al-Si alloys only) to help achieve the desired properties after heat treatment.

It should be noted that large grain size is not solely confined to heavy sections of the casting. Re-radiation of heat in confined complex areas of the casting, considerably increase the solidification time and hence result in a large grain size. Thermal mass of the mold may also be important in areas of confinement in cases, especially where the mold temperature is above the solidification range of the alloy.

In conclusion, the control of grain size is one of the single most important aspects in producing a casting with optimum properties. The increasing trend to design larger and heavier investment castings with more complex configurations leads to slower solidification rates and hence larger grain size. Effective use of grain refiner, chilling and special techniques adapted for each critical casting are thus necessary to produce castings of highest strength and ductility.

OPTIMIZATION OF CHEMISTRY

Basically two types of alloy systems are used in the production of premium quality aircraft and aerospace investment castings (Al-Si-Mg and Al-Cu-Mg). An understanding of elemental effects and impurity levels is essential in matching the chemical composition with the ultimate attainment of required casting properties.

Control of Impurities:

Iron is an impurity in most alloy systems, and drastically reduces elongation by the presence of primary precipitates and needles in the cast alloy. High purity Al-Si-Mg and Al-Cu-Mg alloys are commercially available with iron levels as low as 0.05% and 0.03% respectively, and in order to retain alloy purity upon remelting, special crucibles and tools are required in the foundry. Ladle washes help prevent iron dissolution from steel skimmers, ladles and plungers, however high purity refractories are desired for most applications. For use where steel ladles or tools are necessary, proper iron alloy selection considerably reduces corrosion of iron by aluminium and subsequent iron pickup. (See appendix C)

High silicon alloys (356 and 357) are susceptible to precipitation of the alloying elements, thus forming sludge. The rate of sludge formation increases as the temperature of the molten bath decreases and the concentration of impurities increases. Local high concentrations of Fe, Mn and Cr or a combination of each or all, result in an insoluble sludge compound which segregates to the furnace heel and may subsequently be poured into a casting. Titanium-boron, strontium-silicon and beryllium based hardener alloys as well as iron pickup from foundry tools are some of the sources of Fe, Mn and Cr which may form harmful sludges in the melting furnace. In addition, charging of cold ingot or revert to the molten bath may cause sludge precipitation as a result of the temperature drop. It is therefore recommended to charge preheated metal only. This practice also increases the melting rate of the furnace and discourages hydrogen and oxide pickup from surface moisture and hydrated oxides on the aluminum.

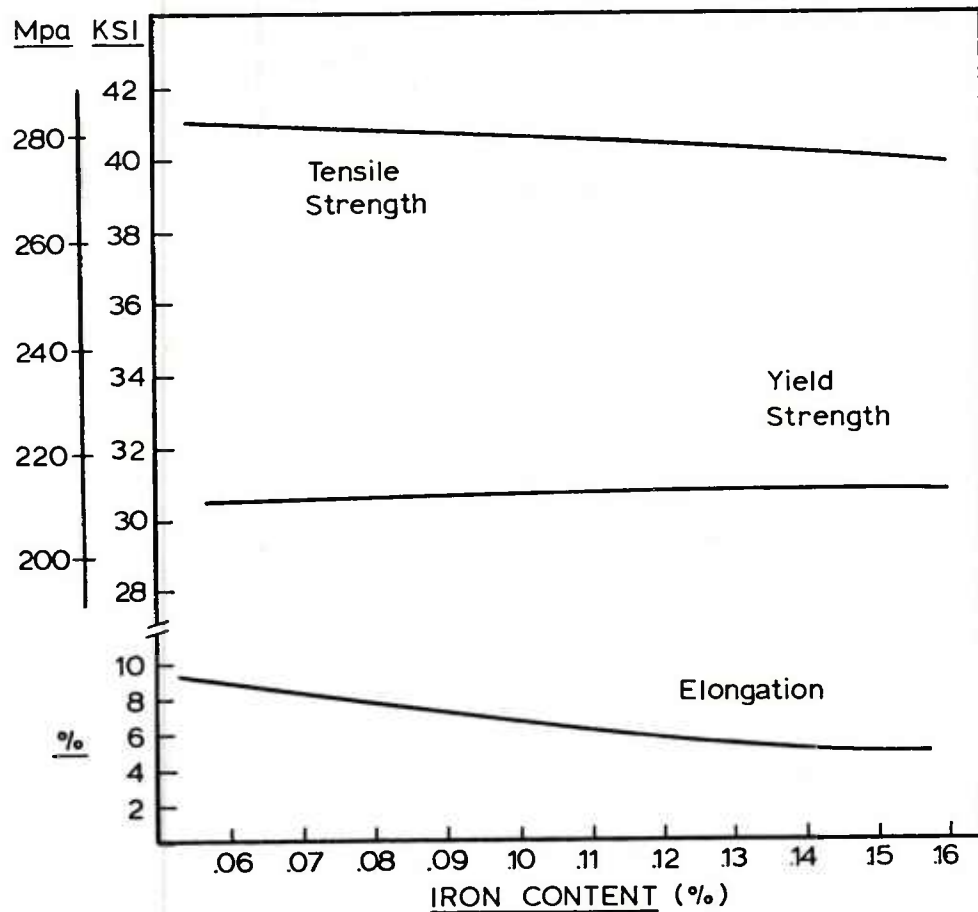
In the quest to obtain maximum grain refinement, the foundry may be adding excessive titanium or using it incorrectly, resulting in TiAl₃ and TiB₂ crystallites settling in the furnace heel. Proper foundry technique, especially small effective ladle additions prevent their formation and resulting harmful inclusions in the casting.

High purity (high property) Al-Cu alloys such as 201 and D25Z require low silicon levels for strength and ductility at room and high temperature applications. Although silicon pickup from various refractories and ladle washes is small, any alloy mix-up resulting in a piece of Al-Si alloy is an Al-Cu melt would have disastrous effects. Here alloy segregation is not only important, it is essential in producing quality castings.

Al-Si alloys modified with sodium must never be mixed with Al-Si alloys modified with strontium (or vice versa) or the subsequent modification effect of future additions will be ineffective. Rather than scavenging phosphorus, the Na and Sr will combine with each other and reduce the available modifying agent. It is thus imperative that the alloys, crucibles and tools used for say Na modification, must not be used in conjunction with Sr modification.

In the following pages, some data relating alloy concentration to mechanical properties of the heat treated alloy, will be presented. These graphs are intended as a guide-line only, as the final mechanical properties depend on many factors, including:

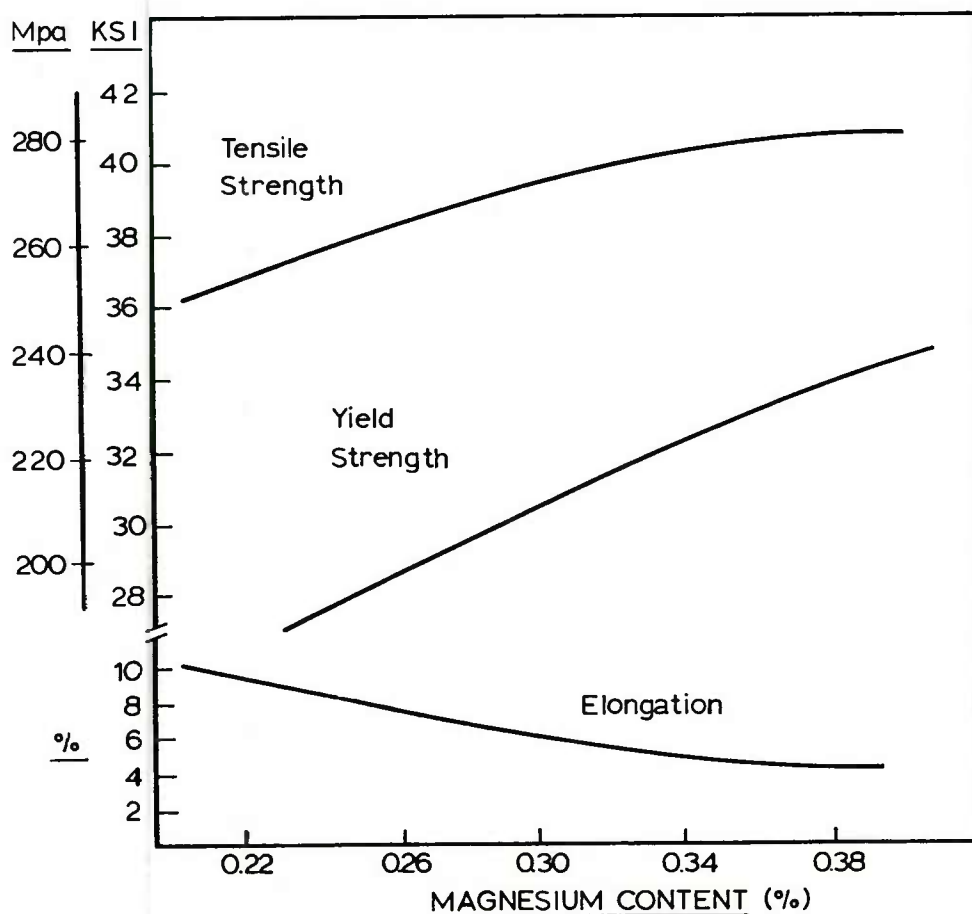
- 1) Solution heat treating time and temperature
- 2) Quench rate
- 3) Ageing cycle
- 4) Grain size of the casting
- 5) Other alloy effects



INVESTMENT CAST PLATE

356 ALLOY

Fig. A



INVESTMENT CAST PLATE

A356 ALLOY

Fig. B

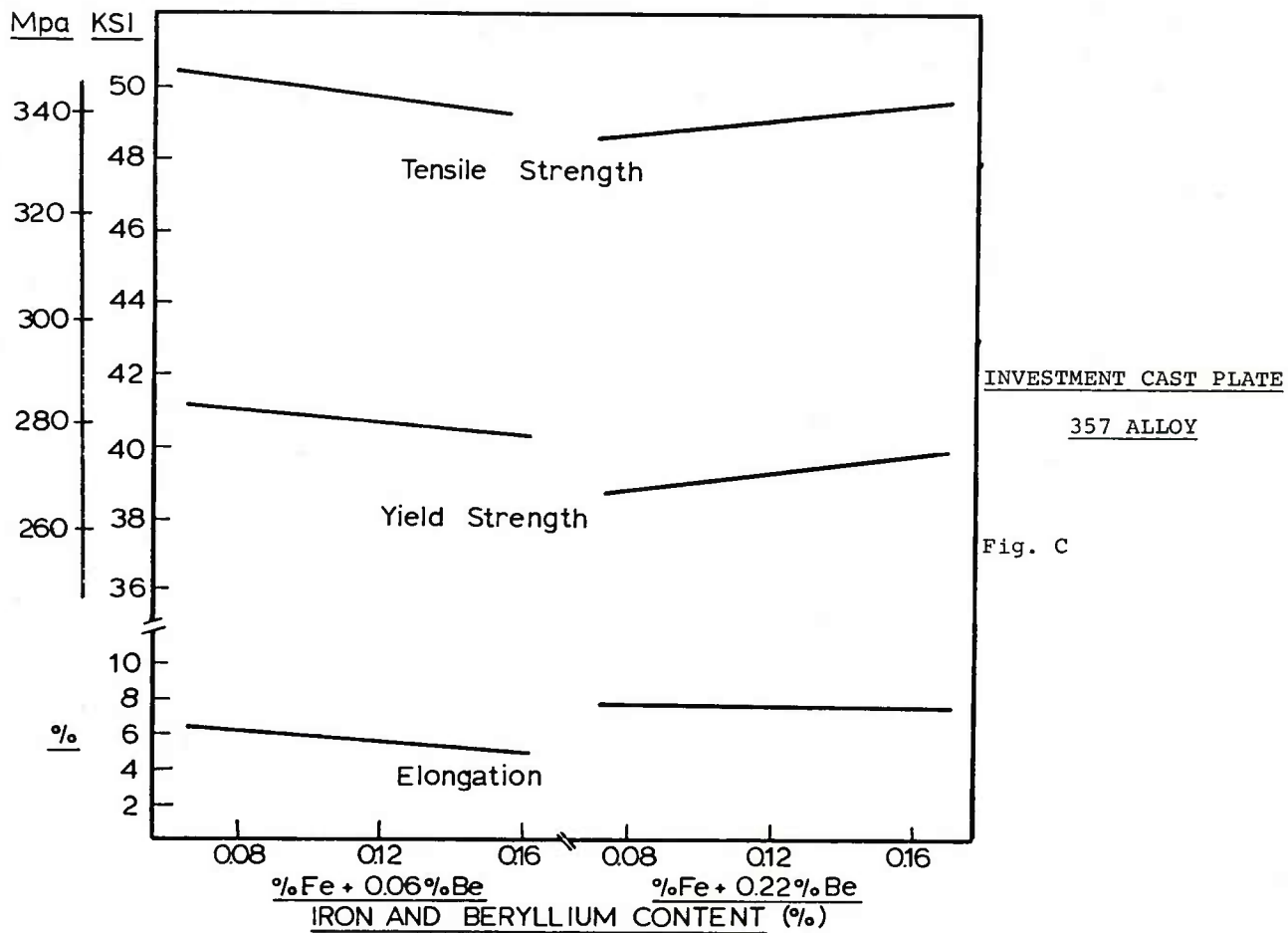


Fig. C

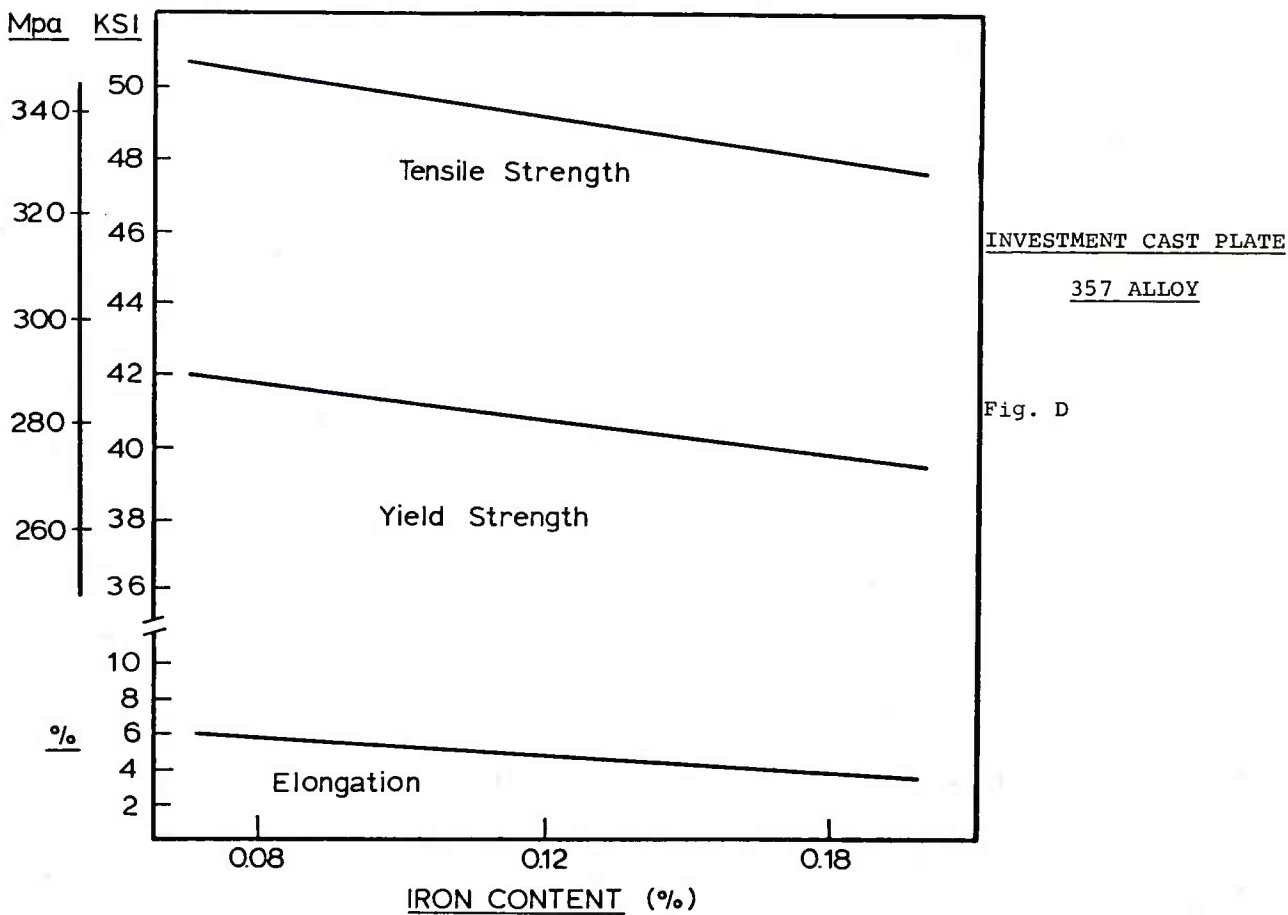
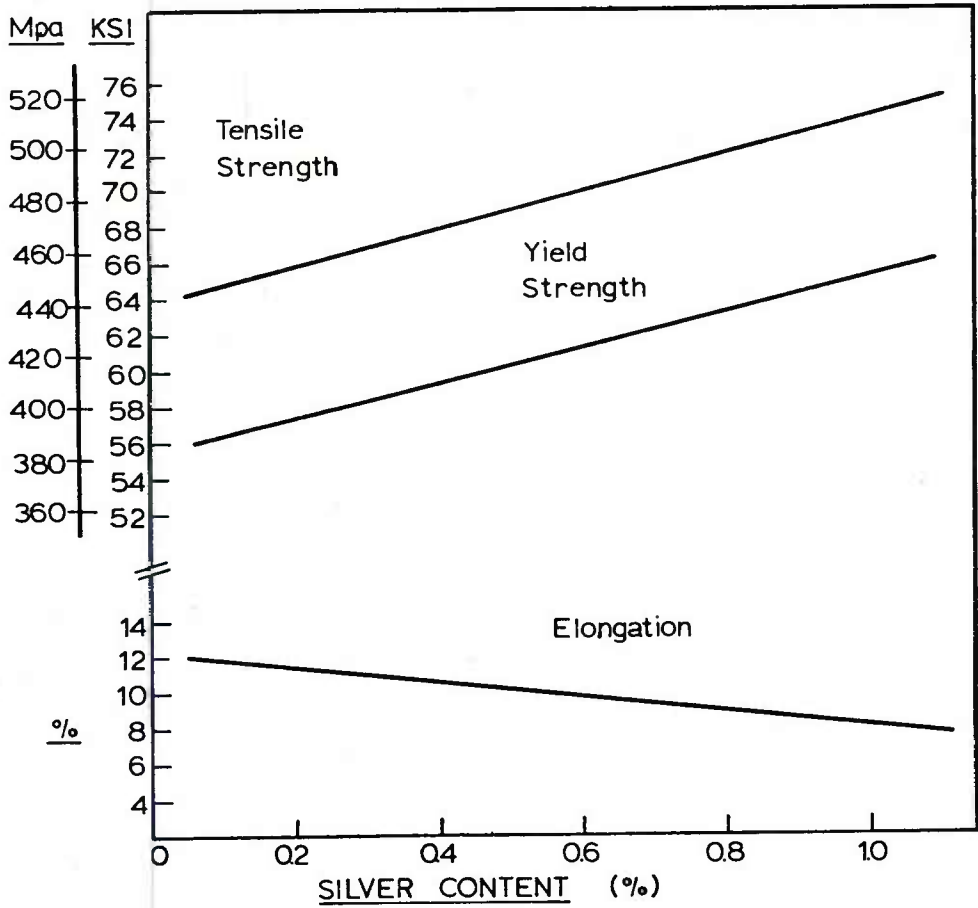


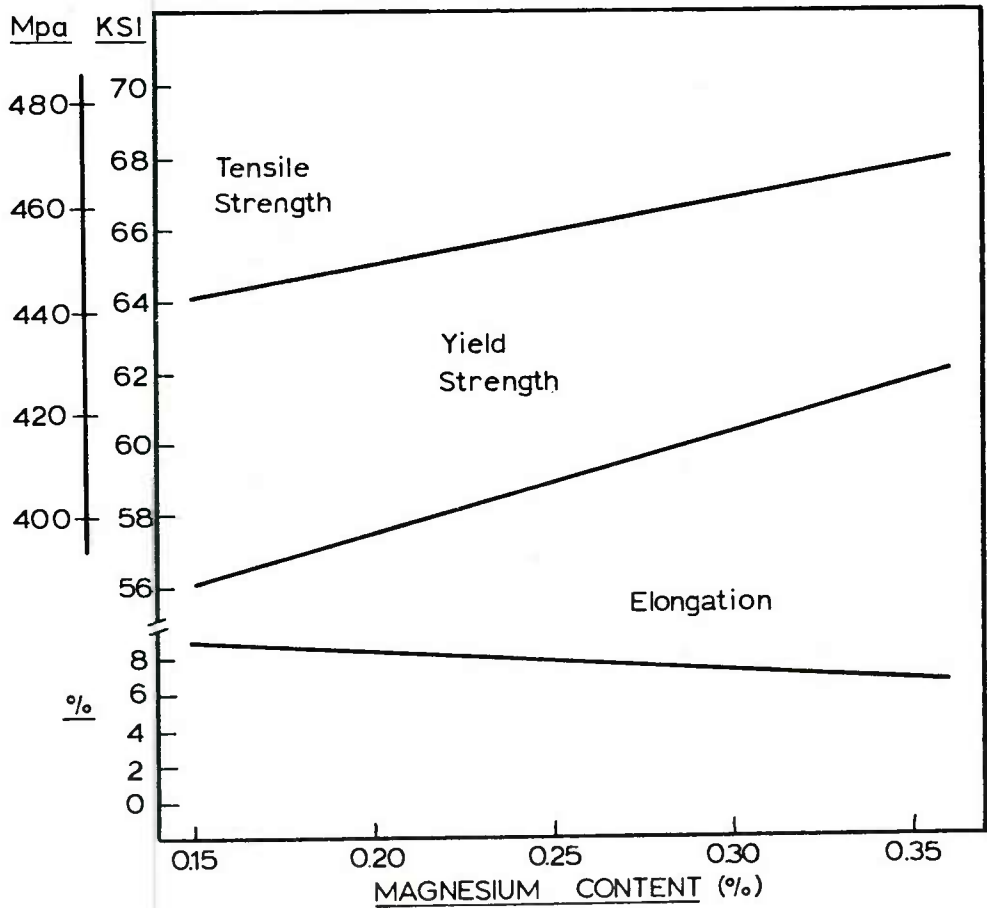
Fig. D



INVESTMENT CAST PLATE

201 ALLOY

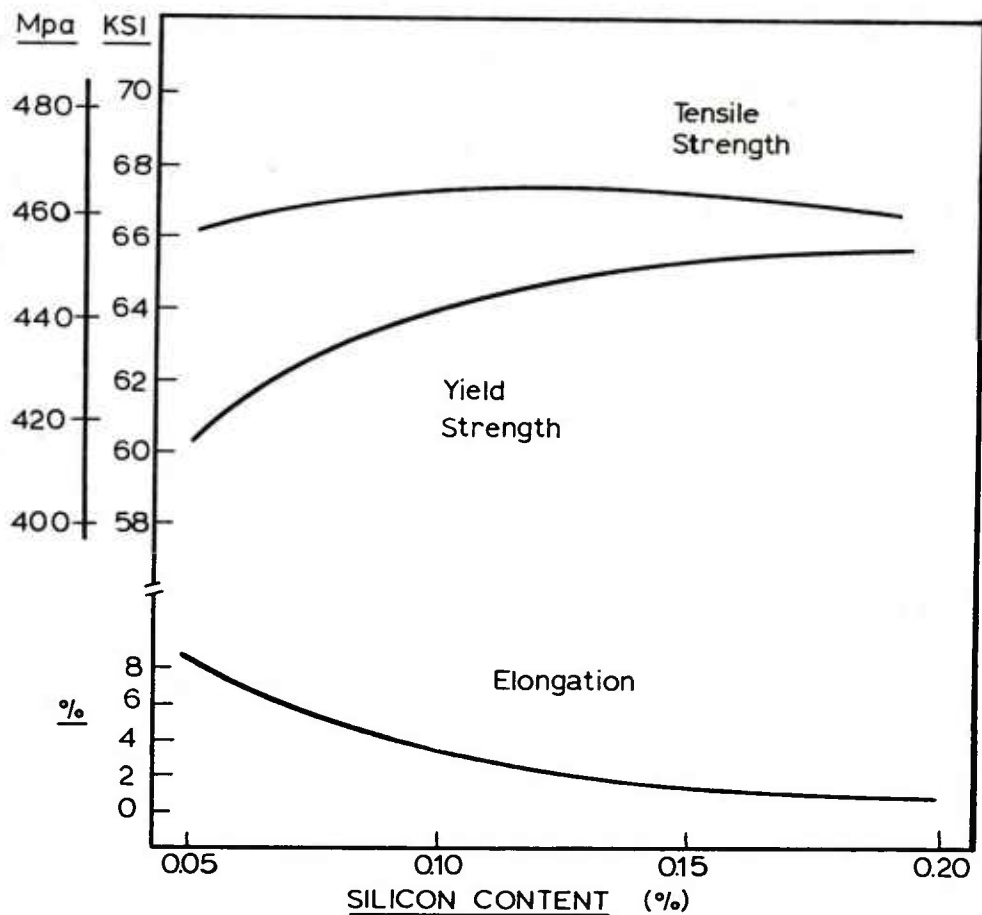
Fig. E



INVESTMENT CAST PLATE

201 ALLOY

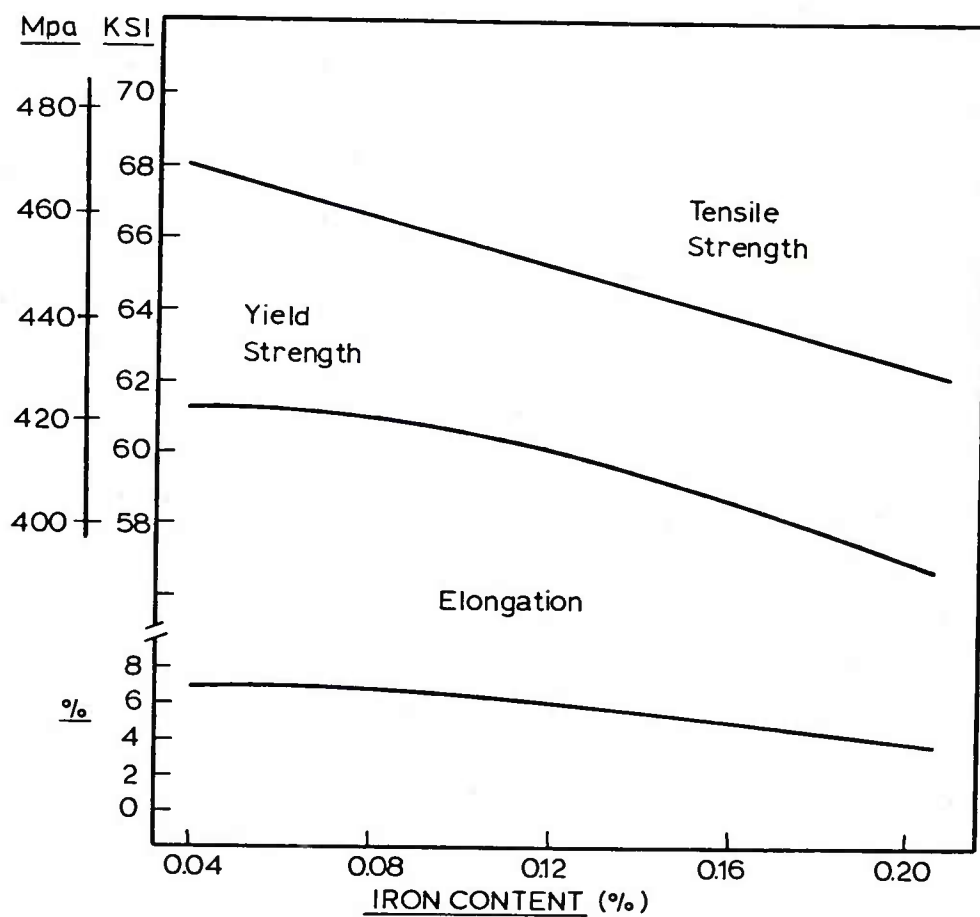
Fig. F



INVESTMENT CAST PLATE

201 ALLOY

Fig. G



INVESTMENT CAST PLATE

201 ALLOY

Fig. H

MODIFICATION

Simply stated, modification is intended to mean the alteration of the silicon particles in the eutectic structure of a hypoeutectic (13% Si) aluminum-silicon alloy from the sharp needlelike pattern normally found in such alloys, when unmodified, to the rounded more finely divided silicon eutectic particles in a modified structure. Both unmodified and modified structures are depicted below in Fig. A for comparison.

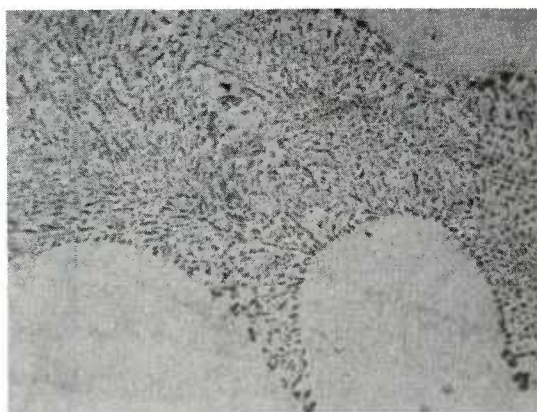


A356 ALLOY

Unmodified Eutectic

400X

Fig. A



A356 ALLOY

Modified Eutectic

400X

Fig. A

Acicular Structure:

The unmodified acicular structure of silicon eutectic is normal in hypoeutectic alloys, due to an impurity found in commercial alloys. The presence of phosphorus from two to ten ppm or greater, results in primary silicon nucleation on sites of aluminum-phosphide. Lack of the Al-P nucleant impurity prevents the formation of primary silicon crystals and yields a finely divided eutectic. Phosphorus concentrations in the range of approximately 0-1.5 ppm P result in a lamellar eutectic structure. The lamellar structure is intermediate between acicular and modified and also results in intermediate type mechanical properties.

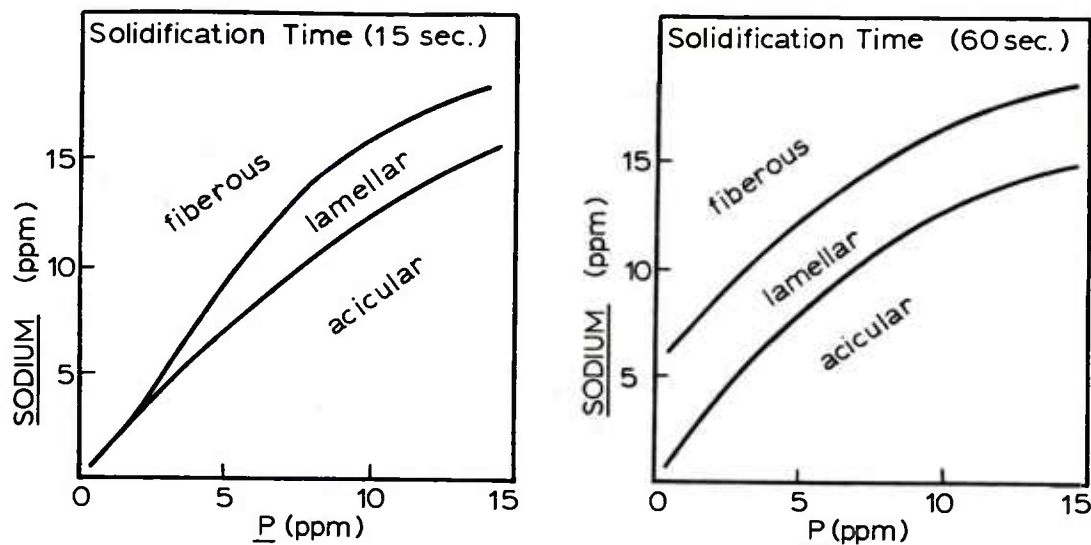
Modified Structure:

The addition of sodium, strontium or antimony in trace amounts (0.002-0.2%) modifies the cast eutectic structure of hypoeutectic alloys. The formation of NaSi_2 , Al-Si-Sr , Al-Sb and Mg_2Sb from these three elements are considered to dissolve phosphorus in solid solution within the compound. This is proven by microprobe analysis of the complex compounds mentioned. The resultant depletion of phosphorus from the liquid alloy results in a modified structure. While Na and Sr additions result in a modified eutectic if properly used, antimony only yields a lamellar type structure. It is therefore considered that sodium and strontium are superior modifying elements, despite other properties which make them more difficult to use.

Depending on the amount of phosphorus in the melt, varying amounts of modifier must be added to dissolve the phosphorus. Too much modifier however will cause coarse intermetallic primary phases to form, which are harmful with respect to mechanical properties.

Sodium Modification:

Sodium was the first element used to modify Al-Si alloys. The higher the phosphorus content of the alloy and the slower the cooling rate, the greater the minimum quantity of sodium needed to modify the eutectic. (see Fig. B)

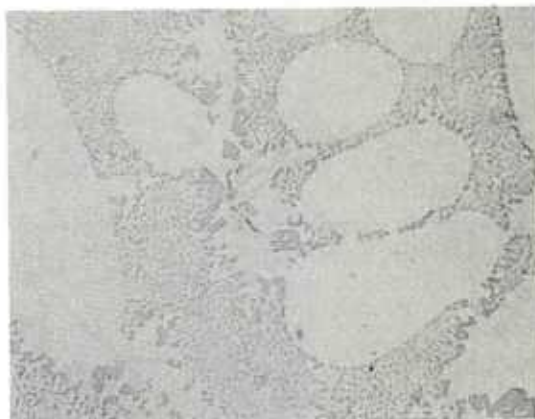


Effect of Sodium and Phosphorus on Modification

Fig. B (8)

Addition of sodium is achieved mainly by two methods: (1) plunging of vacuum packed sodium under the melt until dissolved, or (2) surface treatment of the melt with sodium fluoride salt mixtures. Premodified alloy ingot containing sodium is also available from most aluminum suppliers.

Sodium treatment for modification requires careful control; too much sodium produces an overmodified structure characterized by bands or islands of relatively coarse constituents, too little produces a partially modified structure. Such a treatment is temporary, as sodium oxidizes and evaporates from the melt surface with burn-off rates increasing with melt holding temperatures. With the loss of Na, the cast structure reverts back to its original morphology. Practical holding times for Na modified melts are only a few hours, before significant modification is lost.



Overmodified alloy A356

Fig. C

Strontium Modification:

Strontium qualitatively behaves in a similar manner to that of sodium (see Fig. D) by interacting with phosphorus to promote the formation of a fibrous eutectic. Strontium concentrations required for modification are higher than that of sodium, but the rate of loss of strontium is significantly lower. Stable melts producing modified cast structures may be held in excess of ten hours before significant strontium loss is noted.

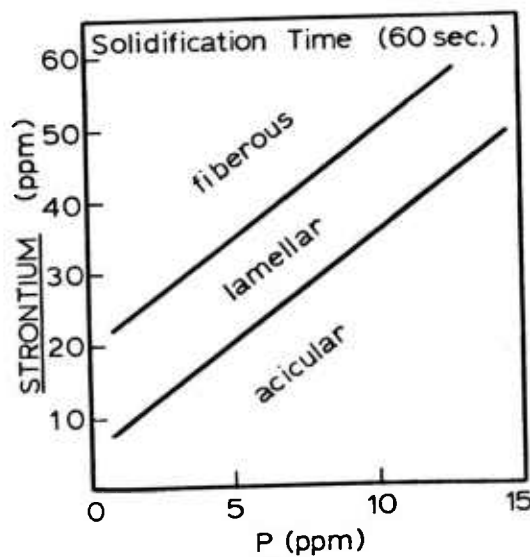
Effect of Strontium and Phosphorus on Modification

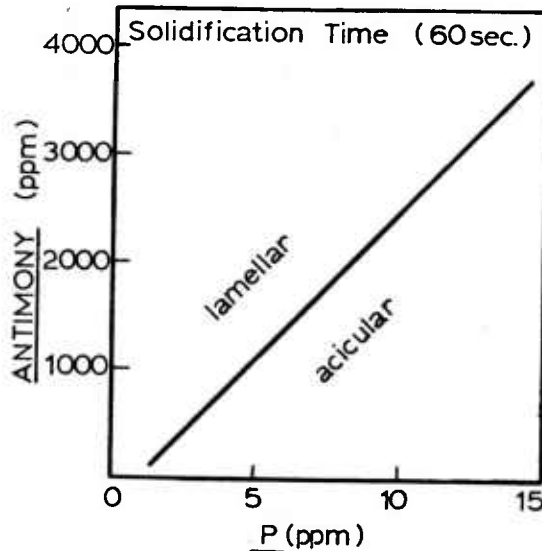
Fig. D (8)

While excess additions of sodium produce coarsening of the eutectic structure, decreased mechanical properties and intermetallic compounds of Na-Al-Si, no disastrous effects were noted with excess strontium additions. No aluminum banding or silicon coarsening results, although large Sr additions ($> 0.3\%$) yield the formation of faceted crystals of SrAl_2Si_2 .

Strontium is commonly added to the melt as (1) pure metal, (2) prealloyed hardener alloys such as $\text{Sr}10\text{-Si}14\text{-Al}$ and $\text{Sr}10\text{-Al}$ and (3) fluoride salt mixtures. Strontium although less dense (2.6 g/cc) than aluminum silicon alloys (2.7 g/cc) does not have as strong a tendency to initially float to the surface upon addition and oxidize, as does Na (1.0 g/cc).

Antimony Modification:

Modification of silicon eutectic with antimony results in a lamellar eutectic rather than a fibrous fully modified one. For rapid solidification this lamellar structure is extremely fine grained but becomes increasingly coarse for slower solidification rates. Neutralization of the phosphorus is by a similar mechanism than Na and Sr modification, ie; by phosphorus dissolution into Mg_2Sb_3 and $AlSb$ compounds. As before, the ability of these compounds to dissolve phosphorus is limited and hence an increase in phosphorus will require more Sb compounds to dissolve it. Quantatively more Sb is required to modify an alloy than Sr or Na, for the same phosphorus content. See Fig. E below.



Effect of Antimony and Phosphorus
on Modification

Fig. E



Antimony Modified A356

Lamellar Eutectic

400X

Fig. F

Due to the rapid fall in mechanical properties with coarsening of the cast structure, antimony modification is recommended primarily for rapid solidification situations.

Rapid solidification leads to small grain size which is easily modified with antimony to yield the lamellar structure. This structure is now easy to spheroidize upon heat treating and will yield excellent mechanical properties. Larger grain size and a coarser lamellar structure however do not spheroidize easily and yield less than spectacular mechanical properties.

Na-Sr-Sb Modification:

-Na and Sr both produce a fibrous eutectic.
 -Sb produces only a lamellar eutectic

-Na, Sr and Sb all show excellent modification potential for fast cooling situations.
 -Na and Sr show excellent potential for modification where slow cooling rates are found.

Sb: permanent modification
 Sr: slow oxidation and fade time (greater than ten hours)
 Na: fast oxidation and fade time (less than two hours)

For a cooling rate producing Sb: $\geq .23\%$
 a cast structure with DAS Sr: $\geq .005\%$
 of 60 μm , we need: (P-10ppm) Na: $\geq .002\%$

Modification for Investment Casting Foundries:

The varied cooling rates found in investment casting operations, coupled with average melt holding times of 1/2 to 12 hours, has resulted in the choice of strontium for an optimum modification agent. The modification effect thus produced, is equal to or better than that of sodium, yet is more stable in the melt. Although antimony produces permanent modification, the effort to remodify each melt with Sr is small, compared to the benefits of the superior microstructure produced with the Sr modification.

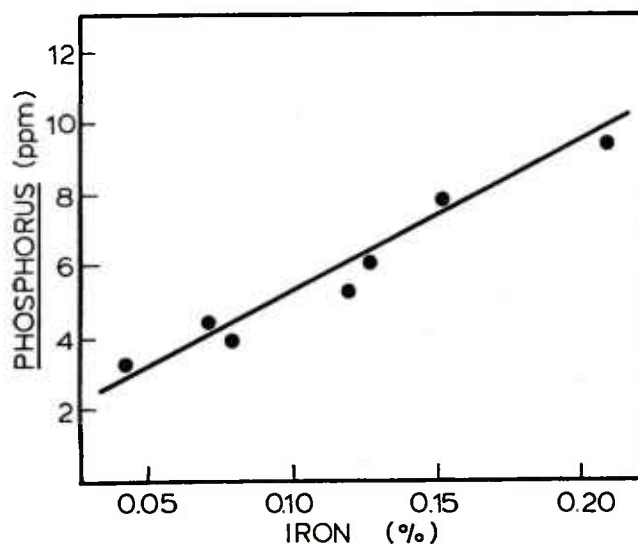
Cercast has launched many investigations into the modification of Al-Si alloys particularly with strontium. The effects of magnesium, phosphorus, cooling rate and form of the modifier have been determined, as well as an evaluation of present methods to predict modification tendencies before casting. Novel methods using thermal, differential thermal and conductivity analysis are currently underway at the Cercast foundry and specialized tests are being conducted in conjunction with McGill University.

Effect and Occurance of Phosphorus:

As seen from previous graphs, the percent concentration of phosphorus determines the degree of modification, for any fixed amount of modifier addition. For larger amounts of phosphorus in the melt, increased amounts of modifier are required, to change the cast structure. The following are only a few of the substances which may poison the aluminum with phosphorus.

- (1) Al-Ti-B grain refiner alloy hardener may contain up to 10 ppm of P.
- (2) Al-Sr-Si master alloy may contain up to 35 ppm of P.
- (3) surface treatment fluxes may contain P impurities.
- (4) some crucible glazes used in gas and electric melting operations may contain P.
- (5) specialized ceramic refractories and/or filters used in the foundry may contain a P based binder.
- (6) alloys high in impurities, particularly iron, may contain 15 ppm P.

An empirical relation has been noted between the Fe and P content of Al-Si alloys. As P and Fe are impurities which are found in the same sources, the following crude graph was plotted. (Fig. F)



Relationship between Fe and P in Commercial Al-Si7% Alloys.

Fig. F

Effect of DAS:

Figure G below shows the effect of cooling rate and hence DAS on an alloy of low (4ppm) phosphorus with variations in residual percent strontium after degassing and melt preparation. We see that for this particular alloy, an increasing amount of strontium is needed to modify the casting sections which cool slower and have a larger grain size.

The test was conducted with a proprietary Al-Sr10%-Si14% master alloy which was added twelve hours before melt preparation. This allowed thorough dissolution and reactivity of the strontium addition.

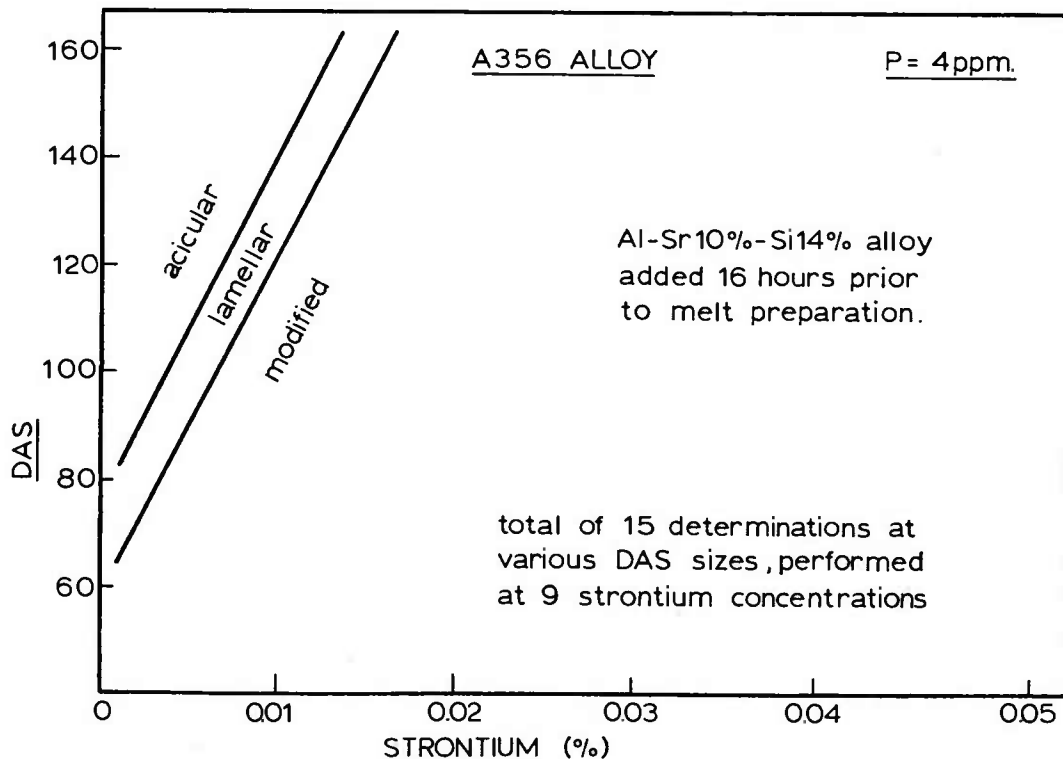
A356 Alloy

Fig. G

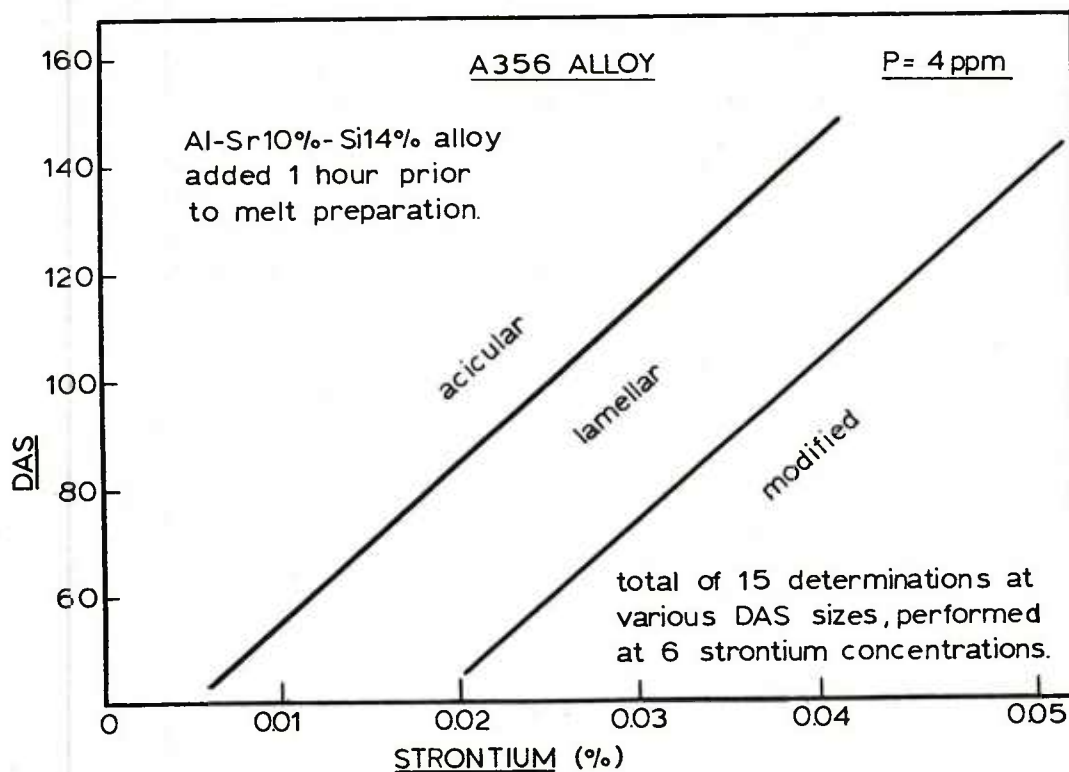
Effect of Holding Time:

Many foundries and alloy suppliers, have found an increase of modification effectiveness with holding time after the master alloy addition. In several cases, an addition of strontium to a melt which was already modified with strontium brought about a deterioration of the cast modified structure, which became coarsely lamellar instead of fibrous. After several hours or so the alloy would progressively revert to the fibrous structure.

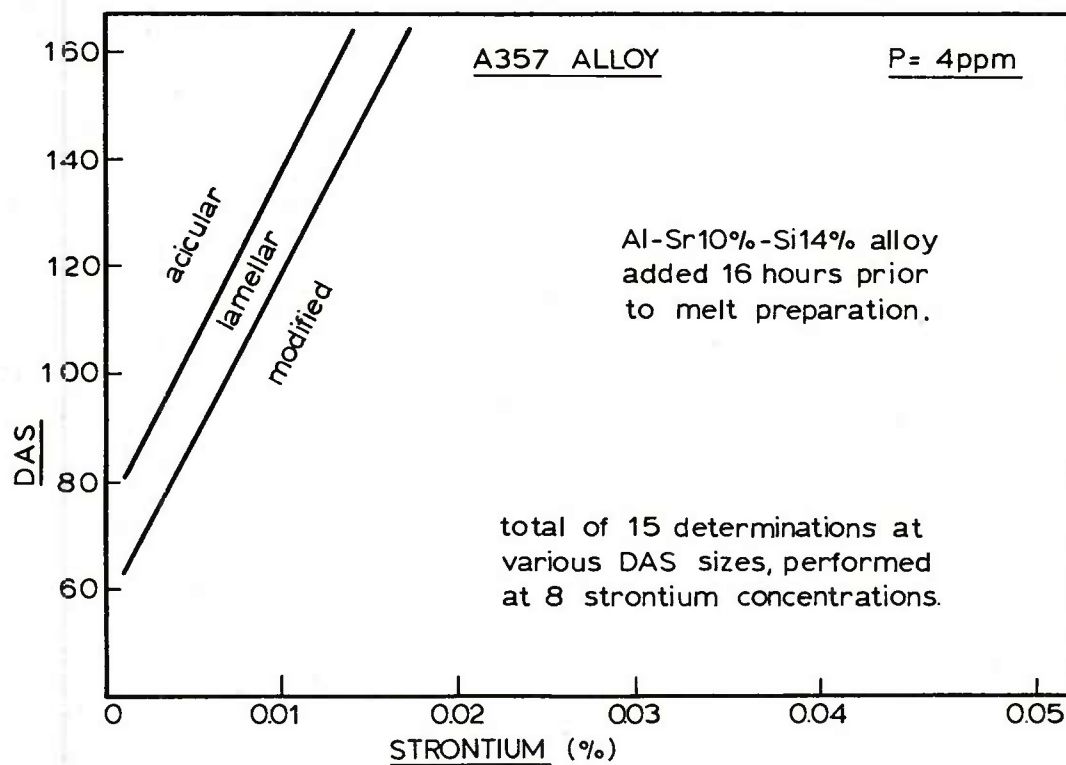
Although a theory has never before been presented, we feel that the inter-metallic strontium compounds formed in casting the master alloy in its production, are drastically less soluble, at normal melt holding temperatures, than is pure strontium. As a result, a holding time is necessary to dissolve these intermetallics and hence increase the strontium dissipation and effectiveness. Melts prepared one hour after master alloy addition proved to be inferior compared to sixteen hours holding, in modification potential as witnessed in Fig. H.

Effect of Magnesium Content:

Although some researchers, claim a 'coarsening effect' on silicon modification, when comparing Al-Si7% and Al-Si7%-Mg0.3%, we find almost no difference between 356 and 357 alloys, prepared under identical conditions. See Fig. I and compare to Fig. G.



A356 Alloy
Fig. H



A357 Alloy
Fig. I

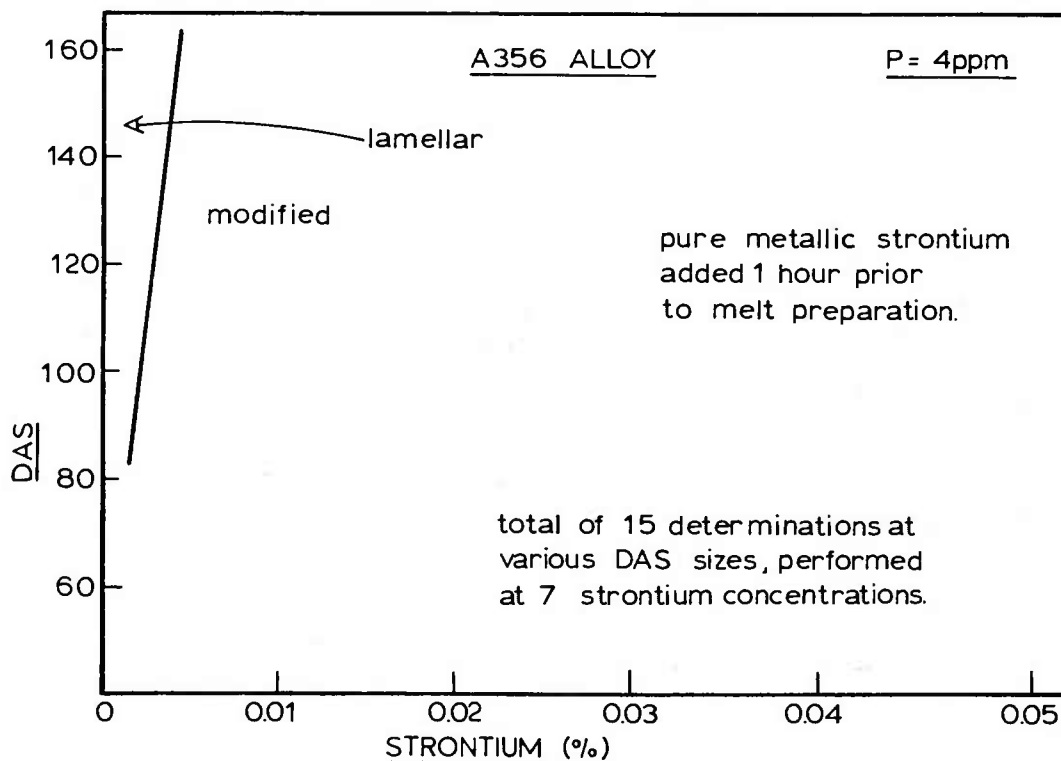
Effect of Modifier Chemistry and Morphology:

Fig. J summarizes the results of alloy melts prepared using a pure Sr addition plunged under the melt surface for a few minutes. The superior effect of the pure Sr addition is attributed to two effects:

- (1) Where as strontium master alloys (particularly those containing Si) are high in Fe and P, pure strontium may be added with little contribution of P to the melt.
- (2) Pure strontium additions dissolve readily compared to the intermetallics found in pre-ingoted master alloys.

Cautions when using Pure Strontium:

- (1) Strontium should be carefully packed and protected from moisture during storage and use.
- (2) A specialized plunger design is necessary to allow thorough dissolution without subsequent melting, floating and partial oxidation of the Sr addition. Such oxidation will hinder the modification effect by limiting the concentration of soluble strontium present in the melt. Also, the harmful oxides thus produced will affect mechanical properties of the casting, as well as interfere with solidification feeding.
- (3) The oxidation and subsequent loss of dissolved strontium may not be apparent in spectrographic chemical analysis, as the oxide particles are readily mixed into the melt as finely divided particles. High and low spot readings however, indicate the presence of non-homogeneous oxide presence and indicate cause for concern regarding the effectiveness of modification.



A356 Alloy

Fig. J

Effect of Modification on Feeding Distance:

Modified alloys have a tendency for increased shrinkage susceptibility compared to the unmodified alloy, especially in thin wall sections where rapid solidification occurs with little temperature gradient. This is attributed to the undercooling resulting from solidification of a modified alloy. In general, gating of a casting must be reviewed when changing from an unmodified to a modified alloy.

Effect on Mechanical Properties:

To evaluate the effect of modification on mechanical properties after heat treatment, we have combined the tensile strength (T.S.) and elongation figures of the test section, to form a quality index, Q, which for 356 and 357 alloys is defined as:

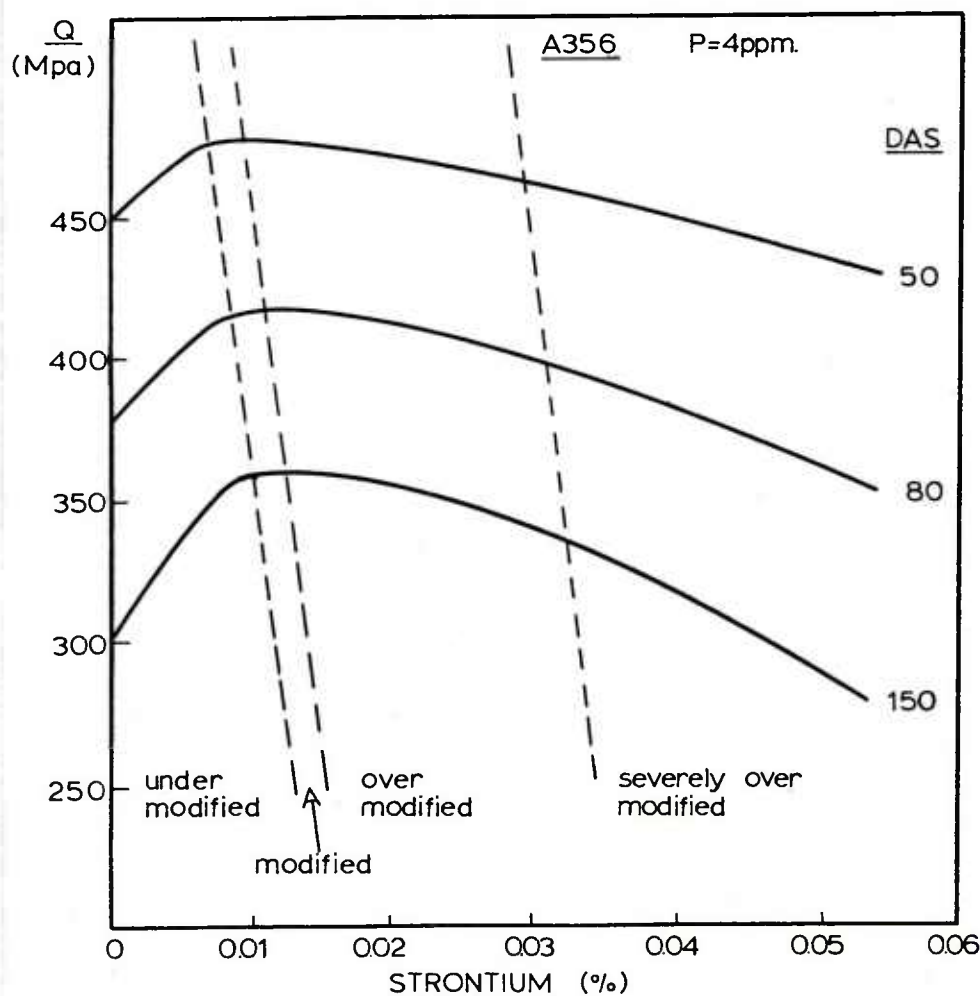
$$Q = T. S. + 150 \log (E\%)$$

This variation in Q is shown in Fig. K for castings of known DAS and freezing rates.

Although elongation is primarily affected by modification, T.S. is also increased. As a result T.S. and E% are represented together in a quality index figure.

Conclusions:

- (1) Mechanical properties are sensitive to Sr level and it is possible to overmodify and undermodify the alloy.
- (2) Sensitivity to residual strontium concentration appears to be more important as the freezing rate of the alloy decreases. In addition, undermodification is more critical than overmodification as seen from the slope of the curves. Hence in practice if determination of modification in the foundry is not adequate, it is preferable to slightly overmodify rather than undermodify.



QUALITY INDEX VS. Sr%

Fig. K

Methods of Determining Modification before Casting:

Due to the compounded effects of:

- (1) cooling rate
- (2) alloy chemistry
- (3) P content
- (4) type of modifier
- (5) melt holding time after addition
- (6) melt preparation and degassing procedures

On modification of the desired casting section, methods have been proposed and devised to determine the alloy's capability of modification prior to casting, to ensure optimum effects.

(1) Electrical Resistivity:

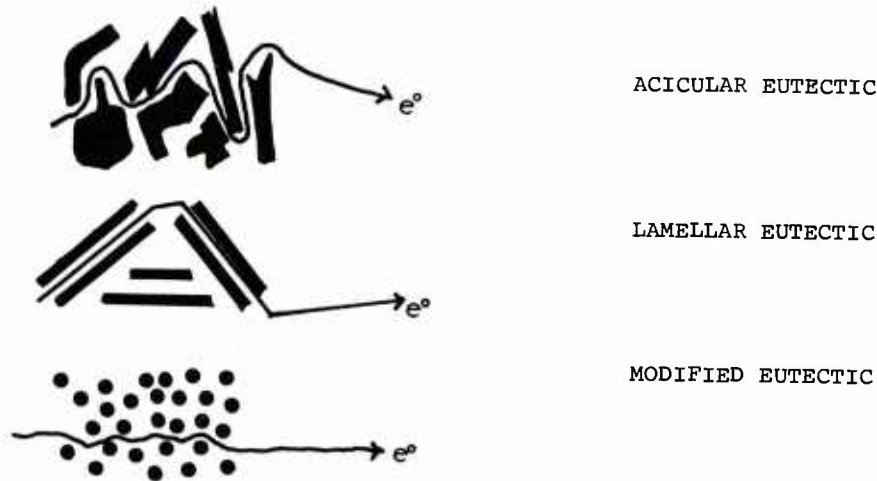


Fig. 1

Fig. 1 depicts the basic logic behind electrical resistivity measurements of modified and unmodified alloys. As the conductivity of aluminium is greater than that of silicon eutectic, electrons will tend to bypass the silicon particles and flow through the aluminum matrix when a potential difference is applied across a sample. Path length of the electrons will be a function of acicular, lamellar and modified configurations (decreasing resistivity).

Current developments have not been very successful or widely recognized but Cercast is re-exploring the possibility of using this method with improved techniques. Preliminary results using optimum shaped as cast test coupons and specific voltage and current levels, distinguish a 5-15% difference in resistivity depending on the degree of modification.

To be effective the coupon must:

- (1) Be of the same DAS as the casting section to be modified.
- (2) Have resistivities measured before and after modification, keeping other element concentrations in the melt constant.

(2) Simple Thermal Analysis:

This procedure entails the production of a time vs. temperature cooling curve of a test casting produced with both unmodified and modified alloys. A set of modified and unmodified curves are kept for comparison purposes with which the unknown is compared. Basically the amount of undercooling and drop in eutectic temperature will signify whether the sample is modified or not.

Advantages:

- (1) The modification potential of a prepared alloy melt may be evaluated as being acceptable or unacceptable for the production of the desired castings. If the melt properties are deemed to be undesirable, the melt may be further changed by altering the amount of modifier or holding for a longer time before casting.
- (2) Proper equipment setup will enable the operator to check for all of the variables which may contribute to the modification effect, provided that the cooling conditions in the test piece are identical to those anticipated in the casting.

Disadvantages:

- (1) The increasing amounts of magnesium, copper, iron and calcium have the effect of decreasing the eutectic temperature of the alloy whether it is modified or not. As a result of the effects of each element, a program would have to be developed to anticipate the combined effects of changing the element concentrations. This is necessary as production melts of Al-Si alloys will vary somewhat in chemical composition from one day to the next. After accounting for the effects of other elements on the drop of eutectic temperature, the effect of modification in lowering the temperature may be isolated. This complicated method may be bypassed however, if a cooling curve is produced from the production melt before and after modification, while keeping other concentrations the same during this period. The difference between the two curves will indicate changes in solidification patterns and indicate whether the sample is modified or not.
- (2) As modification is dependent on cooling rate of the alloy, various test castings would have to be produced at different cooling rates which correspond to the production casting. The cooling curves of these test castings would then be evaluated for suitability.

(3) Differential Thermal Analysis:

This method entails the production of a cooling curve from a test casting having the same cooling rate as that of the production casting. The curve would then be differentiated or analyzed for changes in slope and morphology. It is anticipated that certain aspects of the curve may change only for modification and be independent of changes in other elemental concentrations.

Advantages:

- (1) One curve need only be run at the completion of the modification procedure. The differential analysis on the shape of the curve will tell the operator whether the cast sample is under or over modified. Several test casting configurations will be available for the test so that the operator will pick a test casting mold which will yield the identical DAS and cooling conditions as those expected in the section of production casting desired to be modified. Total time for the analysis will be in the order of 2-10 minutes, depending on the rate of cooling employed for the sample casting.

Currently Available Thermal Analysis Instruments:

Currently available thermal analysis instruments marketed by Leeds and Northrup, Pechiney Aluminum and others have several drawbacks. Mechanical type strip chart recorders have too high an inertia to pick up details in the cooling curves for sensitive changes and thus obliterate these important curve changes. Some instruments do not take into account the effect of cooling rate on modification and use only one test casting mold for all analysis. Some of these instruments do not take into account the effect of other alloying additions in changing the value of eutectic temperature, and thus we expect that an unmodified and modified curve need be made of the same melt to determine whether the sample is modified or not.

Future Developments in Thermal Analysis:

Cercast is presently using a newly developed differential thermal analysis microprocessor unit, which is capable of determining the modification potential of a prepared melt for use in the production of high property investment castings. The unit produces cooling curves of a selected test casting with unequalled accuracy. Duration of the test, including computer manipulation of the stored data is less than ten minutes. The unit is far superior to those previously marketed, as all variables affecting the modification behavior of the alloy are accounted for. Physical set-up of the unit is simple and durable with temperature precision within 0.1°C.

HEAT TREATMENT

Micro and macro-segregation of alloying elements during solidification of the alloy under non-equilibrium conditions, requires specialized heat treatments to obtain optimum properties from each alloy. In most alloy systems, numerous tiny precipitates in the aluminum matrix prevent slip of crystal planes and thus make the alloy stronger than pure aluminum itself. The finer the dispersion of precipitates or 'zones', the more effective is the strengthening mechanism. Grain refinement in casting leading to dispersion of eutectic alloying elements, as well as solution-precipitation heat treatment which creates a finer dispersion, is essential to yield the strongest structure possible from each alloy.

The first stage in heat treatment is solutionizing whereby high temperature (510-543°C/950-1010°F) and concentration gradients promote diffusion of the alloying elements from the grain boundary (where they are concentrated during solidification) to the rest of the aluminum rich phase. This having been accomplished, the alloy is quickly quenched in air, water, oil or other fluid medium, to retain the alloying elements in a supersaturated solution at room temperature. Subsequent ageing at room or moderately high temperatures (149-204°C/300-400°F) promotes precipitation of alloy phases. In general, rapid or long ageing at high temperatures produces coarse precipitates. Slow ageing at lower temperatures produces numerous finer precipitates and result in an optimum alloy structure.

Precipitation in Specific Alloy Systems:

Aluminum-Copper-Magnesium:

In these alloys, room temperature hardening is attributed to localized concentrations of copper atoms forming Guinier-Preston zones. The GP zones are two dimensional disks shaped with a diameter of 30-50 angstroms. As ageing progresses, so do the number of zones, until they are only 100 angstroms apart (fully aged condition). During ageing, the GP zones become three dimensional and eventually form precipitates of CuAl_2 . Maximum hardness and strength occur at a stage intermediate between primary GP zones, and the CuAl_2 precipitates. Additions of magnesium to the Al-Cu alloys accelerate natural age hardening and result in some Al_2CuMg precipitates to form upon final ageing.

Aluminum-Silicon-Magnesium:

Strengthening of this alloy system entails the formation of zones rich in magnesium and silicon. The zones are needle-shaped approximately 200-1000 angstroms in length and are responsible for maximum hardness and strength of the alloy. Subsequent ageing produces coherent precipitates of Mg_2Si yielding an overaged alloy. The precipitation of Mg_2Si is accompanied by a drop in strength and ductility.

Aluminum-Copper-Zinc-Magnesium:

Initial stages of precipitation result in non-coherent GP zones 20-35 angstroms in diameter. Increased time and temperature of ageing results in coherent MgZn_2 , $\text{Mg}_2\text{Zn}_3\text{Al}_2$, as well as CuAl_2 precipitates. Again, optimum strength and ductility occurs before final precipitation of the coarse compounds.

Quenching:

The objective of quenching is to preserve as nearly intact as possible the solid solution formed at the solution heat treat temperature, by rapidly cooling to some lower temperature. While fast quench rates discourage premature precipitation of alloy elements (subsequently resulting in a better ageing cycle and hence better mechanical properties), they may induce warpage, cracking and stress concentrations within the casting which render the structure unusable, prone to stress-corrosion cracking or dimensional instability. In summary, advantages of mechanical properties must be balanced by the end use of the casting when deciding on the severity of the quench. Quench sensitivity of various alloys is depicted in Fig. B

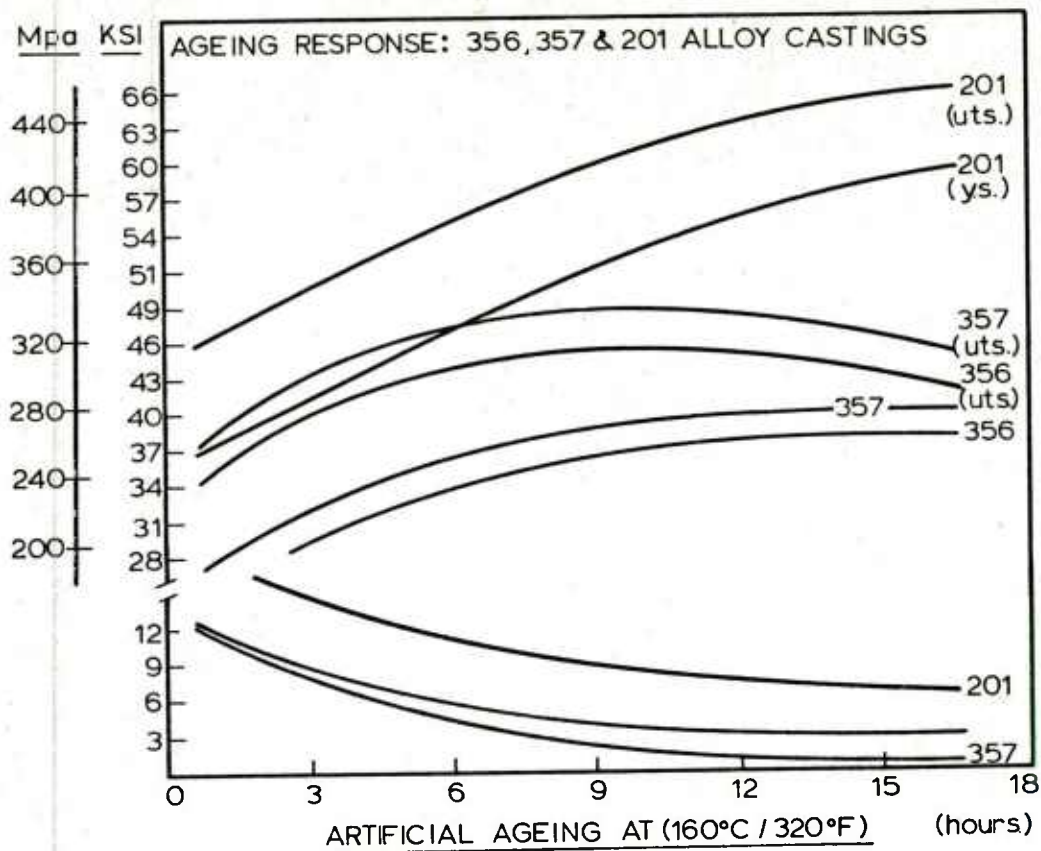


Fig. A

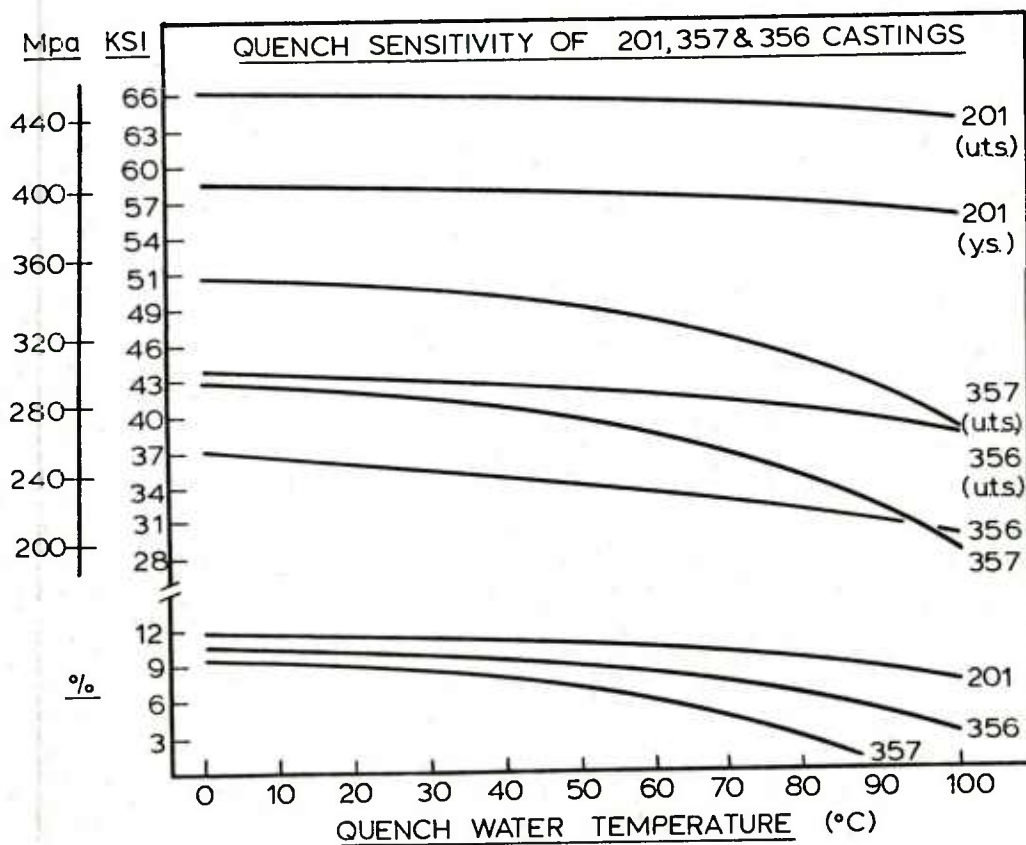


Fig. B

Solution Heat Treatment (Example D25Z Alloy):

Alloy composition:

4.10-4.50% Cu
0.25-0.40% Mn
0.35-0.45% Mg
2.75-3.25% Zn
0.17-0.23% Ti
0.02% max% Others

We may use a nominal composition for calculation of respective alloy phases:

3.0% Zinc
0.4% Magnesium
4.3% Copper

Taking into consideration the molecular weight of each element and its relative abundance, we may express the concentration of each alloy as follows:

31.8%	ZnAl	}
8.4%	Mg ₅ Al ₈	
59.8%	CuAl ₂	

100% of alloy elements

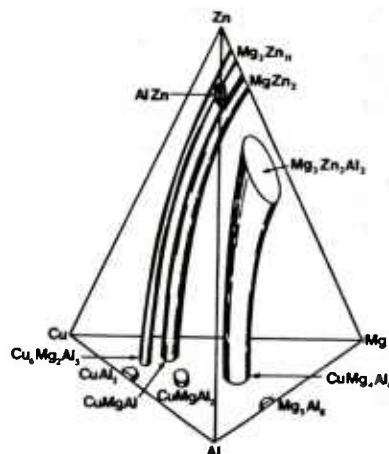
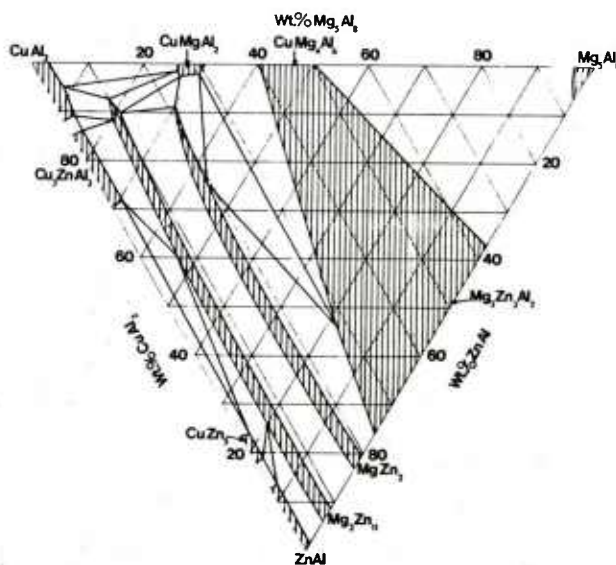


Fig. C

The monophase fields at the aluminum corner of the aluminum-copper-magnesium-zinc diagram.

The complete phase diagram is unfortunately lacking in information and is also extremely complex. One important feature of this diagram is that three of the phases in the Al-Mg-Zn system are isomorphous and completely miscible with three phases in the Al-Cu-Mg system.

Fig. D below depicts a projection of the aluminum corner of the Al-Cu-Mg-Zn diagram-phase distribution in the solid. Upon close examination of the diagram in the area pertinent to the D25Z composition we see that a combination of many compounds may be present in the grain boundaries of the alloy after solidification.



Al-Mg-Zn Phase Diagram

Fig. D

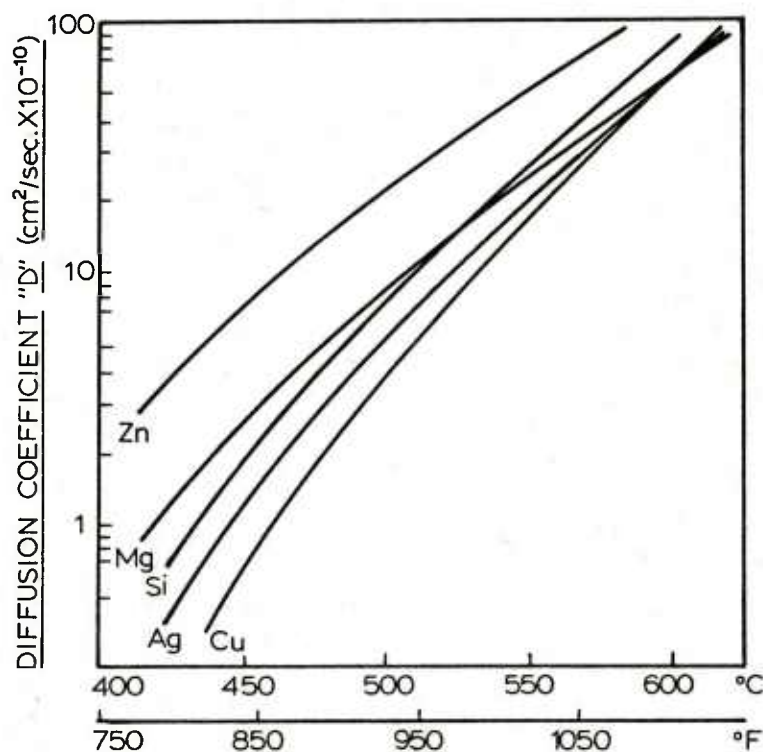
The following low melting eutectic compounds may be present:

<u>Compounds</u>	<u>Melting Point °C (°F)</u>
Mg ₂ Zn ₁₁	547 (1017)
CuAl ₂	548 (1018)
CuMgAl ₂	507 (944)
Cu ₃ ZnAl ₃	555 (1031)

In order to avoid eutectic melting (and subsequent voids in the grain boundary area upon cooling) of the low melting compounds, we conclude that a stage heat treatment is necessary:

Stage 1: Hold at just below 507°C (944°F) and allow the compound CuMgAl₂ to dissociate and diffuse into the aluminum matrix. Holding time will depend on the coarseness of the eutectic but should be approximately six hours.

Stage 2: Hold at a maximum temperature which is limited by other low melting compounds, grain growth at elevated temperatures, and general softening of the cast structure. Highest temperatures selected will reduce the time needed for the alloying elements to diffuse into the aluminum matrix. (for relative diffusion speeds of alloying elements in aluminum, see Fig. E) From experience, we see that we are limited by grain growth of the alloy, to set a maximum temperature. We pick 520°C (970°F) and a time of twelve hours. This should ensure adequate diffusion of the majority of alloying elements.



Diffusion rates as affected by temperature.

Fig. E

RADIOGRAPHY AND PENETRANT EXAMINATION

While radiography and penetrant examination are common non-destructive methods of flaw detection for shrinkage, oxides and gas porosity, they may be used to evaluate other possible metallurgical problems. Solute segregation, hot-tearing, eutectic melting and harmful intermetallic inclusions are some of the more important defects to consider when evaluating a casting by non-destructive testing (NDT).

Eutectic Melting:

A step type solution heat treatment should be used for aluminum-copper alloys (201, 202, 203, 204, 206, 208, D25Z, etc.) because of extreme segregation of the alloying additions during freezing, which results in areas of low melting eutectic compositions within the metal. The progressively increasing temperatures of the solution heat treatment result in the gradual homogenization of the structure so that melting or 'burning' is avoided. A detailed discussion is developed in appendix B.

The tiny voids formed at the grain boundary junctions as a result of eutectic melting are not recognizable by conventional radiographic techniques, yet are revealed by fluorescent penetrant inspection. Shown below in Fig. A are sections of an engine rotor (30 cm. dia.) which was cast in alloy D25Z. Half of the rotor was step heat-treated and the other half was heat-treated without intermediate temperature steps, and subsequently 'burned'. The uniform light green shimmer produced on the burned casting is a result of penetrant entrapped in the millions of microscopic pores of the casting surface.

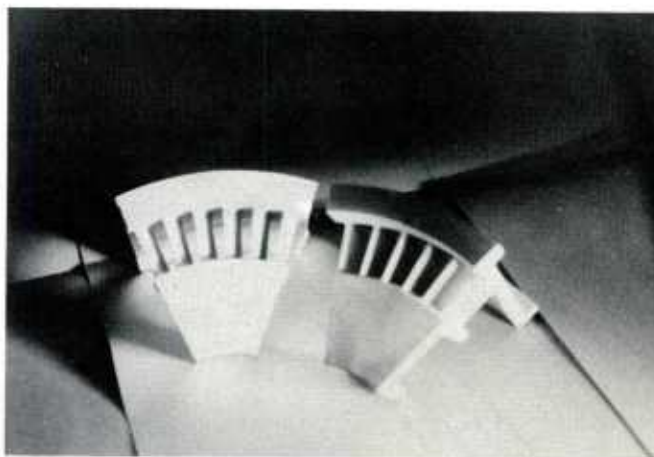


Fig. A

Segregation:

Segregation of alloying elements in a casting is either the result of 1) oversaturation of the alloy with elemental additions, or 2) adverse solidification conditions within the casting. As oversaturation can easily be avoided by temperature and chemistry controls, it will not be mentioned further.

All alloys with significant quantities of alloy additions are prone to segregation. Microsegregation of aluminum-copper alloys is of prime metallurgical importance, as any large areas of copper rich phase will be difficult to homogenize upon heat-treatment and thus result in a localized low strength brittle phase. An understanding of segregation formation, contributing casting conditions and casting geometry, coupled with a reliable and quick method of detection, allows the foundryman to develop techniques to eliminate future segregation and solve his present problems. Although a detailed discussion is developed in appendix A, a brief description of the macrosegregation phenomenon is summarized below.

Conditions which tend to lead to macrosegregation are:

- 1) Solidification of the alloy against a chill will result in solute (copper in Al-Cu alloys) segregation at the chill face.
- 2) Solidification of a casting with a temperature gradient perpendicular or opposite to the force of earth gravity will result in positive segregation in the lower parts of the casting, (for alloys where the solute rich liquid is heavier than the molten alloy).

(3) Feeding a large chilled section of the casting with a small riser (or other small section of the casting) will result in negative segregation of the alloy at the junction of large and small sections, and positive segregation at the extremities of the large section.

(4) Feeding a small section of the casting with a massive section or riser will result in positive segregation in the junction area between small and large sections. This phenomenon is a direct result of the large heat conduction from massive to thin section in that area.

(5) Any abrupt variation in the rate of isotherm movement in the solidifying casting, caused by mold wall buckling or the contracting skin of the solidifying casting (resulting in a temporary thermally nonconductive air space between casting and mold) will result in solute banding. This is characterized by bands of positive and negative segregation perpendicular to the isotherm movement.

Conditions which tend to alleviate the problems of macrosegregation:

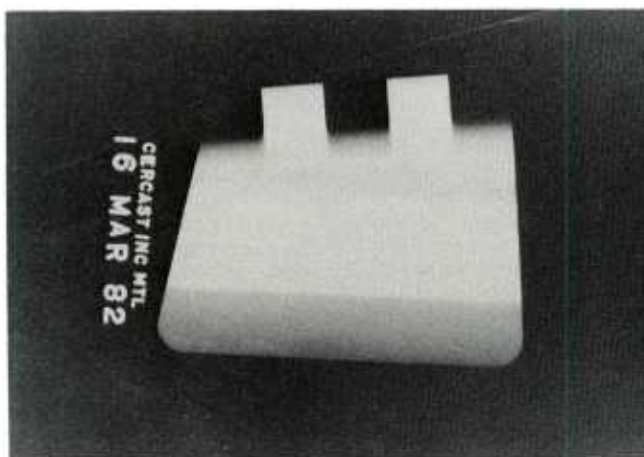
(1) In areas of transition from thin to heavy sections (say 1mm to 10mm), gussets and generous fillets should be employed to prevent localized drastic changes in casting cross-section. Flexibility of the casting designer should be expected from the foundry which is casting a difficult configuration in say perhaps a 201 alloy. Although the foundry is capable of altering the localized heat removal rate of the casting, to prevent segregation, difficult problems require the casting configuration to be altered slightly.

(2) Solute banding as a result of mold wall movement can easily be remedied by the foundry, by the use of varied mold wall materials and thicknesses in conjunction with specialized fixturing or gating techniques. Solute banding resulting from the solidified skin of the casting shrinking away from the mold wall may be alleviated by judicious gating, modified temperature profiles or a change in casting configuration.

(3) Segregation resulting from excessive chilling in localized areas of the casting (to promote directional solidification in short feeding range alloys) may be corrected by proper chill location. (ie. discouraging the placement of chills on thin sections where the alloy will freeze too quickly.)

Steep thermal gradients and a low mold temperature caused copper segregation on the chilled section of this 201 alloy door hinge.

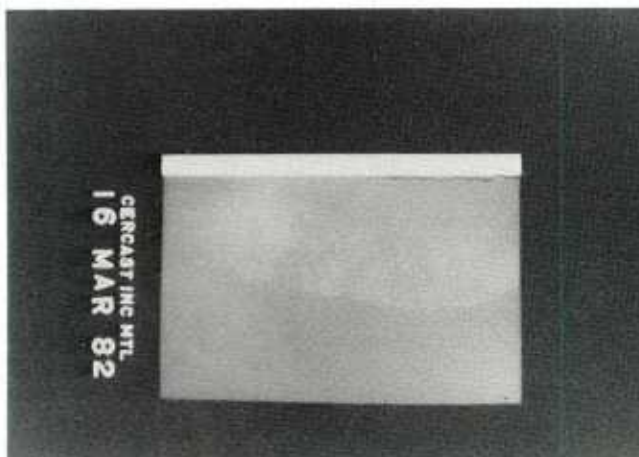
Fig. B



Note that copper segregation is easily visible in conventional radiographs because of the higher density of the alloying element to x-rays. Copper rich areas (sometimes achieving an excess of 9% copper) are depicted as light areas or streaks on the x-ray film.

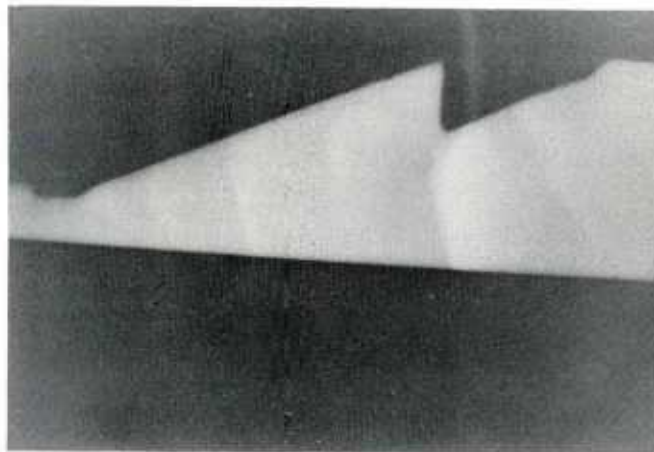
Transition of light to massive sections without adequate fillet or gusset resulted in positive segregation in the experimental thin plate casting.

Fig. C



Banding segregation is revealed here in a section of casting which was subjected to varied cooling conditions during solidification (result of mold wall buckling)

Fig. D



Hot Tearing:

Hot tears are strain caused fractures that occur during solidification or subsequent cooling of a casting, frequently as a result of hindered contraction.

During the mass-feeding stage of a casting, where both solid and liquid move in the early stages of solidification, to compensate for shrinkage, a point is reached where the solid is no longer able to move readily. After a solid skeleton of dendrites has formed, solidification shrinkage must be fed by inter-dendritic flow. The developing strength of the solid network can now cause localized strains which are weakest at the hot spot junction between thick and thin sections. When metal can no longer feed to the hot spot, the contraction strains pull the solid dendrites apart at this location. If the casting is well fed, there is now a stage where eutectic liquid can flow between the separated dendrites to 'heal' the incipient tears. Regions of segregation may thus result in this area.

An important factor affecting hot tearing is grain size. The finer the grain size of the casting, the greater is the resistance to hot tearing. This is now understood to be because the fine-grained semi-solid material is weaker than the coarse-grained material, not stronger. Solidifying alloy develops measurable strength at a later stage of solidification and until that time is free to compensate for strains by movement of both solid and liquid. It is therefore concluded that the fine-grained casting develops strength later in the solidification process, as the smaller solid fragments are still able to flow after the larger fragments have held fast.

Some conditions which promote hot tearing are:

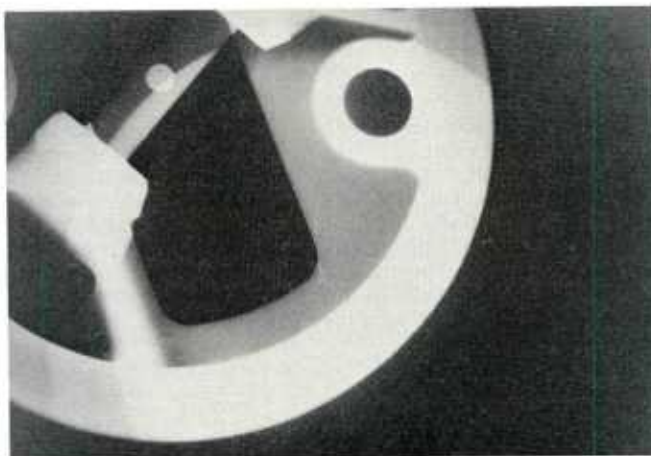
- (1) Mushy freezing range alloys such as Al-Cu alloys form strength earlier in the solidification process than do Al-Si alloys, as a result of a large freezing range. The large interval between solidus and liquidus in the Al-Cu alloys promotes the formation of a mushy phase of dendrites mixed in eutectic liquid. We therefore expect the Al-Cu alloys to be more prone to hot-tearing.
- (2) Poor grain refining especially in the hot tear prone alloys may result in tearing at critical locations. Best grain refining results have been noted with ladle additions of grain refiner prior to casting of the alloy.
- (3) Poor casting design resulting in sharp transitions from thin to thick sections, promote hot spots in the junction area upon casting. Upon solidification, hot tears may develop in the thin wall adjacent to the junction. The use of generous fillets and gussets would eliminate hot-spot formation and discourage the formation of hot tears in susceptible alloys.
- (4) Castings designed for hot-tear prone alloys should make use of an elastic design, such that contractual stresses will not accumulate at one particular section.
- (5) The foundry can, in part, reduce the risk of hot tearing for restricted configurations, by designing a gating system which will yield to the stresses of contractual solidification in the early stages.
- (6) Excessive stresses and hot-tears are most likely to occur under solidification conditions where there is little or no thermal gradient. Proper use of gating design in designing for directional solidification is of great assistance in this respect.

Although hot-tears may fall into the category of cracks, which are easily detected by penetrant examination, some hot-tears are not detected on the surface of the casting.

The example below demonstrates a complex series of events which led to the formation of hot tear in a 201 casting. Low mold temperature in the casting depicted in Fig. A below, resulted in the early stage of copper segregation of the thin deck area. Contractual stresses from the freezing heavy hub area coupled with a brittle copper rich area lead to a hot tear in the corner of an aperture in the deck. The resulting crack was subsequently filled with eutectic fluid and cracked once again upon cooling of the casting to room temperature. Although the crack was not open to the casting surface, where it may have been detected by penetrant examination, a radiograph of the same area revealed an unusually sharp line of copper segregation. The phenomenon was thus recognized and subsequently corrected in future castings.

Radiograph of 201 casting:
note the localized heavy
segregation of copper
(seen as a white line)
in the crack area.

Fig. A



Micrograph of area 100X:
note the copper rich eutectic
liquid which has flowed
into the cracked area during
solidification. (lighter
silver phase)

Fig. B

(Eutectic melting occurred in
Cu rich areas upon heat
treatment)



Intermetallic Compounds:

Because of its reactivity, molten aluminum is easily contaminated. Local high concentrations of undesirable elements may form compounds which are not readily soluble in the alloy, and hence remain as inclusions and precipitates.

(1) Incorrect or excessive additions of an Al5%Ti hardener alloy commonly used for grain refinement, may result in crystals of TiAl, segregating at the bottom of the furnace. These crystals may then be accidentally scooped-up in the pouring ladle and cast into the mold. Brittle phases such as TiAl, are undesirable and may promote fracture in a stressed casting, provided the crystals are in sufficient quantity.

TiAl, 400X:

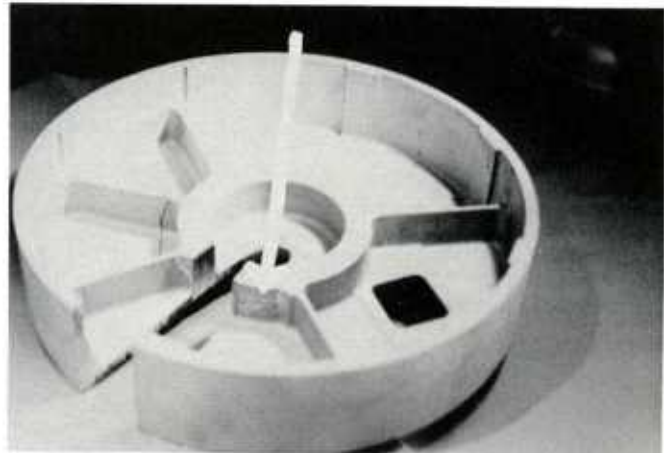
Fig. A



(2) Iron may combine with silicon during solidification to precipitate coarse (Al-Fe-Si) constituents. Also, local high concentrations of iron caused by perhaps a degrading iron furnace thermocouple protection sleeve or sludging (see 'Optimization of Chemistry') may form Al-Fe compounds such as FeAl₃. In sufficient quantity, these crystallized compounds may choke off interdendritic spaces necessary for feeding the casting during solidification. As a result, mysterious shrinkage voids may appear where none were expected or evident before. Intermetallic compounds of Ti and Fe are more dense than liquid aluminum and hence segregate in the lower portions of the casting. Below are two examples of NDT detection of mysterious intermetallics.

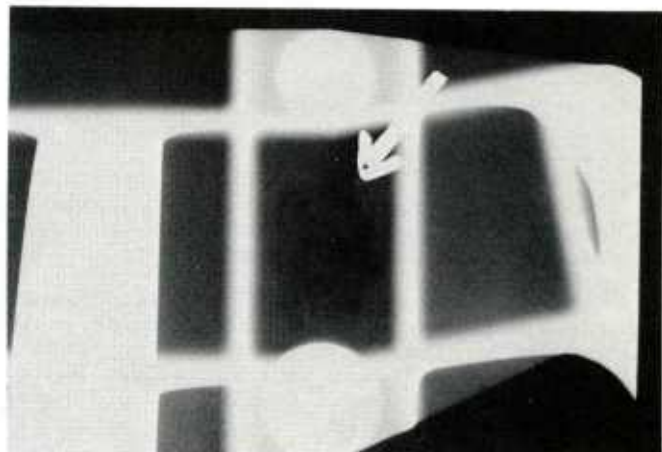
201 Bulkhead casting:
Iron-Titanium based intermetallics
in the lower portions of the
casting, interfered with normal
solidification and resulted in
a porous surface, as detected
by penetrant examination.

Fig. B



201 Structure casting:
Iron based intermetallics
hindered the normal solidification
pattern in this area and resulted
in shrinkage voids, as detected
in normal radiographic QC procedures.

Fig. C



FUTURE PROSPECTS

Vacuum Casting Process:

Preliminary results from castings produced in the Cercast pilot plant vacuum casting installation, indicate a significant increase in mechanical properties and casting integrity. The installation is basically composed of:

- 1) Vacuum melting and processing chamber
- 2) Bottom pour ladle assembly
- 3) Vacuum casting chamber which accommodates the mold and allows it to be cast under reduced pressure.

(A) Vacuum holding and degassing:

Vacuum processing of aluminum alloy melts is not a novel idea, yet it is not widely used in the foundry industry. The quest in recent years to squeeze higher properties out of existing alloy systems requires in part the utilization of a 'super clean' melt. A melt essentially free of dissolved gas and micro-oxides obtained by vacuum degassing is required to yield castings of premium integrity. It is the elimination of micro-oxides, intermetallics and gas voids (undetected in radiographic procedures) from the grain boundary regions, which will result in greater mechanical strength. It is also significant to note that the elimination of these tiny defects is increased an order of magnitude with vacuum melting and degassing as compared to conventional melting and gas fluxing operations.

(B) Vacuum Casting:

The benefits of casting under reduced pressure are basically twofold:

- 1) Transfer and casting of the melted alloy in the absence of oxygen, prevents oxide and micro-oxide formation which are subsequently churned into the alloy.
- 2) The mold may be rapidly filled and hence low mold temperatures are employed. Low mold temperatures encourage chilling and fast cooling rates which yield improved mechanical properties in the casting.

(C) The System:

By combining melting and casting operations under vacuum, Cercast has produced significant improvements in casting strength and integrity, when compared to conventional casting operations. After removal of gas and micro-oxides in the degassing phase, the melt is modified and/or grain refined as well as adjusted to an optimum chemical composition. Subsequent casting of the alloy under vacuum into a mold using a bottom pour ladle configuration, maintains melt cleanliness. The lower mold temperatures employed as a result of the process variables, promotes rapid solidification of the casting.

Hot Isostatic Pressing (H.I.P.):

HIP consists of densifying a casting/PM part by the use of great external pressure at a temperature just below the softening point of the alloy. Such a densification process will reduce internal shrinkage and gas porosity and hence increase the casting's strength.

HIP is commonly used today to salvage expensive titanium superalloy turbine components which would otherwise be unacceptable due to internal porosity. HIPing these critical application castings also narrows the 'band' of mechanical properties usually found from one casting to another. As a result, higher mechanical properties with greater consistency are produced.

Aluminum castings on the other hand, have traditionally not been subjected as frequently to HIP treatment, as a result of economics. Increased casting value and economical HIP installations may however justify large scale use of HIP for aluminum castings in the future. In past years, Cercast has conducted HIP investigations of 201 castings, in the hope of raising mechanical properties high enough to replace forged components of 7075 alloy for aerospace applications. The less than spectacular results were caused by the very nature of 201 cast structures.

Alloy 201 is characterized by microporosity in the grain boundary region for all cast structures except those chilled very rapidly. If this microporosity reaches the casting surface (which it does), any attempt at HIP will fail as a result of pressure equalization between the porosity and the casting surface. Alloy 201 castings would therefore have to be coated or surface impregnated before any HIP operations would be successful.

At present time, Cercast is investigating improving 356/357 alloy cast structures with HIP. Again, a premium quality casting having no detectable micro-oxides or surface porosity will be candidate for such a process. Combining the vacuum casting process for casting production with subsequent HIPing, we anticipate a dramatic increase in casting strength over conventional production. With our present experience and preliminary results, we predict casting quality to rise above MIL-A-21180 specs. for all configurations currently produced.

STATE OF THE ART

The castings pictured in Fig. A are a few of the worlds largest investment castings, produced by Cercast. Increased size and complexity are evident in these structural castings. Guaranteed mechanical properties conforming to military spec's, coupled with intricate design features has opened a new era in functional casting applications.

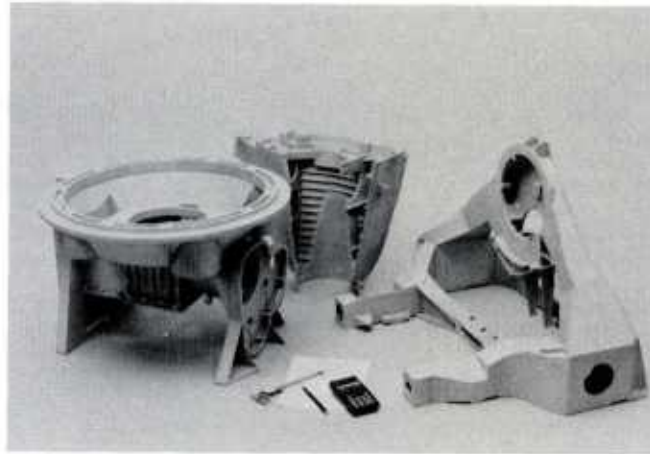


Fig. A

Ultra high strength at room and elevated temperatures with excellent ductility and impact strength are characteristic of the Al-Cu-Mg alloy castings. Figure B depicts a few of the typical cast parts produced by Cercast in 201 and D25Z alloys. Due to the poor casting characteristics of these alloys, a considerable developmental period may be required by the foundry in selecting suitable techniques for casting production. In designing castings to be produced in say 201, the designer should employ:

- 1) Smooth transitions from thin to massive sections
- 2) Adequate fillet radii in junctions
- 3) Flexible designs rather than rigid configurations.

Such considerations will reduce the risk of tearing and segregation and speed the developmental period in producing new cast parts.

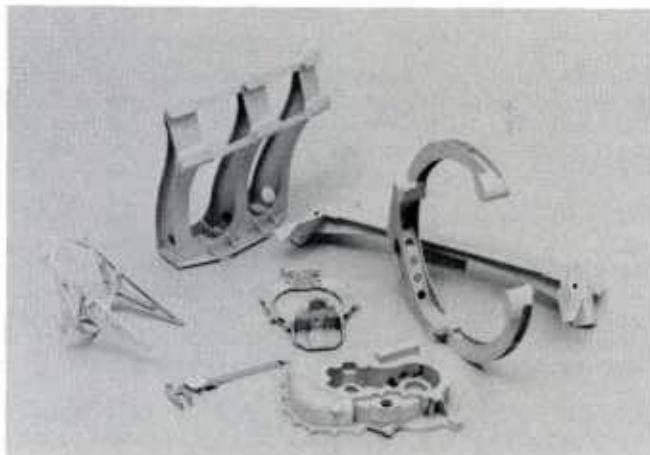


Fig. B

Fig. C shows some impeller type castings produced in 201 alloy. With specialized foundry techniques, even rigid designs prone to tearing, may be cast with success (turbine at left). Castings displayed center and right in the photo (with 20cm and 10 cm hub sections) required extensive dynamic chilling to maintain a fine grain size and high mechanical properties in the casting.

Comments:Al-Si Alloy Castings

- Large complex functional designs are possible.
- Chilling, grain refinement, modification, optimization of chemistry and specialized heat treatments are essential in producing premium quality castings which conform to rigid military specifications.
- Vacuum casting and HIP will improve properties of existing operations and boost casting strength above present military spec's.

Al-Cu Alloy castings

- Non-rigid, simple configurations are desired for casting design.
- Adequate fillet radii with gentle change in section thickness will reduce problems of tearing and segregation in casting production.
- Casting designs lending themselves to directional solidification and chilling will be most successful in the foundry and yield a superior product.
- Longer than normal development times for casting set-up may be required for difficult configurations. Where the foundry is limited in producing an acceptable product, design changes to critical areas may solve inherent difficulties.

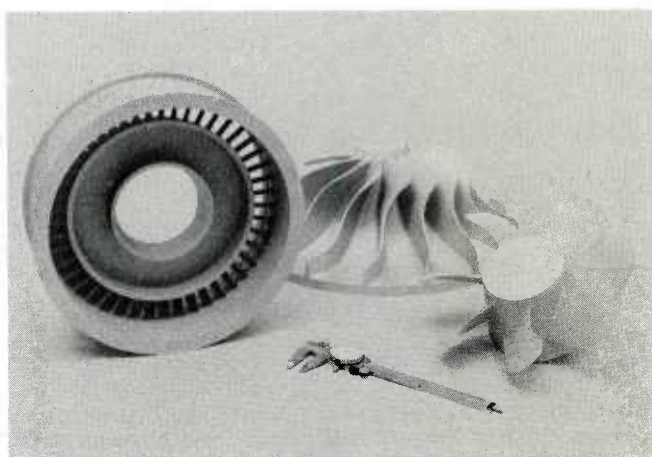


Fig. C

APPENDIX A

Macrosegregation

Macrosegregation is segregation of alloy elements that occurs over distances that are large compared with the dendrite arm spacing or grain size of the casting. Such segregation may lead to local weak or brittle spots in the casting and render it unusable. An understanding of macrosegregation formation allows the foundry to solve particular problems, as well as suggest changes in casting design to prevent future incidents.

Centerline segregation, cone segregation, banding, freckles, inverse segregation and A-segregates are all specific examples of macrosegregation. For a given alloy system, the size and extent of segregation depend on isotherm velocity and interdendritic flow velocity in the solidifying casting. A theoretical equation is developed below to show the effects of solidification conditions on segregation.

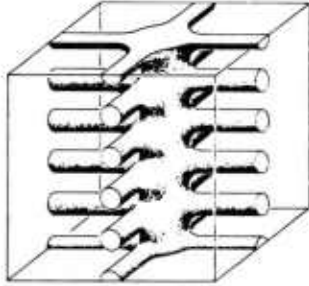


Fig. A

Consider a volume element (Fig. A) containing a solid dendrite, and unsolidified liquid metal. In the model, fluid will be allowed to flow through the element during solidification. Flow occurs here because of solidification shrinkage, contractions of solid and liquid phases as they cool and gravity. The dendrite arms shown are typically 50-150 microns spacing (for investment castings), and so the channels where the liquid must flow through are very small.

Darcy's Law₁ of flow through a fine sieve will adequately represent the interdendritic flow (\vec{v}).

$$\vec{v} = \frac{-k}{\mu f_L} (\nabla P + \rho_L G) \quad (1)$$

where: K- permeability of the medium (constant)
P- pressure
G- acceleration due to gravity
U- viscosity of the fluid
 f_L - volume fraction of liquid

As solidification proceeds in the volume element, the interdendritic flow rate and density of the volume change. This may be expressed as a mass balance on the volume element.

$$\frac{\partial \bar{P}}{\partial t} = -\nabla \cdot \rho_L f_L \vec{v} \quad \text{where } \bar{P} = \rho_S f_S + \rho_L f_L \quad (2)$$

Where: \bar{P} - average density of the volume element
 ρ_L - density of the liquid
 ρ_S - density of the solid

To calculate the effect of interdendritic flow on segregation, we redefine the mass balance in terms of the solute present. Thus, rate of solute flow out minus rate of solute flow in is equal to the rate of solute accumulation in the volume element.

$$\frac{\partial}{\partial t}(\bar{P} \bar{C}) = -\nabla \cdot \rho_L f_L C_L \vec{v} \quad (3)$$

where: C_L - composition of the liquid
 \bar{C} - local average composition of solid and liquid mass fractions.
 \bar{P} - local average density of liquid and solid mass fractions.
 \vec{v} - local velocity of interdendritic liquid, relative to solid.

With suitable manipulations, we derive the following relation:
(detail mathematical derivations are available in reference #2)

$$\frac{\partial f_L}{\partial C_L} = -\left(\frac{1-\beta}{1-k}\right) \left(1 + \frac{\vec{v} \cdot \nabla T}{\epsilon}\right) \frac{f_L}{C_L} \quad (4)$$

where: ϵ - local rate of temperature change
 T - temperature
 β - solidification shrinkage
 k - equilibrium partition ratio (composition of the solid divided by composition of the liquid at the eutectic temp.)

consider: $\frac{\vec{v} \cdot \nabla T}{\epsilon}$ as the local flow velocity which is perpendicular to the isotherms, and relative to the isotherm velocity.

therefore:
$$\frac{\partial F_L}{\partial C_L} = - \left(\frac{1-B}{1-k} \right) \left(1 - \frac{V_P}{u} \right) \frac{F_L}{C_L} \quad (5)$$

where: V_P - component of flow velocity perpendicular to isotherms
 u - isotherm velocity

Equation (5) is the basic "Local Solute Redistribution" equation and is used to calculate macrosegregation from particular solidification conditions. Some assumptions have been made to develop the formula: (a) density of the solid does not change significantly with time spans considered. (b) No solid diffusion of solute. (c) No void formation during solidification.

CASE A:

Theoretical situation: No interdendritic flow
 No liquid - solid shrinkage

From the local solute redistribution eqn.:
$$\frac{\partial F_L}{\partial C_L} = - \left(\frac{1-0}{1-k} \right) (1+0) \frac{F_L}{C_L}$$

Solving the above equation:
$$C_L = C_0 F_L^{(k-1)}$$

where: C_0 - initial concentration of solute in the liquid prior to solidification.

The above simple relation is known as the Scheil equation and states that the absence of interdendritic flow results in no macrosegregation.

CASE B:

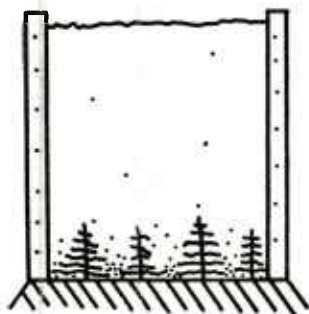


Fig. B

Consider casting an alloy against a chilled surface (Fig. B). Maximum segregation of the solute will occur at the chill face, where interdendritic flow is perpendicular to isotherms and is 0. Therefore:

Note: There is no gravity induced convection in this ingot for alloy systems where the solute is heavier than the solvent (aluminum). This is because the heavier solute rich liquid lies below the lighter liquid.

The redistribution equation yields:
$$\frac{\partial F_L}{\partial C_L} = - \left(\frac{1-B}{1-k} \right) \frac{F_L}{C_L}$$

Integrating the above equation with B and k as constants we have:
$$C_L = C_0 F_L^{-[(1-k)/(1-B)]}$$

This results in maximum segregation of the alloy and occurs in portions of the liquid directly adjacent to a chilled surface. The solute rich region obtained in the vicinity of the chill is called inverse segregation.

CASE C:

Consider solidifying a casting horizontally as shown in Fig. C. Primary dendrites grow outward from the chill surface horizontally, yet the solute rich liquid (formed from rejection of solute into the liquid in front of the growing dendrites) is moved to the left and downward as the result of two forces. Gravity tends to pull the solute rich liquid down, whereas the solidification tends to pull the liquid towards the dendrites. The resultant flow is downward and to the left provided the solute rich liquid is more dense than the liquid (as in the Al-4.5%Cu alloy systems). In cases where the solute rich liquid is lighter than the liquid (as in the Al-7%Si alloy systems) the resultant flow would be upward and to the left.

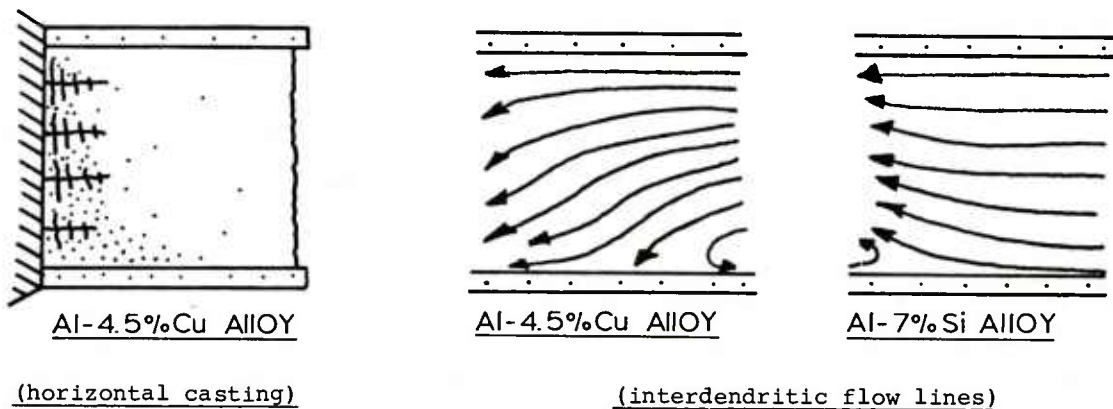


Fig. C

Solute Redistribution Eqn.:
$$\frac{\partial F_L}{\partial C_L} = - \left(\frac{1-B}{1-k} \right) \left(1 + \frac{\vec{v} \cdot \nabla T}{G} \right) \frac{F_L}{C_L}$$

Darcy's Law:

$$\vec{v} = -\frac{k}{\mu F_L} (\nabla P + \rho G)$$

Solving for interdendritic velocity at various locations in the horizontal casting and substituting the values in the Redistribution Equation, we arrive at the following conclusions (by numerical techniques).

Near the chill end of the casting, positive segregation of solute would be evident as shown in case B, previously. This would be valid for both light and heavy solute rich liquid systems.

For heavy solute rich liquid systems (Al-4.5%Cu) away from the chilled surface, we would expect to find the resultant segregation: a) Negative segregation at top of the casting. b) No segregation in the center of the casting. c) Positive segregation in the lower portions of the casting.

For light solute rich liquid systems (Al-7%Si) away from the chilled surface, we expect to find the following pattern: a) Positive segregation at the top of the casting. b) No segregation at the center of the casting. c) Negative segregation in the lower portions of the casting. Because the difference in density between Silicon and Aluminum is not as great as the difference in density between Copper and Aluminum, we expect the magnitude of vertical segregation to be most pronounced in the Al-4.5%Cu alloy casting.

Case D:

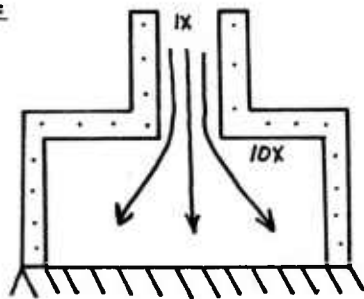


Fig. D

Consider feeding a massive section through a smaller section of the casting.

At the casting base near the chill, v_p remains zero and thus a positive segregation will result as discussed in case B.

In the thin section of casting near junction from thin to thick, the flow rate of interdendritic liquid is 10X higher than normal to feed the solidification below. However, isotherm velocity will be nearly the same in this region, due to heat conduction.

As a result, the ratio v_p/U will increase approximately 10X in the lower neck of the casting. From the Redistribution Equation, we see that this will result in a large area of negative segregation of solute, at the neck of the casting. This negative segregation is balanced by positive segregation at the outer upper portion of the heavy section, where v_p is zero. The resultant segregation is depicted in Fig. E.

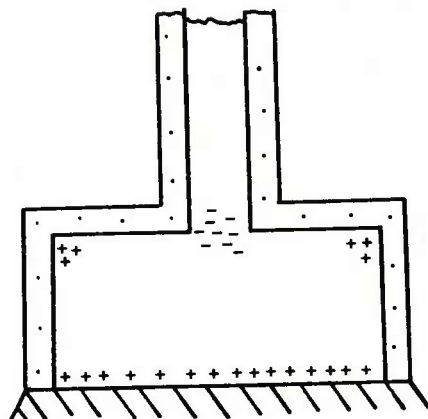


Fig. E

CASE E:

Consider a situation where the mold wall heat removal rate varies. This situation is encountered if the mold wall buckles or pulls away from the solidified skin of metal adjacent to the mold wall. The air space thus produced hampers the rate of heat transfer from the cast metal through and away from the mold wall.

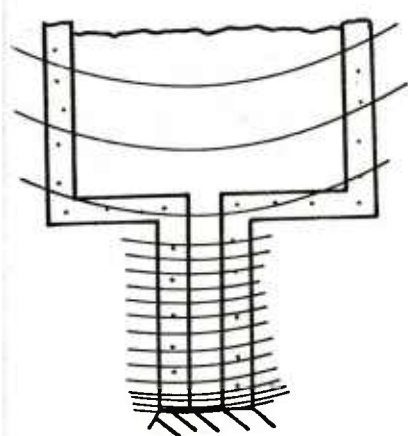
Any abrupt variation in the rate of isotherm movement, causes local variations in V_p/U (since V_p remains almost the same, due to momentum effects). Using the Redistribution Equation, we notice that the above changes lead to solute banding. The frequency of positive and negative alternating bands will depend on the frequency of movement of solidified skin in relation to the mold wall.

CASE F:

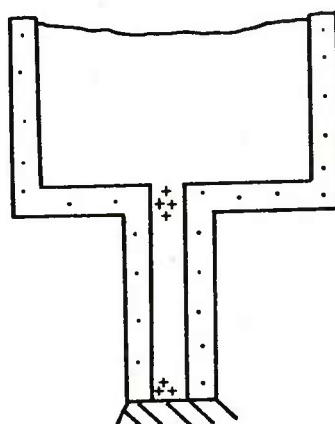
Consider feeding a small section with a massive section of the casting. At the ingot base near the chill, V_p remains zero and thus a positive segregation will result as before.

The major portion of the thin section will solidify rapidly, as indicated by the closely spaced isotherms in Fig. F. Near the neck of the casting in the thin wall, solidification will slow dramatically as a result of the massive heat concentration of the upper section. In this transient stage, the thin solidified section will act as a chill in the neck of the casting. Interdendritic flow will be reduced to almost zero for awhile until the solidification front resumes its movement upwards.

As a consequence, in the neck of the casting, V_p will be reduced momentarily almost to zero in the region of transition from high to low isotherm velocity. If V_p reduces to almost zero and U is momentarily unchanged, we see that the Redistribution Equation tells us that positive segregation will result. The resulting profile is shown in Fig. F below.



Isotherm Profiles



Resultant Segregation

Fig. F

APPENDIX B

EUTECTIC MELTING

Cast aluminum alloys featuring a low melting eutectic phase and requiring a high solution heat treat temperature to obtain maximum strength, must employ a step temperature heat treat cycle.

In order to determine the optimum heat treat cycle for a specific alloy system, we must consider the melting points of the compounds present in a casting, before and during solutionizing.

CASE A: 201 Alloy "K01"

Nominal Composition

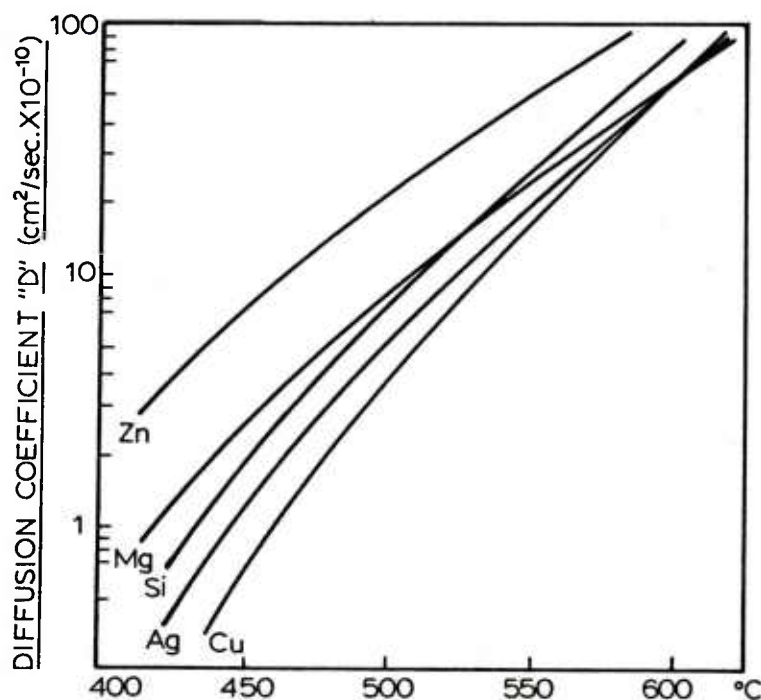
Cu	4.5%
Ag	0.6%
Mn	0.3%
Mg	0.3%
Ti	0.25%

In the initial stages of 201 solidification, dendrites of aluminum start forming, becoming progressively enriched in alloying elements. In the last stages of solidification each dendrite has grown into a grain, rejecting solute into the remaining liquid phase until it reaches the eutectic composition. The eutectic liquid is trapped either between dendrite arms or at grain boundaries and solidifies last. Precipitates of an Al-Cu-Mn phase appear within the copper-rich eutectic, at the grain boundaries, during cooling.

Microprobe analysis of the grain boundary area indicate that copper, magnesium and manganese (as well as impurities such as iron and silicon) are concentrated at the grain boundary area. Analysis of the relevant ternary, quaternary and quinary phase diagrams, of all elements present, indicate the possible formation of the following low melting phases for a solidified 201 alloy.

Phase	Melting Point °C (°F)	
CuAl ₂	591	(1096)
CuMgAl ₂	507	(945)
Ag ₂ Al	727	(1340)
Cu ₂ Mn ₃ Al ₂₀	616	(1141)
(CuFeMn)Al ₆	654	(1209)
(CuFeMn) ₃ Si ₂ Al ₁₅	530	(986)
FeSiAl ₅	611	(1132)
Mg ₂ Si	595	(1103)
(FeMn)Al ₆	656	(1213)
TiAl ₃	1337	(2438)

The lowest melting phase formed in the grain boundary area, of the solidified alloy is CuMgAl₂ with a melting point of 507°C. It is therefore obvious that the first stage of heat treatment should be conducted at or slightly below 507°C to prevent melting of this phase.



(5)

Fig. A

As seen from the graph (Fig. A) of diffusion coefficients 'D', higher heat treatment temperatures than 507°C are needed to promote Cu and Mg diffusion (from the g.b. into the matrix) within reasonable heat treatment times.

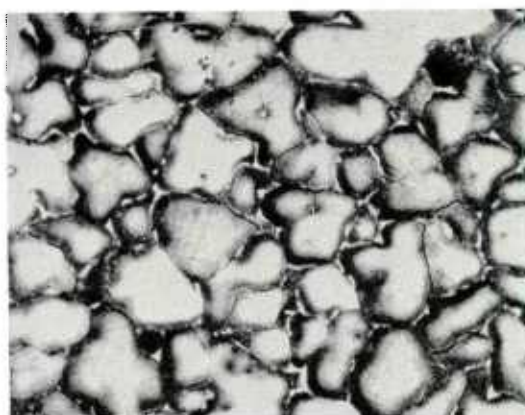
As the low melting phase gradually diffuses into the matrix, in elemental forms, the heat treatment temperature may be gradually raised in steps until a maximum limit is reached, where additional temperature rise would result in distortion of the casting or grain growth of the alloy. Heat treatment experiments have shown that considerable grain growth will take place compared to the cast structure at temperatures exceeding 535°C (995°F), despite additions of manganese.⁴

Manganese additions around 0.30% or more will allow heat treatment temperatures up to 535°C (995°F) without the occurrence of either grain growth or remelting. The presence in the alloy of a stable Al-Cu-Mn phase is credited with pinning the grain boundaries and preventing their migration, thereby eliminating grain growth.

As a result of our investigation into the physical properties of 201 alloy components, we conclude that a step heat treatment is required to homogenize the copper and magnesium in the matrix. The first stage will commence at perhaps 505°C (941°F) and the last will not exceed 535°C (995°F) with one or more intermediate stages.

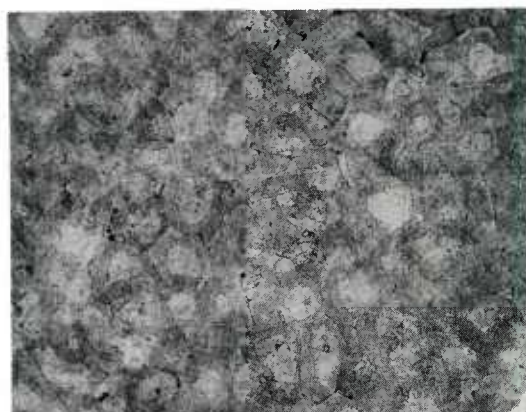
201 alloy: as cast
note the coarse inter-
granular eutectic between
the aluminum rich dendrites

Fig. B



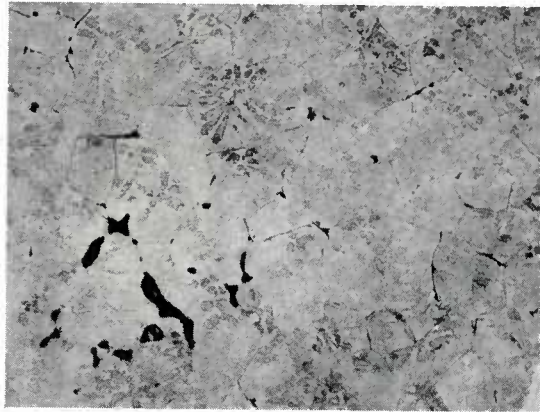
201 alloy: step H.T.
most of the eutectic
phase has diffused into
the matrix, resulting in
maximum alloy strength
upon precipitation H.T.

Fig. C



201 alloy: no step H.T.
lack of a step heat treatment
has resulted in eutectic phase
melting which flowed along the
grain boundaries, where it was
eventually frozen in place during
the quenching operation. Some of
the smaller eutectic particles
trapped between dendrite arms
have been spheroidized to give
the typical rosette appearance.

Fig. D



APPENDIX - C

Selection of alloys resistant to Liquid Aluminum

Experience in handling and experiment both have shown that there are no known metals or alloys totally immune to attack by liquid aluminum. However the coating of an iron tool with inert metallic oxides (Fe_2O_3 , Al_2O_3 , and MgO) are successful in temporary protection against corrosion.

Gray cast iron is found to be more resistant to attack by aluminum than the low carbon steels, Armco iron, or any of the ferrous alloys, including the stainless steels. Graphite neither reacts with nor is readily dissolved by aluminum below 1200°C (2190°F), and the resistance of gray cast iron is attributed to the graphite barrier left behind when the iron is dissolved.⁶

Despite their structural strength at elevated temperatures, ferritic and austenitic stainless steels are strongly susceptible to embrittlement penetration upon exposure to molten aluminum.

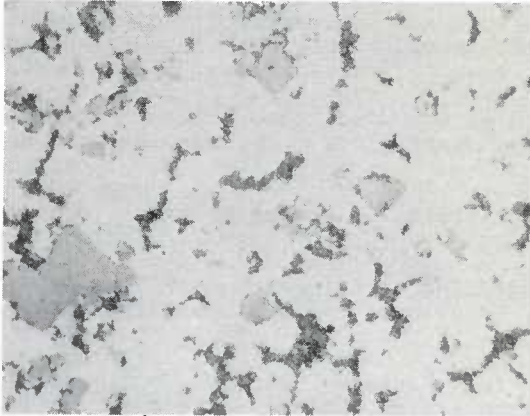
Chrome plate is reported to be resistant⁶ to attack by liquid aluminum at temperatures near its melting point.

Copper and nickel and alloys containing significant quantities of either or both of these elements (monel, Inconel, Incalloy, brasses, bronzes) are severely attacked by aluminum.

Cobalt-based super alloys may be resistant to corrosion by liquid aluminum and resistant to creep at high temperatures, but insufficient data is presently available.

APPENDIX - DTitanium-Boron Hardener Alloy

Experience has shown that optimum grain refining properties are obtained using master-alloys with a titanium:boron ratio of about 5:1. A micrograph of the presently used Kawecki TiBor "I" alloy is shown below;



TiBor "I"

400X

5% Titanium

1% Boron

The alloy has two crystalline intermetallic compounds primarily discernible in the microstructure, namely small crystallites of titanium diboride (TiB_2) and larger crystals of titanium aluminide (TiAl_3). At 400X the TiB_2 appears as dark grains of sand with 80% being $3\mu\text{m}$ and the rest occurring as agglomerates of crystallites ($30\mu\text{m}$). TiAl_3 , seen as light grey crystals, average $20\text{--}30\mu\text{m}$ in diameter; being as large as $90\mu\text{m}$ and as small as $5\mu\text{m}$. Approximately 94% of the alloy is aluminum with trace amounts of iron and silicon. As 40% of the titanium is tied up in the compound TiB_2 , the rest is free to form TiAl_3 , or dissolve in the aluminum matrix.

Upon immersion of the TiBor in an aluminum melt, the matrix melts almost immediately, releasing the TiB_2 and TiAl_3 crystals. Due to the low solubility product of TiB_2 in aluminum, these crystallites remain stable and do not dissolve appreciably (although they are subject to progressive coalescence and sedimentation). The dissolution rate of TiAl_3 in liquid aluminum unsaturated with titanium is high and low for a saturated melt. The crystals are presumed to dissolve within seconds to minutes after contact with the metal.

BIBLIOGRAPHY

1. Solidification Processing - M. C. Flemings, McGraw Hill, 1974
2. Macrosegregation - M. C. Flemings & G. E. Nereo, Trans Aime V239, 1967
3. Aluminum Alloys - L. F. Mondolfo, Butterworths, 1976
4. Conalco R & D Labs, Technical Report CRDL-75-TIR-3 - St. Louis, Missouri
5. Transport Phenomena in Metallurgy - Geiger & Poirier, Addison & Wesley, 1973
6. Liquid Metals Handbook - Dept. of U.S. Navy, Washington, D.C.
7. Solidification Phenomena - J. P. Davies, Mc-Graw-Hill, 1973
8. Recent Casting Alloy Developments - AFS Trans, 1978, M. Garat, Pechiney
9. Communications of M. Garat of Pechiney Aluminum to S. Kennerknecht of Cercast - Pechiney #APV-FD/T-Mg./JM-113/81
10. A Study of the Use of Pure Metallic Strontium in the Modification of Al-Si Casting Alloys - B. Closset & J. E. Gruzleski, MFM. McGill
11. A Review of Grain Refining Practice at Cercast, with Specific Application to 201 Melts - Cercast report, 1981
12. Stability of Intermetallic Aluminides in Liquid Aluminum and Implications for Grain Refinement - Metals Technology, May 1980
13. Factors Affecting the Grain-Refinement of Aluminum Using Titanium and Boron Additives. - Jones & Pearson, Met. Transactions, June 1976
14. Grain Refinement in Aluminum Alloyed with Titanium and Boron - Marcantonio & Mondolfo - Met. Transactions, February 1971
15. Discussions of Grain Refinement in Aluminum Alloyed with Titanium and Boron - Collins, Met. Transactions, August 1972
16. The Influence of Boron on the Mechanism of Grain Refinement in Dilute Aluminum-Titanium Alloys - Cornish, Metal Sci. 1975
17. Grain Refinement of Aluminum Alloys - Warr & Smith, Z. Metallkde, February 1975
18. TiB_2 Particles as Nucleants for Aluminum - Naess & Ronningen, Metallography, August 1975
19. Grain Refinement in Cast Aluminum Alloys - Kotschi & Loper, AFS Transactions, 1977
20. The Nucleation of Aluminum Grains in Alloys of Aluminum with Titanium and Boron - Davies, Met. Trans. January 1971
21. The Mechanisms of Grain Refinement in Dilute Aluminum Alloys - Delamore & Smith, Met. Transactions, June 1971
22. On Grain Refinement in Aluminum Alloys - Naess & Berg, Z. Metallkde, 1974
23. Telephone communications with representatives of Kawecki Berylco Inc., Ray Langdon, Gil Farrior, Ed Hogg.
24. Re-Appraisal of the Tensile Properties of Al-Si-Mg Casting Alloys - Trans. AFS., 1973, B. Chamberlain, Allan Ltd.
25. Strontium as a Modifying Agent for Hypoeutectic Al-Si Alloys - Trans. AFS. 1980 P. D. Hess, Alcoa
26. The Modification of Al-Si Alloys with Strontium - D. C. Jenkinson, Univ. of Queensland, 1971.
27. Controle des Structures de Solidification et des Propriétés des Alliages Al-Si - S. Bercofici, Pechiney

BIBLIOGRAPHY

28. Sodium Versus Strontium for the Modification of Hypoeutectic Al-Si Alloys - AFS Trans, D. D. Kassing, Reynolds Metals
29. Maîtrise de la Structure Eutectic et des caractéristiques Mécaniques des Aluminium Silicium Hypoeutectiques - M. Garat, Pechiney
30. Patents describing Modification by Sr Master Alloys
 U.S. Patent # 4,009,026
 British Patent 1,191,368
 British Patent 388,109
 W.German Patent 1,255,928
 French Patent 723,417
 W.German Patent 2,052,927
 Austrian Patent 136,265
31. R. Redecker Die Thermische Analyse zur Kontrolle des Veredelung bei der Aluminiumlegierung G-AlSi10Mg Giesserei 68 (1981) 1, S. 7/11
32. The Modification of Al-Si Alloys with Strontium - Jenkinson & Hogen, M & M, University of Queensland, 1974
33. Thermal Analysis of Al Alloys to Determine their Suitability for Casting - Pechiney Aluminum, Hommes et Fonderie, November 1975
34. Zum Stand der Betrieblichen Thermischen Analyse in Giessereien - Giesserei (GJ) Heinz Wuebbenhorst
35. Anwendung der Thermischen Analyse Zur Ermittlung des Veredelungsgrades am Beispiel Der Aluminum-Gusslegierungen G-AlSi₈Cu₃ & G-AlSi₁₀Mg - Giesserei (GJ) 1978, Karl Eugen Honer
36. A New Approach for a Modification Study of Al-Si Alloys - Aluminum 1978 Indian Inst. of Technology, Madras
37. Correlation between Castability, Hot Tearing Tendencies & Solidification Properties of Al Casting Alloys - Alumino, 1979, Gianfranco Fortina

SESSION IV

DISCUSSION SUMMARY

by

C.A.Stubbington
Royal Aircraft Establishment
Materials Department
Farnborough, Hants
UK

A NEWLY DEVELOPED PROCESS (THE GKN & COSWORTH PROCESS) FOR THE PRODUCTION OF HIGH INTEGRITY ALUMINIUM ALLOY CASTINGS by P.S.A.WILKINS and DR J.CAMPBELL.

MR G.SWINYARD, Industrial Precision Castings, Rochester, UK complimented Dr Campbell on his presentation of a very new and interesting process. Dr Campbell had referred throughout his paper to the average sand casting and had shown competition with sand castings supplied to the automobile industry. IPC have for some time been supplying the aerospace industry with products superior to the average sand casting. A number of processes were available which gave excellent surface finishes and Mr Swinyard wanted aircraft designers to be aware of the quality of castings on offer and to understand that the founders had a range of approaches to get the right casting of the right type, dimension and price.

In reply Dr Campbell said that the GKN/Cosworth process was not competing with good investment castings in terms of surface finish or of intricacy of detail, neither was it competing with the very thin walled investment castings produced by a hot mould technique. Having said that the process was one which uses comparatively cheap tooling and which can be operated by relatively unskilled personnel to give reproducible castings up to aerospace standards. Dr Campbell said that although this remarkable achievement needed to be brought to the attention of industry he was not attempting to detract from the efforts of foundries such as IPC.

In reply Mr Swinyard said he was not referring to investment castings although these were produced by IPC. Rather he was referring to precision sand castings. He thought that IPC complemented other firms such as Precial, Messier and Cosworth and his intention was to make the designer aware of the range of methods available to obtain required properties and shapes.

MR R.J.HEATH, BAe Weybridge asked whether the impressive tolerances quoted on overall dimensions could be maintained after solution treatment and quenching.

Dr Campbell stated that Cosworth achieve strict dimensional tolerances after solution treatment and quenching, by quenching into a fairly high level of polymer quenchant. Tensile properties are reduced by approximately 10% using this type of quenchant but castings are extremely stable and internal stresses are low. The properties quoted in the paper could therefore be increased from 300 MPa to 330 MPa simply by changing from polymer quenching to water quenching but the resulting high levels of internal stress would result in distortion not only on quenching but also again during machining. Cosworth were not prepared to accept such distortion and had moved away from water quenching.

MR D.DUCKWORTH, British Aerospace, Warton, UK asked where the test bars were situated in the Rolls Royce casting.

Dr Campbell replied that the test bars were taken from the bottom flange. There were other places in that particular casting from which it was more difficult to extract the heat. Hence solidification times were considerably longer and properties were not so good. This illustrated the general problem for foundrymen of having to accept a component design which imposed different cooling rates in different parts and necessarily resulted in different properties.

DR J.R.NEWMAN, Titech International, US referred to Dr Campbell's statement that the lack of shrinkage in Cosworth castings was due to the fact that oxides were not carried turbulently into the cavity. He asked how the shrinkage caused by normal volumetric shrinkage upon solidification was avoided, since there were no feeders and no risers.

Dr Campbell replied that about 19 years ago he had made a purely theoretical prediction that if there were no nuclei in solidifying metal then there would be no porosity, even in materials which would shrink significantly upon solidification.

This was partly because the casting was quite plastic at temperature and the negative pressures generated internally would draw the casting in. Hence instead of a liquid feeding mechanism a solid feeding process would operate and the walls of the casting would collapse inwards. For aluminium alloys there is about six per cent solidification shrinkage to accommodate in total. Four per cent is easily accommodated in liquid feeding, even to the most distant regions of the casting. The remaining one or two per cent, if spread over the casting walls by controlled solid feeding, produces such a small movement of the walls that it is not measurable. Cosworth have, for the first time to Dr Campbell's knowledge, been manipulating this new concept of solid feeding to make sound castings. Good quality metal is, however required; the method is not viable if the metal is loaded with oxide nuclei.

DR T.W.CLYNE, University of Surrey, UK, thought that Dr Campbell's statement was fundamental and fairly controversial. He found it difficult to believe that there would not be a fairly complex interplay between the composition of the alloy, the way in which it solidifies and any feeding mechanism that operates, be it liquid or, as Dr Campbell suggested, solid. He asked Dr Campbell if he had evidence for the importance of the solid contraction idea.

Dr Campbell replied that his theoretical considerations had ranged over a variety of materials, and had included iron and steel, and copper and nickel base alloys, and different solidification models in terms of dendritic and of planar front freezing. He had shown that the nucleation of porosity would be heterogenous rather than homogeneous and so the Cosworth process sets out to remove the heterogeneous nuclei. This has been quite difficult in that some of the pumps and mechanisms used to transfer aluminium do not allow removal of the nuclei to the necessary extent. Cosworth were part of the way to this elusive goal and had attained a degree of success which permitted a start to be made in the use of this principle.

QUALITY ASSURANCE IN TITANIUM AND ALUMINIUM INVESTMENT CASTINGS

by **DR ING. C.LIESNER** – Tital, W. Germany

MR D.L.McLELLAN, Boeing Co., Seattle, US congratulated Dr Liesner for bringing out the relevance of quality assurance which he thought had been lacking in earlier presentations. He suggested that degree of eutectic modification should be added to the other quality criteria discussed by Dr Liesner i.e. porosity, dendrite arm spacing, cell size and inclusions. The audience were reminded that not all aluminium alloy castings were dendritic and he suggested that it was not possible to continue with dendrite arm spacing as a measure of the aluminium cellular structure. Mr McLellan continued with a further comment which he thought might not be totally justified. It was agreed that large scale porosity was deleterious, especially to ductility, but he suggested that there may be a degree of microporosity which is beneficial to ductility in acting as crack arresters for microcracks between particles of the eutectic. He then asked Dr Liesner if he could tell the audience how the quality index can be used as a number to judge the characteristics of a casting.

Dr Liesner said that the quality index Q depends on the soundness, compactness and fineness of the structure of the casting. The primary requirement is a sound casting with very small dendrite arm spacing. It is then possible to obtain the required mechanical properties by changing the tempering treatment to give either high strength and low elongation or low strength and high elongation. Dr Liesner suggested it might be useful to discuss this point again after Dr Kennerknecht had made his presentation.

QUALITE ET CONTROLE DES PIECES DE FONDERIE DE PRECISION POUR PIECES DE TURBOREACTEURS

by **J.THIERY** and **DR ING. J.VOETZEL**

DR E. DE LAMOTTE, FN – Formetal – Herstal, Belgium asked Mr Thiery about the effect of nitrogen on the components produced.

Mr Thiery said that nitrogen content increases as metal is recycled. Contrary to the general view recycled material is satisfactory for the manufacture of components although the more restrictive tolerances are a further complication for the founder. Experience available at present did not permit a more detailed answer to the question.

MR D.A.FORD, Rolls Royce, Bristol, UK, said he thought that evidence of the effect of microporosity in castings was rather scant. He asked Mr Thiery what he considered when determining and establishing a porosity level of acceptance in castings.

Mr Thiery replied that porosity is only dangerous in the most highly stressed parts of a component and it would certainly be appropriate to have a stringent specification for porosity in those areas. Tests on components have shown a considerable reduction in fatigue properties if the porosity content is 3–4%. Mr Thiery asked Mr Ford if he had similar views on porosity level.

Mr Ford replied that it was extremely difficult to establish a satisfactory level of porosity for turbine blades because each engine and each situation demands a different level of porosity. It is normal for the foundry to establish the best achievable level of porosity in turbine blades and then to modify the standard as a result of engine running experience. Mr Ford thought this might also be true for FN – Formetal – Herstal castings.

Mr Thiery agreed saying that they too carried out tests under simulated engine conditions. Predicted porosity levels are not always maintained and although this can result in problems, in practice there are very few accidents attributable to porosity.

METALLURGICAL ASPECTS OF QUALITY CONTROL IN THE PRODUCTION OF PREMIUM QUALITY ALUMINIUM INVESTMENT CASTINGS FOR THE AEROSPACE INDUSTRY

by S.KENNERKNECHT

MR D.DUCKWORTH, British Aerospace, Warton, UK, congratulated Dr Kennerknecht on the excellence of his paper and asked whether the attractive 201 alloy is commercially available.

Dr Kennerknecht replied that CERCAST had been producing castings in this alloy for the last ten years and had demonstrated expertise in controlling all the metallurgical variables to yield the optimum castings for amenable designs.

DR T.W.CLYNE, University of Surrey, UK, also congratulated Dr Kennerknecht on an interesting and wide ranging presentation. He asked Dr Kennerknecht about the modification of the aluminium-silicon eutectic structure saying that most theories envisaged that foreign atom absorption at gross sites was involved in the modification process.

Dr Kennerknecht had proposed that the main factor in the modification process was the presence of phosphorous in the melt and that if this species was removed the growth mode was changed. Dr Clyne asked Dr Kennerknecht to speculate further on the mechanism by which removing phosphorous from the melt results in a change in the growth mode.

Dr Kennerknecht replied that there was proof of the effect of phosphorous from an investigation of alloys with different phosphorous contents. The same modification potential could be applied to each alloy and experiments show that an increasing phosphorous content results in an increased requirement for a modifying agent. In addition, phosphorous compounds which are detected using electron microscopy form as a solid solution in compounds of a modifier added to the melt. Thus removing the phosphorous which initiates primary silicon nucleation results in finely distributed silicon in a eutectic network.

Dr Clyne responded that Dr Kennerknecht was proposing that it was not so much the growth mode that was being changed but the nucleation step. Dr Kennerknecht agreed saying that removing the nucleating particles results in normal eutectic solidification.

DR J.R.NEWMAN, Titech International, US, asked Dr Kennerknecht to indicate the development times required to attain the level of perfection achieved in CERCAST castings.

Dr Kennerknecht replied that the time required depended upon the difficulty of the casting configuration and the type of alloy. For aluminium-silicon alloys which are specifically designed as foundry alloys and have good shrinkage and welding characteristics the development time is short, approximately one week, whereas a month or six months could be required for an identical casting in aluminium-copper alloy, due to the difficulty in obtaining a sound structure in this alloy.

PROFESSOR J.F.WALLACE, Case Western Reserve University, US, asked whether there was any direct evidence of the formation of strontium-phosphorous compounds when strontium is used as a modifying agent.

Dr Kennerknecht replied that there was evidence of the role of phosphorous from electron diffraction studies. There is no compound formation between strontium and phosphorous. Initially a strontium-aluminium silicide zone or precipitate is formed and it is to this zone or precipitate that phosphorous is attracted and dissolved in solid solution.

Professor Wallace then asked Dr Kennerknecht if he would expand on his remarks about the use of thermal analysis to select the amount of modifier.

Dr Kennerknecht replied that the principle was simple. If a casting is required with a given dendrite arm spacing, a test mould would first be obtained which would produce a casting of identical dendrite arm spacing and solidification conditions. A small slug of the alloy would first be cast into the test mould and its time - temperature cooling curve monitored. Then by interpreting the shape of the curve in terms of lowering of the eutectic temperature, the absence of undercooling, the length of the solidification plateau and various other features, areas can be identified which are characteristic of a well modified, under modified or over modified condition. This can be achieved by inspecting the shape of the curve or as CERCAST have done by employing microprocessor control using differential thermal analysis whereby the curve is differentiated to reveal the various deviations and changes of slope.

MR H.J.FEUERSTACK, MBB Hamburg, W. Germany, asked whether stress corrosion tests had been made on the 201 alloy. Dr Kennerknecht replied that he had not done so but tests had been made by other researchers. The -T7 temper has a lower susceptibility to stress corrosion cracking than the -T6 temper and in the limit the user must decide whether to apply corrosion resistant coatings to castings or to specify the -T7 temper.

DISCUSSION SUMMARY – GENERAL DISCUSSION

by

C.A.Stubbington
Royal Aircraft Establishment
Materials Department
Farnborough, Hants
UK

MR C.A.STUBBINGTON referred to Mr Duckworth's paper in which there is mention of machining centres for light alloys and steels able to produce components from the solid at a price that castings find difficult to match. The suggestion is made that such centres are likely to impinge significantly on the small casting market and this perhaps implies that the size trend for castings will be upward. Damage tolerant design is now an important concept for airframe structures fabricated from wrought materials and if castings are to find increasing application it will be necessary to place increasing emphasis on their fracture toughness and resistance to fatigue crack growth.

In the case of Ti-6Al-4V castings with microstructures of 100% beta transformation product there is well documented evidence that the fracture toughness is good and that resistance to fatigue crack growth is high. Evidence is beginning to emerge that the resistance of aluminium alloy castings to fatigue crack growth is also high. An investigation by Dr P.Pitcher at the Royal Aircraft Establishment has shown that the constant amplitude fatigue threshold stress intensity factors for as-cast, homogenised and heat treated 357 alloy are higher than those of wrought aluminium alloys. For both cast titanium and cast aluminium the resistance to fatigue crack growth appears to be associated with the tortuous nature of the fatigue crack path, since there is crack bifurcation and growth on preferred crystal planes away from the plane of maximum tensile stress. Deflected and bifurcated cracks produced by structure-sensitive fatigue crack growth give considerably lower stress intensity factors for a given load and crack length than do planar, structure-insensitive fatigue cracks and result in long energy absorbing fracture paths.

Much of the fatigue crack growth data currently available for castings relates to constant amplitude loading. What is now required for airframe components is an indication of growth resistance under complex loading spectra. To complete the picture for damage tolerant designs K_{IC} and K_{Ic} data will be required since castings exhibit a wide range of section thickness and associated microstructural variations.

The damage tolerant philosophy for wrought components assumes the presence of defects when components enter service. Defects in the form of pores or shrinkage cracks are likely to be present to a greater or less extent in a casting and application of the damage tolerant philosophy to castings seems particularly appropriate. It will however be necessary to determine accurately the size and position of the defects using existing and improved NDE techniques and to study crack growth from defects under appropriate and frequently complex fatigue loading sequences. It will be particularly important to investigate the effect of defects in regions of high stress concentration.

On an unrelated topic Mr Stubbington pointed out that increasing demands for fuel efficient civil and high performance military aircraft were placing requirements on the designer to reduce airframe weight. Weight reduction is particularly important for short and vertical take-off aircraft and helicopters. Efforts are being made to develop wrought lithium containing aluminium alloys with densities $\sim 10\%$ lower than those of the currently available 2000 and 7000 series alloys. Lithium containing aluminium alloys, with compositions modified to optimise casting characteristics and properties would also be attractive for cast components.

MR J.LEE, Westland Helicopters Ltd, UK, referred to the first paper presented and to the statement that for castings to be more widely used they need to be available at the right time, at the right price and of the right quality. He thought that the various sessions had amply demonstrated that more complex castings could now be produced than in the past and that steps were being taken to develop reproducible quality standards. Present requirements are for extensive radiographic examination to cover proof of quality and experience at Westland Helicopters has indicated that for quite small but complex castings of highly variable section the cost of radiography could be 25% of the cost of the casting. He anticipated that the situation might soon be reached where, with automated production and sufficient process control the conventional 100% radiographic coverage could be significantly reduced. This worthwhile target would have an important impact on cost. Mr Lee was very encouraged that we are moving from the past tradition of a casting being totally dependent on individual skills to something that is a numerically controlled production process.

MR D.McLELLAN, Boeing Company, Seattle, US, agreed with Mr Lee that the cost of 100% radiography was prohibitive. Although radiography has its applications it also has limitations in terms of both quantity and geometric complexity. He was concerned that throughout the meeting speakers had not addressed the issue of quality assurance via image analysis techniques. These were available commercially and had been used by the Boeing Company for some years. It is possible using image analysis techniques to quantify the three major microstructural features which determine mechanical properties, particularly elongation. For aluminium based alloys these features are the cell structure, the silicon particle eutectic and the porosity. Mr McLellan thought that until producers and users of castings developed such methods that are reliable and economically feasible the improved real product assurance needed for increased utilisation of castings in primary structures of aircraft will not be achieved.

MR D.DUCKWORTH, Bae Warton, UK, said that a single supplier situation was undesirable and he was concerned that there was no guarantee that the same answers could be obtained from different parts of the foundry industry. He thought that it might be necessary to have a different approach to the writing of British Standards for castings, since the present standards are insufficiently stringent. This action may be necessary to ensure a uniform high quality product from a broad spectrum of the foundry industry.

MR G.SWINYARD, Industrial Precision Casting, Rochester, UK, agreed that aircraft constructors and foundry representatives should cooperate to tighten the specifications to ensure a more uniform quality. He was sure that the founders could, using the range of processes discussed during the meeting, satisfy the aircraft constructors.

DR J.CAMPBELL, Cosworth Research and Development Ltd, Worcester, UK, was concerned that the aerospace industry was concentrating on the 356 and 357 alloys. Although these alloys have reasonable casting characteristics and mechanical properties a founder starting from scratch to design a new alloy would not arrive at these compositions. Rather he would design an alloy that is easier to cast and therefore likely to give a more consistent product of benefit to aerospace industry. The fact that the currently preferred alloys for aerospace applications may not necessarily be the best alloys should be examined as a matter of urgency.

PROFESSOR J.F.WALLACE, Case Western Reserve University, US, asked Dr Campbell to expand on this suggestion.

Dr J.Campbell replied that his choice would be a eutectic silicon material. The reason for this was related to considerations of porosity. An important source of porosity in a casting is that which is initiated at the casting surface and which then creeps into the casting. As it does so it forms a very large region of porous material in the interior, which, on a microsection, looks like dispersed porosity. This apparent dispersed porosity is in fact a large macropore. One of the benefits of a eutectic alloy, solidifying as it does on a planar or substantially planar front, is that the whole problem of interior porosity developing from the surface, particularly in hot spots and at re-entrant angles, would disappear. The founder would have an alloy with at least 50% greater fluidity than current alloys. Such an alloy would be very tolerant to poorly fed sections. The long freezing range of 357, consequent upon the 7% silicon content, tends to maximise casting problems and the alloy would not be Dr Campbell's preferred material for aerospace applications.

MR R.MILLGATE, Industrial Precision Castings, Rochester, UK, agreed with Dr Campbell about the choice of a eutectic alloy but thought that the reason the aerospace industry preferred alloys such as 357 was because high strength castings were required. He too thought it necessary for aerospace and foundry interests to get together to plan the way ahead.

In reply Dr Campbell said he was not advocating reducing the strength of castings. On the contrary, more strength would be obtained from reproducibly sound material. The alloy he had referred to had never been optimised and he thought it important to do so.

MR R.FINCH, British Aerospace, Warton, UK, said he was a designer for a company using castings. He had listened to the presentations with great interest and found it very encouraging to see the extensive amount of both theoretical and practical work aimed at improving metallurgical quality. Important though this was, from the view point of the user company this did not come first on the list of considerations. On numerous occasions when castings had been considered for use they have failed at the first hurdle when weights were considered against the competing article. The reason for failure was partially the strength of the material but also, and quite significantly, the stressing factor which must be applied when castings are used. He was referring primarily to UK applications but was aware of a similar situation in MBB in Germany. These two factors, combined with the inability on occasion to obtain very thin, large surface area components, all combine to produce unfavourable weights. If the cast component does not fail on the basis of weight then another possibility for failure is high tooling costs, particularly for a limited production run. In addition there is often an inability to obtain surfaces smooth enough to use without machining, an operation which adds significantly to cost. In some cases long development times can rule out castings. These various factors should be considered by suppliers of castings and Mr Finch asked for the right emphasis on them in relation to the obvious importance of the metallurgical aspects.

In summing up, **MR J.LEE**, Westland Helicopters Ltd, UK, the Meeting Chairman, said he thought the meeting had been very successful but that with such a wide ranging programme it was difficult to summarise the achievements. The first objective was to bring together designers and specialists in castings and that had certainly been achieved with a

good cross section of users, manufacturers and those working in casting research. As a second objective we had set out to ascertain from designers factors limiting the use of castings and as a third objective to establish from casting specialists the present state-of-the-art. These objectives had also been achieved.

The very significant improvements in technology of the last few years has been clearly demonstrated and these had been coupled with presentations on novel technology which promised very interesting future possibilities.

The last objective was to highlight areas where lack of knowledge is perhaps limiting the use of castings. On this topic Mr Lee suggested that if casting configurations are to be optimised it was necessary to design the component as a casting 'ab initio' rather than convert a component designed as a fabricated wrought assembly into a casting. Maximum use must be made of the science of casting and although traditional individual operator skills are still relevant, it is more and more important to have scientific automated production processes.

In looking at outstanding problems he thought it necessary to demonstrate repeatability of quality and strength and this repeatability must be provided at a constant and acceptable price to a scheduled delivery. Another outstanding problem which requires solution is how the quality of a casting can be proved economically and perhaps with even greater accuracy. If that is possible the designer will be given greater confidence and the various casting factors that lower the efficiency of a casting can be reduced.

Until the discussion there was very little mention of novel alloy development for castings. In the past much effort had gone into the achievement of optimum properties in castings from well established aluminium and titanium alloys but during the discussion suggestions had been made that there is potential for novel alloys developed uniquely for casting or to achieve a superior balance of properties.

Mr Lee then thanked the authors, chairmen and recorders. He complimented the authors on the very high standards of their papers and presentations and in particular thanked the two authors who had prepared papers at short notice. He thanked the long suffering interpreters, the technicians and the audience and finally extended thanks to the hosts, the Belgian Air Force and the Royal Military College for the excellent facilities.

REPORT DOCUMENTATION PAGE

1. Recipient's Reference	2. Originator's Reference AGARD-CP-325	3. Further Reference ISBN 92-835-0314-6	4. Security Classification of Document UNCLASSIFIED
5. Originator	Advisory Group for Aerospace Research and Development North Atlantic Treaty Organization 7 rue Ancelle, 92200 Neuilly sur Seine, France		
6. Title	ADVANCED CASTING TECHNOLOGY		
7. Presented at	the 54th Meeting of the AGARD Structures and Materials Panel in Brussels, Belgium on 4-9 April 1982.		
8. Author(s)/Editor(s) Various	9. Date August 1982		
10. Author's/Editor's Address Various	11. Pages 344		
12. Distribution Statement	This document is distributed in accordance with AGARD policies and regulations, which are outlined on the Outside Back Covers of all AGARD publications.		
13. Keywords/Descriptors Casting Foundry practice Molding techniques Aluminium castings			
14. Abstract Advances in casting technology can lead to a single casting replacing a complex fabrication of wrought components with consequent cost and weight benefits but there is traditionally a reluctance by designers to trust castings. The object of the Specialists' Meeting was to present the current state of development of advanced casting technology, and to bring together designers and materials and processing engineers for a full exchange of views. The papers presented a comprehensive review of the state of casting technology development, and illustrate the significant advances made over the last few years. It became clear from the discussion that the use of castings, especially aluminium alloy castings, for main structural applications is likely to increase significantly in the near future.			

<p>AGARD Conference Proceedings No.325 Advisory Group for Aerospace Research and Development, NATO ADVANCED CASTING TECHNOLOGY Published August 1982 344 pages</p> <p>Advances in casting technology can lead to a single casting replacing a complex fabrication of wrought components with consequent cost and weight benefits but there is traditionally a reluctance by designers to trust castings. The object of the Specialists' Meeting was to present the current state of development of advanced casting technology, and to bring together designers and materials and processing engineers for a full exchange of views.</p> <p>P.T.O.</p>	<p>AGARD-CP-325</p> <p>Casting Foundry practice Molding techniques Aluminium castings</p>	<p>AGARD Conference Proceedings No.325 Advisory Group for Aerospace Research and Development, NATO ADVANCED CASTING TECHNOLOGY Published August 1982 344 pages</p> <p>Advances in casting technology can lead to a single casting replacing a complex fabrication of wrought components with consequent cost and weight benefits but there is traditionally a reluctance by designers to trust castings. The object of the Specialists' Meeting was to present the current state of development of advanced casting technology, and to bring together designers and materials and processing engineers for a full exchange of views.</p> <p>P.T.O.</p>	<p>AGARD-CP-325</p> <p>Casting Foundry practice Molding techniques Aluminium castings</p>
<p>AGARD Conference Proceedings No.325 Advisory Group for Aerospace Research and Development, NATO ADVANCED CASTING TECHNOLOGY Published August 1982 344 pages</p> <p>Advances in casting technology can lead to a single casting replacing a complex fabrication of wrought components with consequent cost and weight benefits but there is traditionally a reluctance by designers to trust castings. The object of the Specialists' Meeting was to present the current state of development of advanced casting technology, and to bring together designers and materials and processing engineers for a full exchange of views.</p> <p>P.T.O.</p>	<p>AGARD-CP-325</p> <p>Casting Foundry practice Molding techniques Aluminium castings</p>	<p>AGARD Conference Proceedings No.325 Advisory Group for Aerospace Research and Development, NATO ADVANCED CASTING TECHNOLOGY Published August 1982 344 pages</p> <p>Advances in casting technology can lead to a single casting replacing a complex fabrication of wrought components with consequent cost and weight benefits but there is traditionally a reluctance by designers to trust castings. The object of the Specialists' Meeting was to present the current state of development of advanced casting technology, and to bring together designers and materials and processing engineers for a full exchange of views.</p> <p>P.T.O.</p>	<p>AGARD-CP-325</p> <p>Casting Foundry practice Molding techniques Aluminium castings</p>

<p>The papers presented a comprehensive review of the state of casting technology development, and illustrate the significant advances made over the last few years. It became clear from the discussion that the use of castings, especially aluminium alloy castings, for main structural applications is likely to increase significantly in the near future.</p> <p>Papers presented at the 54th Meeting of the AGARD Structures and Materials Panel in Brussels, Belgium on 4–9 April 1982.</p> <p>ISBN 92-835-0314-6</p>	<p>The papers presented a comprehensive review of the state of casting technology development, and illustrate the significant advances made over the last few years. It became clear from the discussion that the use of castings, especially aluminium alloy castings, for main structural applications is likely to increase significantly in the near future.</p> <p>Papers presented at the 54th Meeting of the AGARD Structures and Materials Panel in Brussels, Belgium on 4–9 April 1982.</p> <p>ISBN 92-835-0314-6</p>
<p>The papers presented a comprehensive review of the state of casting technology development, and illustrate the significant advances made over the last few years. It became clear from the discussion that the use of castings, especially aluminium alloy castings, for main structural applications is likely to increase significantly in the near future.</p> <p>Papers presented at the 54th Meeting of the AGARD Structures and Materials Panel in Brussels, Belgium on 4–9 April 1982.</p> <p>ISBN 92-835-0314-6</p>	<p>The papers presented a comprehensive review of the state of casting technology development, and illustrate the significant advances made over the last few years. It became clear from the discussion that the use of castings, especially aluminium alloy castings, for main structural applications is likely to increase significantly in the near future.</p> <p>Papers presented at the 54th Meeting of the AGARD Structures and Materials Panel in Brussels, Belgium on 4–9 April 1982.</p> <p>ISBN 92-835-0314-6</p>